

Ultraschall und Theragnostik

Ultraschall in Thera(pie) und (Dia)gnostik

Theragnostik: Diagnostische Systeme mit integrierter Therapie

Prof. Dr. Rainer Brucher

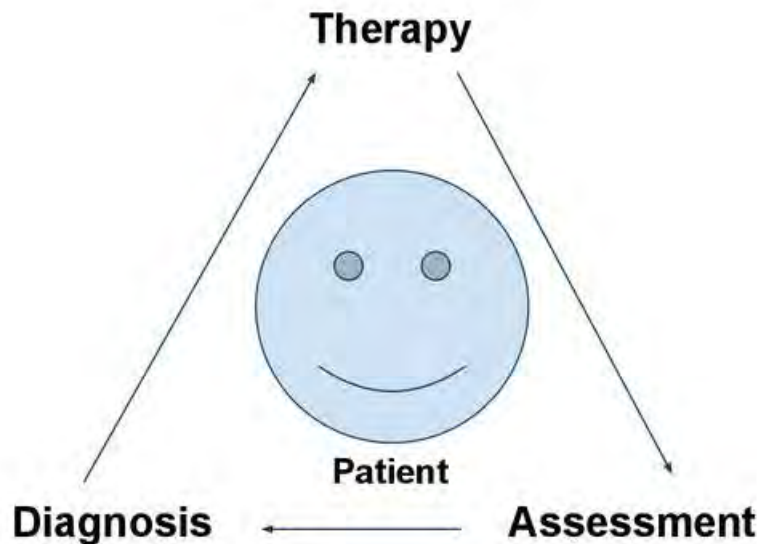
brucher@hs-ulm.de

(Version 1.2)

Theragnostik / Theranostik

Diagnostische Systeme mit integrierter Therapie (Medicine in the loop)

Personen spezifische therapiebegleitende Diagnostik ; individualisierte Medizin



The fundamentals of Theragnostic Medicine, center around personalized patient care.
By this: rapid and sophisticated assessment of the patient's medical condition is attained, followed by a specialized knowledge of the patients diagnosis, which ultimately leads to a custom treatment modality to be applied.

Inhaltsangabe

1. Übersicht der Ultraschallanwendungen
2. Physikalische Grundlagen (Schallausbreitung und Kenngrößen)
3. Ultraschallsonde
 - Einzelemente, Arrays, Abstrahlcharakteristiken
4. Bildgebende Verfahren in der Diagnostik
 - A-Scan, B-Mode, M-Mode, Duplex, Power-Mode, 3D-Verfahren
 - Gerätetechnik
5. Dopplerverfahren in der Blutfluss-Diagnostik
 - Doppler-Effekt, CW/PW-Mode, Strömung, Spektrogramm, Geräteelektronik,
6. Artefakte und Diagnostik
 - Bildgebende Diagnostik → Beispiele mit Artefakten
 - Blutflussdiagnostik → Beispiele mit Artefakten
 - Embolie-Detektion
7. Ultraschall und Kontrastmittel
 - Kontrastmittelverhalten, Anwendung Durchblutung mittels Bolus / Clearance
8. Theragnostik mit Ultraschall
 - Schlaganfall / Embolyse mit und ohne Ultraschallkontrast
9. Therapie mit hochdosierten Ultraschall
10. Gewebecharakterisierung mittels „shear waves“ (Tumordiagnostik)
11. Dosierung / Messverfahren und Sicherheitsaspekte (in der Diagnostik)

Content

1. Introduction and summary of ultrasound and its applications
2. **Basics (physical quantities, sound propagation)**
3. Ultrasound transducer / probes
single elements, phased arrays, beam characteristics
4. Diagnostic and imaging methods
A-Scan, B-Mode, M-Mode, Duplex, Power-Mode, 3D/4D-imaging
Instrumentation
5. Diagnostic and ultrasound Doppler instrumentation
Doppler-Effect, CW/PW-Mode, flow profiles, Spectrograms, Instrumentation,
6. Artefacts and diagnostic
Imaging diagnostics → artefacts
Blood flow diagnosis → artefacts
Embolus-Detection and -Discrimination
7. Ultrasound and contrast agent
Bubble behaviour, Application for flow measurements using Bolus / Clearance
8. Theragnostic and ultrasound
Stroke/ Embolysis with and without ultrasound contrast agent
9. Therapy and high intensity focused ultrasound
10. Tissue characterisation using shear waves (diagnosis in cancer)
11. Ultrasound dosis and safety aspects (in diagnostic)

Was ist Ultraschall

Was ist Ultraschall?

Als **Ultraschall** (US) bezeichnet man Schall mit einer Frequenz, **oberhalb des menschlichen Hörbereichs** (< 20 kHz).



Die US-Wellen werden in einem **Schallkopf** erzeugt. Dieser besteht aus vielen kleinen Elementen die eine spezielle Eigenschaft haben:

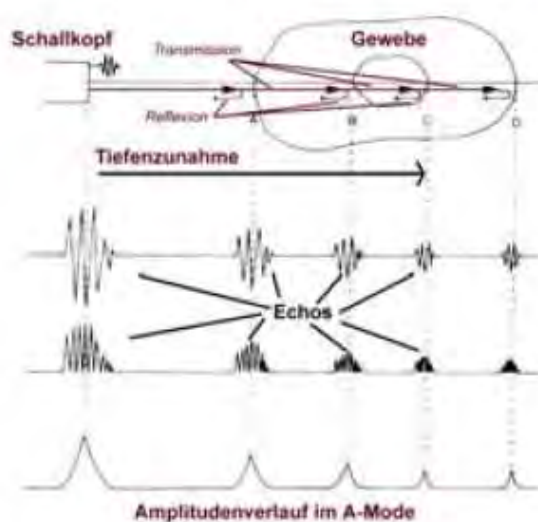
Wird an die Elemente eine elektrische Spannung angelegt, beginnen sie zu schwingen und senden dabei Ultraschall-Wellen aus. (Piezoelektrischer Effekt)



Entstehung eines Ultraschallbilds

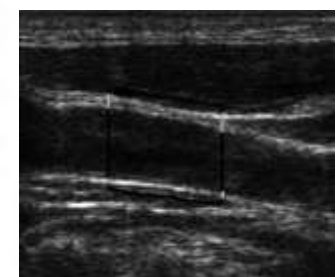
Wie entsteht ein Ultraschall-Bild?

Treffen die Ultraschallwellen im Körper auf **Gewebe / Organ-Grenzen**, so wird ein Teil der zum Schallkopf zurückreflektiert (Echo), der andere Teil breitet sich weiter im Körper aus. Die Echos werden vom Schallkopf aufgefangen, in eine elektrische Spannung (Amplitude) umgewandelt. Je nach spezifischer **Gewebedämpfung** sind die Echos unterschiedlich stark. Die Spannungswerte werden **256** verschiedenen **Grauwertstufen** zugeordnet, die somit die Helligkeit jedes einzelnen Bildpunktes festlegen.



B-Mode oder Grauwertverfahren

Aus der **Zeitdifferenz** zwischen dem Aussenden einer Schallwelle und dem Empfang der Echos kann die **Tiefe** berechnet werden, aus der die Echos stammen. Aus der Abstrahl- und **Empfangscharakteristik** des Schallkopfes ermittelt das Gerät die **Position des Bildpunktes**.



Ein **Ultraschall-Bild** ist ein **zweidimensionales Schnittbild** aus dem Körperinneren, das aus vielen einzelnen Ultraschalllinien in **Echtzeit** (25-100 Bilder/Sekunde) aufgebaut wird.

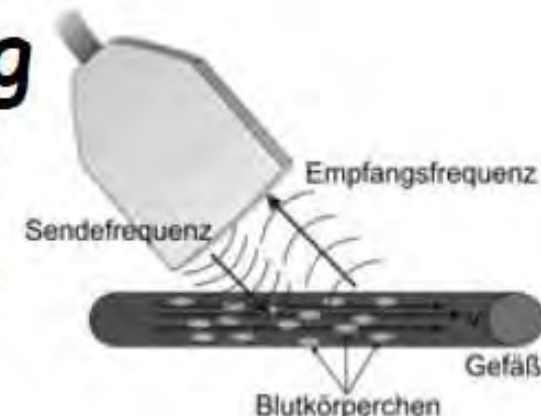


Der Dopplereffekt und Blutflussmessungen

Der Dopplereffekt in der Ultraschall-Bildgebung

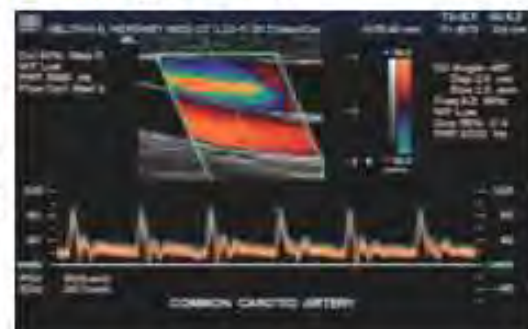
Treffen Ultraschall-Wellen auf ein Objekt, das sich relativ zum Schallkopf bewegt (z.B. Blutkörperchen), so stimmen die ausgesandte und detektierte Frequenz der Wellen nicht mehr überein.

(Doppler-Effekt, Chr. Doppler 1843)



Die **Frequenzverschiebung** wird im Schallkopf ausgewertet und farbig codiert dem Grauwertbild überlagert dargestellt.
(Farbdoppler, Duplexgeräte)

Anhand des Frequenzunterschiedes kann die **Geschwindigkeit und Richtung** des Blutflusses in einem Gefäß berechnet werden.



Anwendungen des Doppler-Ultraschalls:

Detektion von Gefäßverengungen und -verschlüssen (Thrombosen), Kontrolle des Verlaufs von Organtransplantationen, Untersuchung der Funktion der Herzklappen



Anwendungsbereiche Ultraschall

Wo wird Ultraschall angewendet?

Bildgebende Diagnostik in der Medizin

Erkennen von organischen Veränderungen in der inneren Medizin, Gynäkologie,...

Untersuchung von: Leber, Gallenblase, Niere, Diagnose von Verengungen und Verschlüssen von Venen und Arterien, Entwicklung des Fötus während der Schwangerschaft, ...



Normale Niere



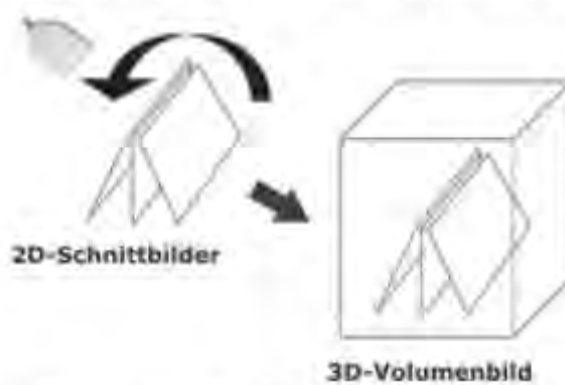
Gallenblase mit Gallenstein

Therapeutischer Ultraschall

Behandlung von Sehnen- und Muskelzerrungen, Schmerzbehandlung bei Gelenksabnützungen (Knie, Hüfte, Schulter)

Räumliche Ultraschall-Verfahren

Werden von einem Organ mehrere 2D Schnittbilder aufgenommen, so kann man daraus mit Hilfe des Computers eine **3 dimensionale Darstellung** des Organs berechnet werden. Voraussetzung dafür ist, dass man die Position der einzelnen Bilder zueinander kennt. Diese wird entweder durch Positions-sensoren oder durch eine gesteuerte Bewegung der Elemente im Schallkopf selbst ermittelt.



Anwendungen:

Diagnose von Fehlbildungen, Vermessung von Strukturen, Quantifizierung von Plaqueablagerungen



Mittlerweile ist das 3D-Verfahren schon so weit entwickelt, dass sogar eine Darstellung der **räumlichen Bilder in "Echtzeit"** also Live auf dem Monitor möglich ist.

(**4D US-Verfahren**)



Gefährlichkeit von Ultraschall

Ist Ultraschall eigentlich gefährlich?

Bei der Anwendung von ***Ultraschall in der Medizin*** handelt es sich um eine durchaus ***sichere Bildgebungs- und Therapiemethode***.

Auch wenn bisher sind keine schädlichen oder negativen Effekte an Patienten für die diagnostischen Verfahren festgestellt worden sind, sollte der Anwendung von Ultraschall in Diagnostik & Therapie folgendes beachtet werden :



Therapie-Verfahren :

potentiell gefährlich durch hohe Energieeinträge
Erwärmung & mechanische Effekte (Gewebezerstörung möglich)

Doppler-Verfahren :

geringst mögliche Leistung & Einsatzzeit verwenden, sofern die diagnostische Information nicht beeinträchtigt wird (prudent use).
Minimierung der Schallexposition an einem Gewebepunkt.
(in Kombi mit US-Kontrastmitteln erhöhtes Risiko !!)

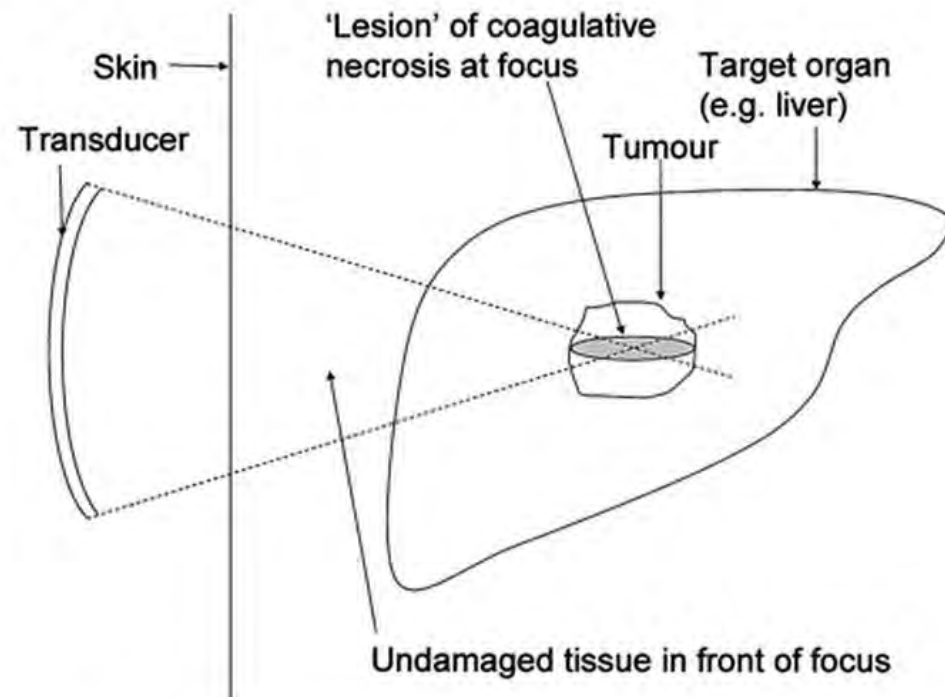
umsichtig

B-Mode / 3D / 4D-Verfahren :

nicht kontraindiziert, keine Einschränkungen
(in Kombi mit US-Kontrastmitteln erhöhtes Risiko !!)

Hochfokussierter Ultraschall

High Intensity Focused Ultrasound: Chirurgie der Zukunft?



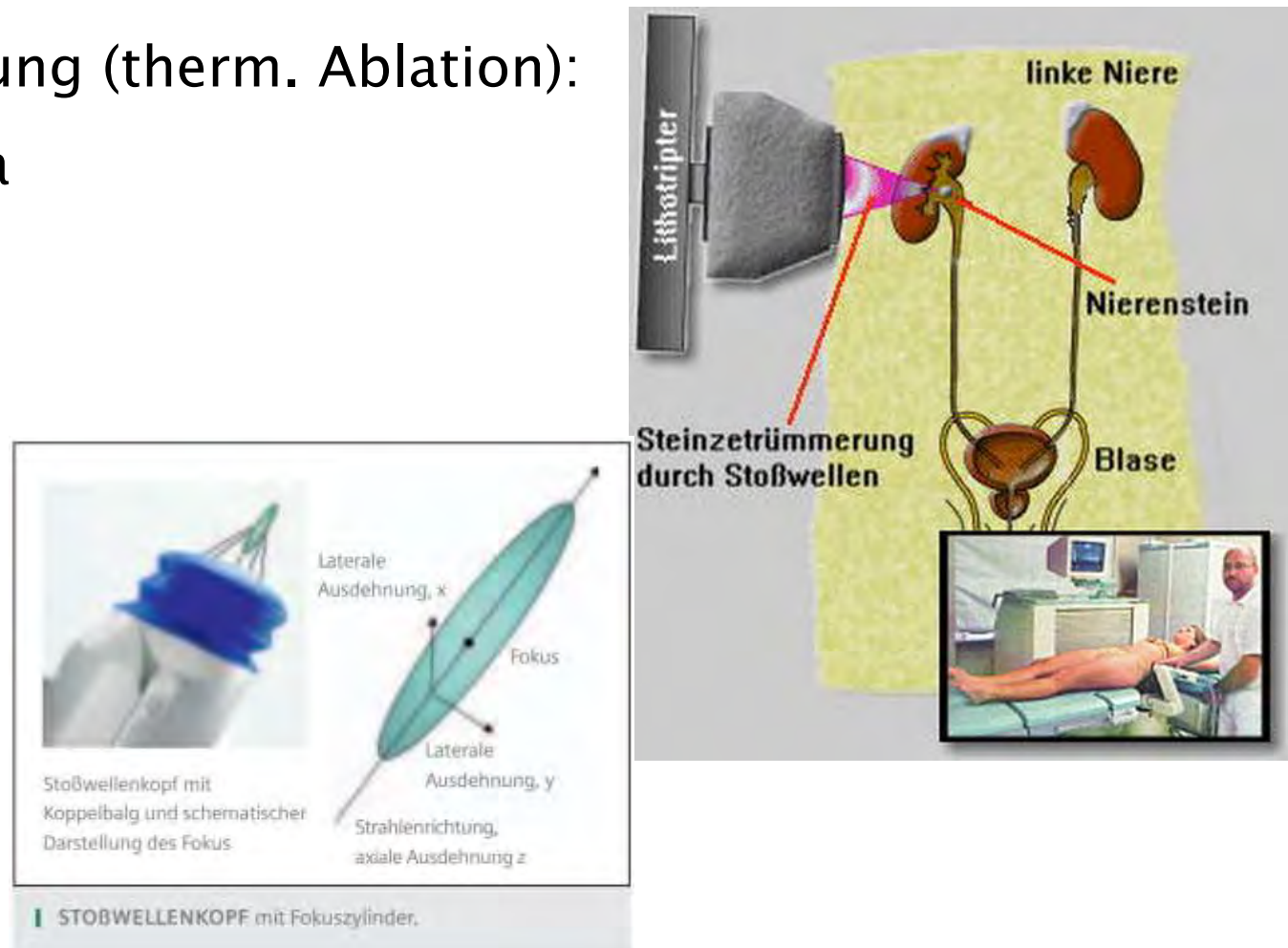
Abbildung

Eine schematische Darstellung der hohen fokussierten Ultraschall Läsion Produktion.

Effekte: Mechanische Energie → Wärme ; Kavitation

Hochdosierter Ultraschall

- Intra-/Extrakorporale Lithotripsie
- Nierensteinzertrümmerer (Stoßwellen)
- Tumorzerstörung (therm. Ablation):
 - Prostata
 - Brust
 - Leber
 - Niere
- Abrasion
(Abkratzen)



Ultraschall und Theragnostik

Ultraschall in Thera(pie) und (Dia)gnostik

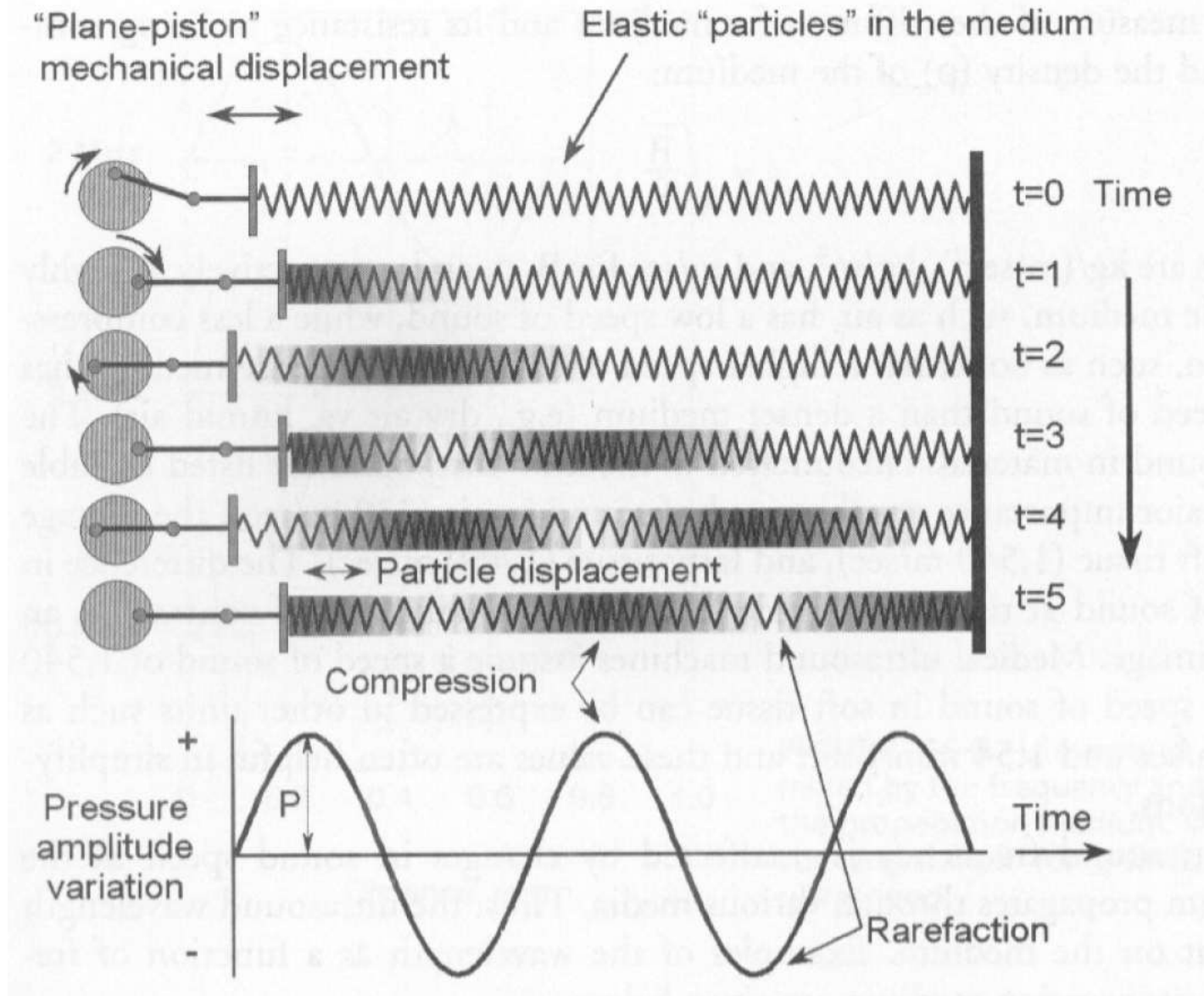
Kapitel 2

Physikalische Grundlagen

Inhaltsangabe

1. Übersicht der Ultraschallanwendungen
2. **Physikalische Grundlagen**
3. Ultraschallsonden
4. Bildgebende Verfahren in der Diagnostik
5. Dopplerverfahren in der Diagnostik
6. Artefakte und Diagnostik
7. Ultraschall und Kontrastmittel
8. Theragnostik mit Ultraschall
9. Therapie mit hochdosierten Ultraschall
10. Gewebecharakterisierung mittels shear waves
11. Dosierung und Sicherheitsaspekte

Physical Basics (quantities of sound field)



Physikalische Grundlagen (Schallfeldgrößen)

Symbol	Einheiten	Bedeutung
I	W/m^2	Schallintensität
p	$\text{Pascal} = \text{N/m}^2$	Schalldruck
u	m/s	Schallschnelle
$Z_0 = c \cdot \rho$	$\text{N} \cdot \text{s/m}^3$	Schallkennimpedanz, Akustische Feldimpedanz
ρ	kg/m^3	Luftdichte, Dichte der Luft (des Mediums)
a	m/s^2	Schallbeschleunigung
ξ	m, Meter	Schallauslenkung
$\omega = 2 \cdot \pi \cdot f$	rad/s	Kreisfrequenz
f	Hertz	Frequenz
E	$\text{W} \cdot \text{s/m}^3$	Schallenergiedichte
P_{ak}	W, Watt	Schallleistung
A	m^2	Durchschallte Fläche
c	m/s	Schallgeschwindigkeit

Physikalische Grundlagen (Schallfeldgrößen)

Schalldruckpegel: $L = 20 \cdot \log_{10} \left\{ \frac{p_1}{p_0} \right\}$ in dB Bezugsschalldruck $p_0 = 1 \mu Pa$
 (Feldgröße)

Schallfluss: $q = u \cdot A$ $[q] = \frac{m}{s} m^2 = m^3 / s$ (Schallschreie u · durchströmte Fläche A)

Akustische Impedanz: $Z_{ak} = \frac{p}{q} = \frac{\text{Schalldruck}}{\text{Schallflus s}}$; $[Z_{ak}] = \frac{N / m^2}{m^3 / s} = \frac{Ns}{m^5}$

Schallintensität $I = p \cdot u \Big|_{Z_0 = \frac{p}{u}} == p^2 / Z_0 = u^2 Z_0$;(im Schallstrahl)
 Pegel: $I_{dB} = 10 \lg \{ I / I_0 \}$

$$[I] = N / m^2 \frac{m}{s} = \frac{Nm}{sm^2} = \frac{W}{m^2}$$

Schallleistung $P_{ak} = I_{ave} \cdot A = p \cdot q = p \cdot u \cdot A$

Vergleich Luft/Flüssigkeit $\frac{Z_{0,Wasser}}{Z_{0,Luft}} = \frac{(\rho \cdot c)_{Wasser}}{(\rho \cdot c)_{Luft}} = \frac{1,485 \cdot 10^6}{408} = 3640$

Physikalische Grundlagen (Wellentheorie)

Schallausbreitung

Die Schallwelle wird über den Druck p (Skalar, entspricht Kraft pro Fläche) angekoppelt. Dadurch entstehen in Ausbreitungsrichtung (z -Richtung) eine dem Druck proportionale Dichteänderung ρ_1 der mittleren Dichte ρ_0 , eine dem Druck proportionale Bewegung der Gewebeteilchen mit der Teilchengeschwindigkeit u und eine Ausbreitungsgeschwindigkeit c der Welle. Beide Geschwindigkeiten sind Vektoren, es werden aber nur ihre Beträge betrachtet, da die Richtung im eindimensionalen Modell stets der z -Richtung entspricht.

Es gilt $\rho_1 / \rho_0 = K \cdot p$ mit K = „adiabatische Kompressibilität“

$[K] = m^2/N = m \cdot s^2/kg$

An einem Volumenelement $\Delta V = A_L \cdot \Delta z$ ergeben sich durch Vergleich

- der Kraft = Masse \times Beschleunigung mit der Kraft = Druckdifferenz \times Fläche:

$$\frac{\partial p}{\partial z} + \rho_0 \frac{\partial u}{\partial t} = 0 \quad (1)$$

- der Massenänderung durch Veränderung des Volumens mit der durch Dichteänderung:

$$\frac{\partial p}{\partial t} + \frac{1}{K} \cdot \frac{\partial u}{\partial z} = 0 \quad (\text{für } \rho_1 \ll \rho_0) \quad (2)$$

Aus (1), (2) folgen

$$\frac{\partial^2 u}{\partial z^2} - \rho_0 \cdot K \frac{\partial^2 u}{\partial t^2} = 0 \quad (3)$$

$$\text{bzw. } \frac{\partial^2 p}{\partial z^2} - \rho_0 \cdot K \frac{\partial^2 p}{\partial t^2} = 0 \quad (4)$$

Diese Wellengleichungen $p(z,t)$ und $u(z,t)$ sind gleich, also muß gelten: $p \sim u$

Die Lösung der Wellengleichung ist jede periodische hin- bzw. rücklaufende Welle, z.B. für p :

$$p = p_{\pm} \cdot f(\omega t \mp kz) \quad (5)$$

$$\text{z.B. } p = p_{+} \cdot \cos(\omega t - kz) \quad (6)$$

mit p_{\pm} = Amplitude der hinlaufenden Welle, $\omega = 2\pi/T$, (T = Periodendauer = $1/f$)
 und k = „Ausbreitungskonstante“ $[k] = 1/m$

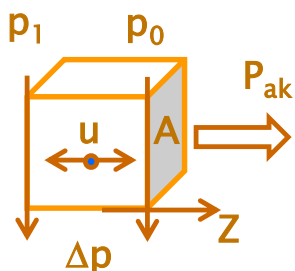
$$(6) \text{ in (4) liefert: } \rho_0 \cdot K \cdot \omega^2 = k^2 \text{ also } k = \omega \cdot \sqrt{\rho_0 \cdot K} \quad (\text{„Dispersionsgleichung“}) \quad (7)$$

Die Ultraschallwelle ist zu jeder Zeit t längs der z -Richtung mit der Wellenlänge λ periodisch,

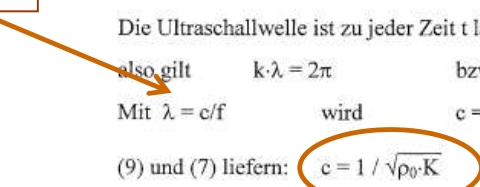
$$\text{also gilt } k \cdot \lambda = 2\pi \quad \text{bzw. } \lambda = 2\pi/k \quad (8)$$

$$\text{Mit } \lambda = c/f \quad \text{wird} \quad c = 2\pi f/k = \omega/k \quad (9)$$

$$(9) \text{ und (7) liefern: } c = 1 / \sqrt{\rho_0 \cdot K} \quad (\text{unabhängig von } \omega !) \quad (10)$$

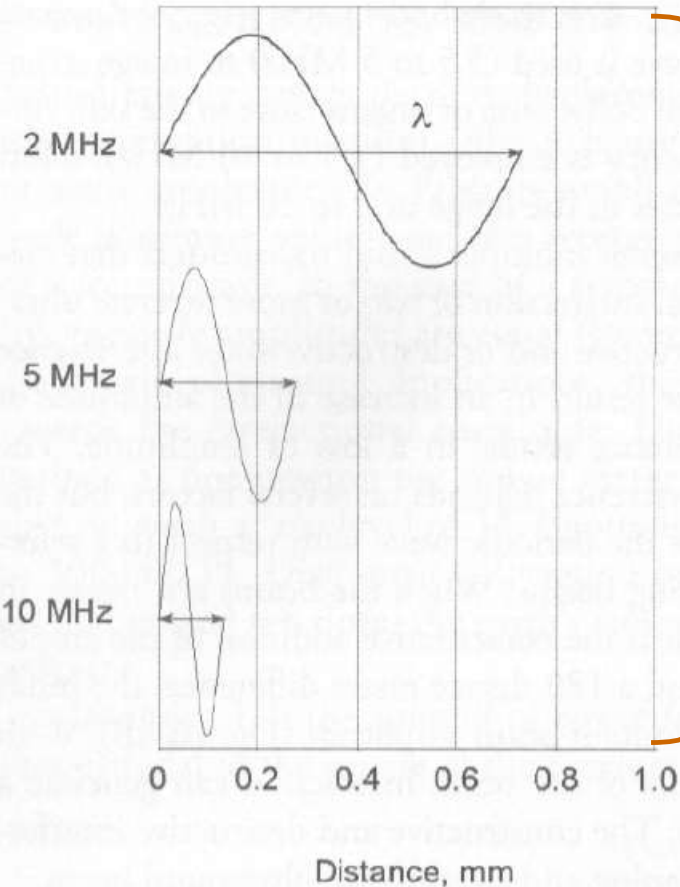


$$c = \lambda \cdot f$$



Physikalische Grundlagen (Schallfeldgrößen)

Wellenlänge (λ), Frequenz (f) und Ausbreitungsgeschwindigkeit (c)



$$c = \lambda \cdot f \quad c = \sqrt{E/\rho} = \sqrt{1/K\rho} \quad \left[\frac{m}{sec} \right] = \sqrt{\frac{kg}{m \cdot sec^2}} / \frac{kg}{m^3}$$

⇒ axiale Auflösung

Example: A 2-MHz beam has a wavelength in soft tissue of

$$\lambda = \frac{c}{f} = \frac{1,540 \text{ m/sec}}{2 \times 10^6/\text{sec}} = 770 \times 10^{-6} = 7.7 \times 10^{-4} \times 1,000 \frac{\text{mm}}{\text{m}} = 0.77 \text{ mm}$$

A 10-MHz ultrasound beam has a corresponding wavelength in soft tissue of

$$= \frac{1,540 \text{ m/sec}}{10 \times 10^6/\text{sec}} = 154 \times 10^{-6} = 1.54 \times 10^{-4} \times 1,000 \frac{\text{mm}}{\text{m}} \approx 0.15 \text{ mm}$$

Physikalische Grundlagen (Schallfeldgrößen)

Wellenlänge (λ), Frequenz (f) und Ausbreitungsgeschwindigkeit (c)

TABLE DENSITY AND SPEED OF SOUND IN TISSUES AND MATERIALS FOR MEDICAL ULTRASOUND

Material	Z ₀ (rayls)	Density (kg/m ³)	c (m/s)	c (mm/μs)
Air	0.0004 × 10 ⁶	1.2	330	0.33
Lung	0.18 × 10 ⁶	300	600	0.60
Fat	1.34 × 10 ⁶	924	1,450	1.45
Water	1.48 × 10 ⁶	1,000	1,480	1.48
Soft tissue	1.63 × 10 ⁶	1,050	1,540	1.54
Kidney	1.65 × 10 ⁶	1,041	1,565	1.57
Blood	1.65 × 10 ⁶	1,058	1,560	1.56
Liver	1.65 × 10 ⁶	1,061	1,555	1.55
Muscle	1.71 × 10 ⁶	1,068	1,600	1.60
Skull bone	7.8 × 10 ⁶	1,912	4,080	4.08
PZT		7,500	4,000	4.00

PZT, lead-zirconate-titanate.

$$\lambda \text{ (mm, soft tissue)} = \frac{c}{f} = \frac{1,540 \text{ mm/μsec}}{f(\text{MHz})} = \frac{1,540 \text{ mm}/10^{-6} \text{ sec}}{f(10^6/\text{sec})} = \frac{1.54 \text{ mm}}{f(\text{MHz})}$$

Kennimpedanz : Z₀ = Z · A = ρ₀ · c

Physikalische Grundlagen (Schallfeldgrößen)

Akustische Kennimpedanz / Akustische Impedanz

$p \sim u$ führt zur Definition der "akustische Kennimpedanz" Z_0

$$p = Z_0 \cdot u$$

bzw.

$$Z_0 = p/u$$

mit

$$[Z_0] = \text{kg}/(\text{m}^2 \cdot \text{s})$$

(11) in (1) liefert mit (6): $k = \rho_0 \cdot \omega / Z$

also: $Z_0 = \rho_0 \cdot \omega / k$

bzw. mit (9):

$$Z_0 = c \cdot \rho_0$$

oder mit (10):

$$Z_0 = \sqrt{\rho_0 / K}$$

(11)

(12a)

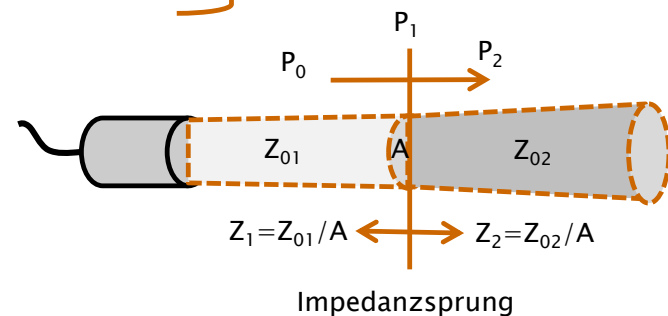
(12b)

(12c)

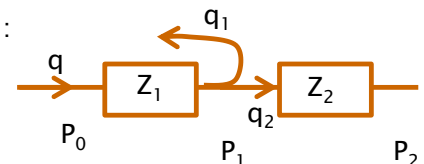
akustische
Kennimpedanz Z_0

TABLE ACOUSTIC IMPEDANCE, $Z_0 = \rho c$, FOR AIR,
WATER AND SELECTED TISSUES

Tissue	Z_0 (rayls)
Air	0.0004×10^6
Lung	0.18×10^6
Fat	1.34×10^6
Water	1.48×10^6
Kidney	1.63×10^6
Blood	1.65×10^6
Liver	1.65×10^6
Muscle	1.71×10^6
Skull bone	7.8×10^6



Modell:



$$\text{akustische Impedanz } Z_{\text{ak}} = \frac{p}{q} = \frac{p}{u \cdot A} = Z_0 / A = \frac{\rho_0 \cdot c}{A}$$

⇒ Kennimpedanz - Dichte

Physikalische Grundlagen (Schallfeldgrößen)

Intensität (Leistungsdichte) I (im Raumpunkt des Schallstrahls)

Es gilt $I(t) = p \cdot u = p^2/Z_0 = u^2 \cdot Z_0$ mit $[I] = \text{Nm}/(\text{m}^2 \cdot \text{s}) = \text{W/m}^2$ (13)

Wenn $p(t)$ und $u(t)$ Sinusfunktionen mit den Amplituden p_+ bzw. u_+ ist der zeitliche Mittelwert:

$$I_{\text{ave}} = p_+^2/(2Z_0) = u_+^2 \cdot Z_0/2 \quad (14)$$

Meist die Intensität I_{ave} vom Schallkopf ausgehend gegeben bzw. aus Leistung und Strahlungsfläche berechenbar, dann folgen aus (14):

Amplitude des Drucks: $p_+ = \sqrt{2 \cdot Z_0 \cdot I_{\text{ave}}}$ (15)

Amplitude der Teilchengeschwindigkeit: $u_+ = \sqrt{2 \cdot Z_0 / I_{\text{ave}}}$ (16)

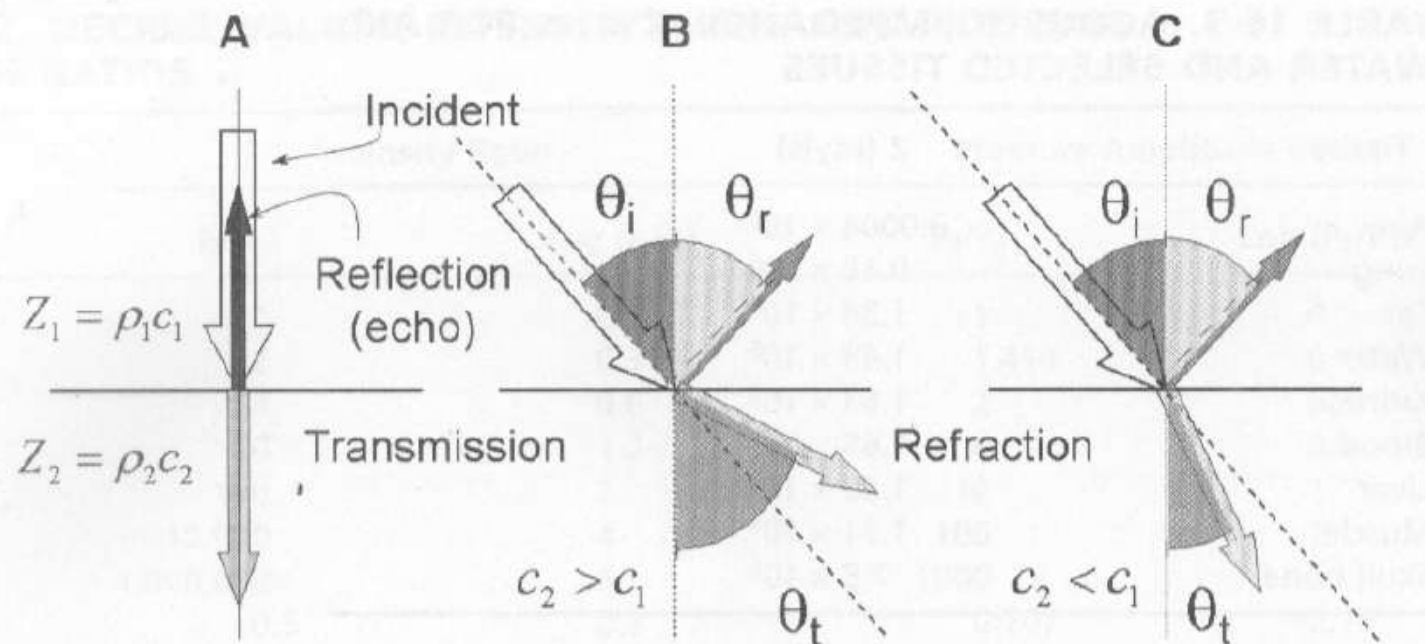
Amplitude der Teilchenauslenkung: $z_+ = u_+/omega$ (17)

Maximale Teilchenbeschleunigung: $b_+ = omega \cdot u_+$ (18)

Schallleistung $P_{\text{ak}} = p \cdot q = Z_{\text{ak}} \cdot q^2 = p^2/Z_{\text{ak}}$ (Gesamtquerschnitt)

$$P_{\text{ak}} = A \cdot I_{\text{ave}} \{A\} = A \cdot u_{\text{mean}}^2 Z_0 = A \cdot u_{\text{mean}}^2 Z_{\text{ak}} \cdot A = Z_{\text{ak}} \cdot A^2 \cdot u_{\text{mean}}^2 = Z_{\text{ak}} \cdot q^2$$

Physikalische Grundlagen (Reflektionen)



$$\frac{\sin\theta_t}{\sin\theta_i} = \frac{c_2}{c_1}$$

$$\frac{\theta_t}{\theta_i} \approx \frac{c_2}{c_1}$$

FIGURE Reflection and refraction of ultrasound occurs at tissue boundaries with differences in acoustic impedance, Z. With perpendicular incidence (90 degrees) to a tissue boundary, a fraction of the beam is transmitted and a fraction of the beam is reflected back to the source. With nonperpendicular incidence, ($\theta_i \neq 90$ degrees), the reflected fraction of the beam is directed away from the transducer at an angle $\theta_r = \theta_i$, and the transmitted fraction is refracted in the second medium ($\theta_t \neq \theta_i$) when $c_1 \neq c_2$.

Physikalische Grundlagen (Reflektionsfaktor)

Reflexion an Grenzflächen unterschiedlicher akustischer Impedanz

Die Schallwelle trifft senkrecht auf die Grenze Z_1 / Z_2 , dann gilt

$$u_i - u_r = u_t \quad \text{sowie} \quad p_i + p_r = p_t \quad (19)$$

Einfallende (Index i = incident) und reflektierte (Index r = reflected) Welle breiten sich im Gewebe mit Z_1 aus, die durchgehende (Index t = transmitted) Welle tritt in das Gewebe mit Z_2 über.

Definition des **Reflexionsfaktors R:** $R = p_r/p_i$ (20)

Es gilt $-1 \leq R \leq +1$, $R < 0$ bedeutet eine Phasenumkehr der rücklaufenden Welle.

Aus (19) und (20) folgt mit (11): $Z_1/Z_2 = (1-R)/(1+R)$, (21)

daraus: **Reflexion** $R = \frac{Z_2 - Z_1}{Z_2 + Z_1}$. (22)

Für die Intensitäten folgt aus (13) und (22): $I_r = R^2 \cdot I_i$ (23)

und $I_t = (1+R)^2 \cdot I_i \cdot Z_1/Z_2$, mit (21): $I_t = (1 - R^2) \cdot I_i$. (24)

Transmission

Physikalische Grundlagen: Reflektion→Streuung

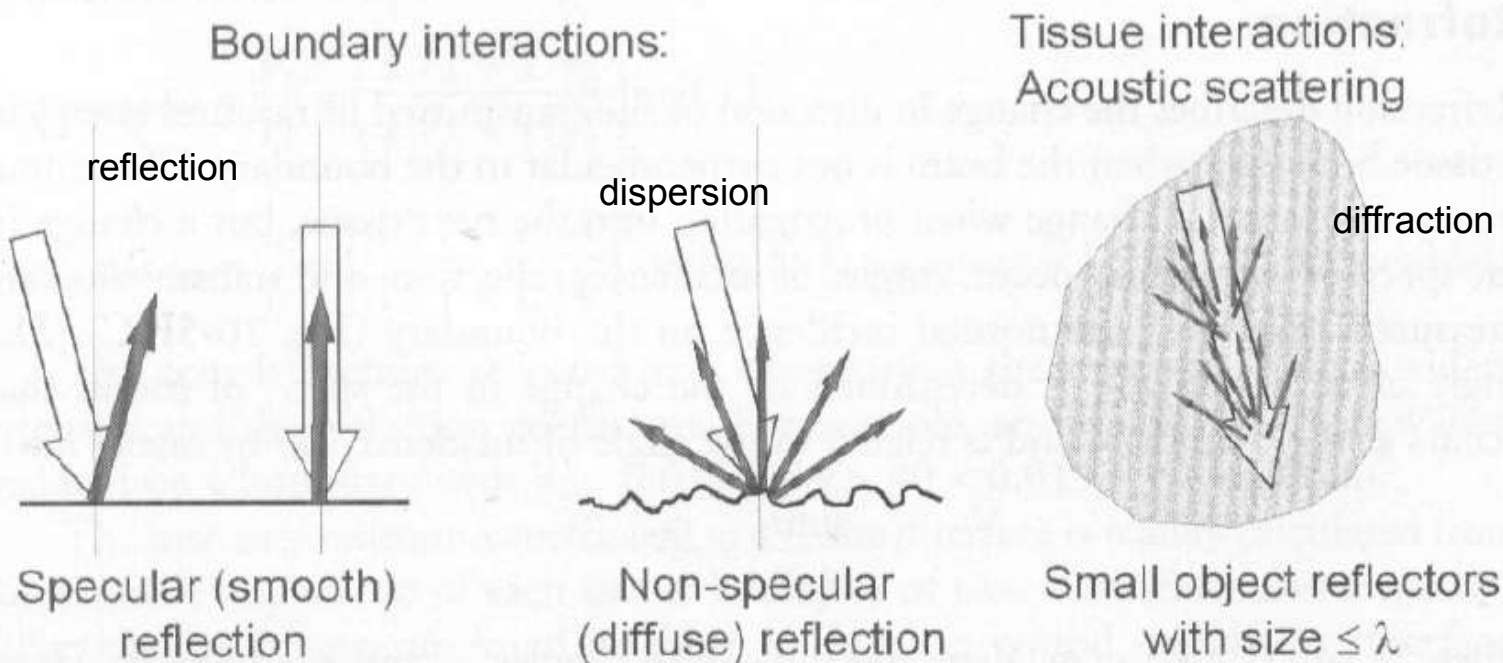


FIGURE Ultrasound interactions with boundaries and particles. The characterization of a boundary as specular and nonspecular is partially dependent on the wavelength of the incident ultrasound. As the wavelength becomes smaller, the boundary becomes "rough," resulting in diffuse reflections from the surface because of irregularities. Small particle reflectors within a tissue or organ cause a diffuse scattering pattern that is characteristic of the particle size, giving rise to specific tissue or organ "signatures."

Physikalische Grundlagen: Wellentheorie-Dämpfung

Schallausbreitung mit Absorption → Dämpfung

Über dem Wegelement Δz fällt infolge der Viskosität der Druck p um einen Anteil p' ab. Dann wird aus (1):

$$\frac{\partial(p-p')}{\partial z} + \rho_0 \frac{\partial u}{\partial t} = 0 \quad (25)$$

mit $p' = (\eta \cdot 4/3 + \eta') \cdot \partial u / \partial z$. (26)

Dabei sind: η = „dynamische Viskosität“, η' = „Scherviskosität“. $[\eta] = \text{Ns/m}^2 = \text{Pa}\cdot\text{s}$

Mit (25) (26) entsteht aus (2) die modifizierte Wellengleichung für p

$$\frac{\partial^2 p}{\partial z^2} + \left(\frac{4}{3}\eta + \eta'\right)K \frac{\partial^3 p}{\partial z^2 \cdot \partial t} - \rho_0 K \frac{\partial^2 p}{\partial t^2} = 0 \quad (27)$$

mit der Lösung:

$$p = p_+ \cdot e^{-\alpha z} \cdot \cos(\omega t - kz) . \quad (28)$$

Dabei ist α die „Dämpfungskonstante“, die den Abfall der p -Amplitude über z charakterisiert:

$$\alpha = \frac{(4\eta/3 + \eta') \cdot \omega^2}{2 \cdot \rho_0 \cdot c^3} \quad (\text{also } \alpha \sim \omega^2) \quad [\alpha] = 1/\text{m} \quad (29)$$

Dabei gilt für $\alpha^2 \ll k^2$:

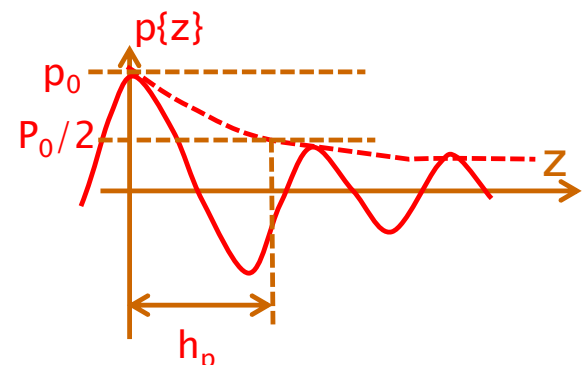
- Es gelten weiter genügend genau (10) und (12), also: $c \approx 1/\sqrt{\rho_0 \cdot K}$ und $Z \approx \rho_0 \cdot c$.

- Die „Hüllkurve“ der mit z abklingenden Zeitfunktion verläuft gemäß $p(z) = p_+ \cdot e^{-\alpha z}$. Aus $e^{-\alpha h_p} = 1/2$ folgt die „Halbwertstiefe“:

$$h_p = (\ln 2)/\alpha \approx 0,7/\alpha \quad (30)$$

$$I = p_+^2 \cdot (1/Z) \cdot e^{-2\alpha z} \cdot \cos^2(\omega t - kz) \quad (31)$$

$$h_I = (\ln 2)/(2\alpha) \approx 0,3466/\alpha \quad (32)$$



Feldgröße

Energetische Größe

Physikalische Grundlagen (Dämpfungsfaktor)

Absorption realer Medien

Es gilt mit dem Meßwert α_0 bei der Meßfrequenz f_0 (meist 1 MHz) bzw. $\omega_0 = 2\pi \cdot f_0$:

$$\alpha/\alpha_0 = (f/f_0)^{\gamma} = (\omega/\omega_0)^{\gamma} \quad , \quad \text{also} \quad \alpha = \alpha_0 \cdot (f/f_0)^{\gamma} = \alpha_0 \cdot (\omega/\omega_0)^{\gamma} \quad . \quad (33)$$

Ideale viskose Flüssigkeiten: $\gamma = 2$, reale Medien: $\gamma < 2$, Weichgewebe meist $\gamma \approx 1$

Die Dämpfungskonstante ist eine Meßgröße, dabei wird manchmal auch das logarithmische „Dämpfungsmaß“ α' angegeben. Dies verwendet das Dezibel (dB), das als Zehnfaches des Zehnerlogarithmus eines Leistungsverhältnisses definiert ist. Es gilt mit Bezug auf z:

$$\alpha'/(dB/cm) = 10 \cdot \lg(I_0/I(z))/(z/cm) = 20 \cdot \lg(p_0/p(z))/(z/cm) \quad (34)$$

Umrechnung α' in α : $\alpha/cm^{-1} = ((\ln 10)/20) \cdot \alpha'/(dB/cm) \approx 0,11513 \cdot \alpha'/(dB/cm)$ (35)

TABLE ATTENUATION COEFFICIENTS FOR SELECTED TISSUES AT 1 MHZ

$$\alpha'_0$$

Tissue Composition	Attenuation coefficient (1 MHz beam, dB/cm)
Water	0.0002
Blood	0.18
Soft tissues	0.3–0.8
Brain	0.3–0.5
Liver	0.4–0.7
Fat	0.5–1.8
Smooth muscle	0.2–0.6
Tendon	0.9–1.1
Bone, cortical	13–26
Lung	40

allgemeiner Dämpfungsfaktor:

$$\alpha = \alpha_0 \cdot f / 1MHz$$

$$\alpha' = \frac{\Delta I_{dB}}{\Delta z} \cdot f$$

$\mu = \text{mean}\{\alpha\}$

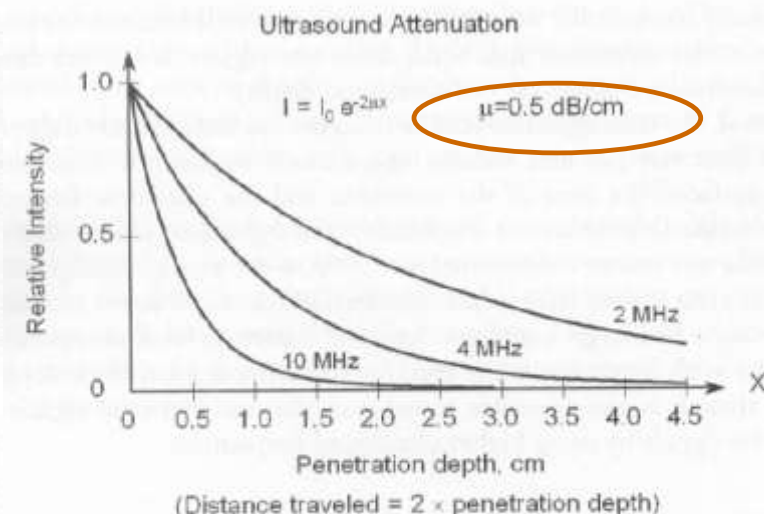


FIGURE Ultrasound attenuation occurs exponentially with penetration depth, and increases with increased frequency. Each curve shows intensity of ultrasound of a particular frequency as a function of penetration depth in a medium whose attenuation coefficient is $(0.5 \text{ dB/cm})/\text{MHz}$. Note that the total distance traveled by the ultrasound pulse and echo is twice the penetration depth.

Physikalische Grundlagen (Dämpfung)

Halbwertstiefe

half value thickness (HVT)

Example: Calculate the approximate intensity HVT in soft tissue for ultrasound beams of 2 MHz and 10 MHz. Determine the number of HVTs the incident beam and the echo travel at a 6-cm depth.

Answer: Information needed is (a) the attenuation coefficient approximation 0.5 (dB/cm)/MHz, and (b) one HVT produces a 3-dB loss. Given this information, the HVT in soft tissue for a f MHz beam is

$$\text{HVT}_{f \text{ MHz}} (\text{cm}) = \frac{3 \text{ dB}}{\text{Attenuation coefficient (dB/cm)}} = \frac{3 \text{ dB}}{\frac{0.5(\text{dB/cm})}{\text{MHz}} \times f \text{ MHz}} = \frac{6}{f}$$

$$\text{HVT}_{2 \text{ MHz}} = \frac{3 \text{ dB}}{\frac{0.5(\text{dB/cm})}{\text{MHz}} \times 2 \text{ MHz}} = 3 \text{ cm}$$

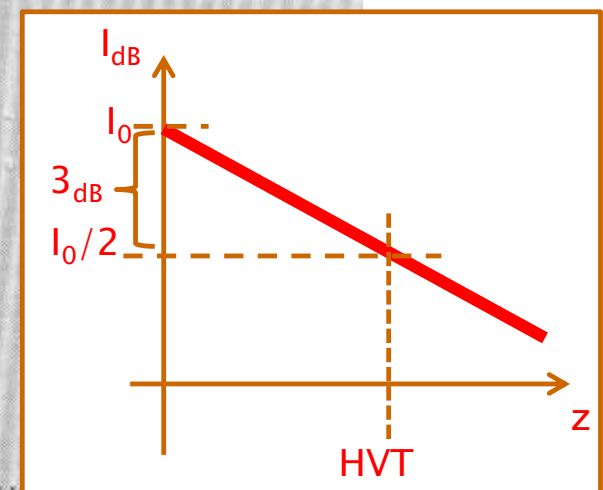
$$\text{HVT}_{10 \text{ MHz}} = \frac{6}{10} = 0.6 \text{ cm}$$

Number of HVTs:

A 6-cm depth requires a travel distance of 12 cm (round trip).

For a 2-MHz beam, this is $12 \text{ cm} / (3 \text{ cm} / \text{HVT}_{2 \text{ MHz}}) = 4 \text{ HVT}_{2 \text{ MHz}}$.

For a 10-MHz beam this is $12 \text{ cm} / (0.6 \text{ cm} / \text{HVT}_{10 \text{ MHz}}) = 20 \text{ HVT}_{10 \text{ MHz}}$.



Gepulstes Beschallungsverfahren im Gewebe

echoes by reflections at tissue layers

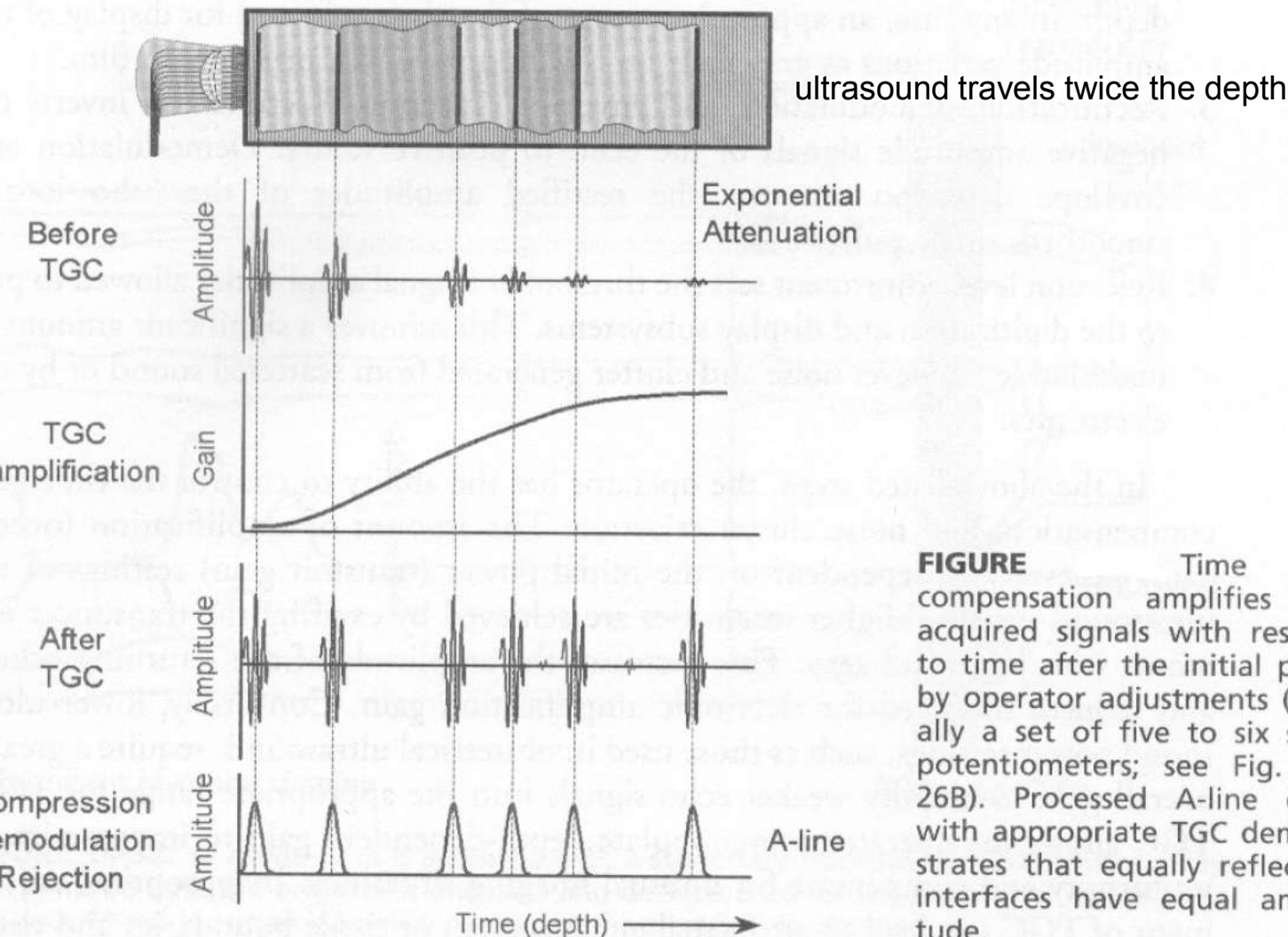


FIGURE Time gain compensation amplifies the acquired signals with respect to time after the initial pulse by operator adjustments (usually a set of five to six slide potentiometers; see Fig. 16-26B). Processed A-line data with appropriate TGC demonstrates that equally reflective interfaces have equal amplitude.

Ultrasound-Basics: Summary

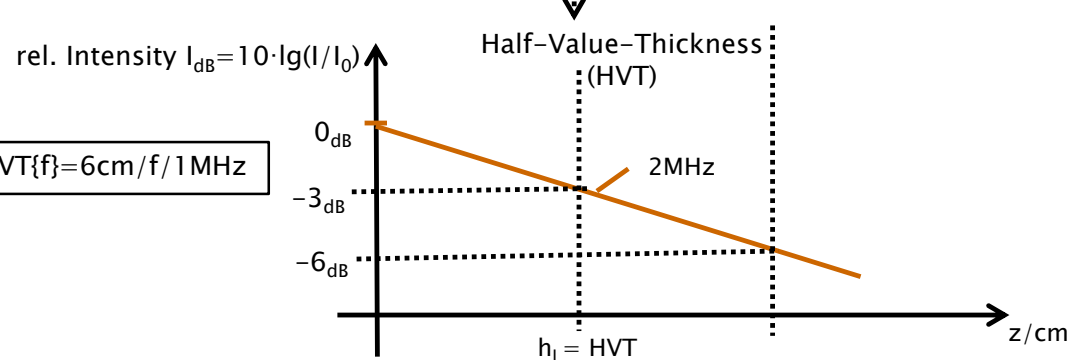
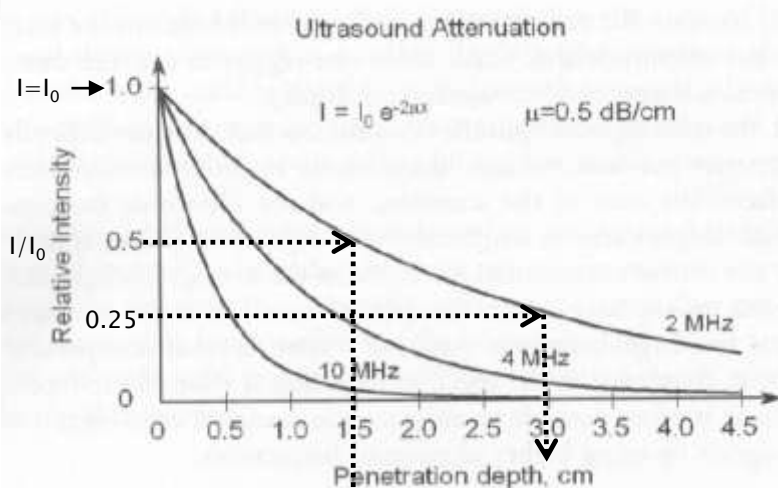
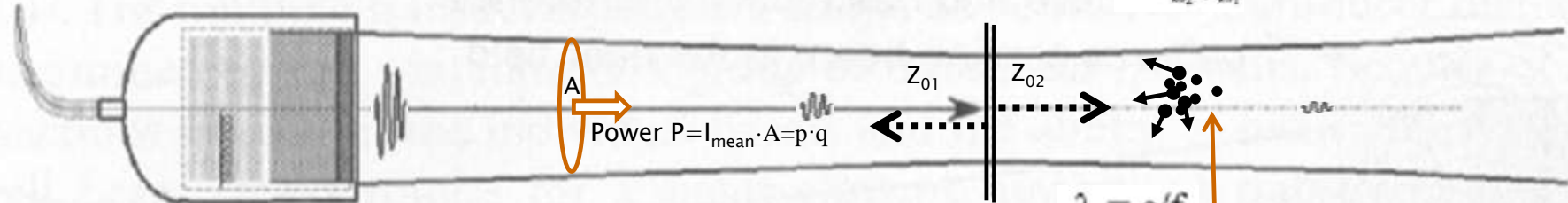
$$q = u \cdot A$$

$$Z_1 = p / q = Z_0 / A = c \cdot \rho_1 / A$$

$$\Delta p$$

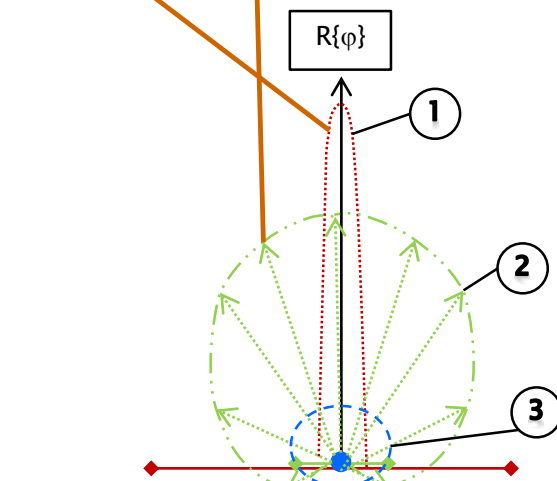
Acoustic Impedance: $Z_1 = p / q = Z_0 / A = c \cdot \rho_1 / A$
 $Z_0 = p / u = c \cdot \rho_1$ = Characteristic Impedance

Layer with P-Reflection factor $R = \frac{Z_2 - Z_1}{Z_2 + Z_1}$



$$\lambda = c/f$$

$$c = 1 / \sqrt{\rho_0 \cdot K} = 1500 \text{ m/s} = 1.5 \text{ mm/}\mu\text{s}$$



- f-dependent reflection/beam characteristics
- 1) Plane reflector, size $\gg \lambda$ (Reflection + refraction)
 - 2) Small reflector, size $\approx \lambda$ (Kidney characteristic)
 - 3) Spherical reflector, size $\ll \lambda$ (Raleigh-reflector)

Ultraschall und Theragnostik

Ultraschall in Thera(pie) und (Dia)gnostik

Kapitel 3

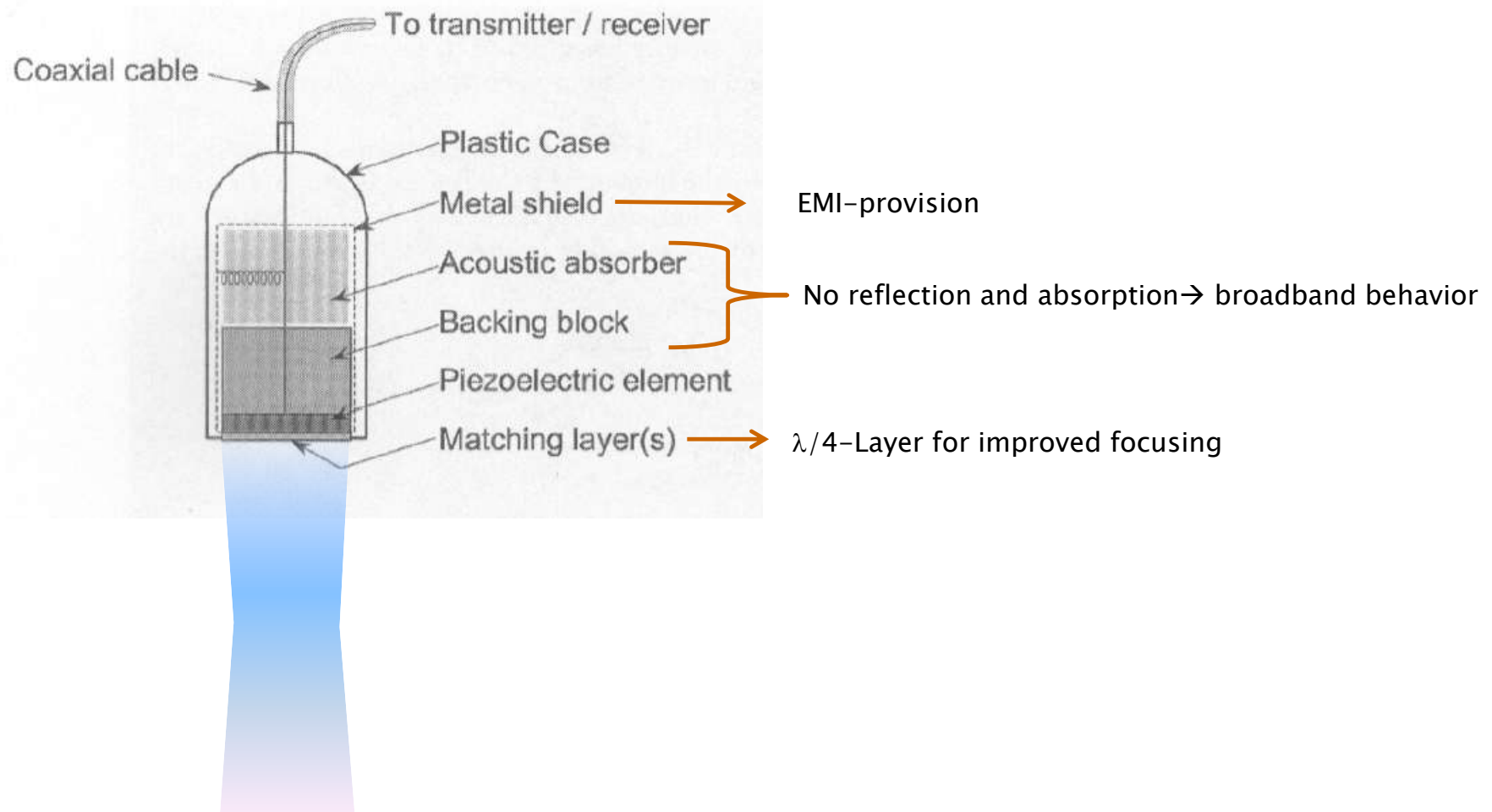
Ultraschallsonden

Inhaltsangabe

1. Übersicht der Ultraschallanwendungen
2. Physikalische Grundlagen
3. **Ultraschallsonden**
4. Bildgebende Verfahren in der Diagnostik
5. Dopplerverfahren in der Diagnostik
6. Artefakte und Diagnostik
7. Ultraschall und Kontrastmittel
8. Theragnostik mit Ultraschall
9. Therapie mit hochdosierten Ultraschall
10. Gewebecharakterisierung mittels shear waves
11. Dosierung und Sicherheitsaspekte

Ultrasound Transducer (Piezo-crystal)

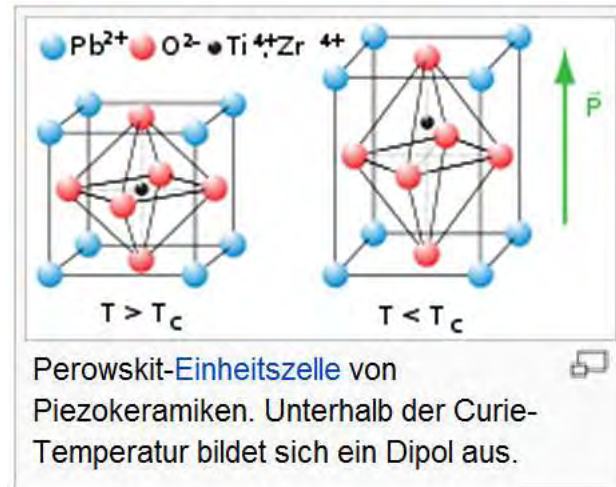
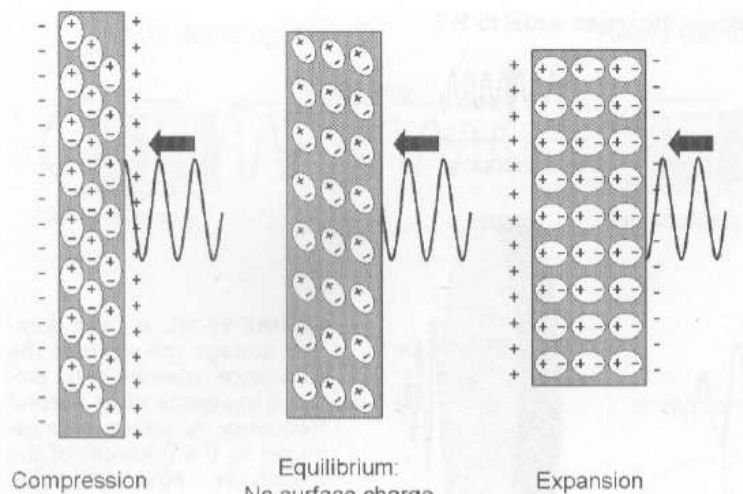
Single Element Transducer



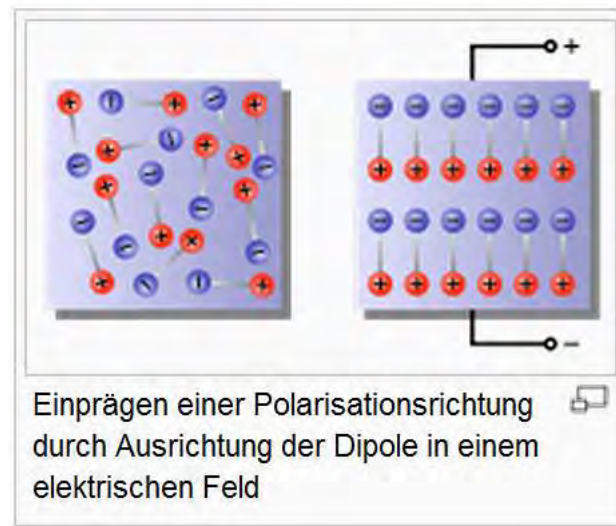
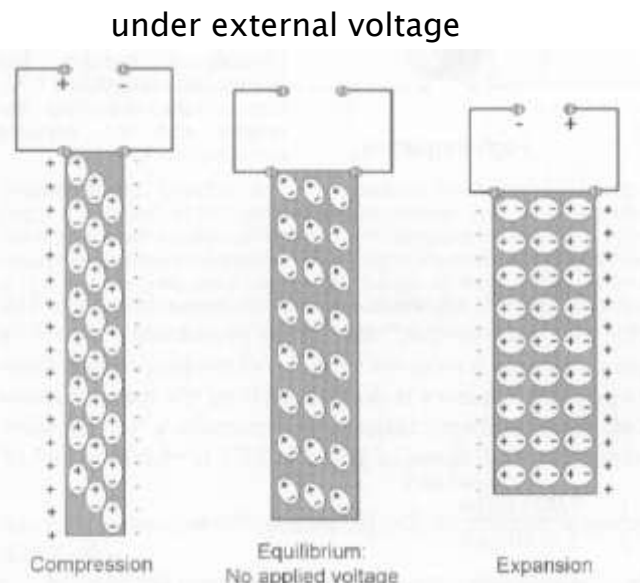


Ultrasound crystal (Physics)

under influence of mechanical pressure (at resonance → stationary wave inside)



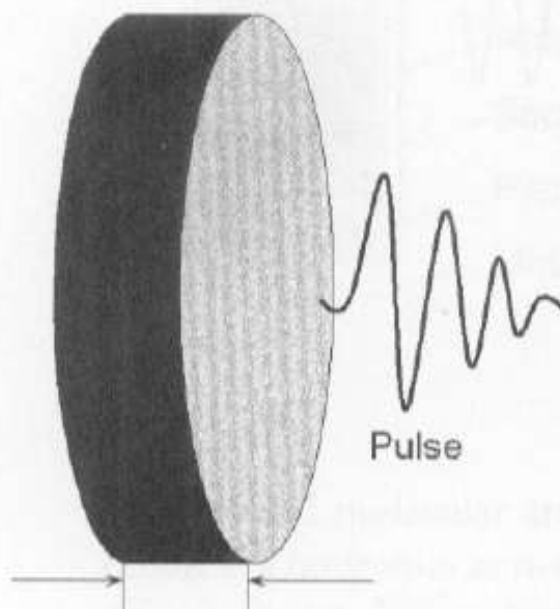
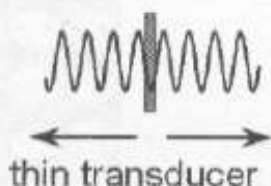
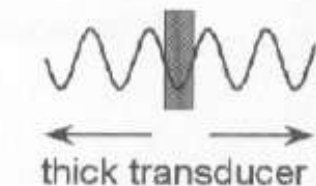
PTZxx: Barium–Tintant–Zirkonat–Material



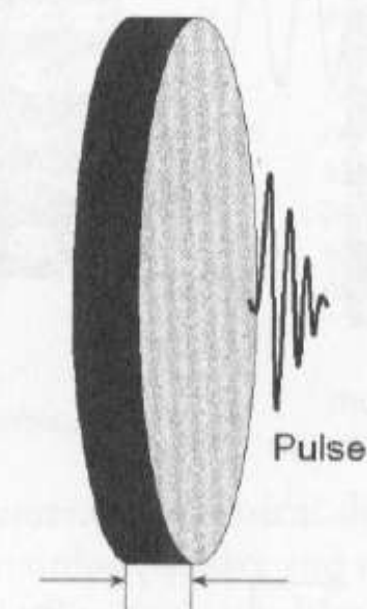
T_c : Curie–Temperatur

Ultrasound crystal (geometry/thickness)

f_0 is determined by the transducer thickness equal to $\frac{1}{2}\lambda$



Low frequency



High frequency

resonance → stationary wave inside)

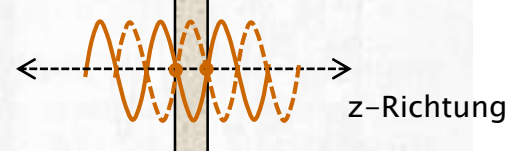
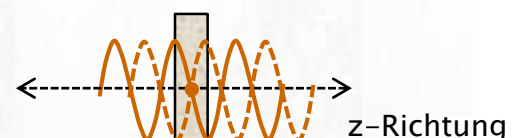


FIGURE A short duration voltage spike causes the resonance piezoelectric element to vibrate at its natural frequency, f_0 , which is determined by the thickness of the transducer equal to $\frac{1}{2}\lambda$. Lower-frequency oscillation is produced with a thicker piezoelectric element. The spatial pulse length is a function of the operating frequency and the adjacent damping block.

$$\lambda = \frac{c}{f} = \frac{4,000 \text{ m/sec}}{5 \times 10^6/\text{sec}} = 8 \times 10^{-4} \text{ m} = 0.80\text{mm}$$

Ultraschallsonden / (Kristallberechnungen)

Piezo-Effekt

Auf die Fläche A eines Kristalls der Dicke l wirkt senkrecht die Kraft F, die den Druck $p = F/A$ erzeugt. Dabei entsteht im Kristall die Feldstärke E gemäß

$$E = -g \cdot p \quad \text{mit } g = \text{"piezoelektrische Spannungskonstante"} \quad [g] = \text{Vm/N} \quad (36)$$

Über dem Kristall entsteht die Spannung U (negatives Vorzeichen: Spannungsquelle):

$$U = E \cdot l = -g \cdot p \cdot l = -g \cdot F \cdot l / A \quad (\text{also } U \sim F, l, 1/A) \quad (37)$$

Dies entspricht der Ladung Q auf der Fläche A:

$$Q = C \cdot U = \epsilon \cdot A / l = -g \cdot \epsilon \cdot F \quad (\text{also } Q \sim F \text{ aber unabhängig von } l, A) \quad (38)$$

Umkehrung des Piezo-Effektes (Spannung U erzeugt Kraft F bzw. Druck p):

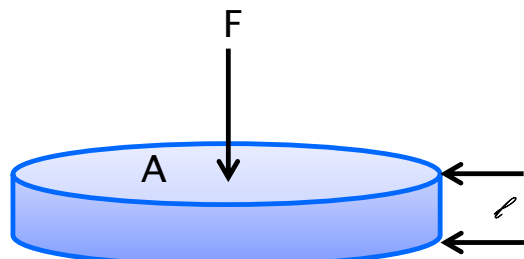
$$\text{Aus (37) mit Vorzeichenumkehr: } F = +U \cdot A / (g \cdot l) = A \cdot E / g \quad (39)$$

$$\text{Weitergabe als Druck } p \text{ ins Gewebe: } p = F / A = U / (g \cdot l) = E / g \quad (40)$$

Damit wird bei totaler Energieabgabe auf der Gewebeseite (mit Totalreflexion auf der Grenze Kristall / Luft der anderen Seite, d.h. $p_{\text{ges}} = 2p$) im zeitlichen Mittel abgegeben:

$$\text{Aus (14) und (40): } I_{\text{ave}} = (2p_+)^2 / (2 \cdot Z_{\text{Gewebe}}) = 2U_0^2 / (g^2 \cdot l^2 \cdot Z_{\text{Gewebe}}) \quad (41)$$

mit U_0 = Amplitude der angelegten Spannung



Ultraschallsonden (Kristall, elektrisches Modell)

Schallschwinger mit Piezokristall

Elektrische Ersatzschaltung: C_0 parallel zur Reihenschaltung von C , L und R

mit $C_0 = \epsilon_0 \cdot \epsilon_r \cdot A / l$, Kapazität des Plattenkondensators (Größenordnung 1 nF)

C = Ersatzkapazität infolge der Steifigkeit des Kristalls (Größenordnung 0,1 pF)

L = Ersatzinduktivität infolge der Masse des Kristalls (Größenordnung 100 mH)

$R = R_i + R_{Pat} \approx R_{Pat}$, da R_i (innere Reibung, Größenordnung 1 Ω) << R_{Pat} (für die an den Patient abgegebene Leistung P_{Pat} , Größenordnung 50 Ω)

Aus

$$P_{Pat} = I_{ave} \cdot A = U^2 / R_{Pat} = U_0^2 / (2 \cdot R_{Pat}) \quad \text{folgt mit (41):}$$

$$R_{Pat} = U_0^2 / (2 \cdot I_{ave} \cdot A) = g^2 \cdot l^2 \cdot Z_{Gewebe} / (4 \cdot A) \quad (42)$$

Die komplexe elektrische Impedanz der Ersatzschaltung folgt aus

$$\underline{Z}_{el} = [1/(j\omega C_0)] \parallel [j(\omega L - 1/(\omega C)) + R]$$

für $\omega C_0 R \ll C_0/C$:

$$\underline{Z}_{el} = \frac{R}{1 - \omega^2 C_0 L - C_0/C} + j \frac{(\omega L - 1/(\omega C))}{1 - \omega^2 C_0 L - C_0/C} \quad . \quad (43)$$

Aus (43) folgt bei *Reihenresonanz* aus $\text{Im}\{\underline{Z}_{el}\} = 0$:

$$\omega_r = 1/\sqrt{L \cdot C} \quad (44)$$

Bei ω_r werden $\text{Re}\{\underline{Z}_{el}\} = R$ und $\text{Im}\{\underline{Z}_{el}\} = 0$.

Aus (43) folgt bei *Parallelresonanz* aus $\text{Im}\{\underline{Z}_{el}\} \rightarrow \infty$, also $1 - \omega^2 C_0 L - C_0/C = 0$:

$$\omega_p = \sqrt{(1+C_0/C)/(L \cdot C)} = \omega_r \sqrt{(1+C_0/C)}$$

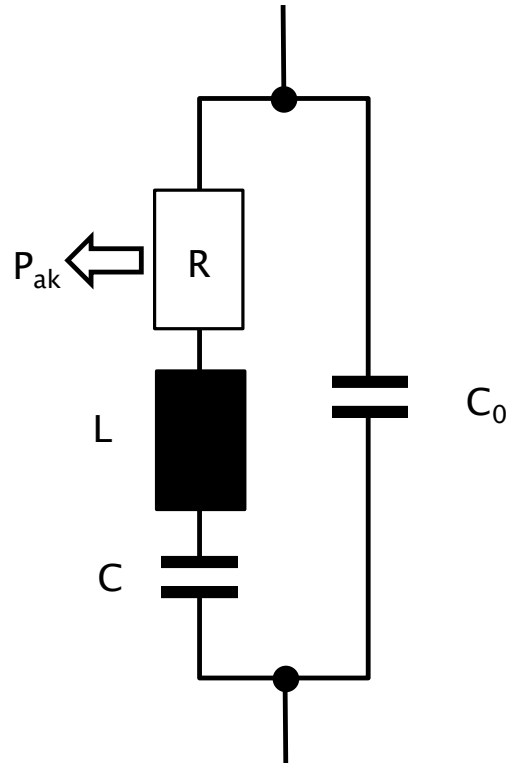
Bei ω_p werden $\text{Re}\{\underline{Z}_{el}\} \approx R/(\omega_r \cdot C_0 \cdot R)^2$ und $\text{Im}\{\underline{Z}_{el}\} \approx -1/(\omega_p \cdot C_0)$

Wegen $\omega C_0 R \ll 1$ werden $\text{Re}\{\underline{Z}_{el}\} \gg R$ und $-\text{Im}\{\underline{Z}_{el}\} \gg R$

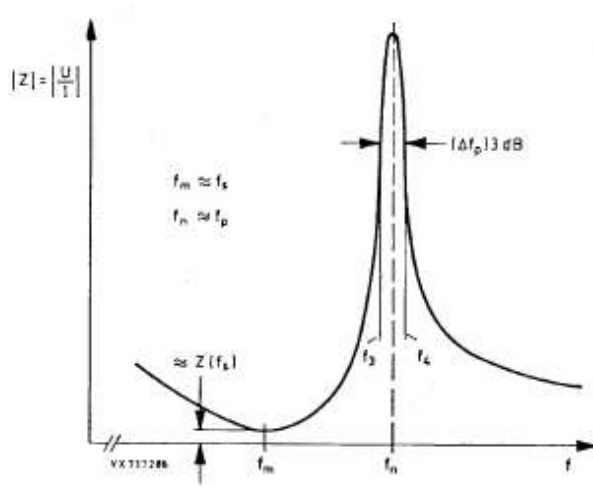
Aus (46) folgt mit $C_0 \gg C$:

$$\omega_p \approx \omega_r \quad \text{aber stets} \quad \omega_p > \omega_r \quad (48)$$

Die größte Leistungsabgabe an den Patienten erfolgt bei ω_r und wegen $P_{Pat} = U^2 / R_{Pat}$ bei möglichst kleinem R_{Pat} , deshalb muß der Hochfrequenz-Generator auf die Reihenresonanzfrequenz ω_r stabil abgestimmt werden.



Ultraschallsonden (Kristall–Impedance–Matching)



Bild

Scheinleitwert und Scheinwiderstand als Funktion der Frequenz. Die Serienresonanzfrequenz f_s liegt in der Nähe der Minimalimpedanzfrequenz f_m , die Parallelresonanzfrequenz f_p in der Nähe der Maximalimpedanzfrequenz f_n . Unterhalb f_m und oberhalb f_n verhält sich der Wandler kapazitiv, zwischen f_m und f_n induktiv.

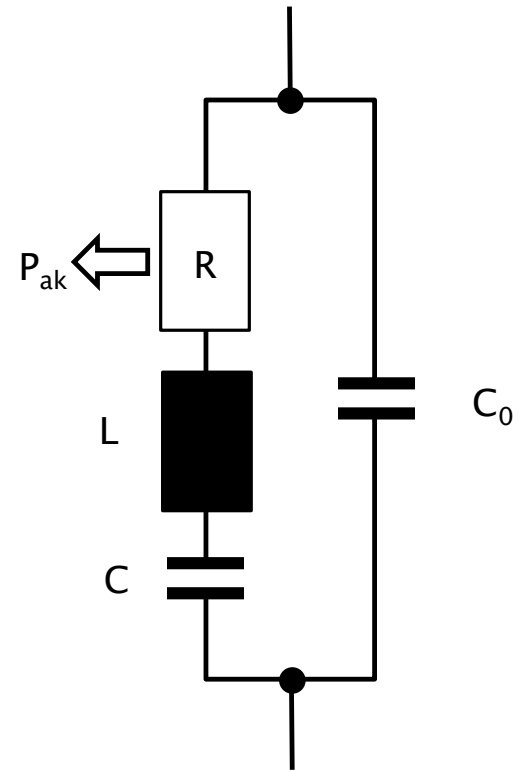
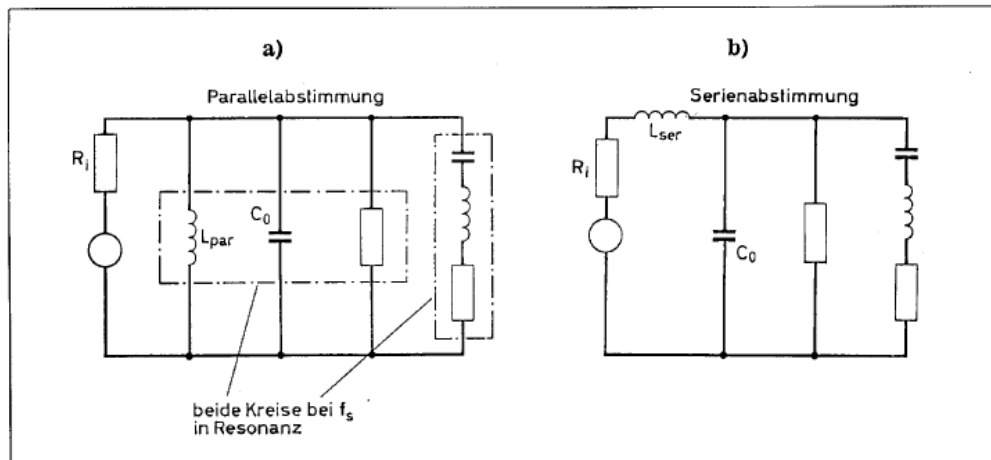


Bild Ersatzschaltungen für abgestimmte Wandler



$$L_{\text{par}} = \frac{1}{\omega_s^2 C_0} \quad (\omega_s = 2\pi f_s)$$

$$L_{\text{ser}} = \frac{1}{\omega_p^2 C_0} \quad (\omega_p = 2\pi f_p)$$

Ultrasound probe : beam basics

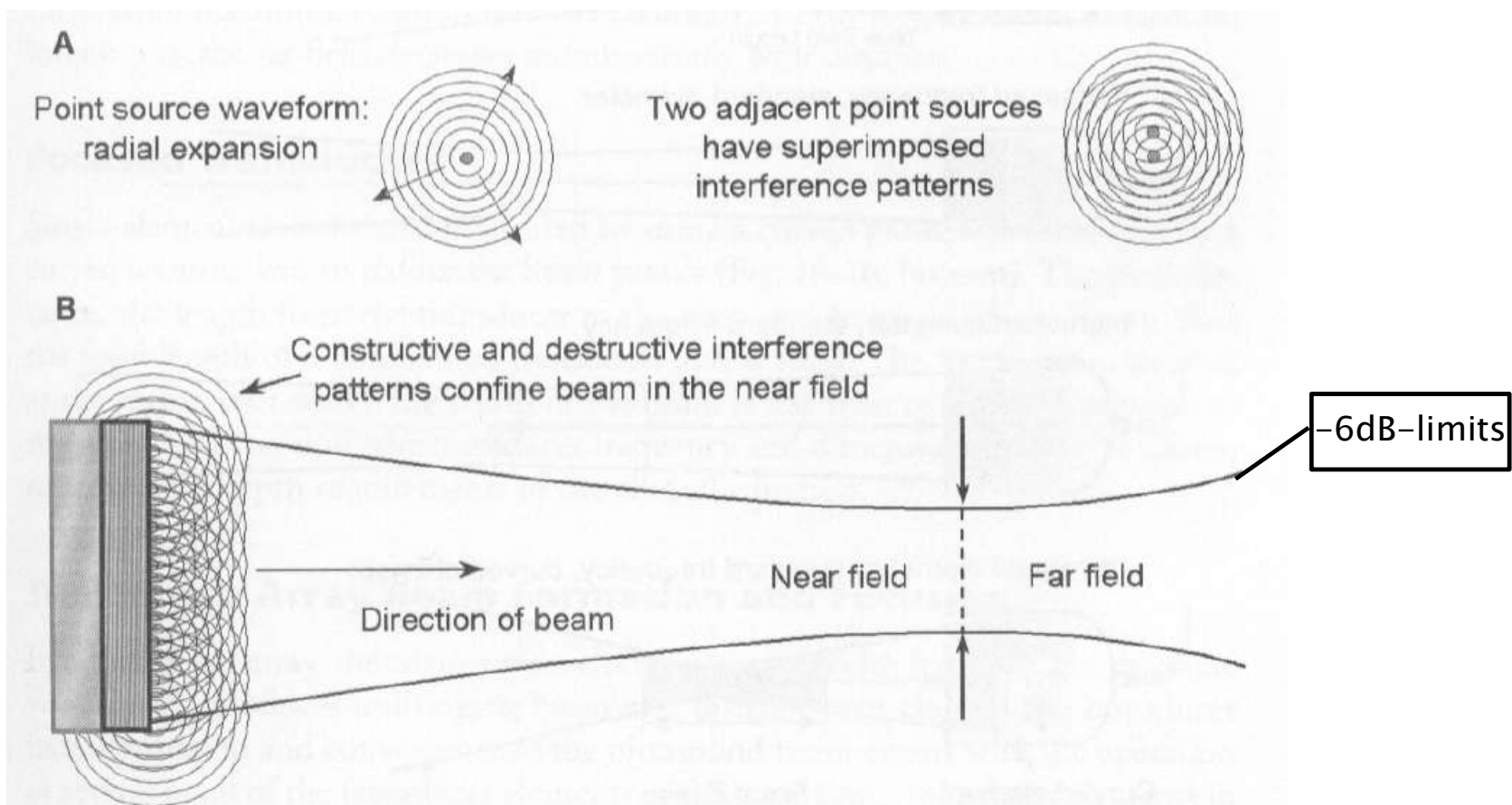


FIGURE **A:** A point source radiates the ultrasound beam as a radially expanding wave. Two adjacent point sources generate constructive and destructive interference patterns. **B:** Huygen's principle considers the plane of the transducer element to be an "infinite" number of point radiators, each emitting a radially expanding wave. The interference pattern results in a converging ultrasound beam in the near field, with subsequent divergence in the far field.

Ultraschallsonden / (Schallfeld-Charakteristik)

Schallfeld-Charakteristik (kreisförmiger Schwinger mit dem Radius a)

Radius $a \rightarrow$ Durchmesser d

Aus Laufwegunterschied von $\lambda/2$:

$$\text{Nahfeld bis etwa} \quad z_R = a^2/\lambda = a^2 \cdot f/c \quad (52)$$

Im *Nahfeld* etwa konstante Fläche der Schallwelle, es treten durch Interferenzen Maxima und Minima der Intensitäten auf. Im daran anschließenden *Fernfeld* treten keine Interferenzen mehr auf aber es erfolgt ein Auseinanderlaufen der Wellenfront mit dem halben Öffnungswinkel ϕ_d („Dispersionswinkel“).

ϕ_d folgt in Näherung aus der Geometrie zu

$$\phi_d \approx \arctan (\lambda/a) \quad (53)$$

oder exakt aus der Wellentheorie (für die Haupt-Strahlungskeule) zu

$$\phi_d \approx \arcsin (0,61 \cdot \lambda/a) \quad (54)$$

focus diameter: $=x_F=2Z_R\sin\{\Theta\}=0,61d$

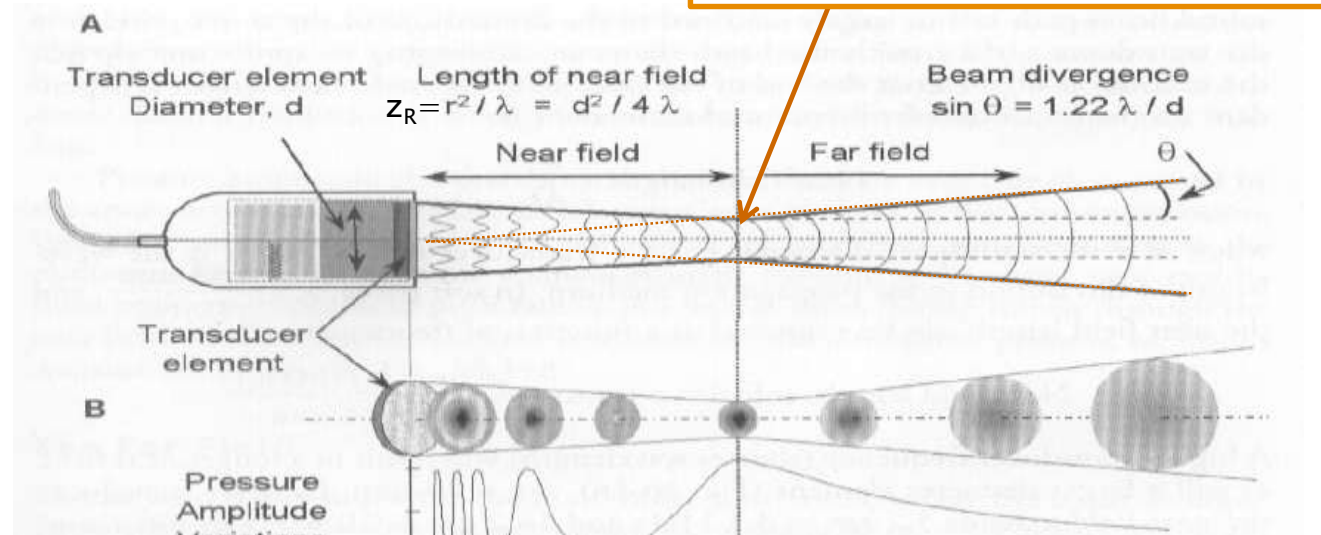
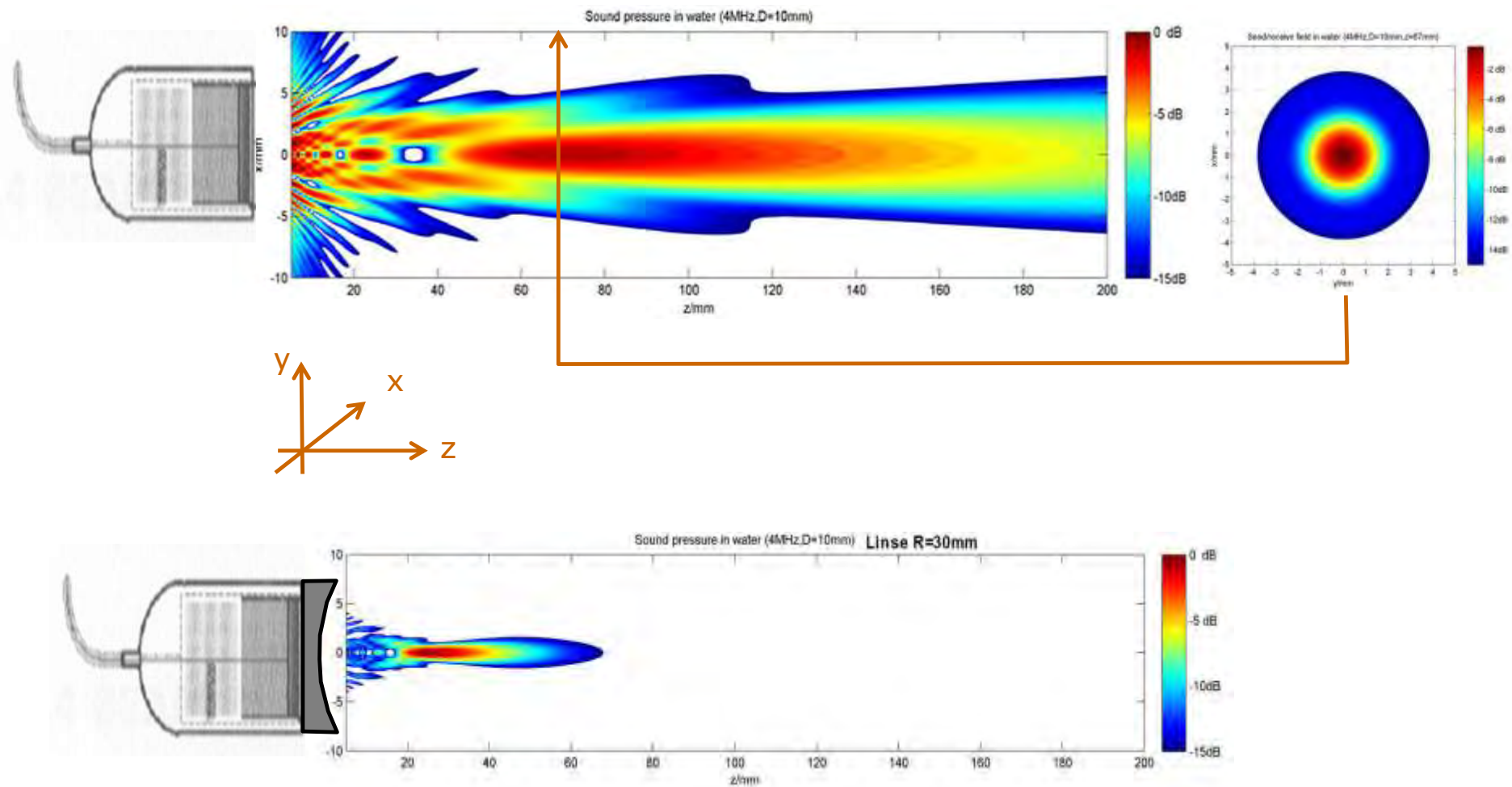
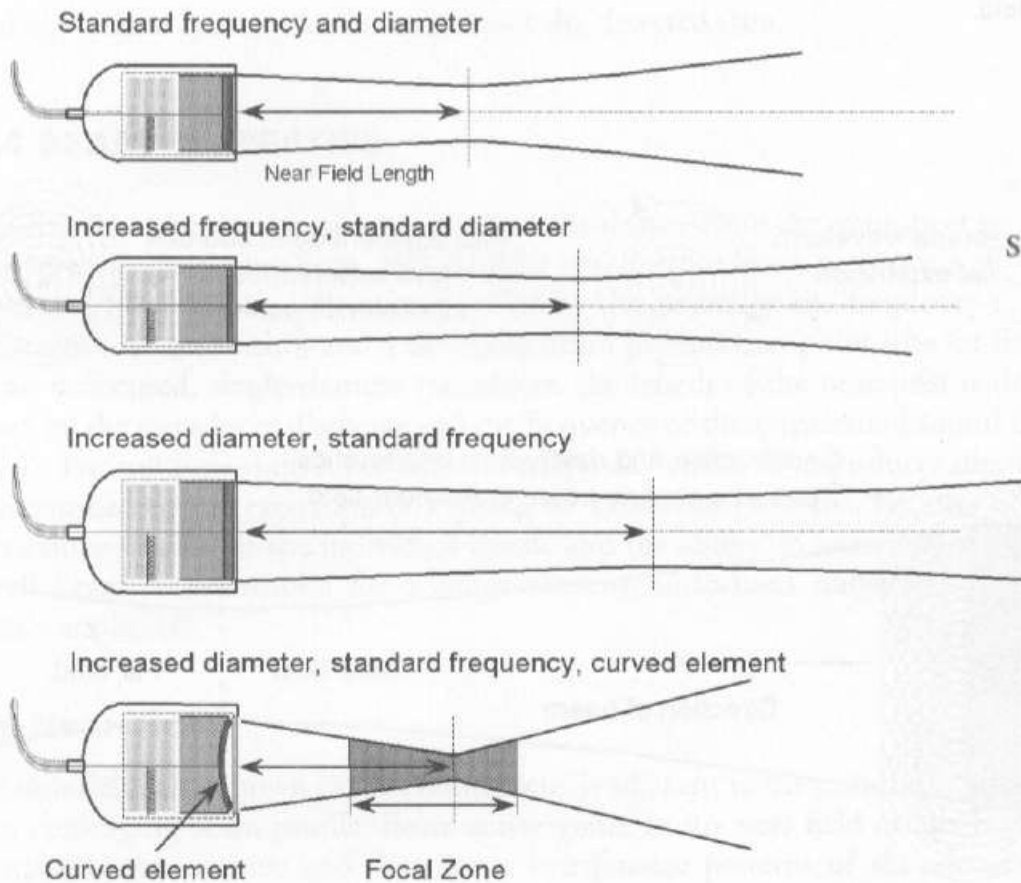


FIGURE **A:** The ultrasound beam from a single, circular transducer element is characterized by the near field and far field regions. **B:** Pressure amplitude variations in the near field are quite complex and rapidly changing, and monotonically decreasing in the far field.

Ultrasound transducer (beam characteristics)



Ultrasound probe (beam parameter variationen)



$$\text{Near field length} = \frac{d^2}{4\lambda} = \frac{r^2}{\lambda}$$

$$\text{soft tissue (mm)} = \frac{d^2(\text{mm}^2) f(\text{MHz})}{4 \times 1.54 \text{ mm}}$$

FIGURE For an unfocused transducer, the near field length is a function of the transducer frequency and diameter; as either increases, the near field length increases. **Bottom:** A focused single element transducer uses either a curved element (shown) or an acoustic lens. The focal distance (near field length) is brought closer to the transducer surface than the corresponding unfocused transducer, with a decrease in the beam diameter at the focal distance and an increase in the beam divergence angle. A "focal zone" describes the region of best lateral resolution.

Ultraschallsonden / (Piezokristall)

Schallkopf-Kennwerte

ERA: Effective-Radiating-Area (tatsächliche Strahlungsfläche)

$$\text{Europa: } \text{ERA} = A_{\text{Blende}}(I = 0,9 \cdot I_{\text{ave}}) \cdot 1,11$$

$$\text{USA: } \text{ERA} = A(I > 0,05 \cdot I_{\text{max}})$$

BNR: Beam-Nonuniformity-Ratio (Strahlungsungleichmäßigkeitsverhältnis)

$$\text{BNR} = I_{\text{max}}/I_{\text{ave}}$$

mit I_{max} = Spitzenintensität im Schallfeld, I_{ave} = mittlere Intensität in der ERA

IV: Intensitätsverhältnis (nur für Schallköpfe mit Durchmesser $\geq 2 \text{ cm}$)

$$\text{IV} = \frac{\text{mittlere Intensität in der zentralen Kreisfläche mit } 1 \text{ cm Durchmesser}}{\text{mittlere Intensität in der ERA}}$$

also

$$\text{IV} = \frac{(1/A_1) \cdot \int_{A_1} I \cdot dA}{(1/A_2) \cdot \int_{A_2} I \cdot dA}$$

mit A_1 = Kreisfläche (zentral) mit $D = 1 \text{ cm}$, A_2 = Europa-ERA

Werte realer Schallköpfe: $\text{ERA} \approx (0,7 \dots 0,9) \cdot A_{\text{Schallkopf}}$

$$\text{BNR} \approx 2 \dots 6$$

$$\text{IV} \leq 2$$

Hinweis: Alle Schallkopf-Messungen sind in 5 mm Abstand vom Schallkopf in entgastem Wasser durchzuführen. (für $d > 2 \text{ cm}$; ansonsten im Fokus)

Ultraschallsonden / (Dosierung)

Diathermie

Sicherheitsgrenze für Langzeitanwendungen: $I_{\max} \leq 0,1 \text{ W/cm}^2$

Sicherheitsgrenze für höhere Intensitäten: $\int I \cdot dt \leq 50 \text{ Ws/cm}^2$ (55)

Daraus Begrenzung der Behandlungszeit bei vorgegebener Intensität ($I = \text{konstant}$):

$$t_{\max}/s = \frac{50}{I/(W/cm^2)} \quad (56)$$

oder Begrenzung der Intensität bei vorgegebener Behandlungszeit t:

$$I_{\max}/(W/cm^2) = \frac{50}{t/s} \quad (57)$$

Diese Grenzen gelten für *statische* Beschallung. Für höhere Dosiswerte ist die *semistatische* Beschallung (kleine kreisende Bewegungen über dem Zielgebiet) oder die *dynamische* Beschallung (Bewegung des Kopfes über größere Gebiete) zu wählen. Die semistatische Beschallung führt zur höchsten Temperaturerhöhung, die dynamische Beschallung kann mit höchster Dosis längere Zeit erfolgen, sie fördert die athermischen Wirkungen des Ultraschalls.

**Dosierung
bei
Diagnostik
/ Therapie**

Aerosol-Bildung

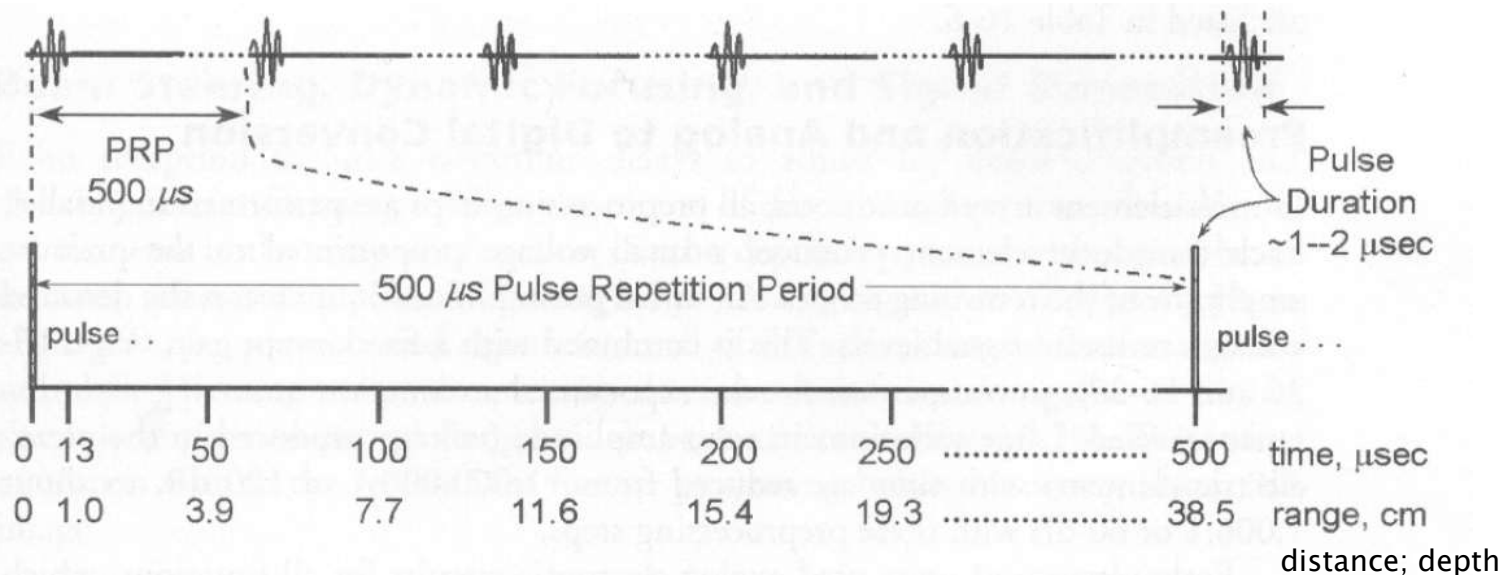
Der Tröpfchendurchmesser D hängt nur von der Schwingerfrequenz f sowie von der Dichte ρ und der Oberflächenspannung σ des Medikaments ab ($[\rho] = \text{N/m}$, $[\sigma] = \text{kg/m}^3$):

$$\text{Aus Kapillarwellen-Theorie: } D \approx \frac{\sqrt[3]{\sigma/(\rho \cdot f^2)}}{\sqrt[6]{2\pi}} \approx 0,73 \cdot \sqrt[3]{\sigma/(\rho \cdot f^2)} \quad (\text{also } D \sim f^{-2/3}) . \quad (58)$$

Pulsed Ultrasound and its parameter

$$\text{Time } (\mu\text{sec}) = \frac{2D(\text{cm})}{c(\text{cm}/\mu\text{sec})} = \frac{2D(\text{cm})}{0.154 \text{ cm}/\mu\text{sec}} = 13 \mu\text{sec} \times D(\text{cm})$$

$$\text{Distance (cm)} = \frac{c(\text{cm}/\mu\text{sec}) \times \text{Time } (\mu\text{sec})}{2} = 0.077 \times \text{Time } (\mu\text{sec})$$

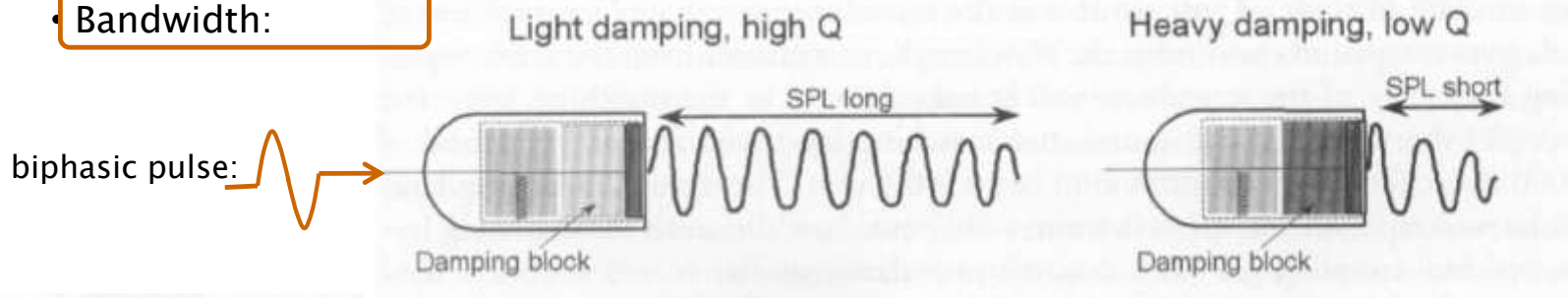


$$\text{PRF} = \frac{1}{\text{PRP}} = \frac{1}{500 \mu\text{s}} = \frac{1}{500 \times 10^{-6} \text{s}} = \frac{2000}{\text{s}} = 2 \text{ kHz}$$

FIGURE This diagram shows the initial pulse occurring in a very short time span, pulse duration of 1 to 2 μ sec, and the time between pulses equal to the pulse repetition period (PRP) of 500 μ sec. The pulse repetition frequency (PRF) is 2,000/sec, or 2 kHz. Range (one-half the round-trip distance) is calculated assuming a speed of sound = 1,540 m/sec.

Ultrasound using pulsed/echoe mode

- Bandwidth:



Q-Factor:

$$Q = \frac{f_0}{\text{Bandwidth}}$$

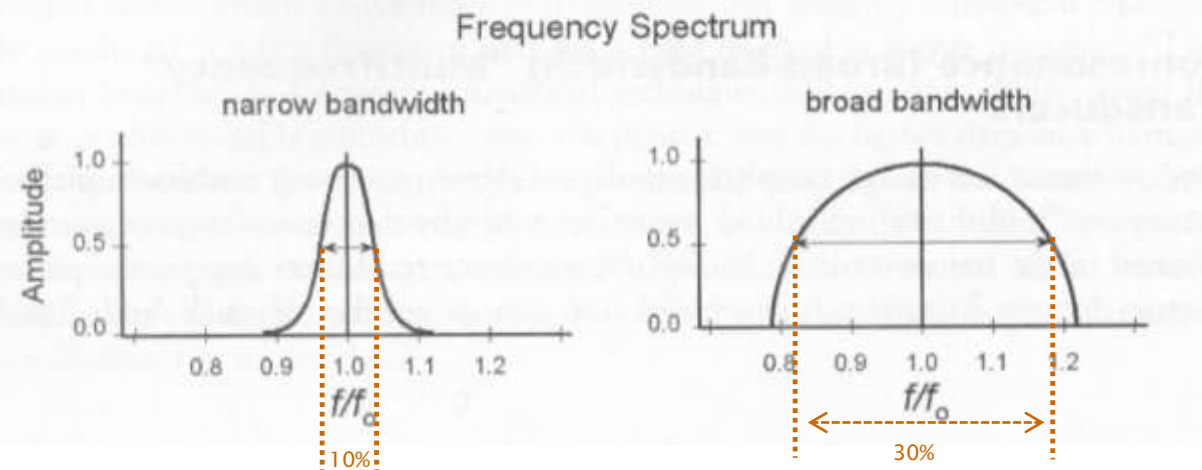
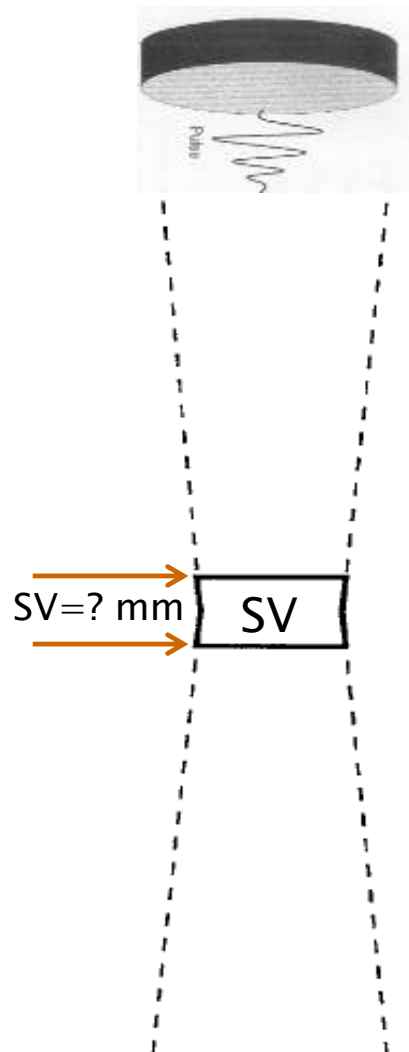


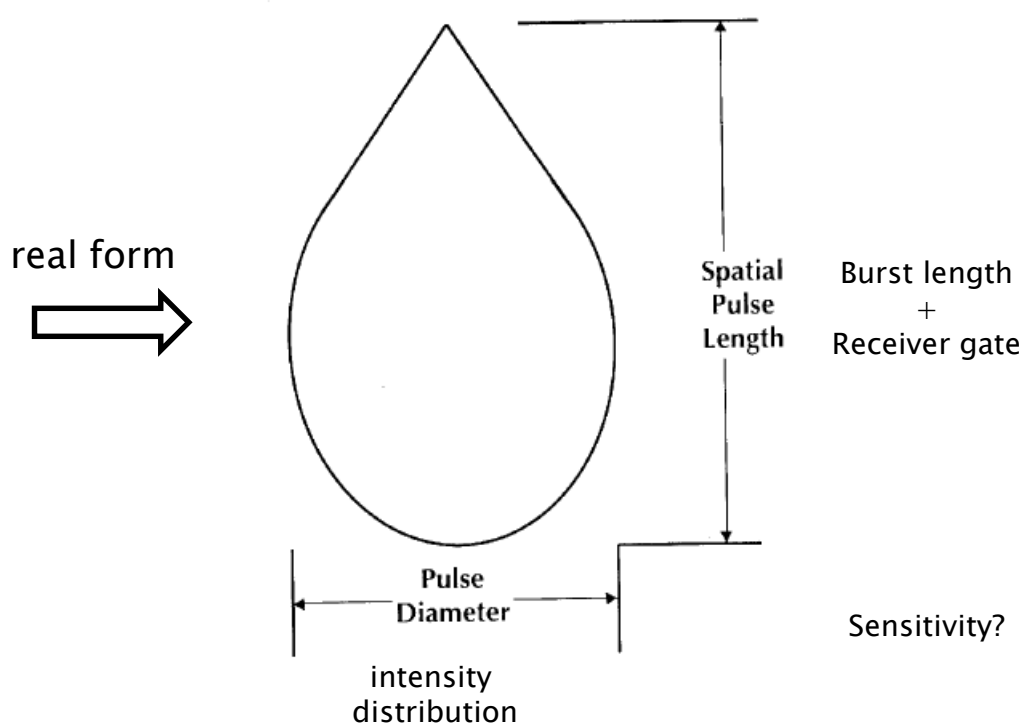
FIGURE Effect of damping block on the frequency spectrum. The damping block is adjacent to the back of the transducer and limits the vibration of the element to a small number of cycles. Light damping allows many cycles to occur, which results in an extended spatial pulse length (number of cycles times the wavelength) and a narrow frequency bandwidth (range of frequencies contained in the pulse). Heavy damping reduces the **spatial pulse length** and broadens the frequency bandwidth. The Q factor is the center frequency divided by the bandwidth.

Ultrasound and spacial resolution (Pulsed/echo-mode)

Abtastvolumen / Sample Volume SV due to beam form and burst length B →
 tear drop form using one short gate



Example: $B=10\mu\text{m}$ without ringing



Ultraschallsonden / (Arrays)

Punktstrahler / Kugelstrahler 0.Ordnung = Monopol (pulsierende Kugel Radius R mit Schallschnelle v_0)

Lösung Wellengleichung:

$$p \sim \frac{1}{r}$$

$$v \sim \frac{1}{r} \left(1 + \frac{1}{jkr} \right)$$

r = Entfernung vom Mittelpunkt der Kugel-schallquelle
(Ortskoordinate)

$k = \omega/c = 2\pi/\lambda$ = **Wellenzahl**

Im **Fernfeld** $\left(kr = \frac{2\pi r}{\lambda} \gg 1 \right)$ ist $1/kr \ll 1$, d.h.

Schalldruck und **Schallschnelle** sind phasengleich.

– Läßt man den Radius des Kugelstrahlers gegen Null gehen, und führt man ferner den Schallfluß

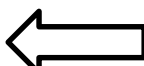
$$q = v_0 \cdot 4\pi R^2 \quad (\text{Ruheradius: } R)$$

ein, so gehen die obigen beiden Gleichungen über in die:

Schallfeldgleichungen für den Punktstrahler 0. Ordnung:

$$p = \frac{j\omega \rho_-}{4\pi} \cdot q \cdot \frac{e^{jkr}}{r}$$

$$v = \frac{p}{\rho_- \cdot c} \cdot \left(1 + \frac{1}{jkr} \right)$$



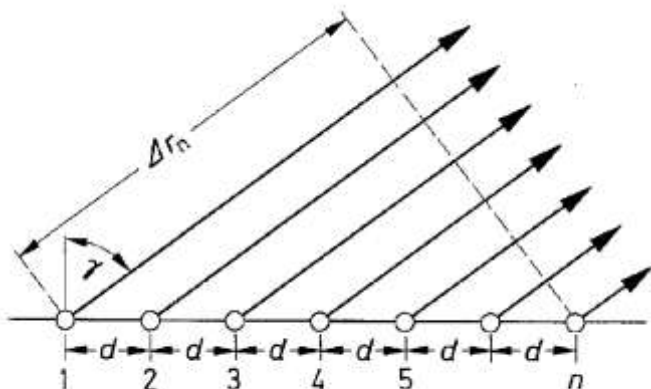
Die von einem Kugelstrahler 0. Ordnung insgesamt abgestrahlte Schalleistung beträgt im Fernfeld:

$$P_a = I \cdot A = \frac{\tilde{P}^2}{\rho_- \cdot c} \cdot 4\pi R^2$$

Als einen Punktstrahler 0. Ordnung kann man grundsätzlich jede beliebige einseitig Schall abstrahlende Quelle ansehen, deren lineare Abmessungen vernachlässigbar klein gegenüber der Wellenlänge des abgestrahlten Schalls sind und für die man einen Schallfluß q angeben kann.

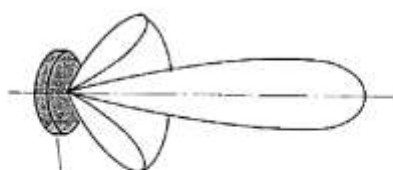
Ultraschallsonden / (Arrays)

- Linear Arrays von Punktstrahler
- Hauptkeule und Nebenkeule



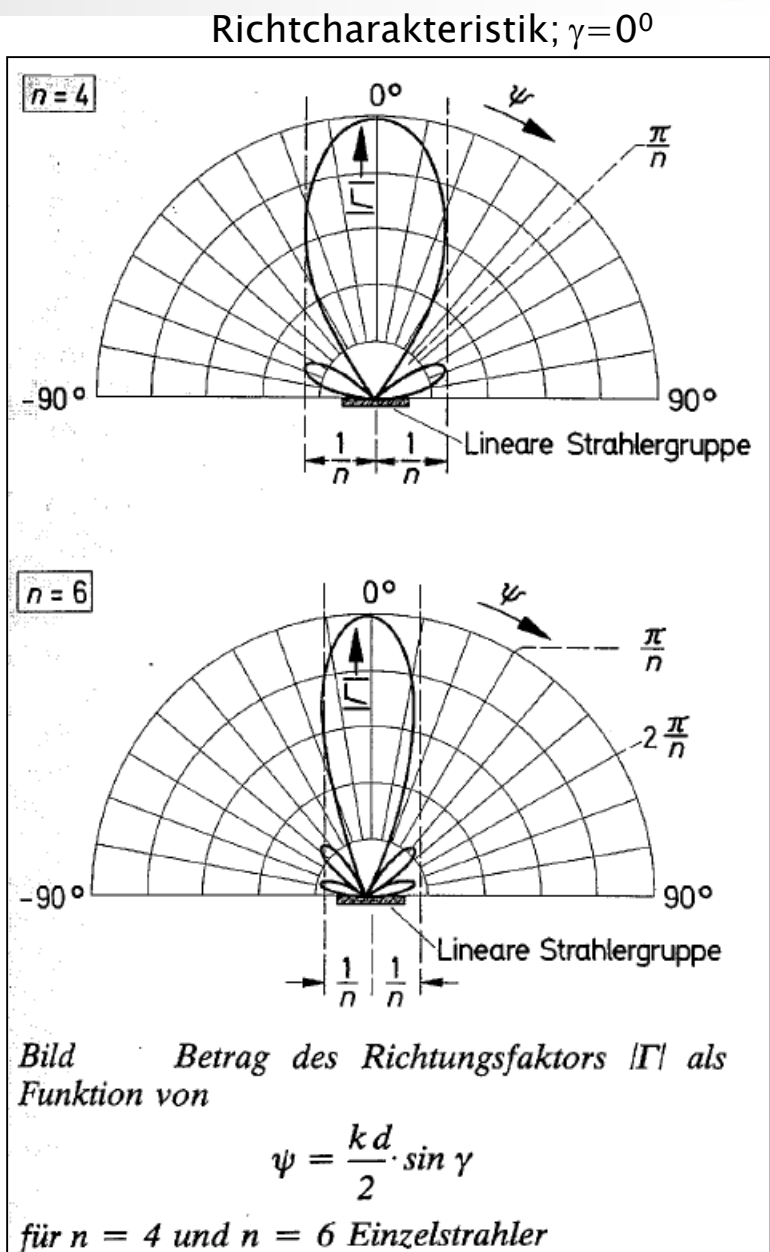
alle in Phase

Lineare Strahlergruppe



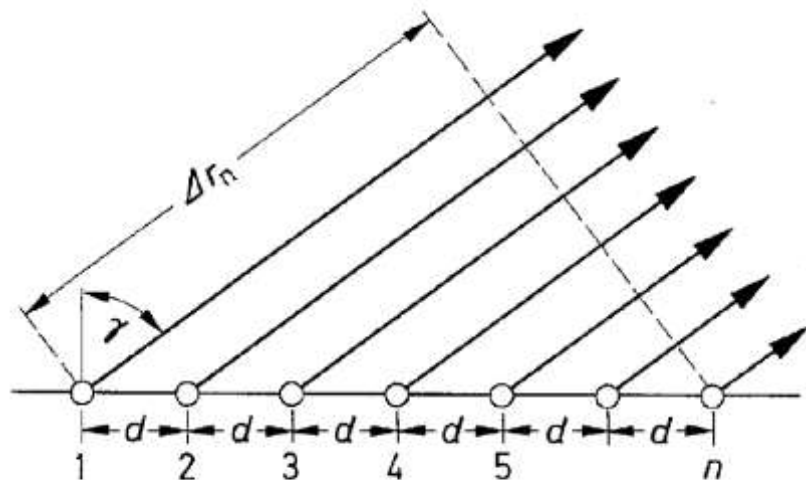
Kreisrunder Flächenstrahler

Bild Richtcharakteristik eines kreisrunden Flächenstrahlers (schematische Darstellung)

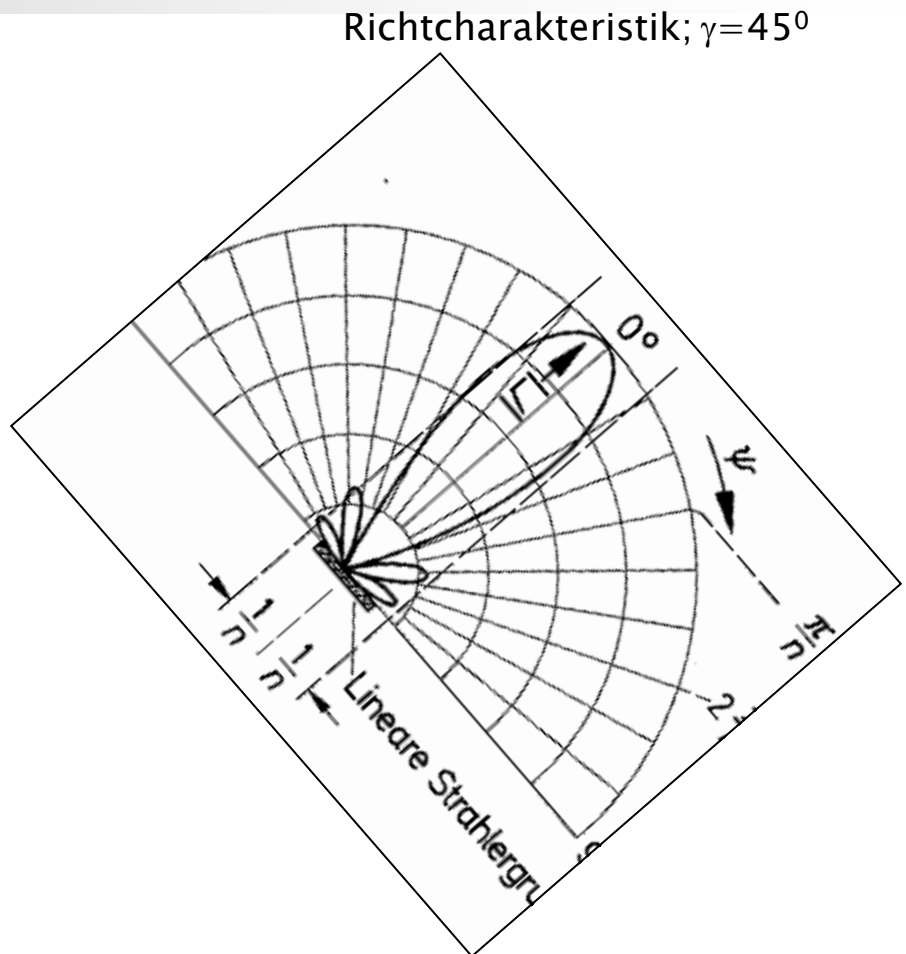


Ultraschallsonden / (Arrays)

- Linear Arrays von Punktstrahler
- Hauptkeule und Nebenkeule



Lineare Strahlergruppe



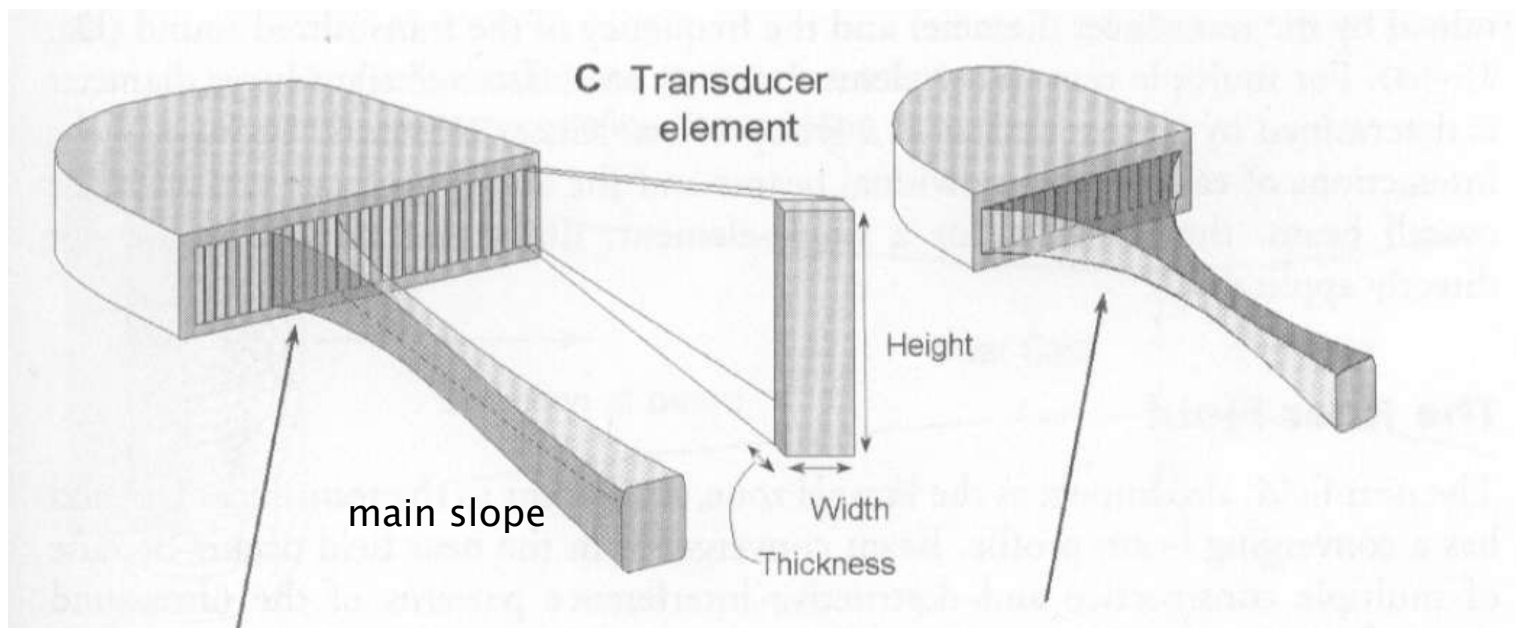
Gangunterschied $\Delta r_n = (n - 1) \cdot d \cdot \sin \gamma$ wird durch Zeitverzögerungen kompensiert → Schwenken der Keule

Ultrasound transducer (arrays: 6dB-beam limits)

A) Linear Arrays

(A-Scan-Beams)

B) Phased Array



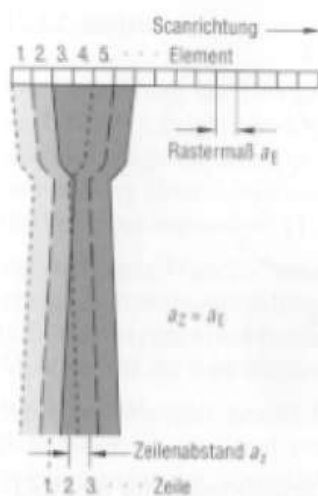
A subset of transducer elements activated

All transducer elements activated

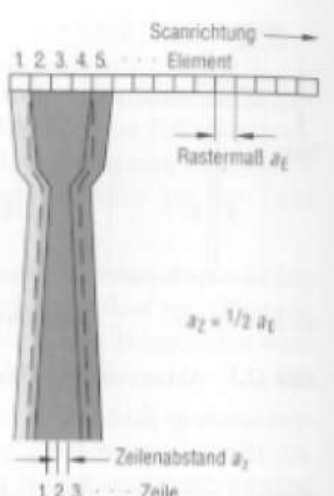
FIGURE Multielement transducer arrays. **A:** A linear (or curvilinear) array produces a beam by firing a subset of the total number of transducer elements as a group. **B:** A phased array produces a beam from all of the transducer elements fired with fractional time delays in order to steer and focus the beam. **C:** The transducer element in an array has a thickness, width, and height; the width is typically on the order of $\frac{1}{2}$ wavelength; the height depends on the transducer design.

Ultraschallsonden / (Arrays)

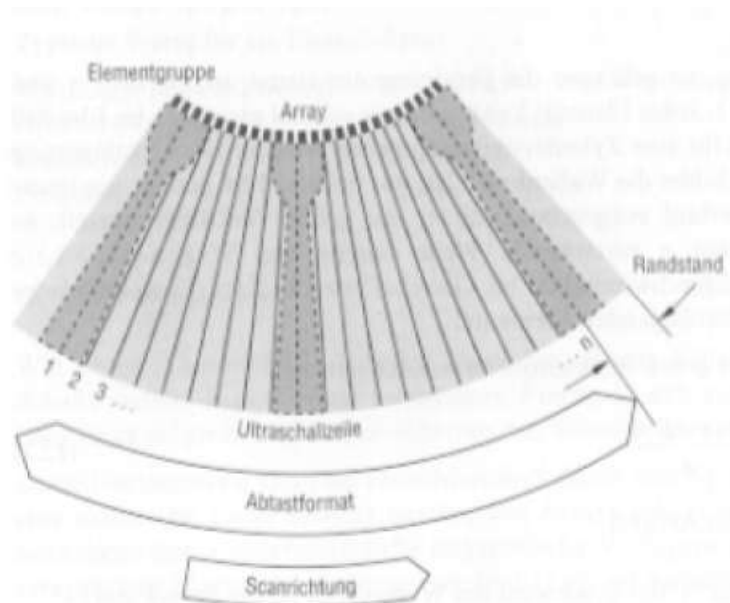
A) Prinzip Linear A-Scan und Sektor Scan (2D-Bild)



a) Prinzip des Linearscans (Zeilenabstand a_z ist der Elementabstand bzw. das Rastermaß a_E)



b) Prinzip der Gruppenfortschaltung mit Verdopplung der Zeilendichte

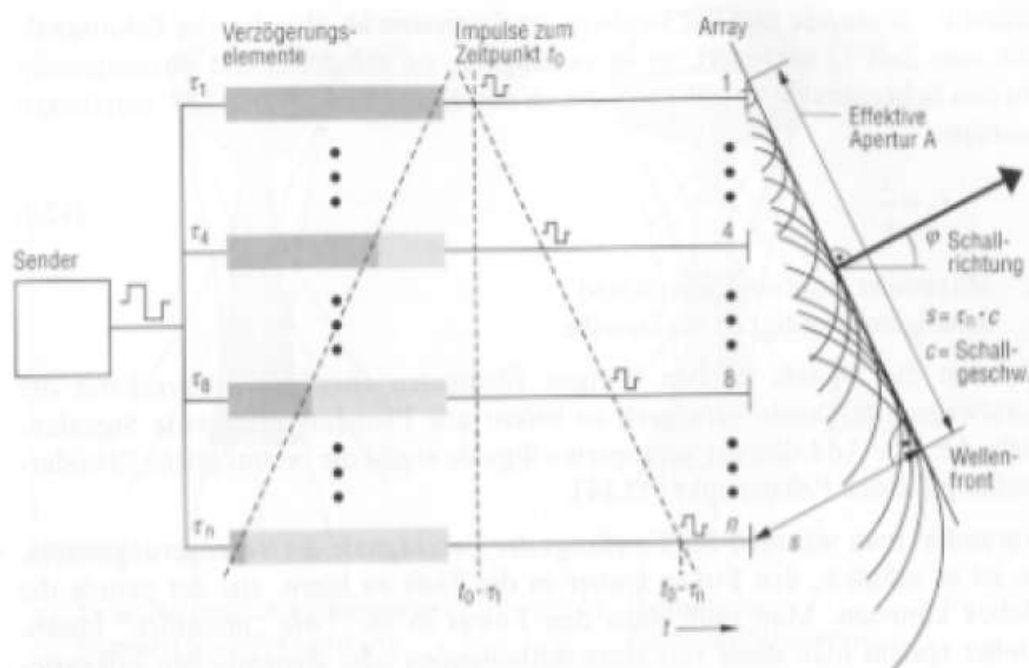


Typische Werte für ein Linear-Array

Gesamtzahl der Elemente	n	60 bis 196	Elemente
Elementbreite	b	1 bis 4	λ
Gruppenbreite	$B = m \cdot b$	8 bis 128	Elemente
Frequenzen	f	3,5 bis 7,5	MHz
Länge der Keramik	L	2 bis 11,5	cm
Scanlänge (Bildbreite)	$S \approx L - B$	10 bis 2	cm
Breite der Keramik		6 bis 14	mm

Ultraschallsonden / (Arrays)

Elektronisch schwenbarer Schallstrahl bei Linear phased array



Typische Werte für ein Phased-Array

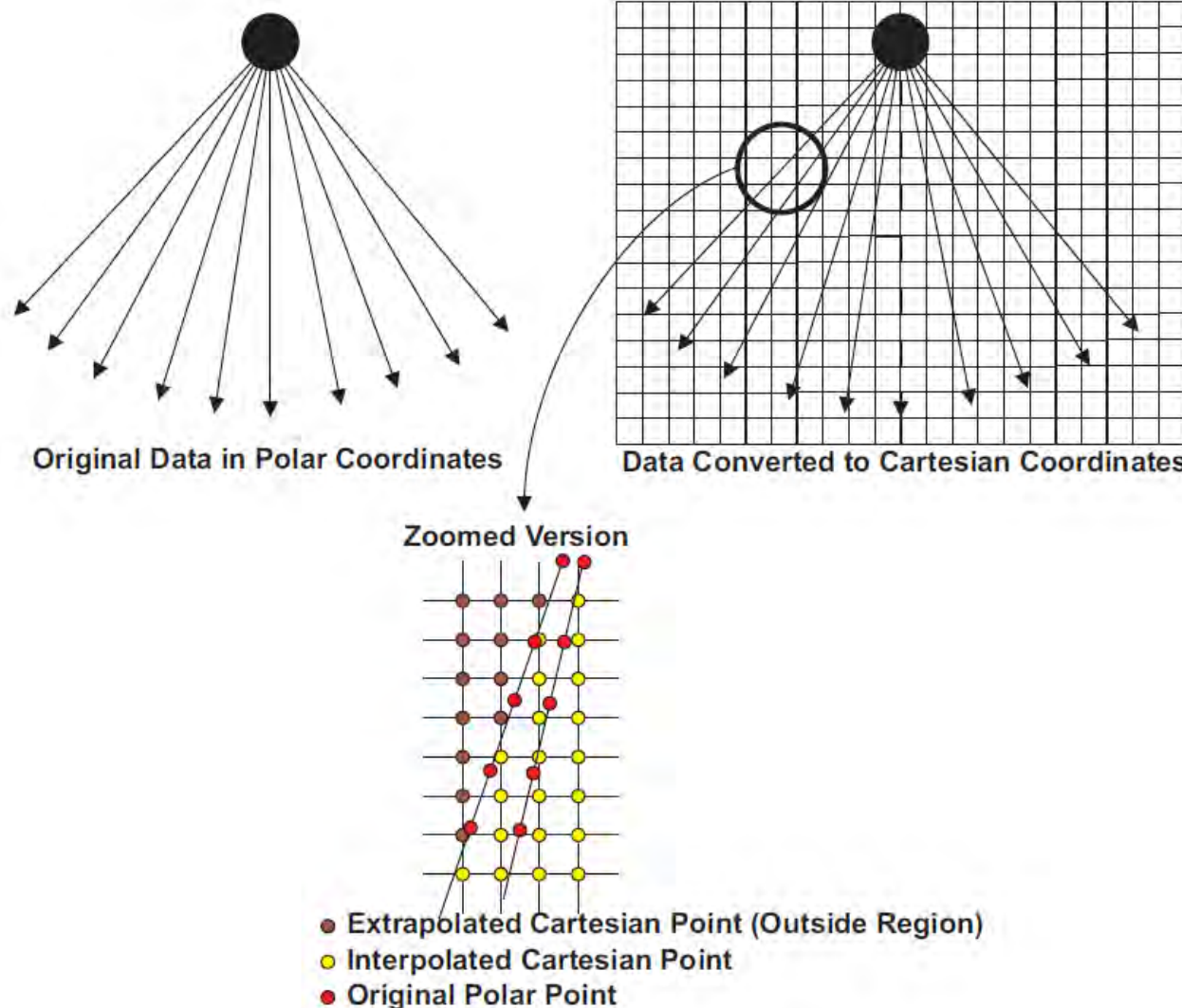
Maximaler Schwenkwinkel	40 bis 45°
Apertur (Arraylänge)	14 bis 28 mm
Elementzahl	48 bis 128
Frequenz	2,5 bis 7 MHz

Bild

Phased-Array: Erzeugung einer elektronisch schwenkbaren Wellenfront.
 Die Steuerung des Scanwinkels geschieht durch zeitversetzte Anregung (τ_1 bis τ_n) der Elemente des Arrays (Sendefall)

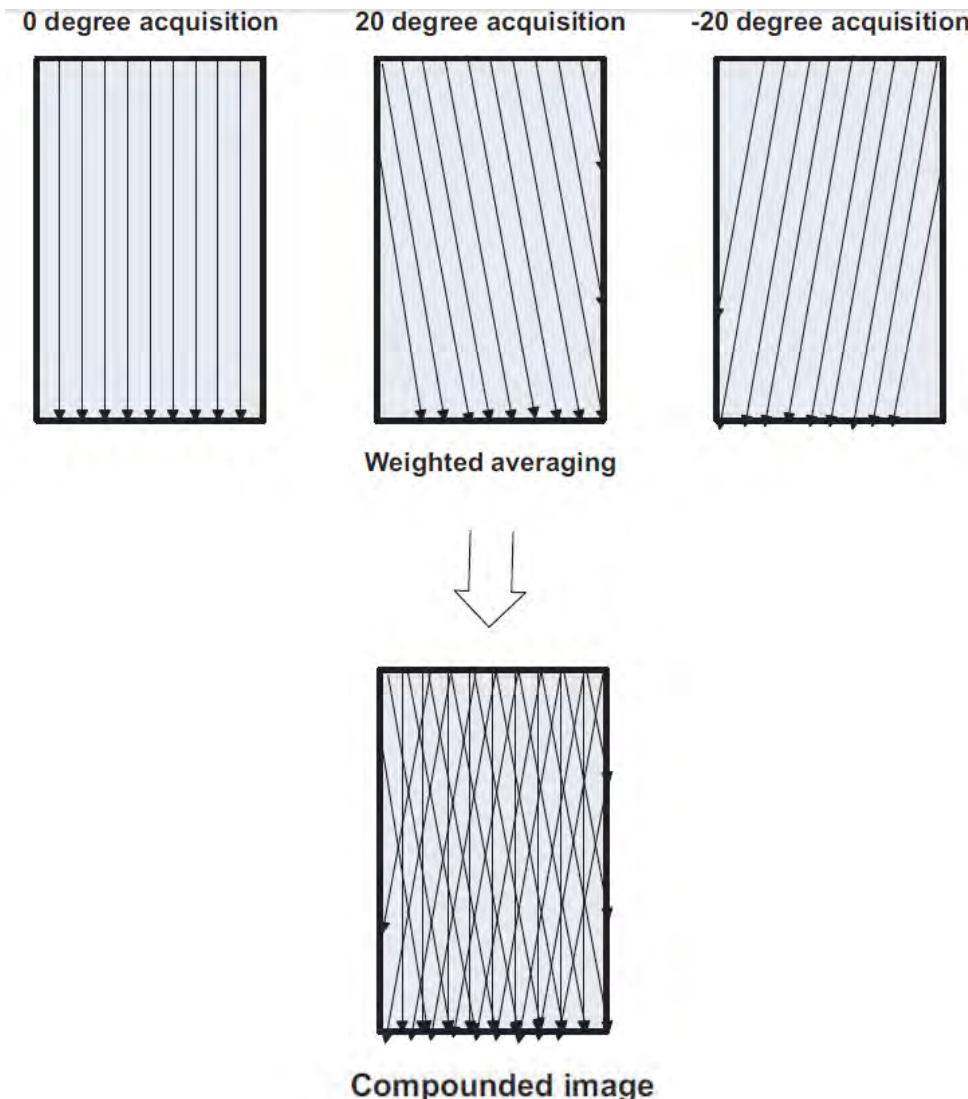
Ultrasound probe (Arrays)

Scan Conversion from radial → karthesic coordinates



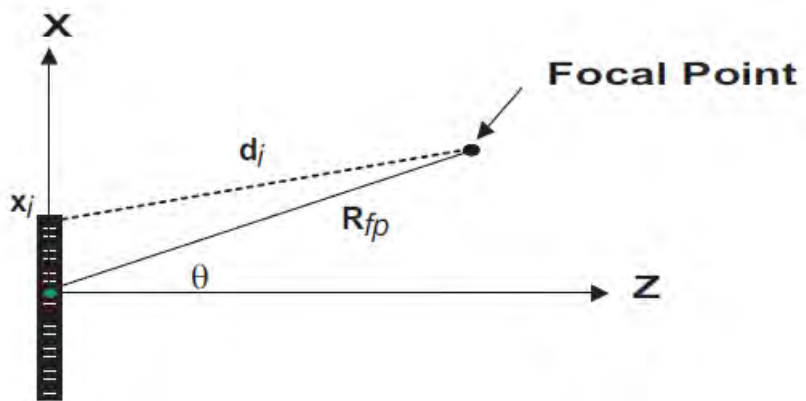
Ultrasound probe (Arrays)

Spatial Compound imaging by reducing frame rate



Ultrasound probe (Arrays)

Beamforming



Focal Point Representation - Polar Coordinates

Suppose that each piezo-electric element is driven with the same pulse waveform, $p(t)$. The propagation time, t_i , for the i th piezo-electric element to the focal point can be written as:

$$t_i = \frac{\sqrt{R_{fp}^2 + x_i^2 - 2x_i R_{fp} \sin(\theta)}}{c} \quad \text{Propagation time} \quad (6)$$

where x_i is the x-axis coordinate of the i th piezo-electric element, R_{fp} is the radial distance from the origin to the focal point, θ is the angle of the focal point with respect to the z-axis, and c is the speed of sound. Notice that θ defines the scan line of interest. In general, multiple focal points are analyzed for a given scan line that makes R_{fp} a function of time.

Ultrasound probe (arrays)

Beamforming

To ensure that the sound waves from each piezo-electric element arrive at the focal point at the same time, the pulse waveform to each element must be delayed by this amount. By studying [Equation 6](#), the maximum propagation time for a given (R_{fp} , θ) configuration (i.e., focal point) becomes:

$$t_{max} = \frac{\sqrt{R_{fp}^2 + x_{max}^2 + 2x_{max}R_{fp} \sin(\theta)}}{c} \quad (7)$$

This value is used to bias the time-delay values so that the pulse start time for the piezo-electric element that is furthest away from the focal point is time zero. Therefore, the pulse waveform for the i th piezo-electric element becomes:

$$p_i(t) = p(t - \tau_i) \quad (8)$$

where $\tau_i = t_{max} - t_i$

Pulse Wave and Delay

Once the sound waves reach the focal point, some of the sound waves will reflect back towards the transducer. One can assume that the focal point is emitting a sound wave and the transducer is recording the received sound wave at each piezo-electric element. As a result, the propagation time from the focal point back to the i th piezo-electric element is the same value as that given in [Equation 6](#). The received signal, $r(t)$, from a given focal point after it has been time ligned can be written as:

$$r(t) = \sum_{i=1}^N A_{ri} \sum_{j=1}^N A_{tj} p(t - \tau_{ri} - \tau_{tj}) \quad (9)$$

Received Signal

where A_{ri} is the apodization applied to each receive signal, A_{tj} is the apodization applied to each transmit signal, τ_{ri} is the time-delay value applied to each received signal, and τ_{tj} is the time-delay value applied to each transmitted signal. The apodization factors are used to shape the transmitted beam and to weight the received signals. Sidelobes can be dramatically reduced by properly adjusting these factors.



Ultrasound probe (arrays)

Beamforming

The process of beamforming can be broken down into two main components: steering and focusing. Steering is performed by adjusting the angle, θ , which controls the direction of the beam and focusing is performed at various time intervals along a given scan line. An efficient implementation will have the largest ΔR_{fp} possible so that multiple image points can be retrieved for a single pulse sequence to the piezo-electric elements. Unfortunately, [Equation 6](#) cannot be separated into terms that just depend on R_{fp} and θ . One common solution is to approximate this equation with a Taylor series expansion that yields:

$$t_i \approx \frac{R_{fp} - \sin(\theta)x_i + \frac{\cos^2(\theta)}{2R_{fp}}x_i^2}{c} \quad (10)$$

This second order approximation minimizes the mean squared error for the values of R_{fp} under consideration. Peak errors are less than 1/8 wavelength. Other approximations can also be used.

The linear term,

$$-\frac{\sin(\theta)}{c}x_i$$

is often referred to as the beamsteering component because it only depends upon θ and is fixed over all the focal points along a particular scan line. The quadratic term,

$$\frac{\cos^2(\theta)}{2cR_{fp}}x_i^2$$

is referred to as the dynamic focusing component because it depends on the focal point and can be used to adjust the focal point of the received data from the piezo-electric elements. Also notice that $x_1 = i \Delta x$, where i is the channel number and Δx is the piezo-electric element spacing. Therefore, these terms can be easily expressed in terms of channel number for easy implementation.

Ultrasound probe (arrays)

A) Side lobes

B) 3D-Resolution Main Lobe

(A-Scan-Beams)

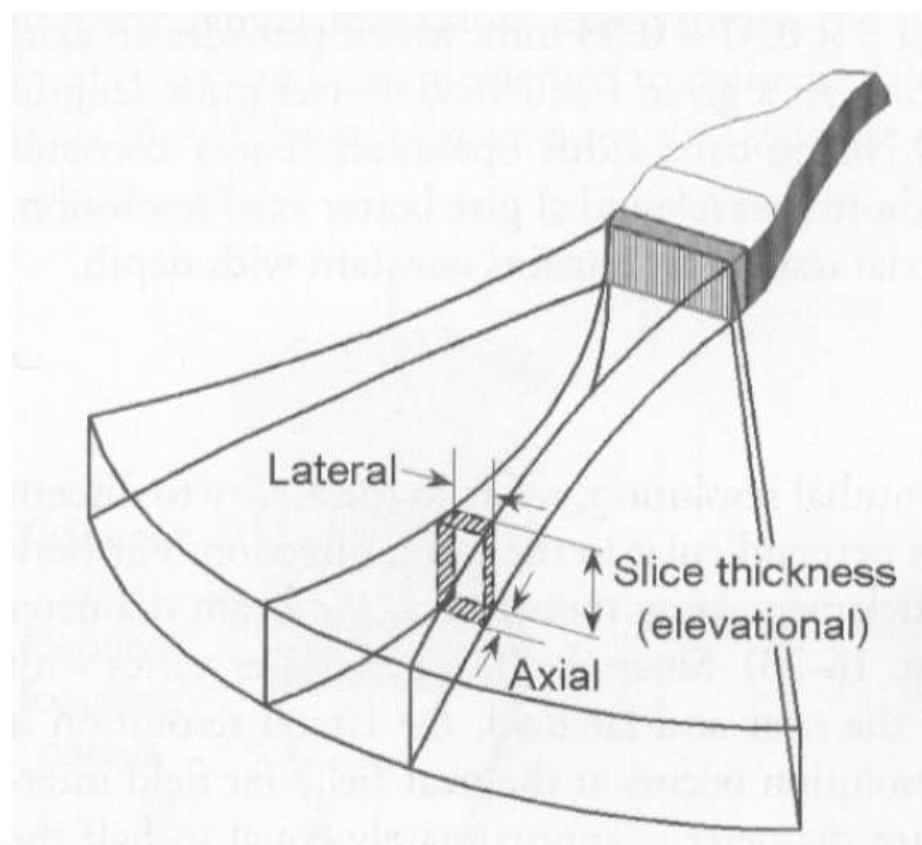
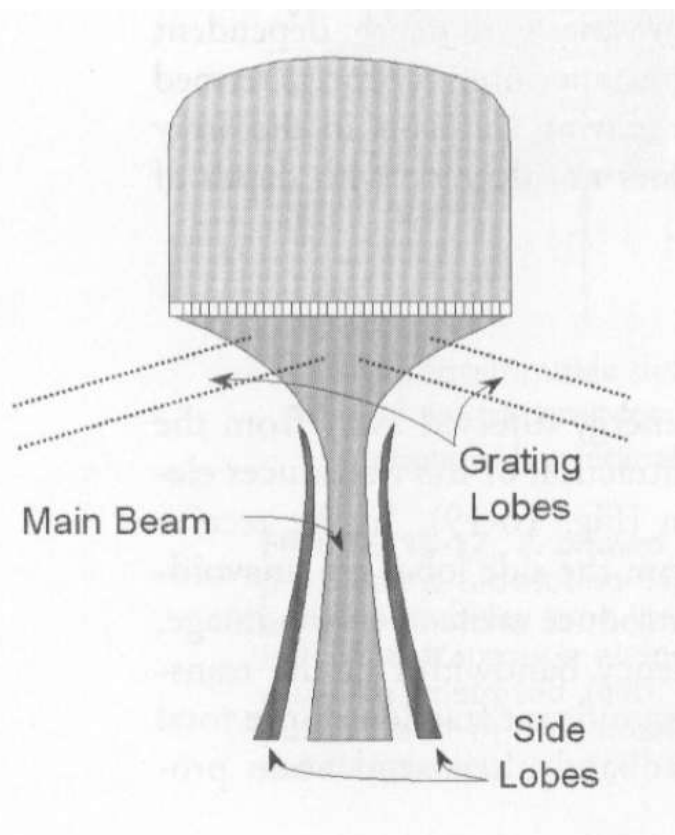


FIGURE Side and grating lobes are off-axis energy emissions produced by linear and phased array transducers. Side lobes are forward directed; grating lobes are emitted from the array surface at very large angles.

Ultrasound probe (arrays)

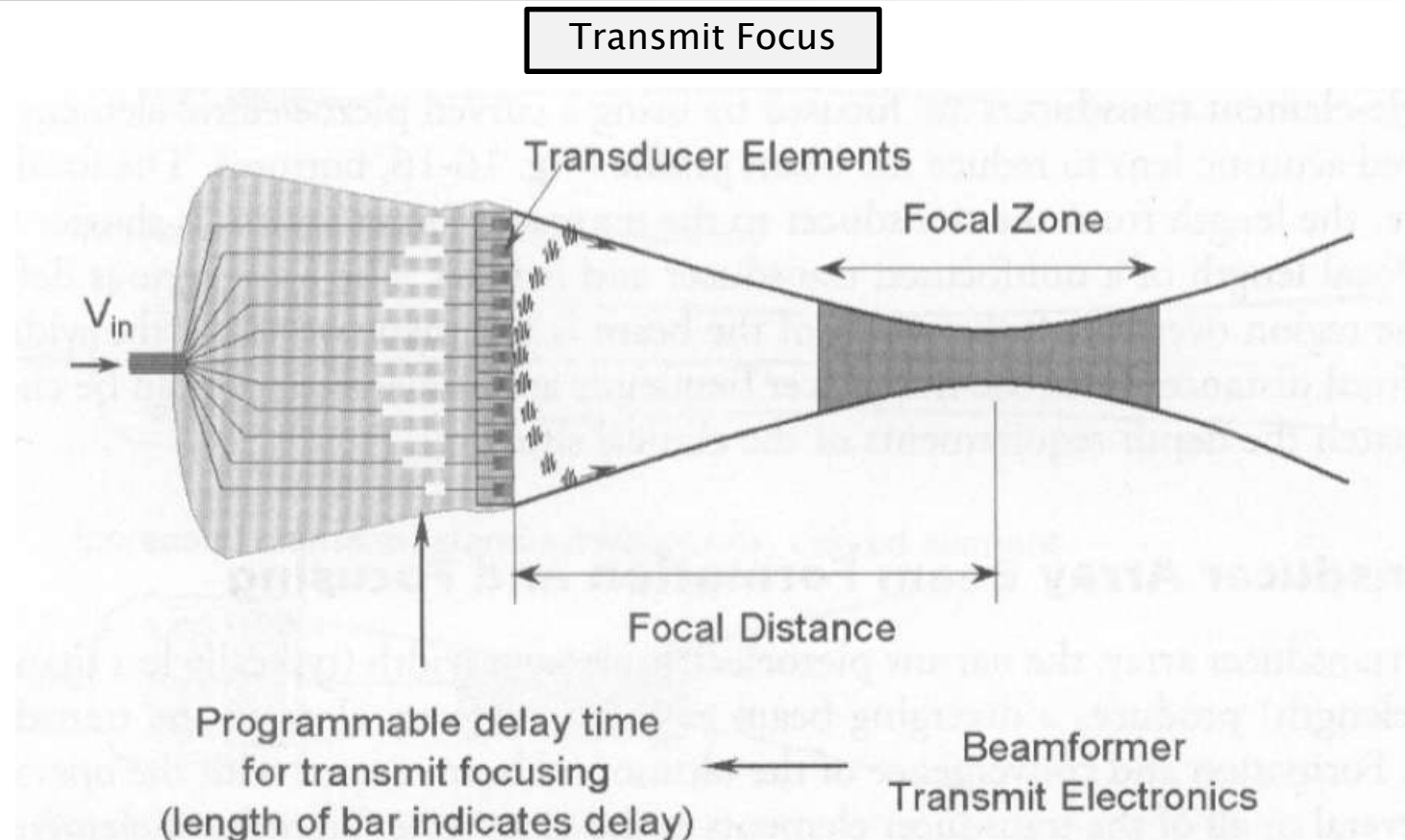


FIGURE A phased array transducer assembly uses all elements to produce the ultrasound beam. Focusing is achieved by implementing a programmable delay time (beam-former electronics) for the excitation of the individual transducer elements (focusing requires the outer elements in the array be energized first). Phase differences of the individual ultrasound pulses result in a minimum beam diameter (the focal distance) at a predictable depth.

Ultrasound probe (arrays)

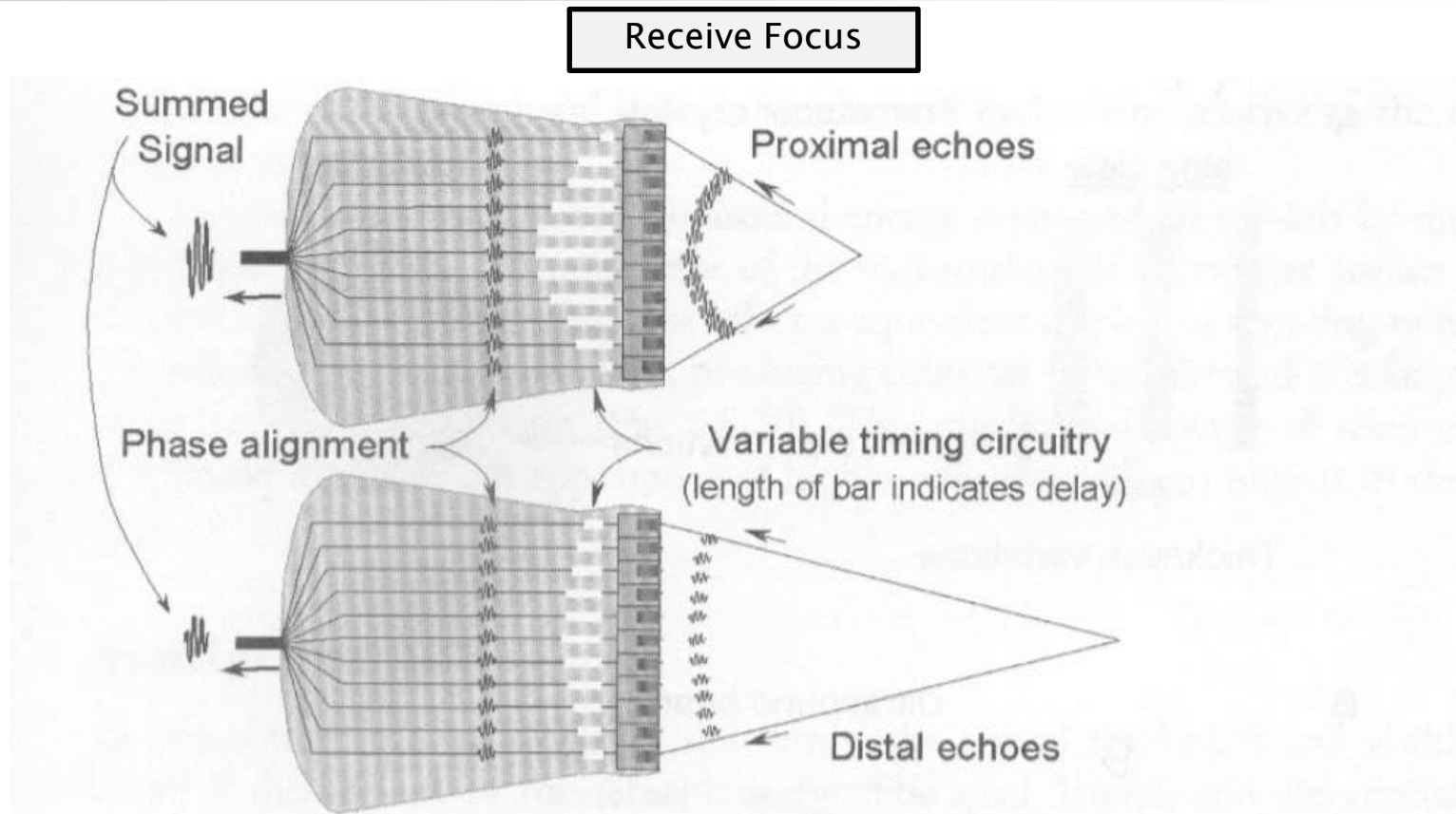


FIGURE Dynamic receive focusing. All transducer elements in the phased array are active during the receive mode, and to maintain focus, the receive focus timing must be continuously adjusted to compensate for differences in arrival time across the array as a function of time (depth of the echo). Depicted are an early time (**top**) of proximal echo arrival, and a later time of distal echo arrival. To achieve phase alignment of the echo responses by all elements, variable timing is implemented as a function of element position after the transmit pulse in the beam former. The output of all phase-aligned echoes is summed.



Ultrasound probe (arrays)

Dynamic Focusing

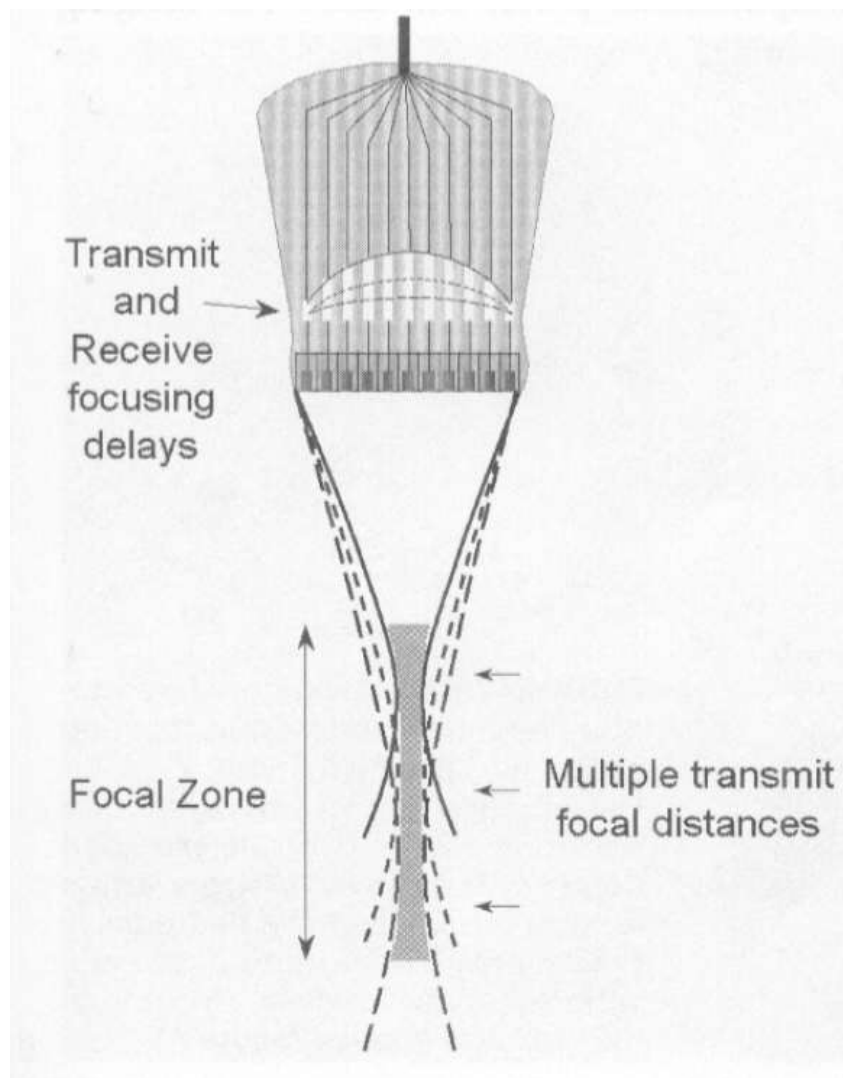


FIGURE Phased array transducers permit multiple user selectable transmit and receive focal zones implemented by the beam former electronics. Each focal zone requires the excitation of the entire array for a given focal distance. Good lateral resolution over an extended depth is achieved, but the image rate is reduced.

Ultrasound probe (arrays)

Receive Focus

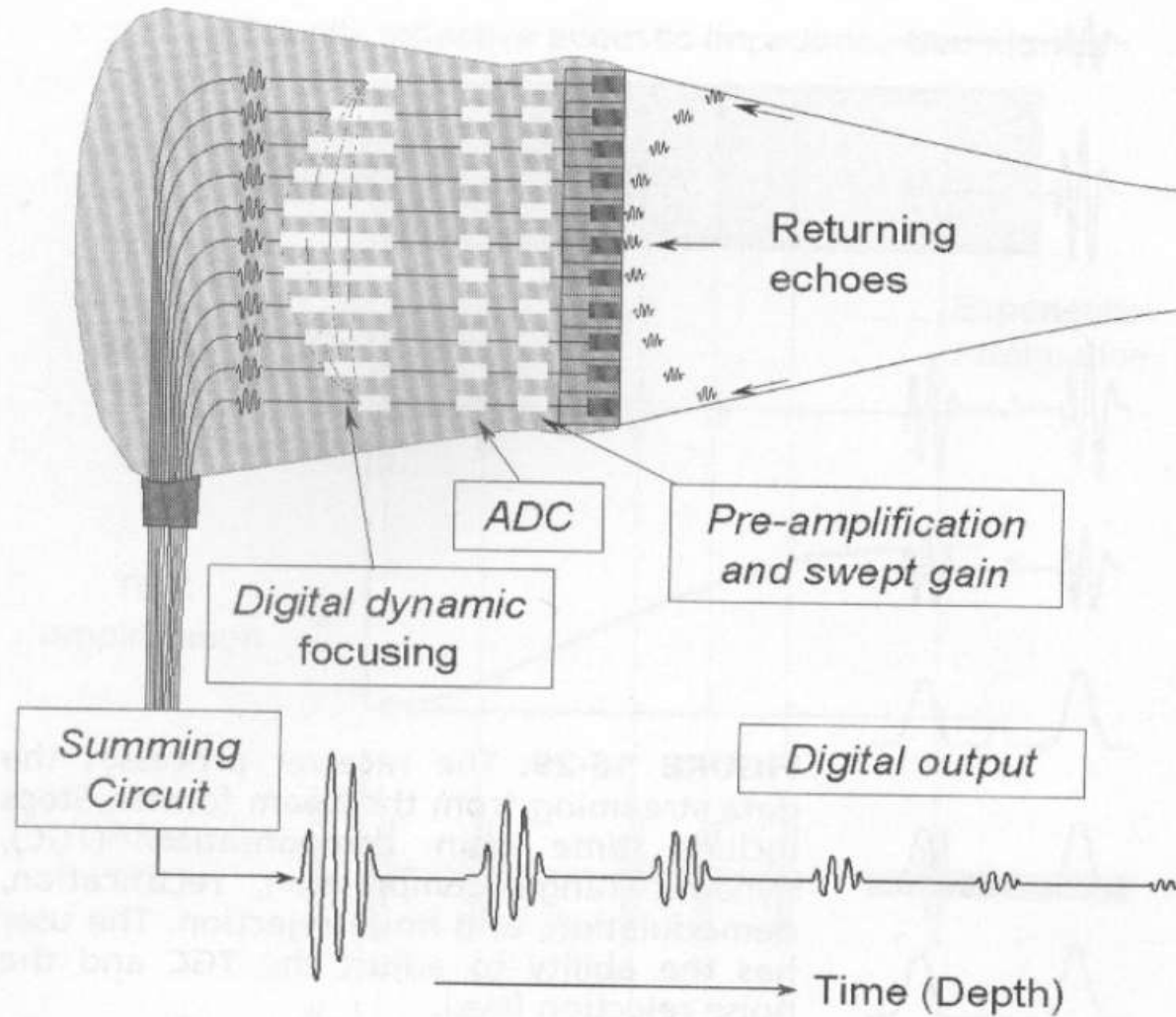
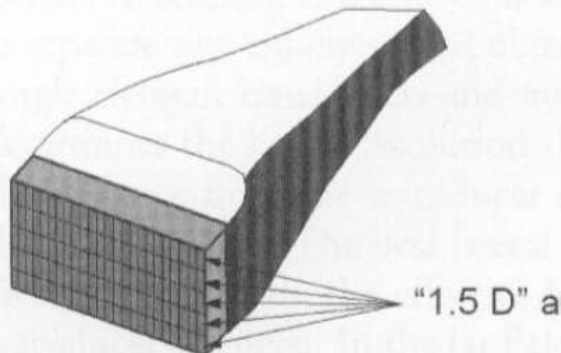


FIGURE A phased array transducer produces a pulsed beam that is focused at a programmable depth, and receives echoes during the pulse repetition period. In this digital beam-former system, the analog-to-digital converter (ADC) converts the signals before the beam focus and steering manipulation. Timed electronic delays phase align the echoes, with the output summed to form the ultrasound echo train along a specific beam direction.

Ultrasound probe (arrays)

Dynamic Focusing elevational



Multiple transmit focal zones: elevational plane

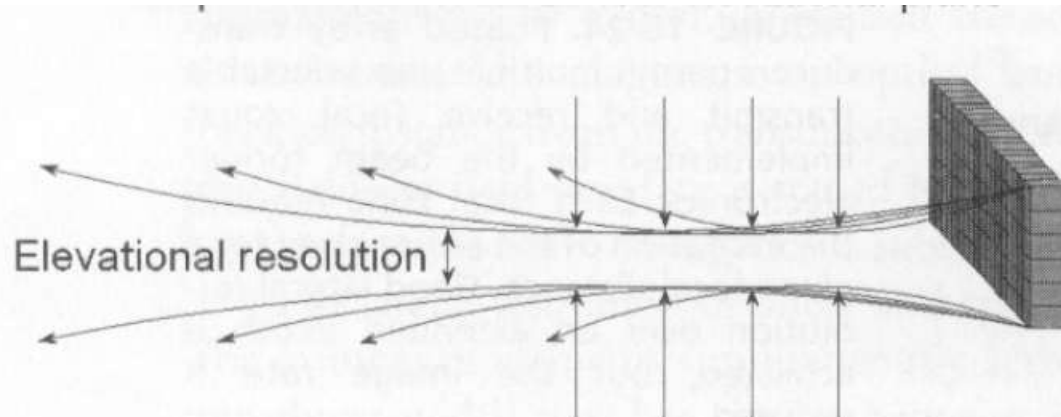
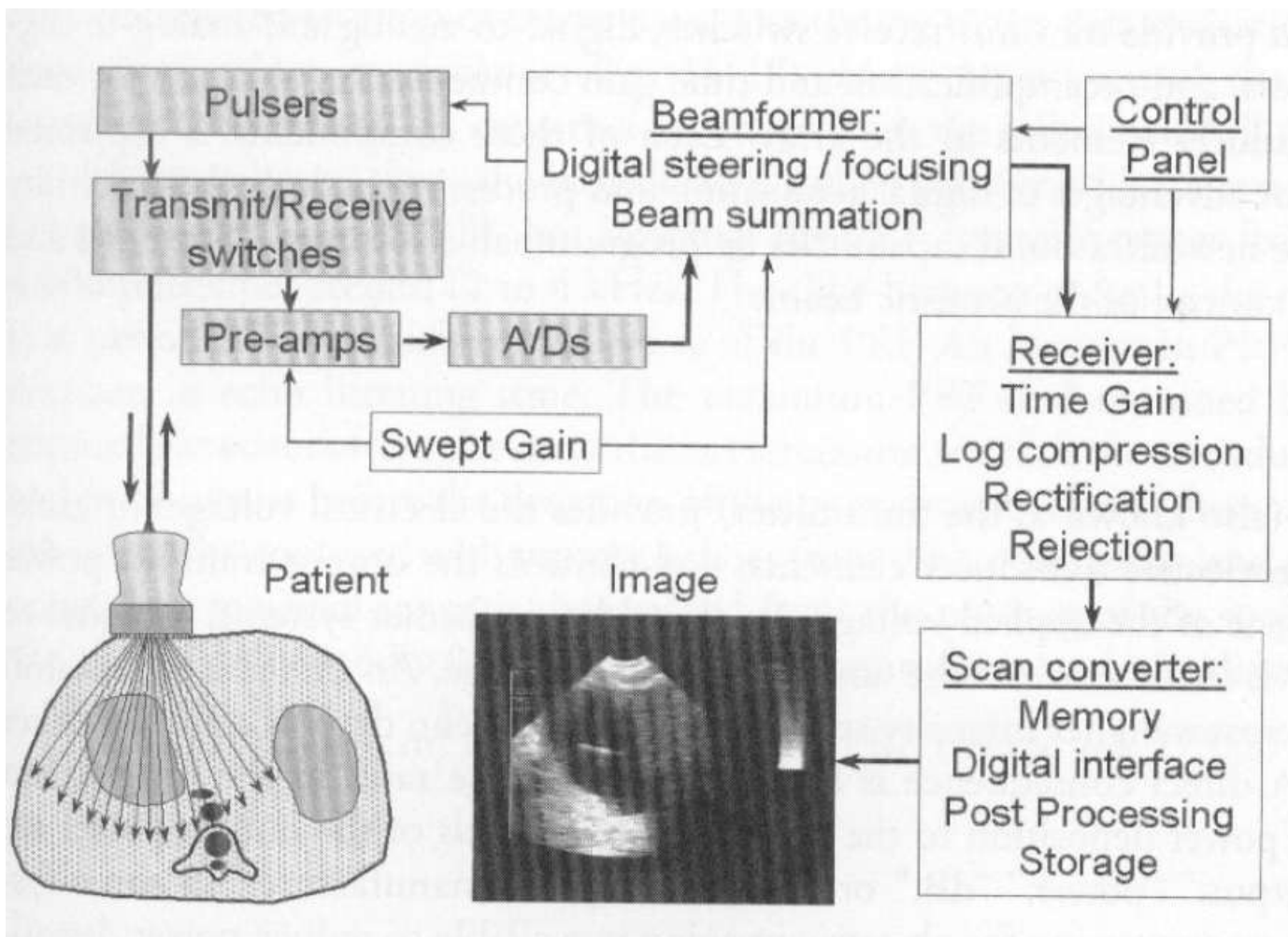


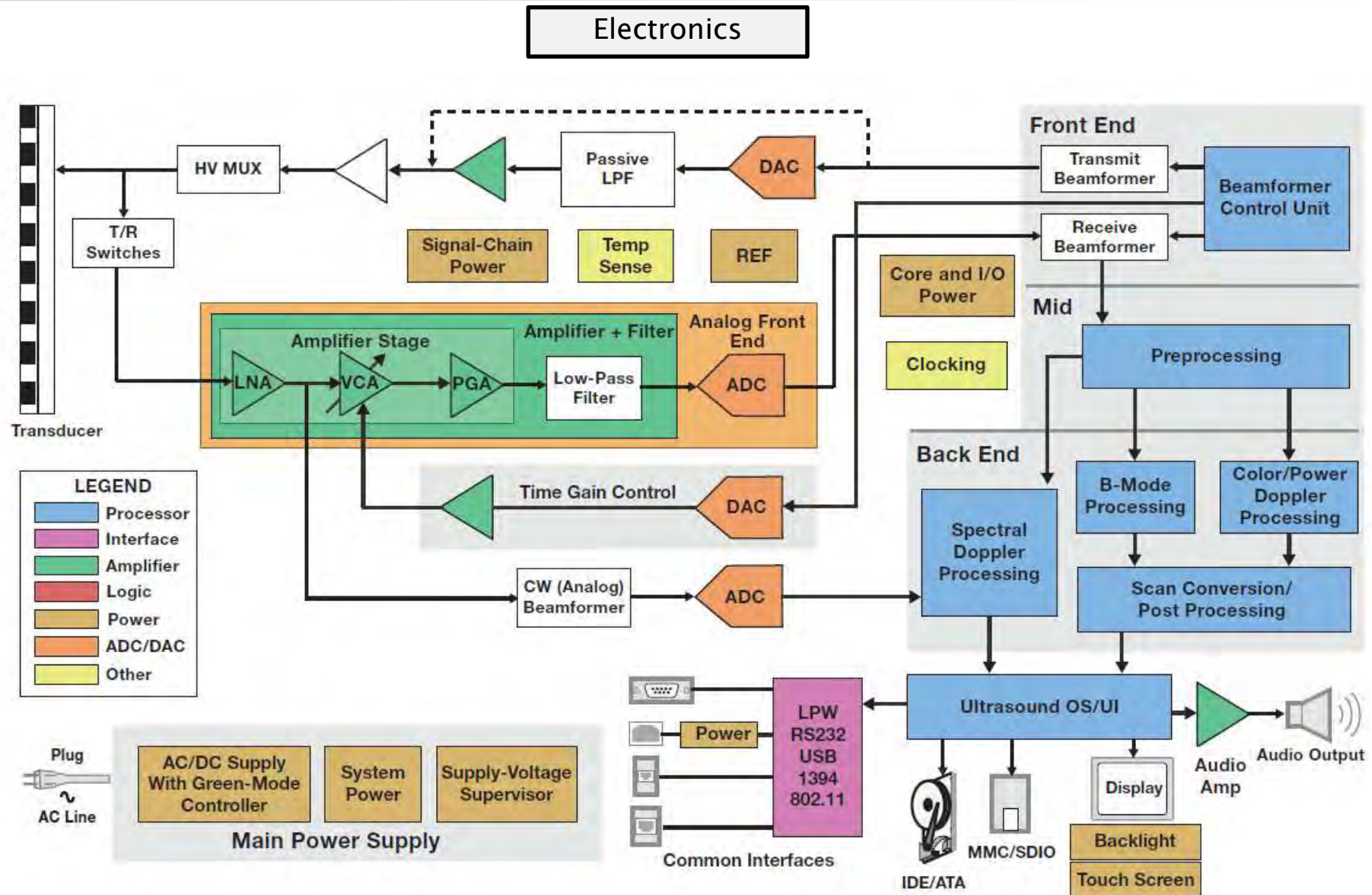
FIGURE E elevational resolution with multiple transmit focusing zones is achieved with "1.5-D" transducer arrays to reduce the slice thickness profile over an extended depth. Five to seven discrete arrays replace the single array. Phase delay timing provides focusing in the elevational plane (similar to lateral transmit and receive focusing).

Image acquisition and processing

Summary of instrumentation in diagnostics



Summary: Electronics and Imaging in detail



Ultraschall und Theragnostik

Ultraschall in Thera(pie) und (Dia)gnostik

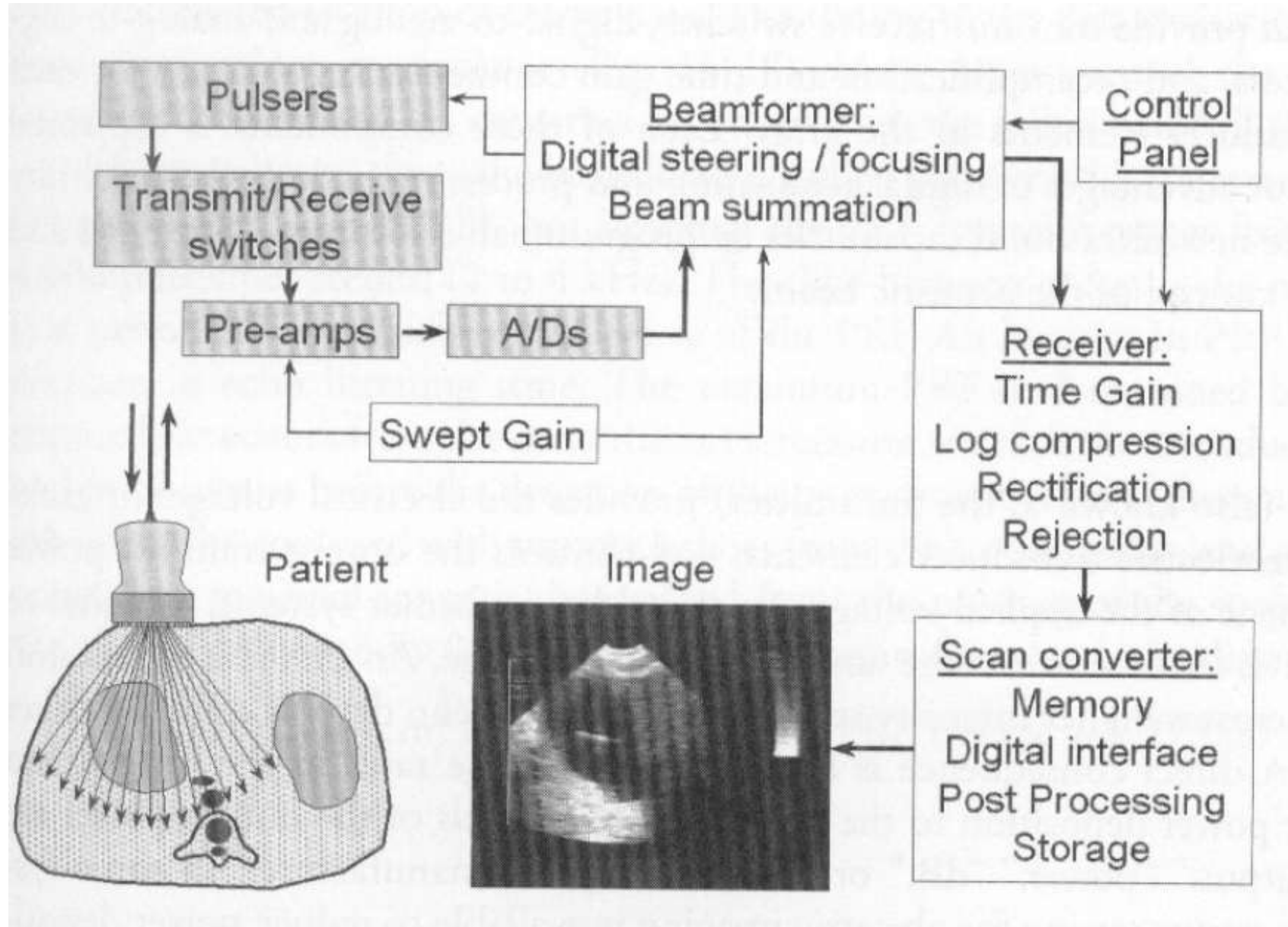
Kapitel 4

Bildgebende Verfahren in der Diagnostik

Inhaltsangabe

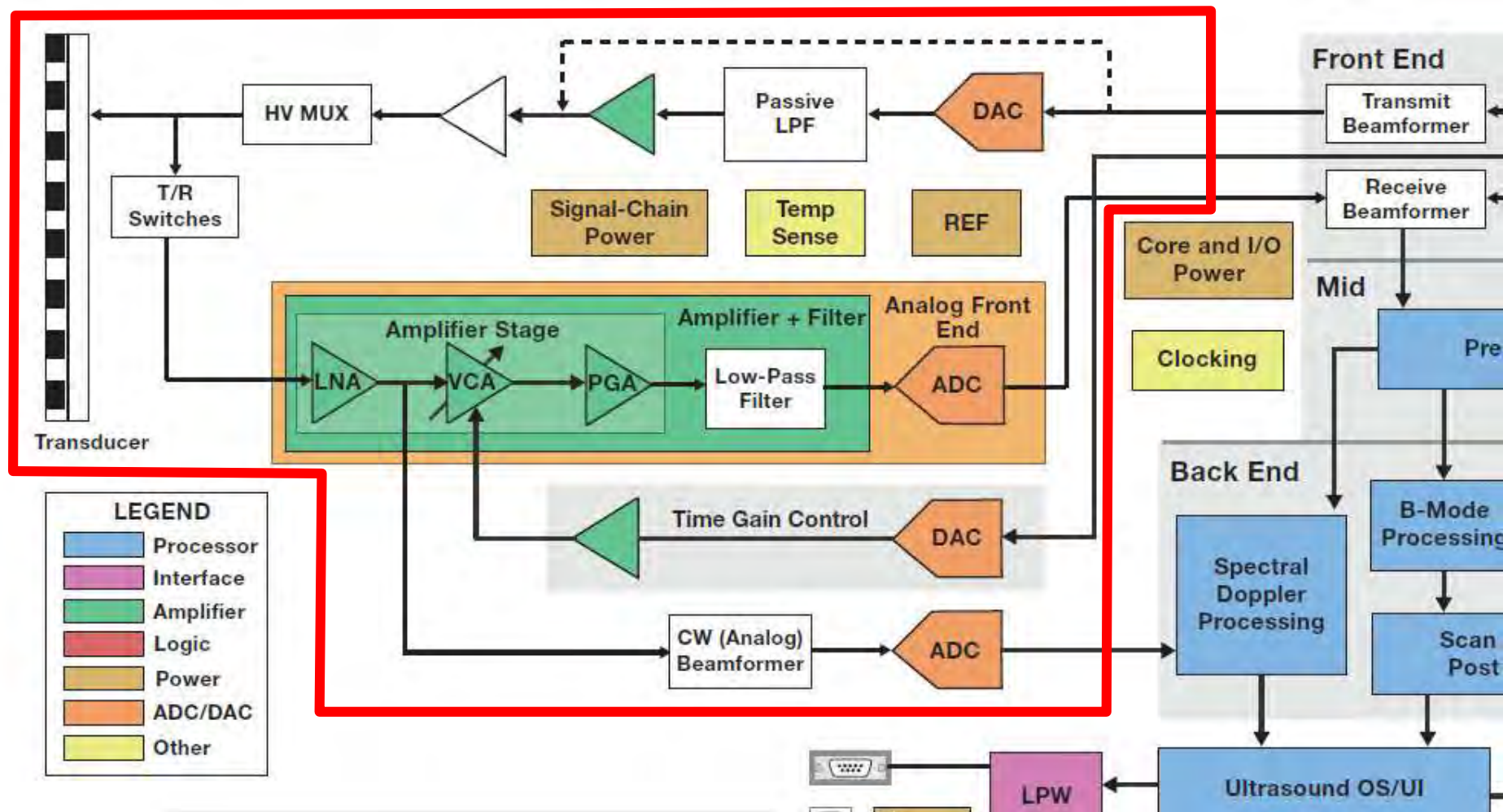
1. Übersicht der Ultraschallanwendungen
2. Physikalische Grundlagen
3. Ultraschallsonden
4. **Bildgebende Verfahren in der Diagnostik**
5. Dopplerverfahren in der Diagnostik
6. Artefakte und Diagnostik
7. Ultraschall und Kontrastmittel
8. Theragnostik mit Ultraschall
9. Therapie mit hochdosierten Ultraschall
10. Gewebecharakterisierung mittels shear waves
11. Dosierung und Sicherheitsaspekte

Imaging method: Principle

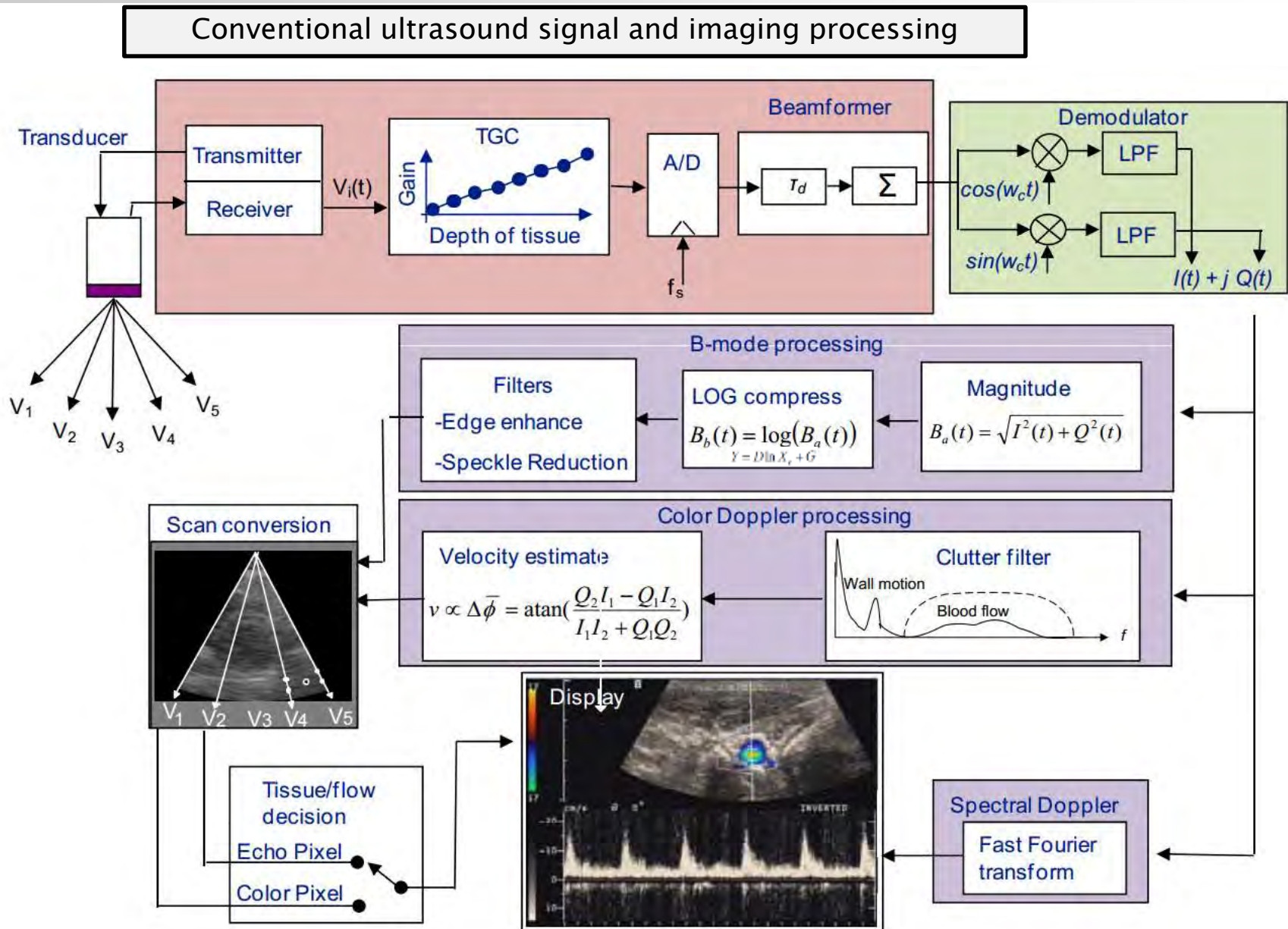


Ultrasound Imager-Instrumentation (TI)

RF-Front and Electronics

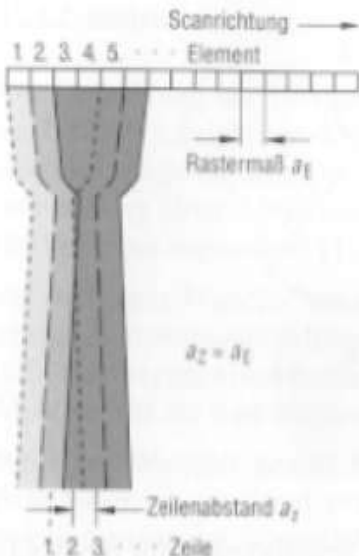


Ultrasound B-Mode imaging

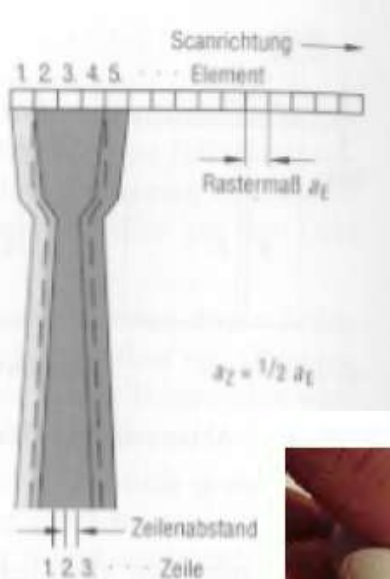


Beamformer: Linear Scan

Prinzip Linear Scan (2D-Bild)



a) Prinzip des Linearscans (Zeilenabstand a_z ist der Elementabstand bzw. das Rastermaß a_L)



b) Prinzip der Gruppenforts mit Verdopplung der Zeil

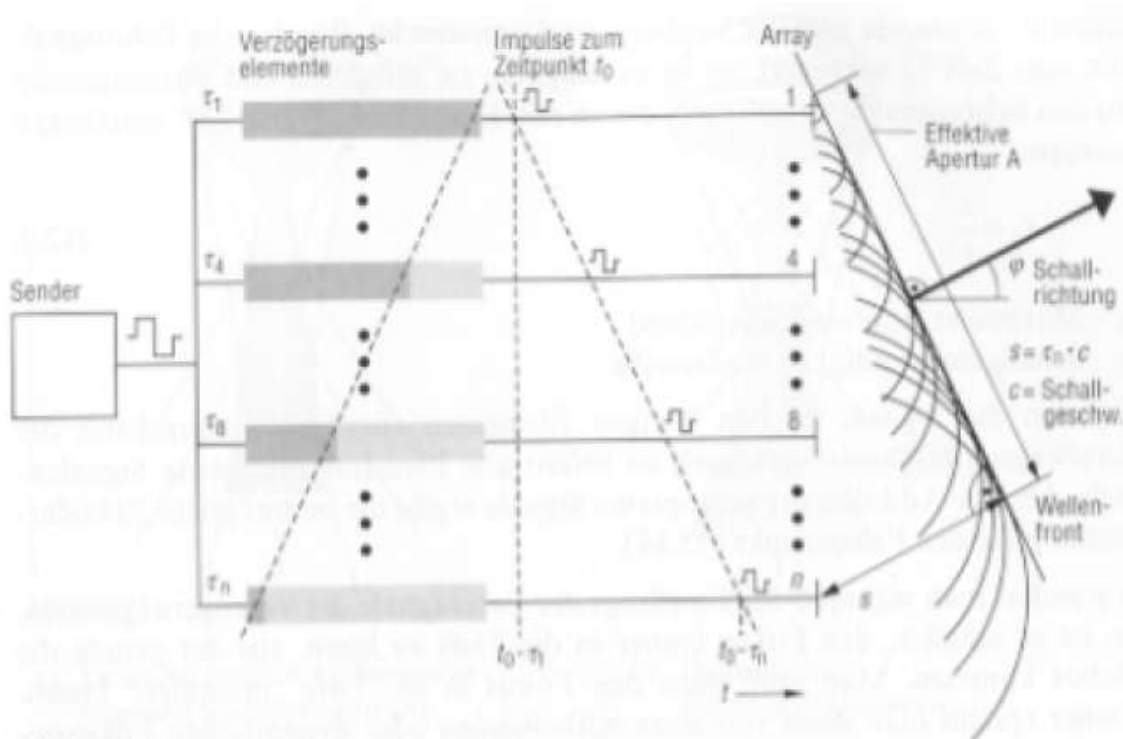


Left: Linear array transducer.

Right: Phased array transducer

Beamformer: Phased array

Beamformer durch Phased Array



Bild

Phased-Array: Erzeugung einer elektronisch schwenkbaren Wellenfront.
 Die Steuerung des Scanwinkels geschieht durch zeitversetzte Anregung (τ_1 bis τ_n) der Elemente des Arrays (Sendefall)

Typische Werte für ein Phased-Array

Maximaler Schwenkwinkel	40 bis 45°
Apertur (Arraylänge)	14 bis 28 mm
Elementzahl	48 bis 128
Frequenz	2,5 bis 7 MHz

Schwenkwinkel φ der Wellenfront

$$\varphi = \arcsin \frac{(\tau_1 - \tau_n) \cdot c}{A}$$

effektive Apertur A'

$$A' = A \cdot \cos \varphi.$$

Beamformer: Phase control transmitter

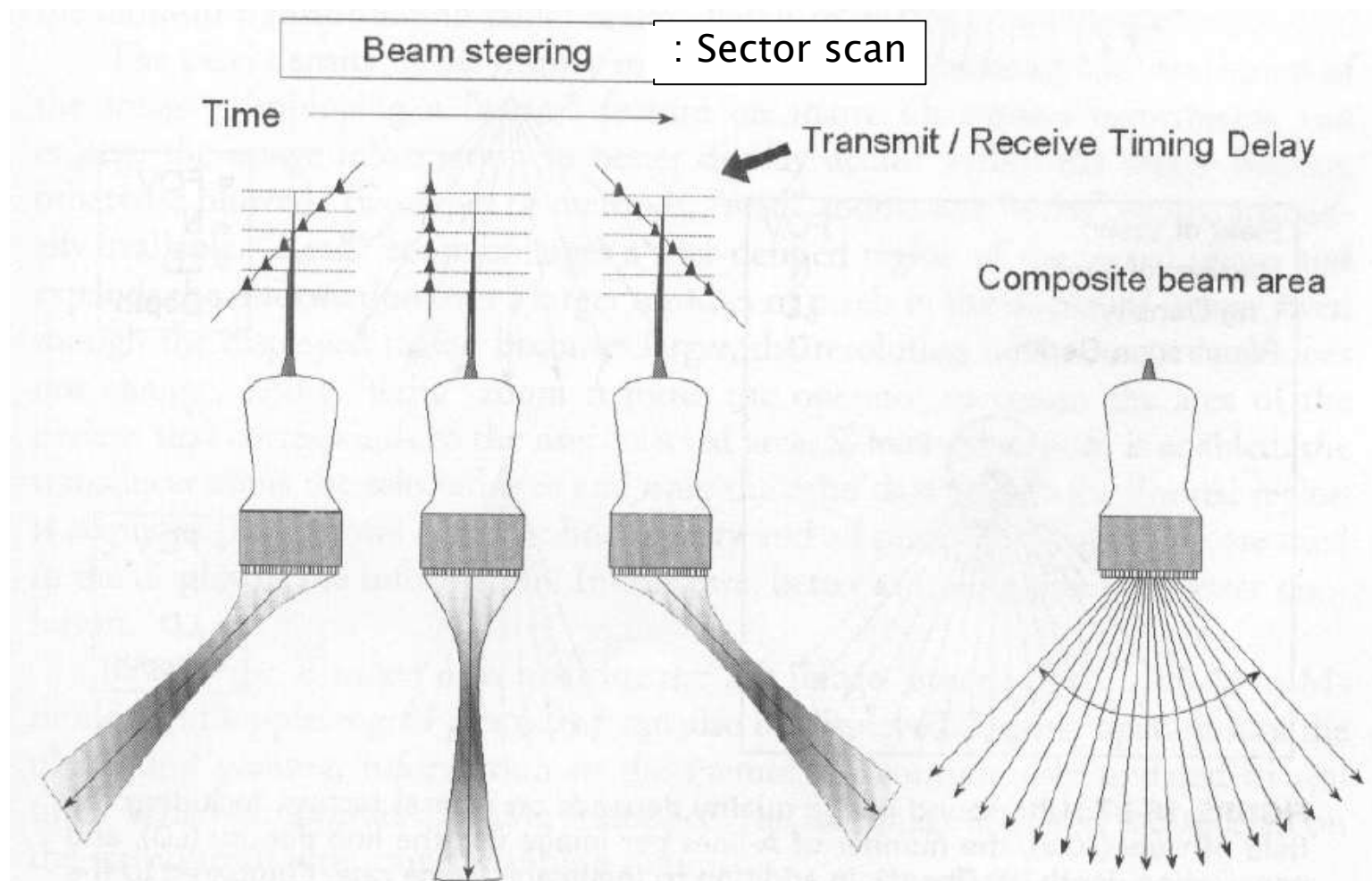
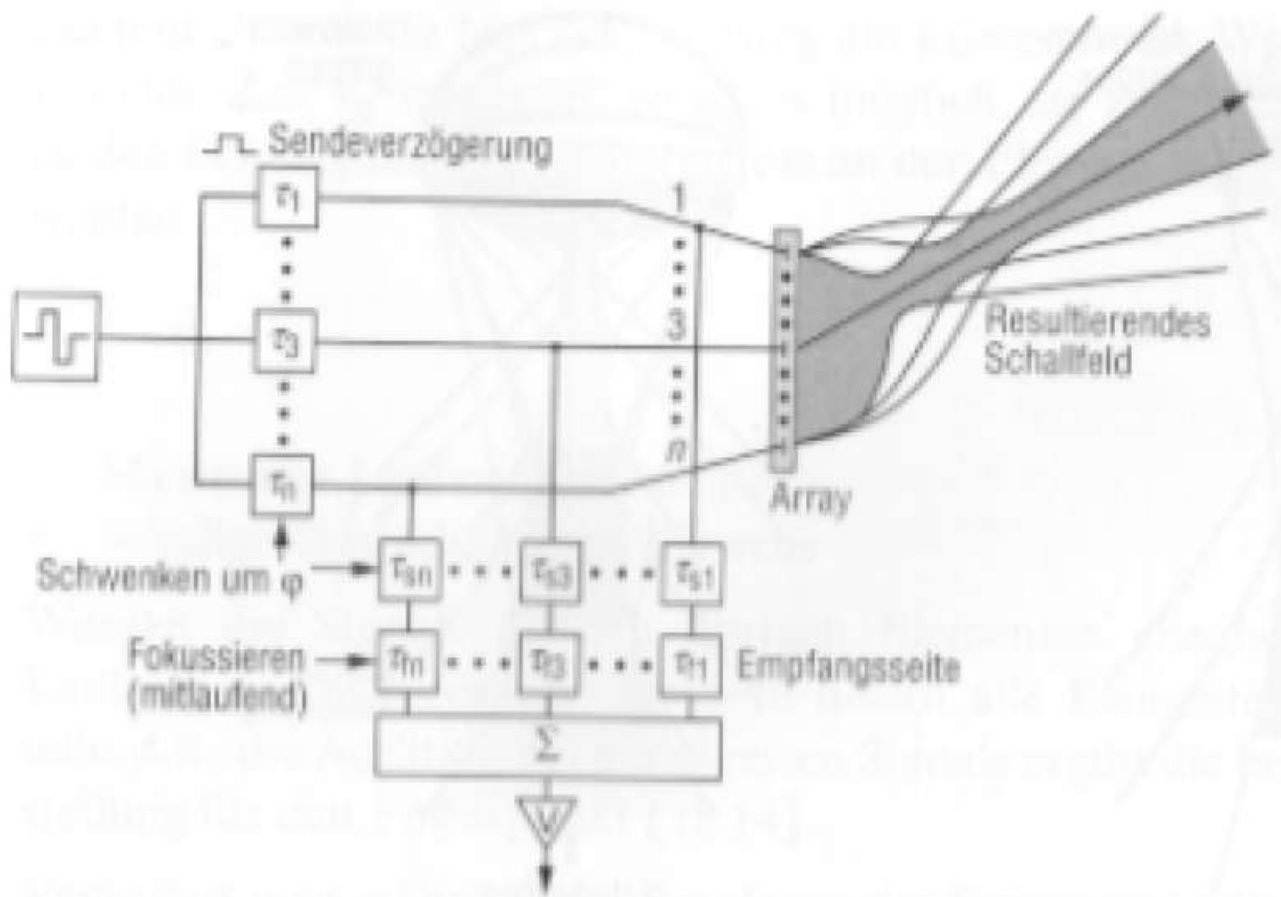


FIGURE The beam former electronically steers the ultrasound beam by introducing phase delays during the transmit and receive timing of the phased-array transducer. Lateral focusing also occurs along the beam direction. A sector format composite image is produced (right), with the number of A-lines dependent on several imaging factors discussed in the text.

Beamformer : Phase control Receiver

Elektronisch schwenkbarer Schallstrahl durch Zeitverzögerungen

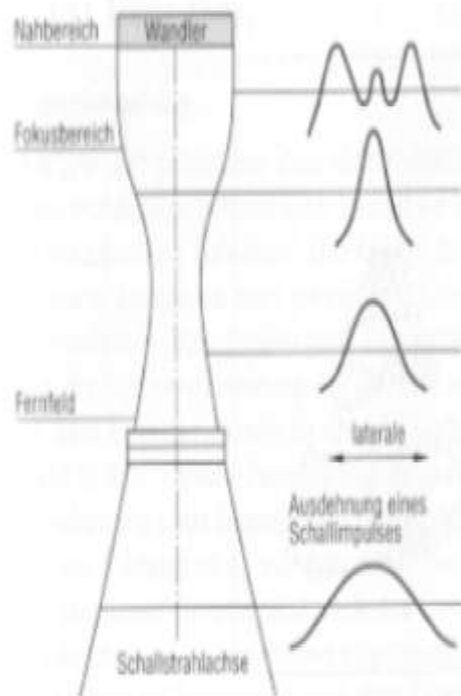


Bild

Phased-Array mit dynamischer Empfangsfokussierung

Beamformer : A-Scan

A-Scan und Auflösung und TGC



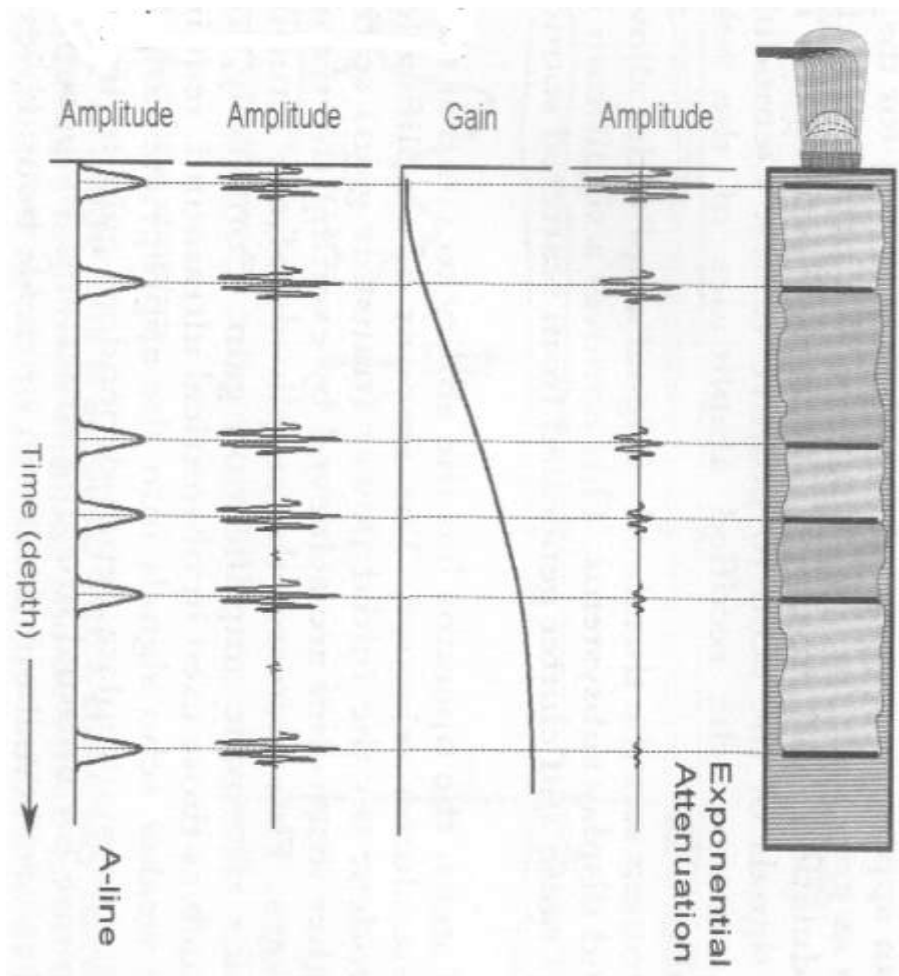
a) Schallfeld



b) Laterale Querschnitte
durch das Schallfeld

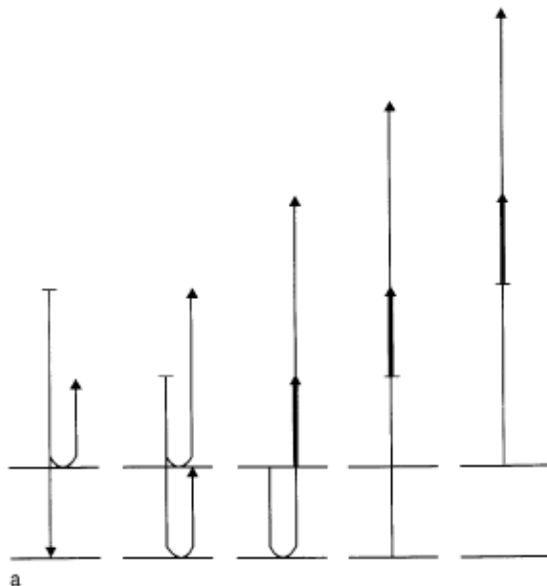
Bild Schallfeld eines Ultraschallwandlers

c) Intensität
auf Mittellinie



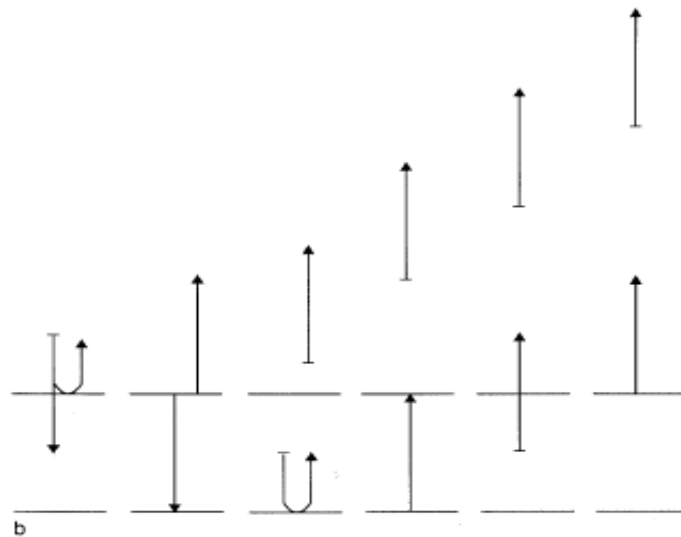
Beamformer : Axiale Auflösung

A-Scan und axiale Auflösung infolge Puls-Länge



a

Figure ... Axial resolution. (a) The separation of the reflectors is less than half the spatial pulse length, so that echo overlap occurs. Separate echoes are not produced. The reflectors are not resolved on the display.



b

Figure ... *Continued.* (b) The reflector separation is increased so that it is greater than half the spatial pulse length. Therefore, echo overlap does not occur. Separate echoes are produced and the reflectors are resolved on the display.

$$\text{axial resolution (mm)} = \frac{\text{spatial pulse length (mm)}}{2} \quad R_A = \frac{SPL}{2}$$

spatial pulse length ↑ axial resolution ↑ (worsened)

cycles per pulse ↑ axial resolution ↑ (worsened)

frequency ↑ axial resolution ↓ (improved)

Beamformer : Axiale Auflösung

A-Scan und axiale Auflösung infolge der Puls-Länge

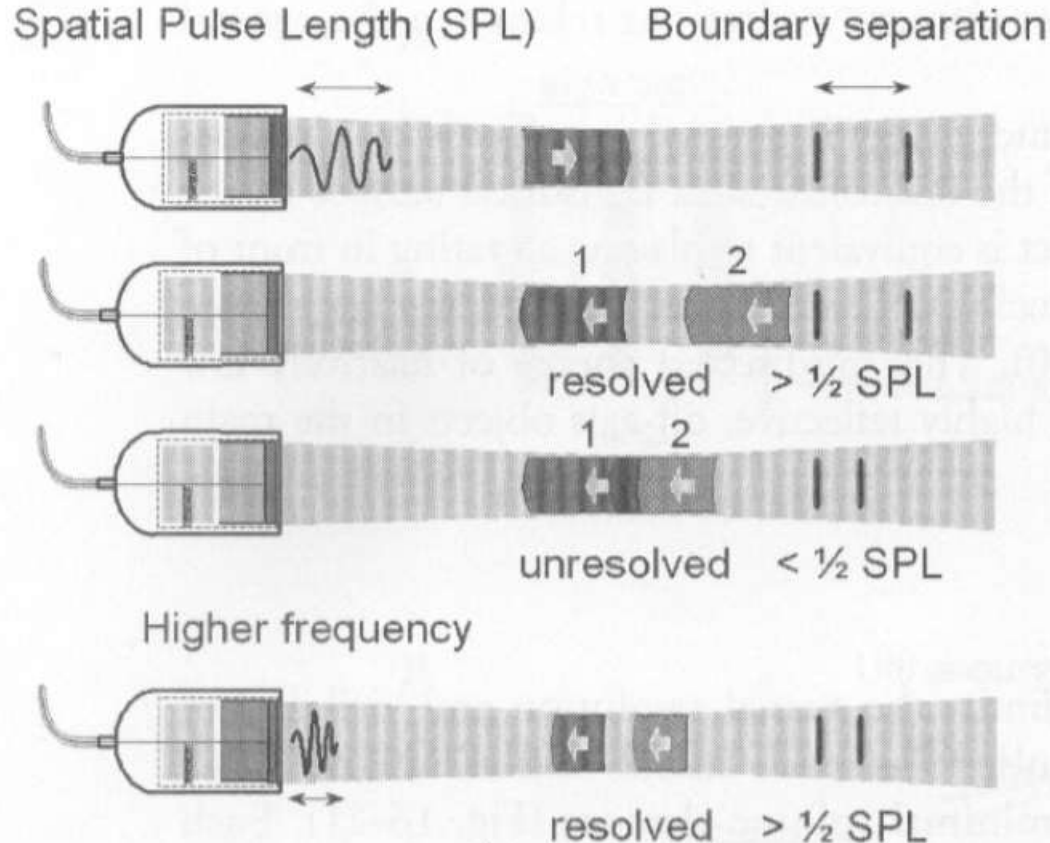


FIGURE Axial resolution is equal to $\frac{1}{2}$ spatial pulse length (SPL). Tissue boundaries that are separated by a distance greater than $\frac{1}{2}$ SPL produce echoes from the first boundary that are completely distinct from echoes reflected from the second boundary, whereas boundaries with less than $\frac{1}{2}$ SPL result in overlap of the returning echoes. Higher frequencies reduce the SPL and thus improve the axial resolution (**bottom**).

Beamformer : Laterale Auflösung

A-Scan und laterale Auflösung mittels dynamischer Fokusierung

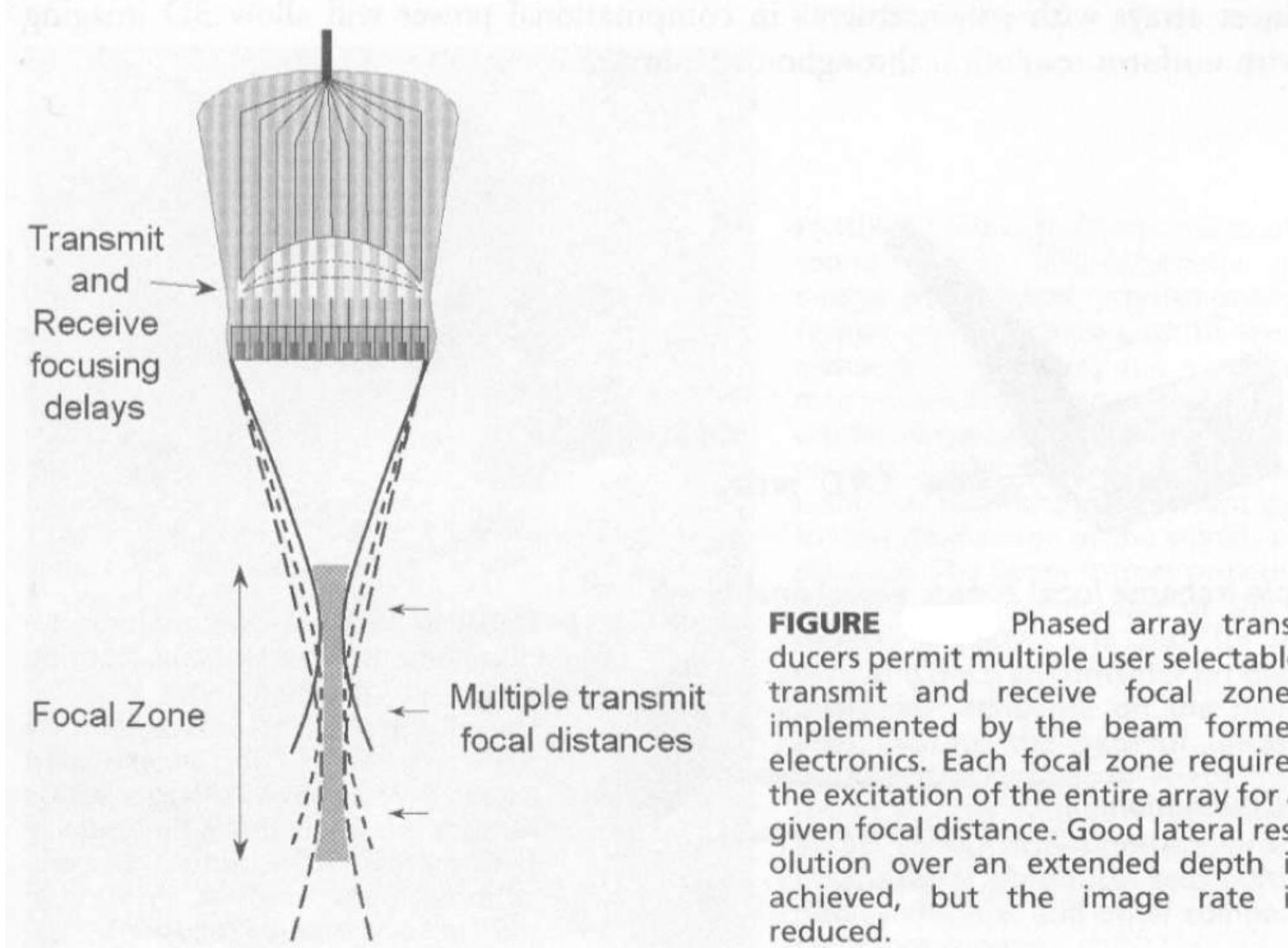
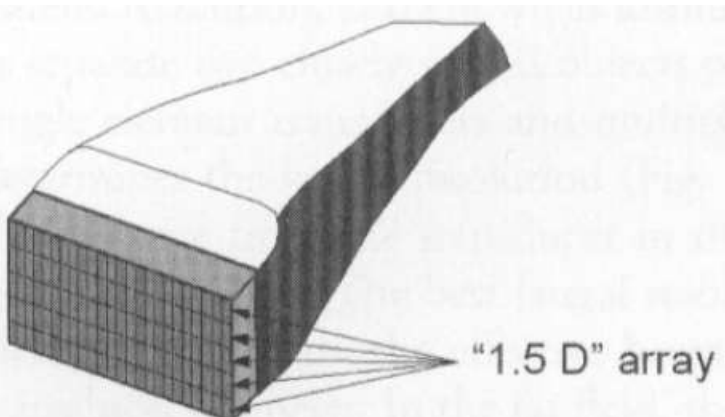


FIGURE Phased array transducers permit multiple user selectable transmit and receive focal zones implemented by the beam former electronics. Each focal zone requires the excitation of the entire array for a given focal distance. Good lateral resolution over an extended depth is achieved, but the image rate is reduced.

Beamformer : Laterale Auflösung

A-Scan und Schicht-Auflösung infolge 1.5D-Mode



Multiple transmit focal zones: elevational plane

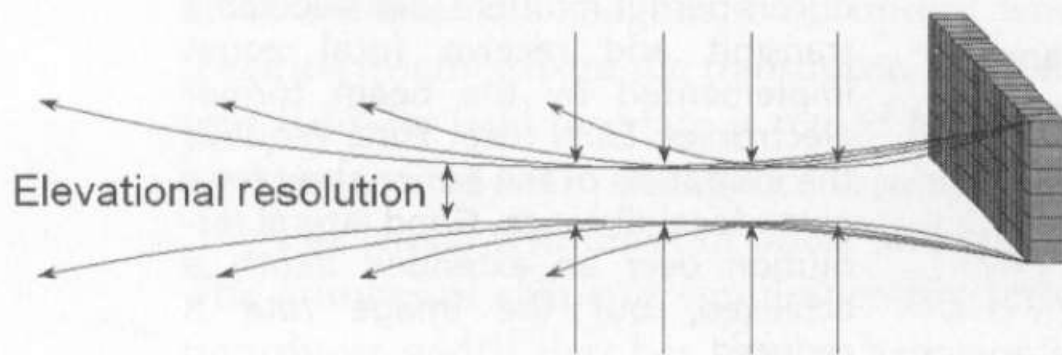
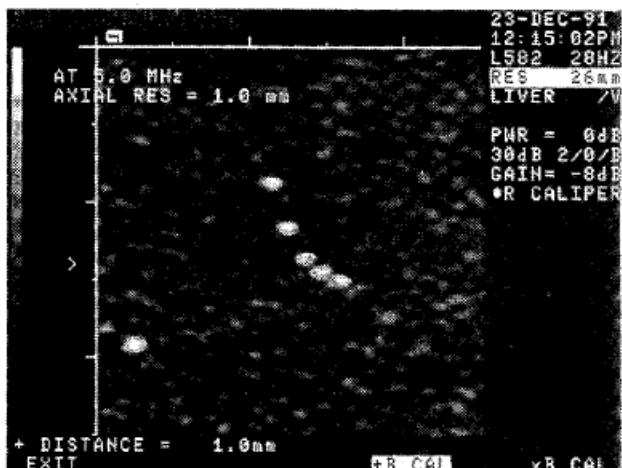


FIGURE E elevational resolution with multiple transmit focusing zones is achieved with "1.5-D" transducer arrays to reduce the slice thickness profile over an extended depth. Five to seven discrete arrays replace the single array. Phase delay timing provides focusing in the elevational plane (similar to lateral transmit and receive focusing).

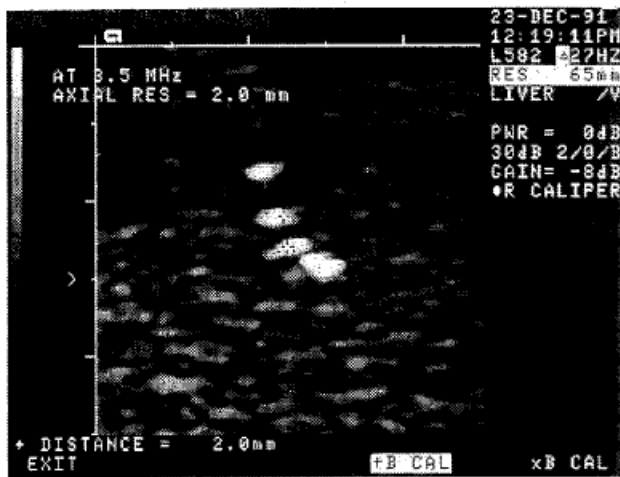
Ultraschall-Bildverfahren: Phantom Beispiel

Auflösung infolge Frequenz am Phantom

Figure Axial resolution improves as frequency increases: 3.5 MHz, with a resolution of 2.0 mm (*a*); 5.0 MHz, with a resolution of 1.0 mm (*b*); 7.0 MHz, with a resolution of 0.5 mm (*c*). Detail resolution is like a golf score (*d*); that is, smaller is better.



b



a



c

Ultraschall-Bildverfahren: M-Mode

Echoe-Display-Mode: Fast Single A-Scan Mode

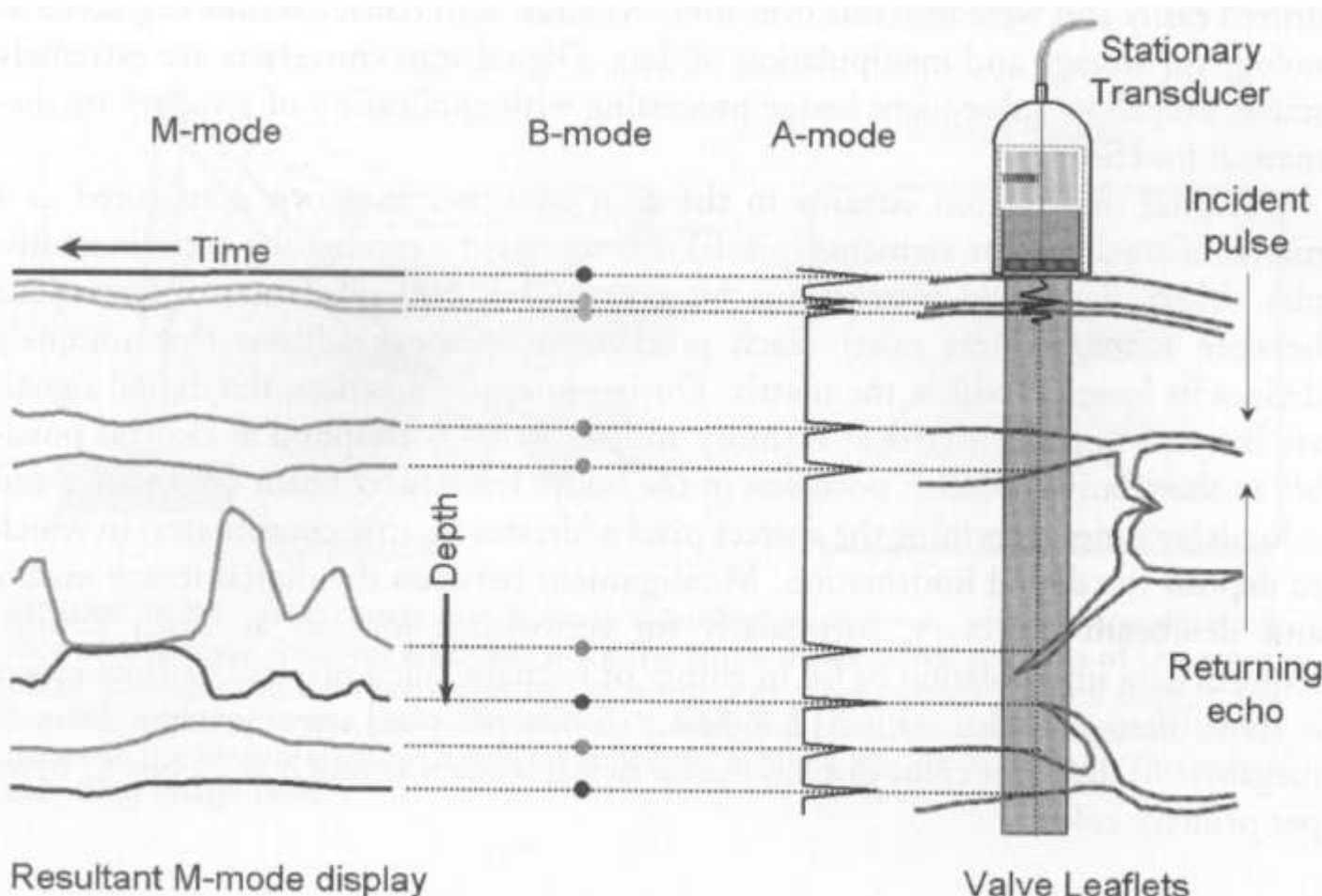
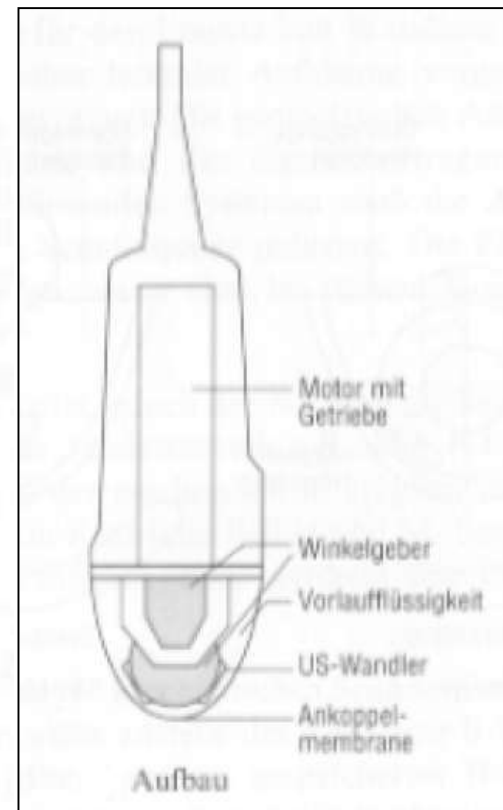
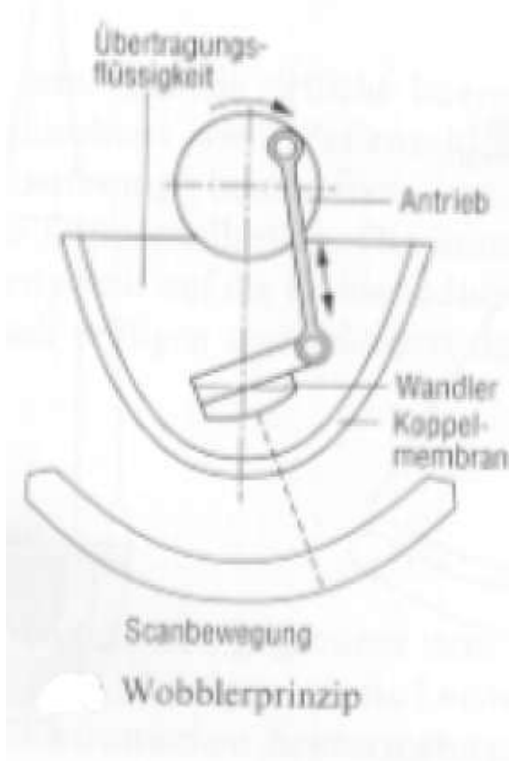
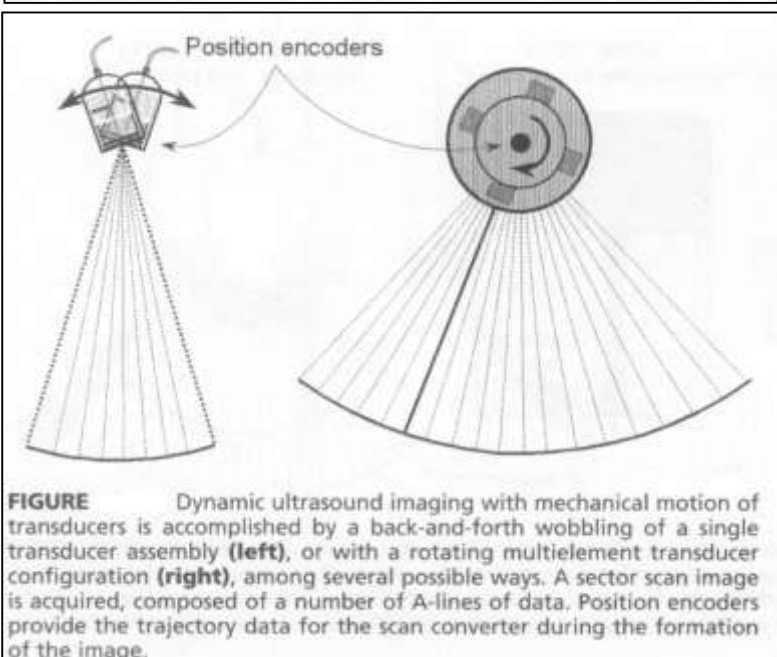
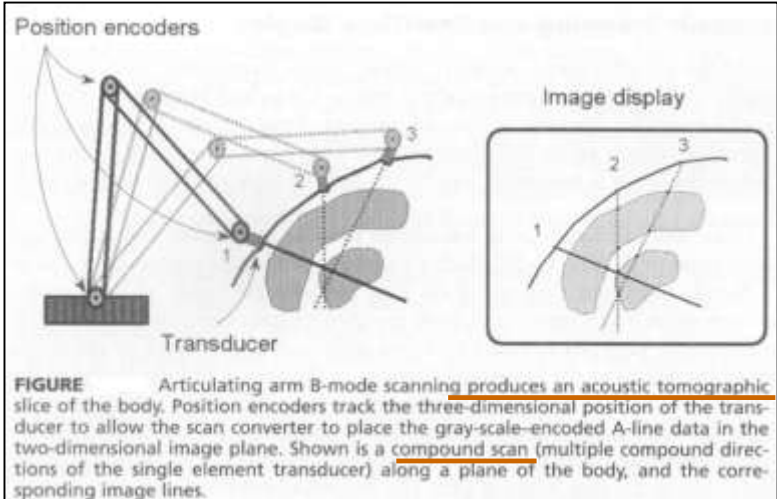


FIGURE M-mode data is acquired with a stationary transducer or transducer array. The A-mode data are brightness encoded and deflected across the horizontal direction to produce M-mode curves. M-mode display of valve leaflets is depicted.

Ultraschall-Bildverfahren: Mechanische Methoden

Historisch



Ultraschall-Bildverfahren: Elektronischer Scan

2D-Electronic Scanning → Frame Rate

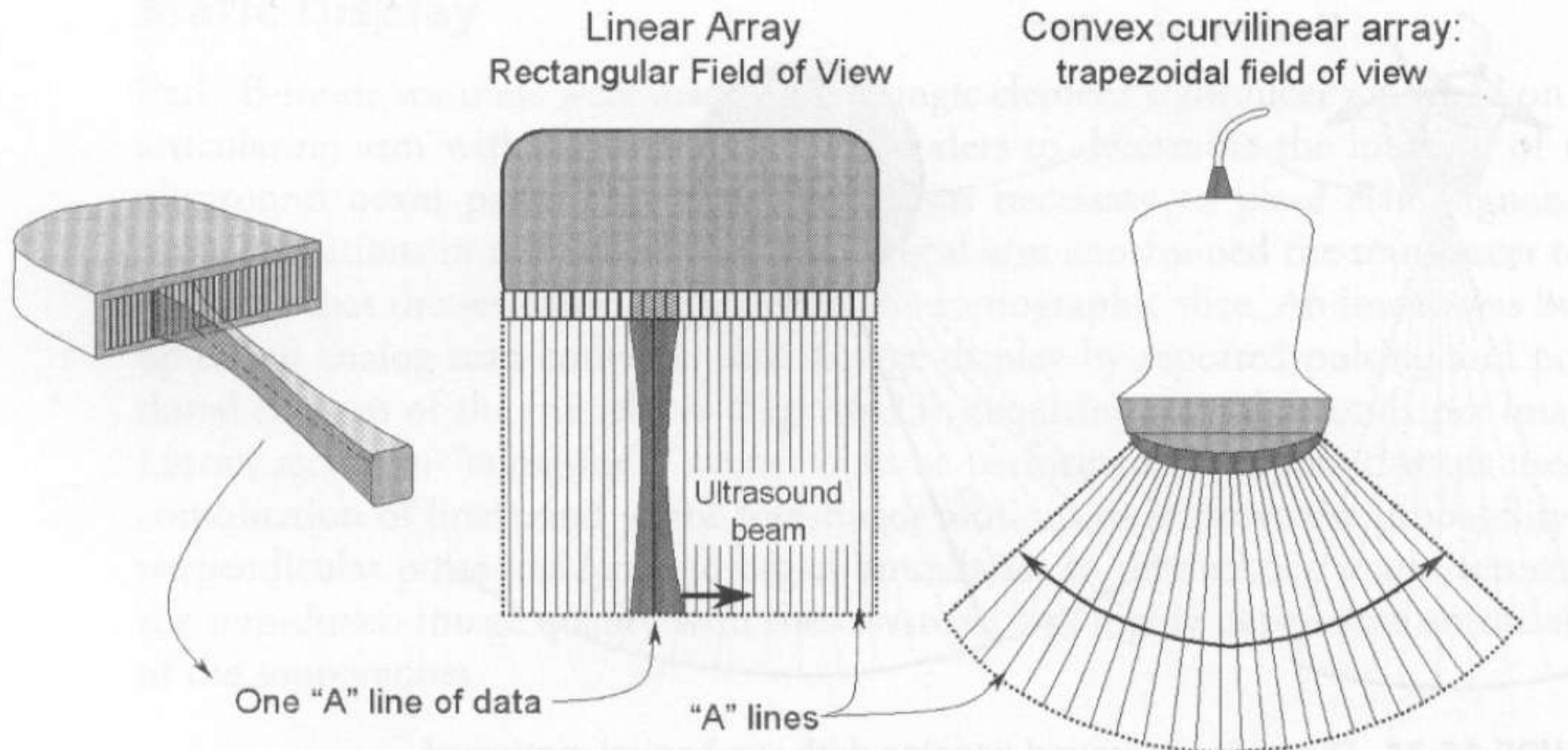
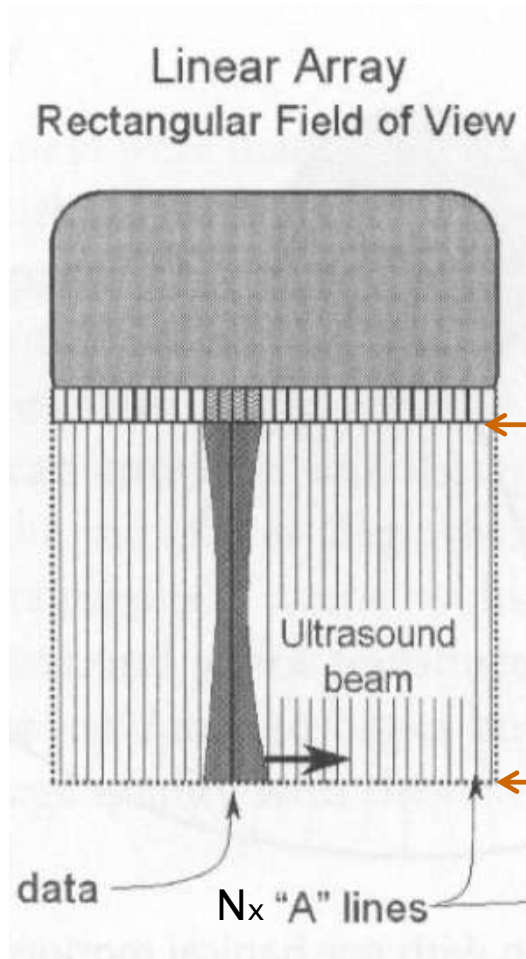


FIGURE The linear and curvilinear array transducers produce an image by activating a subgroup of the transducer elements that form one A-line of data in the scanned object, and shifting the active elements by one to acquire the next line of data. Linear arrays produce rectangular image formats; curvilinear arrays produce a trapezoidal format with a wide field of view.

Ultraschall-Bildverfahren: Elektronischer Scan

Frame Rate



$$\text{Frame rate} = \frac{1}{T_{frame}} = \frac{1}{N \cdot 15\mu\text{sec} \cdot D(\text{cm})}$$

Ultraschall-Bildverfahren: Bildrate

Sector- B-Mode-Bilder und Bildrate

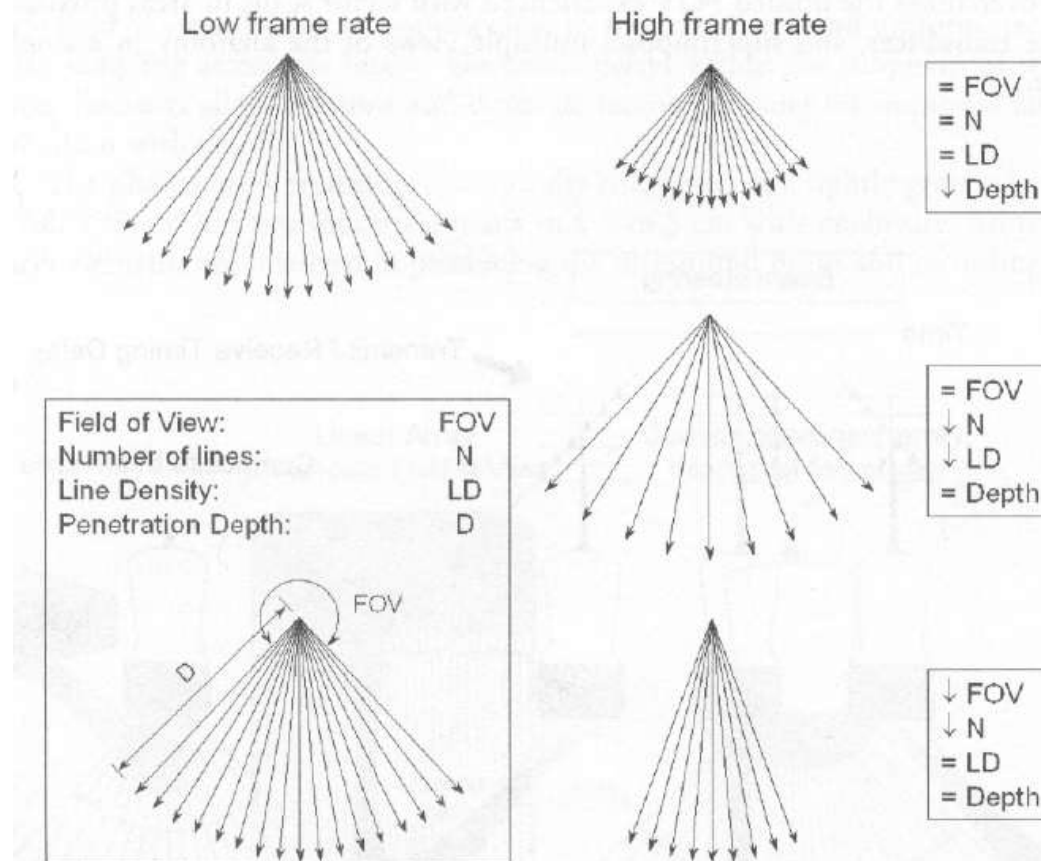
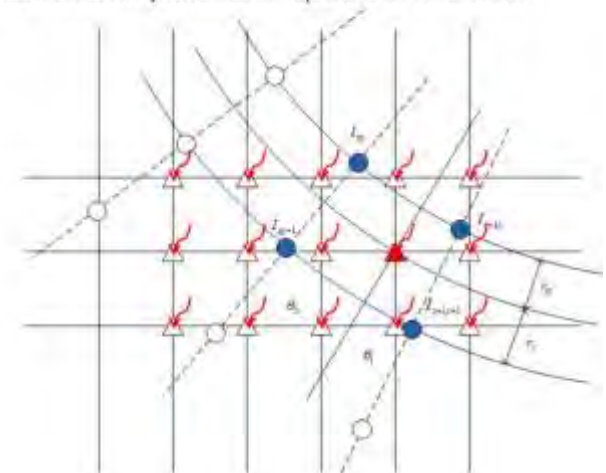
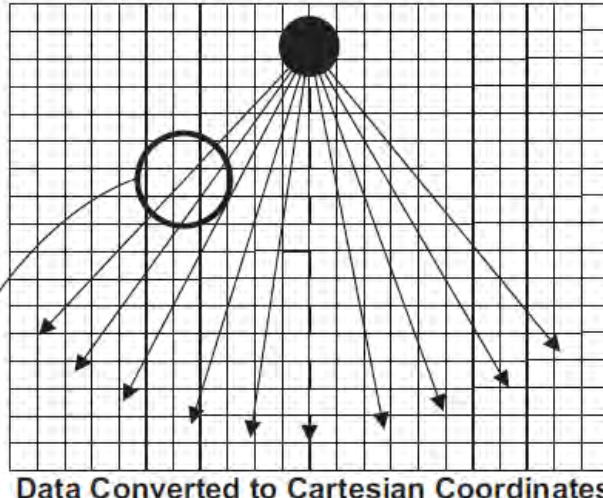
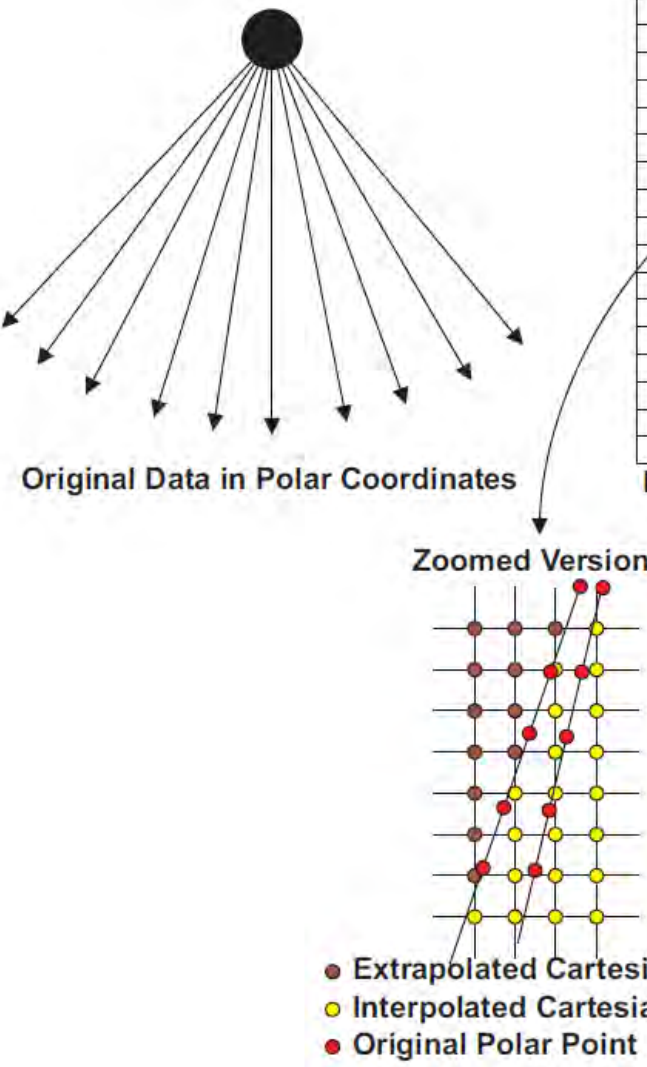


FIGURE Ultrasound image quality depends on several factors, including the field of view (FOV), the number of A-lines per image (N), the line density (LD), and penetration depth (D) (**inset**), in addition to the image frame rate. Compared to the low frame rate acquisition parameters with excellent factors (*upper left diagram*), a high frame rate (to improve temporal resolution) involves tradeoffs. To maintain a constant FOV, number of A-lines, and line density, penetration depth must be sacrificed (*upper right*). To maintain penetration depth and FOV, the number of A-lines and line density must be decreased (*middle right*). To maintain line density and penetration depth, the FOV and number of A-lines must be decreased (*bottom right*).

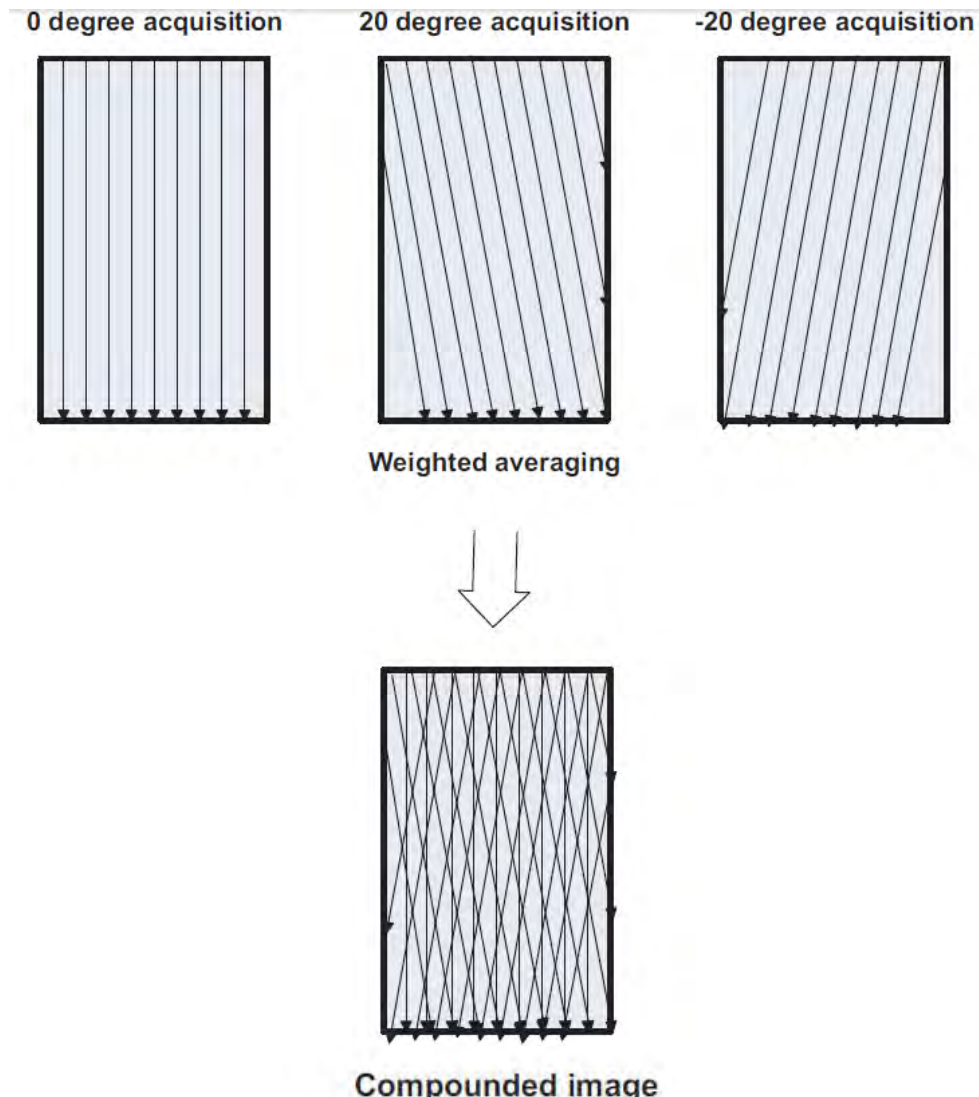
Ultraschall-Bildverfahren: Scan Converter

B-Mode-Scan-converter: Polar to Cartesian



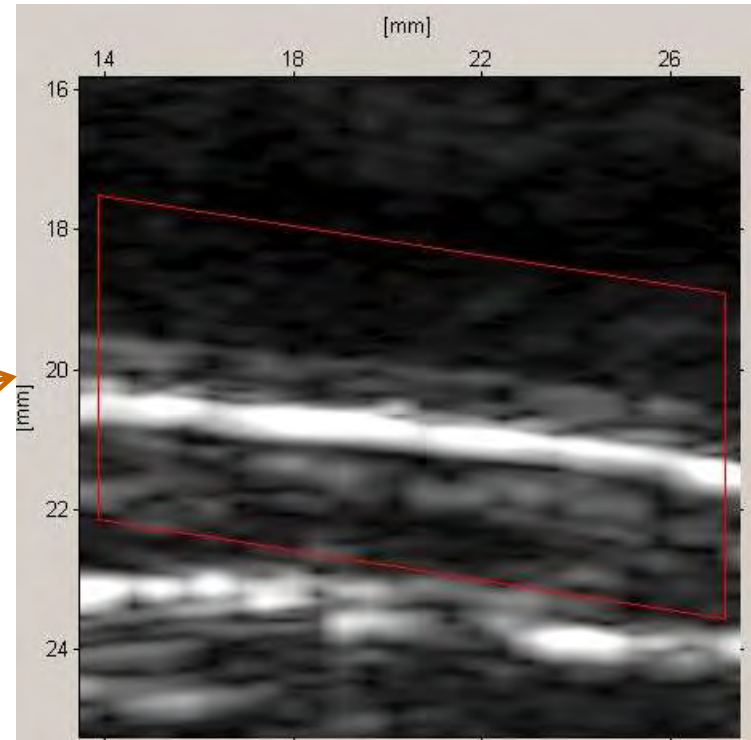
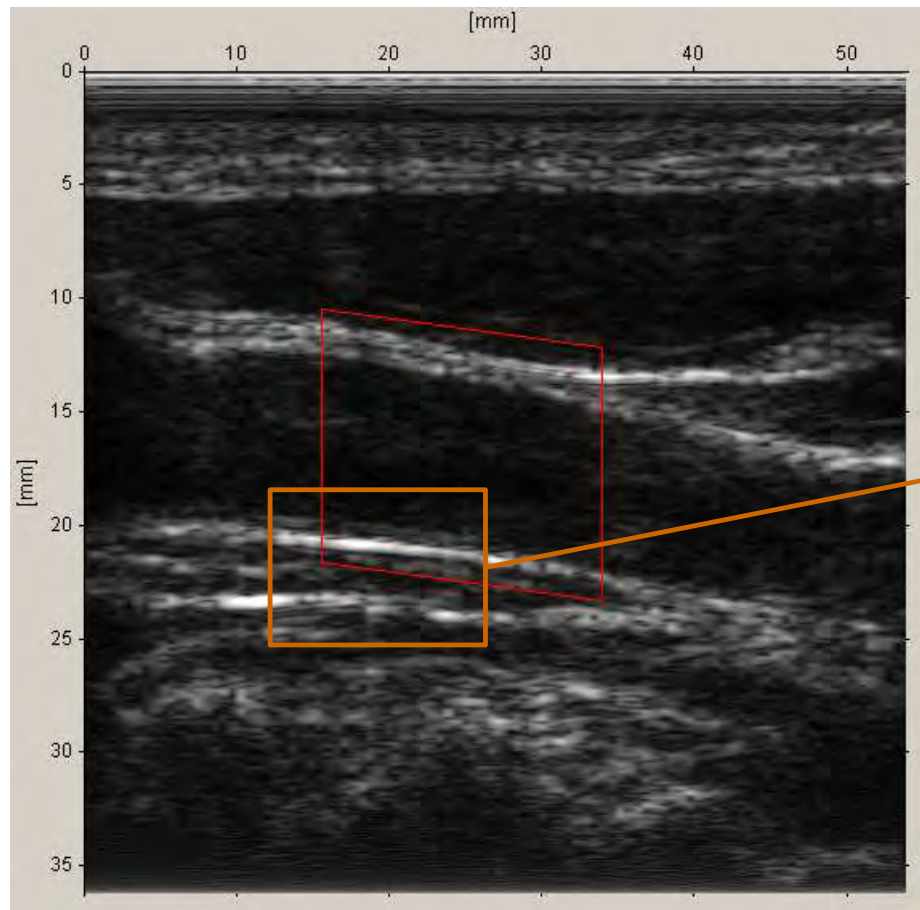
Ultrasound Tomography

Spatial Compound imaging by reducing frame rate (Ultrasound Tomography)



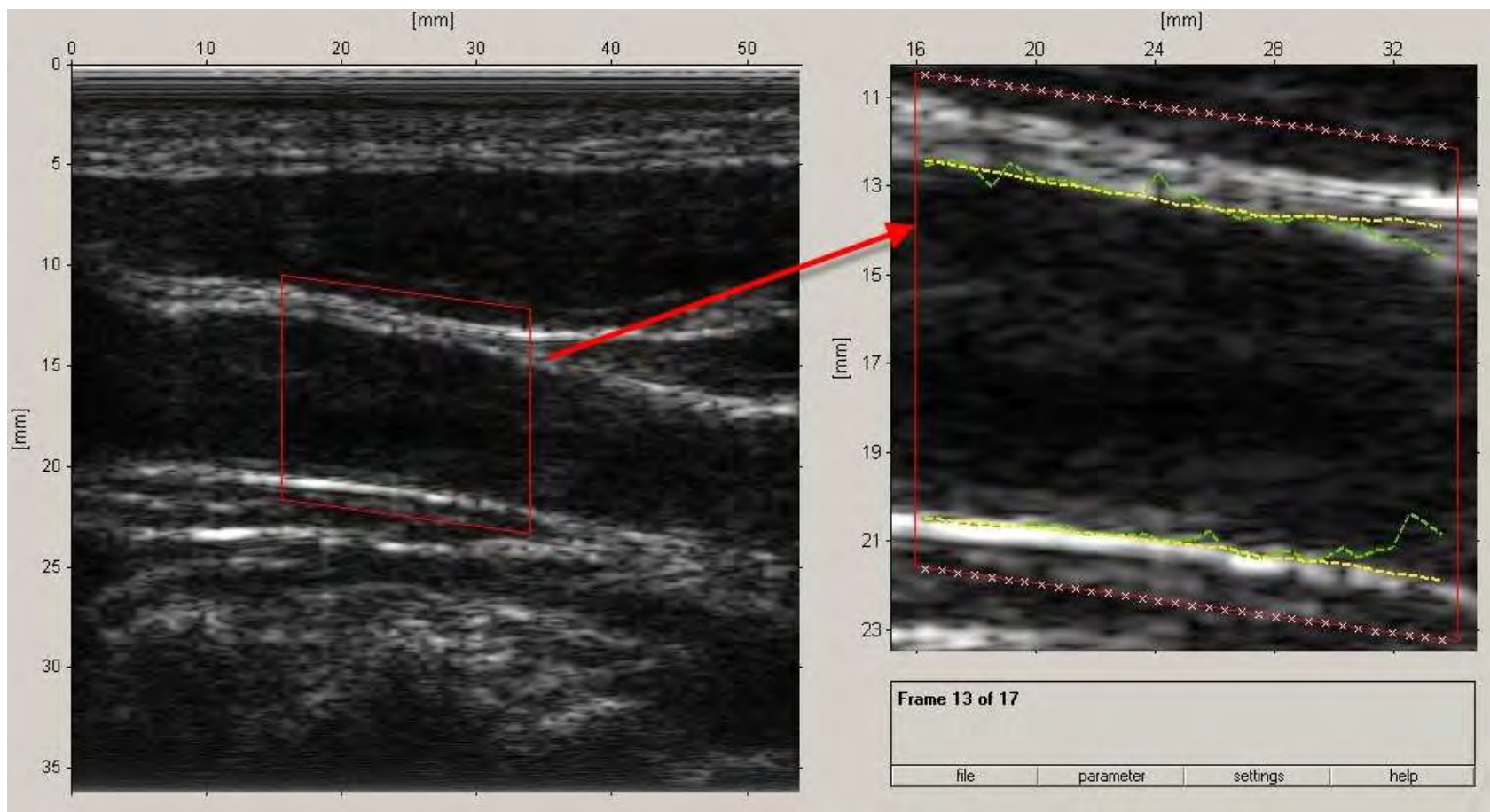
Ultraschall-Linear-Scan: Carotis Verkalkung

B-Mode: Intima – Dicke → Verkalkung / Elastizität der Wände



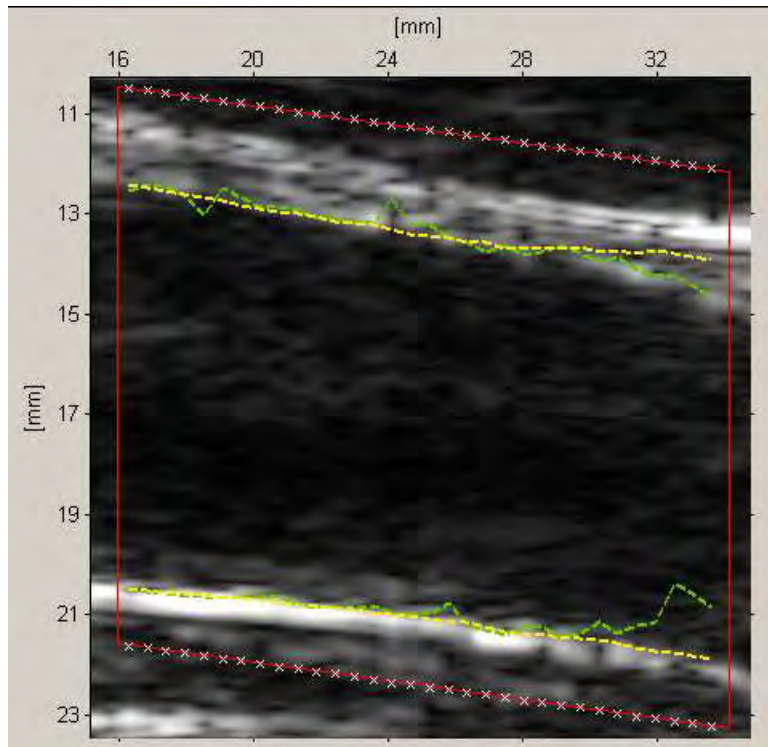
Ultraschall-Bildverfahren: Region of Interest

B-Mode: ROI

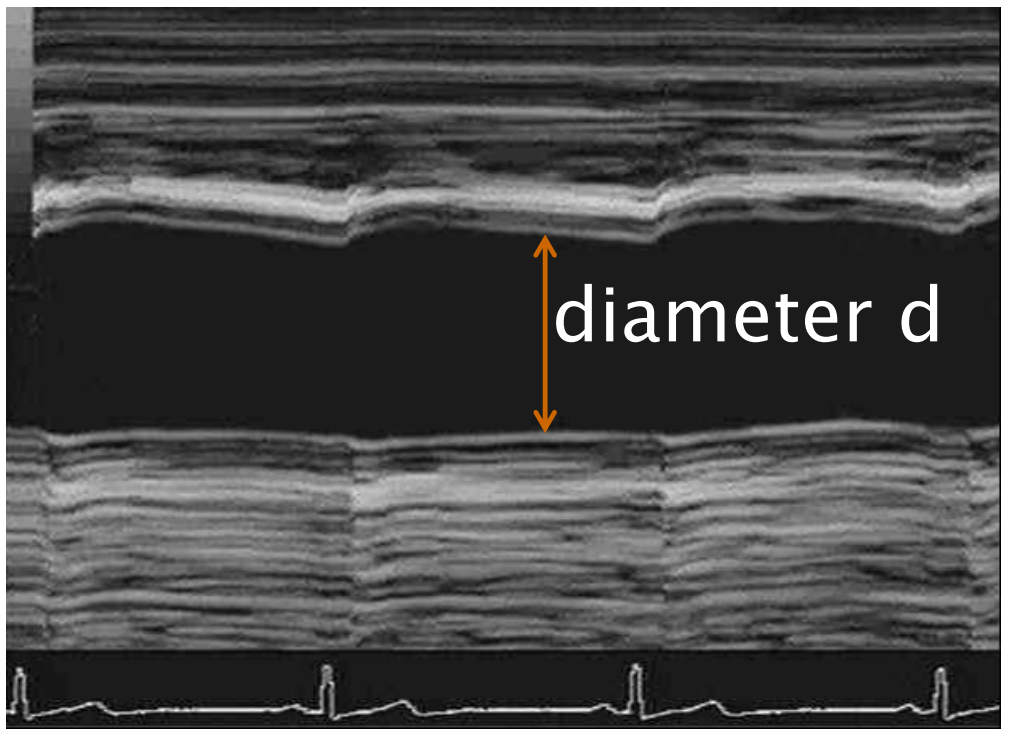


Ultraschall-Bildverfahren: Carotis Elastizität

ROI-B-Mode → M-Mode



M-Mode



Real-time Diameter Variation

Ultraschall-Bildverfahren: PV-Diagramme

M-Mode: Vessel Elasticity

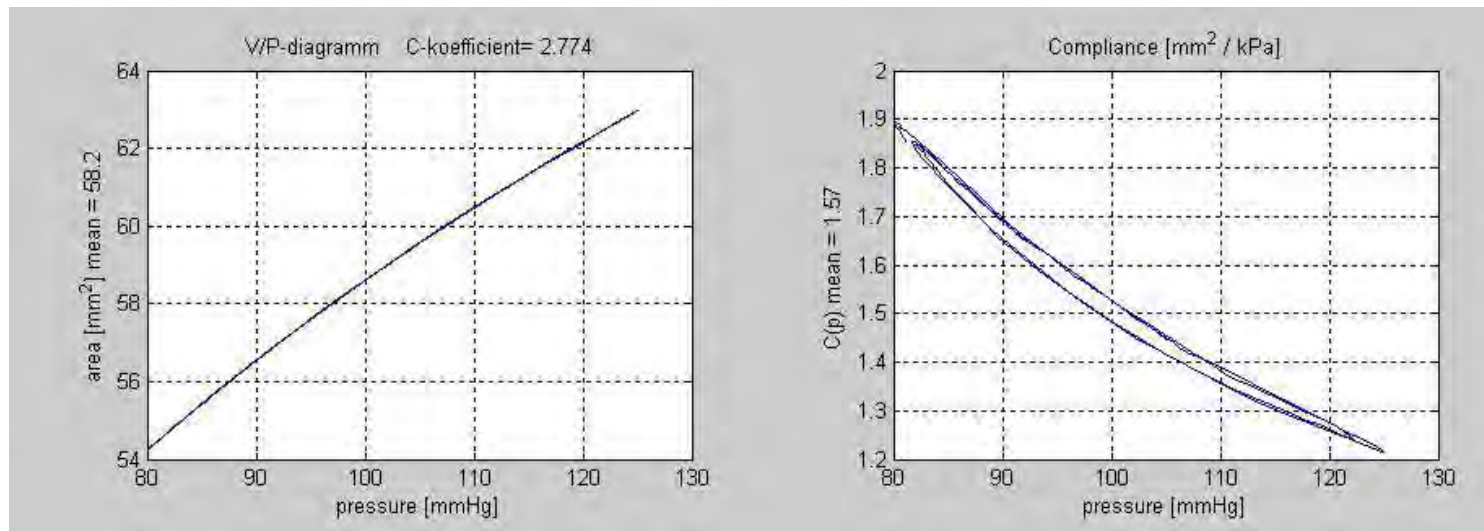
$$p\{t\} = p_0 e^{\gamma A\{t\}} \quad ; \quad A\{t\} = \pi d^2 \{t\}/4$$

$$p\{t\} = p_d e^{\alpha \left(\frac{A\{t\}}{A_d} - 1 \right)} \quad ; \quad \alpha = \frac{A_d \ln \{p_s / p_d\}}{A_s - A_d}$$

P_s : pressure systole at a. brachialis

P_D : pressure diastole at a. brachialis

$$C\{p\} = \frac{\partial A\{p\}}{\partial p} \quad ; \text{ Compliance of the vessel}$$



Ultraschall-Bildverfahren: Beispiel

B-Mode: Sector Scan Pränatal (Beamconverter)

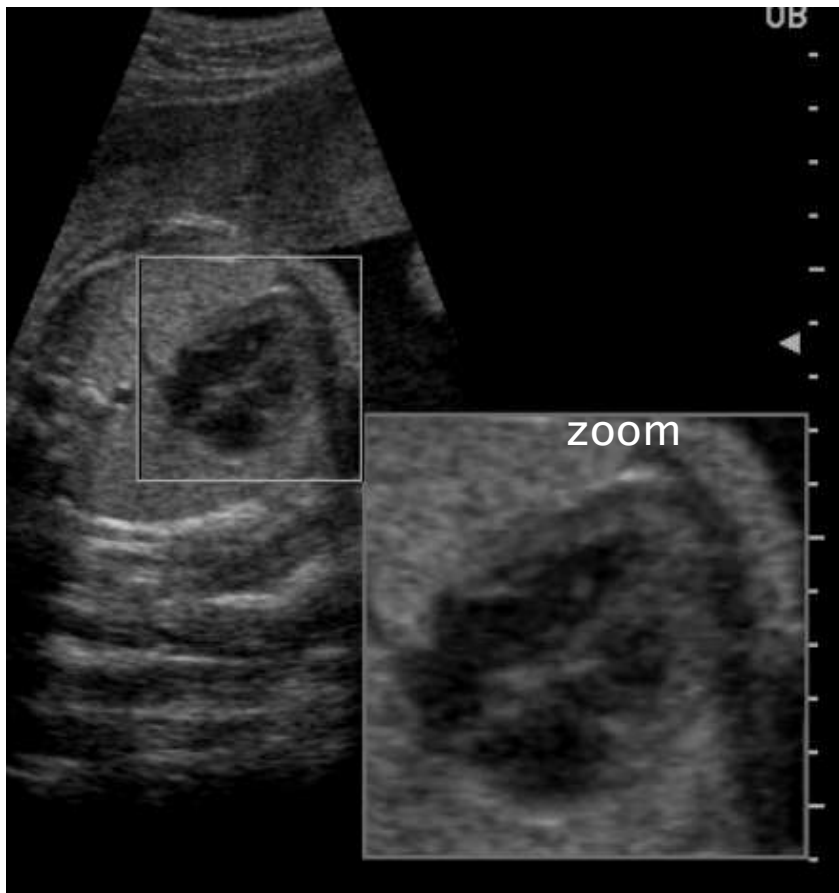


Mittels Sonographie erstellte Aufnahme eines elf Wochen alten Fetus,
die auch als Video in Real-Zeit die Bewegung erfasst

Link: <http://de.wikipedia.org/wiki/Sonografie>

Ultraschall-Bildverfahren

B-Mode: Sector Scan Pränatal (Beamconverter)

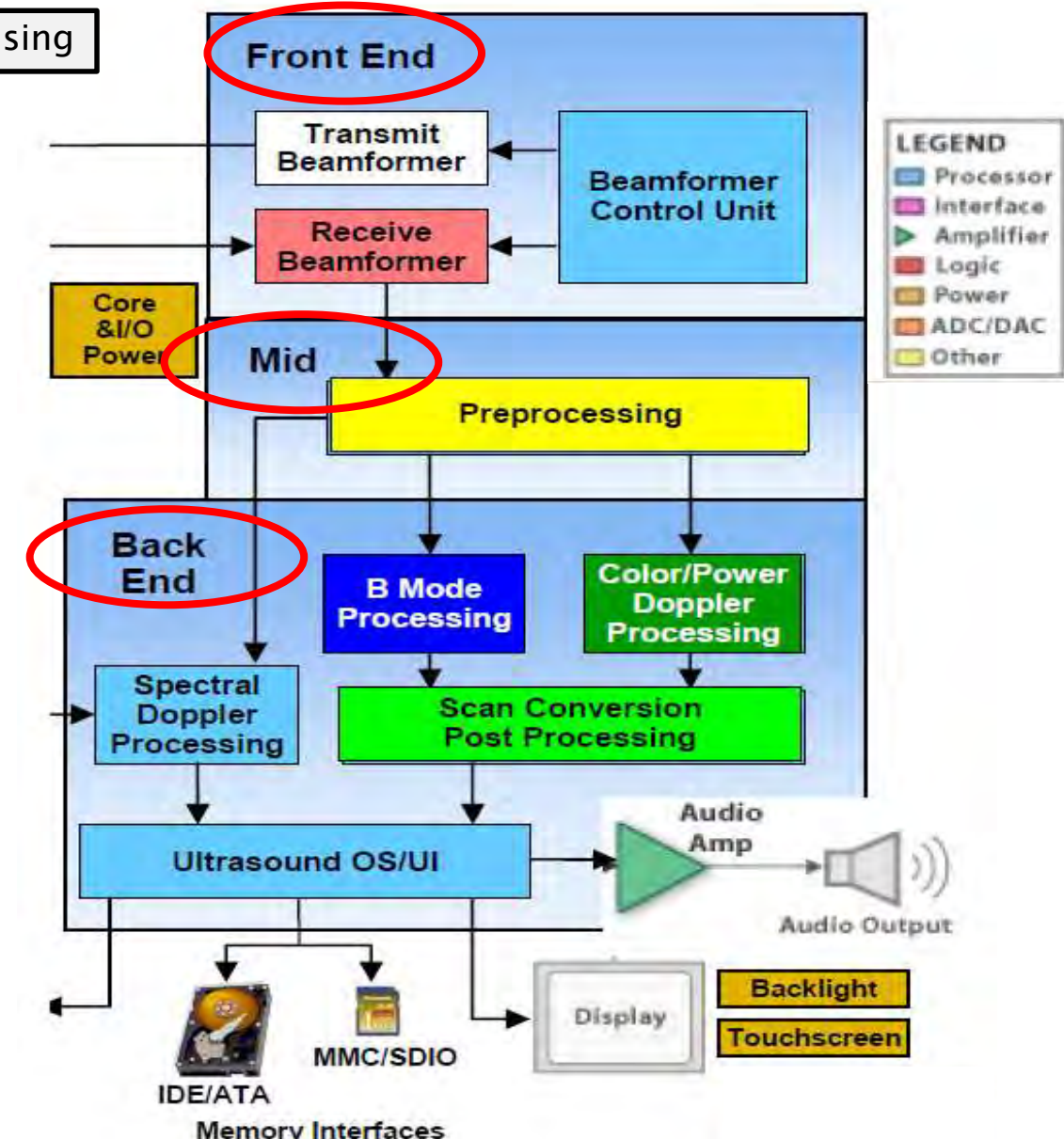


Mittels Sonographie erstellte Aufnahme eines schlagenden Herzens
(Herzkammern) beim Fetus

Ultrasound Imager-Instrumentation Techniques

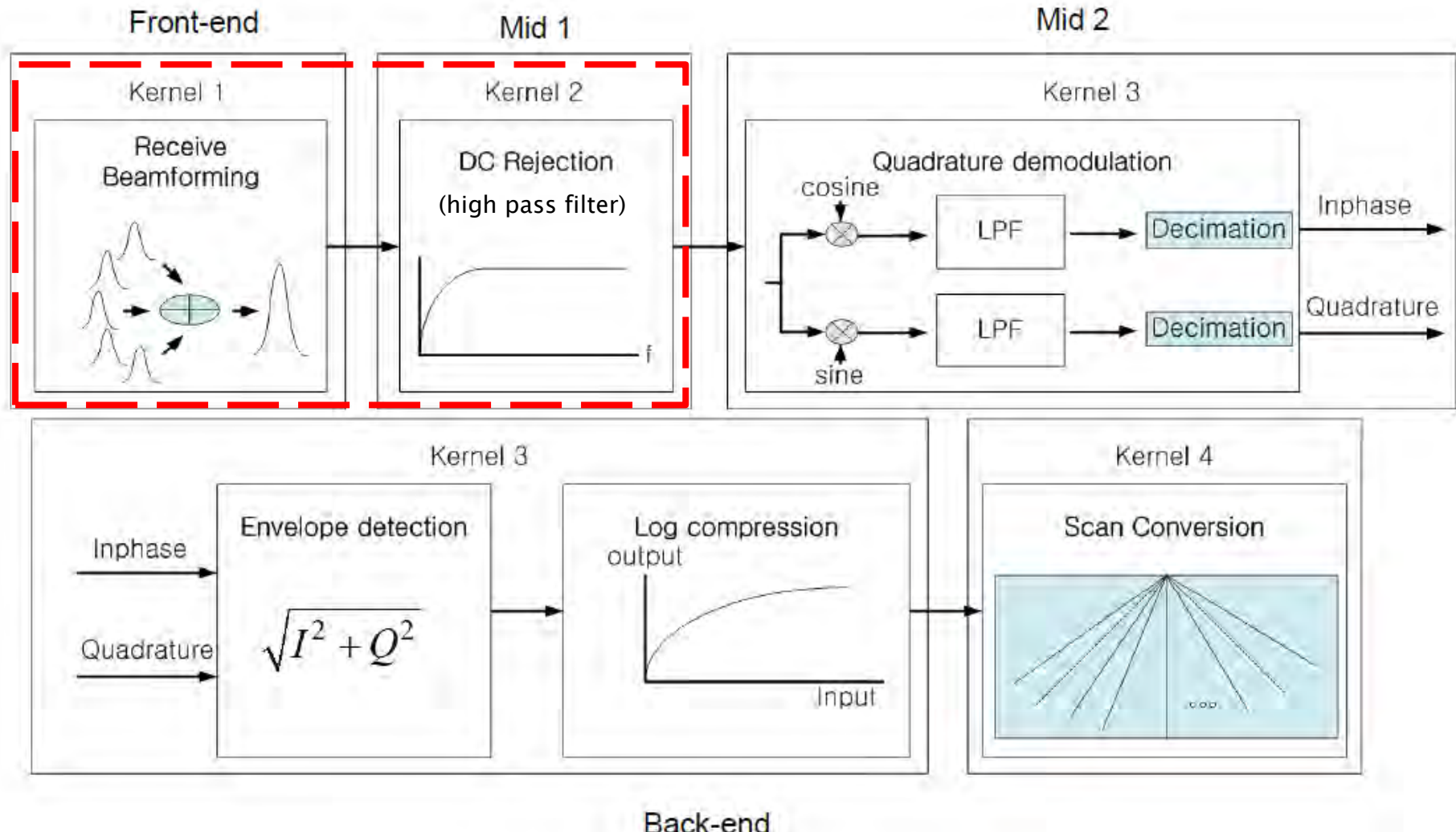
Component

Image processing
Delay and Sum (DAS) receive beam-forming
RF demodulation and decimation
B-Mode
Wall Filter for Color Flow
1D Color Flow
2D Color Flow
Power Estimator
Scan Conversion



Ultrasound Imager-processing

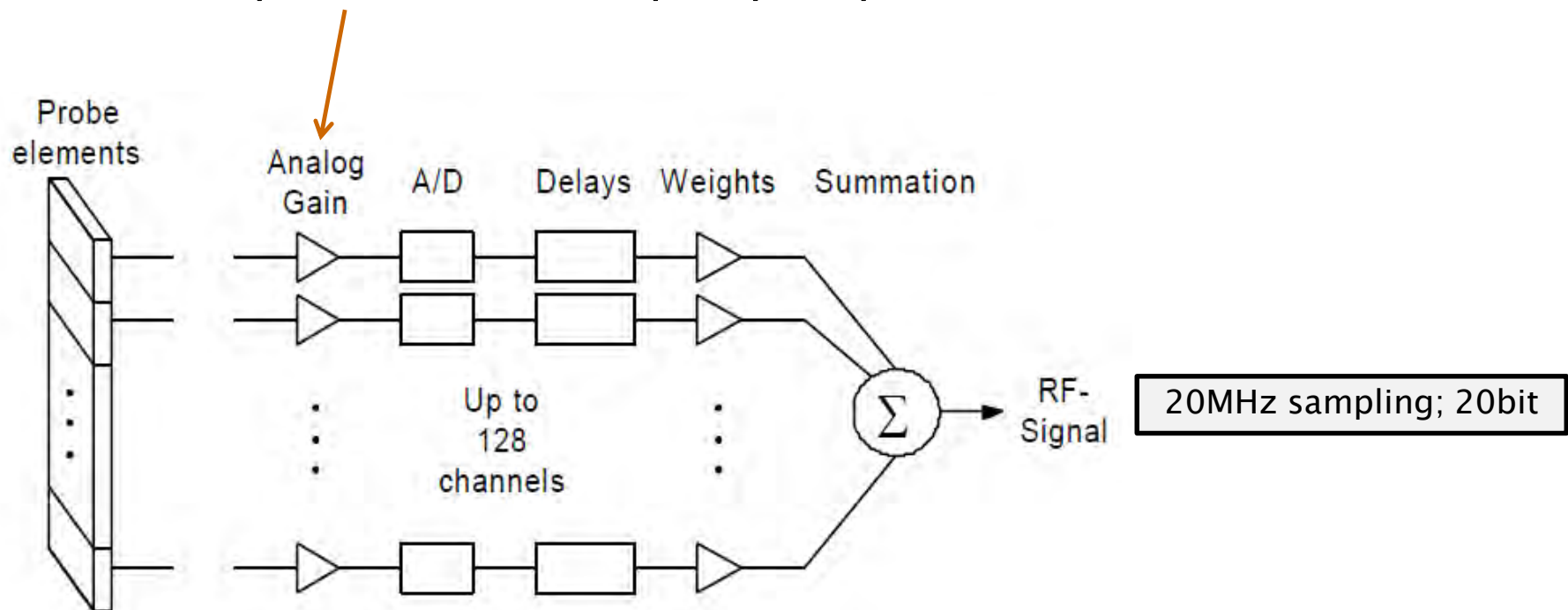
Signal processing



Ultrasound Imager-processing: Beamformer

Front-end

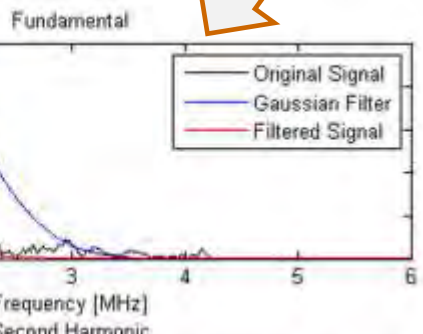
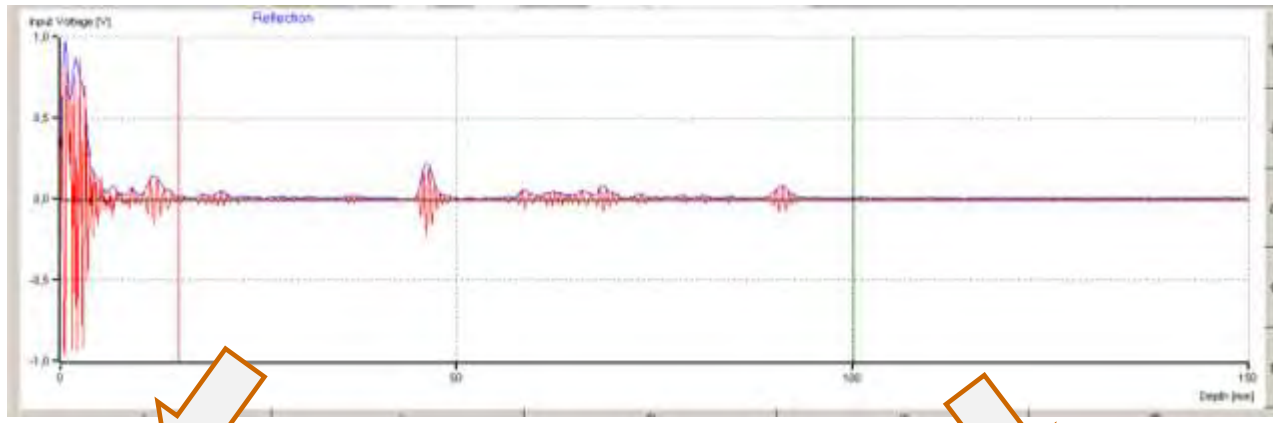
Time Gain Compensation / Time Frequency compensation (Back-end)



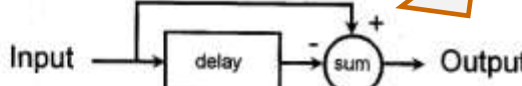
Ultrasound Imager-processing: DC-rejection

mid 1

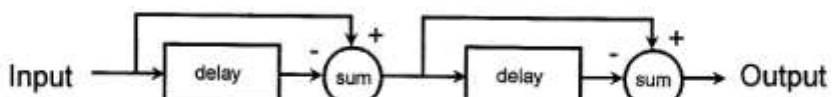
20MHz sampling; 20bit → Scan-line



(a)



(b)



(c)

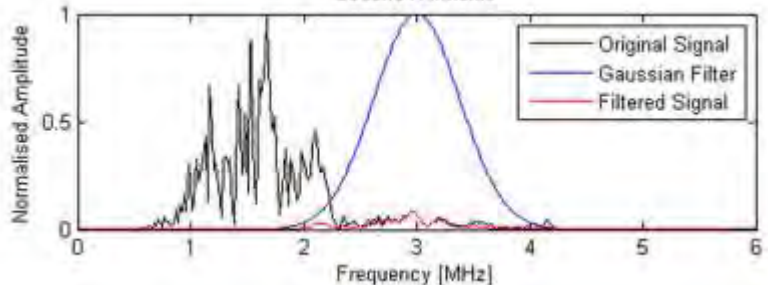
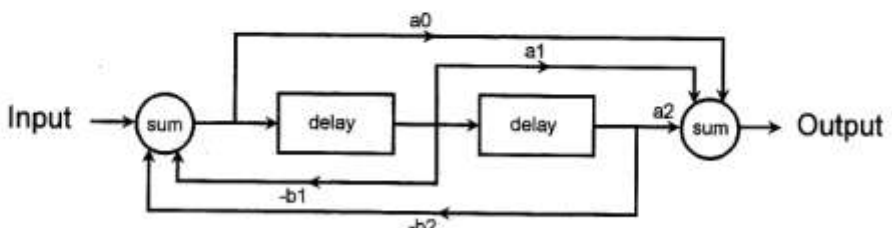
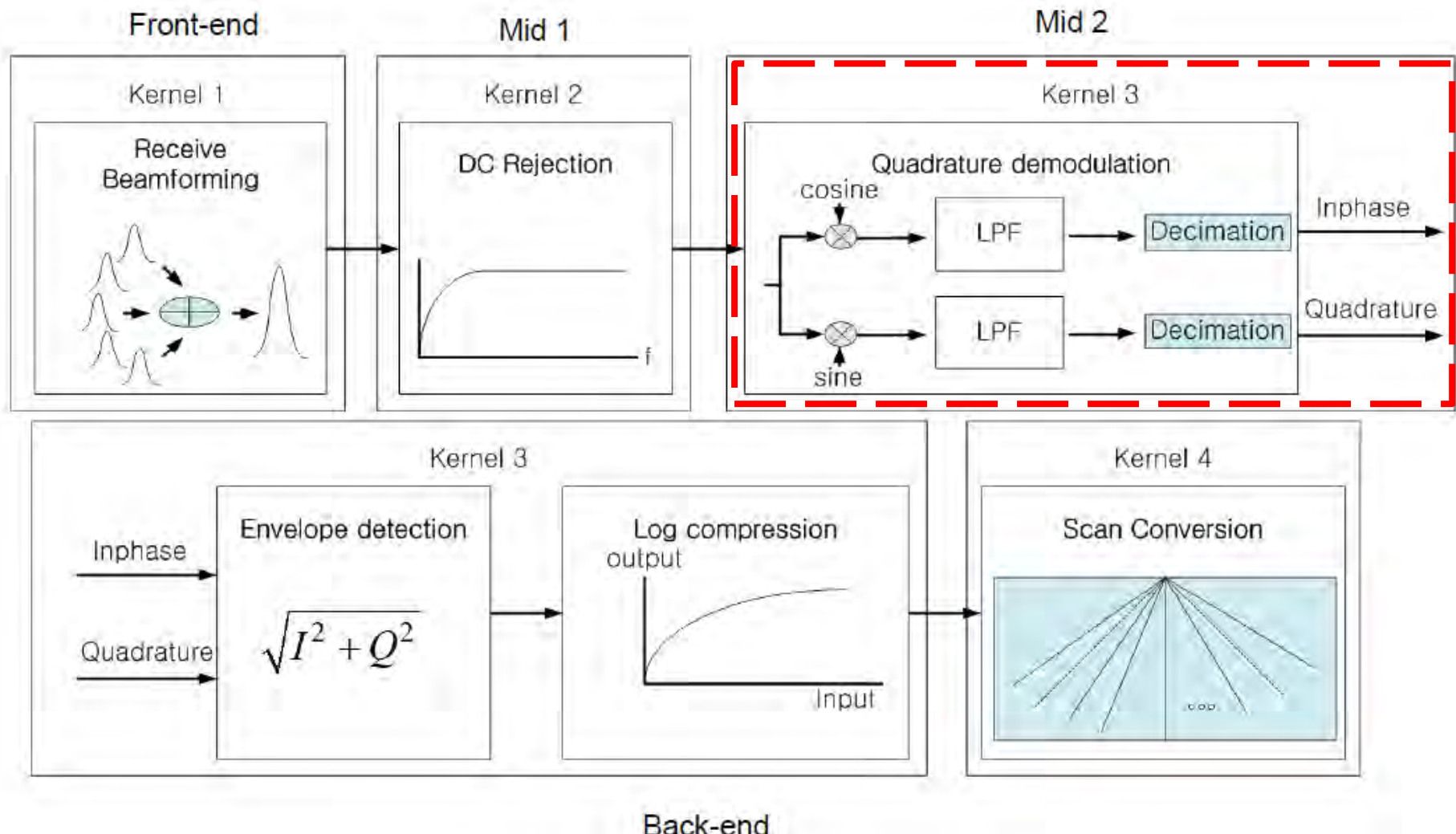


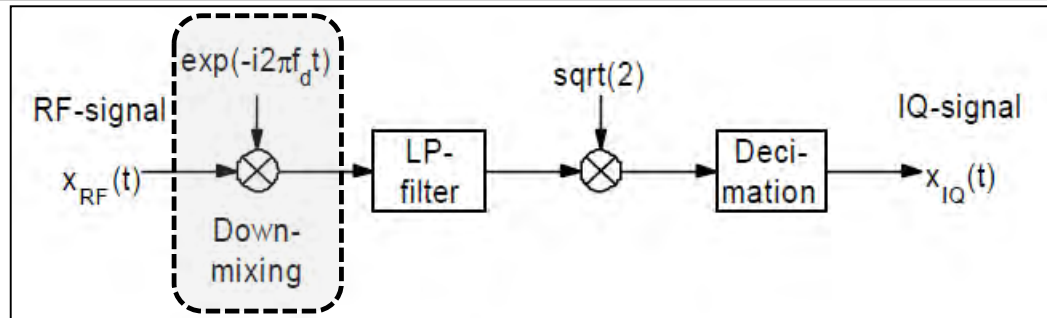
Figure Clutter rejection filters: (a) simple single echo canceller; (b) simple double echo canceller; (c) second order infinite impulse response filter. All delays are equal to one pulse repetition period

Ultrasound Imager-processing

B-Mode Signal processing



Ultrasound Imager-processing: Demodulator

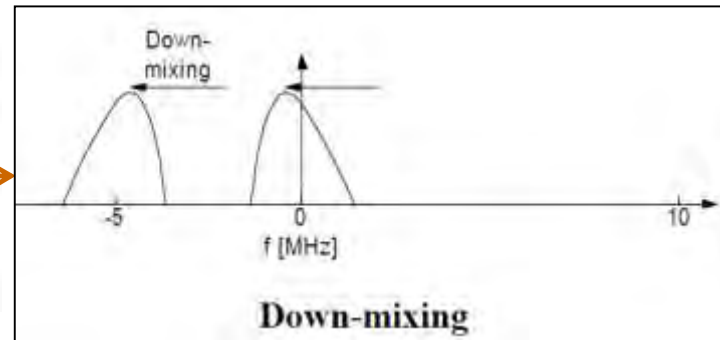
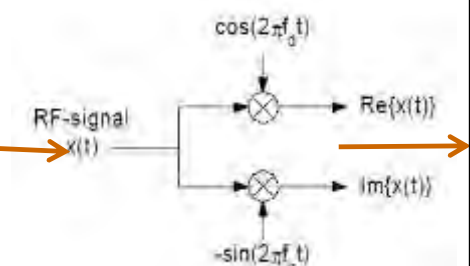
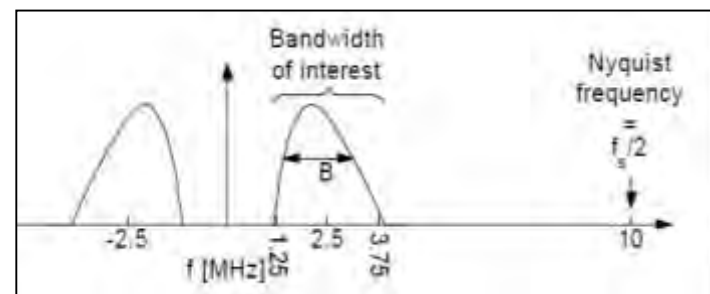


mid 2

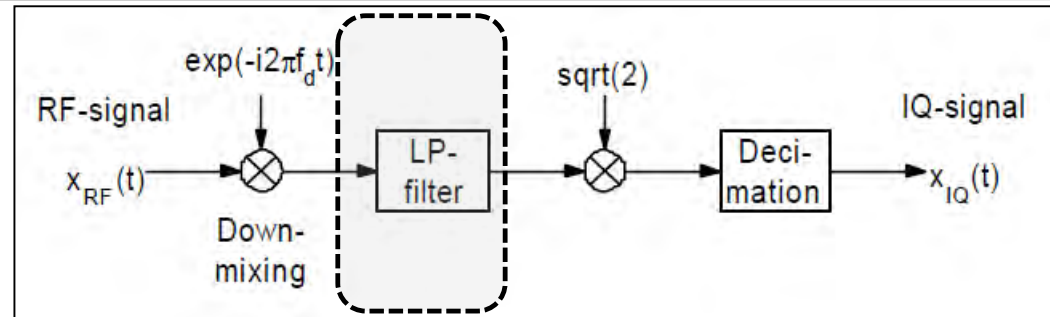
$$t = 2 * r / c$$

$$x_{IQ}(t) = x_{RF}(t) \cdot \exp(-i2\pi f_{Demod} \cdot t)$$

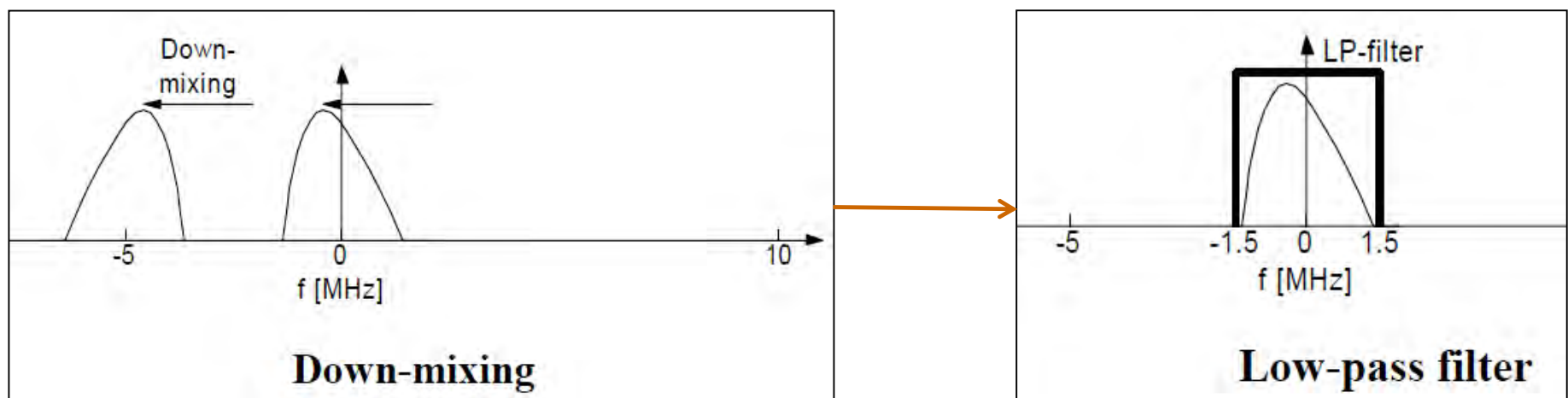
Signal processing



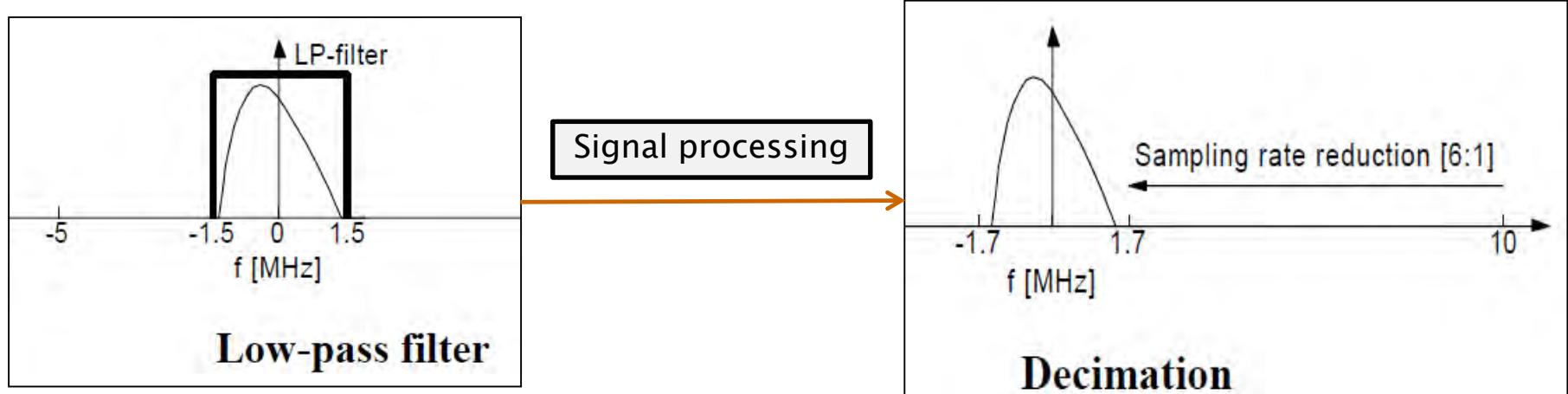
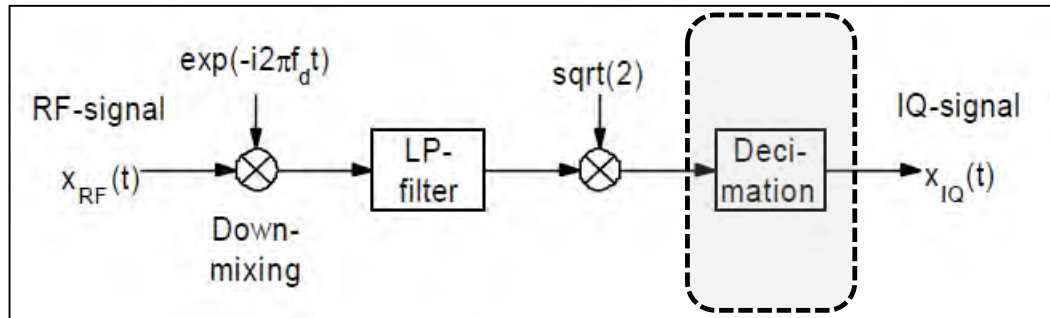
Ultrasound Imager-processing: LP-Filter



Signal processing



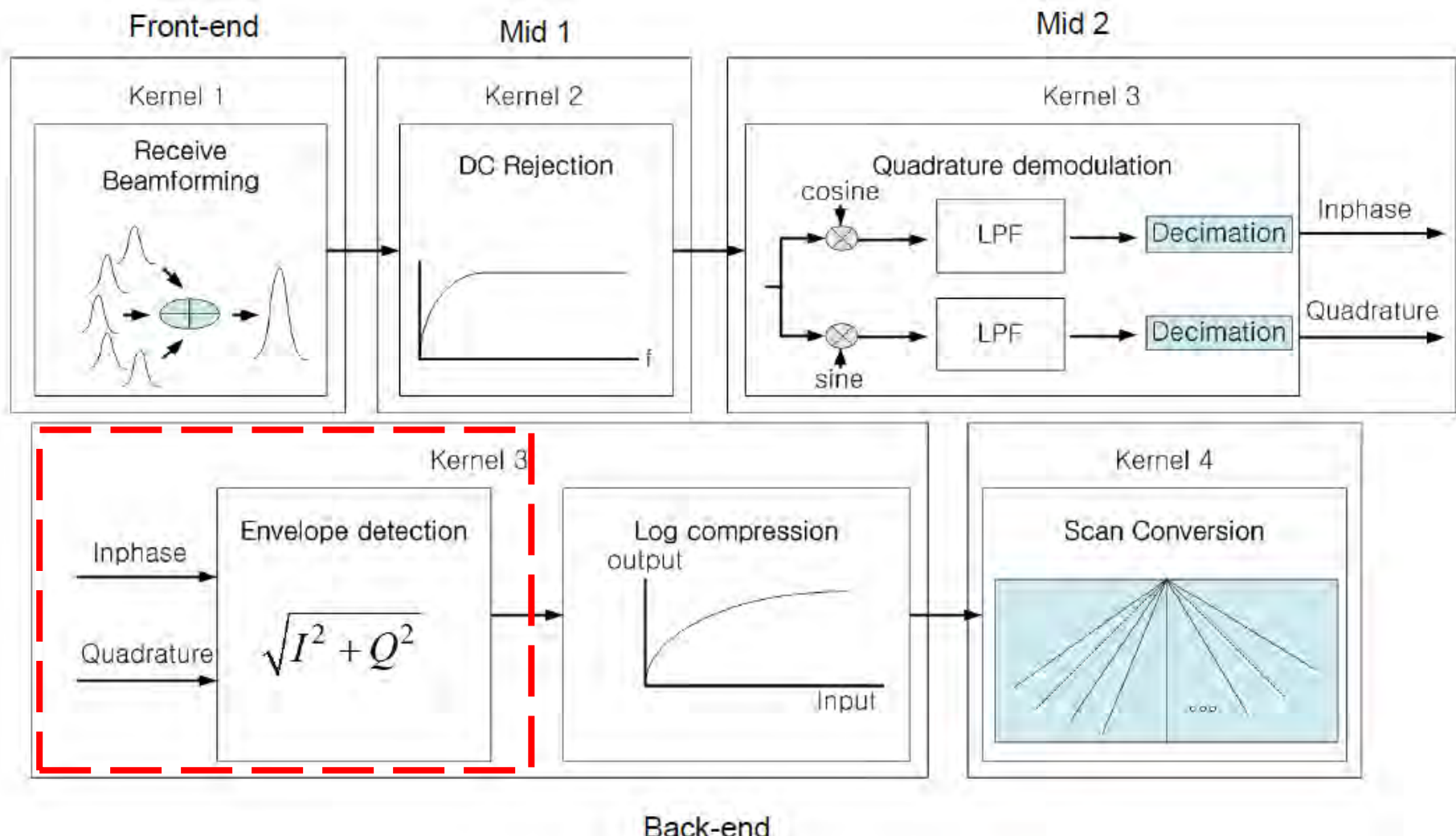
Ultrasound Imager-processing: Decimation



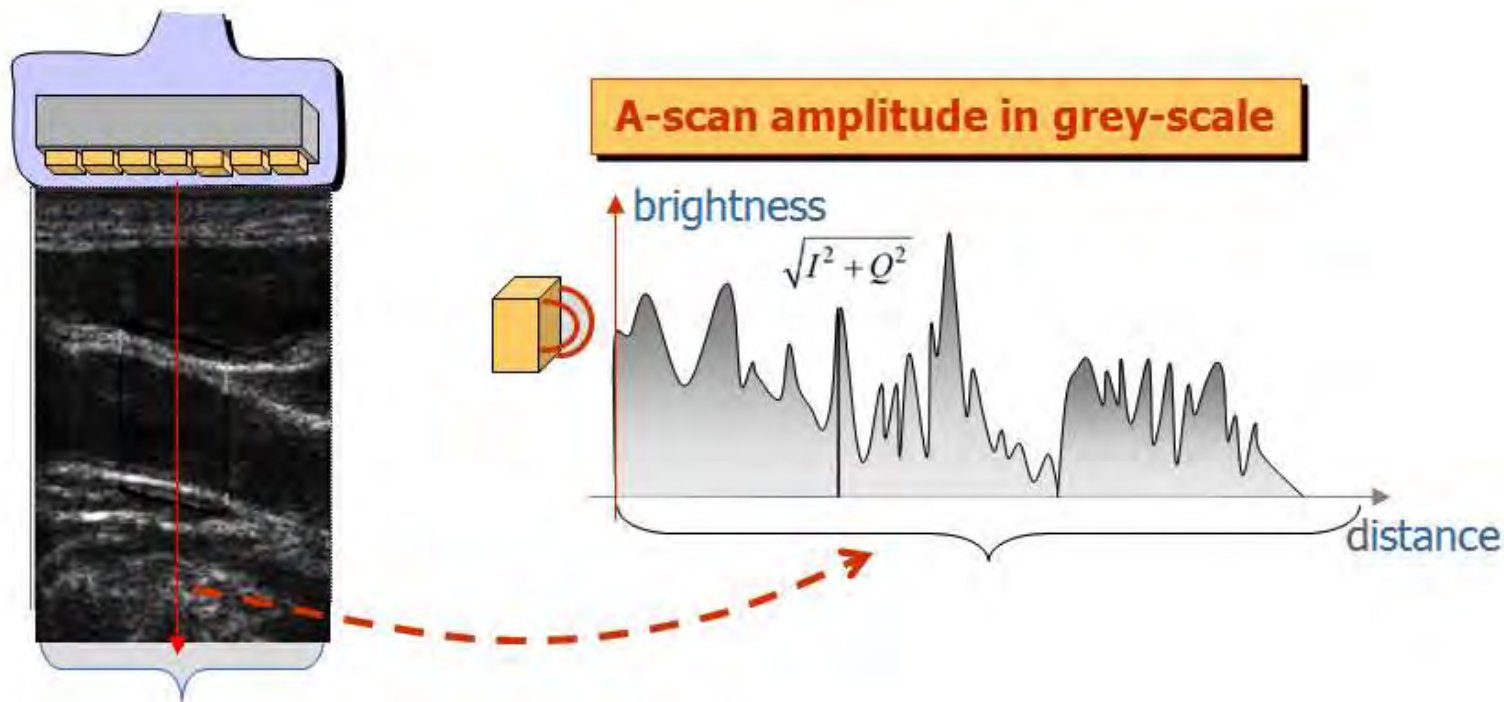
20 MHz → 3.33 MHz

Ultrasound Imager-processing

B-Mode signal processing



Ultrasound Imager-processing: Envelope detection

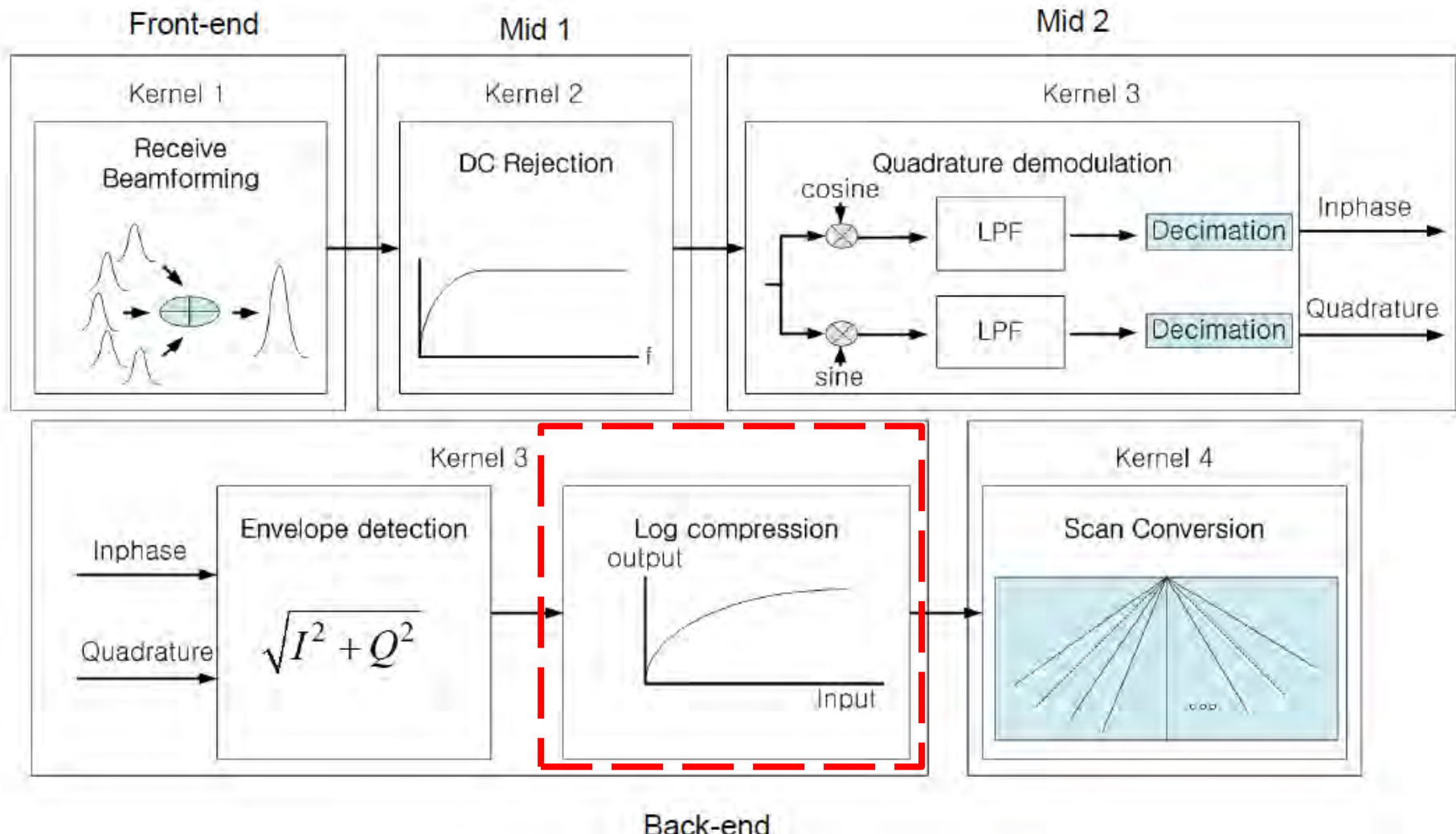


Time-Frequency-Compensation (TFC):

- Reduction of changing in center frequency with penetration in depth
- Attenuation is frequency dependant

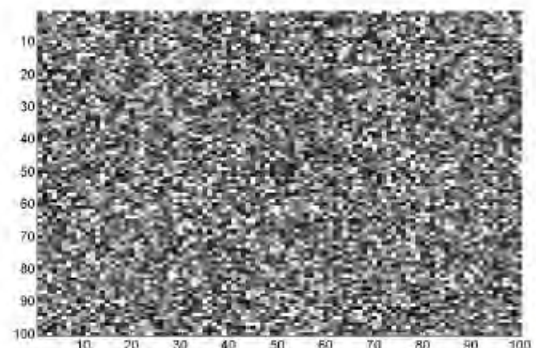
Ultrasound Imager-processing

Signal processing

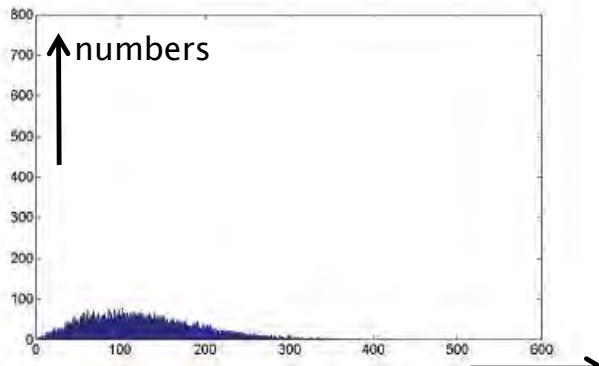


Ultraschall-Bildverfahren

B-Mode: log-compression



(a)



(b)

$$Y = D \ln X_e + G$$

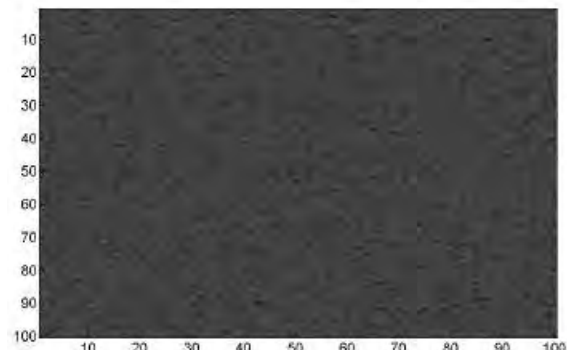
Xe: Envelope

G: Offset

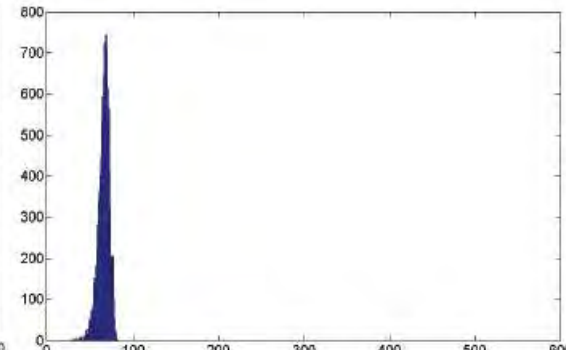
D: Shape parameter

(a) Computer generated signal with Rayleigh distribution; (b) Its histogram.

- Adapting dynamic range (D)-Parameter
- Improving S/N (G-Parameter) in picture



(a)



(b)

(a) Signal after log-compression. (b) Its histogram.

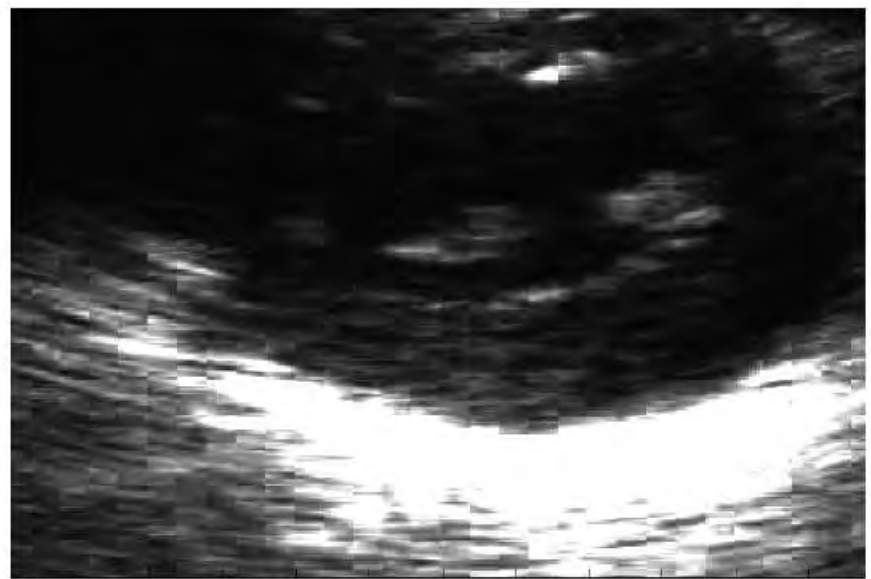
Ultraschall-Bildverfahren

B-Mode: Log-Compression-Example

decompressed



Log-compressed image.



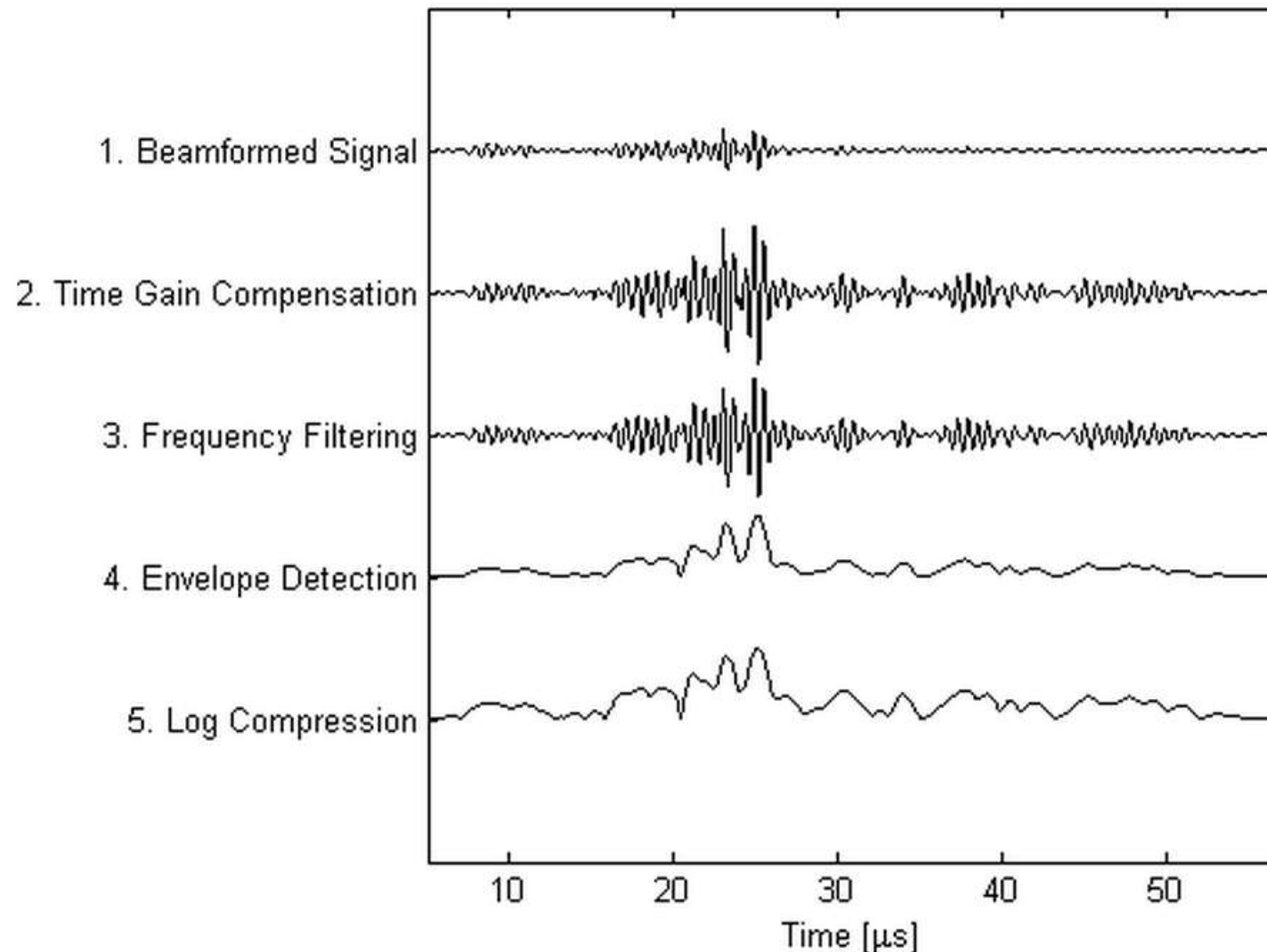
Reconstructed signal.



Log-compressed

Ultraschall-Bildverfahren

B-Mode: Signal processing A-scan summary



Ultraschall-Bildverfahren

B-Mode: Signal processing: Speckle due to scattering

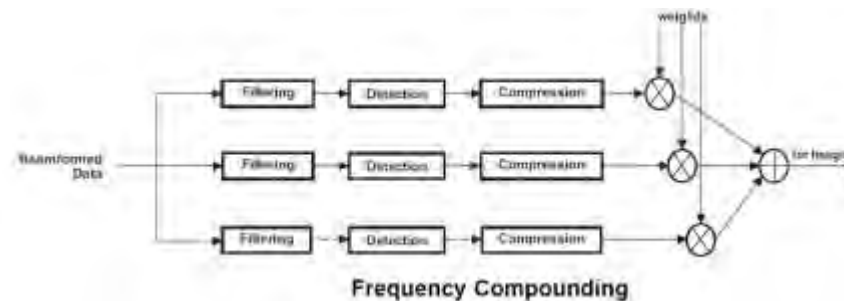
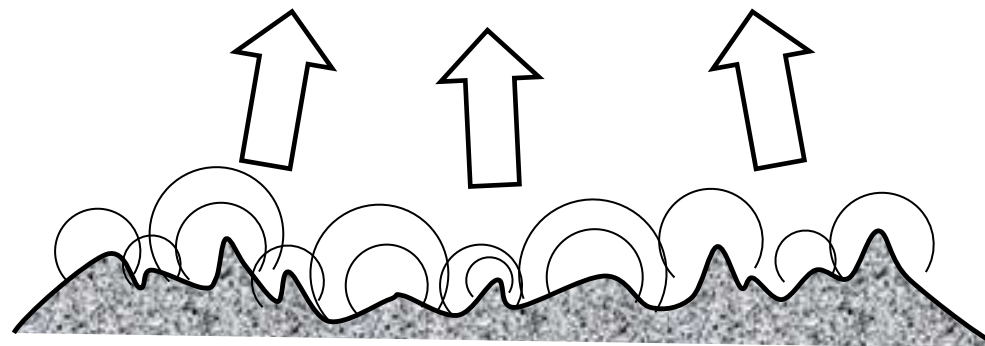
specular scattering: size $\gg \lambda$

Diffractive scattering: size $\approx \lambda$

diffusive scattering: size $\ll \lambda$

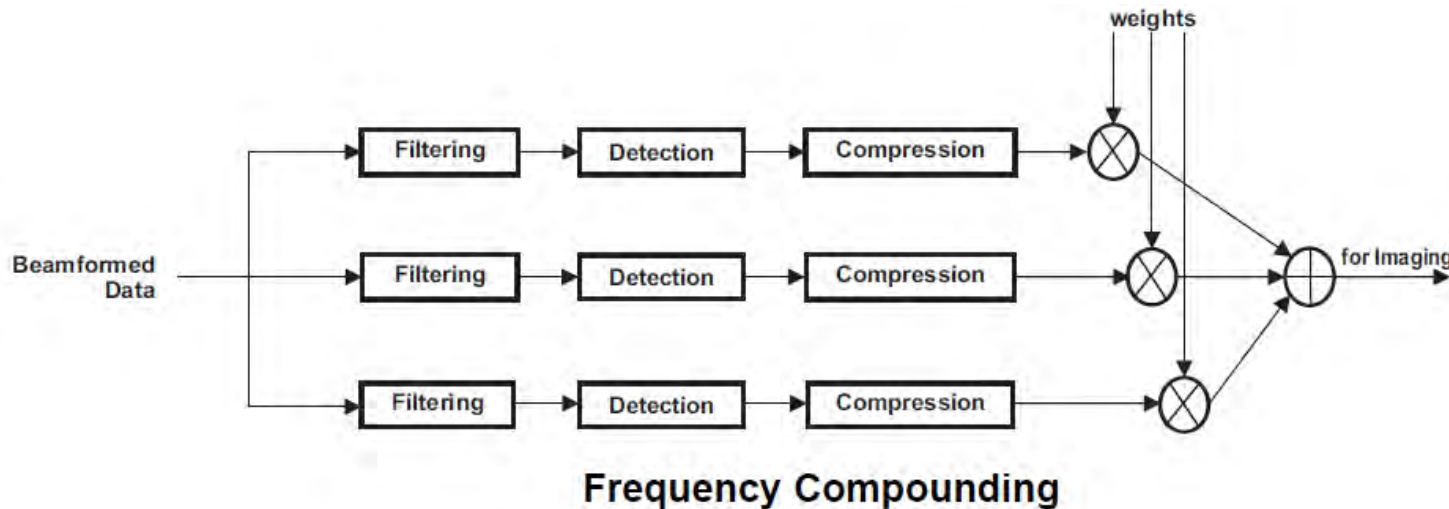
Tissue = aggregate of small sub wavelength point scatters

→ complex Gaussian random variable



Ultraschall-Bildverfahren

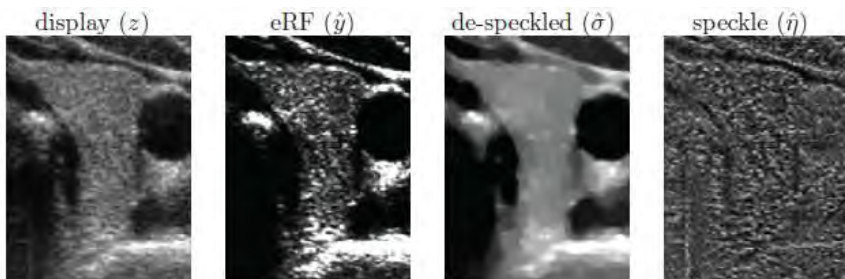
B-Mode: Signal processing: Speckle reduction



Median-Filter
Gaussian Filter

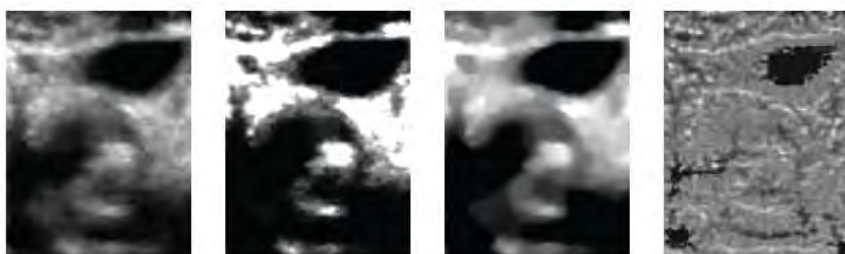
Ultraschall-Bildverfahren

B-Mode: Signal processing: Despeckle



eRF: raw data – decompressed → despeckled

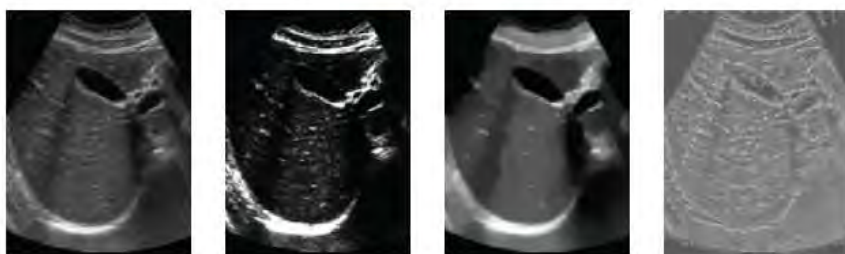
(a) Thyroid



Methods from TI-Basic-Imager:

- Wavelet decomposition
- Anisotropic Filtering
- Bilateral Filterng

(b) Carotid Plaque



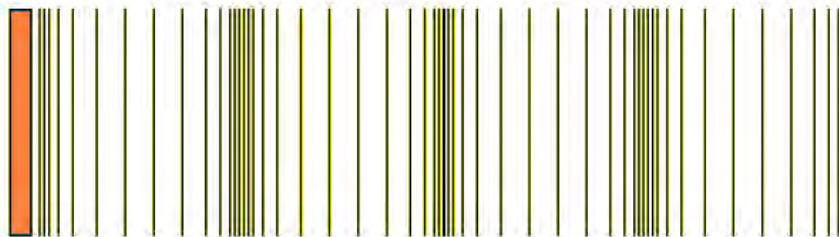
(c) Liver

Fig. Illustrative results of the ultrasound speckle decomposition method applied to different tissue types.

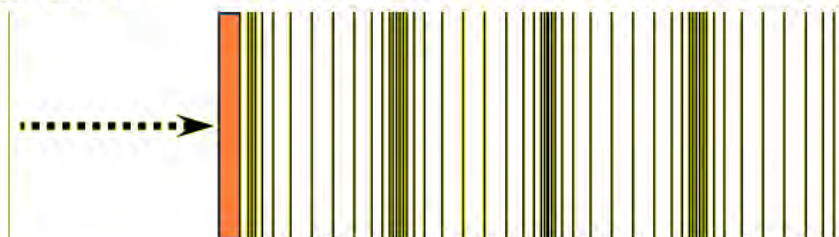
Ultraschall-Bildverfahren: Signal processing

Duplex (Doppler) + signal processing: Demodulation

Stationary Source



Moving Source

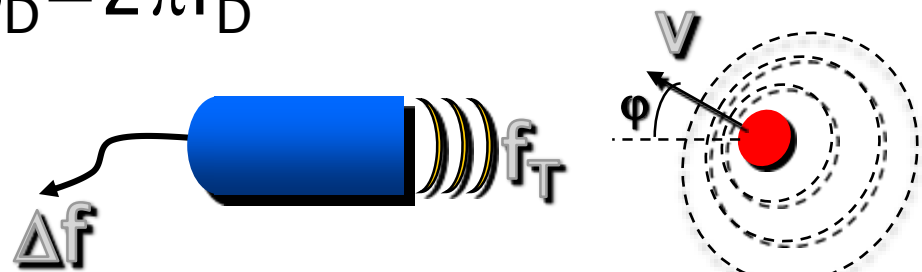


Decreased wavelength

Increased frequency

2xDoppler effect for $\omega_D = 2\pi f_D$

$$f_D = \Delta f = [2(\frac{v}{c_0}) \cos \theta] \cdot f_0$$



Ultraschall-Bildverfahren: Signal processing

Duplex + signal processing: Demodulation

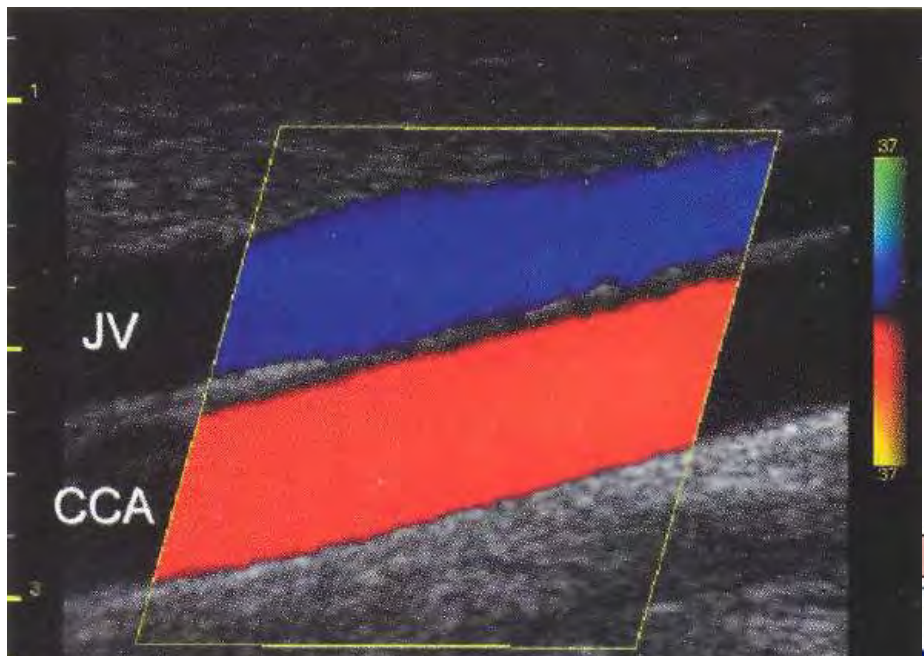
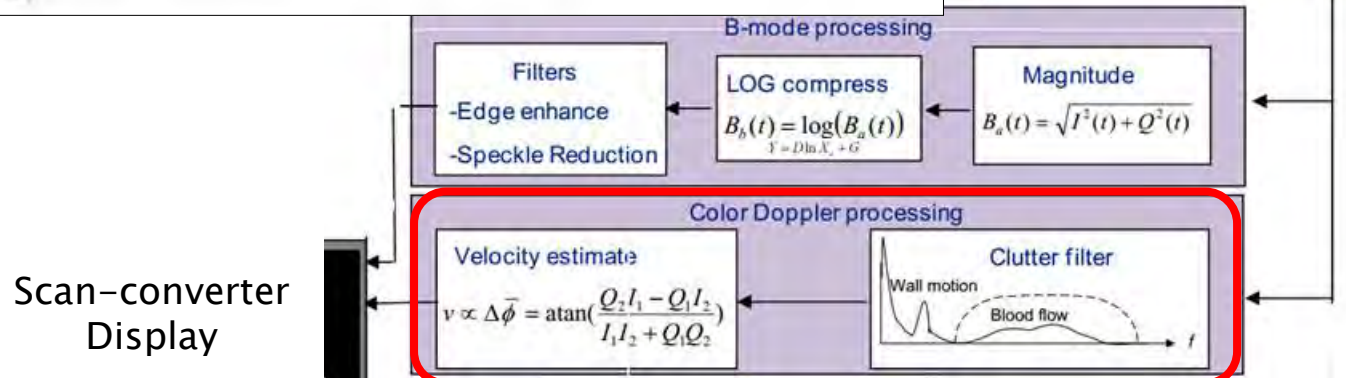
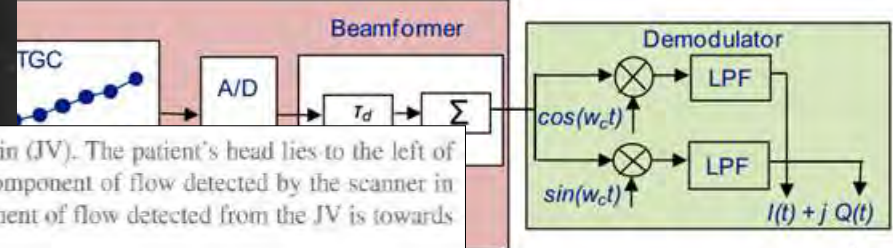
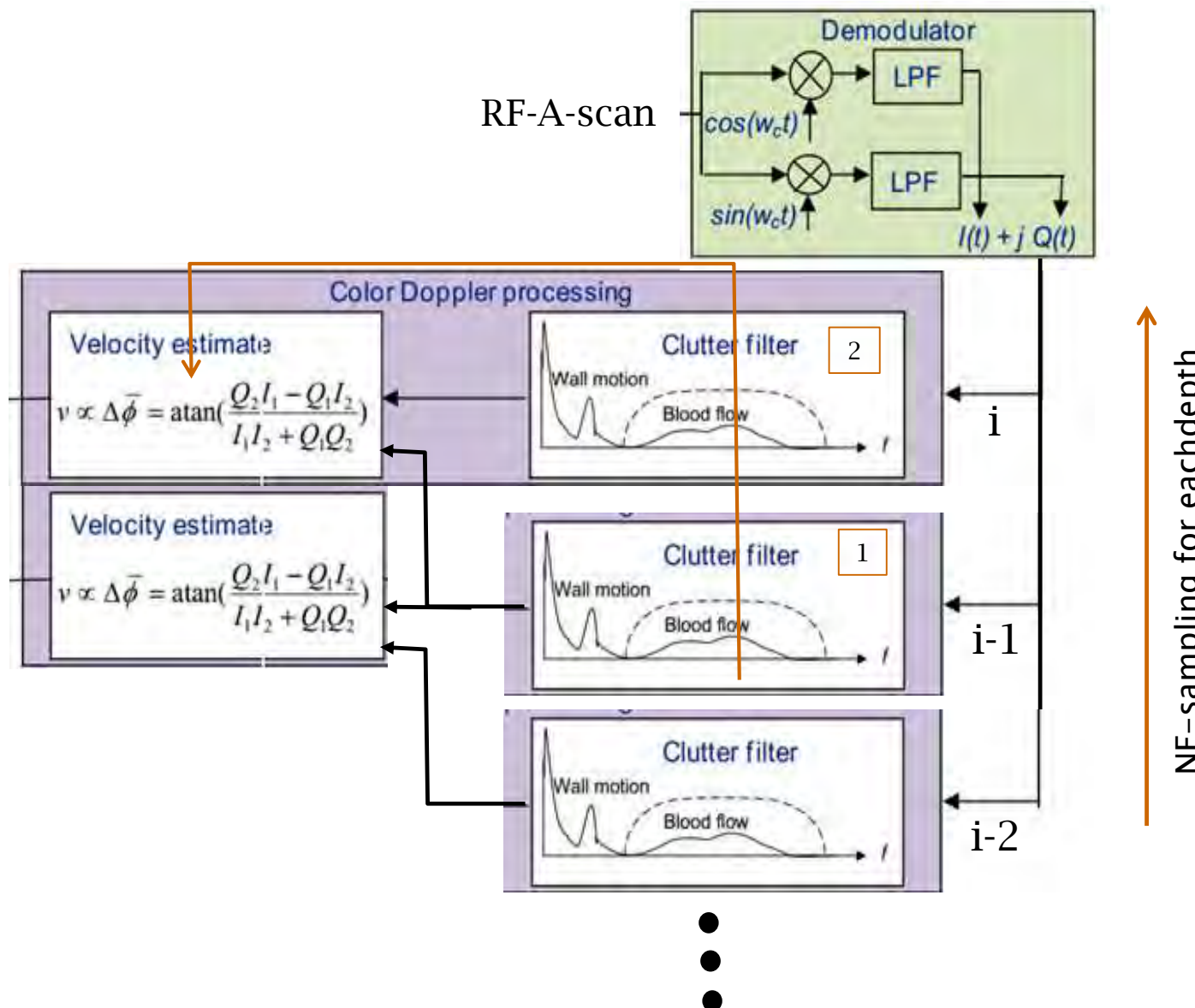


Figure Colour Doppler flow image of a common carotid artery (CCA) and jugular vein (JV). The patient's head lies to the left of the scan, his feet to the right. The colour scale on the right of the image indicates that the component of flow detected by the scanner in the CCA is away from the transducer (i.e. moving from right to left). Conversely, the component of flow detected from the JV is towards the transducer (image courtesy of GE Ultrasound)



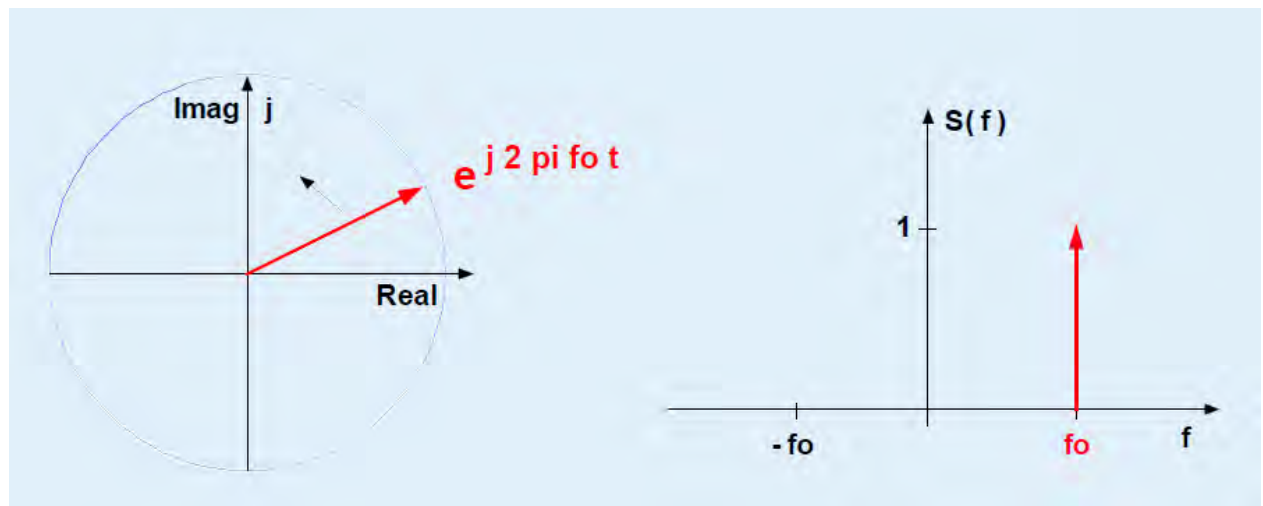
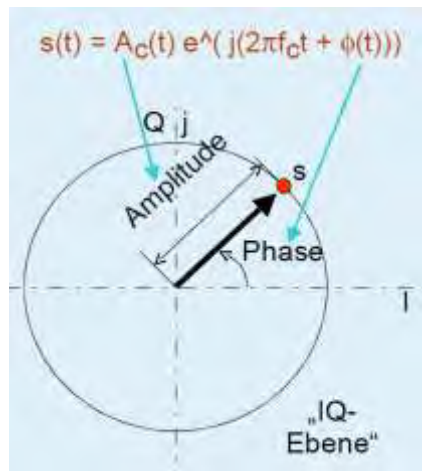
Ultraschall-Bildverfahren: Signal processing

Doppler Color coded – M-Mode-line (single A-Scan running over time)



Ultraschall-Bildverfahren: Signal processing

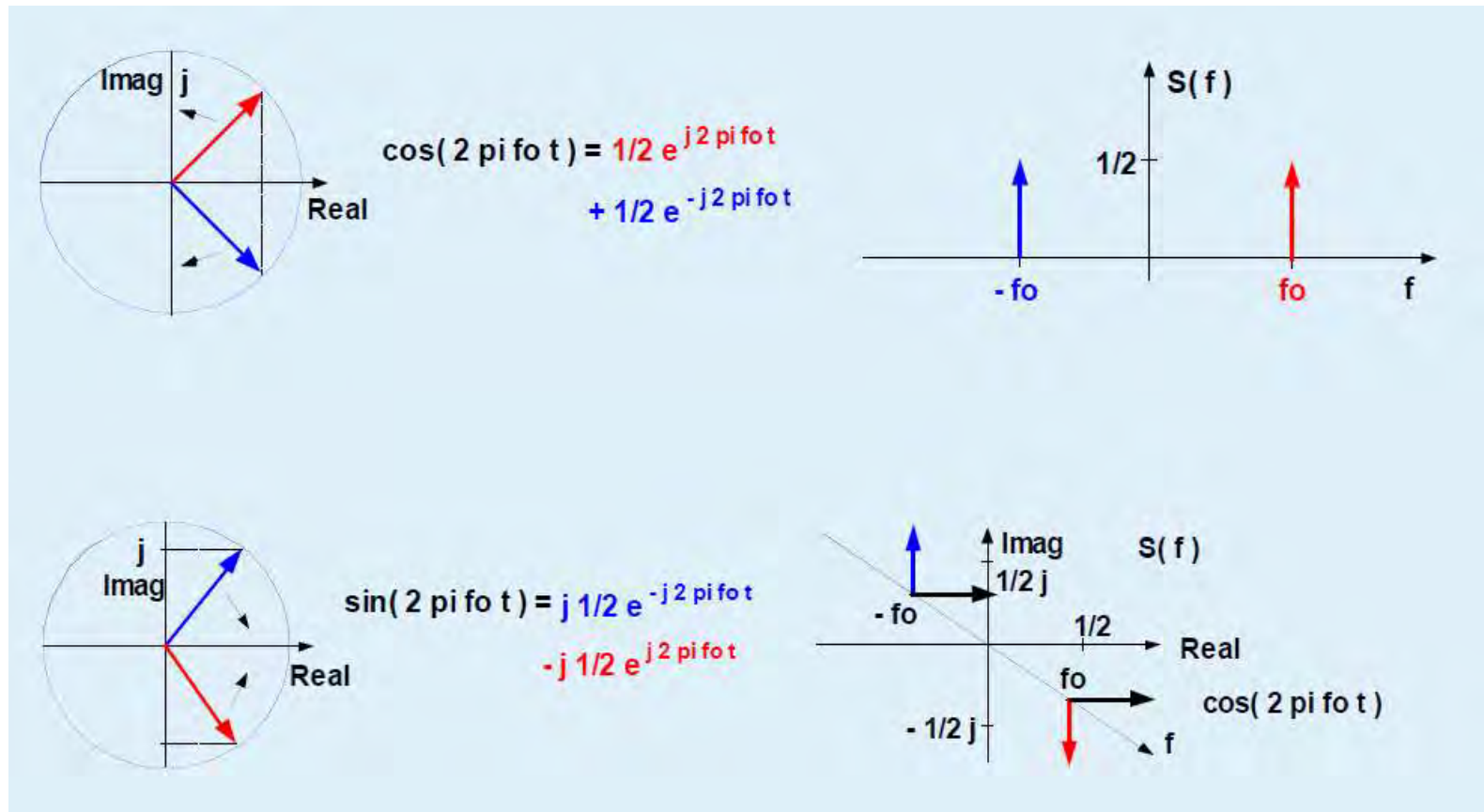
Demodulation; complex signals in frequency domain → flow directionality



The sign of the exponent is corresponding to the positive and negative frequency

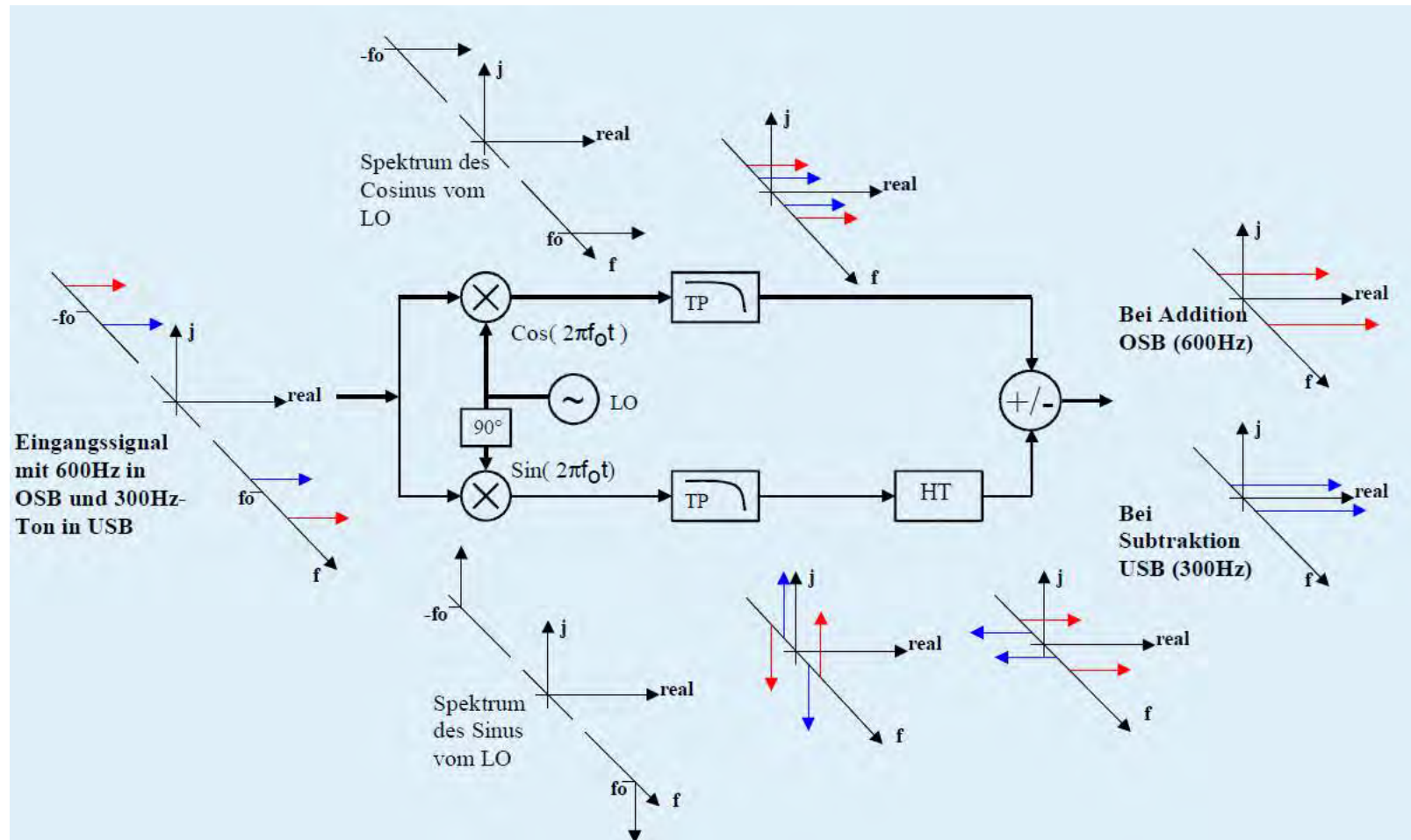
Ultraschall-Bildverfahren: Signal processing

signal processing: Demodulation; Sinus + Cosinus in frequency domain



Ultraschall-Bildverfahren: Signal processing

signal processing: Demodulation, upper and lower sideband → flow directionality

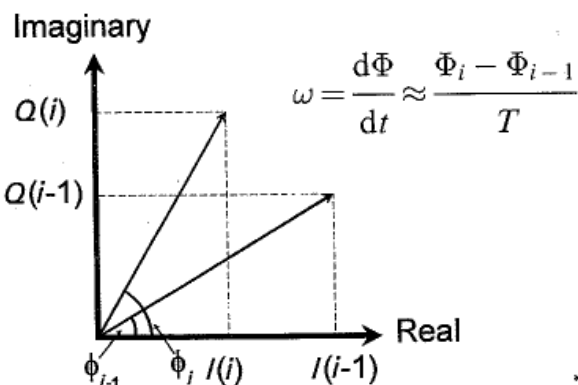
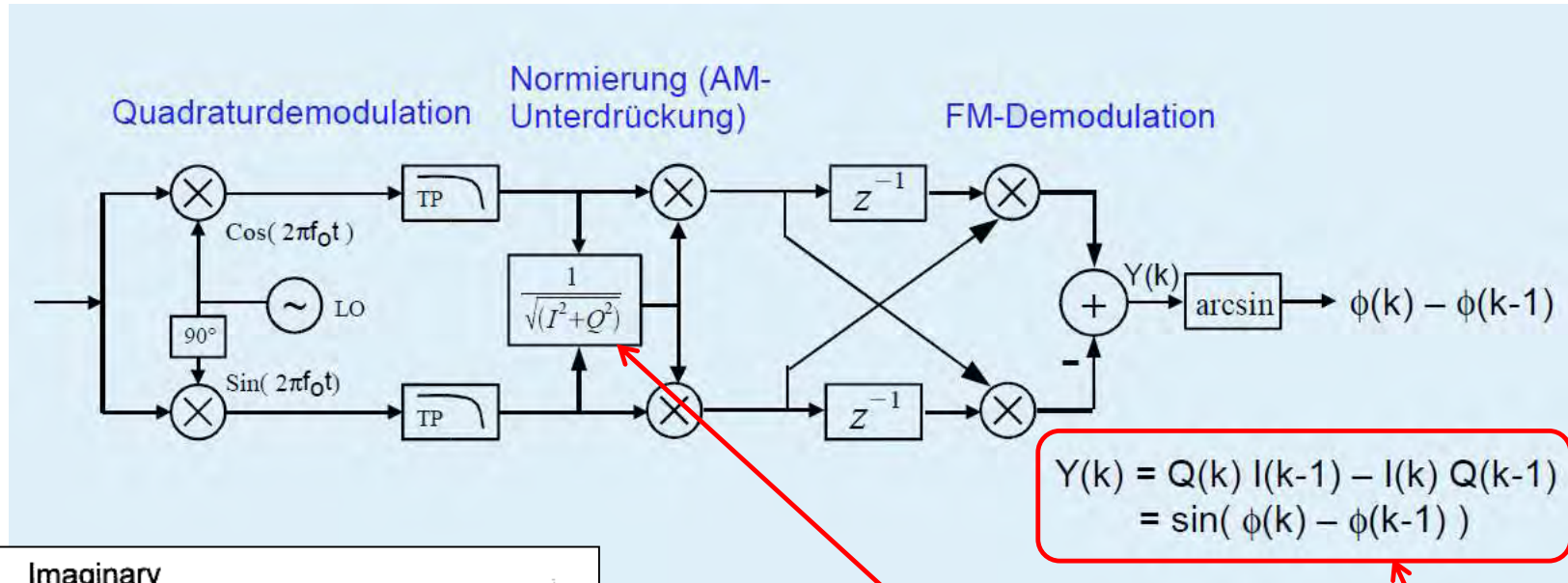


Demodulation of upper and lower frequency band

Ultraschall-Bildverfahren: Signal processing

Demodulation to mean velocity

FM-Demodulation using quadratur signals



$$\begin{aligned} & \tan(\Phi_i - \Phi_{i-1}) \\ &= \frac{\sin(\Phi_i - \Phi_{i-1})}{\cos(\Phi_i - \Phi_{i-1})} \\ &= \frac{\sin \Phi_i \cos \Phi_{i-1} - \cos \Phi_i \sin \Phi_{i-1}}{\cos \Phi_i \cos \Phi_{i-1} - \sin \Phi_i \sin \Phi_{i-1}} \end{aligned}$$

$$\hat{\omega} = \frac{1}{T} \tan^{-1} \left\{ \frac{\sum_{i=1}^N Q(i)I(i-1) - I(i)Q(i-1)}{\sum_{i=1}^N I(i)I(i-1) + Q(i)Q(i-1)} \right\}$$

Figure Position of a rotating signal vector during two successive samples $(i-1)$ and (i) , showing the in-phase components $I(i-1)$ and $I(i)$, and quadrature components $Q(i-1)$ and $Q(i)$.

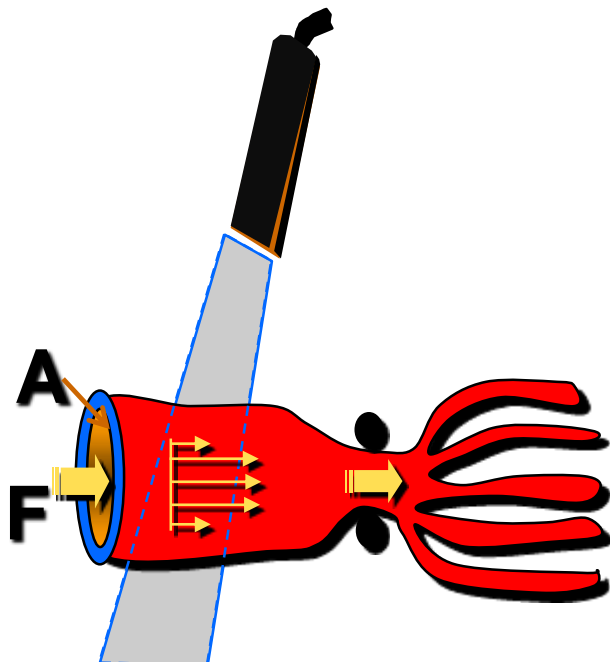
Ultraschall-Bildverfahren: Signal processing

signal processing: Demodulation, upper and lower sideband

Directional mean velocity in sample volume/local area (spacial point):

$$\hat{\bar{\omega}} = \frac{1}{T} \tan^{-1} \left\{ \frac{\sum_{i=1}^N Q(i)I(i-1) - I(i)Q(i-1)}{\sum_{i=1}^N I(i)I(i-1) + Q(i)Q(i-1)} \right\}$$

$$\bar{\omega} = \frac{\int_{-\infty}^{\infty} \omega P(\omega) d\omega}{\int_{-\infty}^{\infty} P(\omega) d\omega}$$



Flow-index and Area index:

$$\sum_i \omega_i P\{\omega_i\} \cdot \Delta\omega = \bar{\omega}_{mean} \cdot \sum_i P\{\omega_i\} \cdot \Delta\omega$$

$$\int \omega P\{\omega\} \cdot d\omega = \bar{\omega}_{mean} \cdot \int P\{\omega\} \cdot d\omega$$

$$F = v_{mean} \cdot A$$

Ultraschall-Bildverfahren: Signalprocessing

Color- flow imaging examples: Carotis stenosis

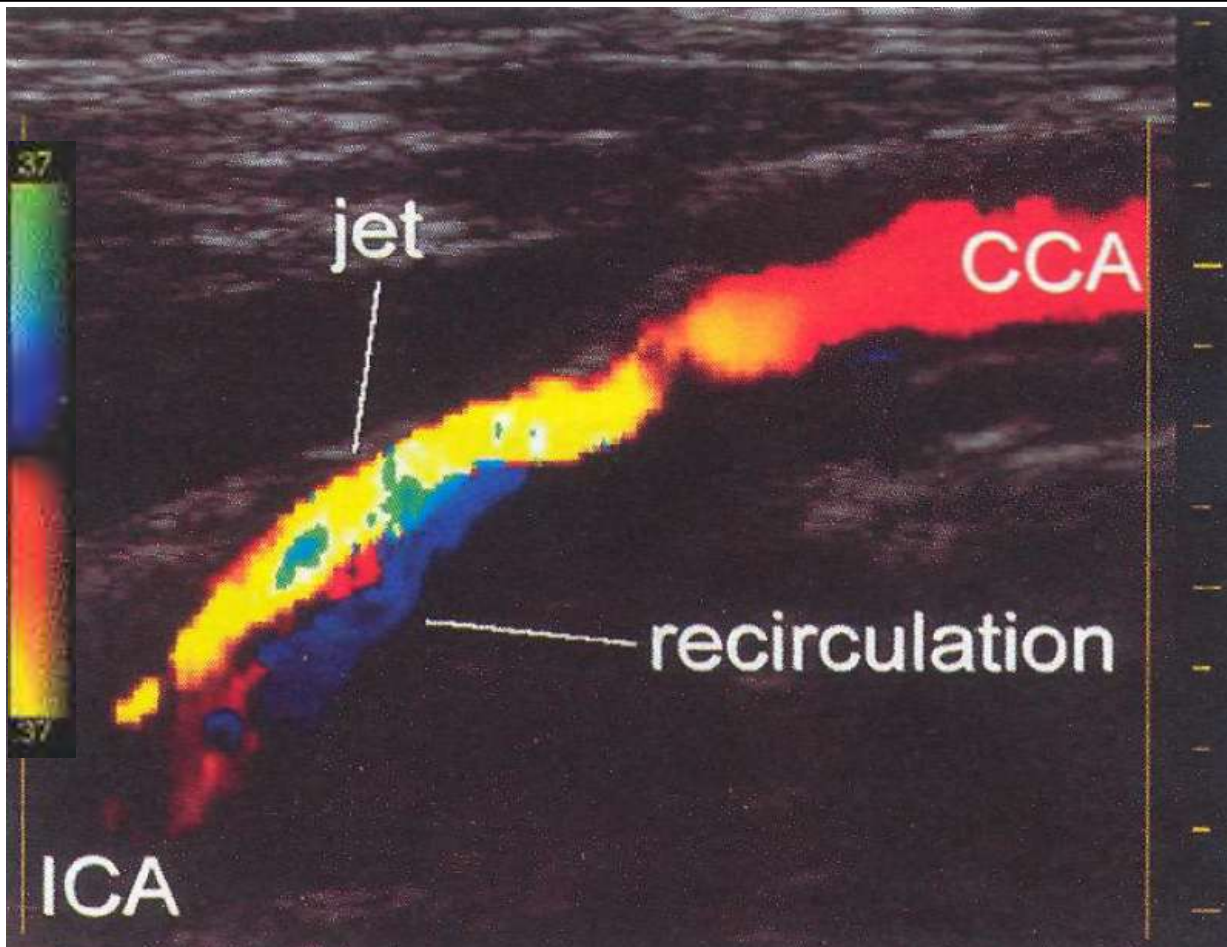
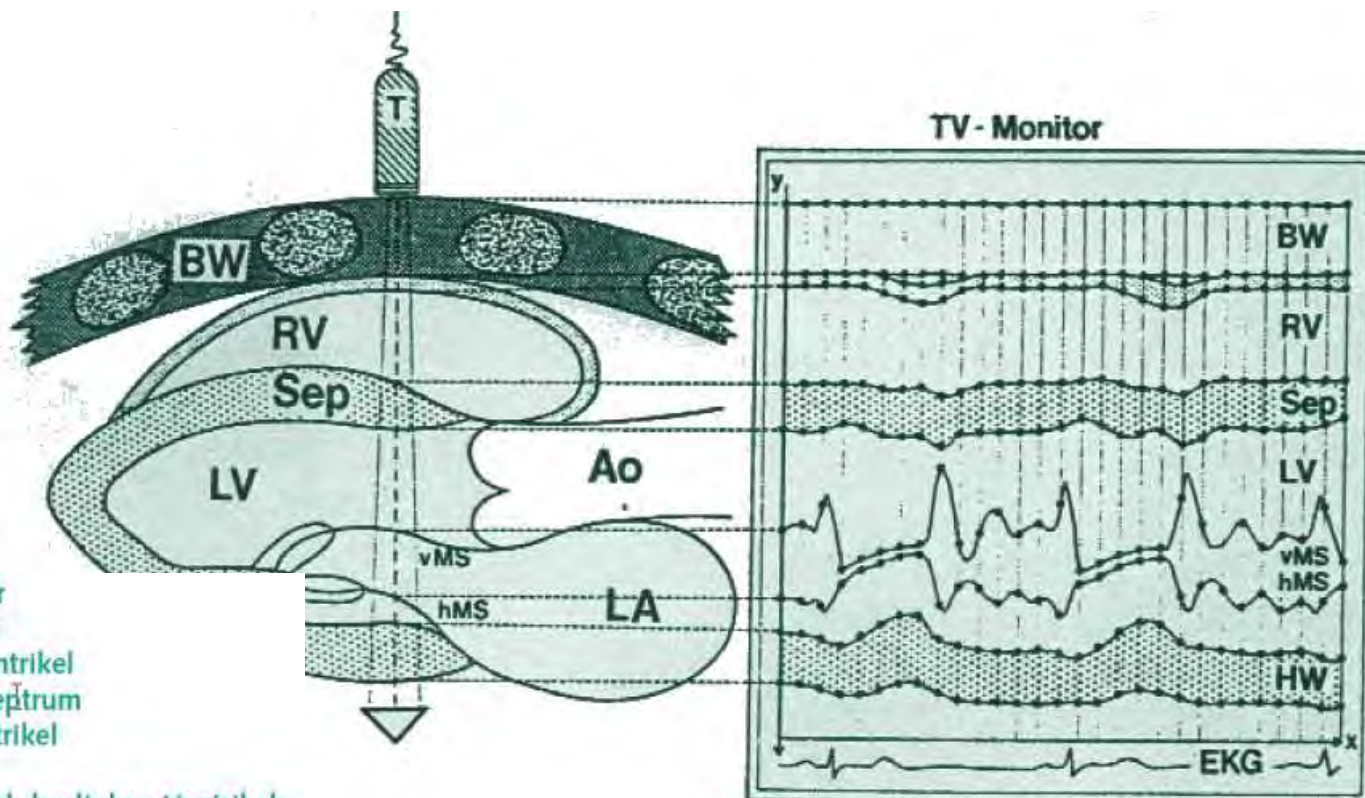


Figure Colour Doppler flow image of an internal carotid artery (ICA) stenosis. The patient's head lies to the left of the scan. The colour coding scale is similar to that shown in Fig. 4.17. The colour of the flow changes from red to yellow (and then to green) for two reasons. First, the Doppler angle is increasing as the vessel curves deeper into the tissue, but also because the velocity increases as the same volume of flow has to pass through the stenosis. Once the blood has passed through the stenosis, the jet continues for some distance and gives rise to a region of recirculation (coded in blue because the component of flow is towards the transducer in this region). Note that the region of green in the jet is not reverse flow but aliasing, due to the Doppler shift exceeding half the pulse repetition frequency (image courtesy of GE Ultrasound)

Ultraschall-Bildverfahren: Demodulation

M-Mode-Picture-Principle for Color-M-Mode-Example



T	= Transclucer
BW	= Brustwand
RV	= rechter Ventrikel
SEP	= Ventrikelseptum
LV	= linker Ventrikel
AO	= Aorta
HW	= Hinterwand des linken Ventrikels
LA	= linker Vorhof
VMS	= vorderes Mitalsegel
HMS	= hinteres Mitalsegel

Ultraschall-Bildverfahren: Demodulation

Color- flow imaging examples:M-Mode

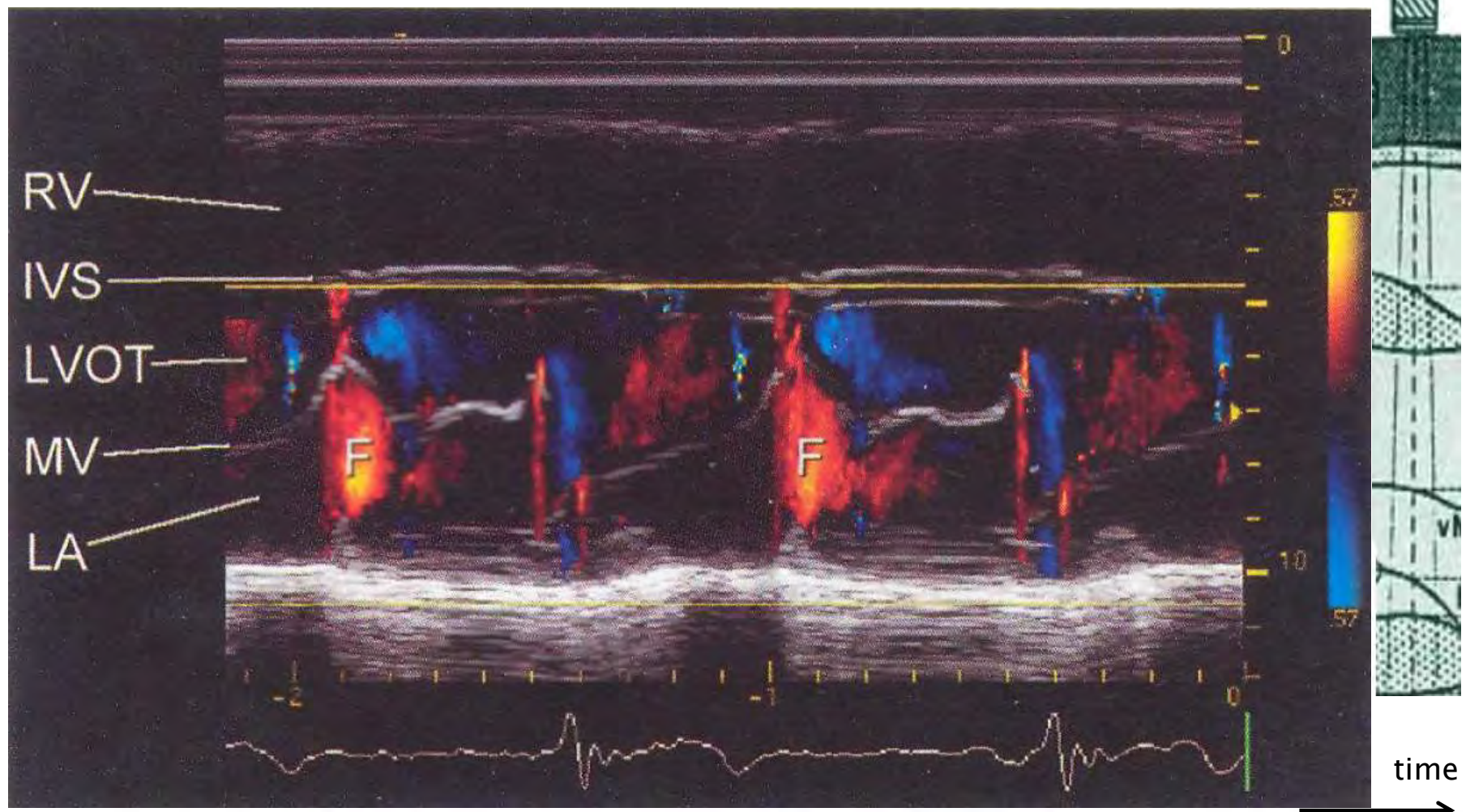


Figure Parasternal long axis, M-mode, through the mitral valve leaflets of the heart with colour Doppler overlaid, showing diastolic ventricular filling through the open mitral leaflets and into the left ventricular outflow tract. RV, right ventricle; IVS, intra-ventricular septum; LVOT, left ventricular outflow tract; MV, mitral valve; LA, left atrium. F indicates the ventricular filling phase (image courtesy of GE Ultrasound)

Ultraschall-Bildverfahren: Power-Doppler

Power-Doppler imaging. No velocities!!!

$$\hat{\bar{\omega}} = \frac{1}{T} \tan^{-1} \left\{ \frac{\sum_{i=1}^N Q(i)I(i-1) - I(i)Q(i-1)}{\sum_{i=1}^N I(i)I(i-1) + Q(i)Q(i-1)} \right\}$$

$\int_{-\infty}^{\infty} \omega P(\omega) d\omega$

$$\bar{\omega} = \frac{\int_{-\infty}^{\infty} \omega P(\omega) d\omega}{\int_{-\infty}^{\infty} P(\omega) d\omega}$$

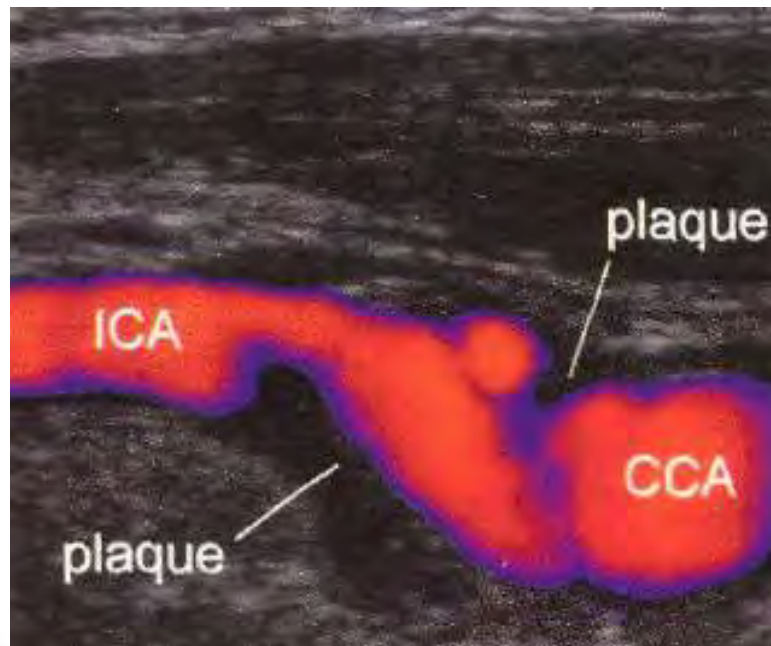
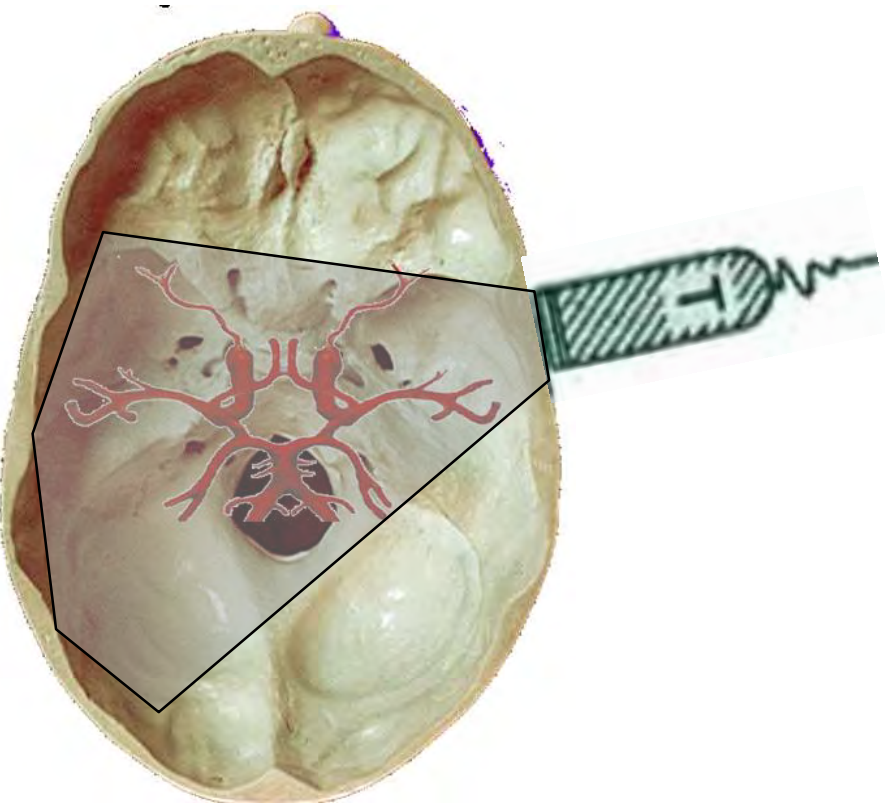
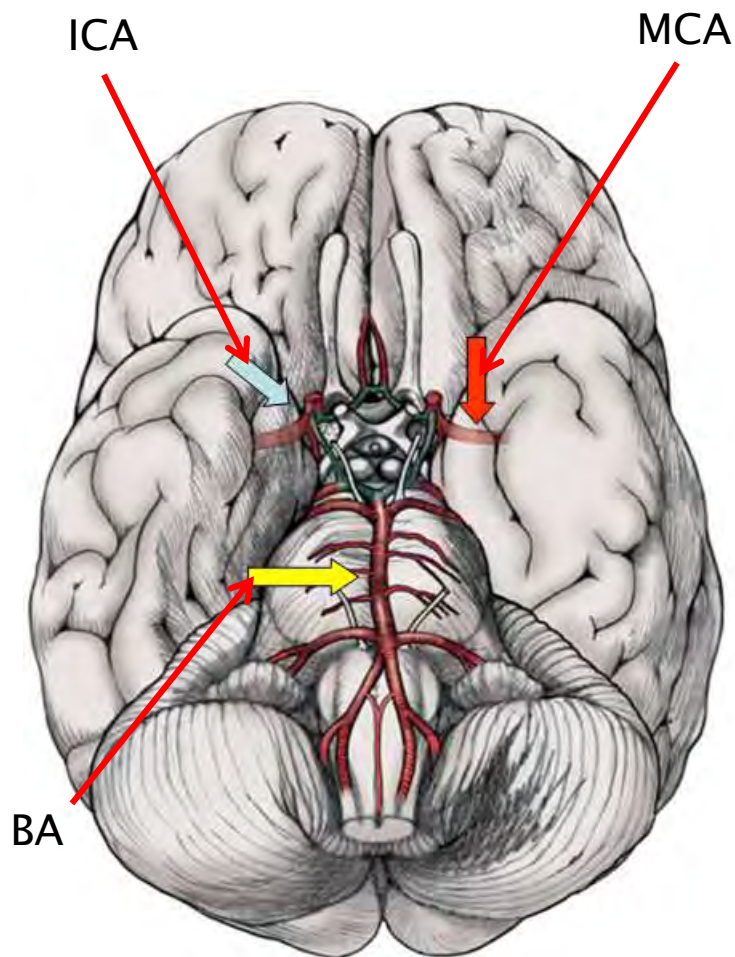


Figure Power Doppler image showing narrowing of the internal carotid artery (ICA) lumen due to the presence of atheromatous plaque. Note once again that there is no velocity (speed or direction) information available from this type of image (image courtesy of GE Ultrasound)

Ultraschall-Bildverfahren: Color-coded-Doppler

TCCD-Imaging (Transcranial-Colour-Coded-Dopplersonography)



Ultraschall-Bildverfahren: Color-coded-Doppler

TCCD-Imaging (Transcranial-Colour-Coded-Dopplersonography)

Contrast-Enhanced Transcranial Color-Coded Duplexsonography in Stroke Patients with Limited Bone Windows

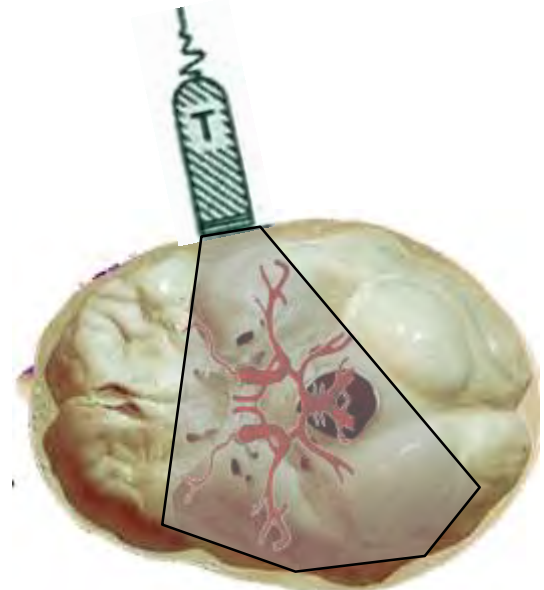
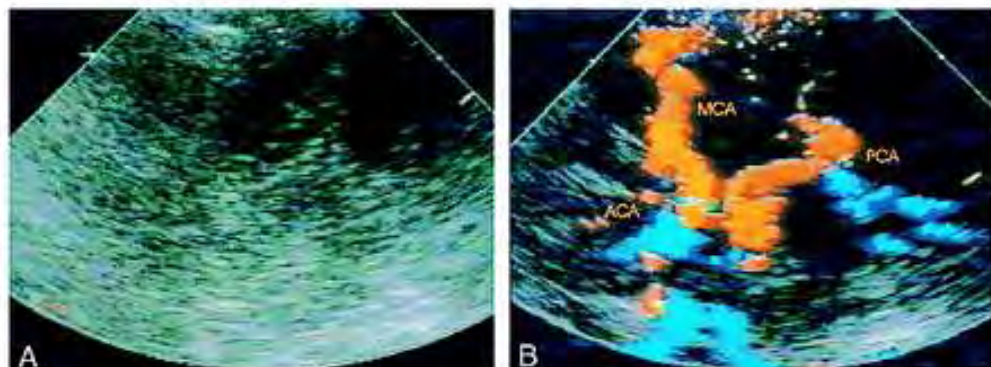
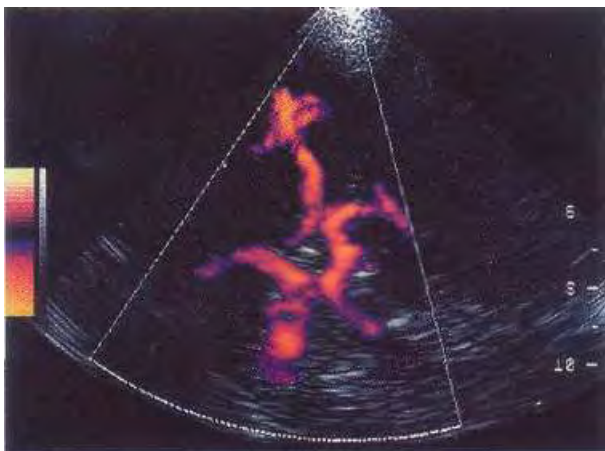


FIG 1.

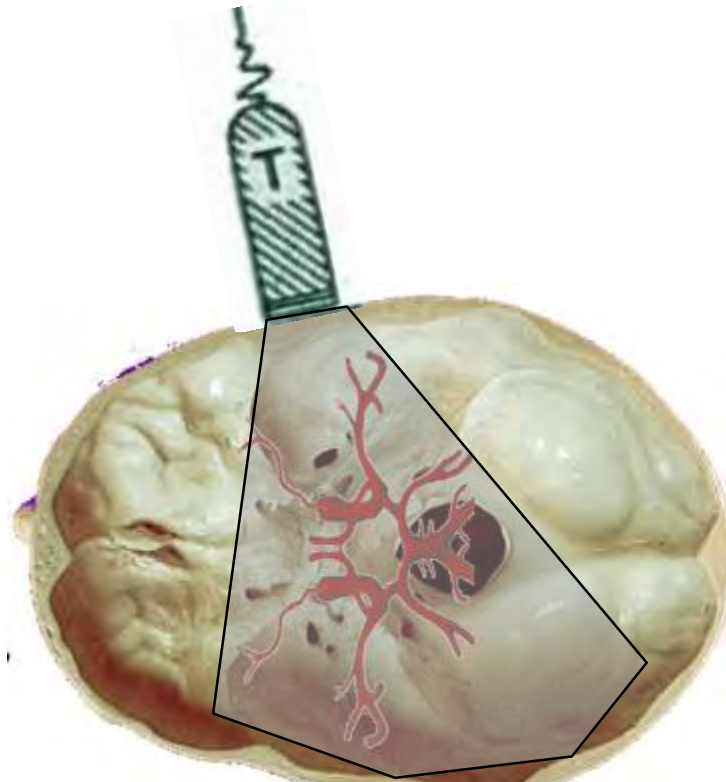
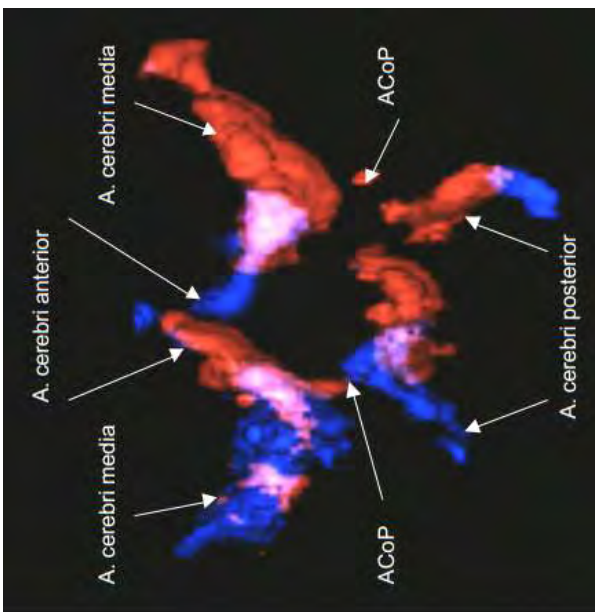
A and B, Unenhanced TCCD (A) provides no detectable colorflow signals, contrast-enhanced TCCD (B) of same patient shows the complete circle of Willis

Ultraschall-Bildverfahren: Color-coded-Doppler

TCD-Imaging



Difference = ? = Type



Ultraschall-Bildverfahren: Color-coded-Doppler

3D- TCCD-imaging

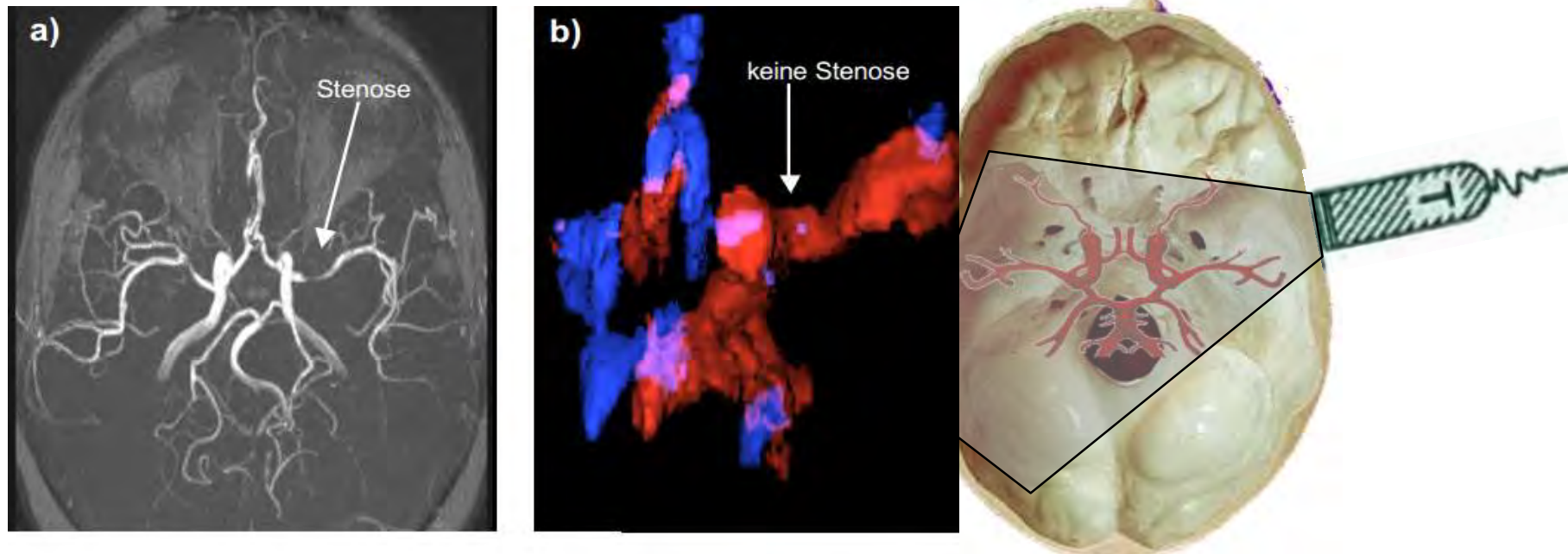
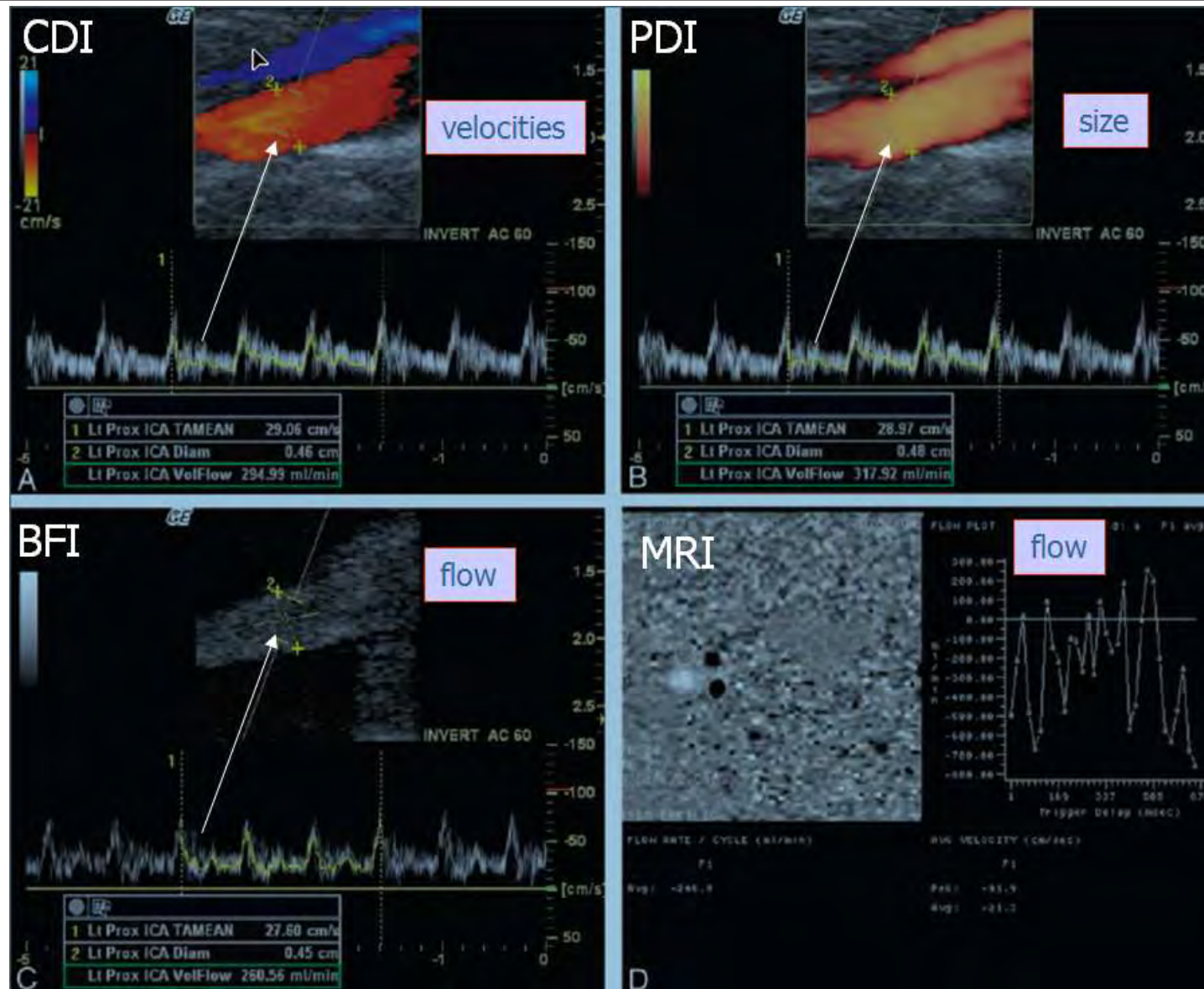


Abb. Beispiel für einen falsch negativen Befund in der Diagnostik von Stenosen der A. cerebri media mittels der 3-D CM-TCCD (Abbildung 13b)) im Veraleich mit der MRA (Abbildung 13 a))

Ultraschall-Bildverfahren: Color-coded-Doppler

Types of Imaging



Ultraschall-Bildverfahren-3D

B-Mode-3D-4D (mechanically tilting)

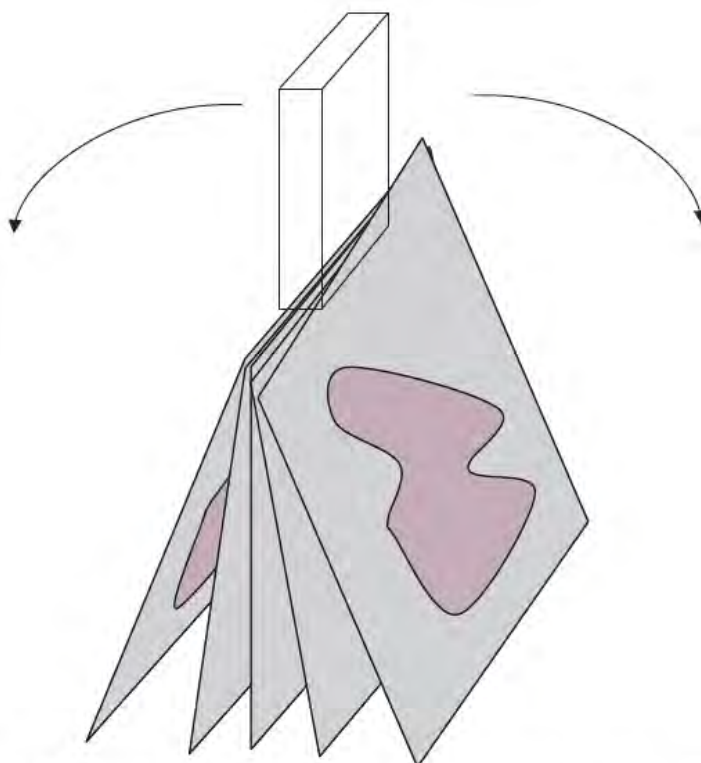
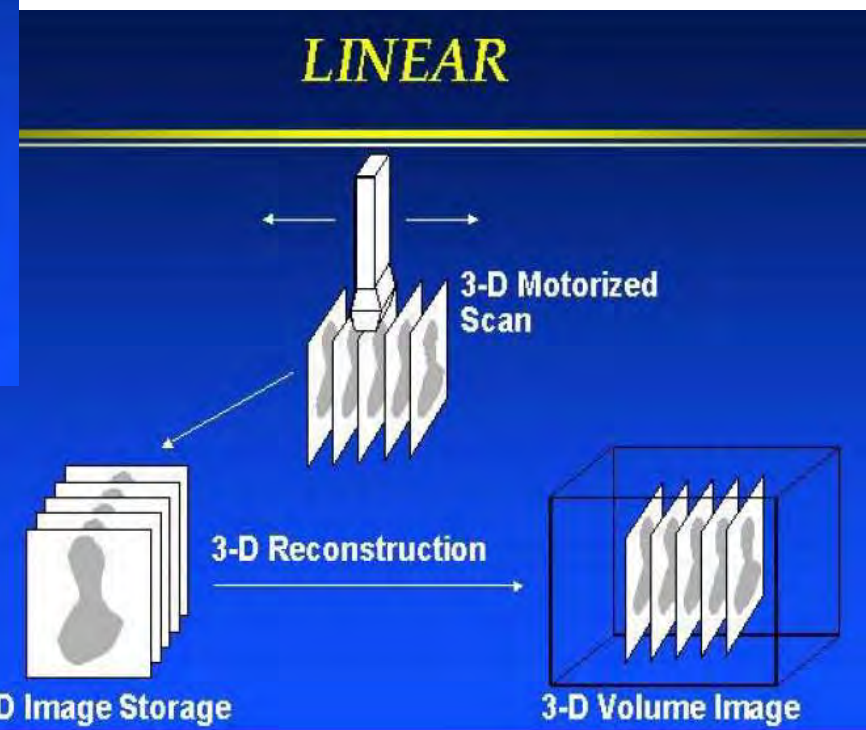
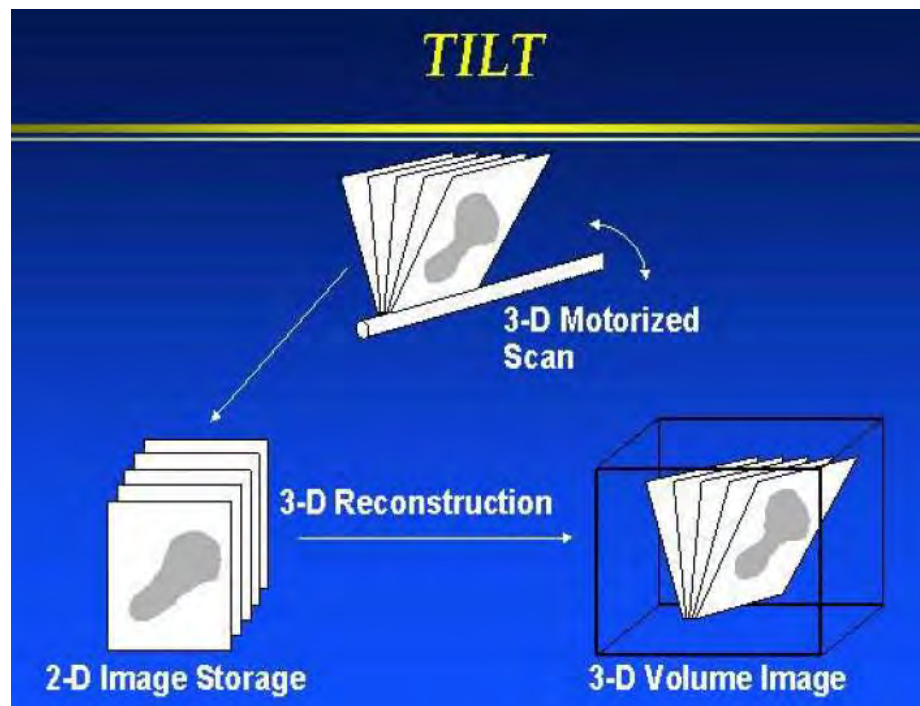


Figure . . 3D Ultrasound Acquisition Based on Mechanical Tilting of Transducer Assembly

Based on the transducer (linear, curvilinear, phased array, etc.) and movement used (tilting, rotational or linear displacement, etc.), the image is acquired in cylindrical, spherical or Cartesian coordinates.

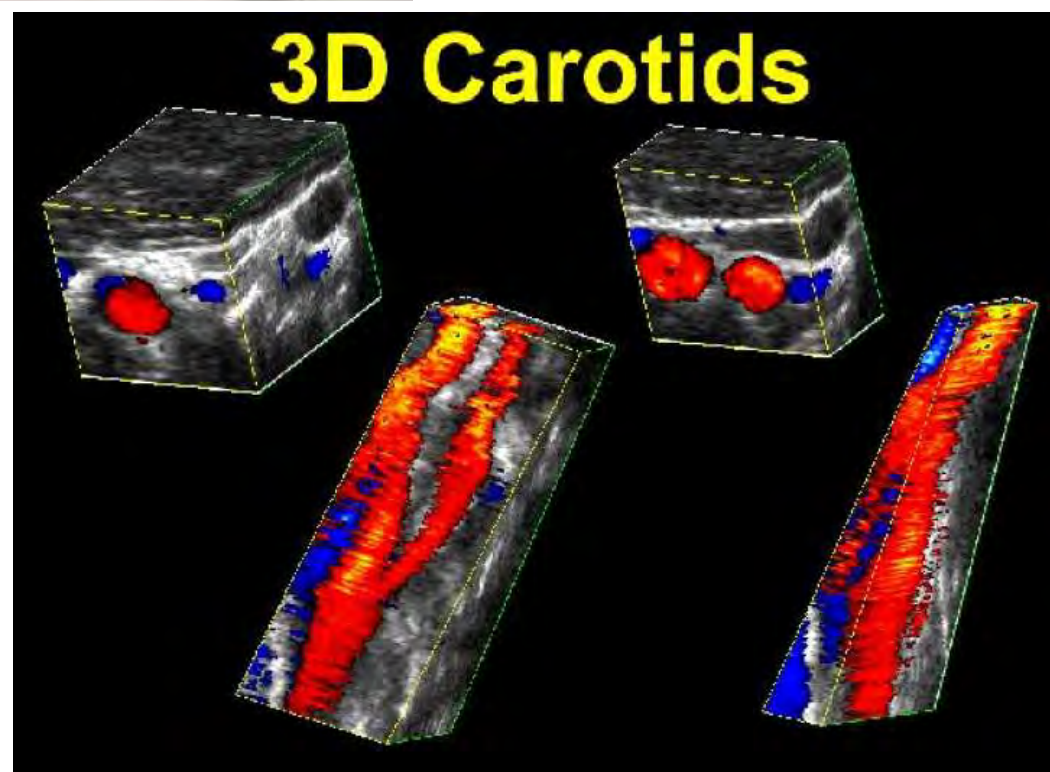
Ultraschall-Bildverfahren-3D

B-Mode-3D-4D? (mechanical)



Ultraschall-Bildverfahren-3D

B-Mode-3D (mechanical)



Ultraschall-Bildverfahren-3D

B-Mode-3D (mechanically tilting)



1999, Dreidimensionale Darstellung eines Feten

Ultraschall-Bildverfahren

B-Mode-3D-4D (electronically)

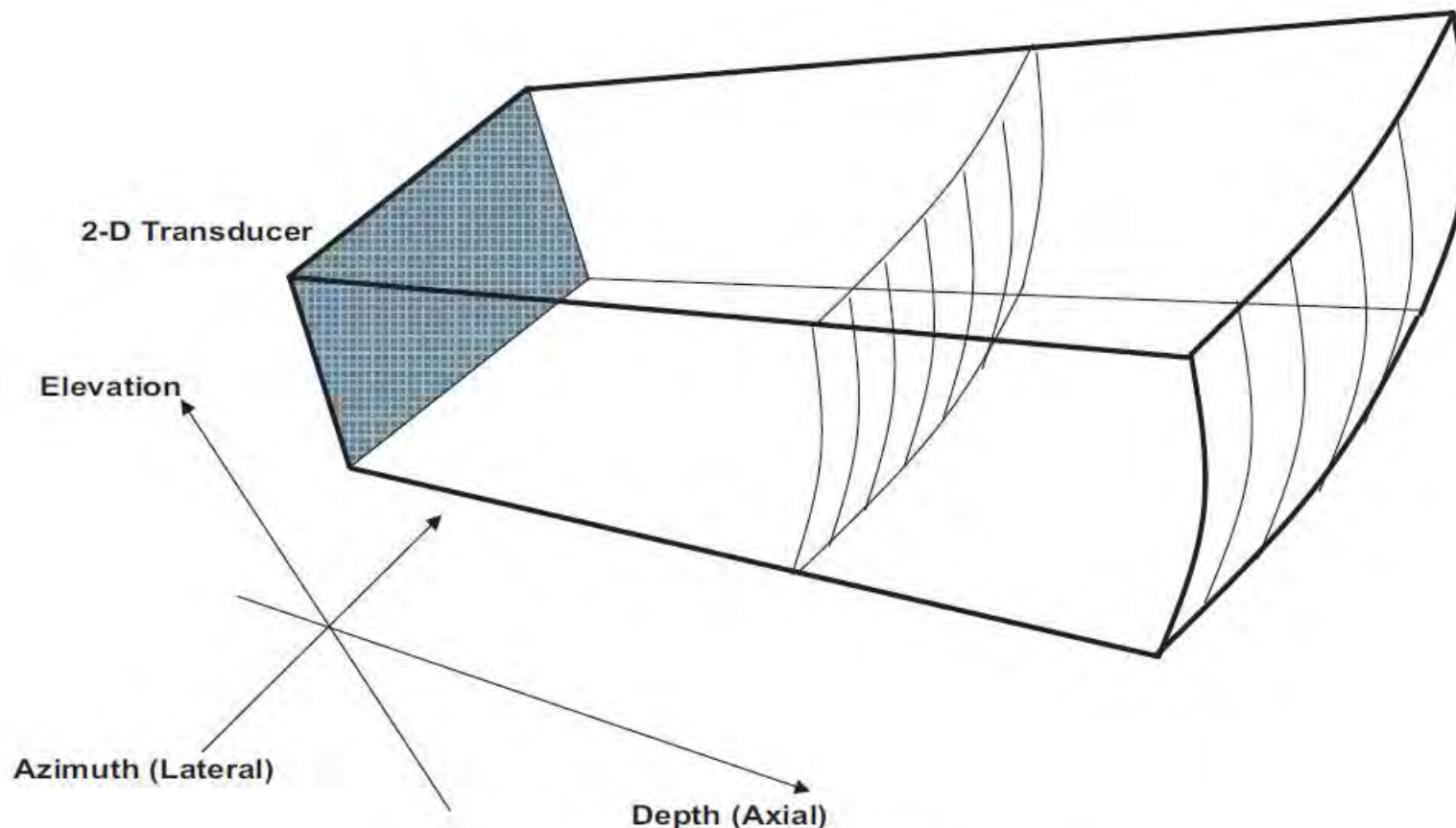


Figure Scanning Using 2D Transducer

Ultraschall-Bildverfahren

B-Mode-3D-4D (scan conversion+ smoothing)

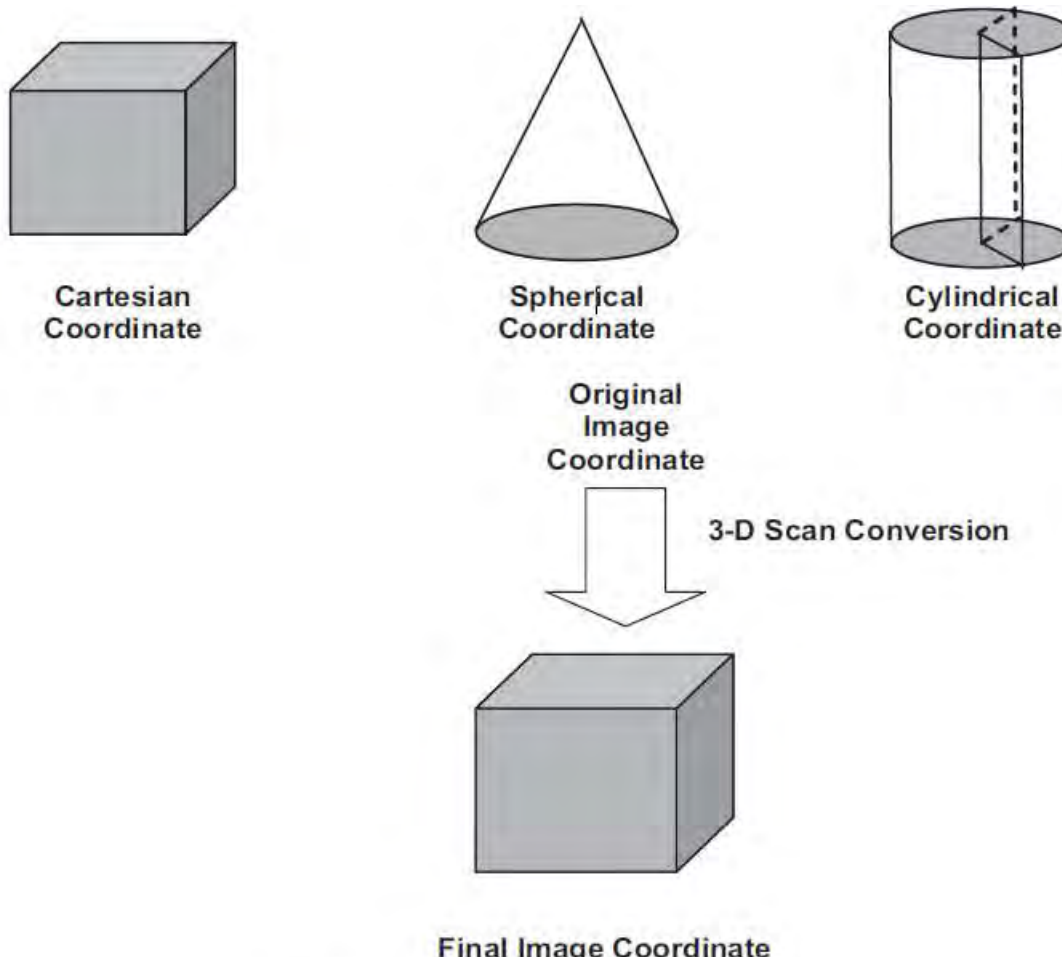


Figure 3D Scan Conversion

Ultraschall-Bildverfahren

B-Mode-3D-4D (tissue extraction, realtime to physician !?)
 Method of Volume rendering: Multiplanar ; Raycasting

Multi-planar rendering (MPR): In this rendering mode, three orthogonal planes are chosen for viewing by the physician as shown in Figure. Computer interface is provided so that the user can choose the planes. The values of the pixels on these planes are extracted and presented for display.

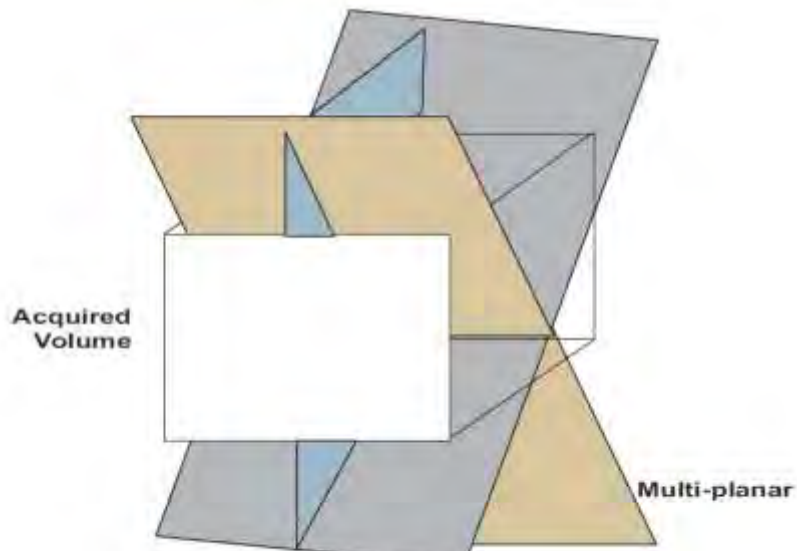


Figure Slices for Multi-Planar Viewing

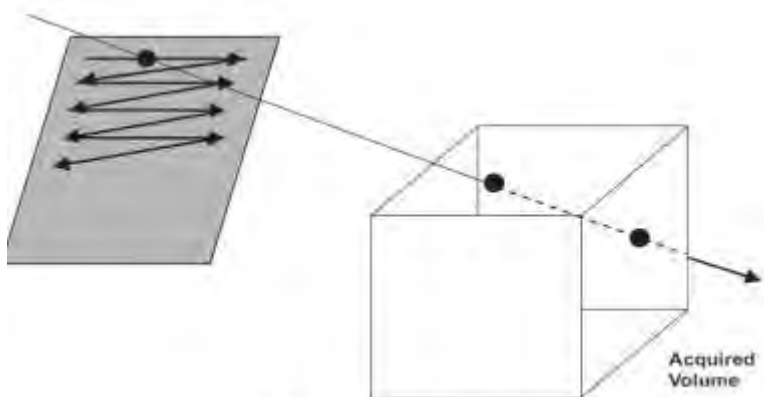
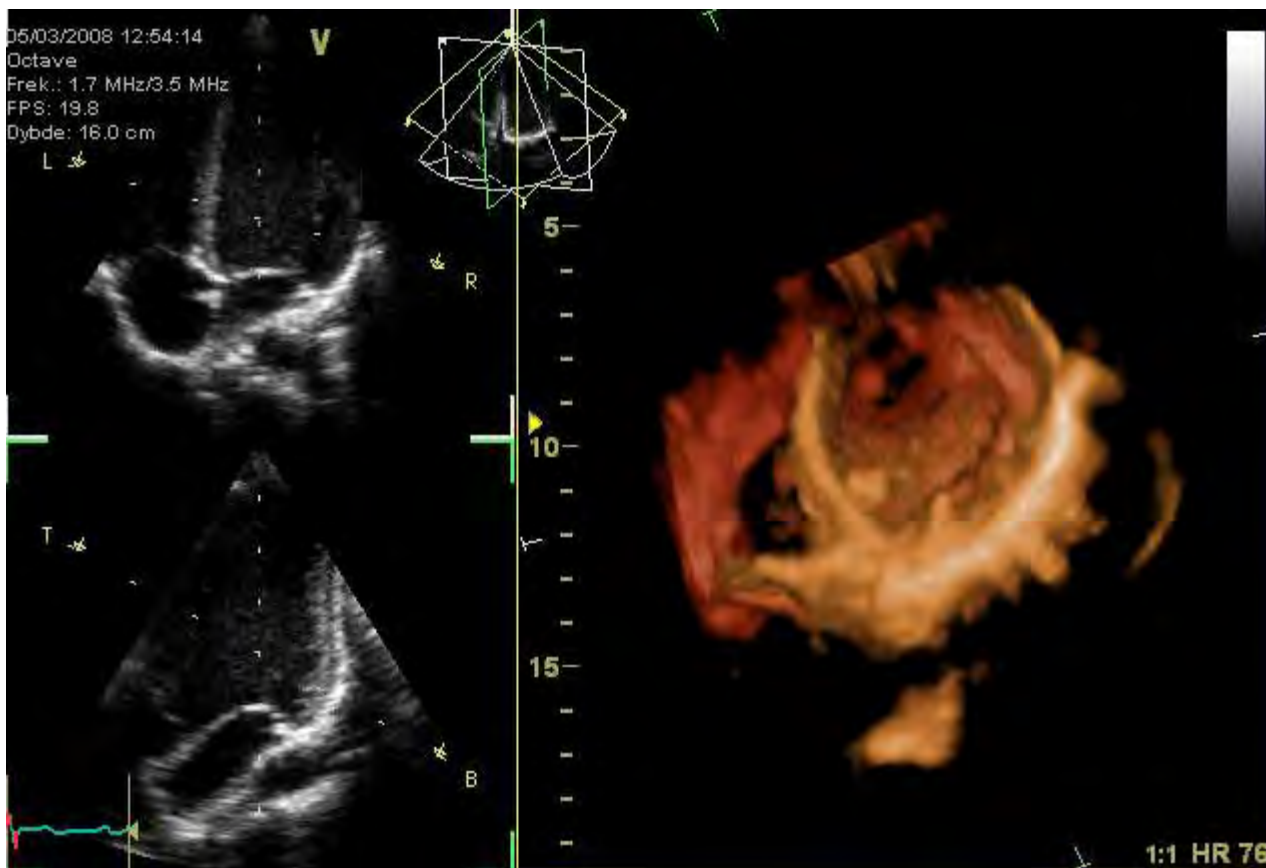


Figure Ray Casting

- Volume rendering: The most common method of volume rendering is ray casting. In this rendering method, an imaginary ray perpendicular to the plane is drawn through the volume for each pixel in the viewing plane (Figure). Since the ray cannot lie exactly on the voxels, trilinear interpolation is usually used to determine the value inside the volume on that ray. The contribution of each point in that ray is then accumulated to determine the overall value of the pixel in the viewing plane. The following methods of accumulation are the most popular for volume rendering.
- Maximum Intensity projection (MIP): Only the maximum value along the ray is taken as the value of pixel in the image plane.
- Opacity accumulation: An opacity value, $a(i)$, and a luminance value, $c(i)$, is assigned to every point in the ray. The opacity is usually dependent on the local value of the pixel and luminance on the local gradient. Then, the rendered value along the ray can be calculated as a weighted accumulated sum, which is given below.

$$V(i) = V(i-1)(1-a(i)) + c(i)a(i)$$

Kardiografie



Ultraschall-Bildverfahren

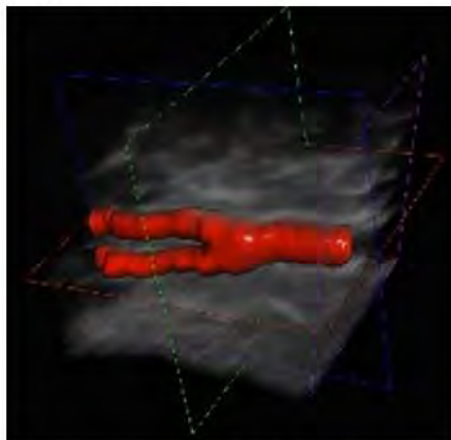
B-Mode-3D-4D (tissue extraction, realtime in real-time today)

<http://www.privatpraxis-gyn.de/3d-4d-ultraschall-frauenarzt.html>



<http://curefab.com/applications/vascular/>

Vascular

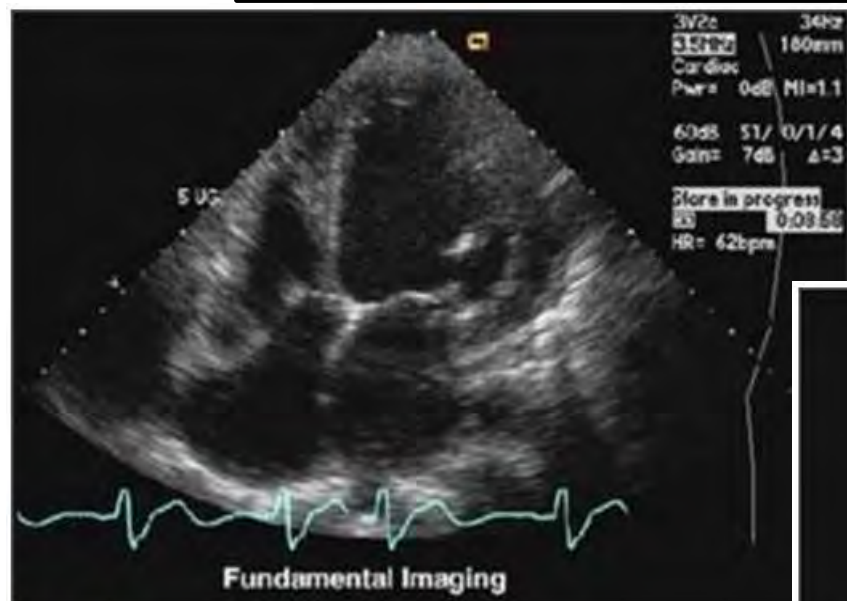


Diagnosing limited functions in arteries and veins with ultrasound is a common clinical practice. Now there even can be accurate quantified data.

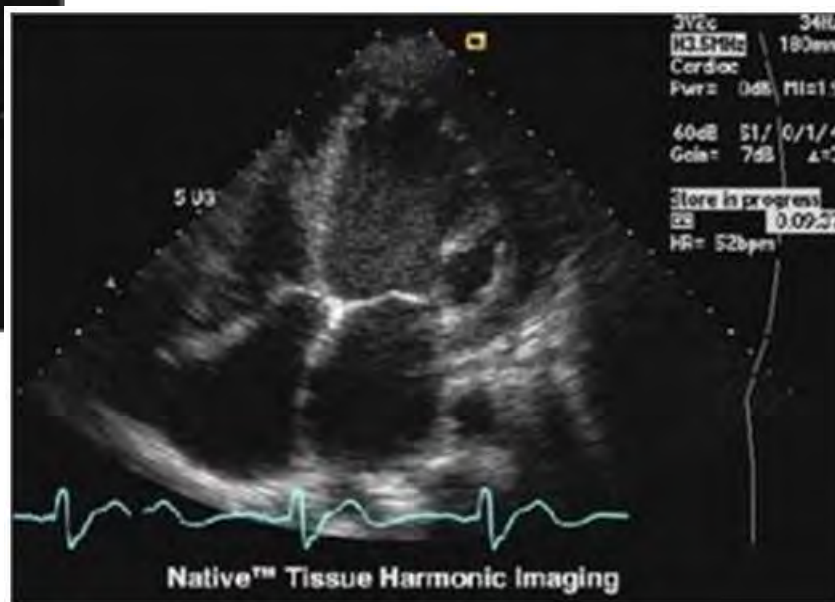


Ultraschall-Bildverfahren

Tissue Harmonic Imager (THI) due to non-linear effects
 (detected using contrast agent for perfusion)



ohne THI



mit THI

$$\text{Tx-frequency } f_0 = \text{Rx-frequency } f_0$$

$\text{Tx-frequency } f_0 < \text{Rx-frequency } 2 \cdot f_0$
 → shows higher spacial resolution
 → As deeper as more second harmonics

Ultraschall und Theragnostik

Ultraschall in Thera(pie) und (Dia)gnostik

Kapitel 5

Doppler-Verfahren in der Diagnostik und Therapie

Inhaltsangabe

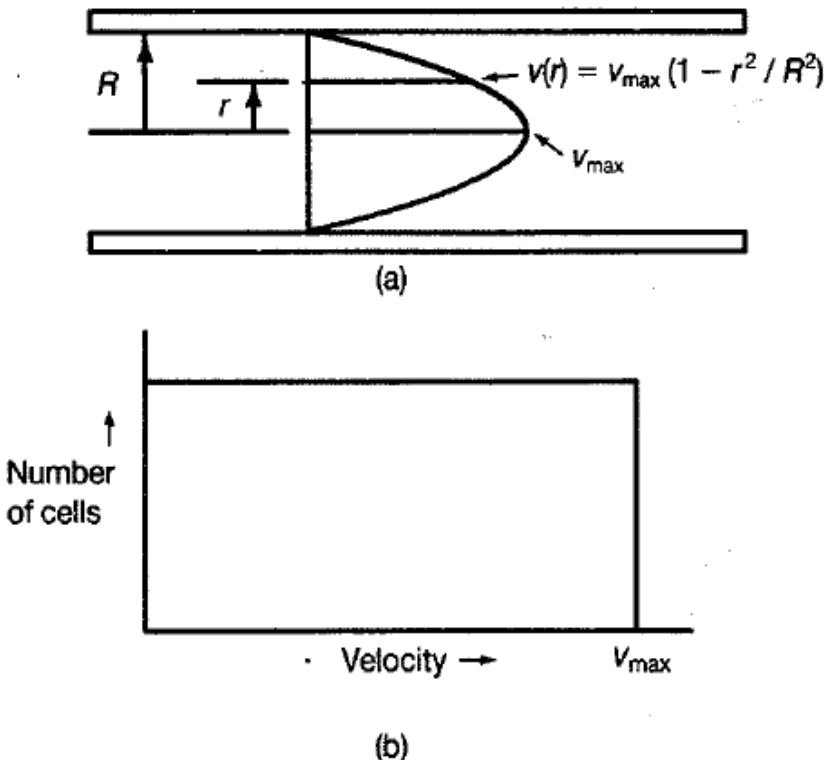
1. Übersicht der Ultraschallanwendungen
2. Physikalische Grundlagen
3. Ultraschallsonden
4. Bildgebende Verfahren in der Diagnostik
5. **Dopplerverfahren in der Diagnostik und Therapie**
6. Artefakte und Diagnostik
7. Ultraschall und Kontrastmittel
8. Theragnostik mit Ultraschall
9. Therapie mit hochdosierten Ultraschall
10. Gewebecharakterisierung mittels shear waves
11. Dosierung und Sicherheitsaspekte

Doppler Ultrasound key words

- Bloodflow ;
- Velocity profiles
- Doppler Effect
- Doppler Shift Frequencies
- Spectral Doppler \leftrightarrow Spectrogram
- Power M-Mode Doppler
- Emboli detection /HITs
- Contrast agent ; Bolus ; Medication
- Embolyse, TPA-plus

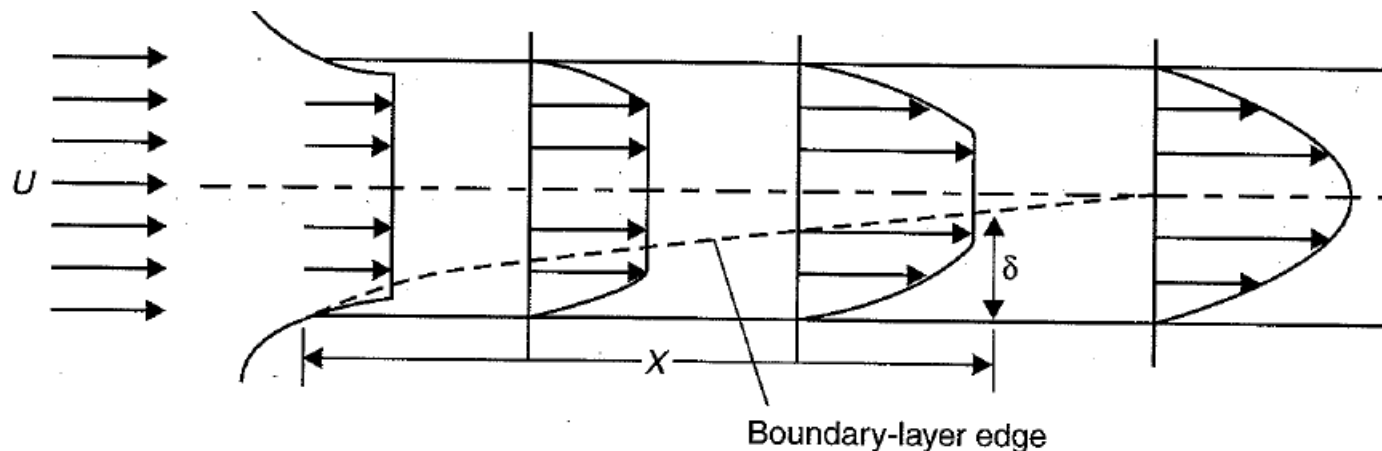
Doppler Basics: Blood flow profiles

Flow resistance: $\Delta p = 8\mu QL/\pi R^4$

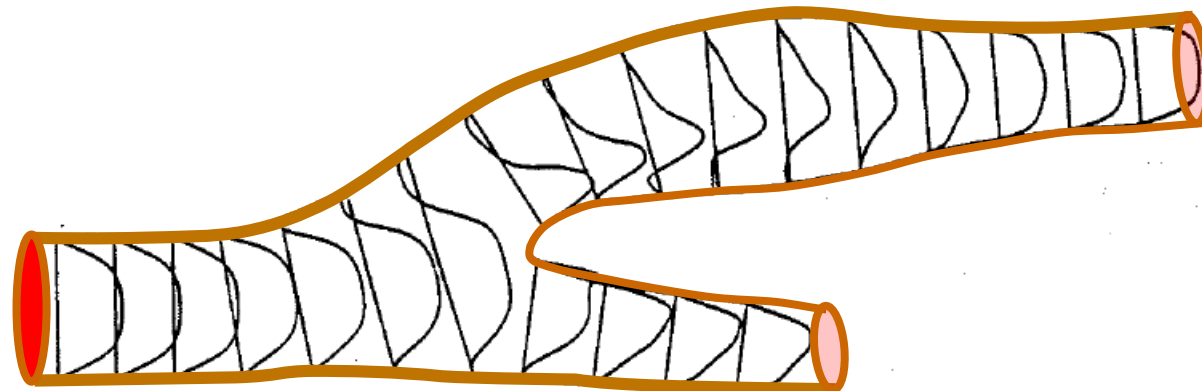


(a) Parabolic velocity profile found in steady laminar flow in a long cylindrical pipe. (b) Histogram illustrating the number of cells moving with a given velocity in the profile shown in (a). From this it follows that for this type of profile the maximum velocity is twice the mean velocity

Doppler Basics: Blood flow profiles

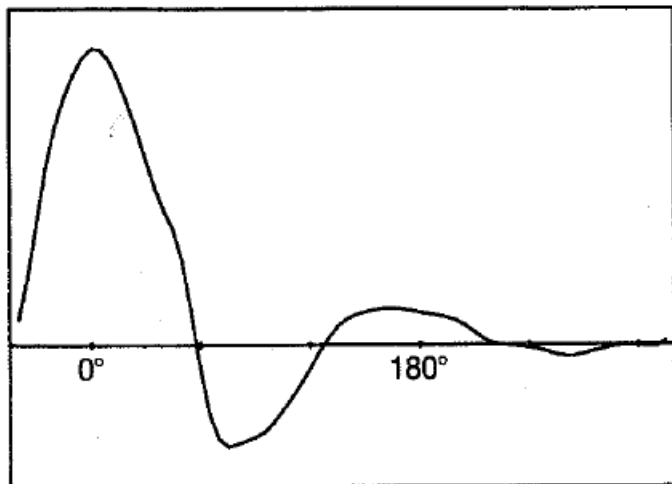


The development of the steady-state parabolic velocity profile at the entrance to a tube. The initially flat profile becomes progressively modified as the boundary layer grows with distance from the inlet (reproduced by permission from Caro et al 1978, Oxford University Press)

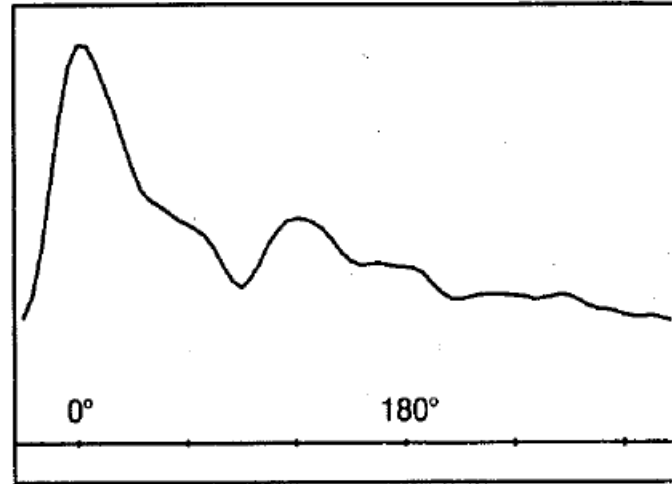


Velocity profiles calculated from a mathematical model of the human carotid bifurcation (in the branching plane)

Doppler Basics: Blood flow profiles



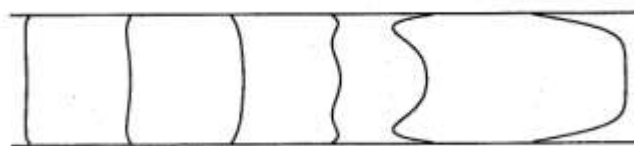
(a)



(b)

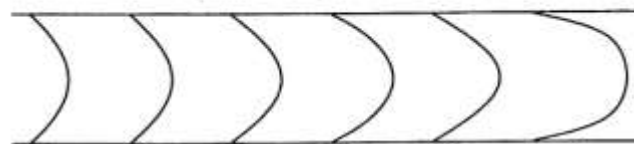
Mean velocity waveforms recorded from (a) the common femoral and (b) the common carotid arteries

profile common femoral artery



360° 240° 180° 120° 90° 0°

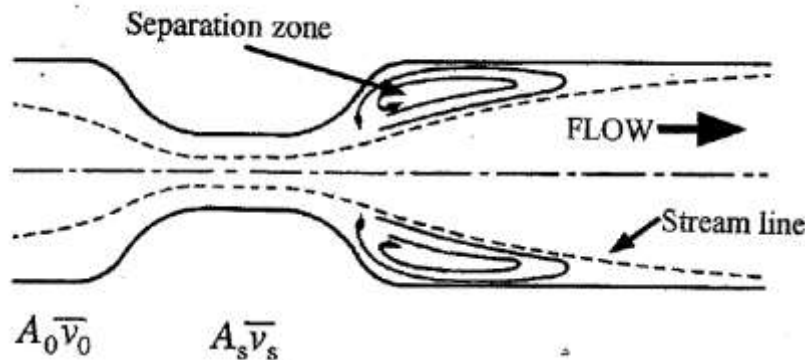
profile common carotid artery



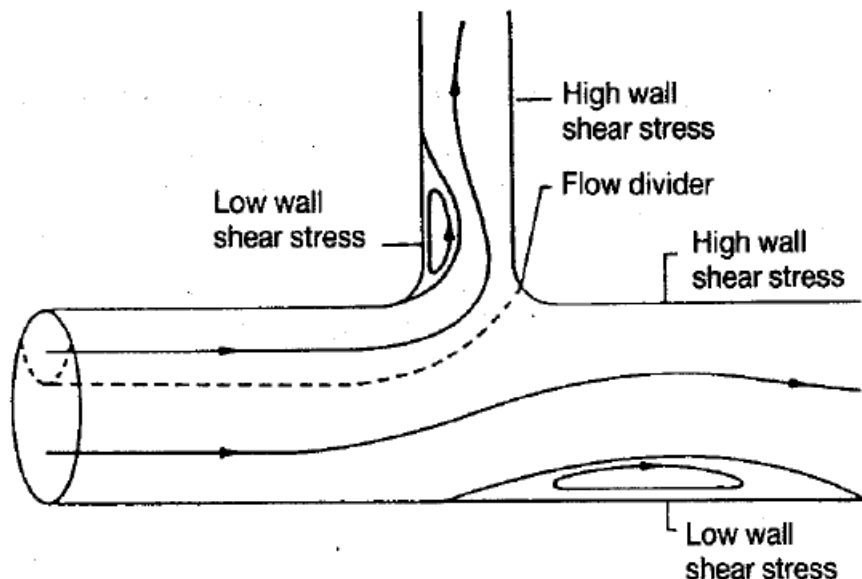
Doppler Basics: Blood flow profiles

bifurcation

stenosis



Schematic diagram of flow through a simple smooth stenosis, showing convergence of the stream-lines (and hence a velocity increase) and post-stenotic recirculation



Flow at right-angled junction. The dashed line is the surface dividing the fluid which flows down the side branch from that continuing in the main tube; the solid lines are stream lines. Note the closed eddies in the two regions of separated flow. Regions of high and low shear are also indicated

Physics: Doppler Effect

Doppler Effect

Doppler Formula:

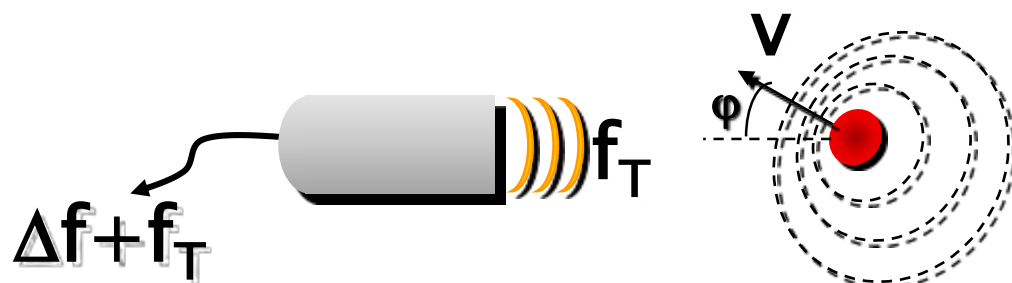
$$\Delta f = 2 f_T (v / c) \cos\{\varphi\}$$

$\Delta f = f_D$: Doppler shift frequency

f_T : transmitting frequency

c : Sound velocity

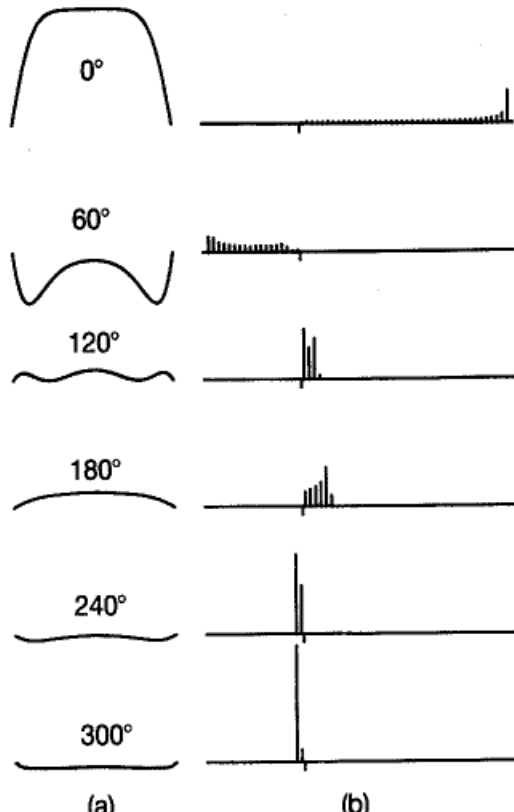
v : target velocity



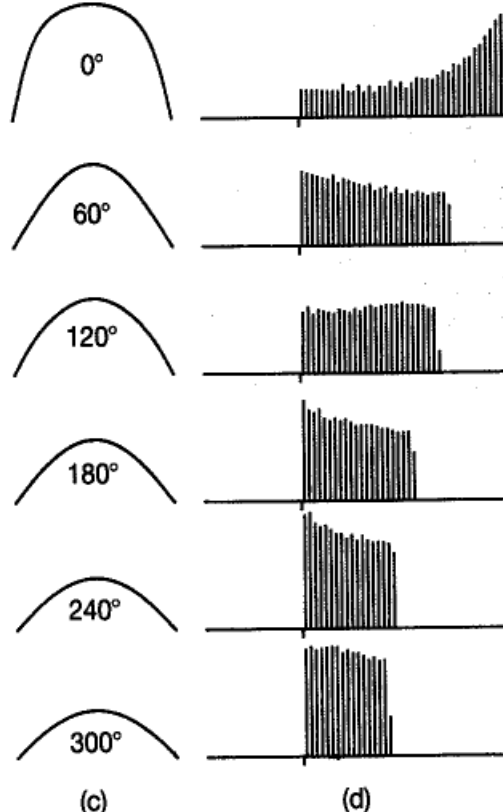
Velocity profiles and Doppler shift frequency

Doppler Power Spectrum (Audiosignals) <-> Velocity profile

A. femoralis



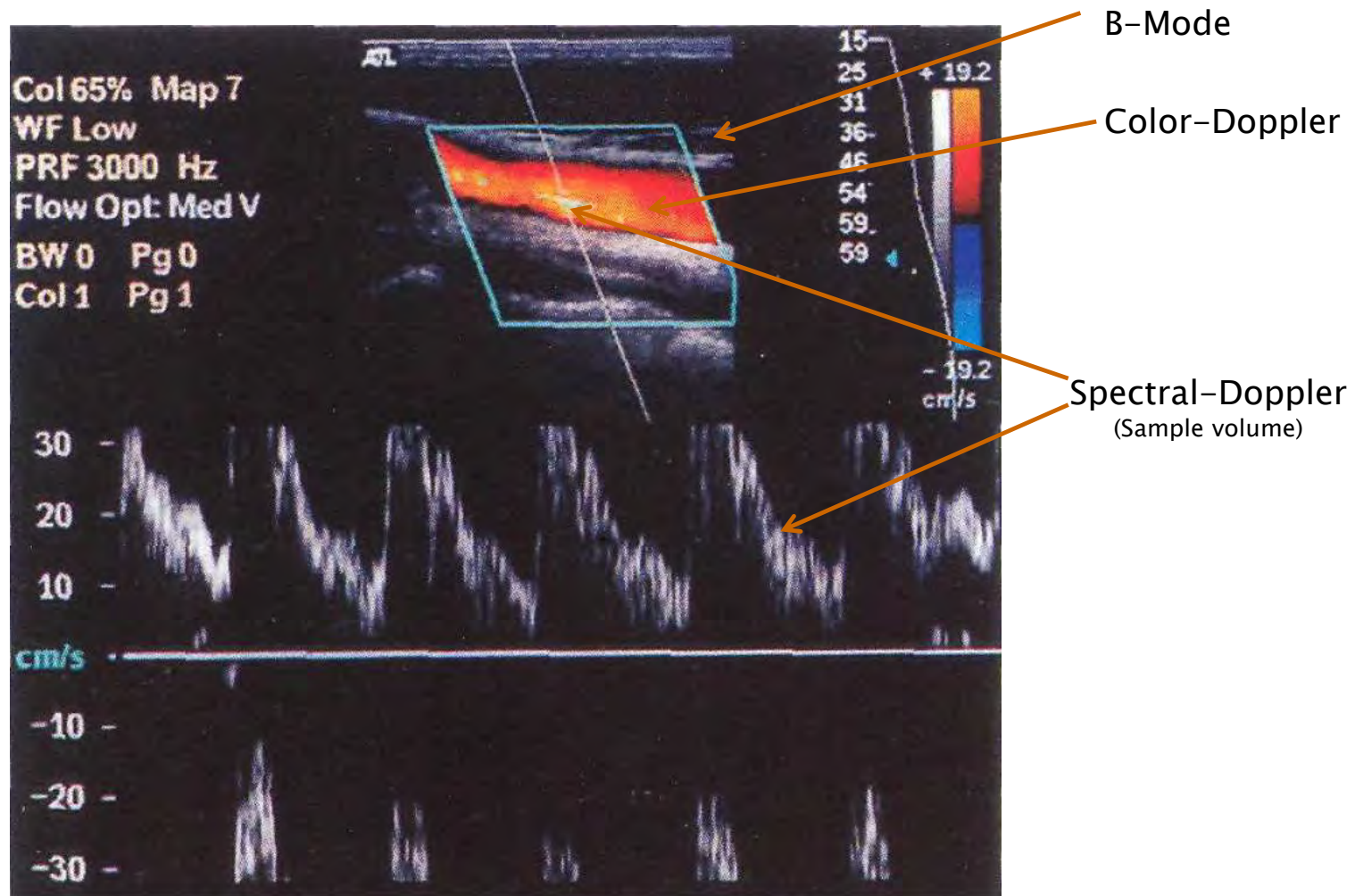
A. Common carotid



Series of velocity profiles for a common femoral artery (a) and common carotid artery (c), together with corresponding velocity distribution histograms (b) and (d). The peak of forward flow has been arbitrarily called 0° and the maximum velocities have been scaled to have the same amplitude

Summary: Doppler Imaging Systems

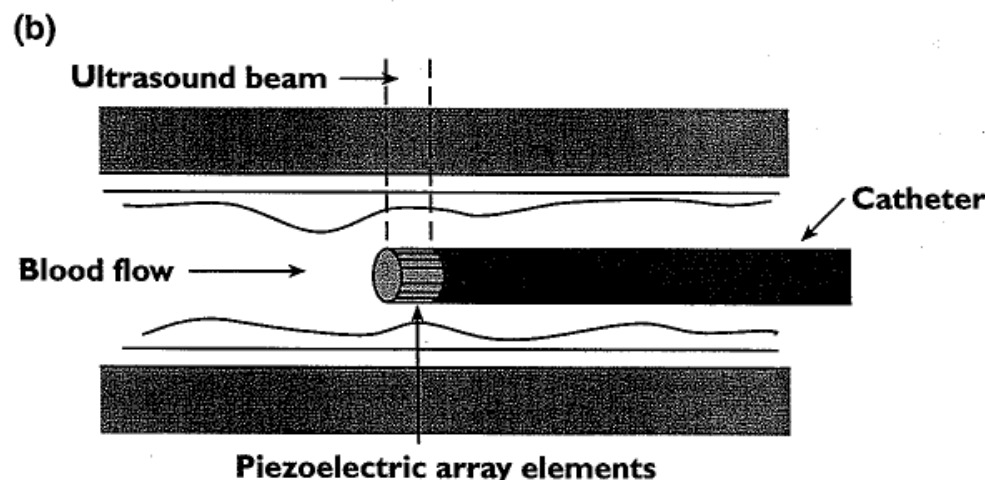
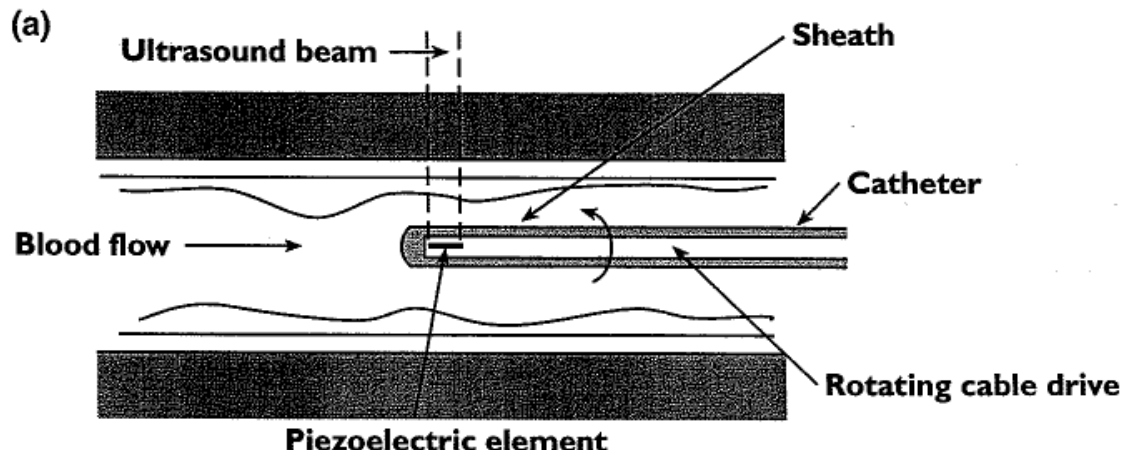
Duplex Imaging + Spectral Doppler



A triplex image representing B-mode, colour Doppler velocity image and spectral Doppler in the same display. The aliasing artefact is seen in both the colour Doppler velocity image and in the corresponding spectral Doppler

Summary: Katheder Doppler Systems

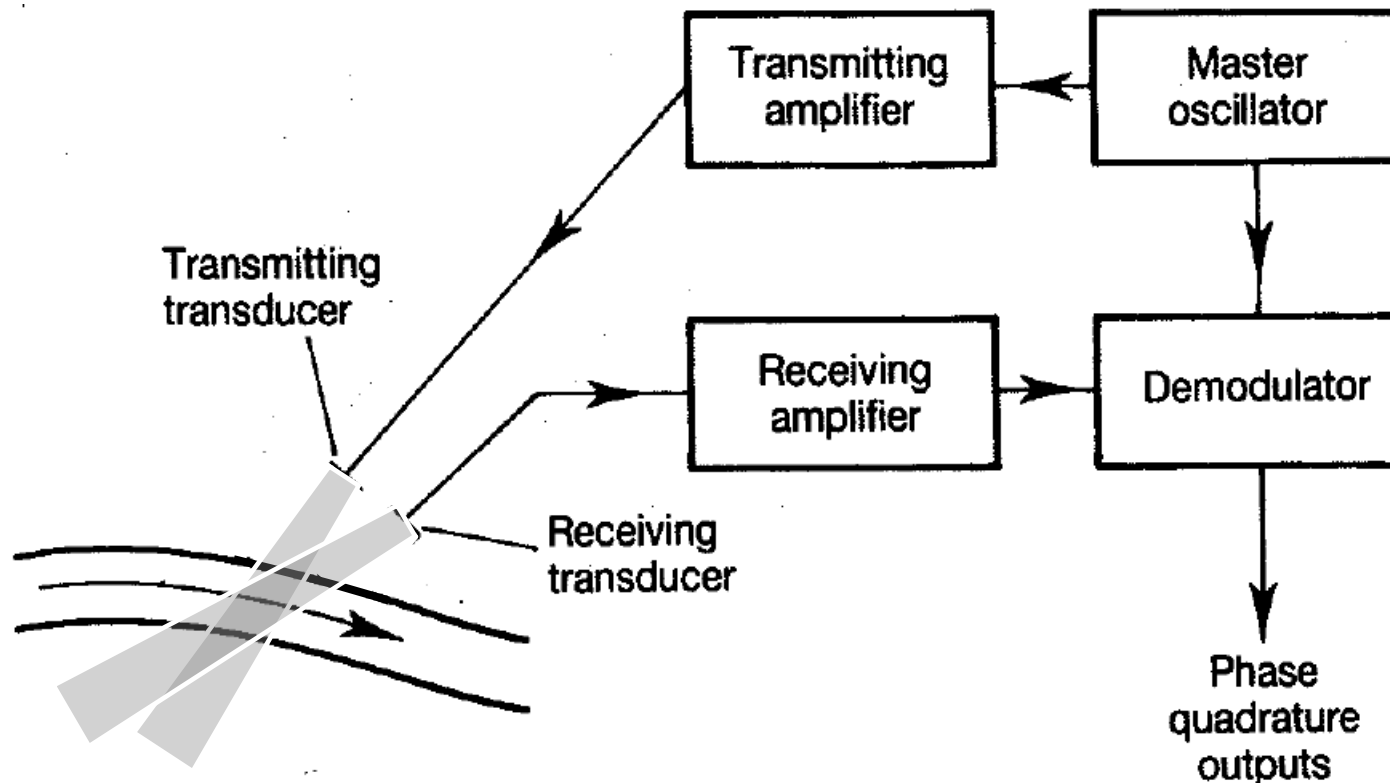
Intravascular Ultrasound



Intravascular ultrasound (IVUS) imaging catheters, (a) mechanical scanner, (b) phased array. Field of view is 360°

Summary: CW–Doppler Systems

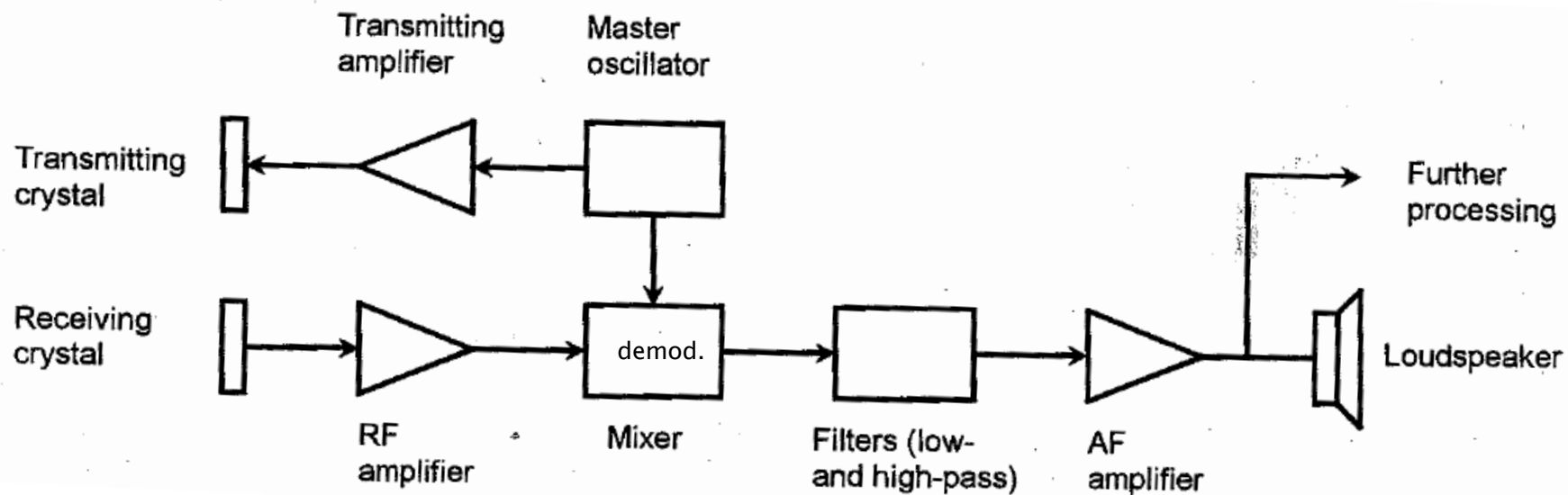
Application Continuous Wave System (single beam)



Block diagram of a continuous wave Doppler system

Summary: CW–Doppler Systems

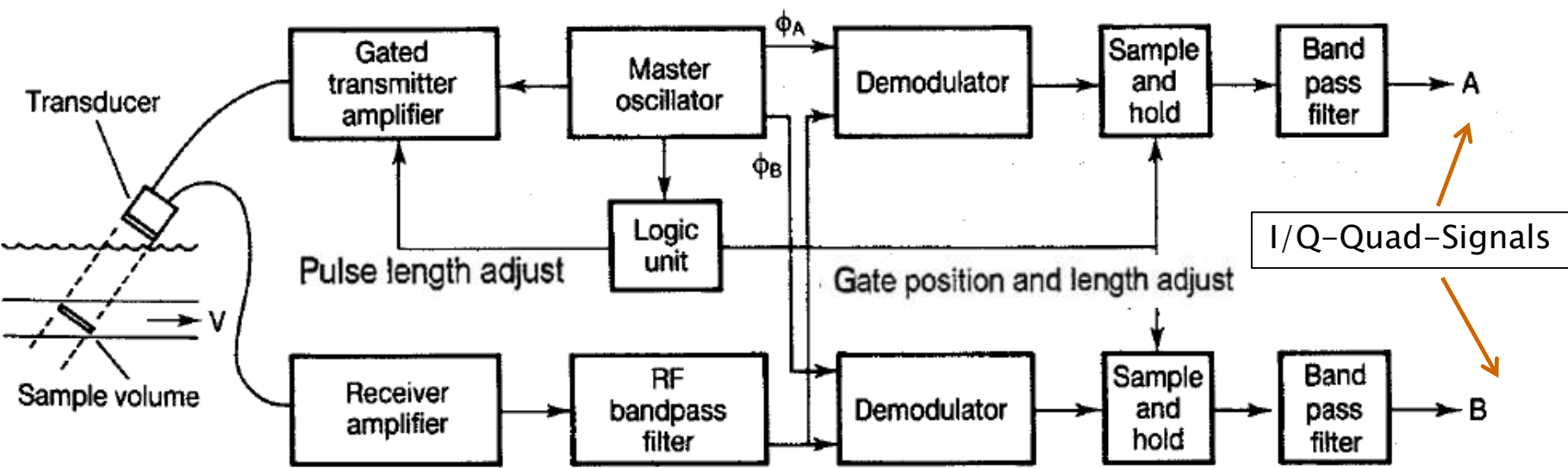
Continuous Wave System signal conditioning and electronics



Block diagram of a continuous wave Doppler system → no depth-sensitive

Summary: PW-Doppler Systems

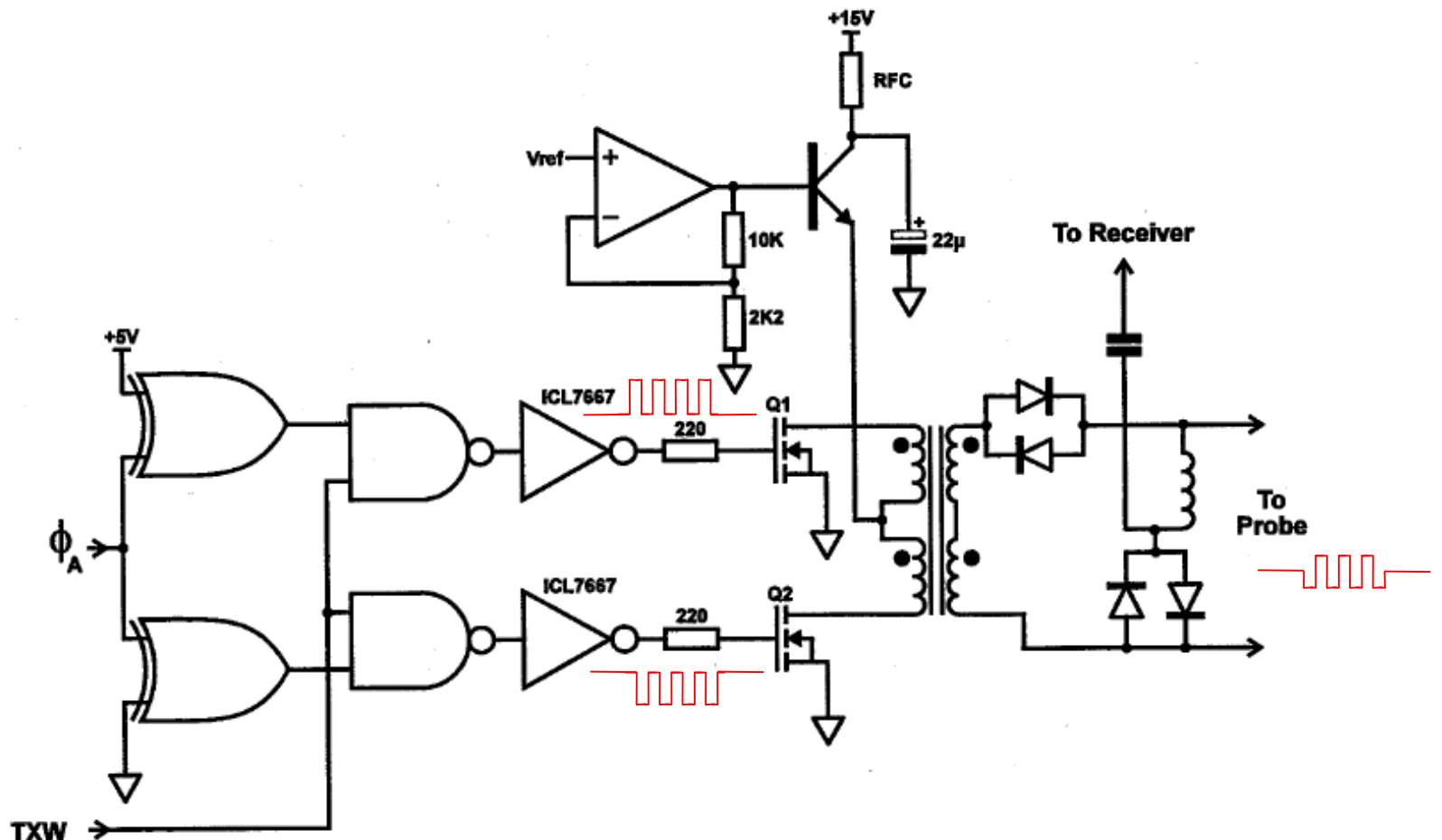
Signal conditioning of Pulsed Wave System (single beam) and electronics



Block diagram of a pulsed Doppler system

Summary: CW/PW-Doppler Systems

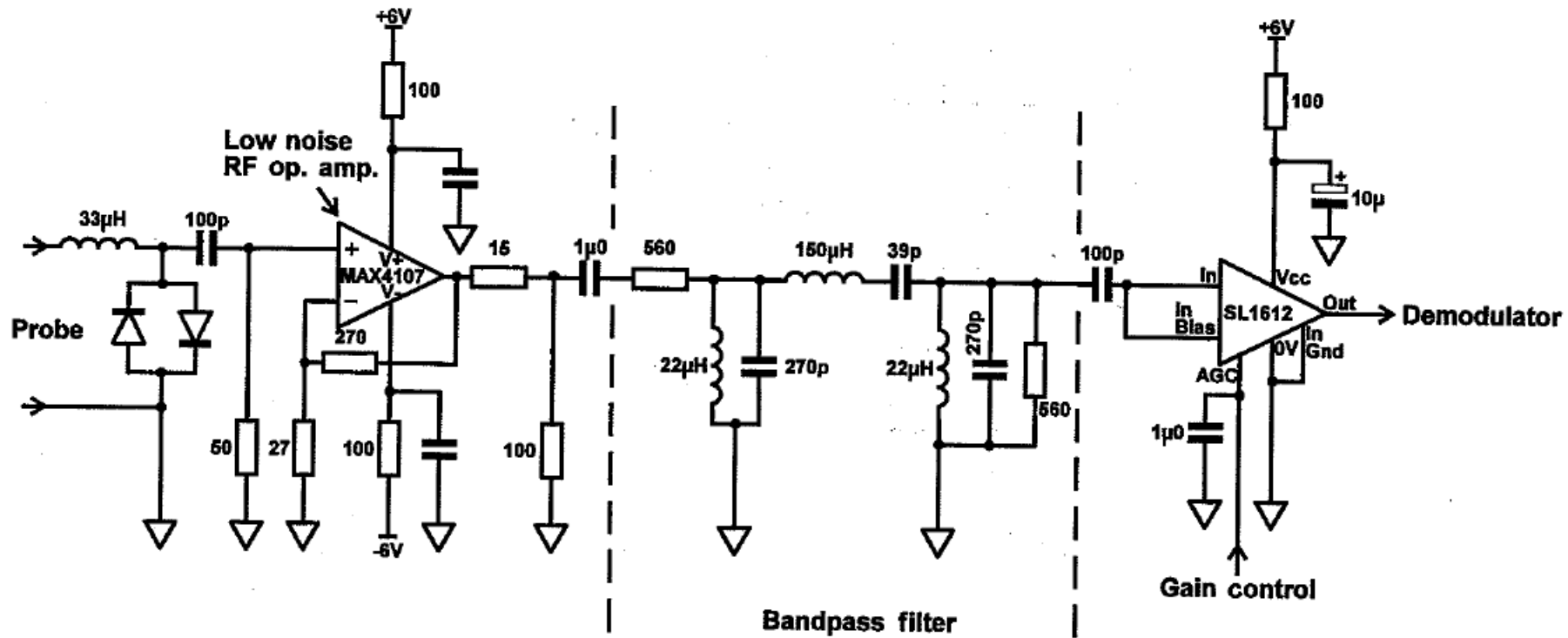
Pulsed Wave System : RF-Transmitter



Circuit diagram of a wideband transmitter system for continuous and pulsed wave applications. ϕ_A , operating clock frequency; TXW, transmission burst width (PW operation only); Vref, output voltage control. Q₁, Q₂ are MOSFET devices

Summary: CW/PW-Doppler Systems

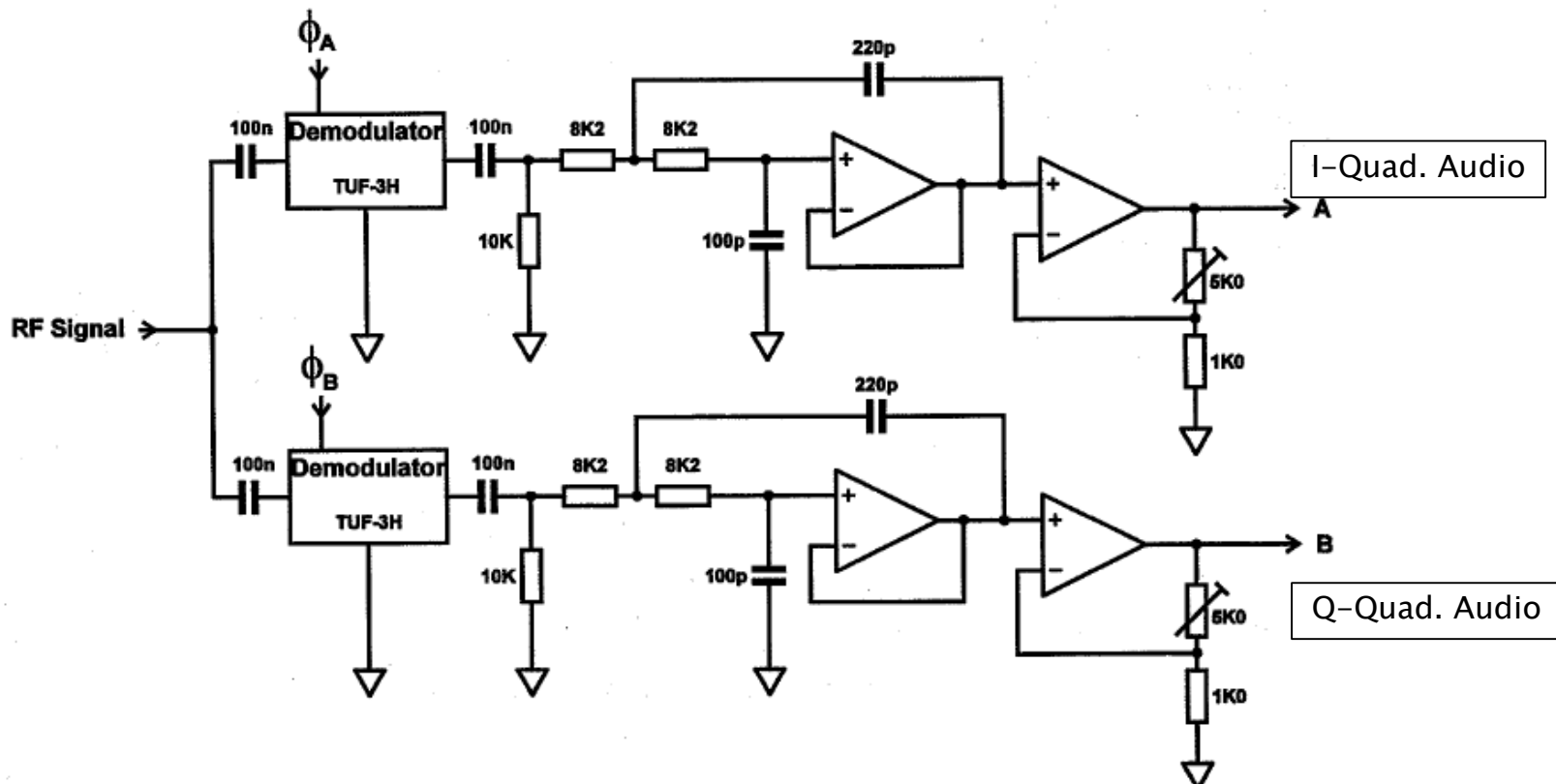
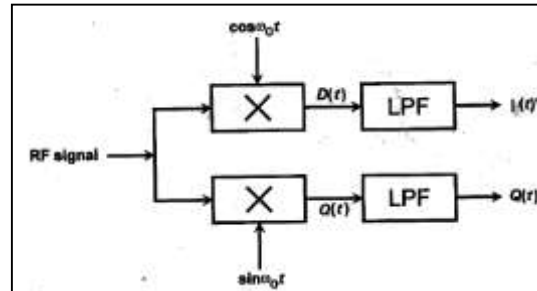
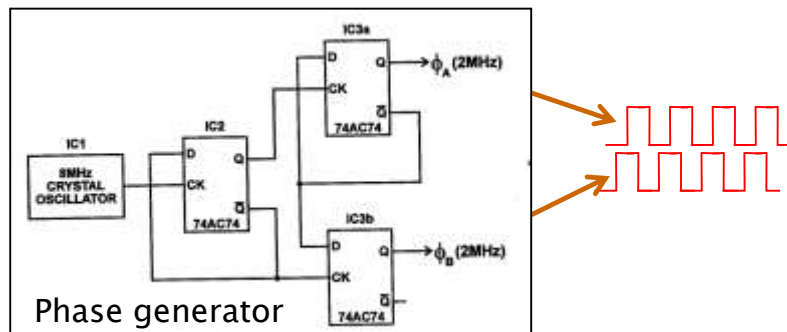
Pulsed Wave System : Analog RF-Receiver



Circuit diagram of a wideband continuous or pulsed wave Doppler receiver. The 33 μ H coil and the diode combination are protection from the transmission burst for pulsed Doppler applications. The bandpass filter illustrated is for a 2 MHz system. The final amplification stage is a voltage-controlled amplifier

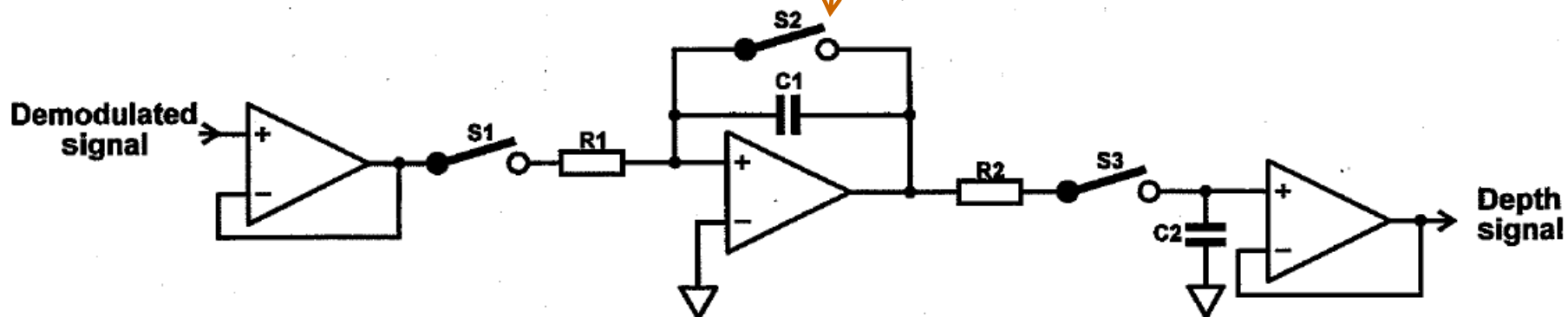
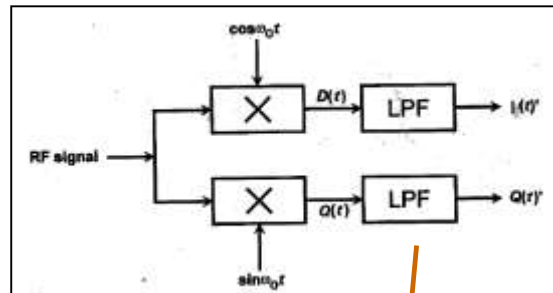
Summary: CW/PW-Doppler Systems

Pulsed Wave System : Receiver analog signal processing ; I/Q-Modulator



Summary: PW-Doppler Systems

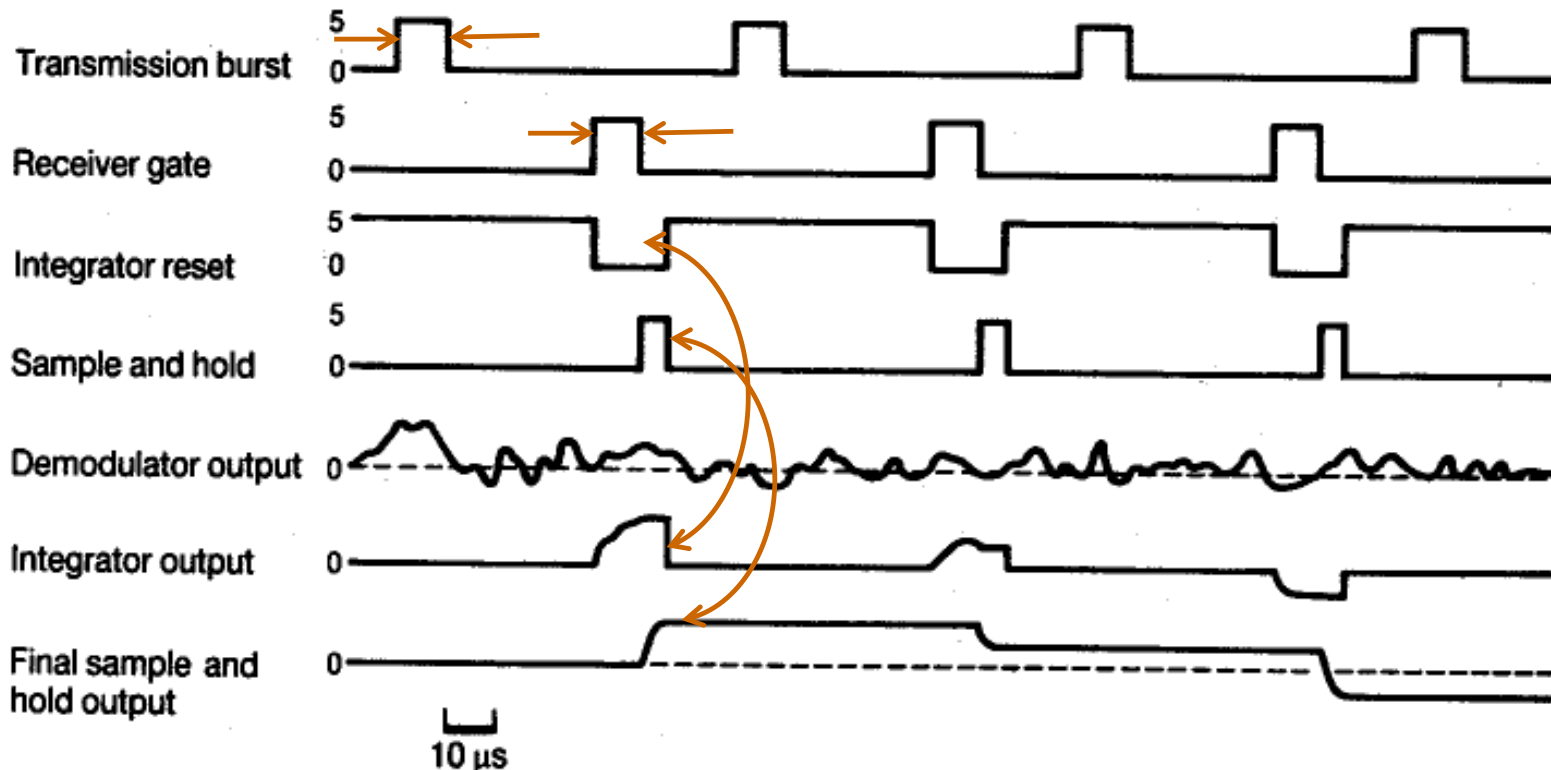
Pulsed Wave System : LF-part of Receiver and signal processing → Sample Volume (SV)



Pulsed Doppler integrating sample and hold system. Switch S1 samples the signal for a period defined by the gate length. During this time the signal is integrated. The final integrated voltage is then sampled and held via S3/C2. The integrator is then reset by switch S2 and the sequence restarted on the next pulse repetition cycle

Summary: PW-Doppler Systems

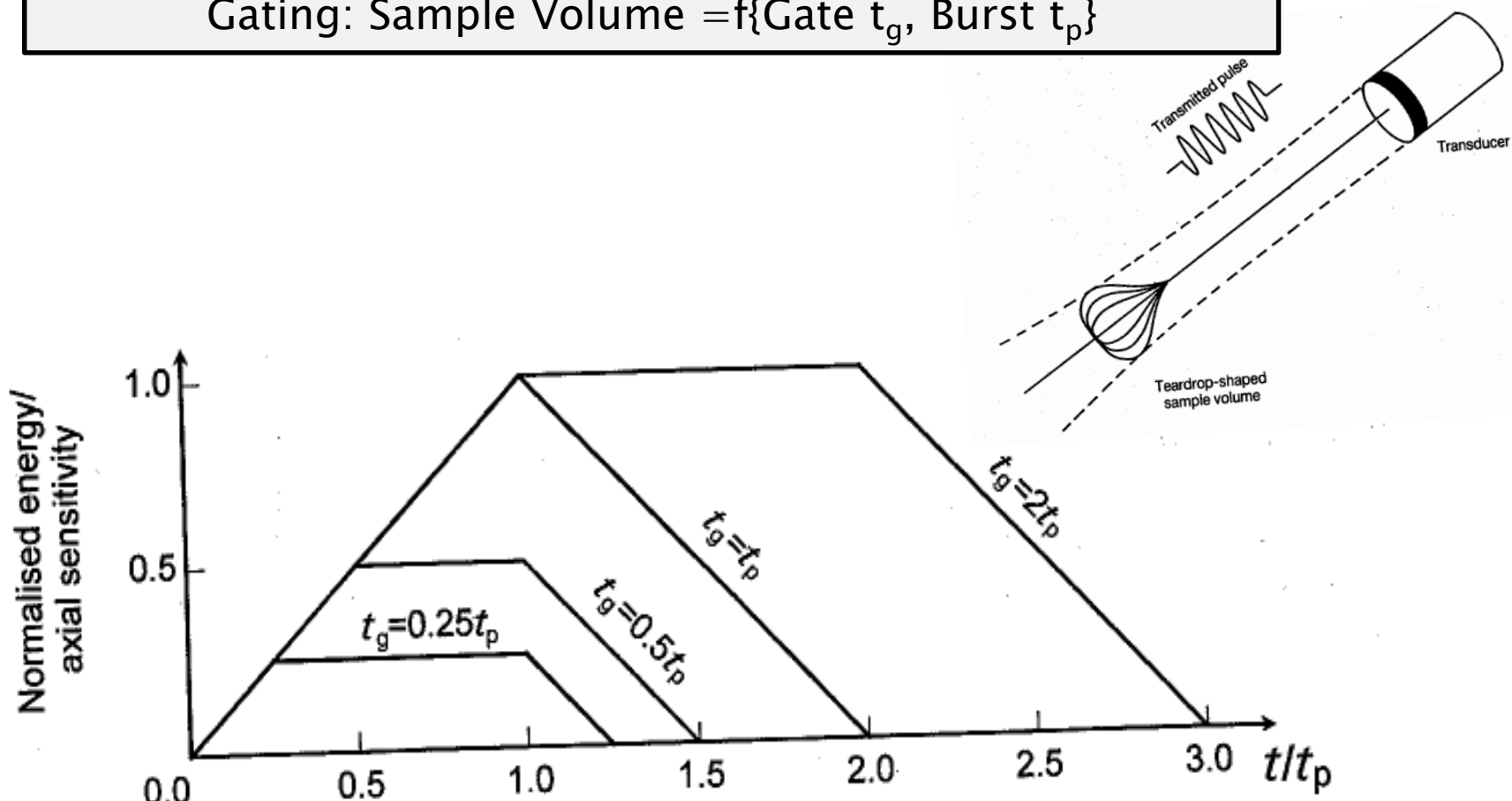
Signal detection and pre-processing in PW_Receiver with gating



Timing diagram illustrating the sequence of events during the sampling of a Doppler signal in a PW system

Summary: PW-Doppler Systems

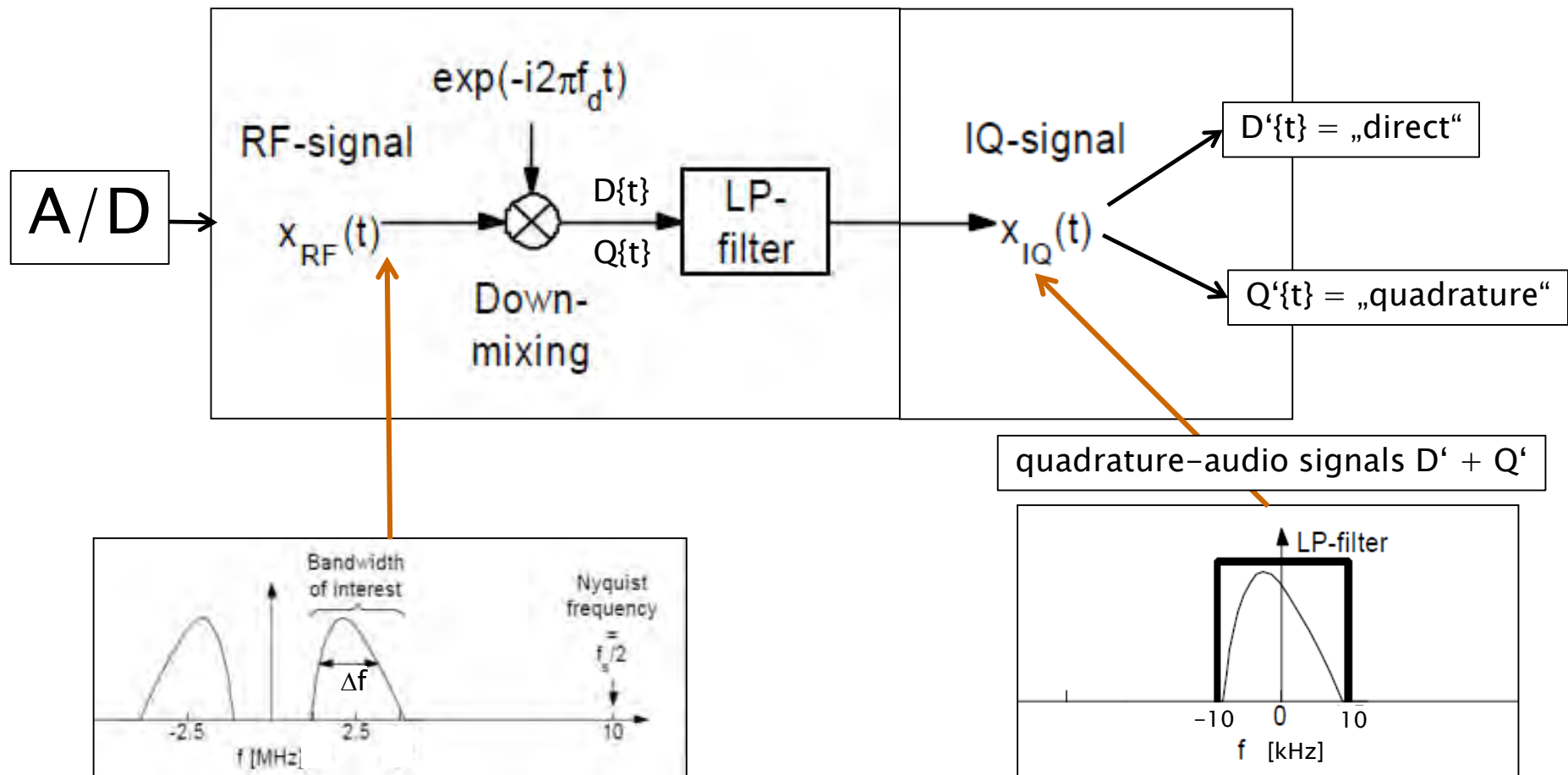
Gating: Sample Volume =f{Gate t_g , Burst t_p }



Axial sensitivity of a PW sample volume for a rectangular pulse of length t_p , and a rectangular receive gate of length t_g . The abscissa is scaled in terms of pulse length and can be converted to distance by multiplying by $(t_p c)/2$ where c is the velocity of ultrasound. The sensitivity, plotted along the ordinate, is normalised to the maximum attained using a value of $t_g \geq t_p$.

Summary: Doppler Systems

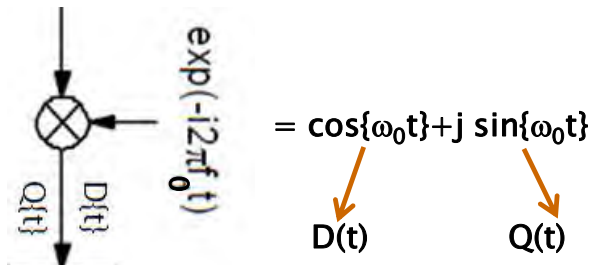
Digital/Analog-Doppler Receiver/Demodulator):
 forward-, reverse flow/frequency



Summary: Doppler Systems

Principle Doppler Receiver/Demodulator):
 Forward (f_f), reverse (f_r) flow/frequency

$$X_{RF} = S(t) = A_0 \cos(\omega_0 t + \phi_0) + A_f \cos(\omega_0 t + \omega_f t + \phi_f) \\ + A_r \cos(\omega_0 t - \omega_r t + \phi_r)$$



$$D(t) = \frac{1}{2}A_0[\cos(\phi_0) + \cos(2\omega_0 t + \phi_0)] \\ + \frac{1}{2}A_f[\cos(\omega_f t + \phi_f) \\ + \cos(2\omega_0 t + \omega_f t + \phi_f)] \\ + \frac{1}{2}A_r[\cos(\omega_r t - \phi_r) \\ + \cos(2\omega_0 t + \omega_r t + \phi_r)]$$

LPF

$$D(t)' = \frac{1}{2}A_f \cos(\omega_f t + \phi_f) \\ + \frac{1}{2}A_r \cos(\omega_r t - \phi_r)$$

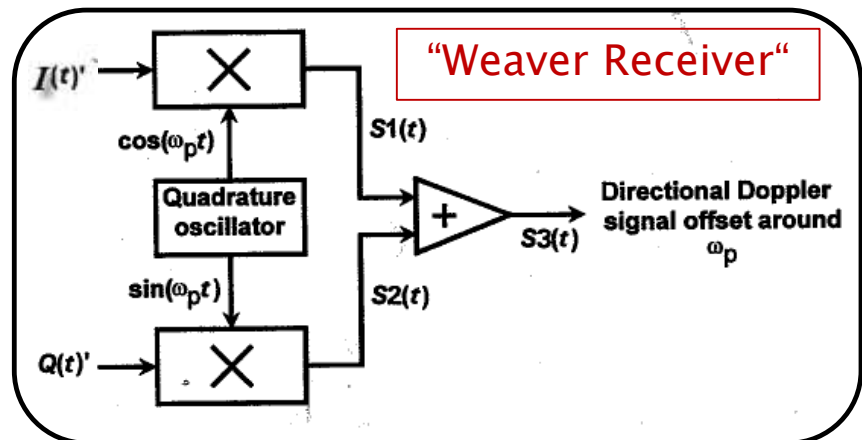
$Q(t) = \dots$

→

$$Q(t)' = -\frac{1}{2}A_f \sin(\omega_f t + \phi_f) \\ + \frac{1}{2}A_r \sin(\omega_r t - \phi_r)$$

Summary: Doppler Systems

Directional flow detection → Weaver method



Multiplying by $A_p \cos(\omega_p t)$ results in:

$$S1(t) = \frac{1}{2}A_p \{ A_f \cos(\omega_f t + \phi_f) \cos(\omega_p t) + A_r \cos(\omega_r t - \phi_r) \cos(\omega_p t) \} \quad 6.14$$

which can be expanded to give:

$$S1(t) = \frac{1}{4}A_p \{ A_f [\cos(\omega_p t - \omega_f t - \phi_f) + \cos(\omega_p t + \omega_f t + \phi_f)] + A_r [\cos(\omega_p t - \omega_r t + \phi_r) + \cos(\omega_p t + \omega_r t - \phi_r)] \} \quad 6.15$$

Multiplying by $A_p \sin(\omega_p t)$ results in:

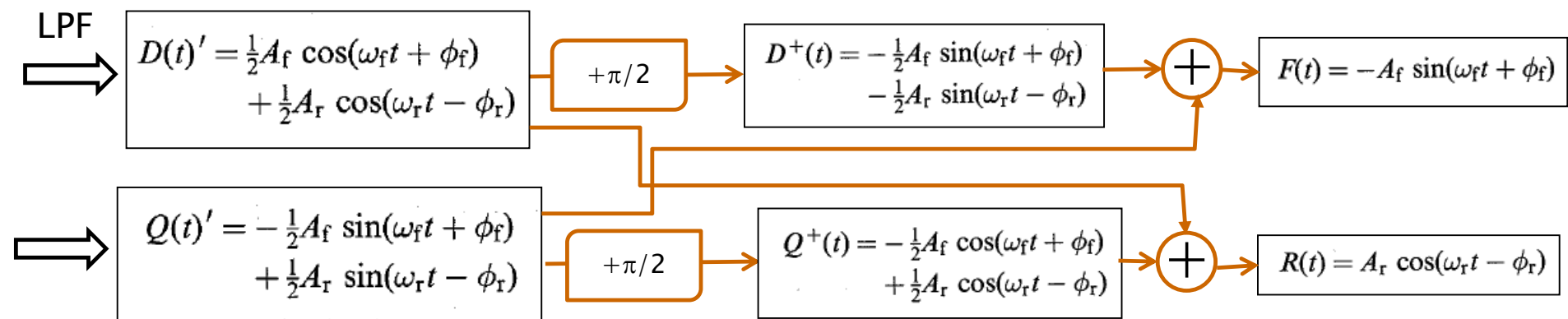
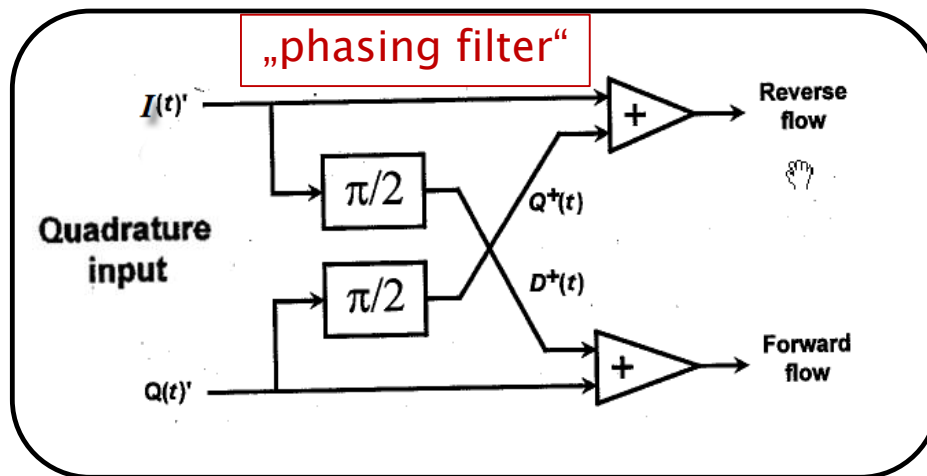
$$S2(t) = \frac{1}{4}A_p \{ A_f [-\cos(\omega_p t - \omega_f t - \phi_f) + \cos(\omega_p t + \omega_f t + \phi_f)] + A_r [\cos(\omega_p t - \omega_r t + \phi_r) - \cos(\omega_p t + \omega_r t - \phi_r)] \} \quad 6.16$$

Finally, adding eqns 6.15 and 6.16 results in:

$$\begin{aligned} S3(t) &= S1(t) + S2(t) \\ &= \frac{1}{2}A_p \{ A_f \cos[(\omega_p + \omega_f)t + \phi_f] + A_r \cos[(\omega_p - \omega_r)t + \phi_r] \} \end{aligned} \quad 6.17$$

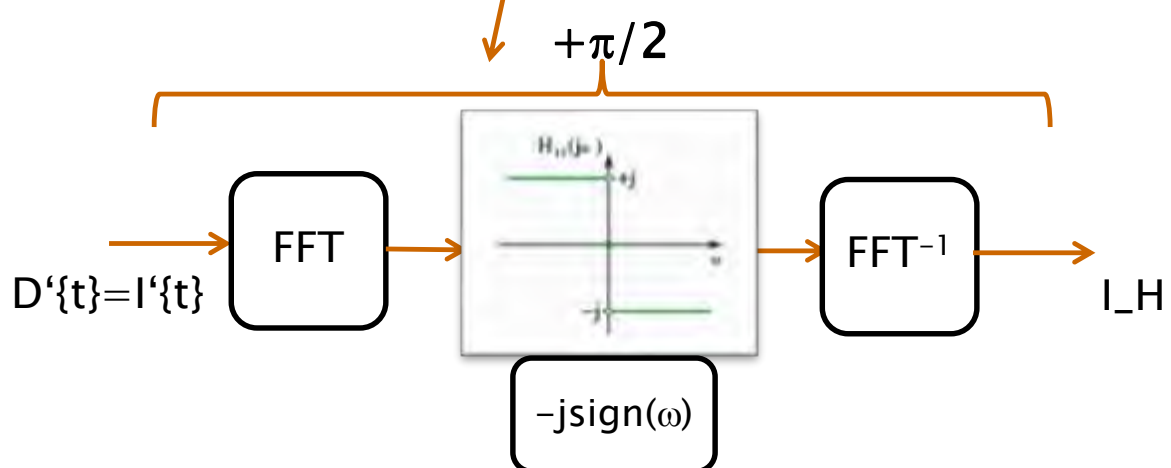
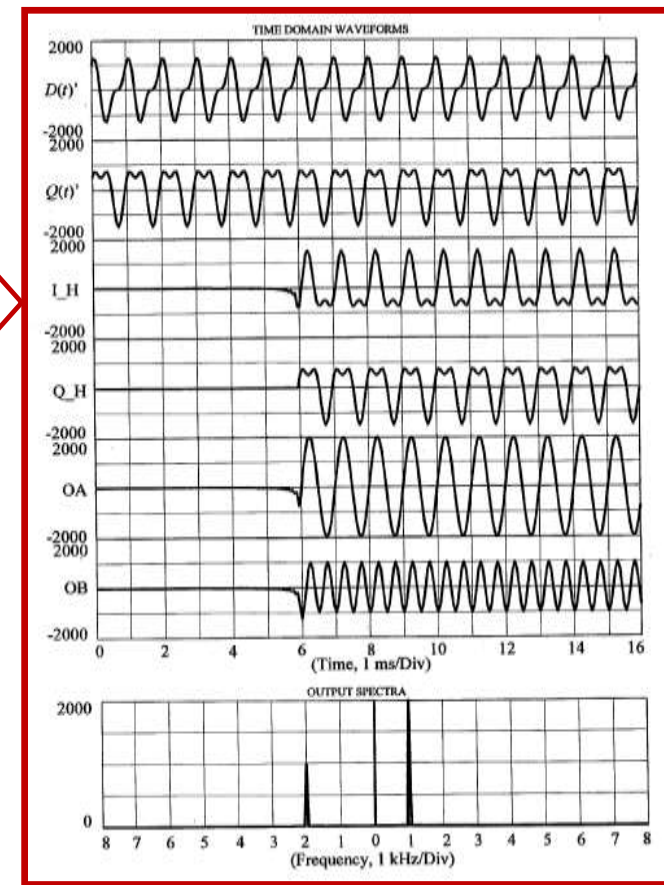
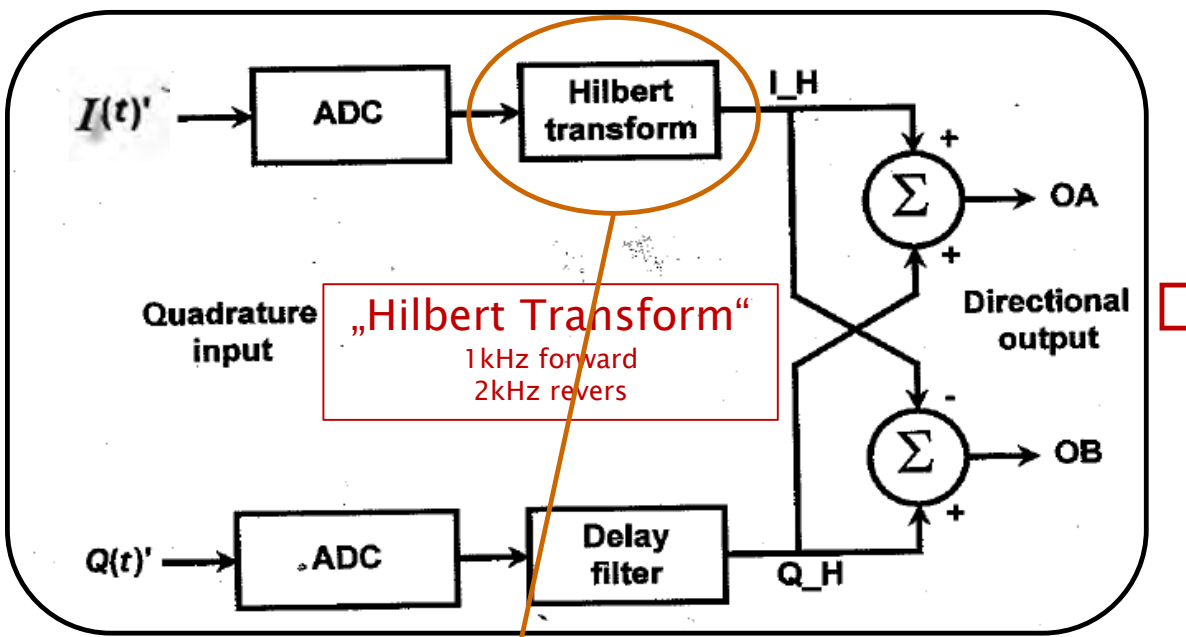
Summary: Doppler Systems

Directional flow detection by „phasing technique“
 Index „f“: forward flow velocities
 Index „r“: reverse flow velocities



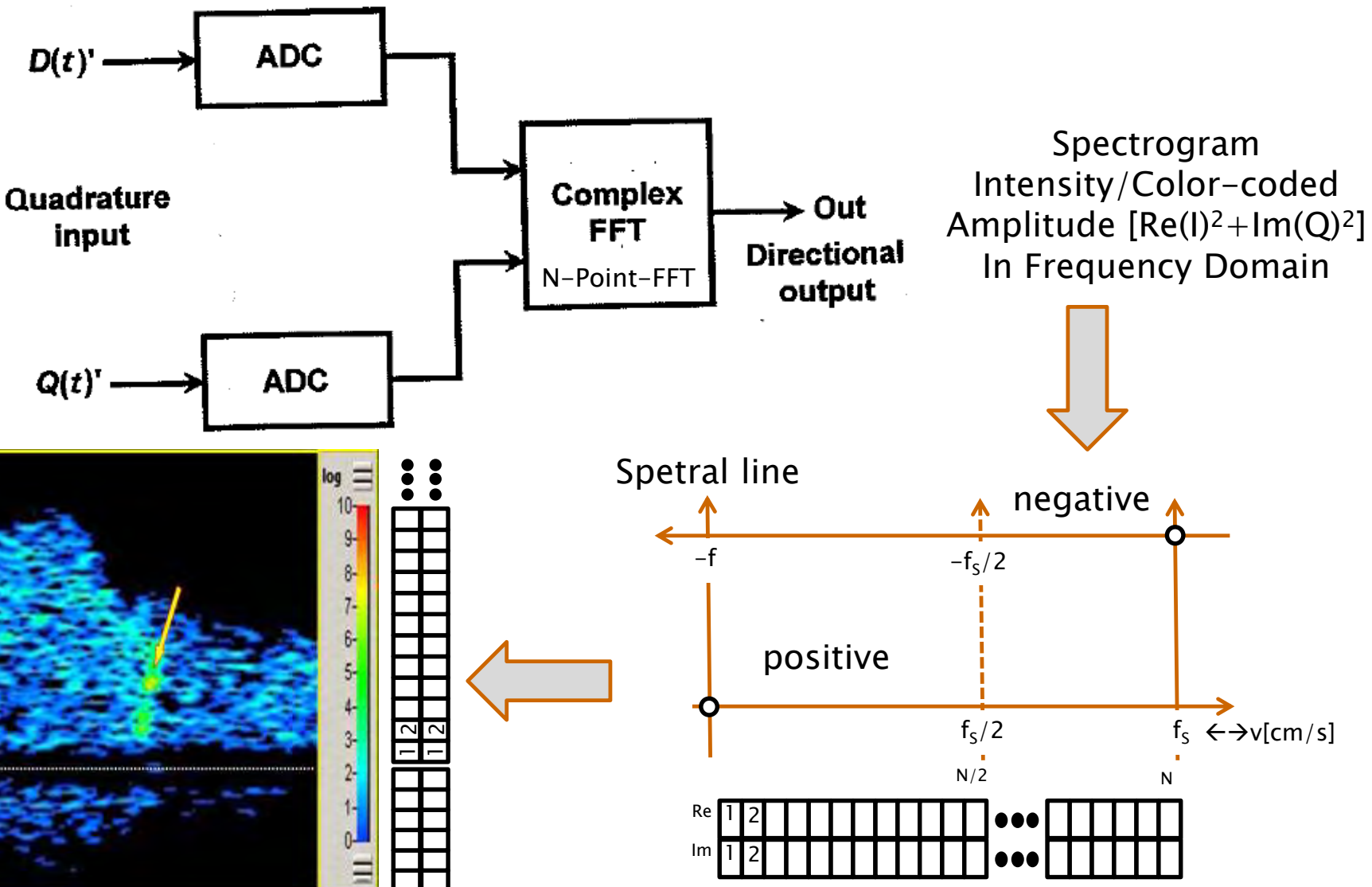
Summary: Doppler Systems

Directional flow detection by „diskret Hilbert Transform“
 with corresponding Delay in corresponding channel



Summary: Doppler Systems

Directional flow detection by „FFT“ → Spectrogram

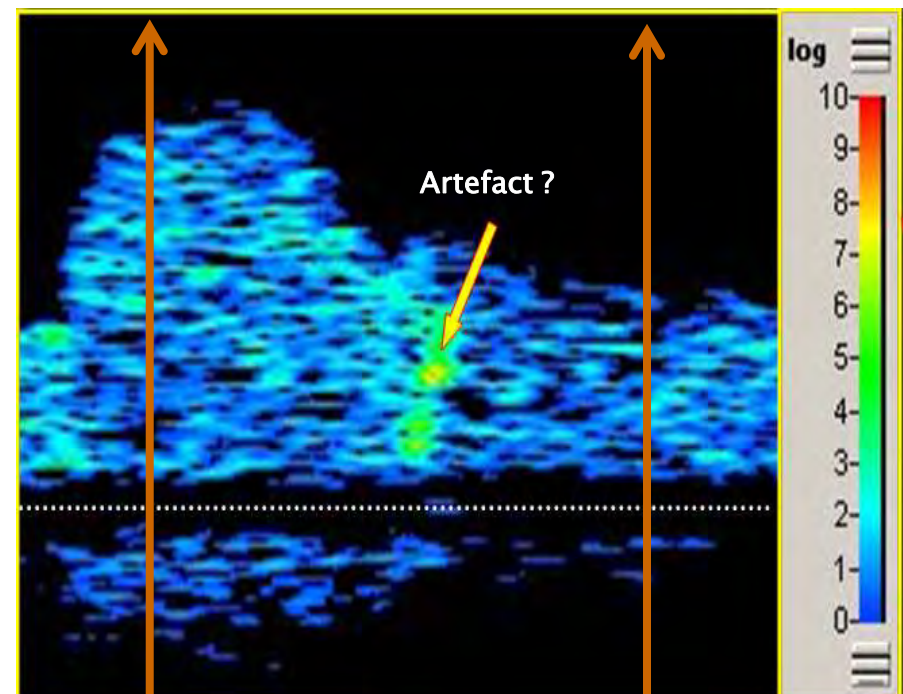
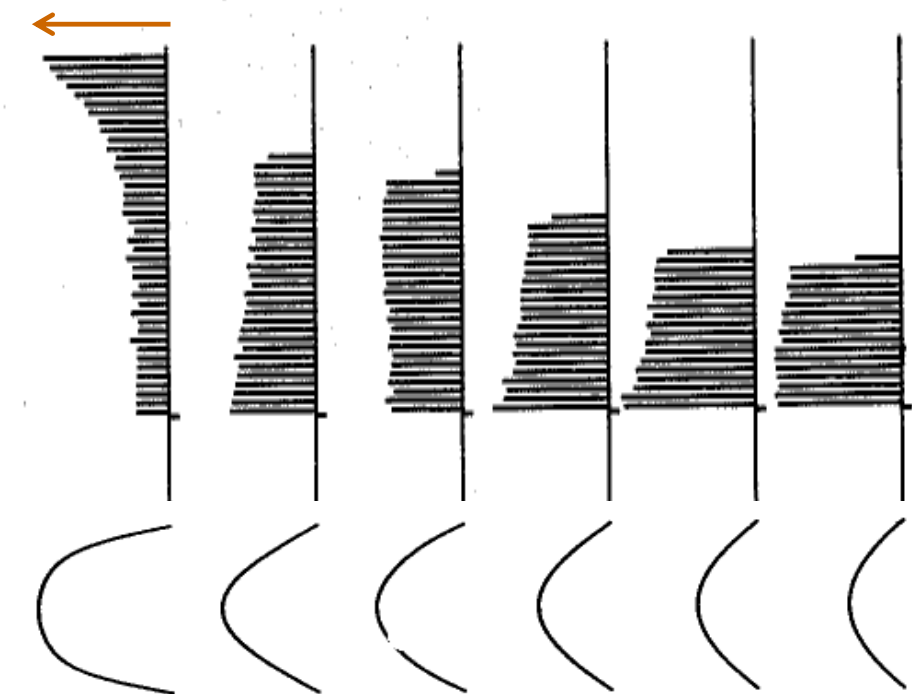


Summary: Doppler Systems

Spectrogram/ Power \leftrightarrow velocity profile

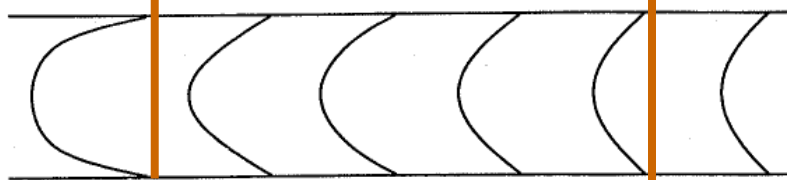
profile common carotid artery

Color coded

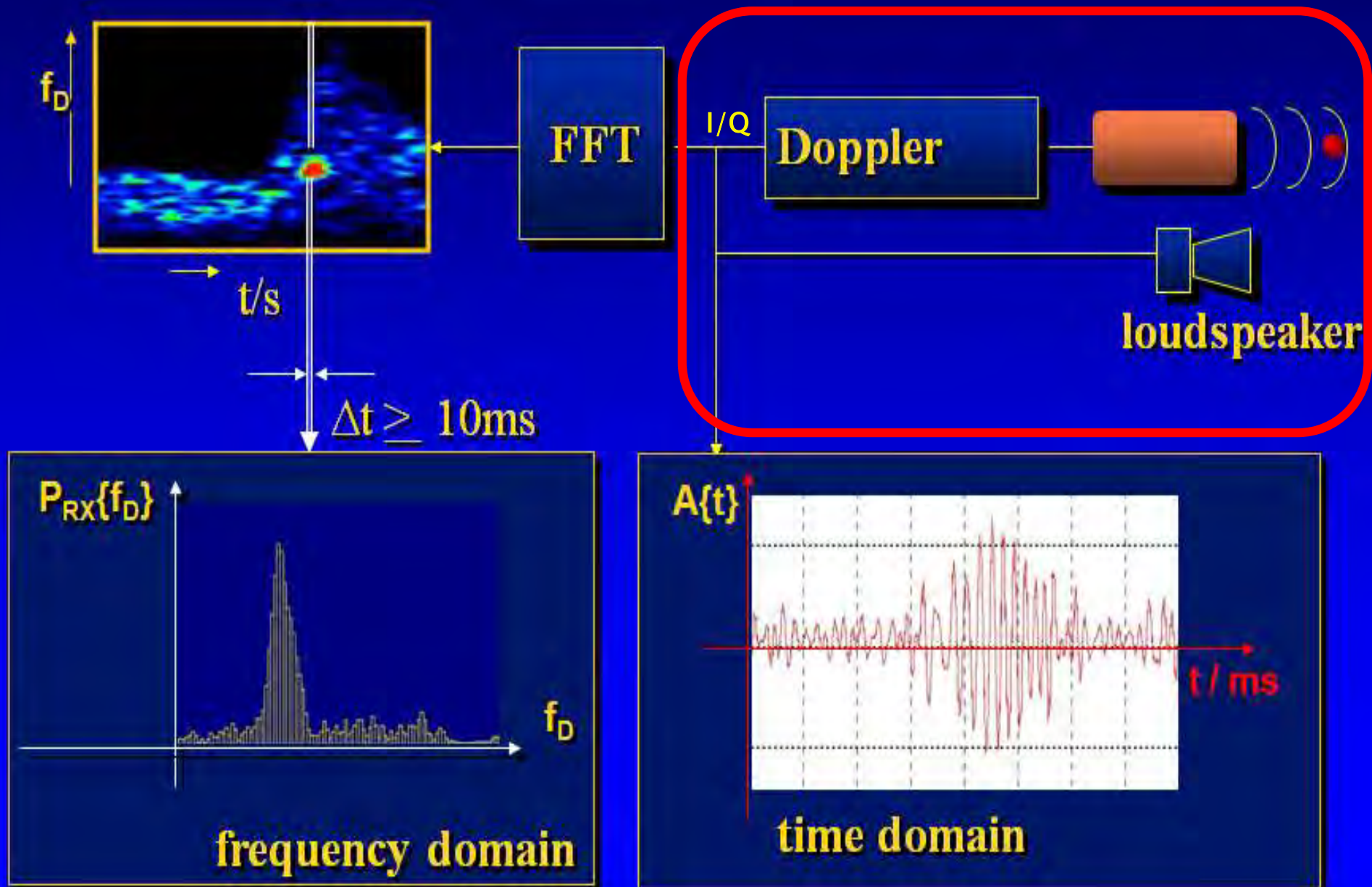


systole

diastole

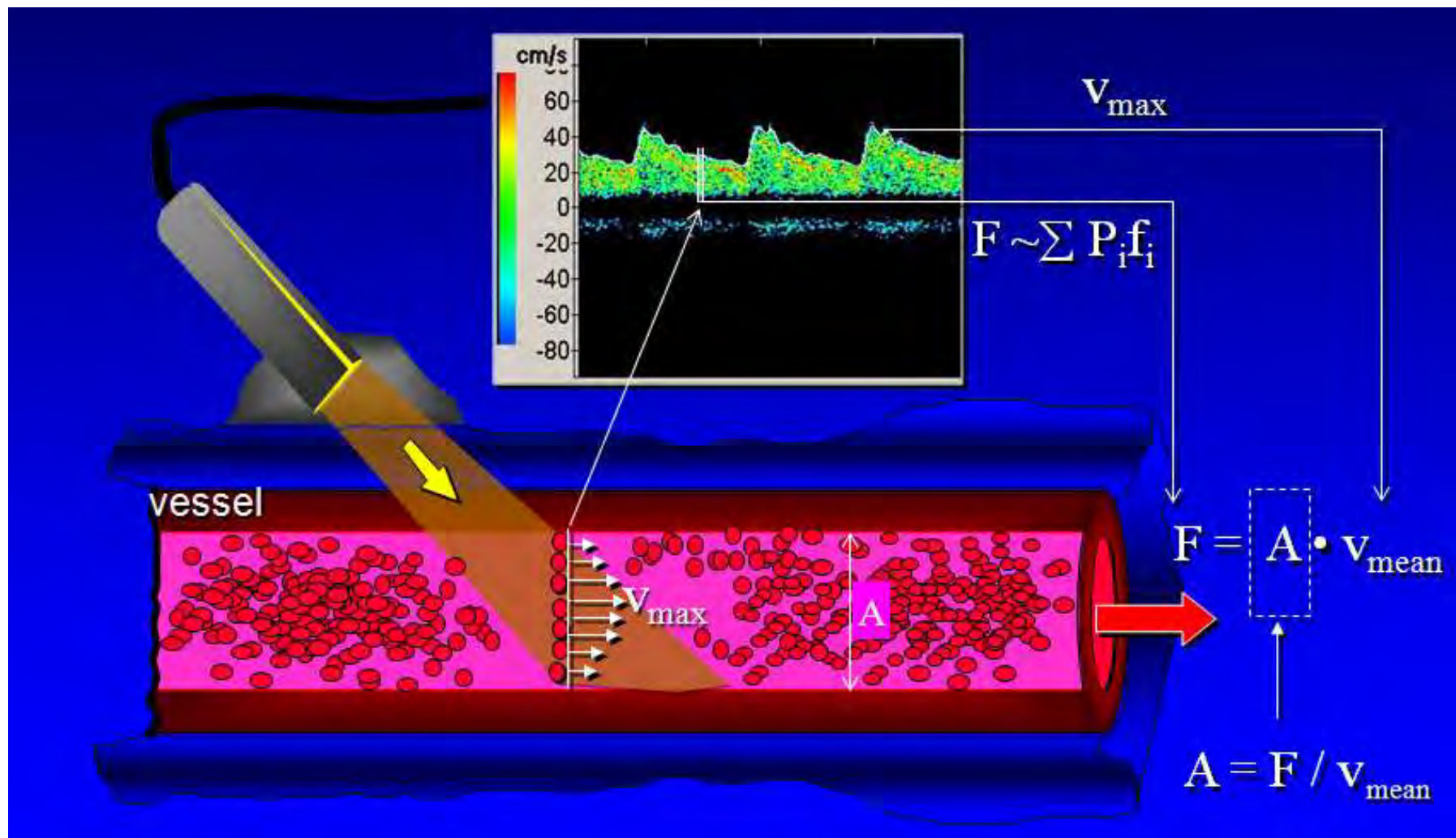


Summary: Doppler System → single gate



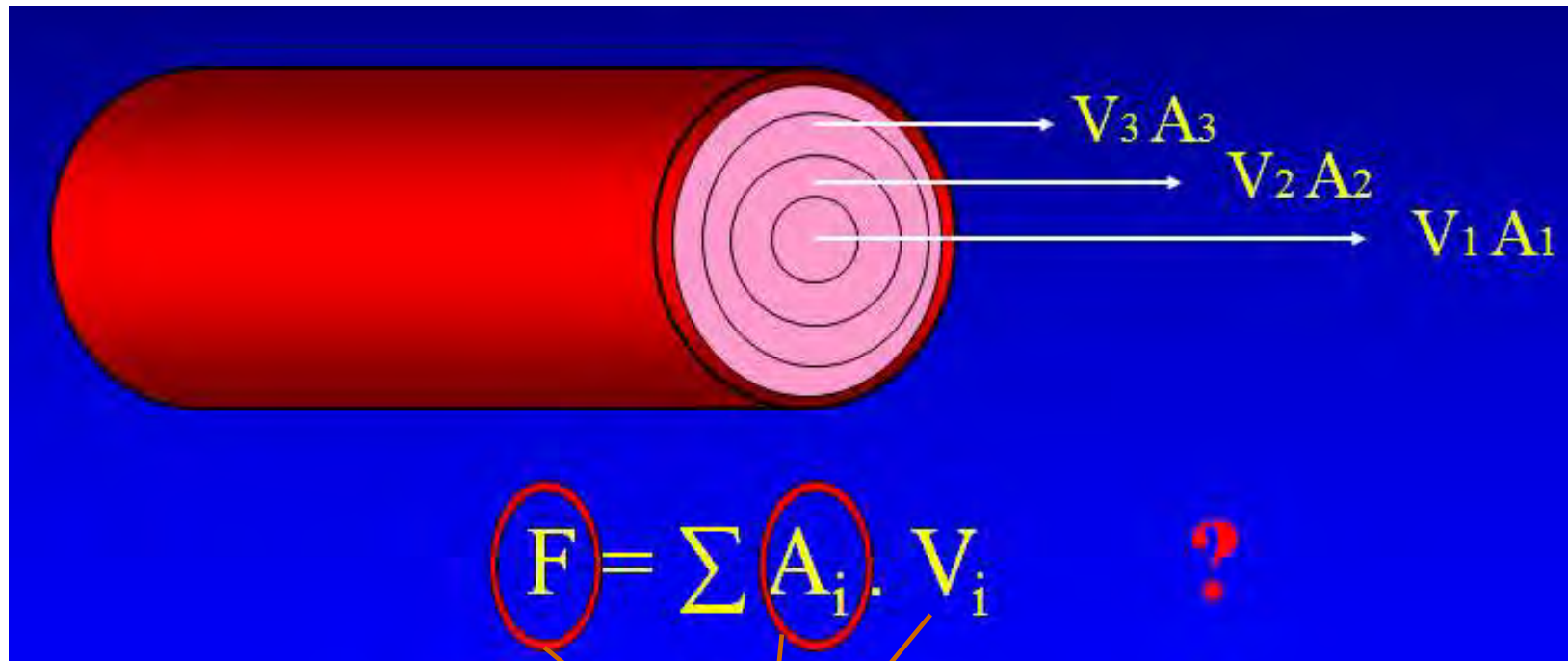
Summary: Doppler Systems

Spectrogram/ Power \leftrightarrow volume flow



Summary: Doppler Systems Power Analysis

Spectrogram/ Power \leftrightarrow volume flow F



- Flow Index - $F_{ix} = \sum P_i \cdot f_i$

- Velocity - $v_{max} \sim v_{mean}$

- If... $F = A \cdot v_{mean}$

$$A_{ix} = \sum P_i = F_{ix} / v_{max \approx mean}$$

$$f_{mean} = \sum P_i \cdot f_i / \sum P_i$$

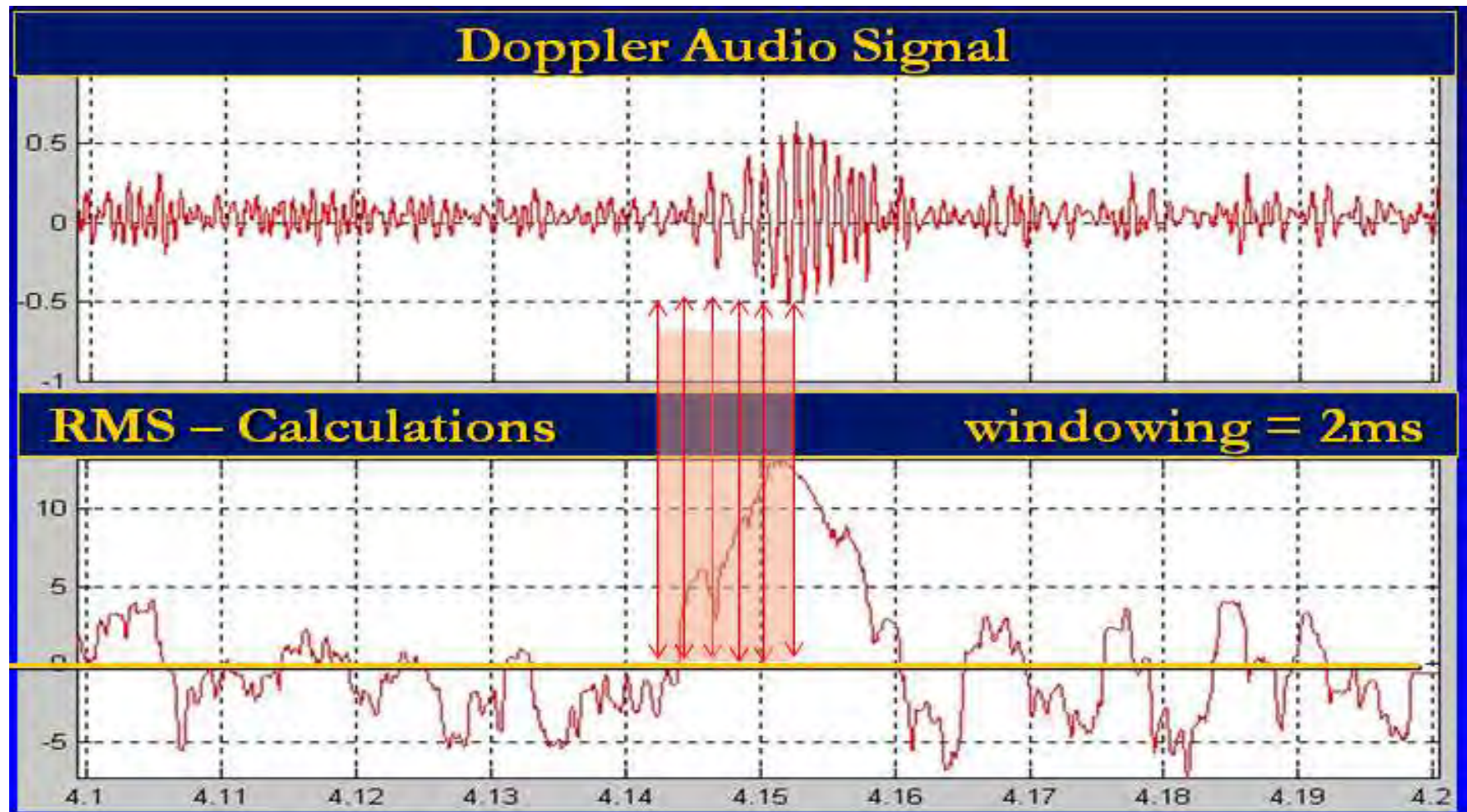
Doppler Formula

$$v_{mean} = f_{mean}$$

$$F = A \cdot v_{mean}$$

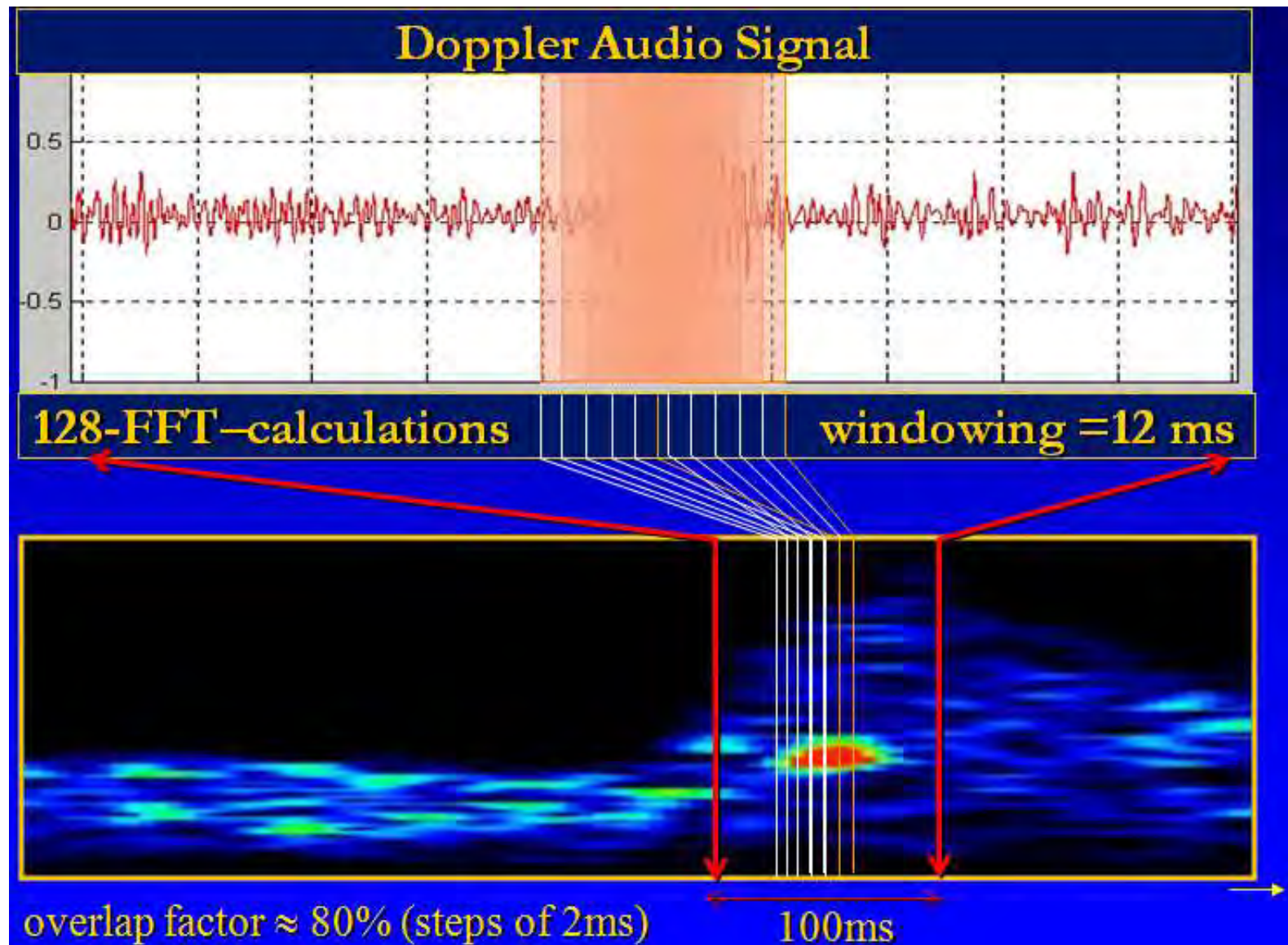
Summary: Doppler Systems Events

Spectrogram/ Power \leftrightarrow transit time single event



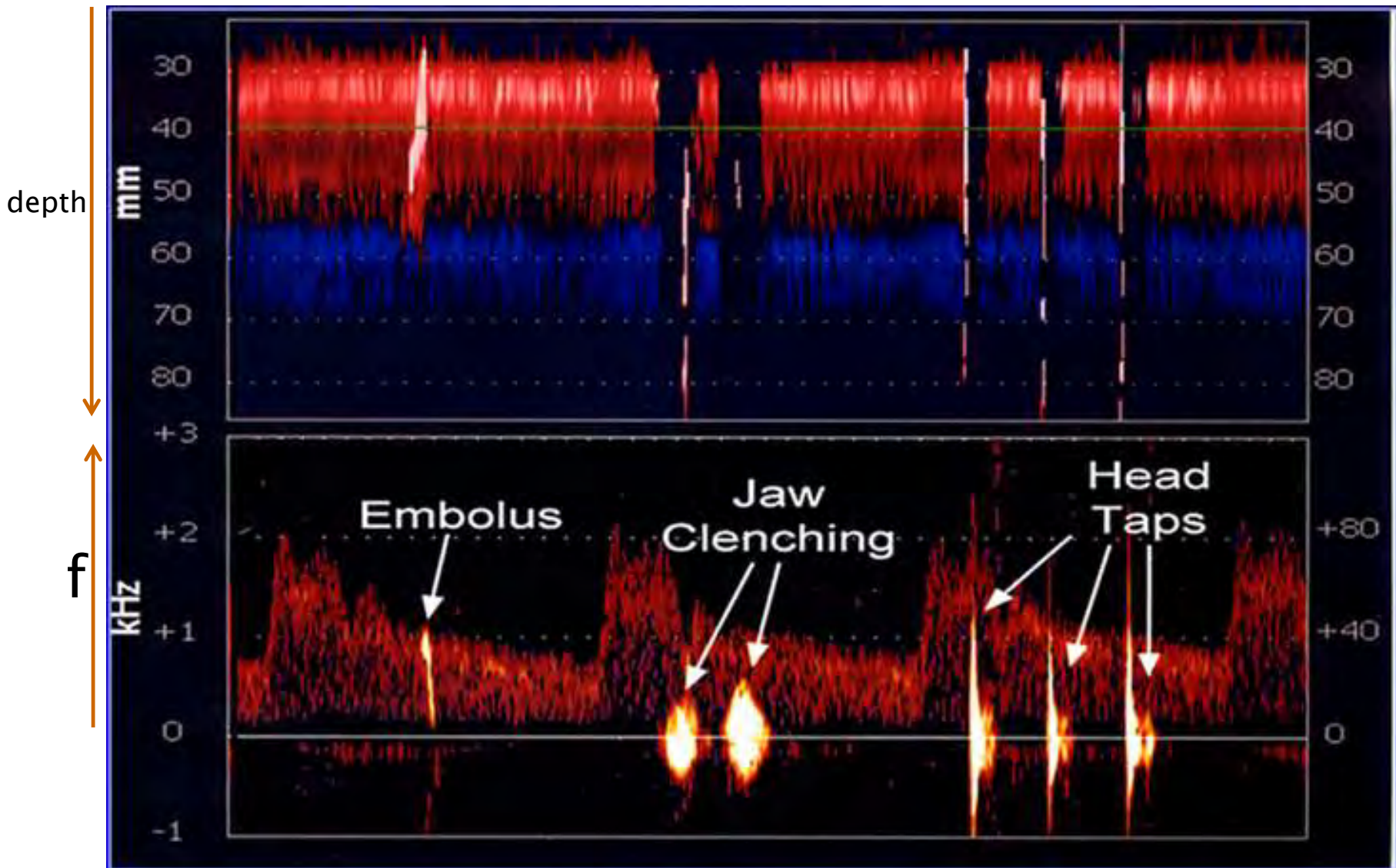
Summary: Doppler Systems Spectral Events

Spectrogram/ Power \leftrightarrow transit time single event



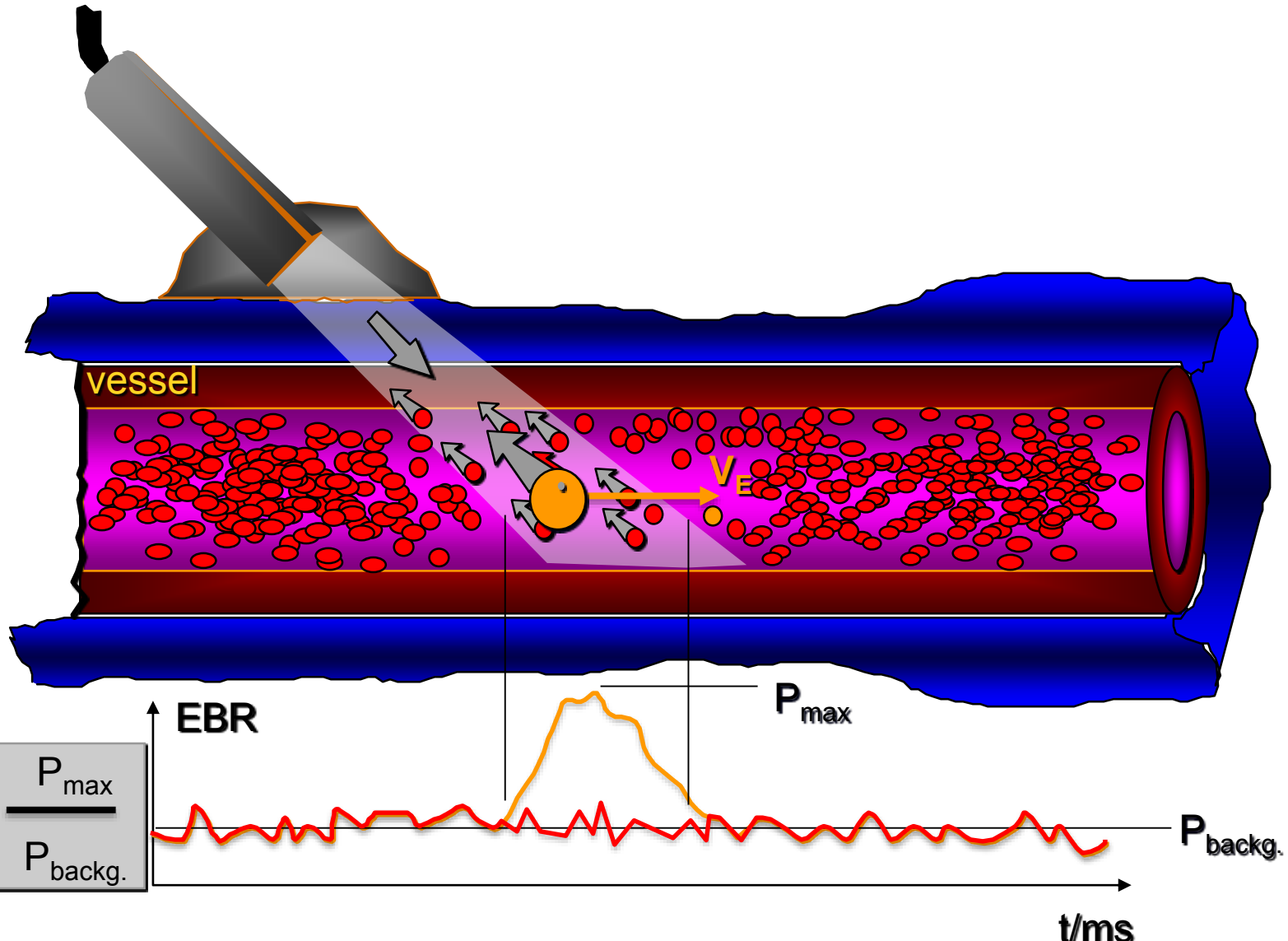
Summary: Doppler Systems Power M-Mode

Single / Multigate Doppler – M-Mode–Power Doppler



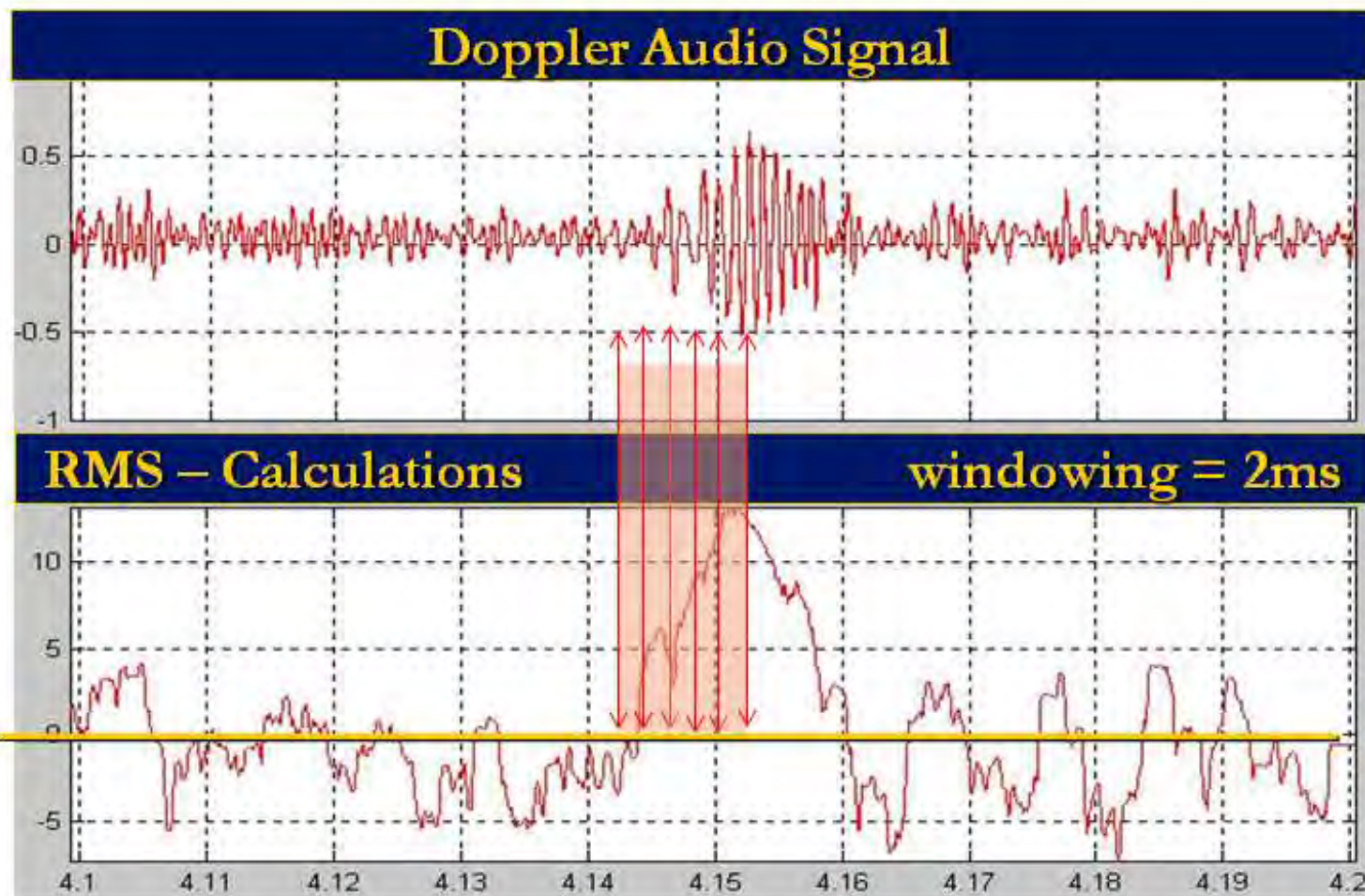
Summary: Emboli Detection

Power \leftrightarrow High Intensity Transient Signal (HITS)



Summary: Emboli Detection

Power \leftrightarrow High Intensity Transient Signal (HITS)



Summary: Emboli Detection

Power \leftrightarrow HITS Theory

$$\sigma_E = \left(\frac{c}{2\pi f} \right)^2 \left| \sum_{m=0}^{\infty} (-1)^m (2m+1) a_m P_m (\cos \theta) i^{m+1} \right|^2$$

σ_E : Differential scattering cross section

c, \bar{c} : Ultrasound propagation velocity in medium and embolus

f : Insonated frequency

$\rho, \bar{\rho}$: Mass density of the medium and embolus

$P_m \{\cos \theta\}$: Legendre polynomial of order m ; θ = reflectttion angle

$$a_m = (-i)^m \frac{\bar{\rho} Z_0 J_{m+1} \bar{J}_m - \rho \bar{Z}_0 J_m \bar{J}_{m+1} + (\rho - \bar{\rho}) m \bar{J}_m J_m}{\bar{\rho} Z_0 H_{m+1} \bar{J}_m - \rho \bar{Z}_0 H_m \bar{J}_{m+1} + (\rho - \bar{\rho}) m H_m \bar{J}_m}$$

$$Z_0 = 2\pi f r_0 / c ; \bar{Z}_0 = 2\pi f r_0 / \bar{c} ; r_0 : \text{Embolus radius}$$

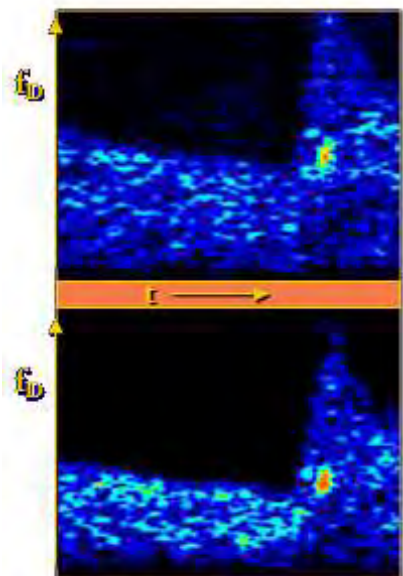
$J_m \{Z\}$: Sperical Bessel-functions of order m

$H_m \{Z\}$: Sperical Hankel-functions of order m

Summary: Emboli Detection

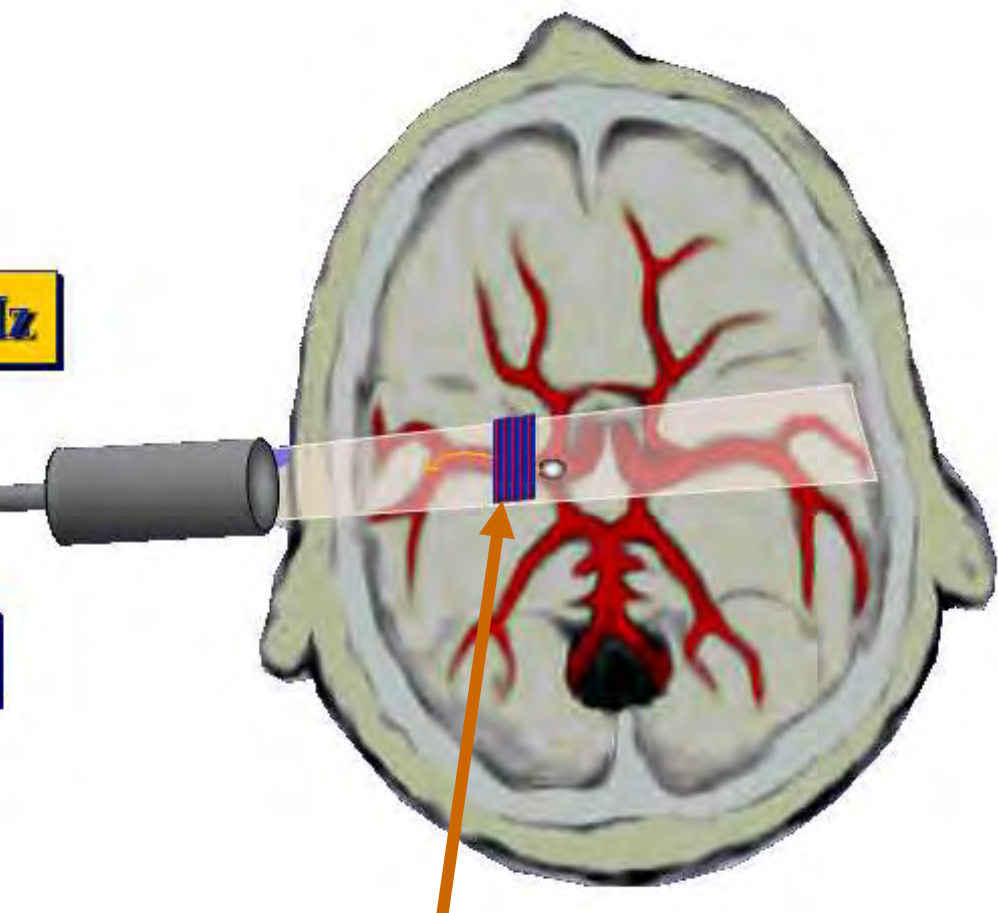
Dual-Frequency Ultrasound-Doppler

Horizontal cross section skull



$f_2 = 2.5\text{MHz}$

$f_1 = 2\text{MHz}$

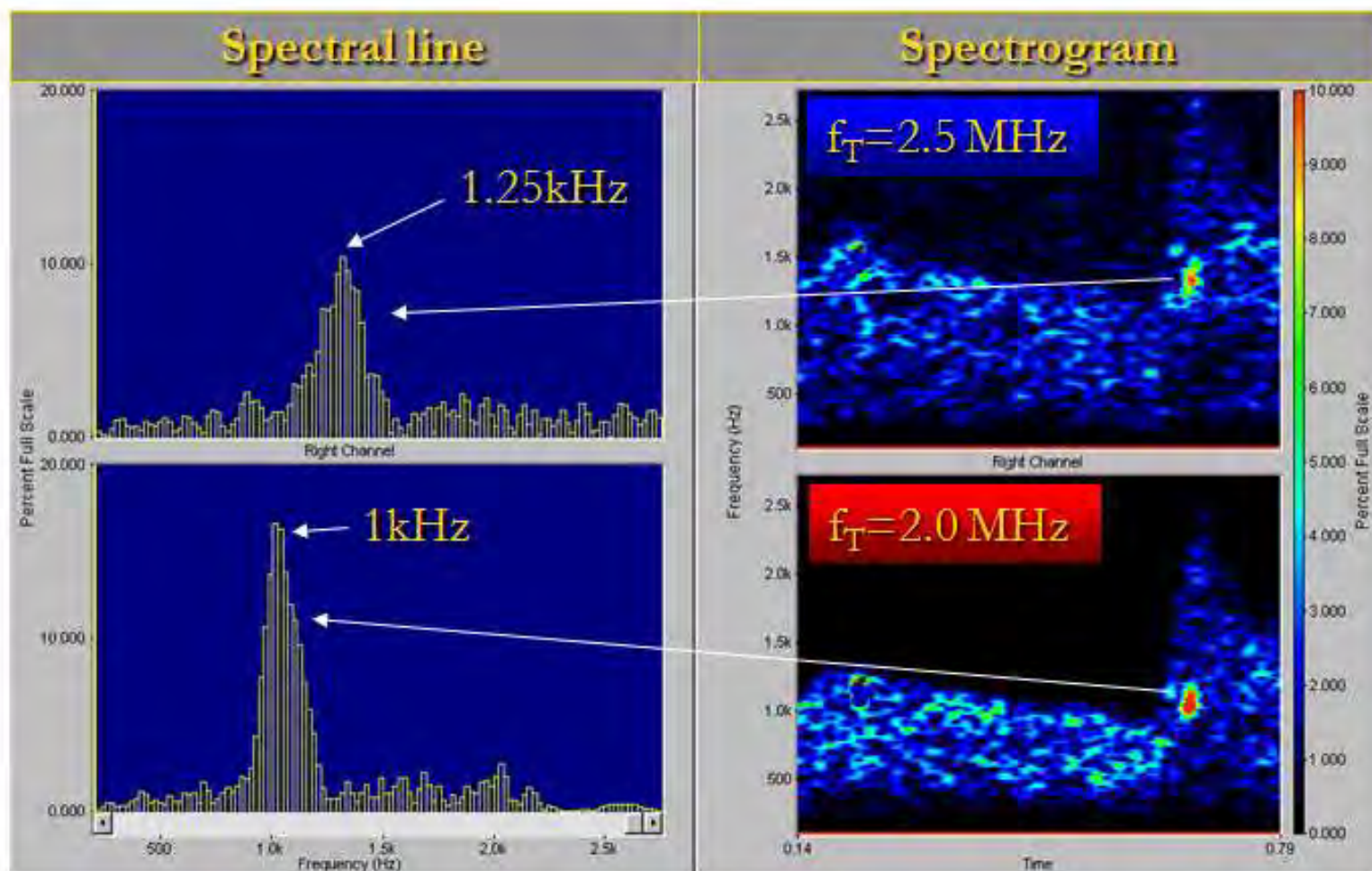


Sample volume
at

Middle Cerebral Artery (MCA)

Summary: Emboli Detection

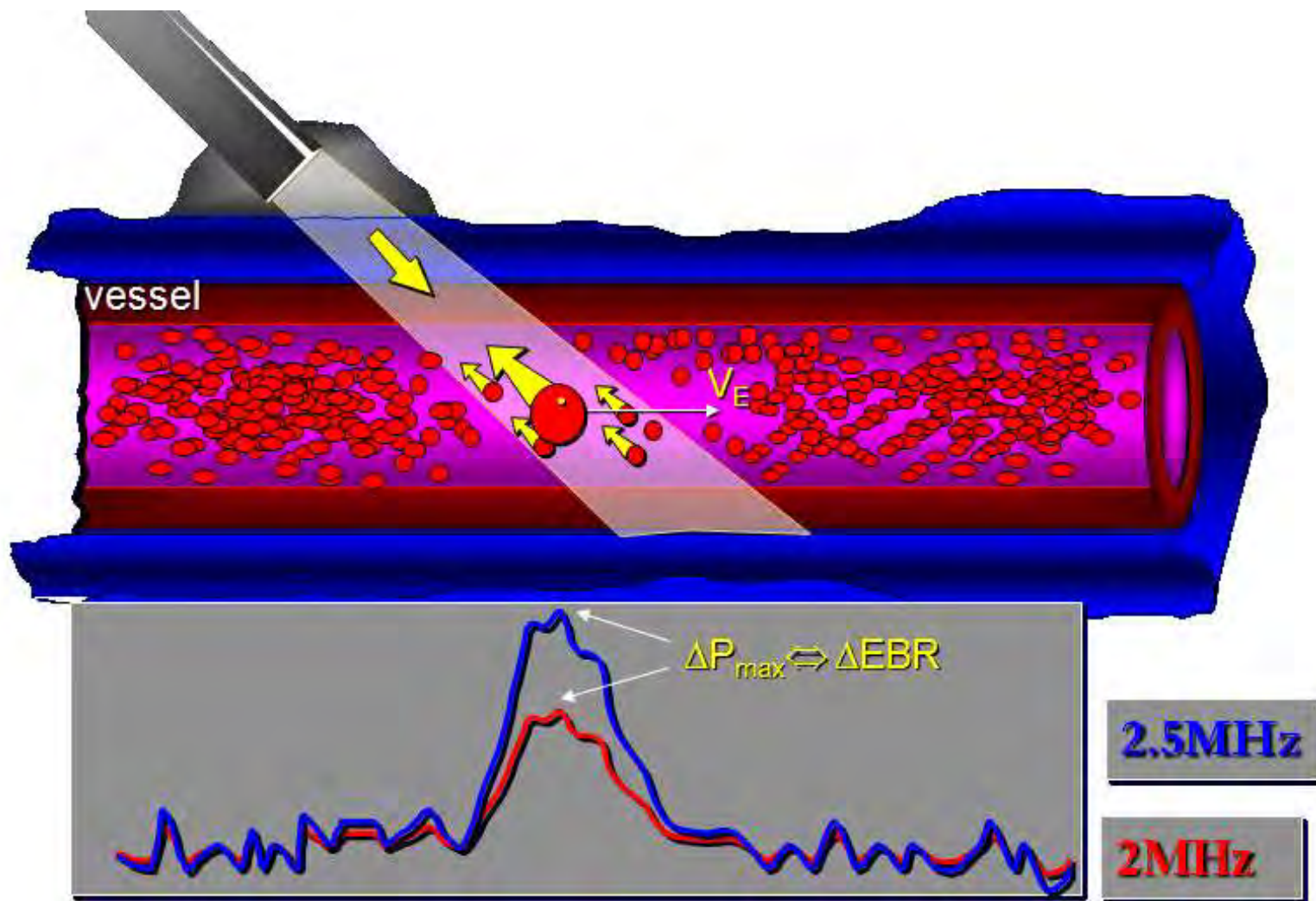
Dual-Frequency Doppler



MCA bubble: $v \approx 40 \text{ cm/s}$; $SV_{\text{axial}} = 10 \text{ mm}$

Summary: Emboli Detection

Dual-Frequency Doppler

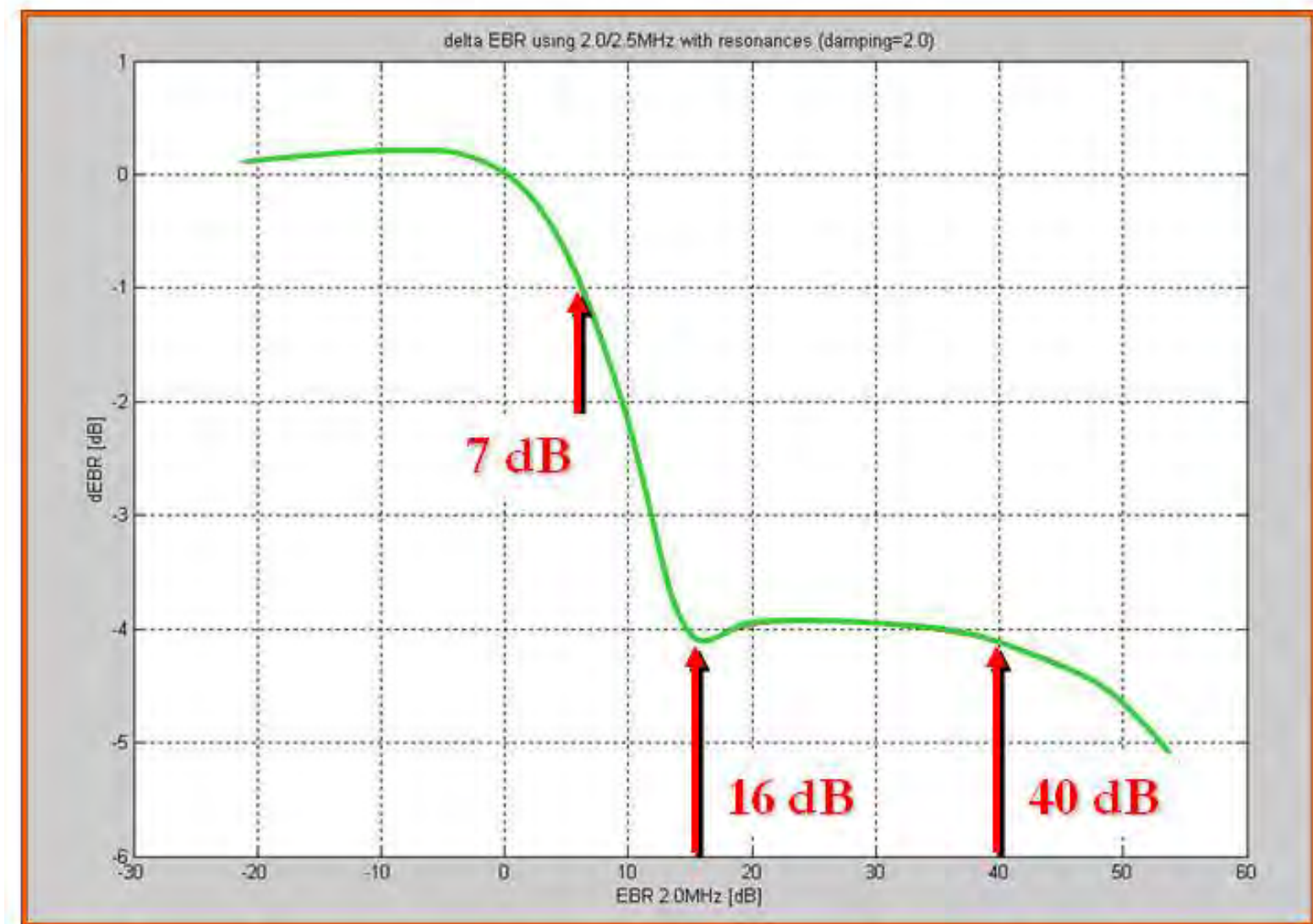


2.5MHz

2MHz

Summary: Emboli Discrimination

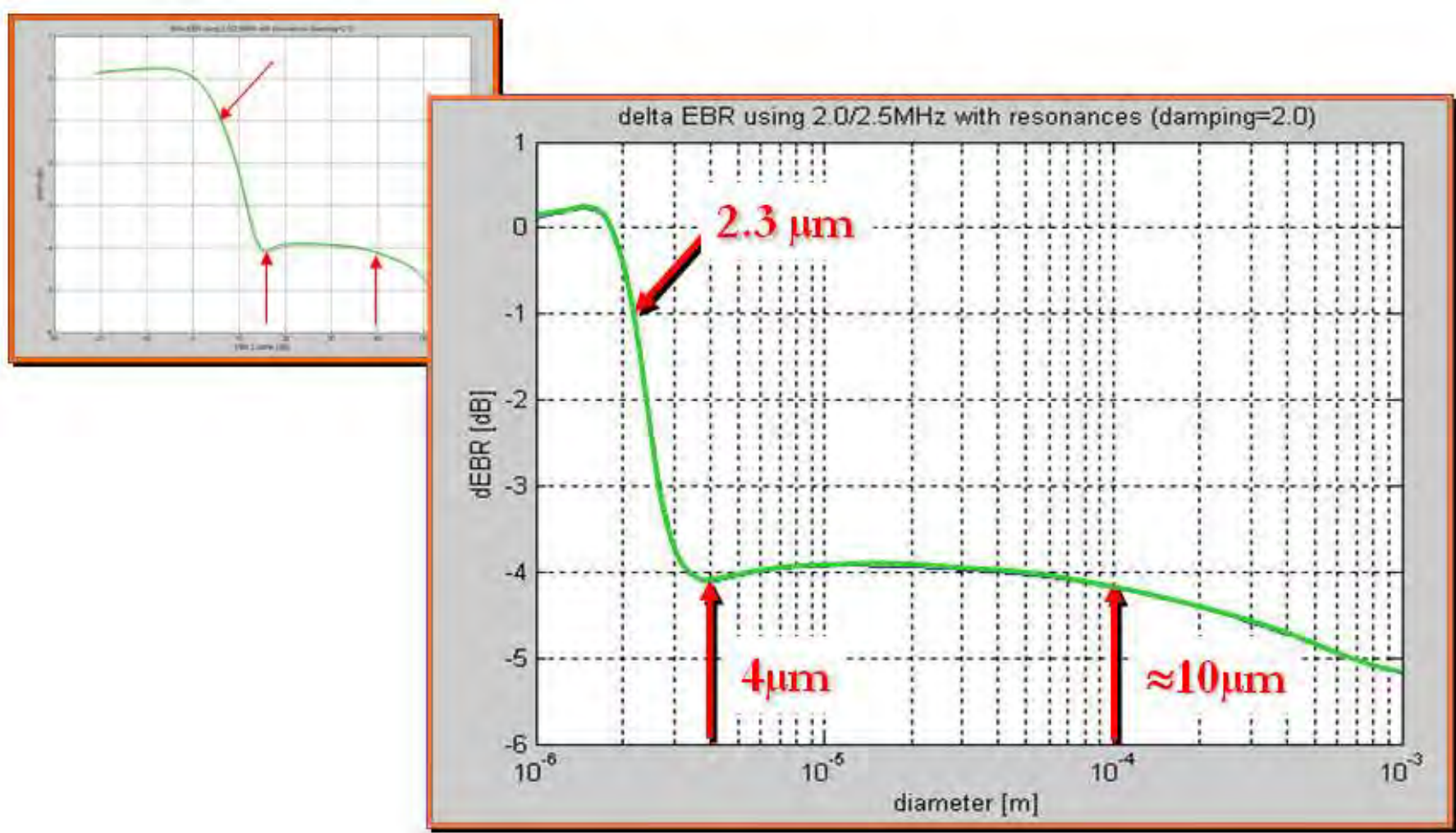
ΔEBR vs EBR of bubbles (Theory)



Sample volume length = 10mm, vessel diameter 0.3mm

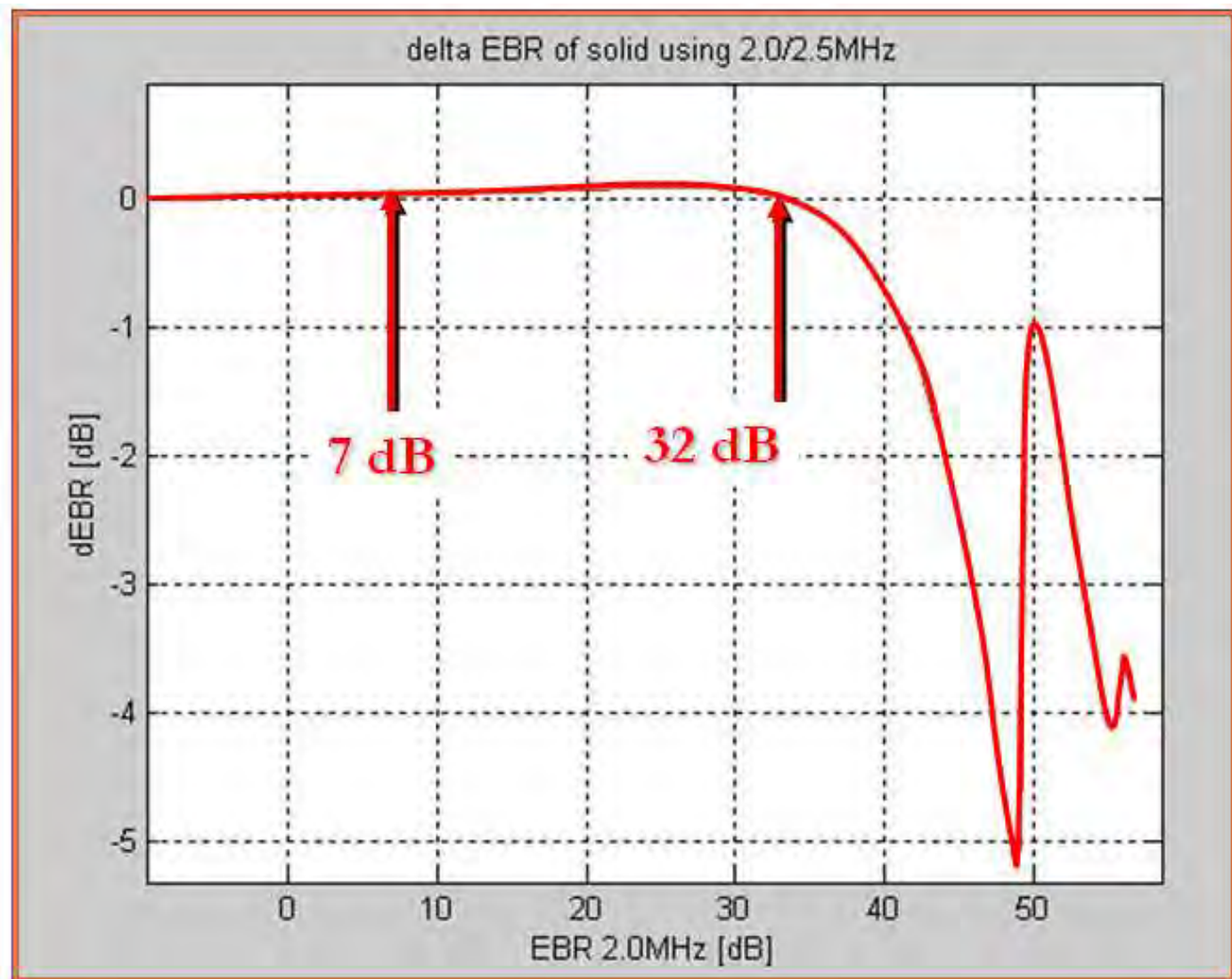
Summary: Emboli Discrimination

ΔEBR vs EBR of bubbles (Theory)



Summary: Emboli Discrimination

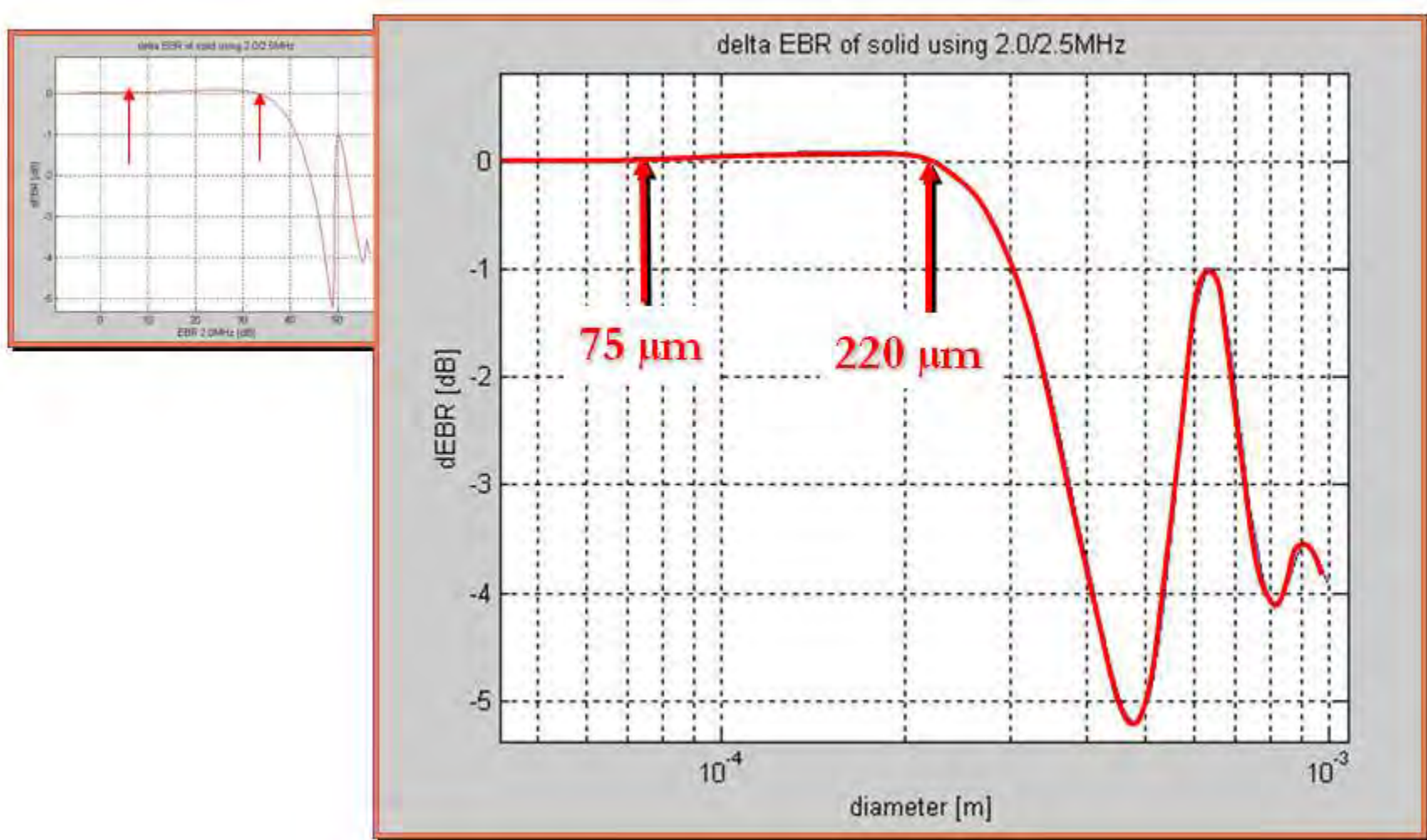
ΔEBR vs EBR of solid (Theory)



Sample volume length = 10mm, vessel diameter 0.3mm

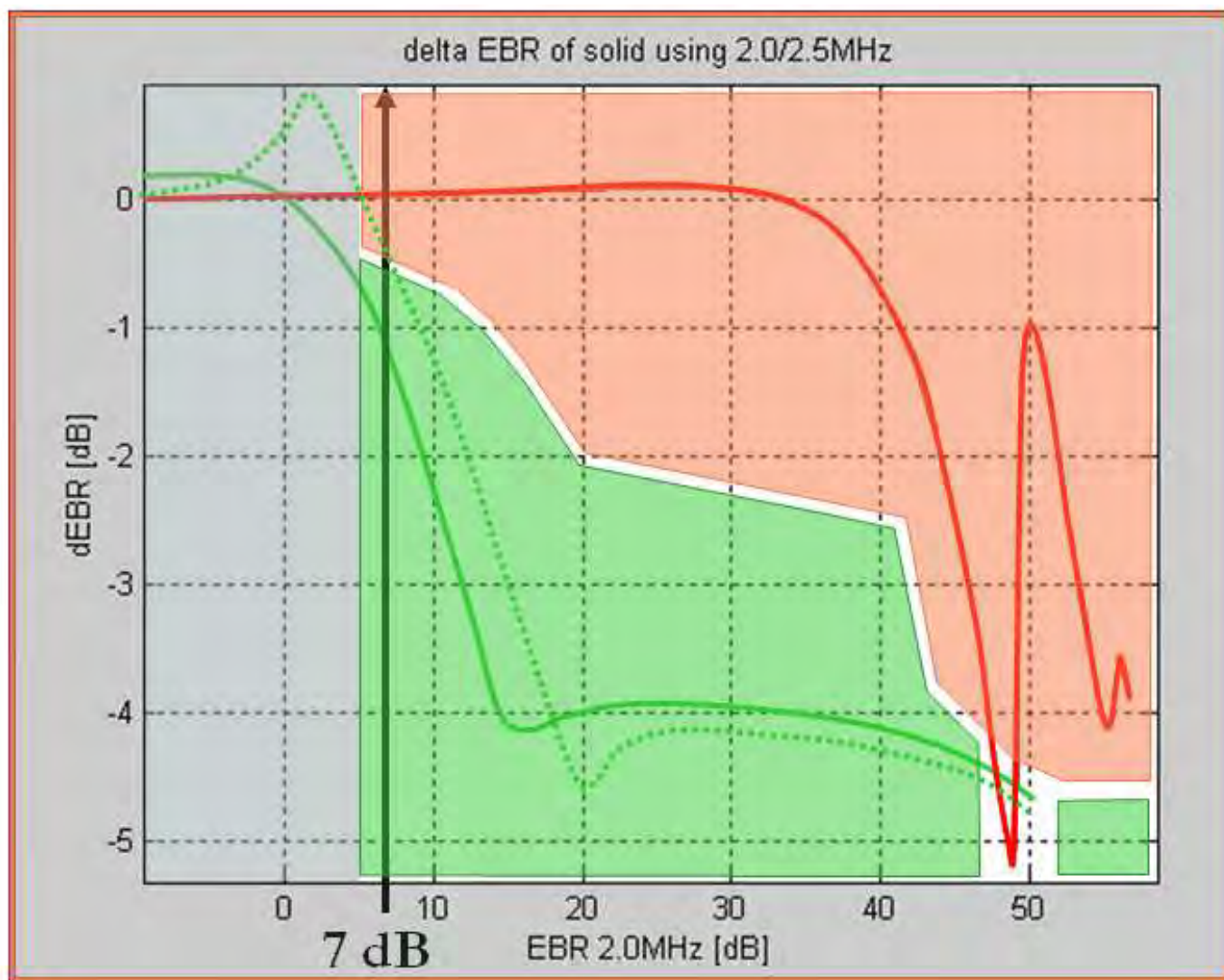
Summary: Emboli Discrimination

ΔEBR vs EBR of solid (Theory)



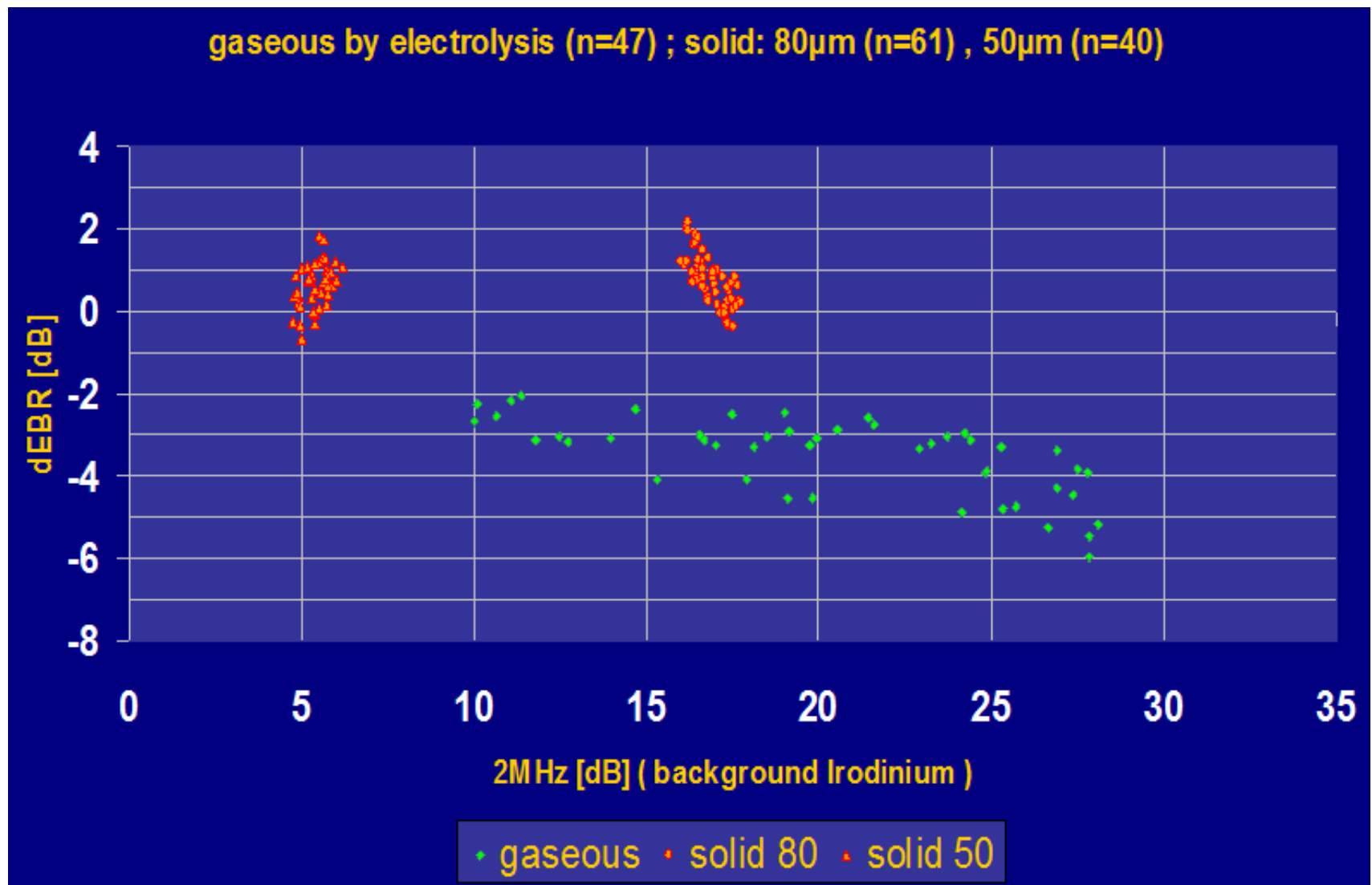
Summary: Emboli Discrimination

ΔEBR vs EBR of solid and gaseous (Theory)



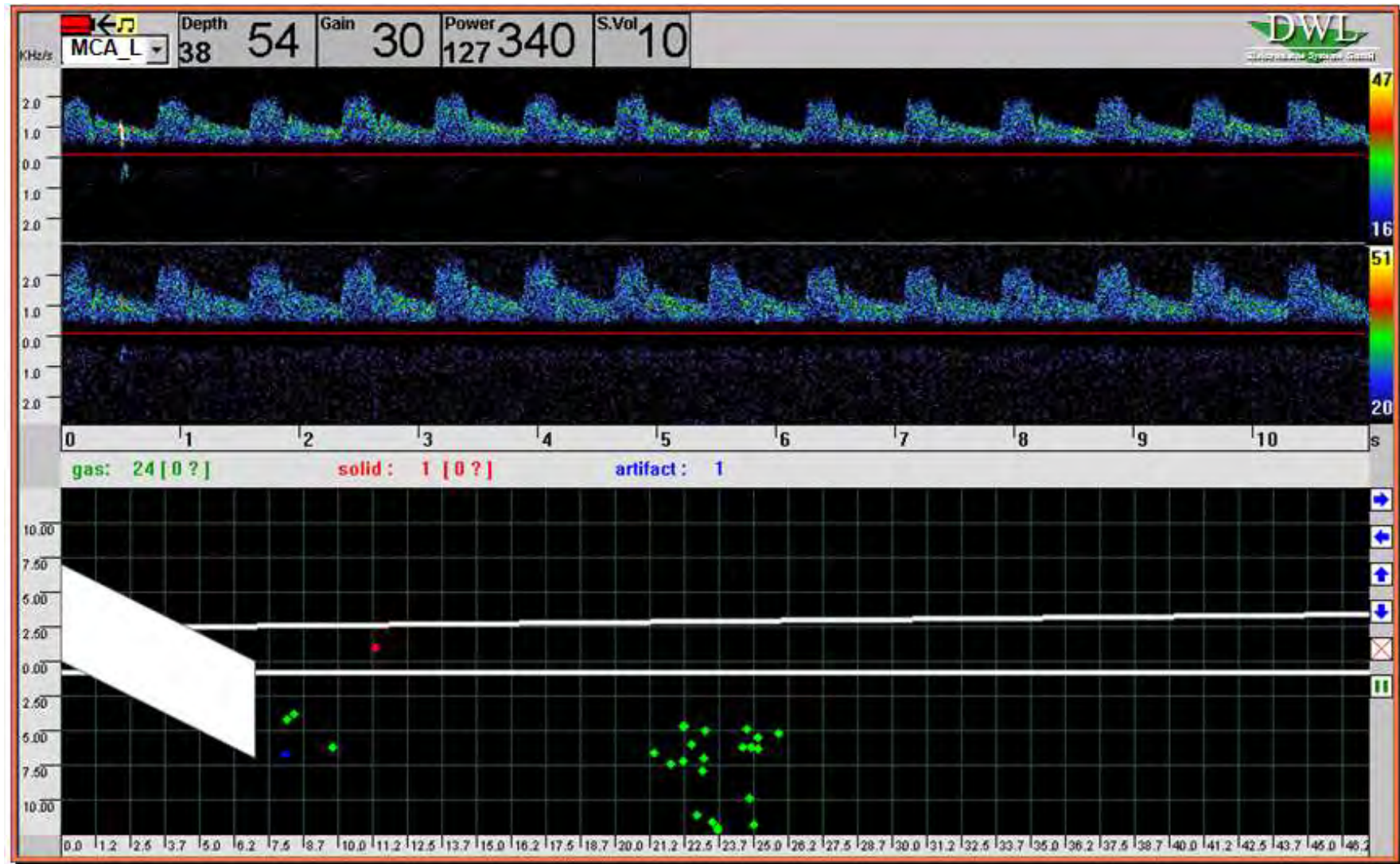
Summary: Emboli Discrimination

ΔEBR vs EBR of solid and gaseous (Experiment in artificial circulatory)



Summary: Emboli Discrimination

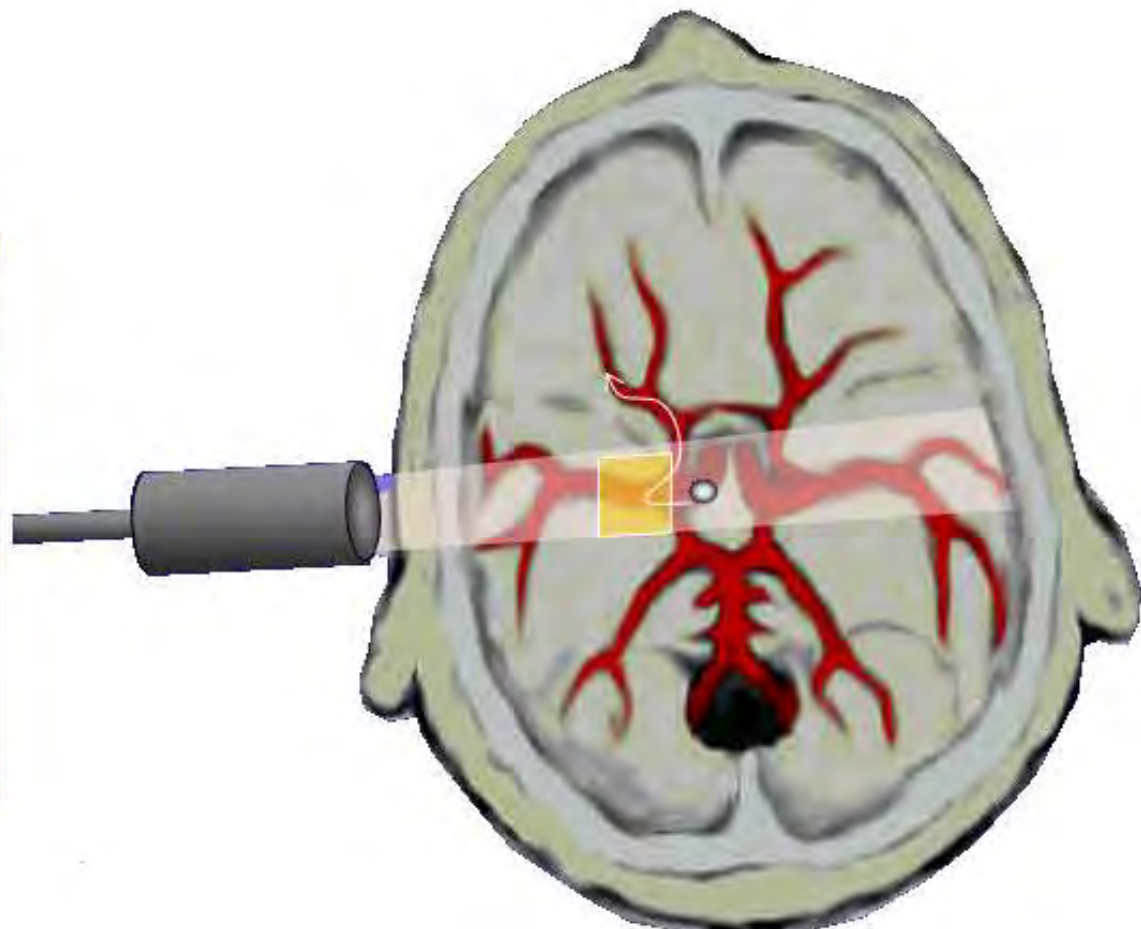
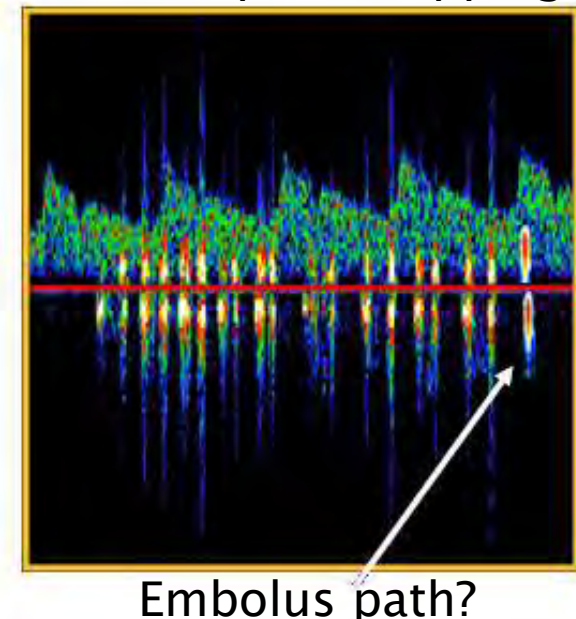
Patient with artificial heart valve



Summary: Emboli /Artifacts-supression

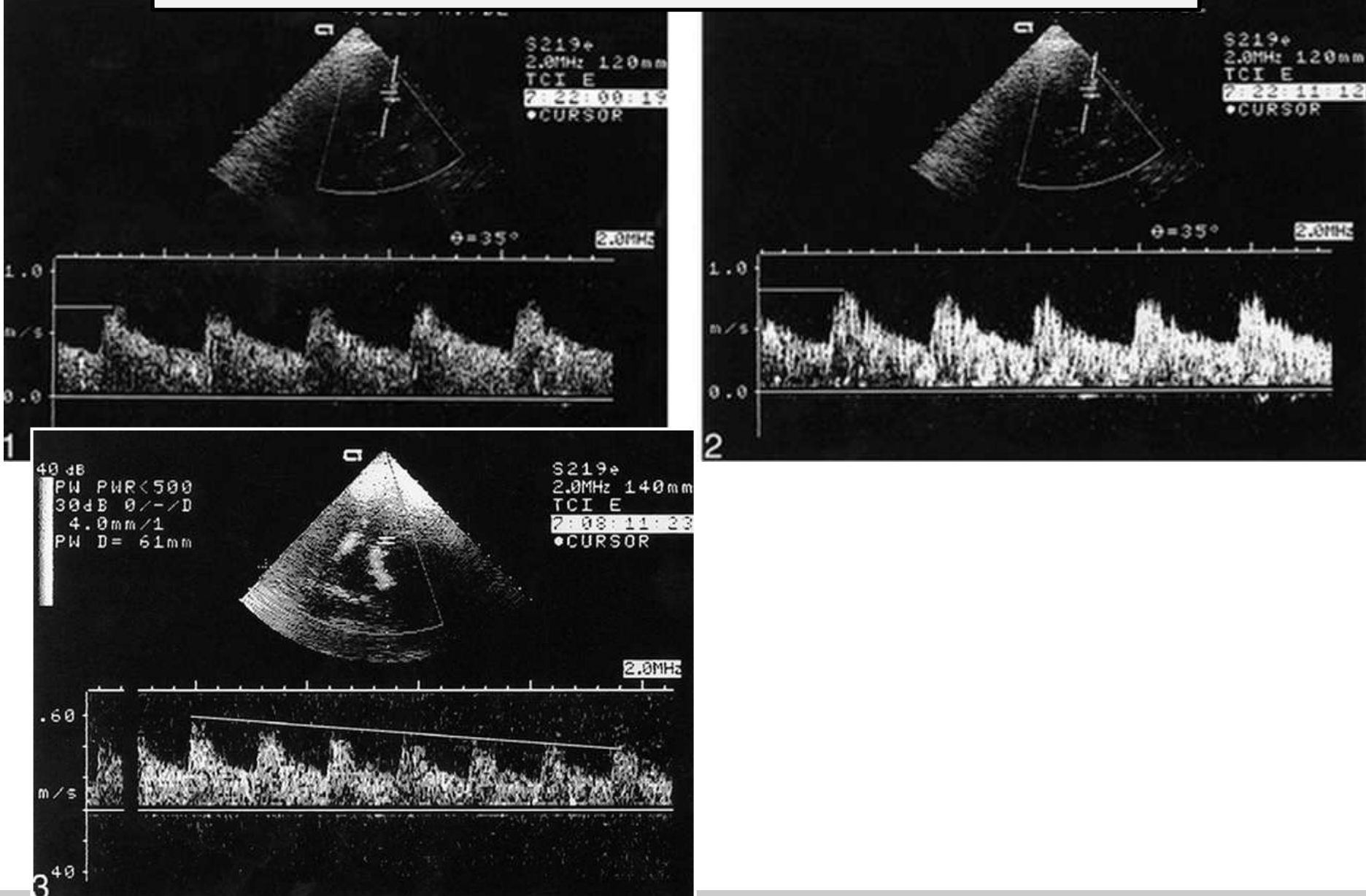
Artefacts and Emboli

Artifact probe tapping



Summary: Contrast agent bubbles

Contrast agent bolus (early pictures)



Ultraschall und Theragnostik

Ultraschall in Thera(pie) und (Dia)gnostik

Kapitel 6

Artefakte und Diagnostik

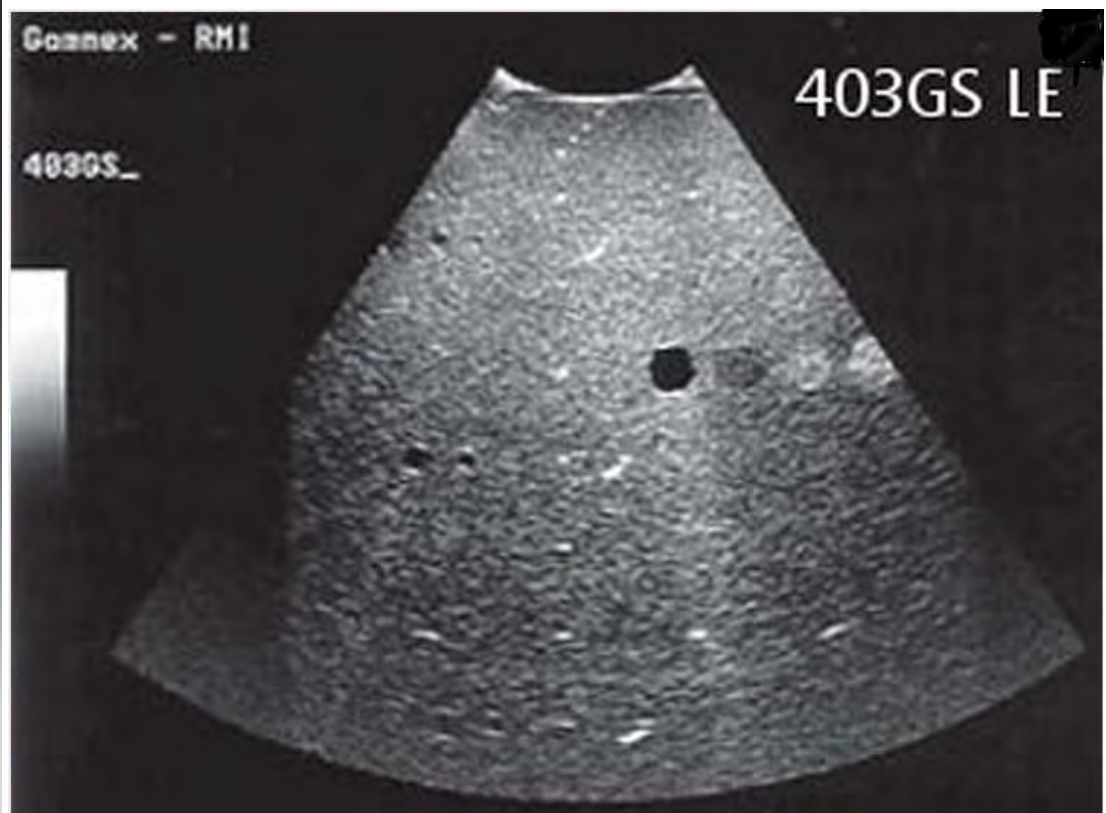
Inhaltsangabe

1. Übersicht der Ultraschallanwendungen
2. Physikalische Grundlagen
3. Ultraschallsonden
4. Bildgebende Verfahren in der Diagnostik
5. Dopplerverfahren in der Diagnostik und Therapie
6. **Artefakte und Diagnostik**
7. Ultraschall und Kontrastmittel
8. Theragnostik mit Ultraschall
9. Therapie mit hochdosierten Ultraschall
10. Gewebecharakterisierung mittels shear waves
11. Dosierung und Sicherheitsaspekte



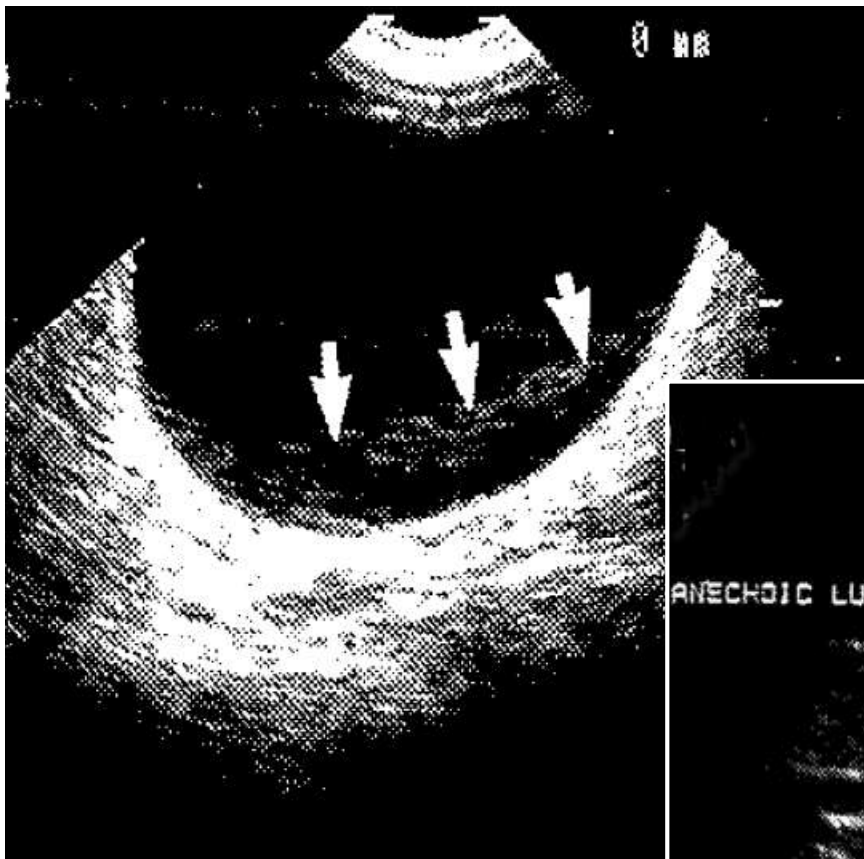
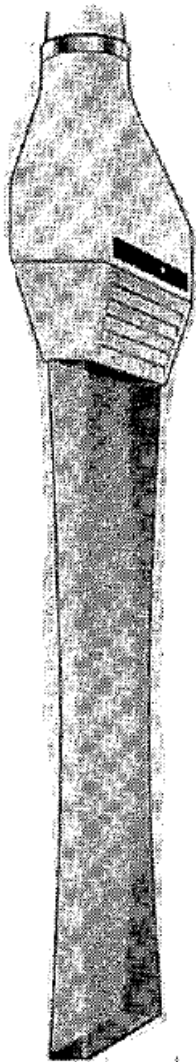
Ultrasound Test equipment: imager

Phantoms: Gammex 403GS LE und 403 LE with special located echogenic targets



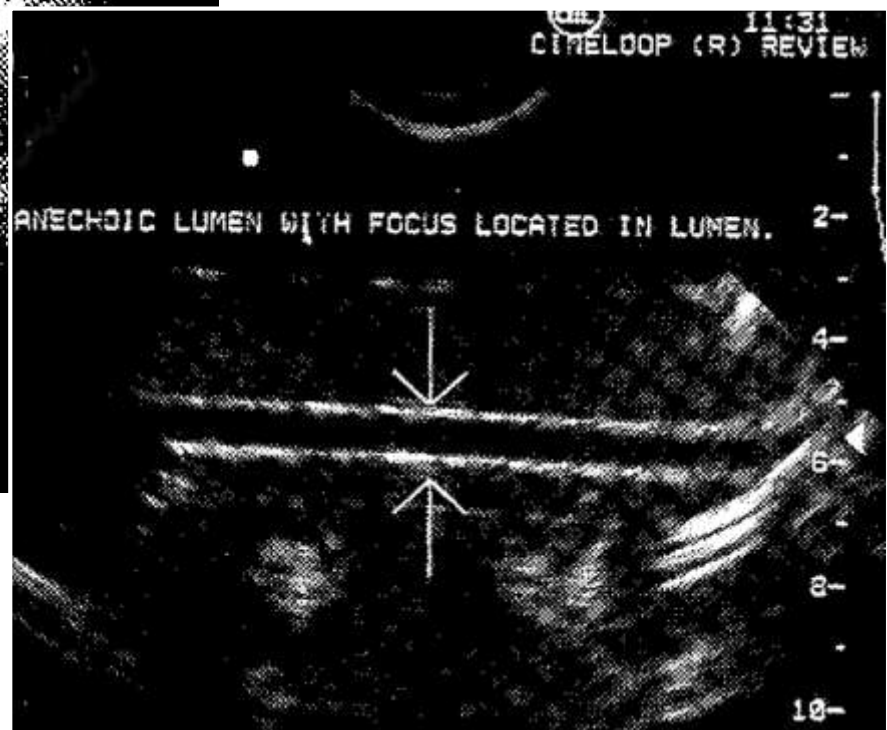
Ultrasound imager: Artifacts

Beam is 3D → thickness:



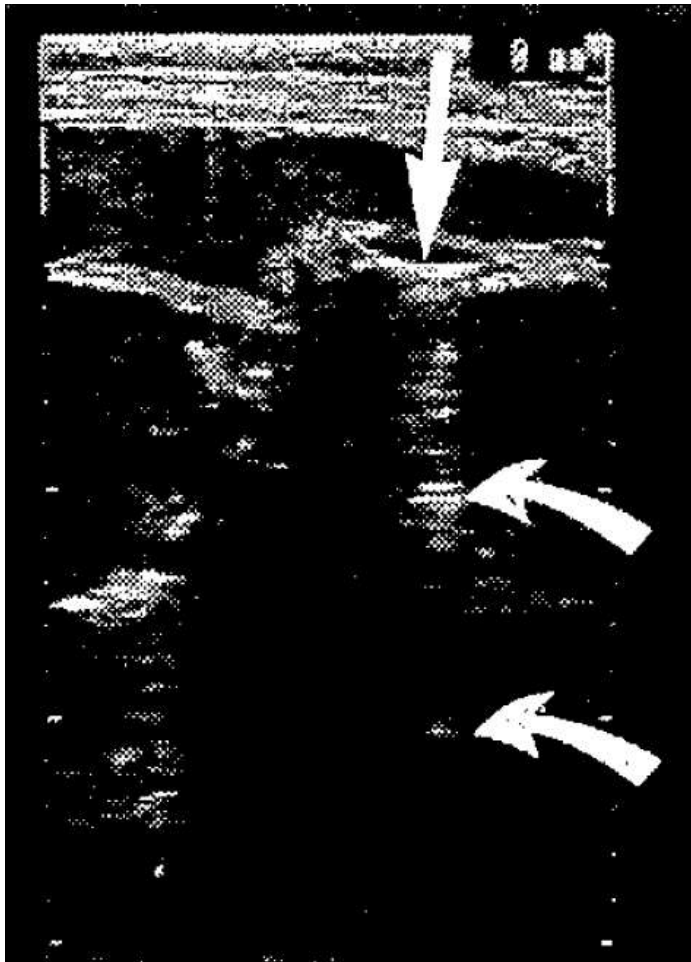
a)

b)

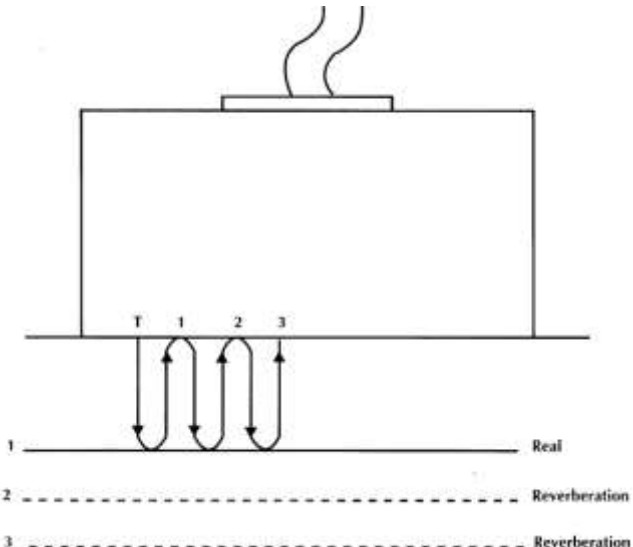


Ultrasound imager: Artifacts – Multireflection

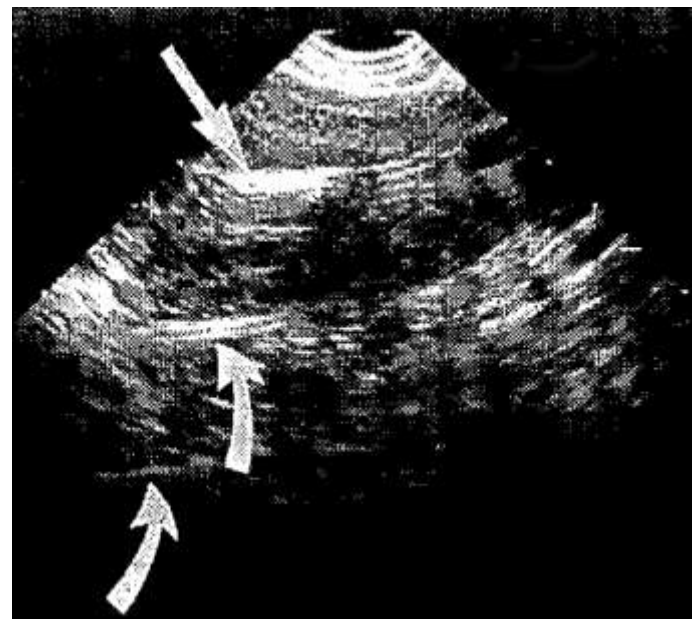
c)



a)

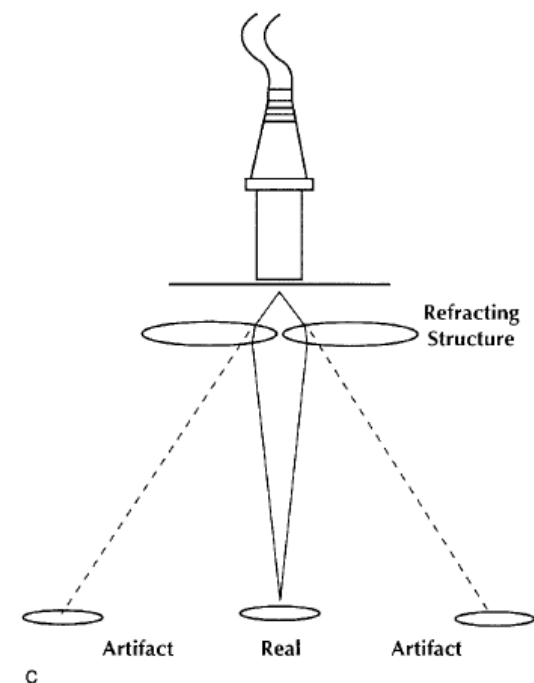
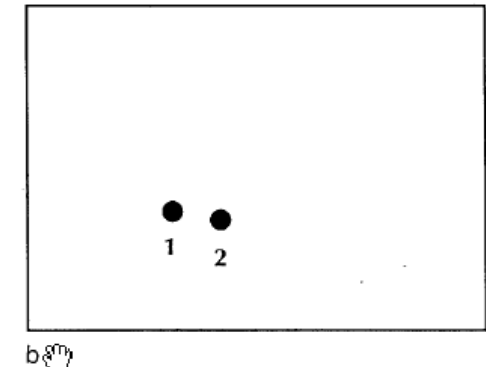
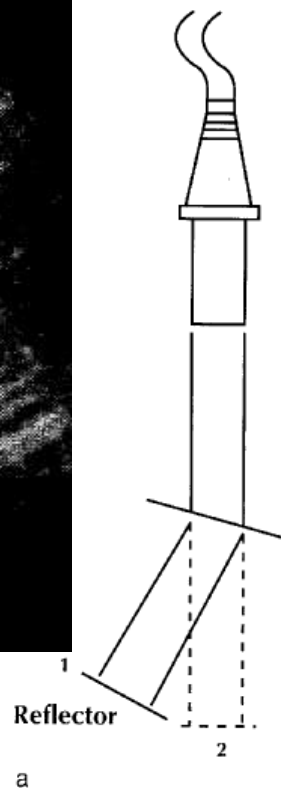
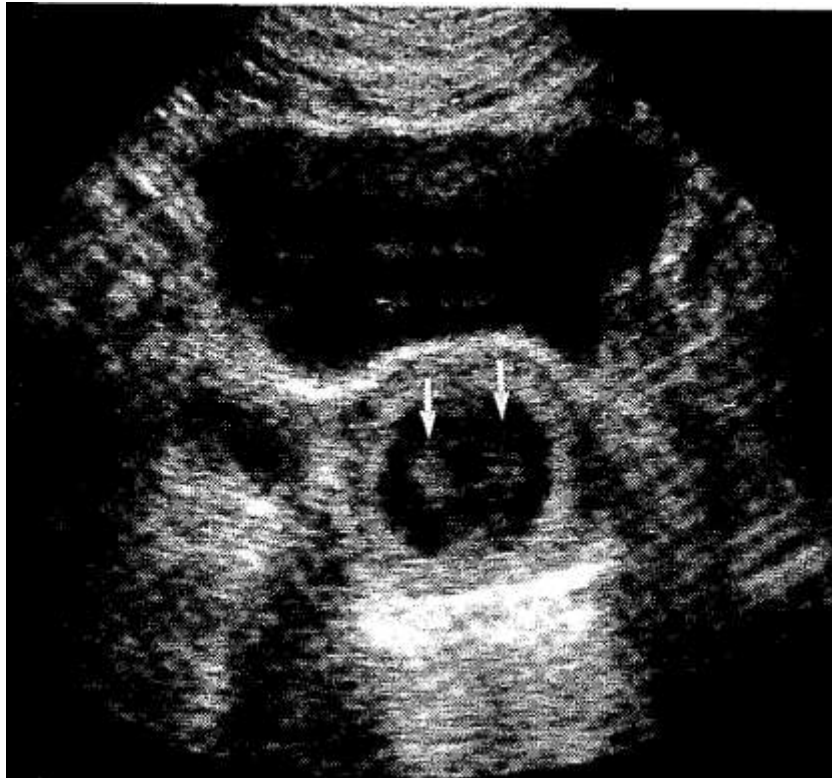


b)



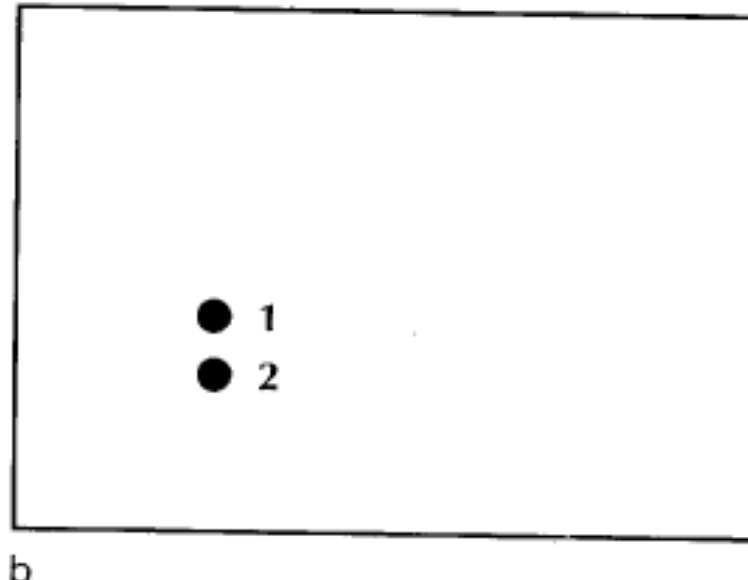
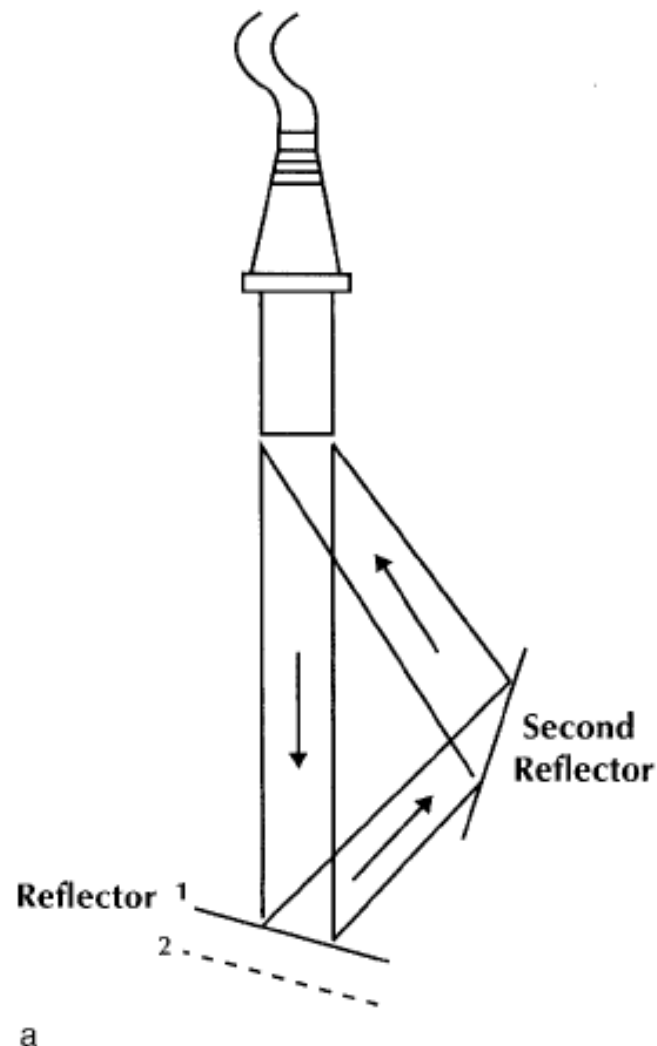
(a) A pulse (T) is transmitted from the transducer. A strong echo is generated at the real reflector and is received (I) at the transducer, allowing correct imaging of the reflector. However, the echo is partially reflected by the transducer so that a second echo (2) is received, as well as a third (3). These later echoes appear deeper on the display, where there are no reflectors. (b) A chorionic villi sampling catheter (straight arrow) and two reverberations (curved arrows). (c) A fetal scapula (straight arrow) and two reverberations (curved arrows).

Ultrasound imager: Artifacts–refraction



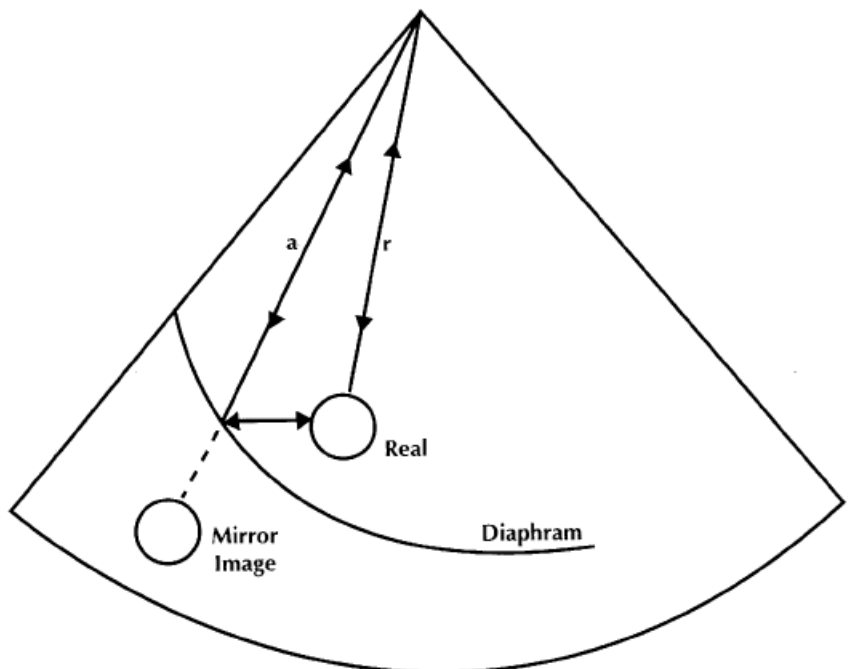
Refraction (a) results in improper positioning of the reflector on the display (b). The system thinks the reflector is at position 2 because that is the direction from which the echo was received when, in fact, the reflector is actually at position 1. (c) One real structure is imaged as two artifactual objects because of the refracting structure close to the transducer. If unrefracted pulses can propagate to the real structure, a triple presentation (one correct, two artifactual) can result.

Ultrasound imager: Artifact – Multipath

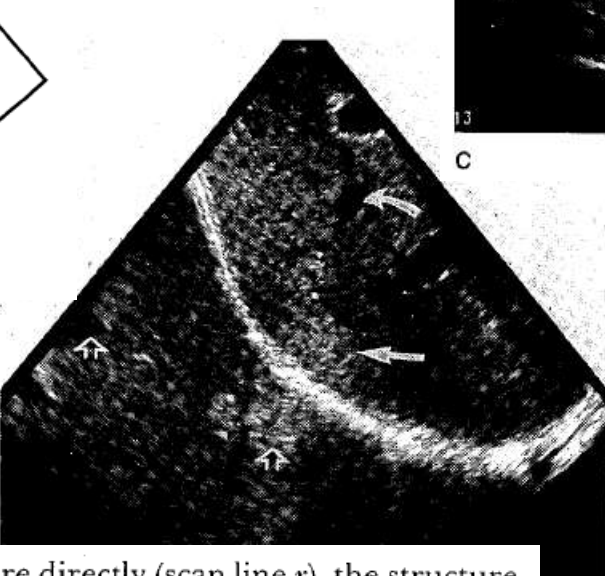


Multipath (*a*) causing improper positioning of the reflector on the display (*b*). The instrument thinks that the reflector is at position 2 because of the increased round-trip travel time required for a longer return path. The reflector is actually at position 1. The second reflector is not imaged.

Ultrasound imager: Artifacts – Mirror

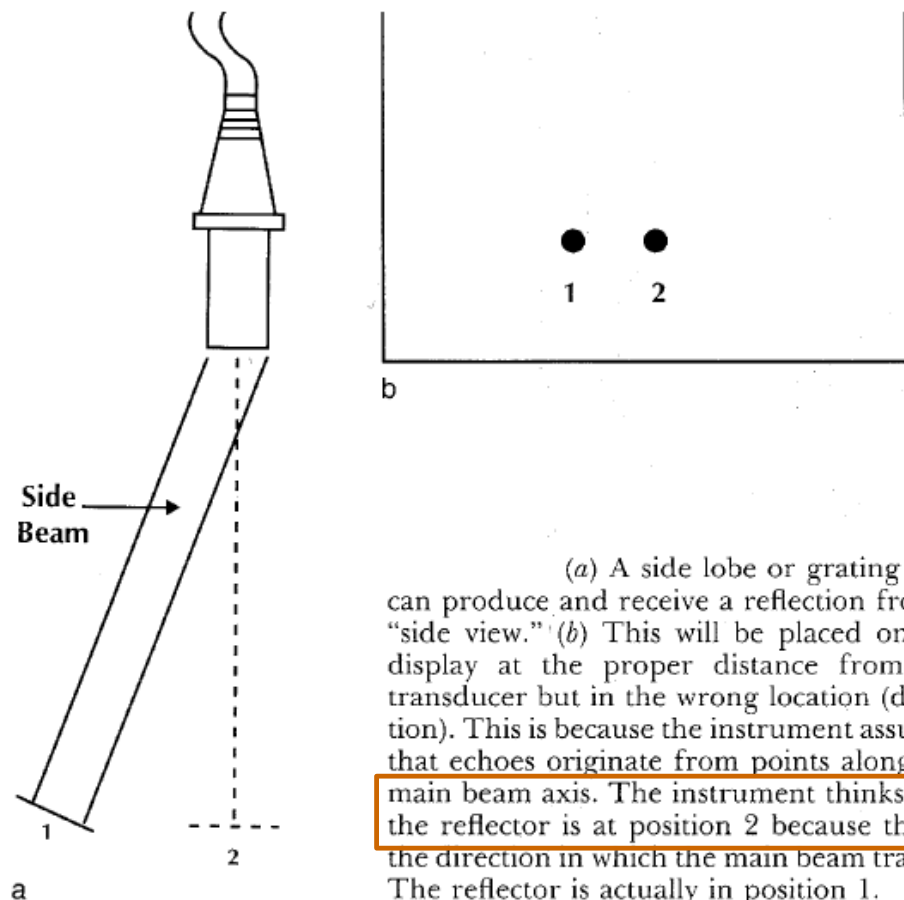
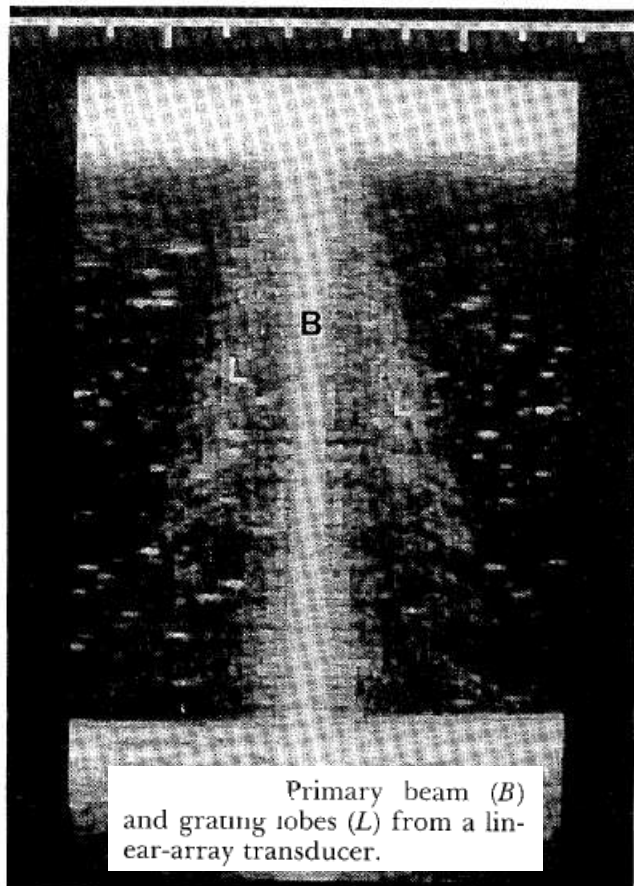


a



(a) When pulses encounter a (real) structure directly (scan line *r*), the structure is imaged correctly. If the pulse first reflects off the diaphragm (also the returning echo) (scan line *a*), the structure is imaged on the other side of the diaphragm. (b) A hemangioma (straight arrow) and vessel (curved arrow) with their mirror images (open arrows). (c) A vessel is mirror-imaged (arrow) superior to the diaphragm, but does not appear inferior because it is outside the unmirrored scan plane.

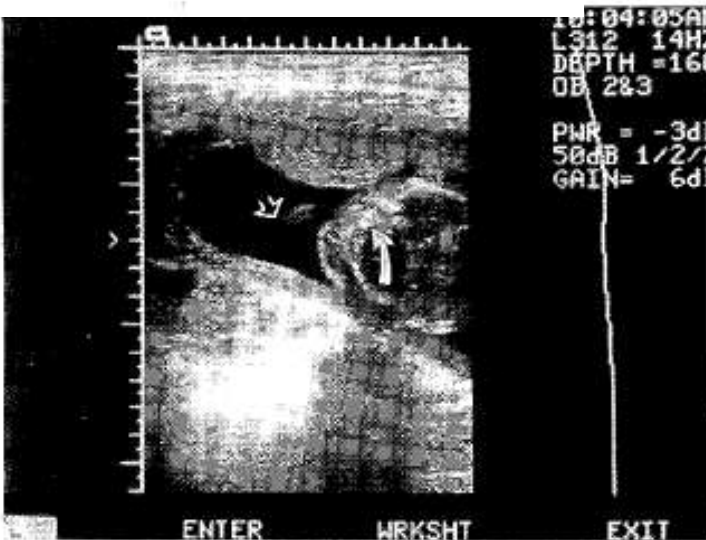
Ultrasound imager: Artifacts – slopes



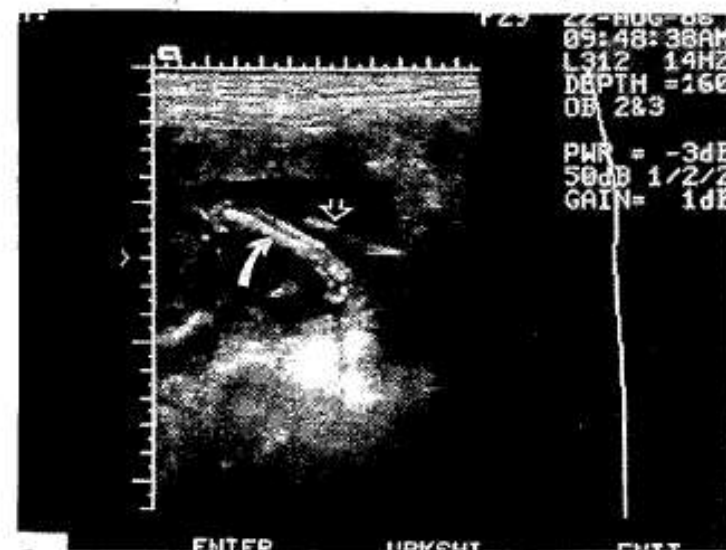
Ultrasound imager: Artifacts – slopes



a



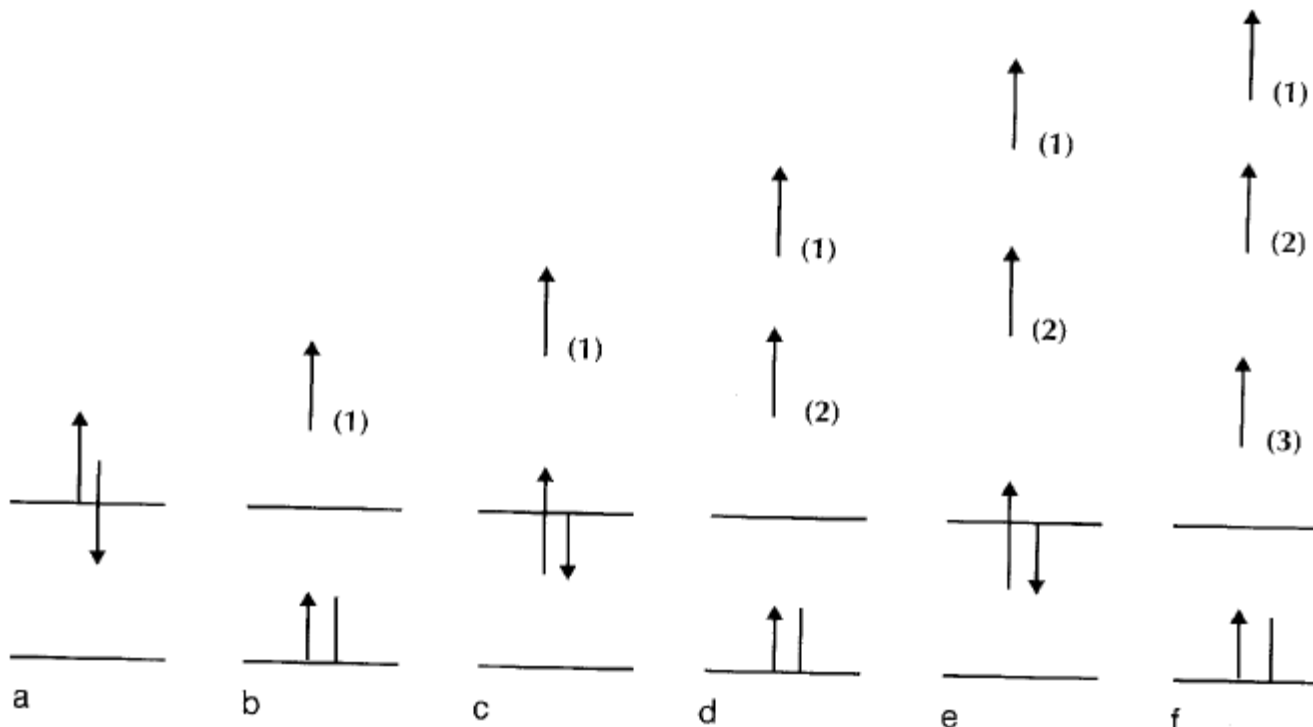
b



c

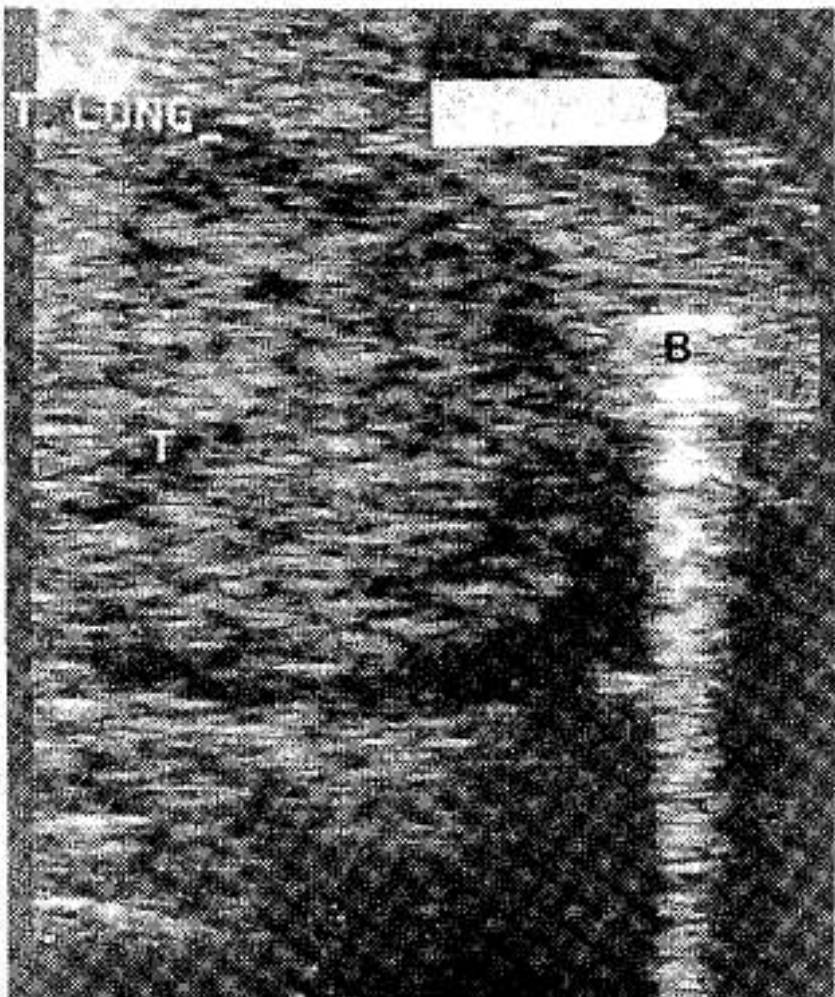
Side and grating lobes in obstetrical scans can produce the appearance of amniotic sheets or bands. (a) A real amniotic sheet (arrow). (b) and (c) Grating lobe (open arrow) **duplication of fetal bones** (curved arrow) appearing like amniotic bands or sheets.

Ultrasound imager: Artifacts – comet tail



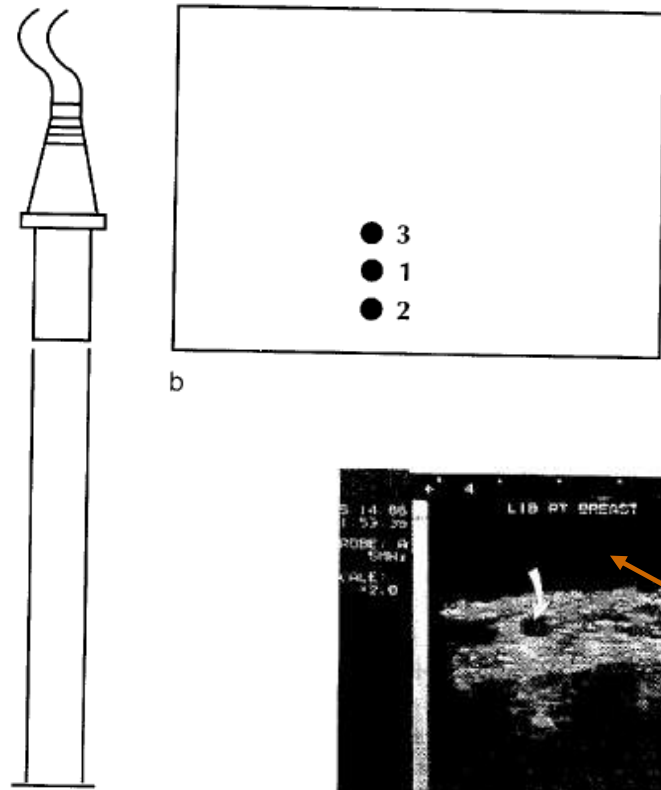
The generation of comet tail (closely spaced reverberations). Action progresses in time from left to right. (a) An ultrasound pulse encounters the first reflector and is partially reflected and partially transmitted. (b) Reflection and transmission at the first reflector are complete. Reflection at the second reflector is occurring. (c) Reflection at the second reflector is complete. Partial transmission and partial reflection are again occurring at the first reflector. (d) The echoes from the first (1) and second (2) reflectors are traveling toward the transducer. A second reflection (repeat of b) is occurring at the second reflector. (e) Partial transmission and reflection are again occurring at the first reflector. (f) Three echoes are now returning: the echo from the first reflector (1); the echo from the second reflector (2); and the echo from the second reflector (3), reflected from the back side of the first reflector (c) and reflected again from the second reflector (d). A fourth echo is being generated at the second reflector (f).

Ultrasound imager: Artifacts – comet tail

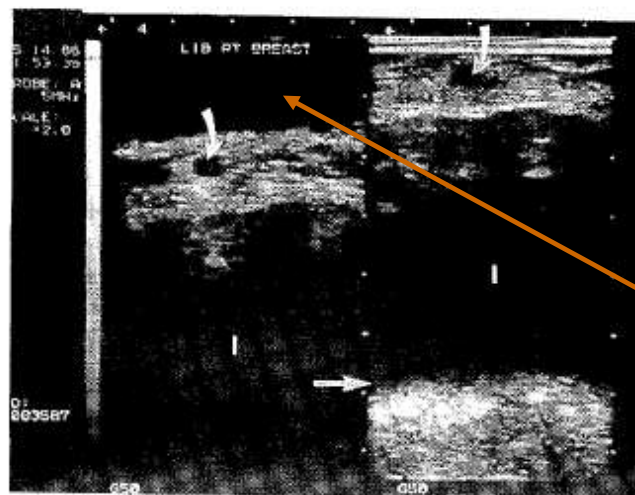


(g) Comet tail from an air rifle BB shot pellet (*B*) adjacent to the testicle (*T*). The front and rear surface of the BB are the two reflecting surfaces involved in this example.

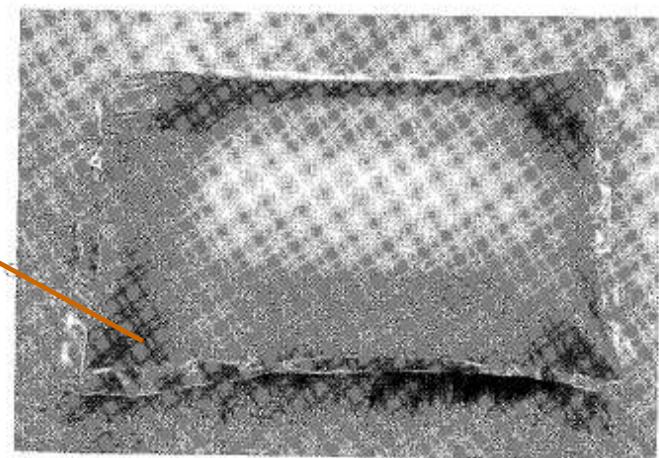
Ultrasound imager: Artifacts – speed variation



The propagation speed over the traveled path (a) determines reflector position on the display (b). The reflector is actually in position 1. If the actual propagation speed is less than that assumed, the reflector will appear in position 2. If the actual speed is more than that assumed, the reflector will appear in position 3.



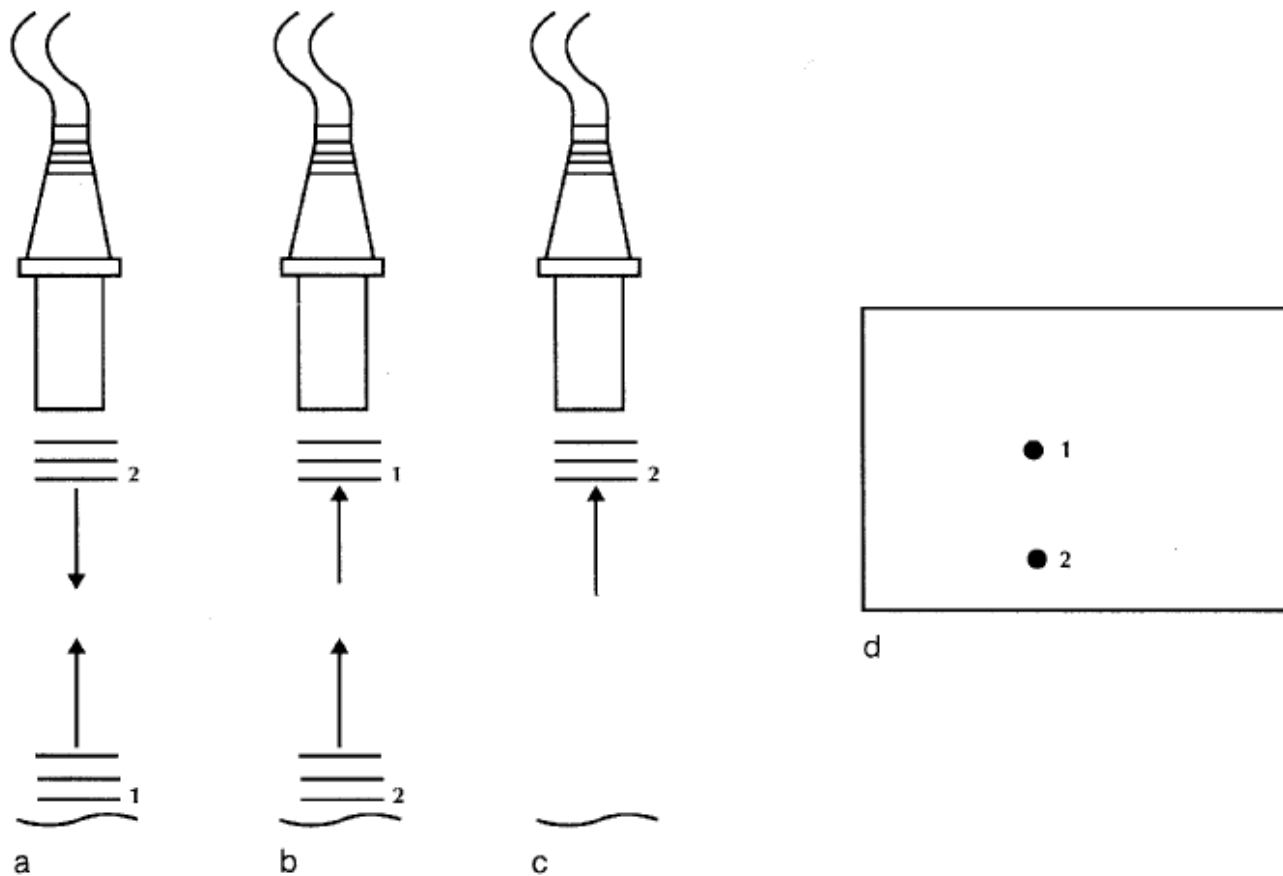
a



b

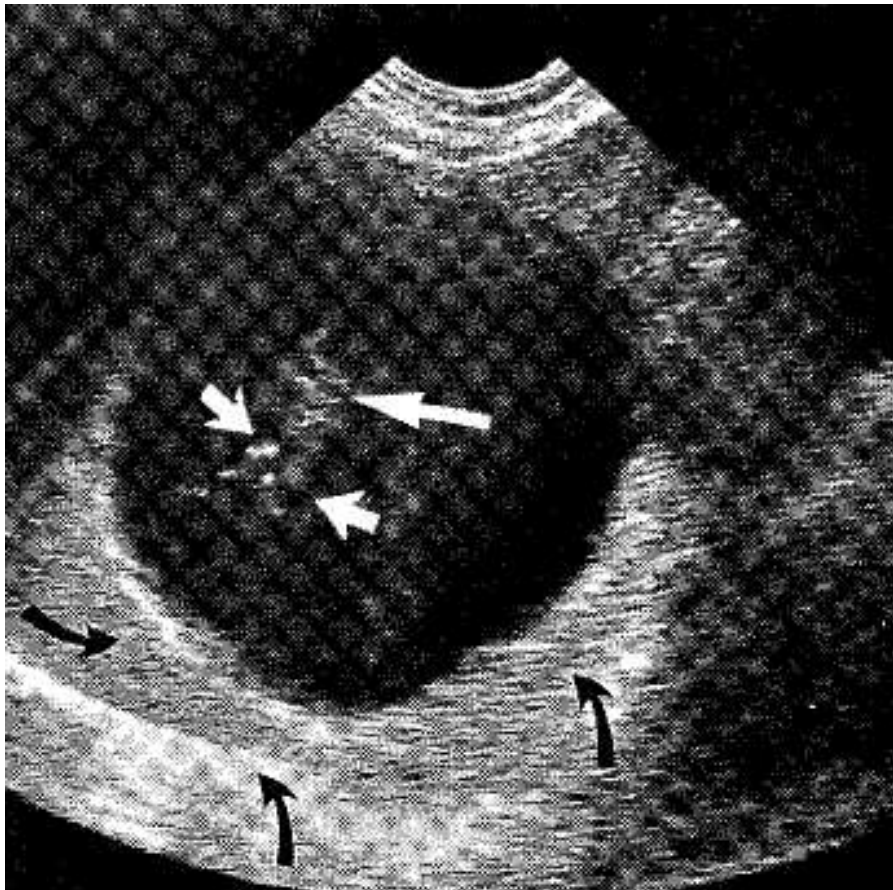
(a) The low propagation speed in a silicone breast implant (I) causes the chest wall (straight arrow) to appear deeper than it should. Note that a cyst (curved arrow) is shown more clearly on the left image than on the right. That is because a gel standoff pad (b) has been placed between the transducer and the breast, moving the beam focus closer to the cyst.

Ultrasound imager: Artifacts – doubled echoes



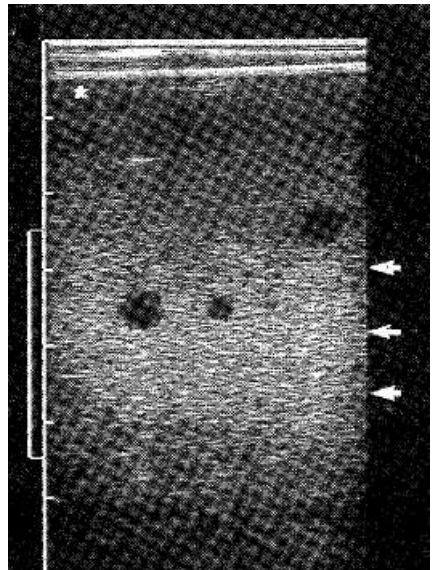
Ambiguity caused by sending out a pulse before an echo from the previous pulse is received. (a) A pulse (2) is sent out just as a previous pulse (1) is reflected. (b) The first echo arrives at the transducer when the second pulse reflects. (c) The second echo arrives at the transducer. (d) The spot (1) in the center of the display resulting from the arrival of the earlier pulse indicates a reflector at a location where there is none. The spot below (2) is in the correct reflector location.

Ultrasound imager: Artifacts – doubled echoes

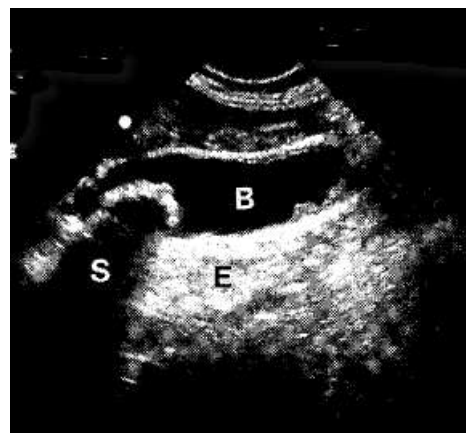


A large renal cyst (having a diameter of about 10 cm) has artifactual range-ambiguity echoes within it (*white arrows*). These came from structure(s) below the display. These deep echoes arrived after the next pulse was emitted, so they were thought to have arrived earlier and were placed closer to the transducer than they should have been. Echoes arrived from much deeper (later) than usual in this case because the sound passed through the long, low-attenuation paths in the cyst. These echoes may have come from bone or a far body wall. Low attenuation in the cyst is indicated by the strong echoes (enhancement) below it (*curved black arrows*).

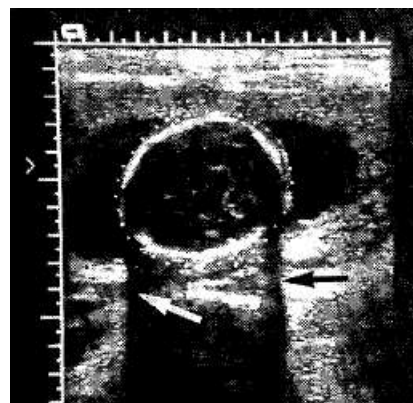
Ultrasound imager: Artifacts – shadowing



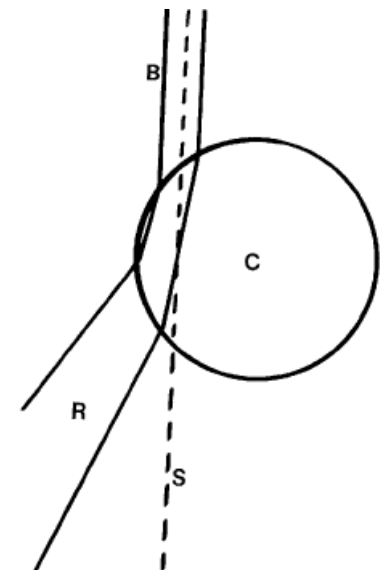
Focal banding (*arrows*) is the brightening of echoes around the focus where intensity is increased by the narrowing of the beam.



Shadowing (*S*) from a gallstone and enhancement (*E*) caused by the low attenuation of bile (*B*).



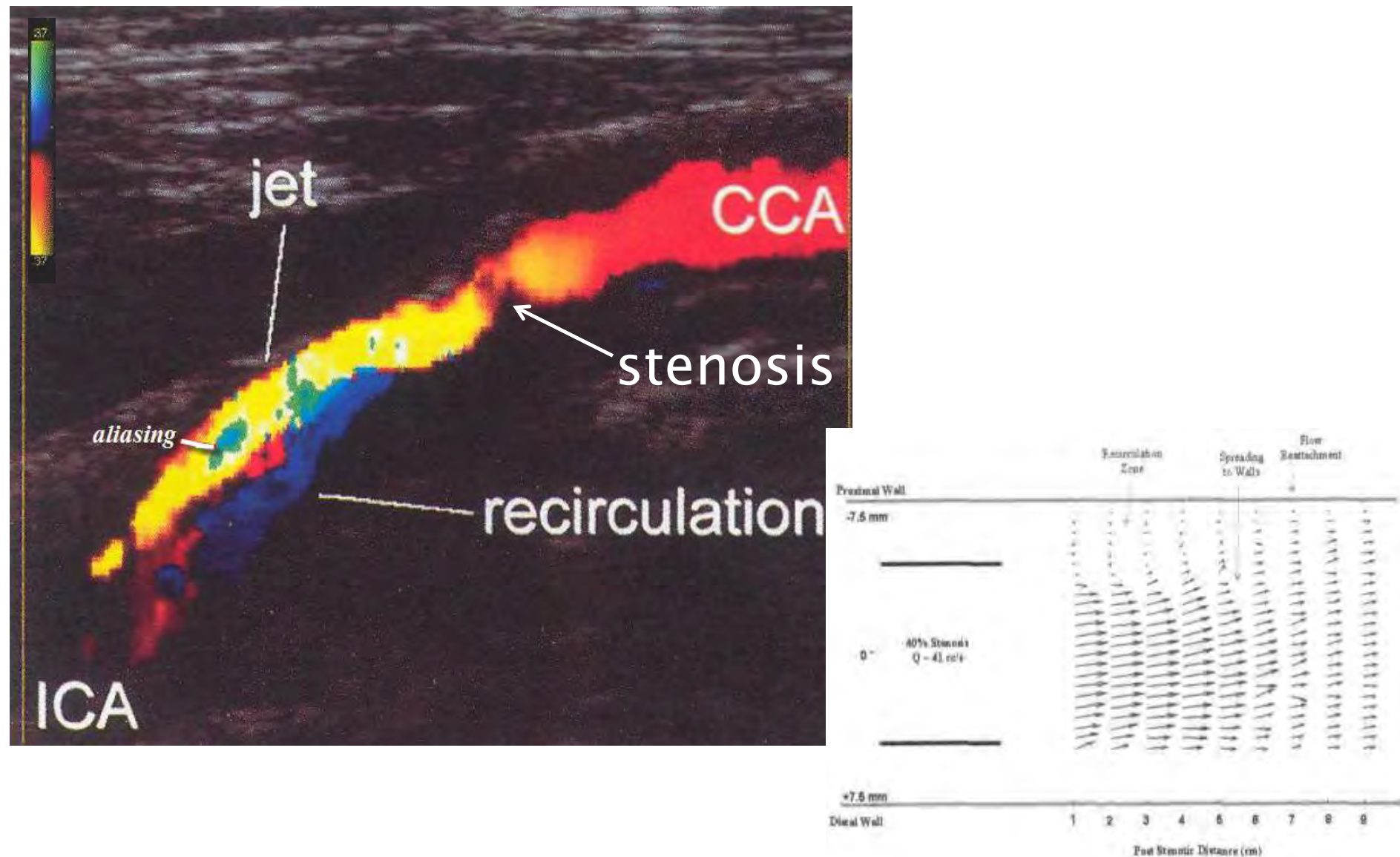
Edge shadows (*arrows*) from a fetal skull.



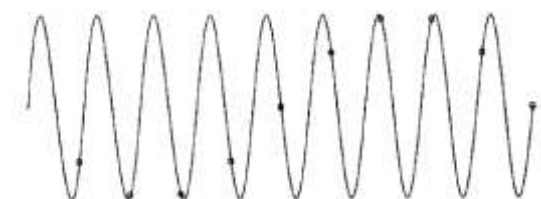
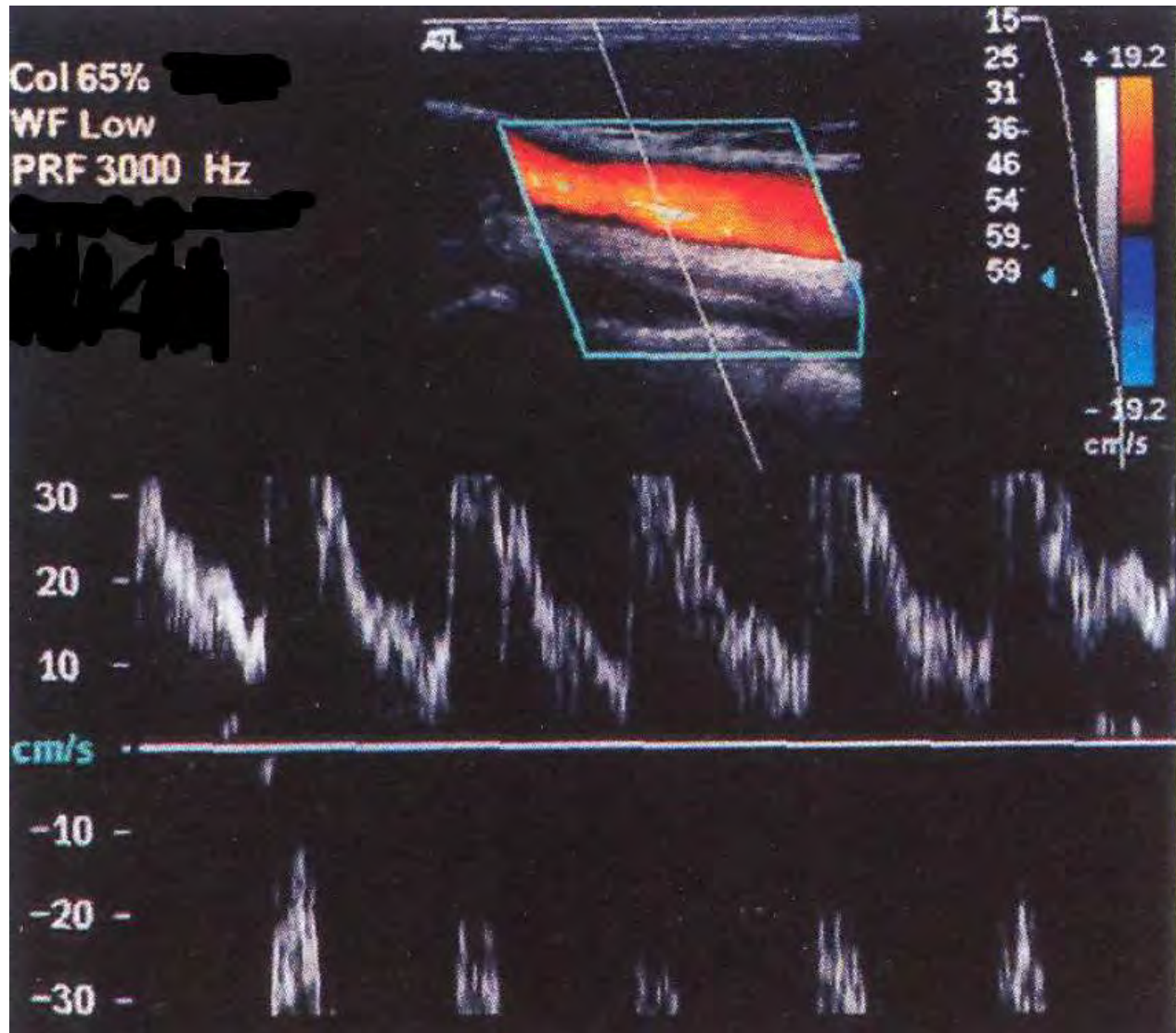
As a sound beam (*B*) enters a circular region (*C*) of higher propagation speed, it is refracted, and refraction occurs again as it leaves. This causes spreading of the beam with decreased intensity. The echoes from region *R* are presented deep to the circular region in the neighborhood of the dashed line. They are weak owing to the beam spread, thus giving the shadow in the region *S*.

Ultrasound Color Doppler Artifacts

Stenosis; variation of Doppler angle; jet-stream, recirculation and Aliasing



Ultrasound Spectral Doppler-Artifacts (Aliasing)

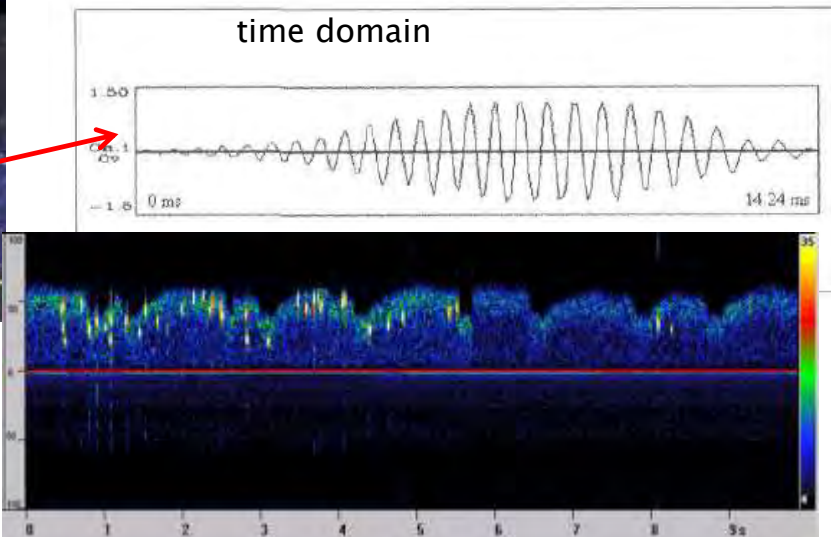
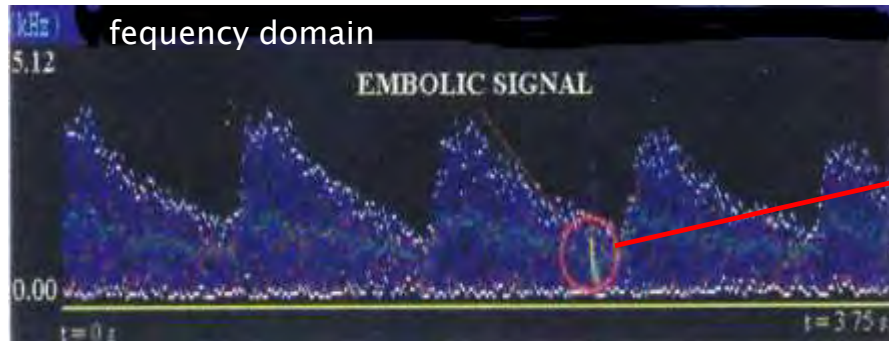


11 point/9 cycles

} wrap around /
 f_D -rotation

A triplex image representing B-mode, colour Doppler velocity image and spectral Doppler in the same display. The aliasing artefact is seen in both the colour Doppler velocity image and in the corresponding spectral Doppler

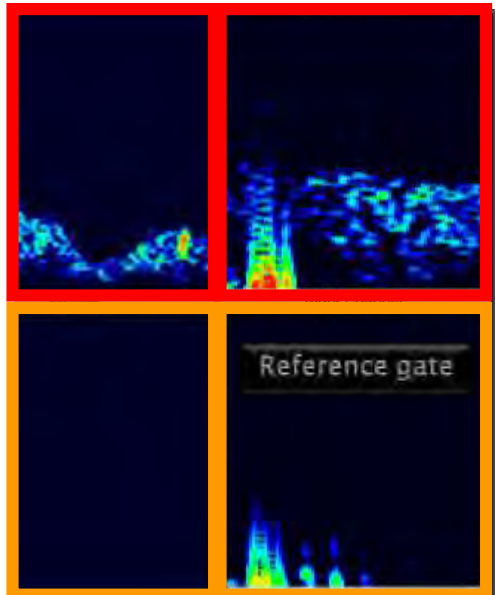
Ultrasound Spectral Doppler-Embolus/Artifacts



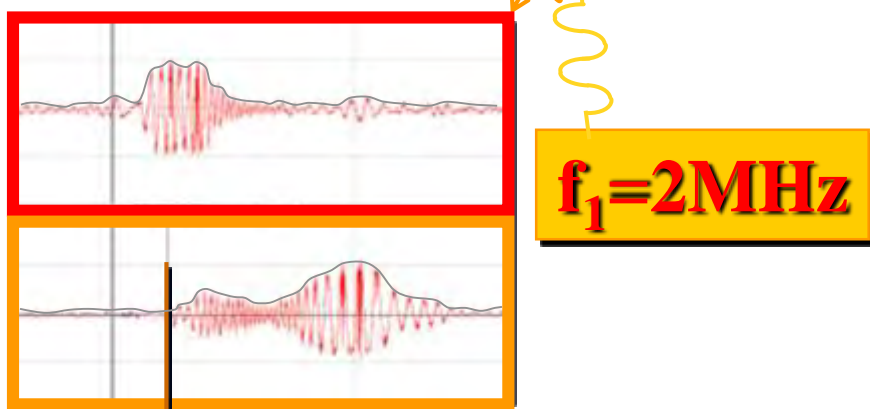
Sonogram showing the effect of overload as two emboli with large cross-sections move through the Doppler sample volume

Spectral Doppler: Artifacts rejection

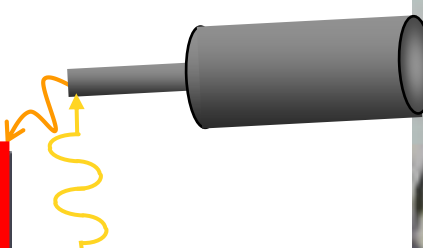
Embolus Artefact



Dual gate Doppler

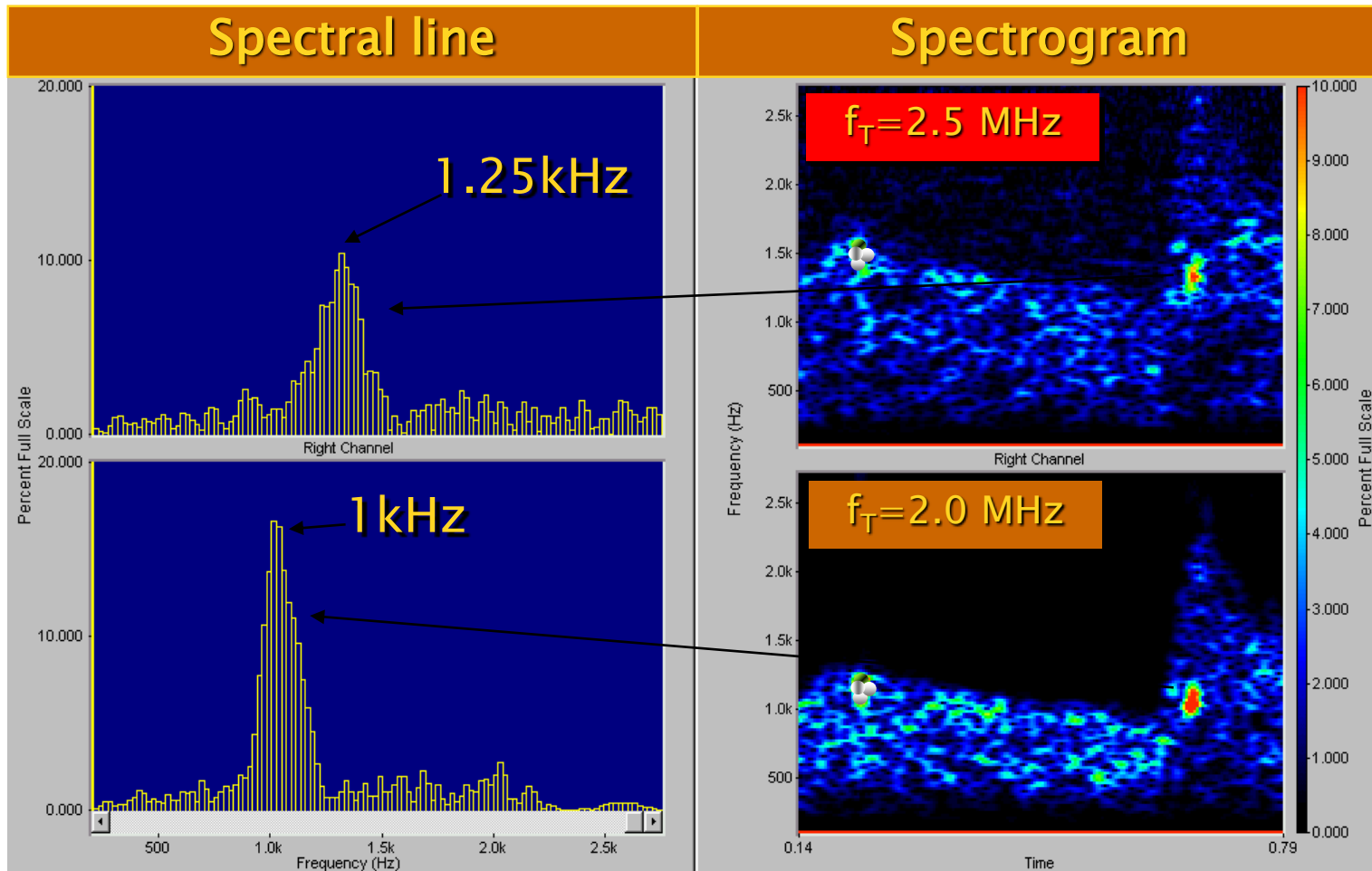


$$\Delta d = ?$$



Spectral Doppler: Artifacts rejection

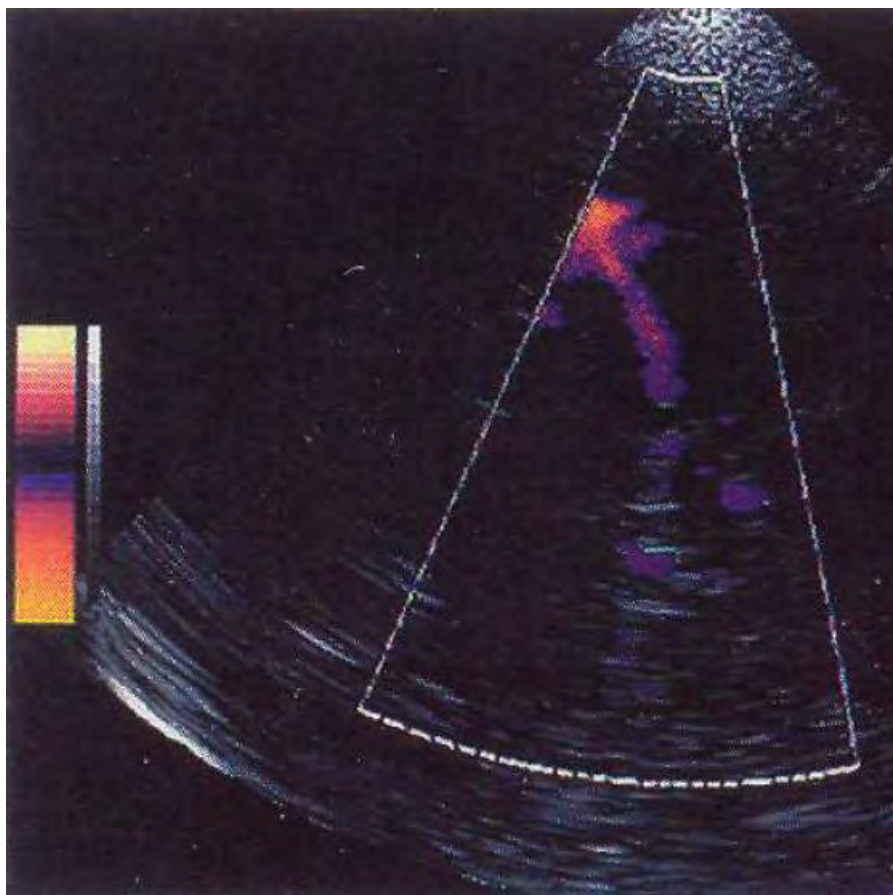
Quarter Doppler shift using Dual frequency



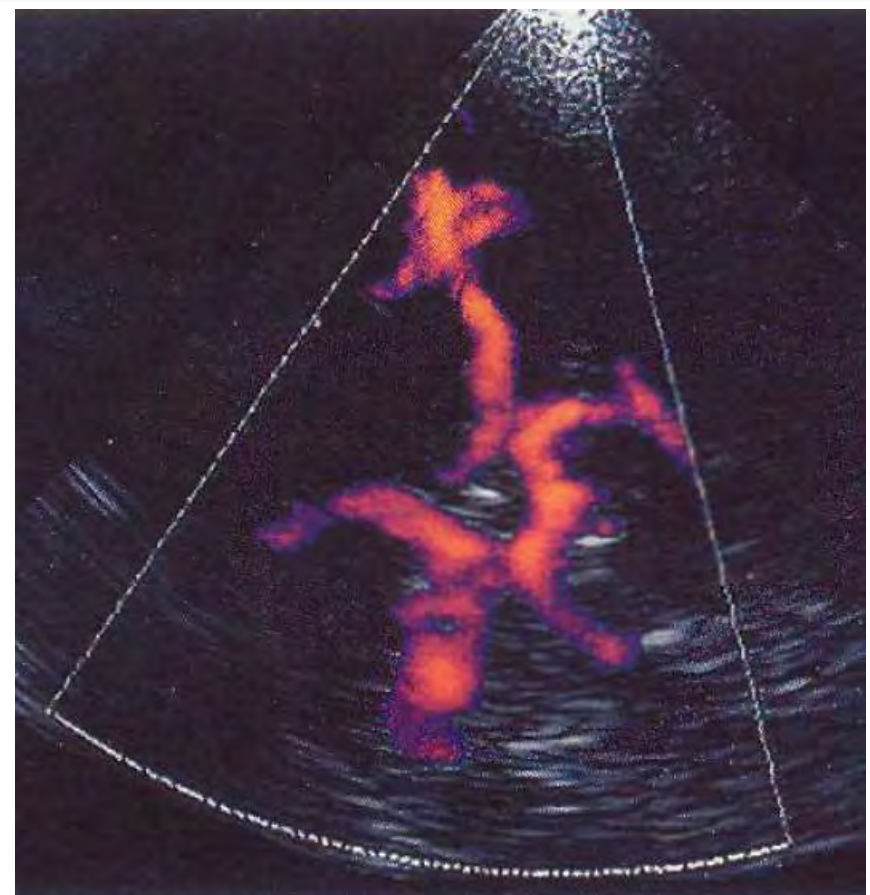
MCA bubble: $v \approx 40\text{cm/s}$; $SV_{\text{axial}} = 10\text{mm}$

Ultrasound Contrast agent → blooming

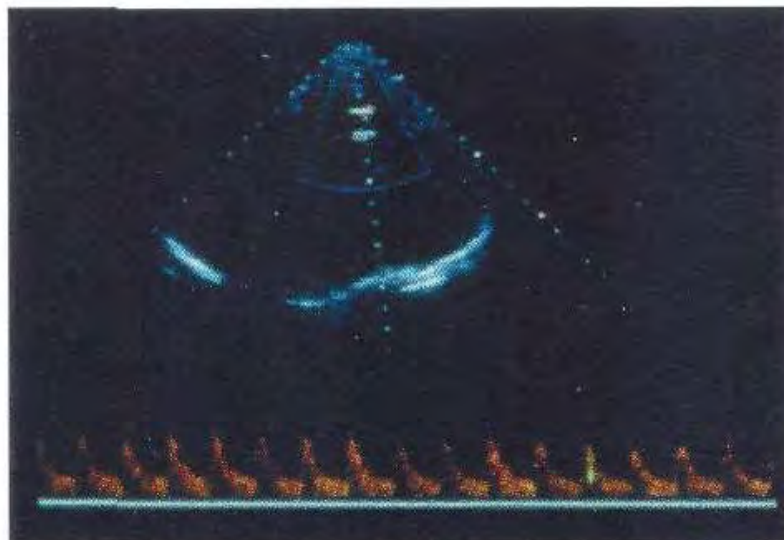
TCCI Power Doppler: No bubbles



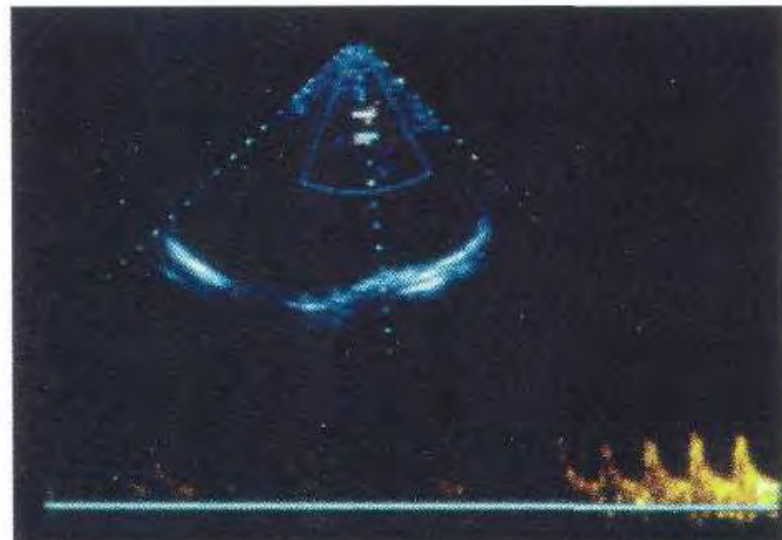
TCCI Power Doppler: Bubble bolus → blooming



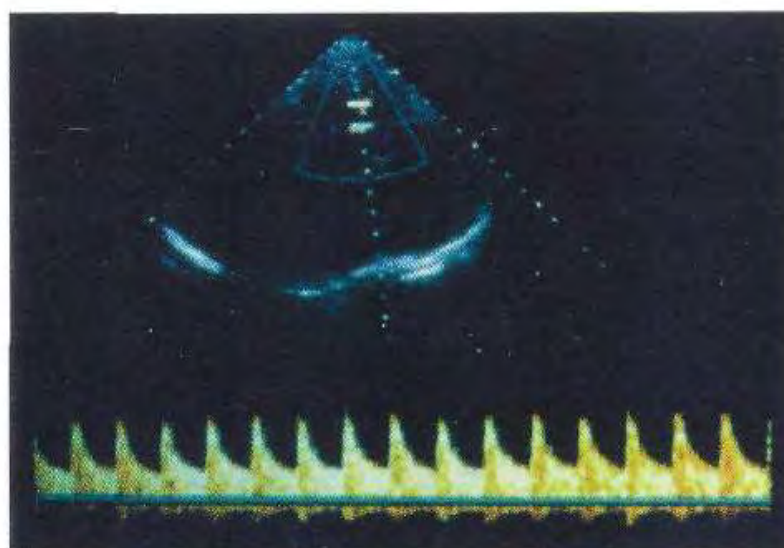
Spectral Doppler: Contrast agent → enhancement



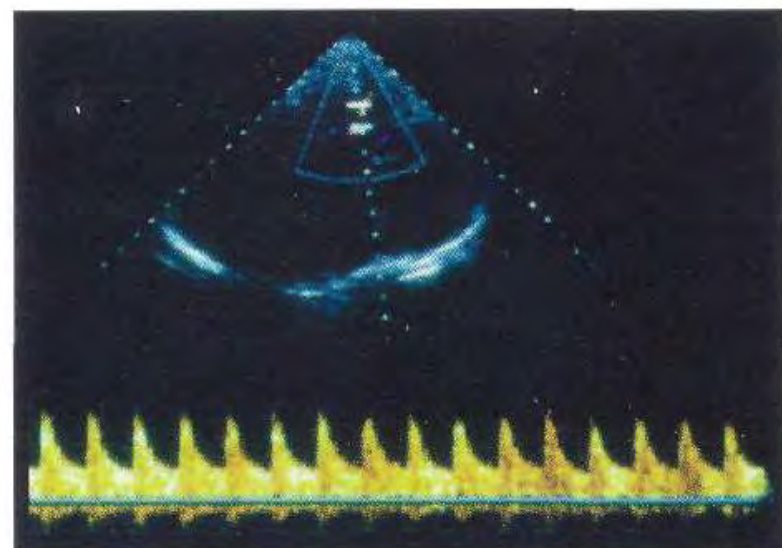
a) MCA no contrast agent



b) Gain reduced to avoid overload



c) Maximum intensity of the bolus



d) Descend of the intensity/bolus

Ultraschall und Theragnostik

Ultraschall in Thera(pie) und (Dia)gnostik

Kapitel 7

Ultraschall und Kontrastmittel

1. Übersicht der Ultraschallanwendungen
2. Physikalische Grundlagen
3. Ultraschallsonden
4. Bildgebende Verfahren in der Diagnostik
5. Dopplerverfahren in der Diagnostik und Therapie
6. Artefakte und Diagnostik
7. **Ultraschall und Kontrastmittel**
8. Theragnostik mit Ultraschall
9. Therapie mit hochdosierten Ultraschall
10. Gewebecharakterisierung mittels shear waves
11. Dosierung und Sicherheitsaspekte

ultrasound contrast agent → applications

contrast agent/encapsulated micro-bubbles = gas-filled microspheres

Applications of contrast agent and targeted microbubbles:

- strong reflection due to low acoustic impedance → enhancement
- low acoustic pressure – nonlinearity reflections (Harmonics)
- Ultrasound and bubble destruction →
cavitation, microstreaming, permeability of membranes
- bubbles as vehicle for drugs and genes (local delivery)
- microbubbles and thrombolysis
- Enhancement left ventricular image
- Myocardial perfusion imaging
- Cerebral perfusion imaging
- Increase Doppler signal intensity

History and Physics

- 1968: saline water with microbubbles enhanced aortic delineation
- air-filled bubbles disappear by solubility and filtered especially during lung passage
- Stability by shell out of Albumin (Albunex), Galactose (Levovist)
- Gas with heavy-molecular-weight (Sonovue; 2,5 μ m) → improvement capillary and lung passage with recirculation
- MI (PNP/\sqrt{Ftx})>0.05 causes nonlinear behaviour → harmonics
- potential use for drug delivery → cavitation, destruction
- Since 2001 Sonovue microbubbles (loaded with nanospheres → targeted)
- microbubbles exposed to ultrasound could cause mechanical stress to act on cells and consequently lead to cell injury/permeability and Embolysis

Ultrasound contrast agent – basics

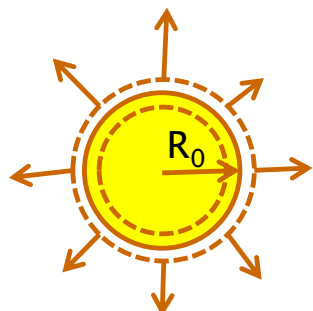
Commercial contrast agent list (IEEE short course Hawaii 2003)

Manufacturer	Name	Gas	Shell	Status
Acusphere	AI-700	Decafluorobutane	Polymer	Pre-clinical
Alliance/Schering	Imavist	Perfluorohexne	Surfactant	Approved
Bracco	Sonovue	Sulfurhex/Fluoride	Phospholipid	Available EU
Bracco	BR14	Perfluorocarbon	Phospholipid	Clinical
Byk-Gulden	BY963	Air	Lipid	Research Only
Dupont-	Definity	Octafluoropropane	Liposome	Available USA/Canada
IMARx	Aersomes	Perfluoropropane	Lipid bilayer	Clinical
Mallinckrodt	Albunex	Air	Albumin	Available
Mallinckrodt	Optison	Octafluoropropane	Albumin	Available
Nycomed	Sonazoid	Perfluorocarbon	Lipid	Late Clinical
Point Biomedical	BiSphere	Air	Polymer bilayer	Late Clinical
Porter	PESDA	Perfluorocarbon	Albumin	Research
Quadrant	Quantison	Air	Albumin	Clinical/hold
Schering	Echovist	Air	No	Available
Schering	Levovist	Air	Fatty acid	Available
Schering	Sonavist	Air	Polymer	Clinical
Sonus	Echogen	Deodecafluoropentane	Surfactant	Withdrawn 2000

Ultrasound contrast agent – basics

Mathematics: non-linear Rayleigh–Plasset equation

$$P\ddot{R} + \frac{3}{2}\dot{R}^2 = \frac{1}{\rho_l} \left[p_g - p_l - \frac{2\sigma}{R} - \frac{4\mu}{R} \dot{R} \right]$$



R = bubble radius

\dot{R} = velocity of bubble wall motion

\ddot{R} = bubble boundary acceleration

P_l = ambient pressure with liquid

p_g = internal bubble gas pressure

ρ_l = liquid density

μ = liquid viscosity

σ = surface tension

Resonance frequency with compression↔expansion
model for adiabatic air bubbles in water:

$$f_{reson} = \frac{329}{R_0}$$

$$R_0 = 2 \text{ } \mu\text{m}, f_{reson} \sim 1.645 \text{ MHz}$$

Ultrasound contrast agent – harmonics

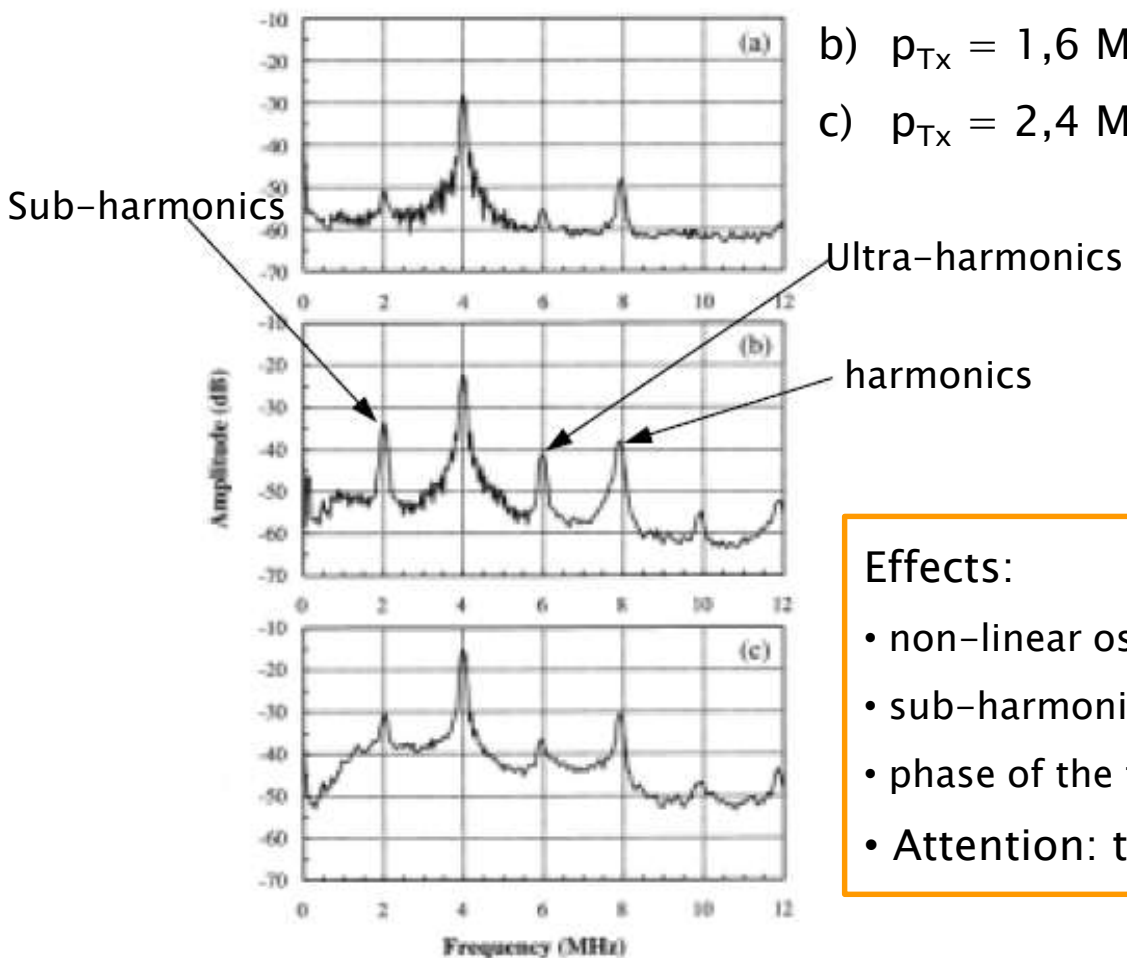
Harmonic behaviour → non-linear response

Spectra of the scattered signal insonified by p_{Tx}

a) $p_{Tx} = 0,8 \text{ MPa}$: linear at 4MHz

b) $p_{Tx} = 1,6 \text{ MPa}$: non-linear at 4MHz

c) $p_{Tx} = 2,4 \text{ MPa}$: non-linear at 4MHz



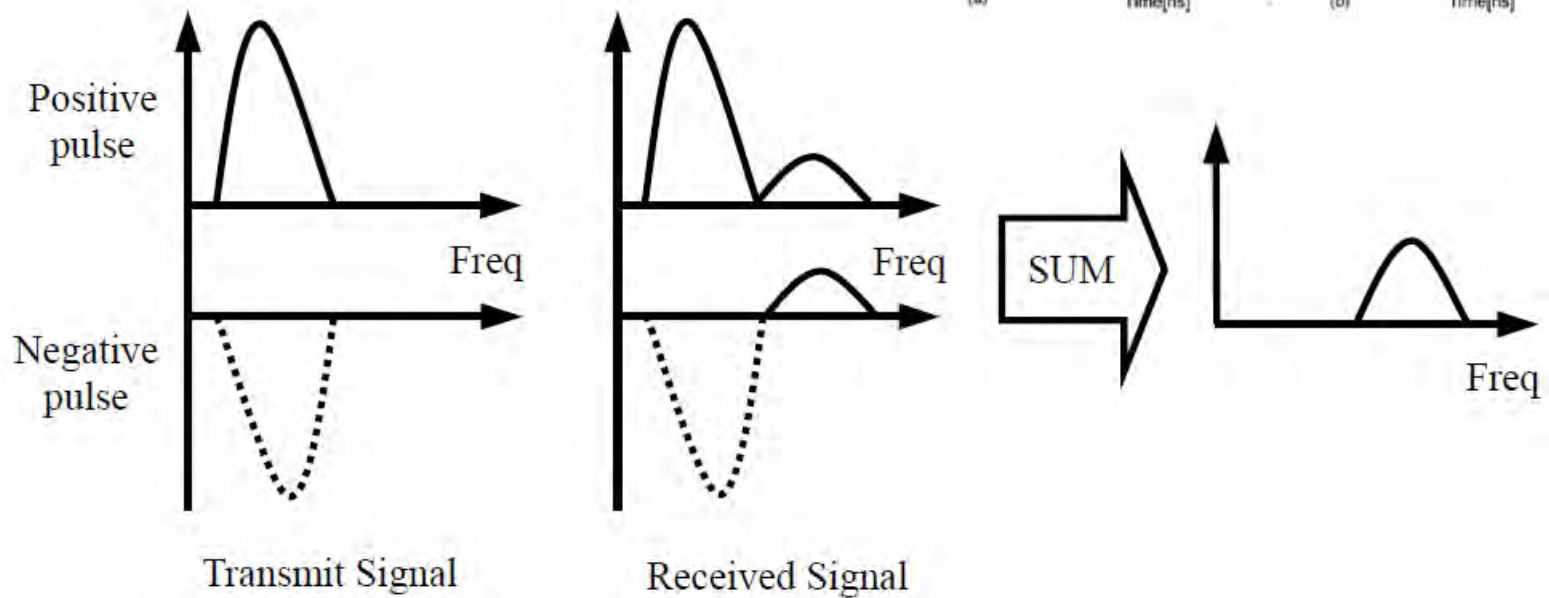
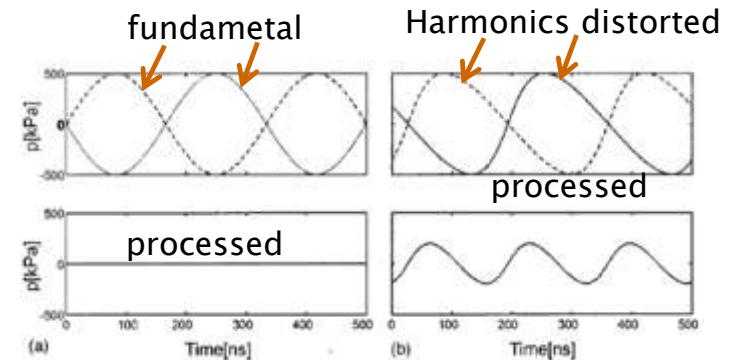
Effects:

- non-linear oscillation by sufficient acoustic pulse
- sub-harmonics, ultra-harmonics
- phase of the transmitted pulse → phase inversion
- Attention: tissue shows also small harmonics

Ultrasound contrast agent – harmonics

Harmonic behaviour → Phase inversion technique

Principle : Pulses succession into tissue
→ tissue subtraction
→ Sensitive bubble extraction

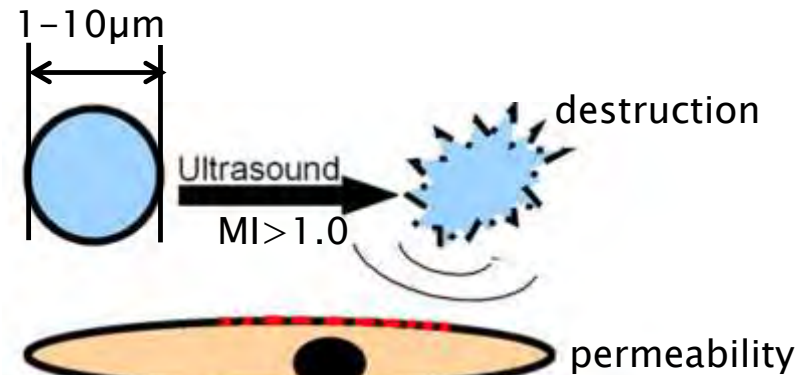
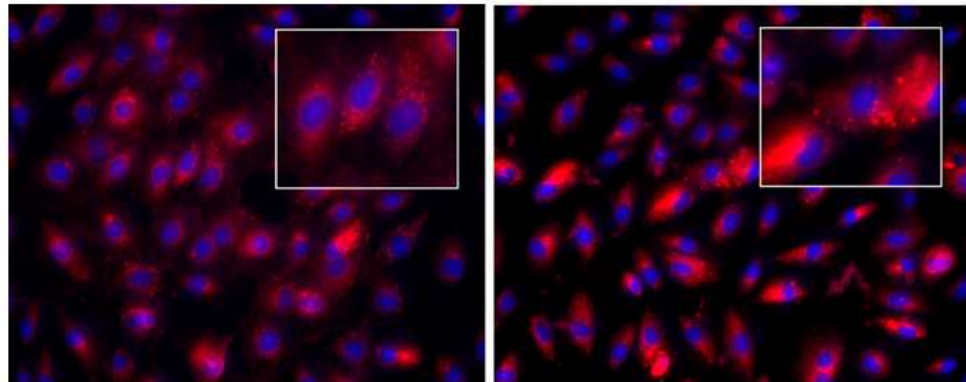


Ultrasound contrast agent – drugs

Microbubbles and their bioeffects

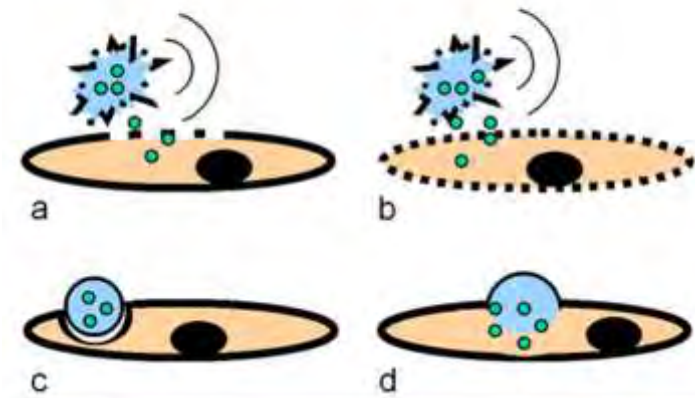
- Vehicles for delivery drugs to cells (blue nucleus)

Uptake of red fluorescent nanospheres



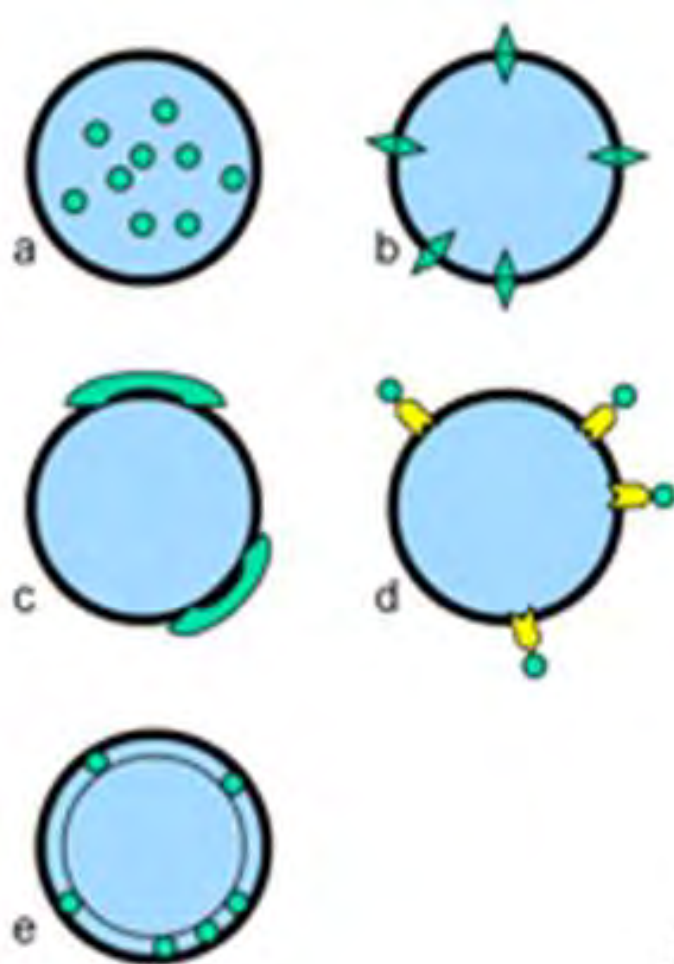
drug delivery:

- a) transient holes
- b) membrane fluidity
- c) endocytosis
- d) fusion



Ultrasound contrast agent – drugs

Microbubbles and attached drugs

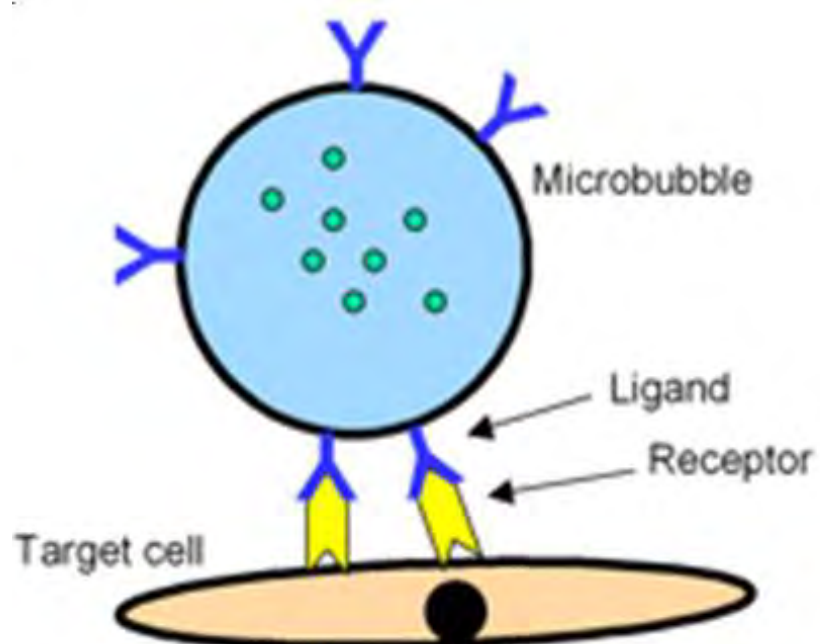


drug attachment:

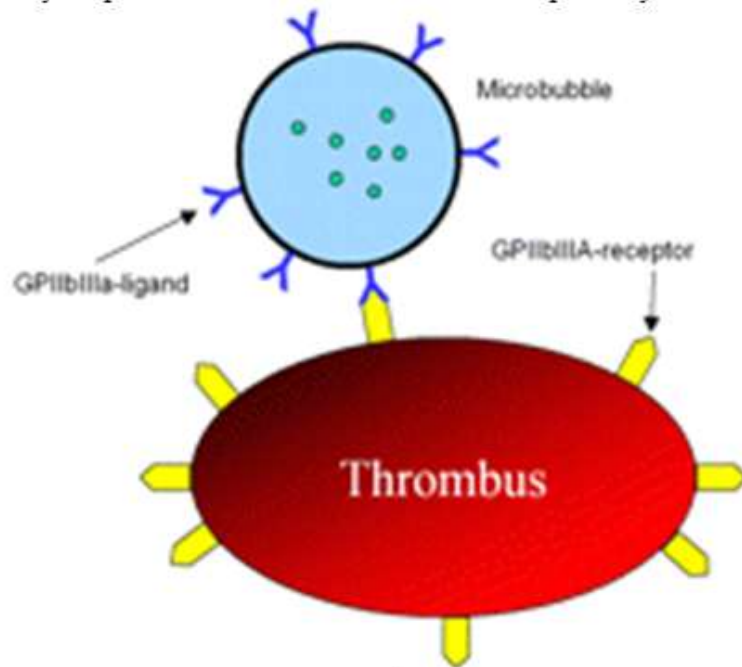
- a) incorporation in the bubble
- b) Incorporation in the membrane
- c) attachment to the membrane
- d) attachment to a ligand
(koordinative /non-kovalent)
- e) Incorporation in a multilayer

Ultrasound contrast agent – drugs

Targeted microbubbles and drugs delivery



connected by ligand and receptor

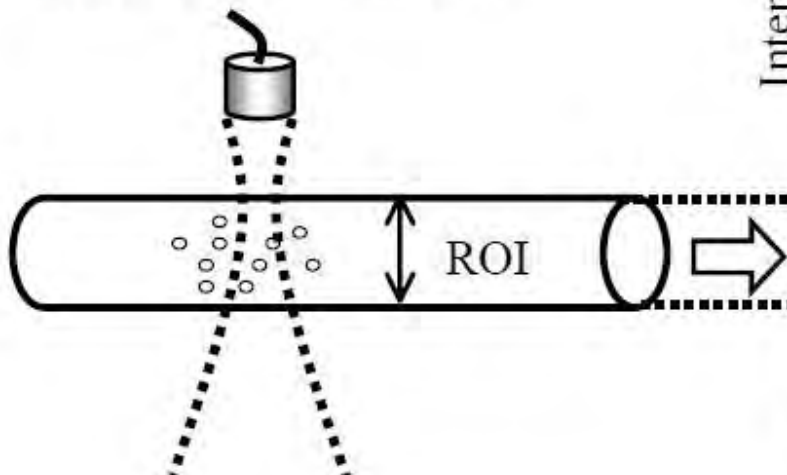


binding to vascular thrombus
for accelerating lyses

Ultrasound contrast agent – Enhancement

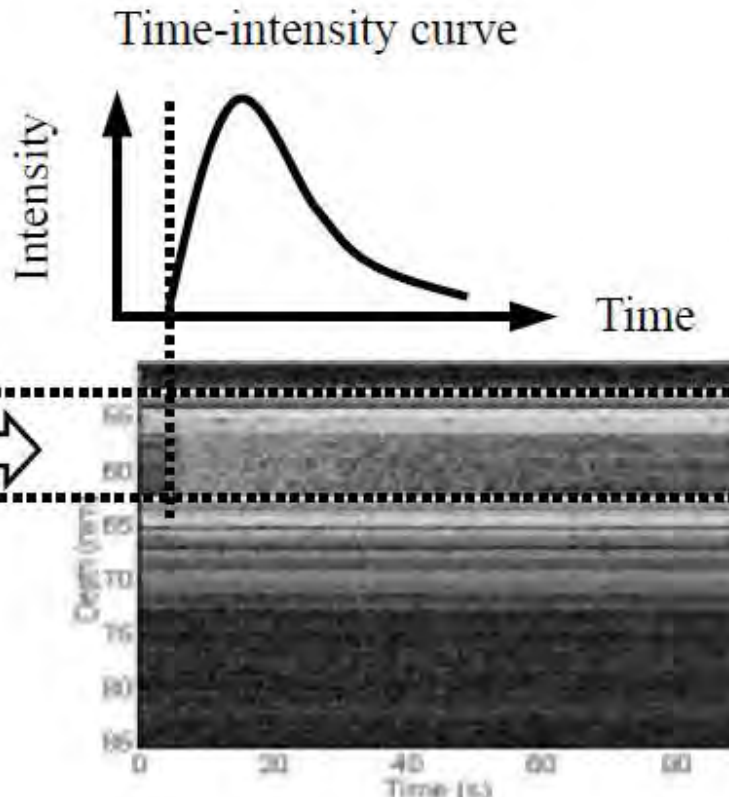
Dilution and destruction : time-intensity curve
plus time variance imaging (TVI)

ROI : Region of Interest



Signal processing:

- Bolus harmonic imaging
- contrast burst imaging
- Harmonic Power Doppler
- Disadvantage → shadowing



Ultrasound contrast agent – bolus → perfusion

Principle of perfusion: Bolus with in-flow → out-flow

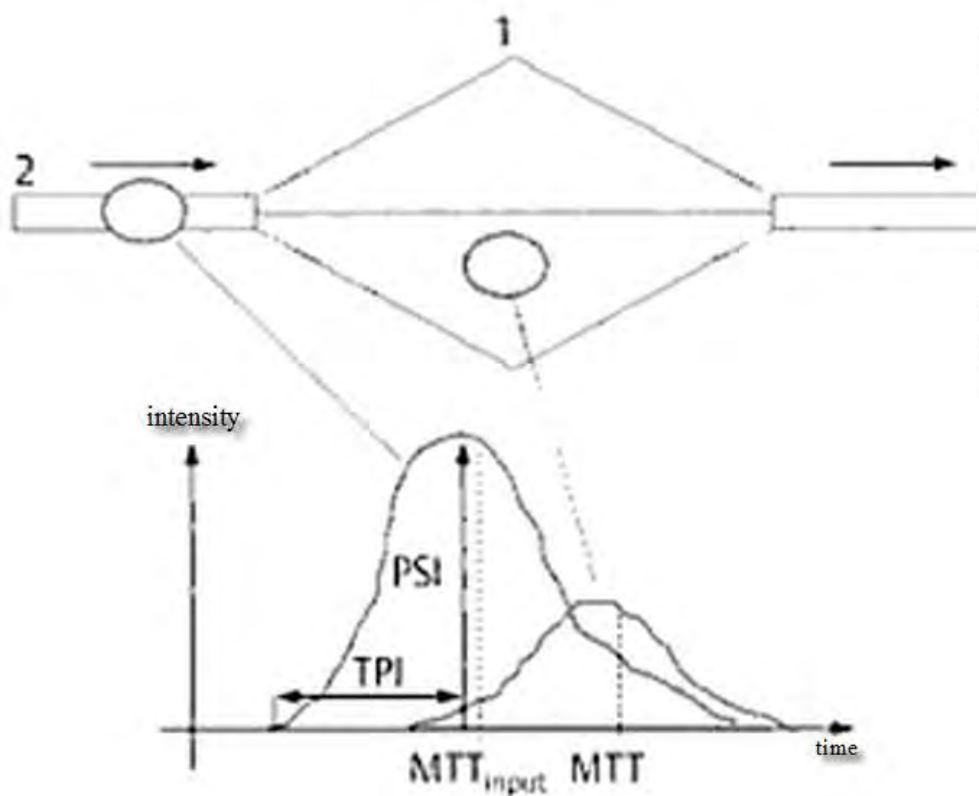


Abb. Boluskinetik. Schematische Darstellung des Kapillarnetzes (1) mit dem zuführenden Gefäß (2). Zeit-Intensitäts-Kurven nach Kontrastverstärker-Bolusinjektion eines Inputgefäßes (weiß) und einer hiervon abhängigen Parenchymregion (grün). Gemäß der GI lässt sich aus der Fläche unter der Zeit-Intensitäts-Kurve (AUC) und der mittleren Transitzeit (MTT) der Blutfluss pro Volumeneinheit berechnen. Der maximale Signalanstieg wird als PSI (Peak Signal Increase) und die Zeit zwischen Kontrastbeginn und maximaler Kontrastierung als TPI (Time-to-Peak-Intensity) bezeichnet

In der Arbeit von Heidenreich (Heidenreich et al. 1993) ist die Formel zur Berechnung der Flussrate pro Volumeneinheit nach Kontrastverstärker-Bolusinjektion beschrieben (Gl. 21.1).

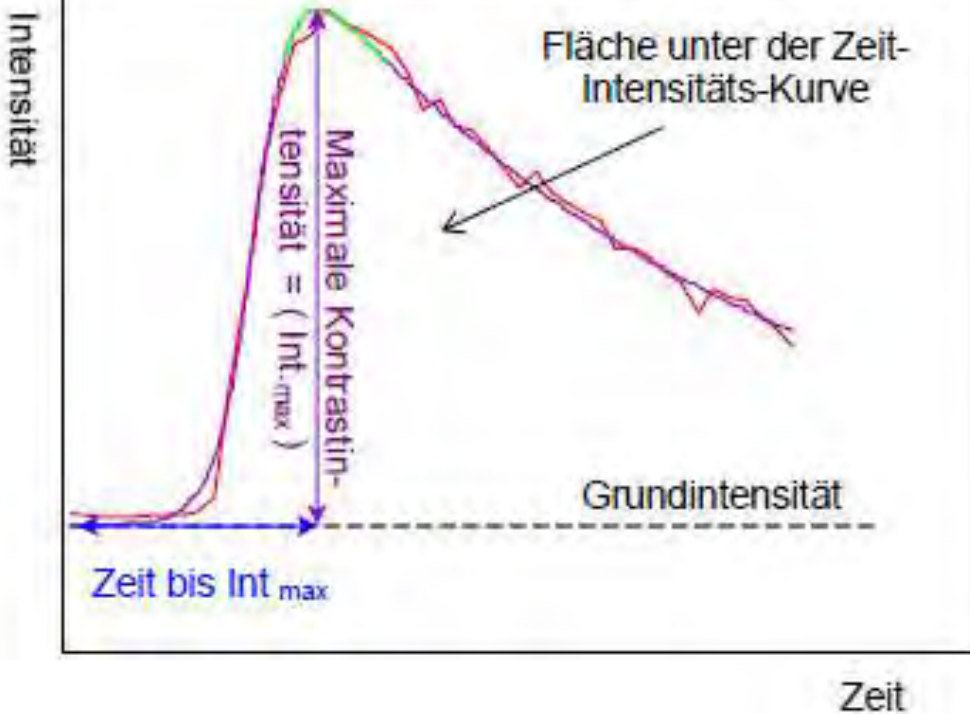
$$F_V \sim AUC_R/2 AUC_I (MTT_R - MTT_I)$$

F_V = Blutfluss pro Volumeneinheit, AUC_R = Fläche unter der primären Transitkurve des Indikators im Gewebe, AUC_I = Fläche unter der primären Eingangskurve in das Gewebe, MTT_R = mittlere Transitzeit der primären Transitkurve des Indikators im Gewebe, MTT_I = mittlere Transitzeit der primären Eingangskurve in das Gewebe.

Ultrasound contrast agent – bolus → perfusion

Methods of contrast (second) harmonic imaging sHI / CHI and / or pulse inversion (phase technique) → S/N-increase

Non-destructive in ROI (e.g. cerebral perfusion)



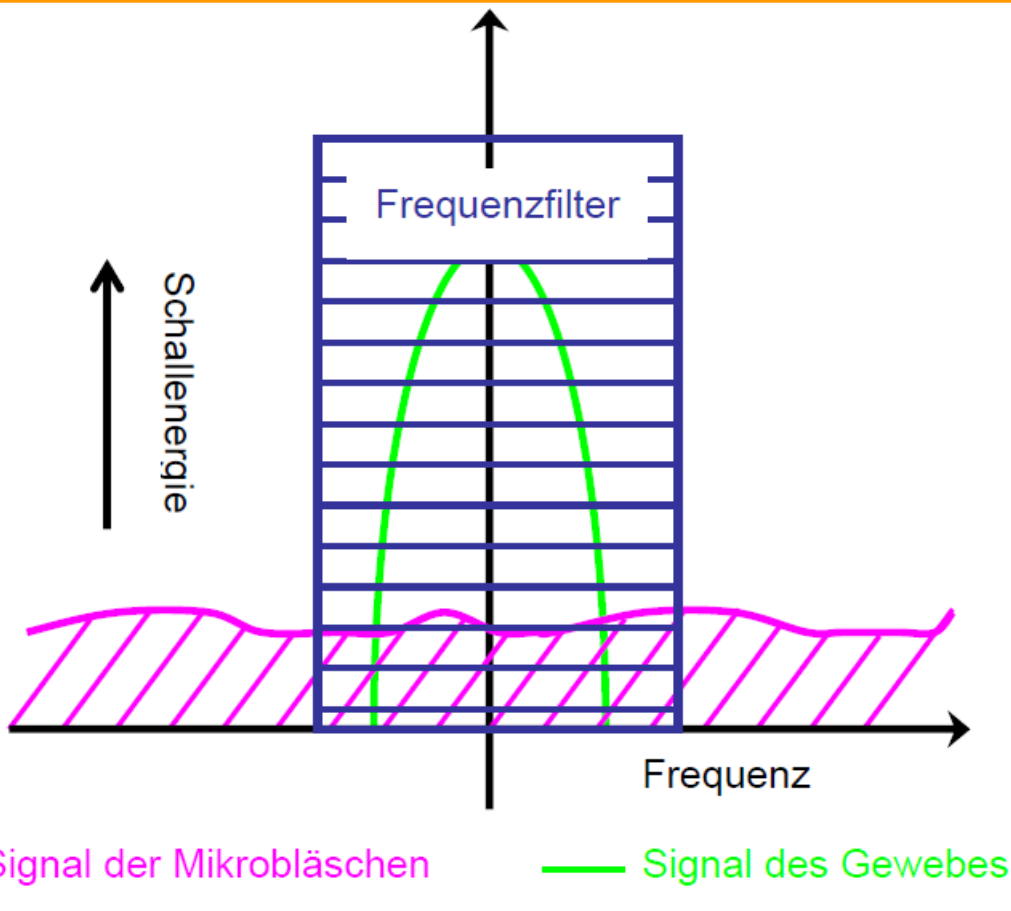
Studien:

- Postert et al. (1998)
- Seidel et al. (2000)
- Federlein et al. (2000)
- Schlachetzki und Hoelscher et al. (2000)
- Wiesmann und Seidel (2000)

Methods of contrast burst imaging (CBI)

destructive in ROI (e.g. cerebral perfusion)

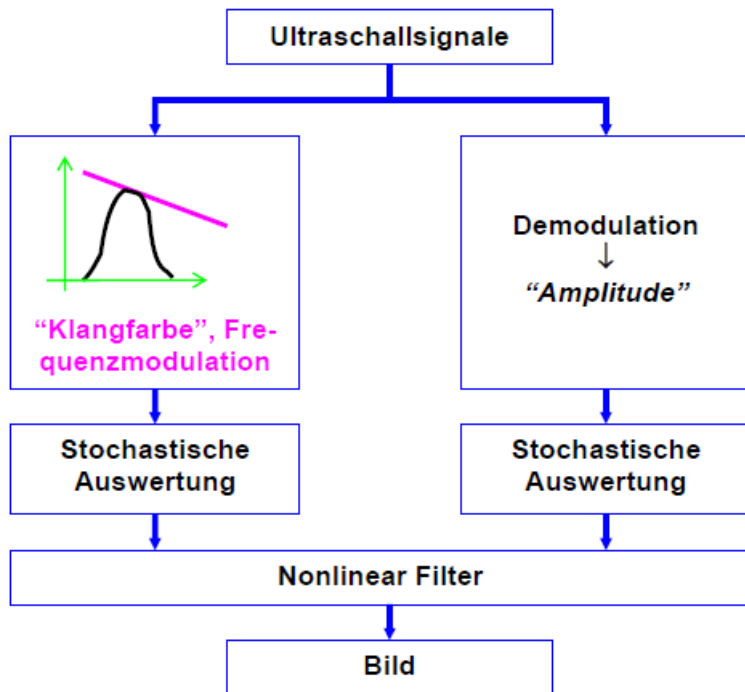
Improvement 1



Methods of Time Variant Imaging (TVI)

destructive in ROI (e.g. cerebral perfusion)

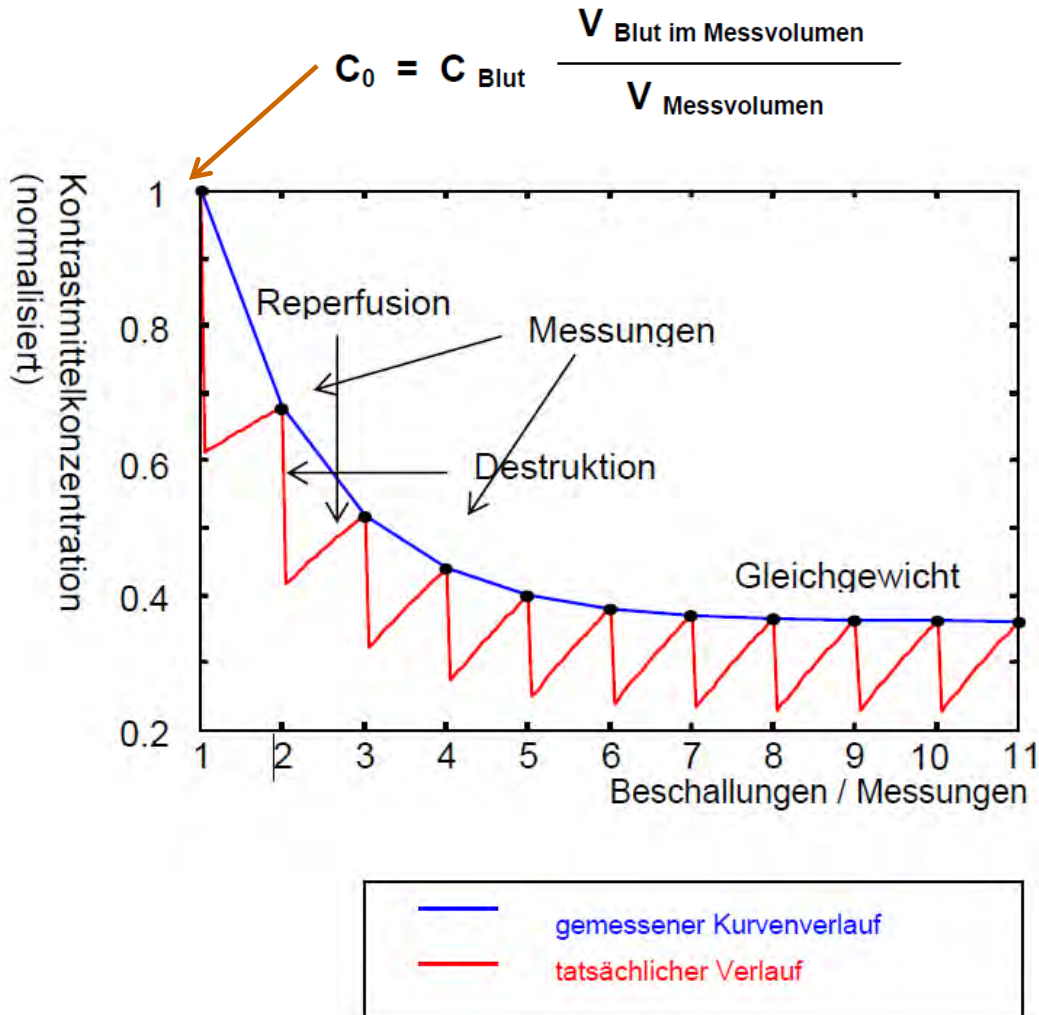
Improvement 2



Ultrasound contrast agent – bolus → perfusion

Methods of Contrast Burst Depletion Imaging (CODIM)

destructive in ROI (enrichment after constant contrast using CBI in addition)



Durch Destruktion und Reperfusion der Mikrobläschen bestimmter (tatsächlicher) Verlauf der Mikrobläschen-Konzentration (rot). Die blaue Linie verbindet die Messpunkte und veranschaulicht, wie sich ein Gleichgewichtszustand von Destruktion und Reperfusion einstellt

$$c(n+1) = c(n) \cdot e^{-p\Delta t} - e^{-d} + c^0 \cdot (1 - e^{-p\Delta t})$$

Abflusskinetik ("wash-out") Destruktion Auffüllkinetik ("wash-in")

Dabei sind:
 n = Anzahl der Beschallungen, Δt = 1/Bildwiederholungsrate
 d = Destruktionskoeffizient
 p = Perfusionskoeffizient

$$c(n) = c_0 \cdot \left(x^{n-1} + Y \cdot \frac{x^{n-1} - 1}{x - 1} \right)$$

$$x = e^{-d} \cdot e^{-p\Delta t}$$
$$y = (1 - e^{-p\Delta t})$$

Ultrasound contrast agent – bolus → perfusion

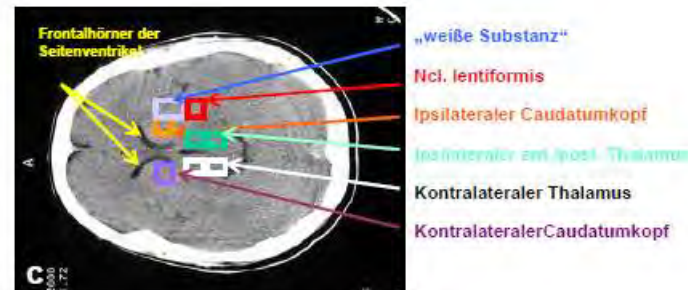
Methods of Contrast Burst Depletion Imaging (CODIM)



„weiße Substanz“
Ncl. lenticularis
Ipsilateraler Caudatumkopf
Ipsilateraler ant./post. Thalamus
Kontralateraler Thalamus
Kontralateraler Caudatumkopf



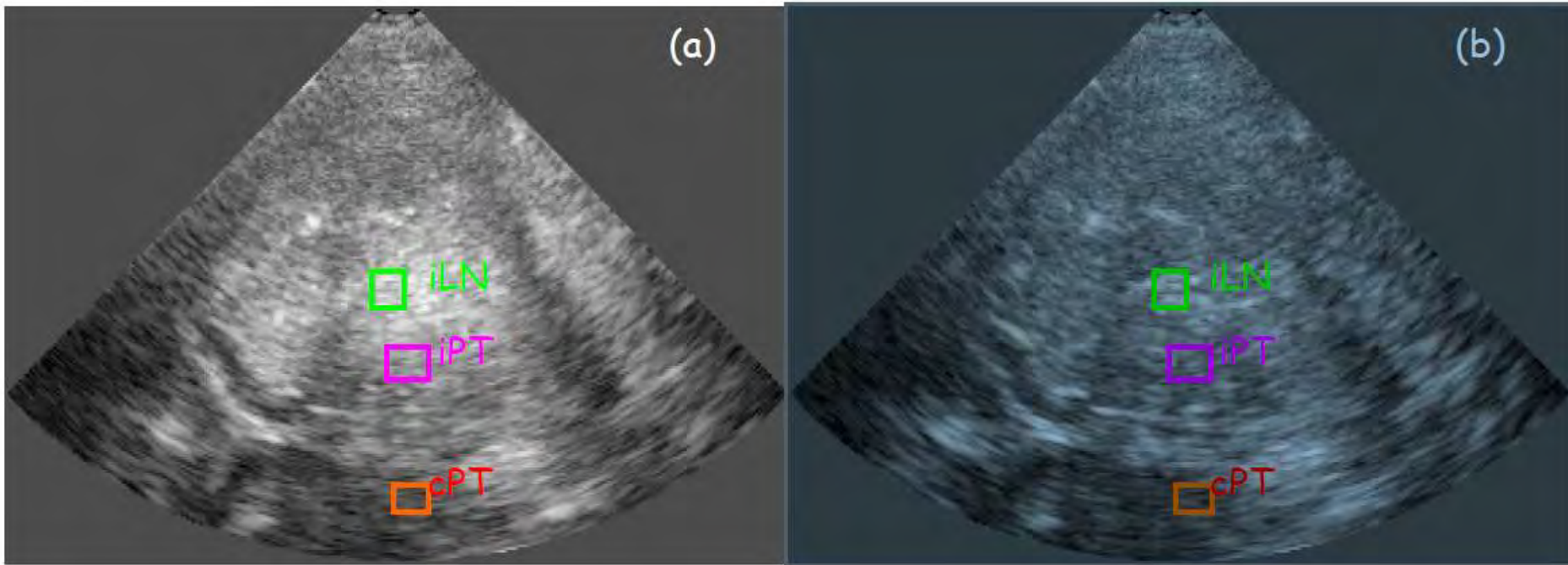
- a) Ausgewählte Hirnregionen in der Standarduntersuchungsebene
- b) Standarduntersuchungsebene als CT-Darstellung mit einngezeichnetem Ultraschallsektor
- c) Ausgewählte Hirnregionen in der CT-Darstellung



Ultrasound contrast agent – bolus → perfusion

Methods of Phase Inversion Depletion Imaging (CODIM)

destructive in ROI (enrichment after constant contrast using Pulse Inversion in addition)

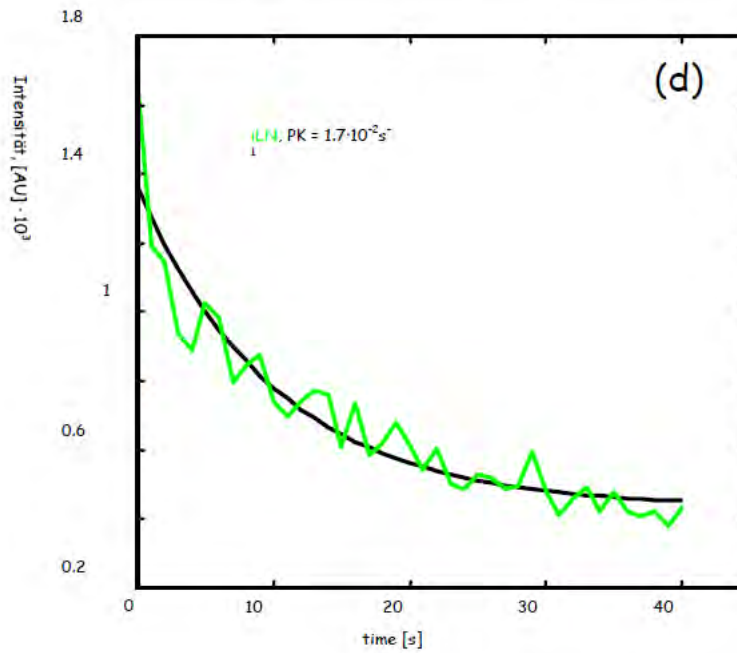
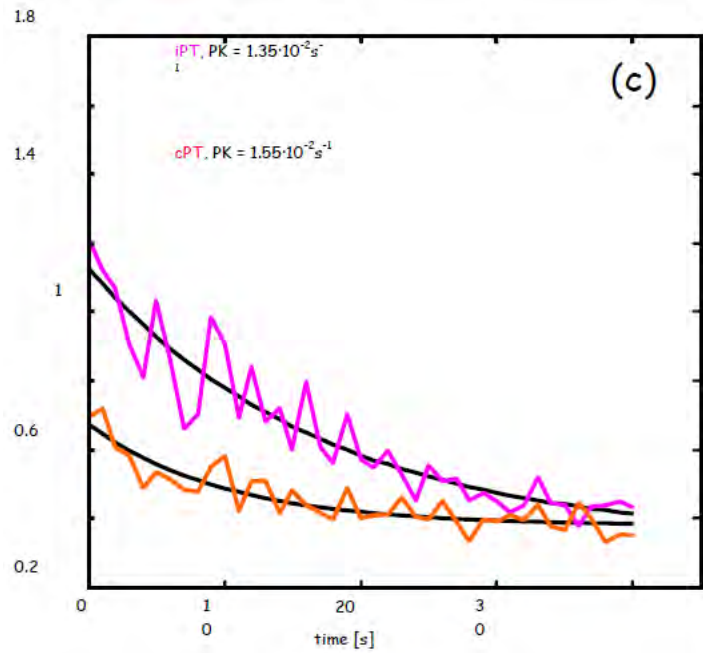


- Abb. a-b: B-Bild-Darstellung der Untersuchungsebene im Verlauf der CODIM Untersuchung
- Abb. c-d: Zeit-Intensitätskurven aus **ipsilateralem Nucleus lentiformis**, **ipsilateralem posterioren Thalamus** und **kontralateralem posteriorem Thalamus** mit angepasster Modellfunktion (schwarz) zur Bestimmung von PK und DK
- Abb. e-h: Darstellung der auch im B-Bild sichtbaren Abnahme des Kontrastmittels
- Abb. i: Lokalisation von Ultraschallsektor in einer computertomographischen Darstellung der Standard-Untersuchungsebene.

Ultrasound contrast agent – bolus → perfusion

Methods of Phase Inversion Depletion Imaging (CODIM)

destructive in ROI (enrichment after constant contrast using Pulse Inversion in addition)

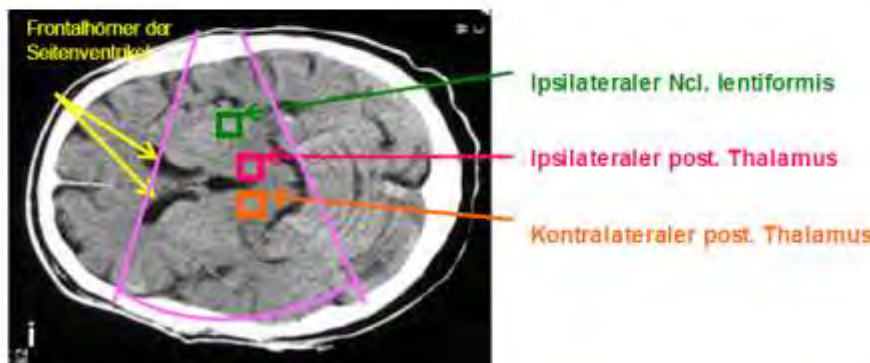
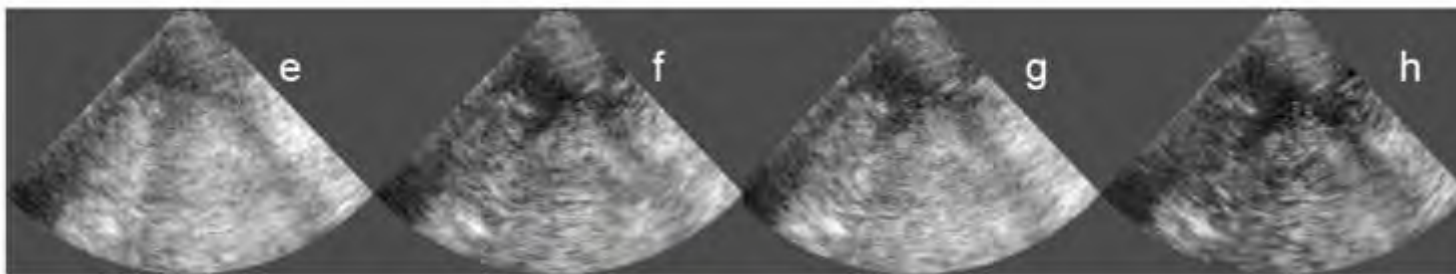


- Abb. a-b: B-Bild-Darstellung der Untersuchungsebene im Verlauf der CODIM Untersuchung
Abb. c-d: Zeit-Intensitätskurven aus **ipsilateralem Nucleus lentiformis**, **ipsilateralem posterioren Thalamus** und **kontralateralem posteriorem Thalamus** mit angepasster Modellfunktion (schwarz) zur Bestimmung von PK und DK
Abb. e-h: Darstellung der auch im B-Bild sichtbaren Abnahme des Kontrastmittels
Abb. i: Lokalisation von Ultraschallsektor in einer computertomographischen Darstellung der Standard-Untersuchungsebene.

Ultrasound contrast agent – bolus → perfusion

Methods of Phase Inversion Depletion Imaging (CODIM)

destructive in ROI (enrichment after constant contrast using Pulse Inversion in addition)

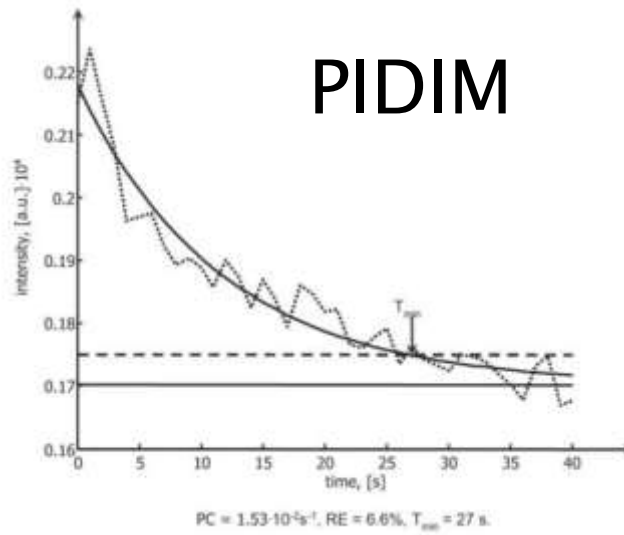
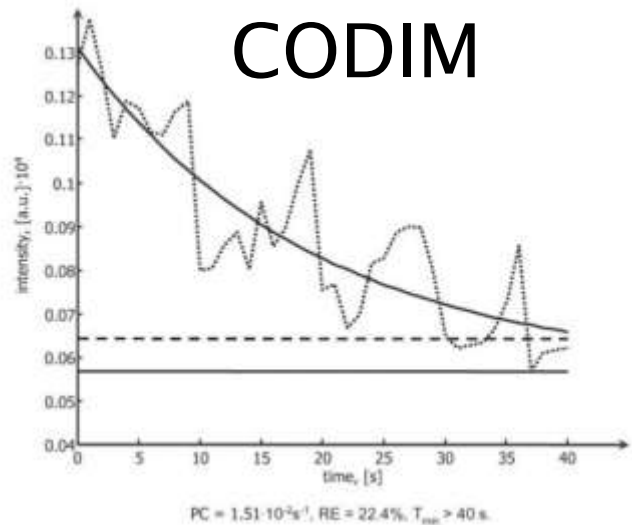


- Abb. a-b:** B-Bild-Darstellung der Untersuchungsebene im Verlauf der CODIM Untersuchung
- Abb. c-d:** Zeit-Intensitätskurven aus **ipsilateralem Nucleus lentiformis**, **ipsilateralem posteriorem Thalamus** und **kontralateralem posteriorem Thalamus** mit angepasster Modellfunktion (schwarz) zur Bestimmung von PK und DK
- Abb. e-h:** Darstellung der auch im B-Bild sichtbaren Abnahme des Kontrastmittels
- Abb. i:** Lokalisation von Ultraschallsektor in einer computertomographischen Darstellung der Standard-Untersuchungsebene.

Ultrasound contrast agent – bolus → perfusion

Methods of Contrast Burst Depletion Imaging (PIDIM)

destructive in ROI (enrichment after constant contrast using Phase inversion technique in addition



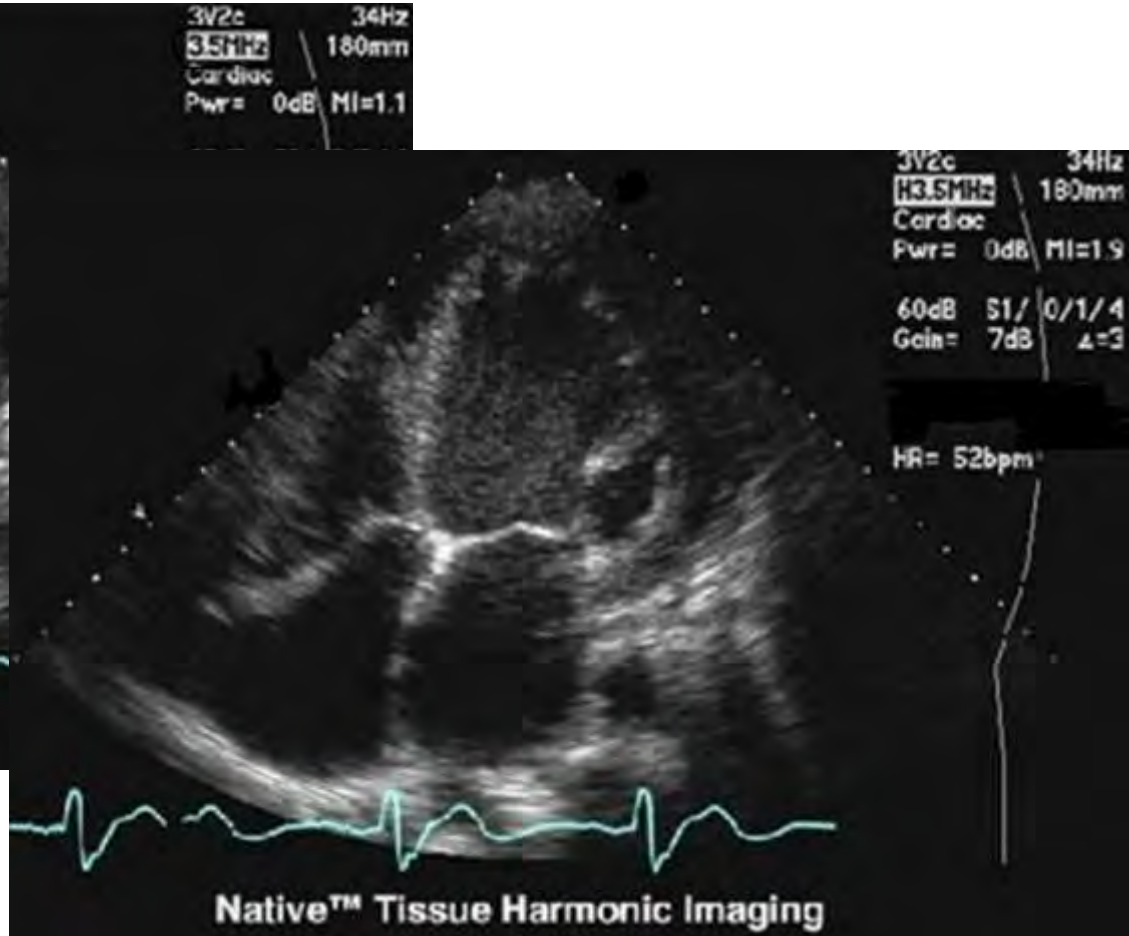
Phase inversion harmonic depletion imaging proved to be more reliable than CODIM because values of the relative error were significantly lower in PIDIM even in this relatively small cohort. This is of interest because the underlying technique, phase inversion harmonic imaging, is more widely available than contrast burst imaging.

Ultrasound contrast agent – non-linear imaging

Tissue harmonic imaging (THI) no contrast agent!!!!

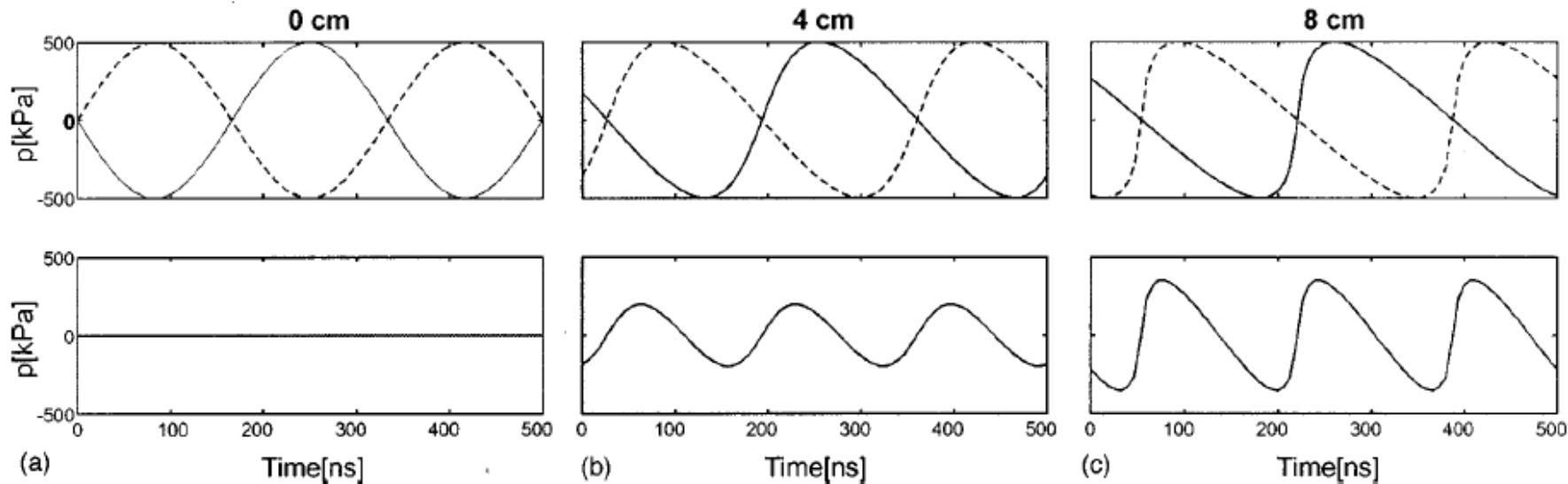


Separation by HP-Filtering /
Subtraction-filter



Ultrasound contrast agent – non-linear imaging

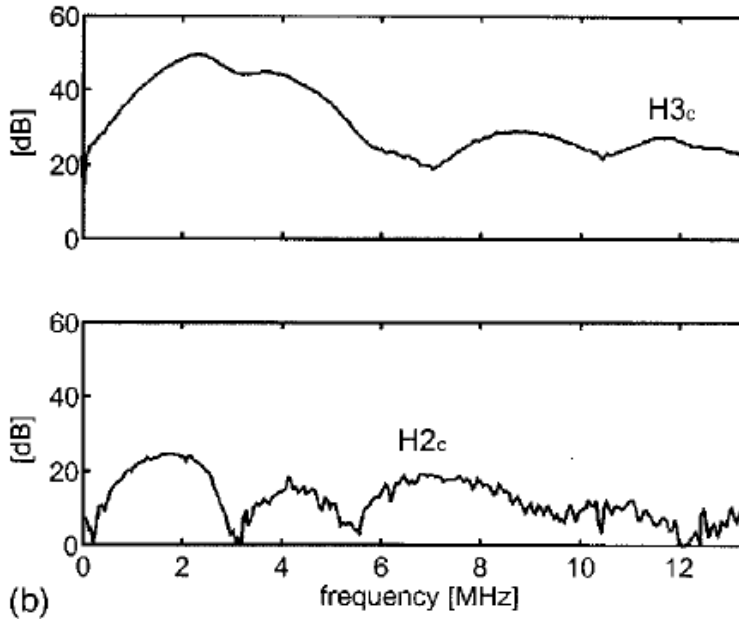
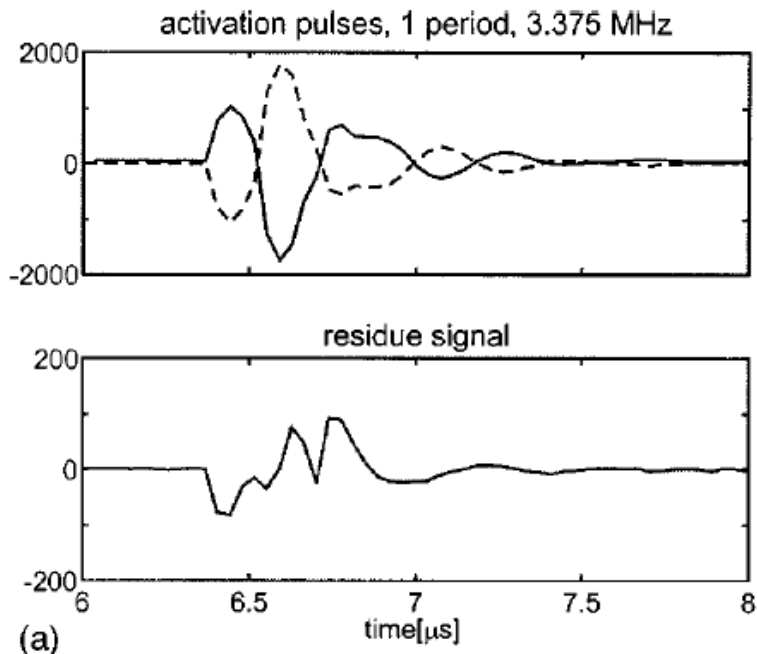
Tissue harmonic imaging (THI): basic principles



Pulse inversion technique:

Gradual distortion of an initial sinusoidal plane wave (solid line) and inverted sinusoidal wave (dashed line) as a function of time measured at a fixed location from the source. (a) At the source, (b) at 4 cm, and (c) at 8 cm from the source. Also shown, at the bottom of each figure, is the pulse inversion residue signal, which is the sum of the inverted and non-inverted distorted waves.

Tissue harmonic imaging (THI): Pulse examples



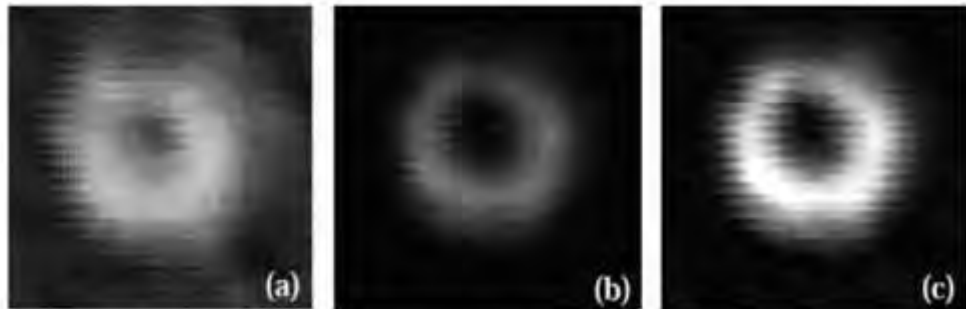
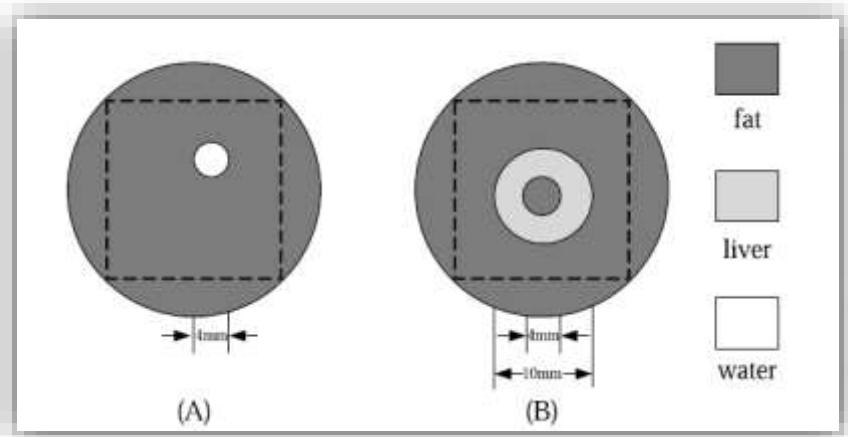
Pulse inversion technique:

Normal (solid line) and inverted (dashed line) activation pulses, their residue signals and corresponding spectra. Measurements were performed at the transmitter-board output, which was loaded with the 3.5-MHz transducer, for a square wave activation pulse of (a) one period and a frequency of 3.375 MHz. Synchronous sampling was performed at frequencies of 27 MHz. The spectra (b) reveal the contaminating second ($H2_c$) and third ($H3_c$) harmonics. Note the difference in vertical scale between the normal/inverted pulses and the residue signal.

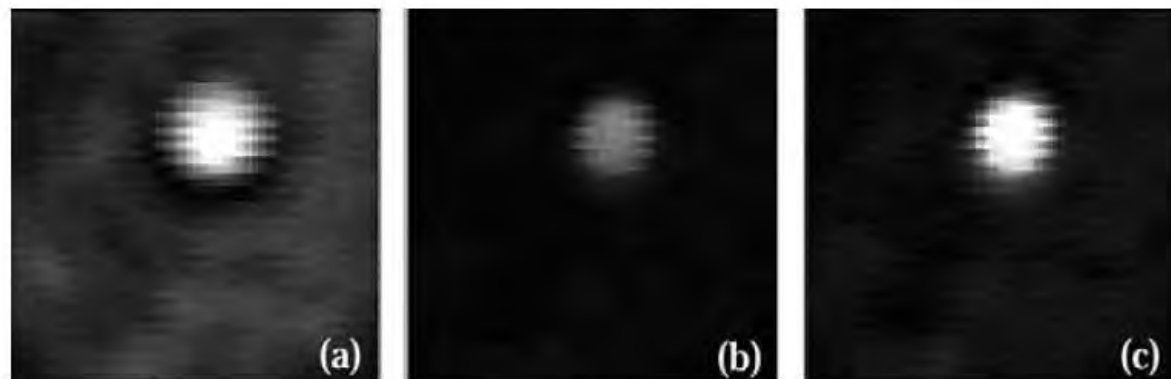
Ultrasound contrast agent – non-linear imaging

Tissue harmonic imaging (THI): examples

Sample models (A) (B) with different tissue combinations



Reconstructed images of sample model (B): (a) fundamental frequency image, (b) second harmonic image obtained before and (c) after use of pulse-inversion technique.



Reconstructed images of sample model (A): (a) fundamental frequency image, (b) second harmonic image obtained before and (c) after use of pulse-inversion technique.

Ultraschall und Theragnostik

Ultraschall in Thera(pie) und (Dia)gnostik

Kapitel 8

Theragnostik und Ultraschall

Inhaltsangabe

1. Übersicht der Ultraschallanwendungen
2. Physikalische Grundlagen
3. Ultraschallsonden
4. Bildgebende Verfahren in der Diagnostik
5. Dopplerverfahren in der Diagnostik und Therapie
6. Artefakte und Diagnostik
7. Ultraschall und Kontrastmittel
8. Theragnostik mit Ultraschall
9. Therapie mit hochdosierten Ultraschall
10. Gewebecharakterisierung mittels shear waves
11. Dosierung und Sicherheitsaspekte

Keywords

Applications of different ultrasound dosis:

- wound healing with and without drug by microbubbles with higher US-Dosis
- Liver/Cancer blood perfusion with targeted microbubbles
- Stroke Unit: flow monitoring plus Embolysis with/without (targeted microbubbles) and Diagnostic US-Dosis
- Monitoring surgery and improvement of operational techniques
 - Open heart surgery
 - Cathederization of heart an carotid area
 - Coronary stenting
 - Bypass surgery

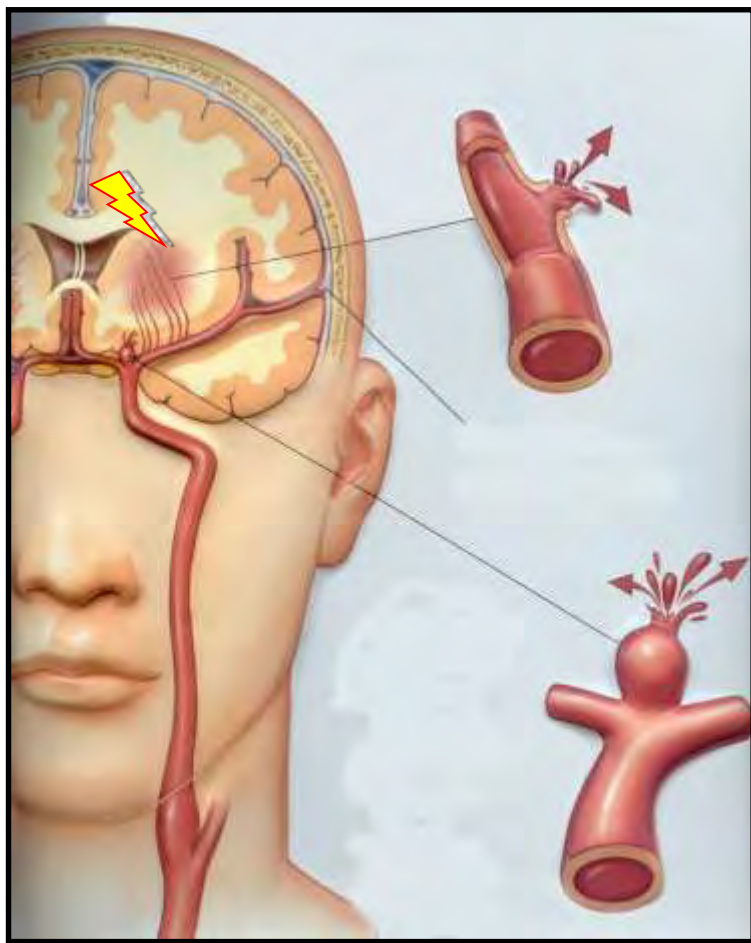
Wound healing

- Thermal effect: Heat transport via Ultrasound 1–1.5 Watts/cm²
- Non-thermal effect via Ultrasound <0.3–1 Watts/cm²: These effects cause changes in cell membrane permeability and thus the diffusion of cellular metabolites.
 - cellular recruitment, collagen synthesis, increased collagen tensile strength, angiogenesis, wound contraction, fibroblast and macrophage stimulation, fibrinolysis, and reduction of the inflammatory phase and promotion of the proliferative phase of healing.

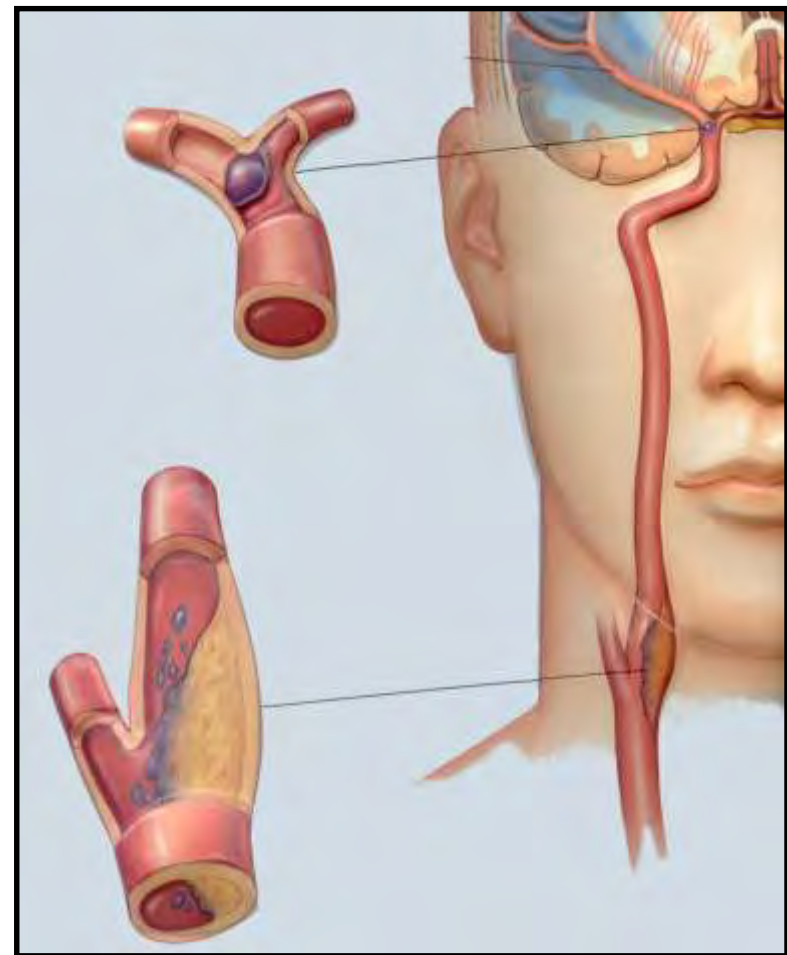
ultrasound Diagnostic plus Therapy → Embolysis

Basics: Stroke/Flow and Monitoring

Aneurism, hemorrhage



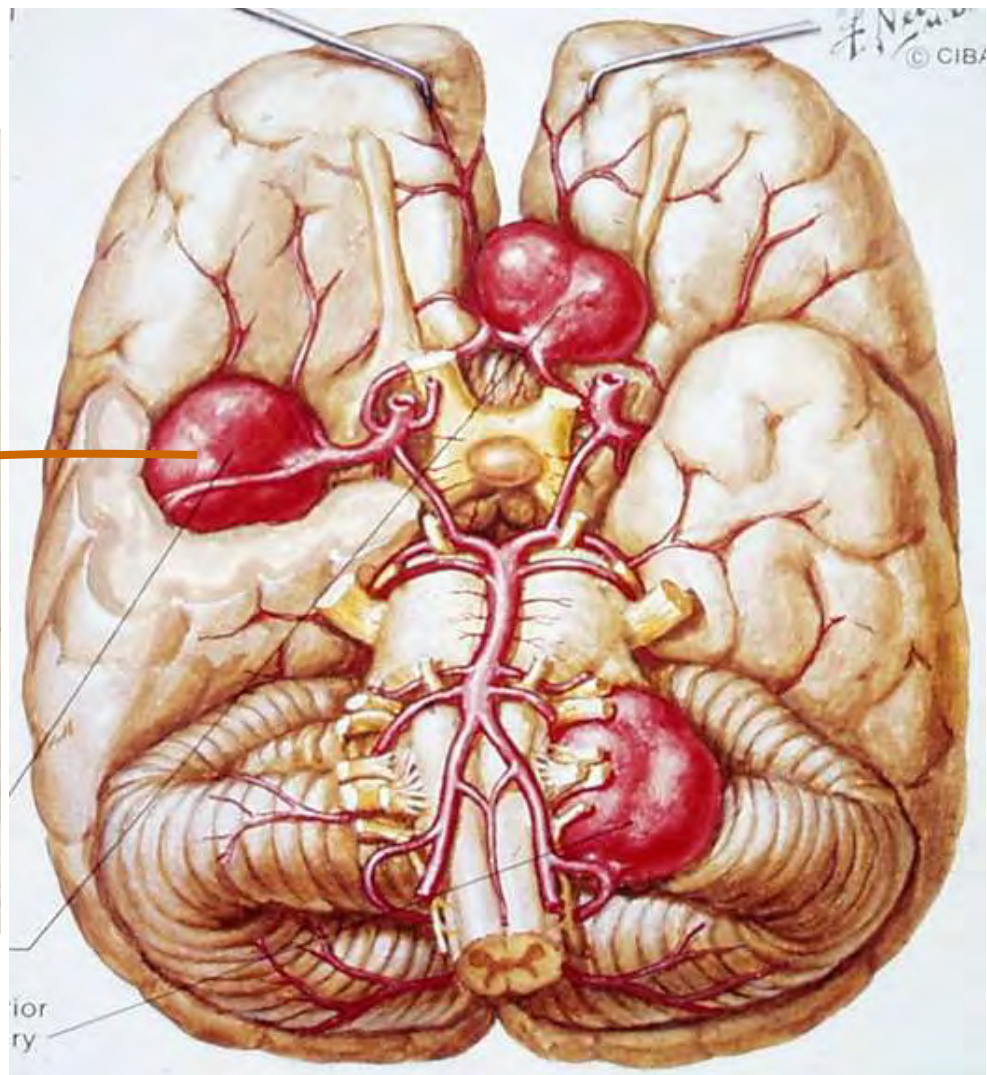
Cerebral embolism
due to arteriosclerosis



ultrasound Diagnostic plus Therapy → Embolysis

Basics: Aneurism in the MCA

Cerebral Angiography



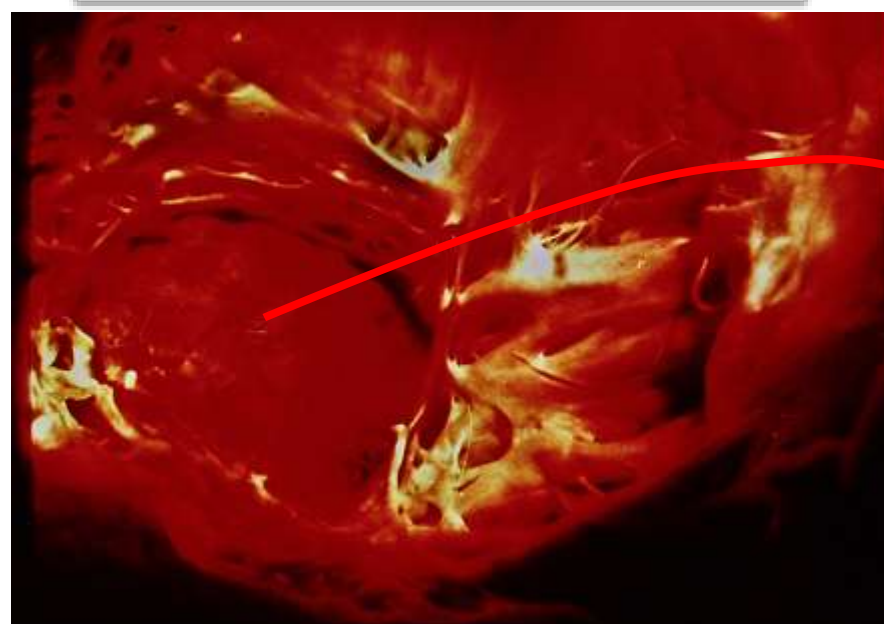
Basics: Stroke/Flow and Monitoring

- Ischemia 80%
- Cerebral haemorrhage 15%
- Subarachnoid bleeding 5%

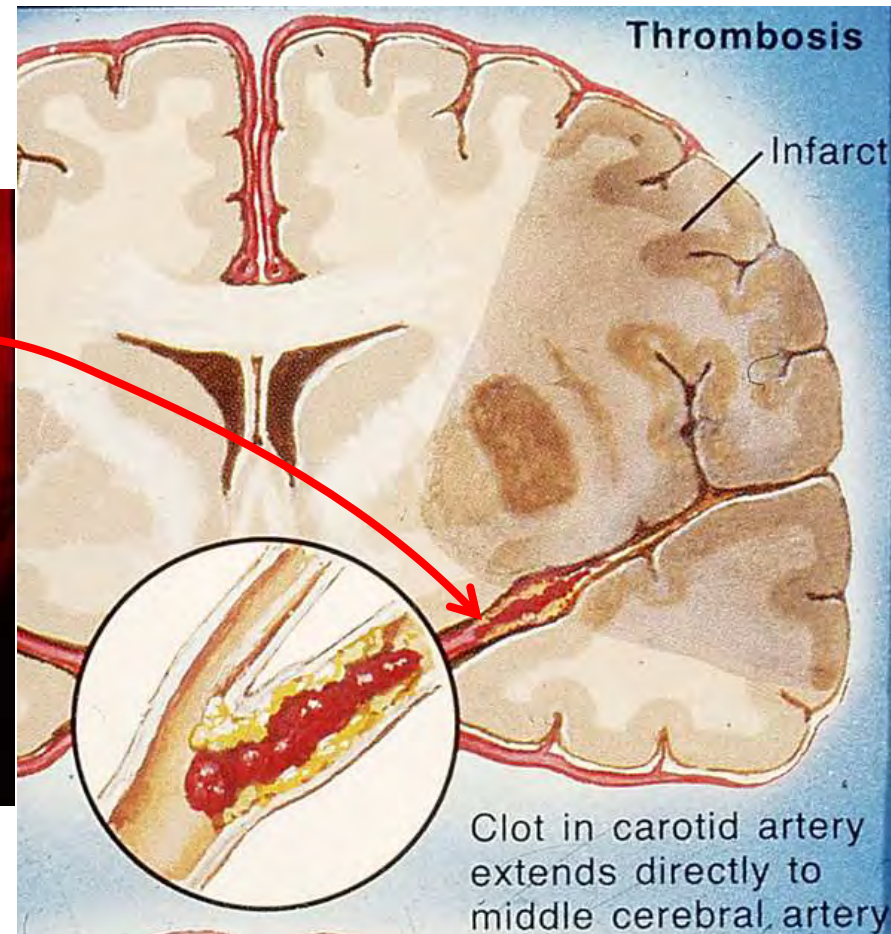
Thrombotic
Embolic
Hemodynamic



Basics: Thrombotic Stroke

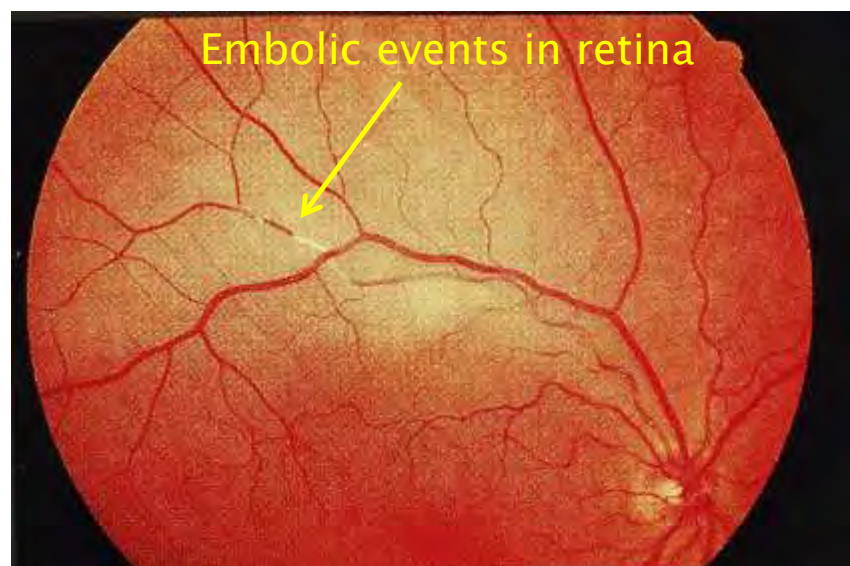
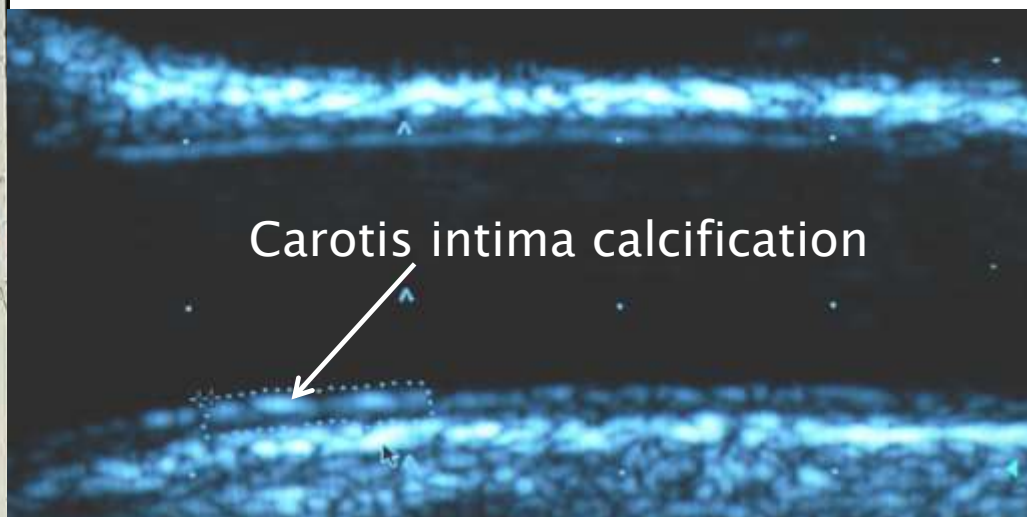
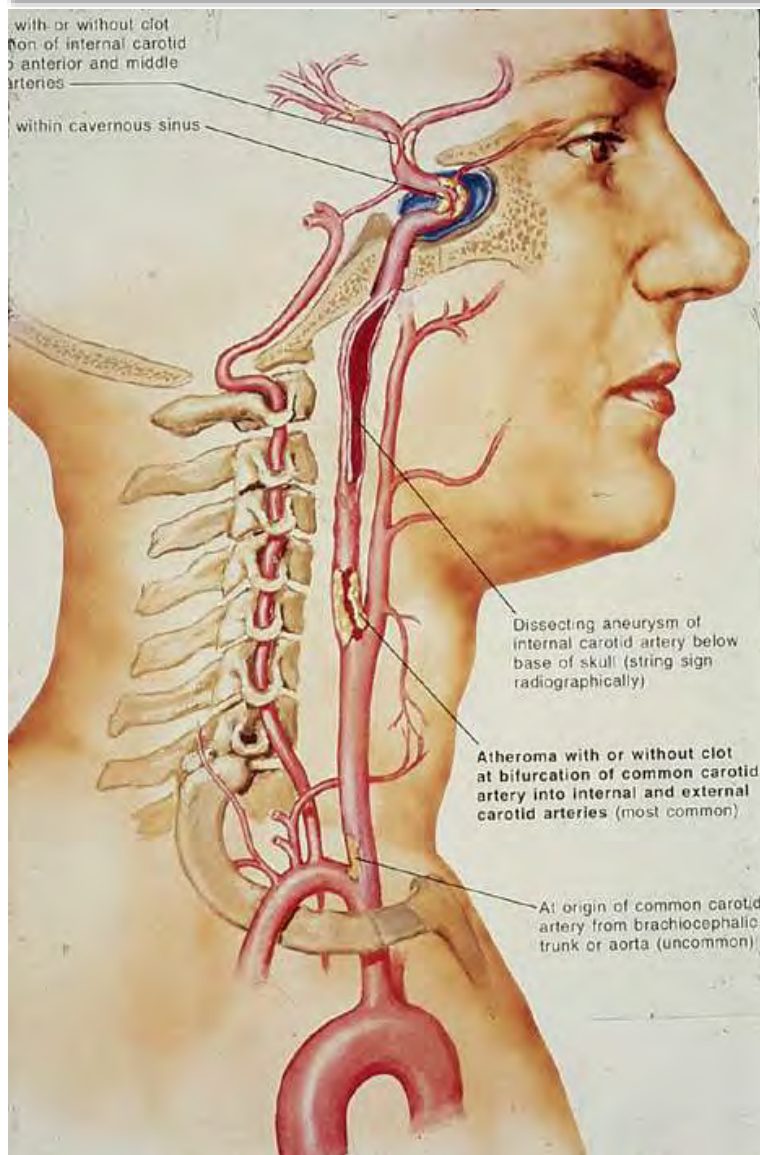


Thrombus in the left atrium due to atrial fibrillation



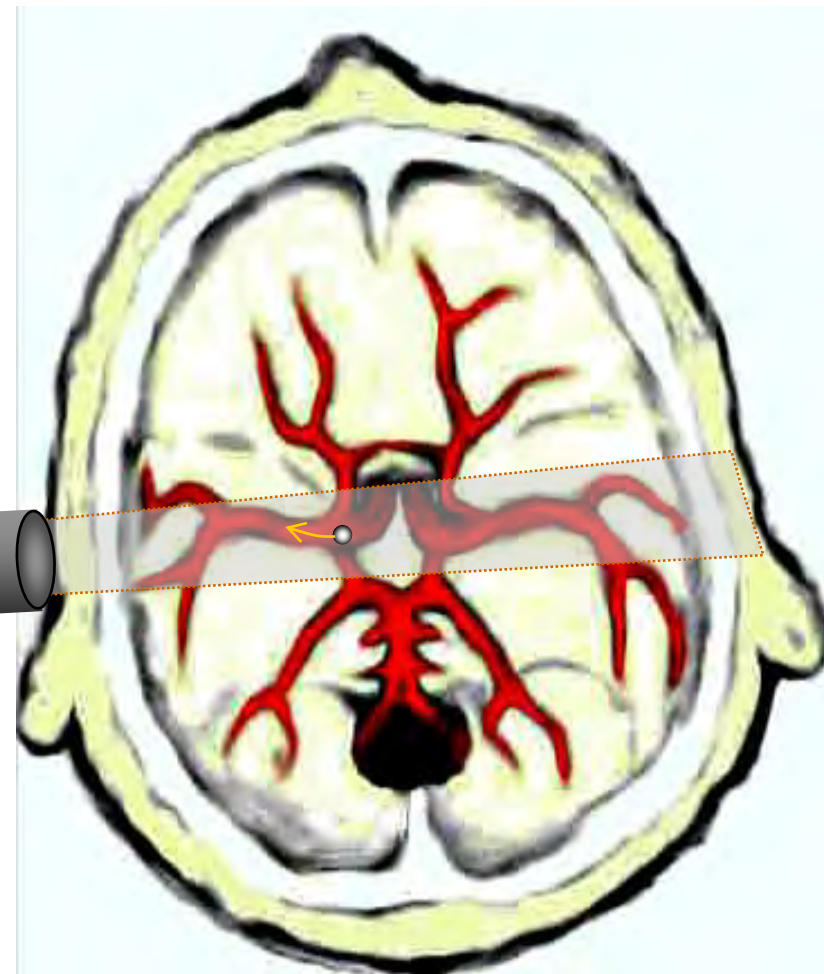
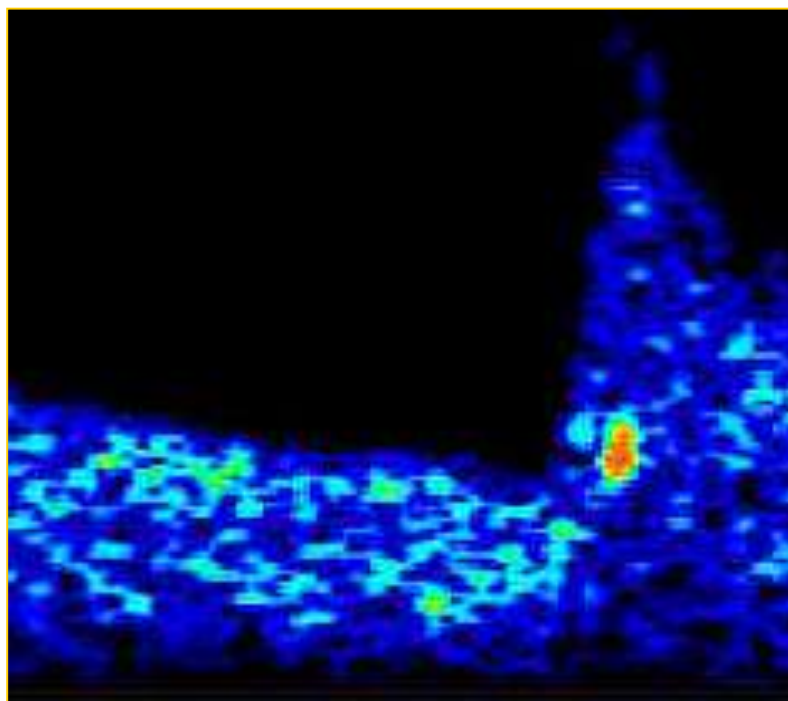
ultrasound Diagnostic plus Therapy →Embolysis

Basics: Embolic Stroke



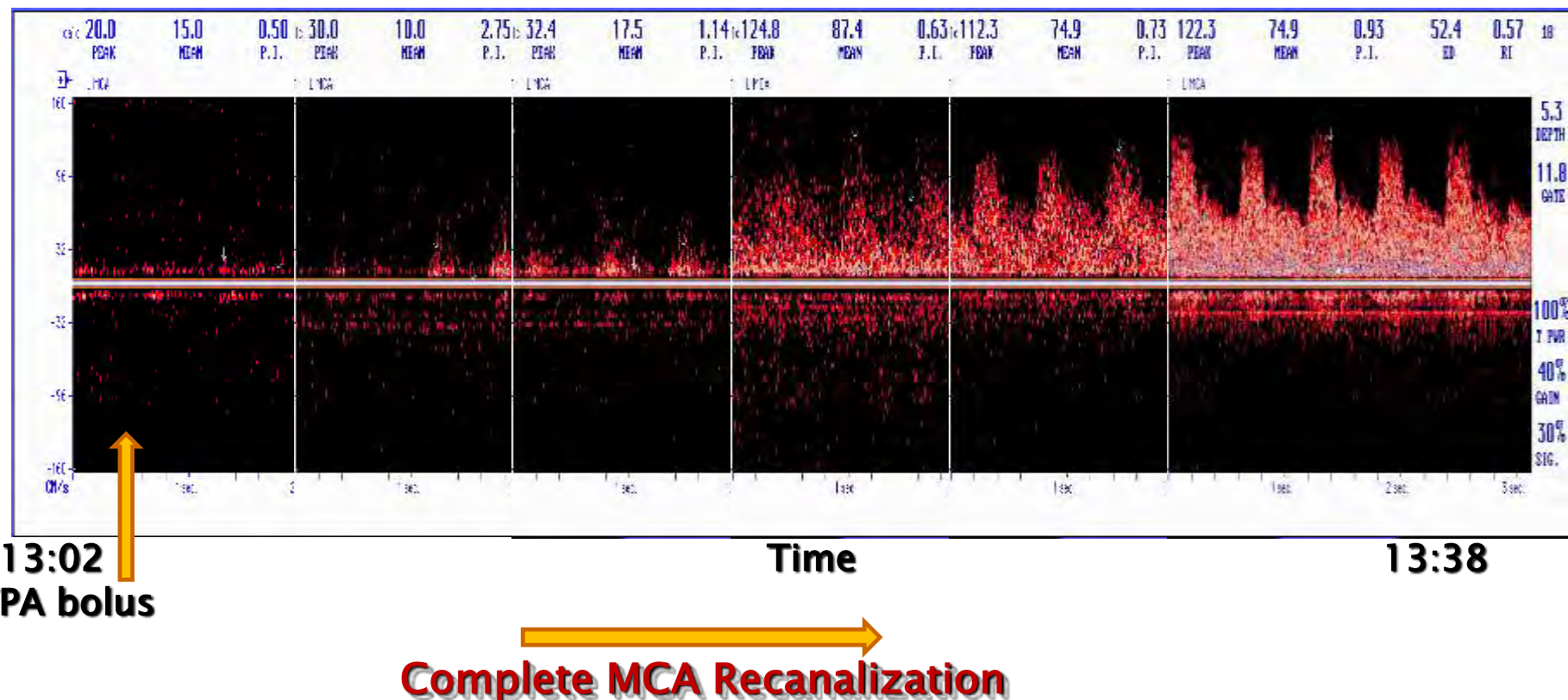
ultrasound Diagnostic plusTherapy →Embolysis

Basics: Embolic event monitoring



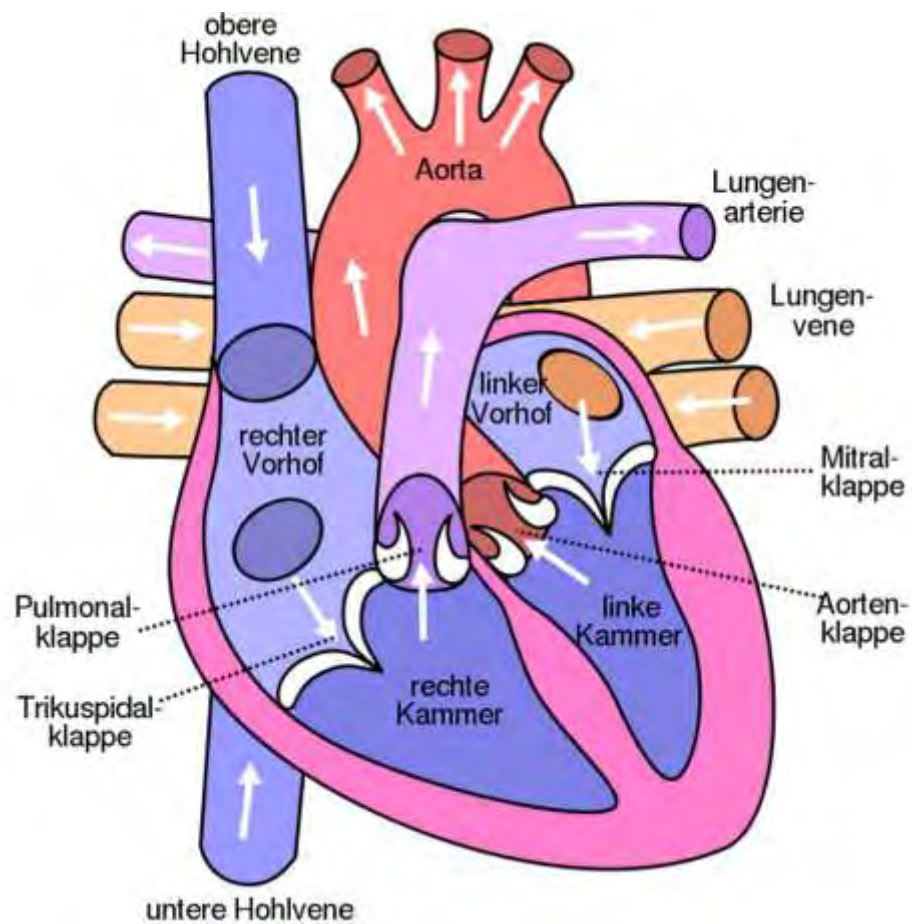
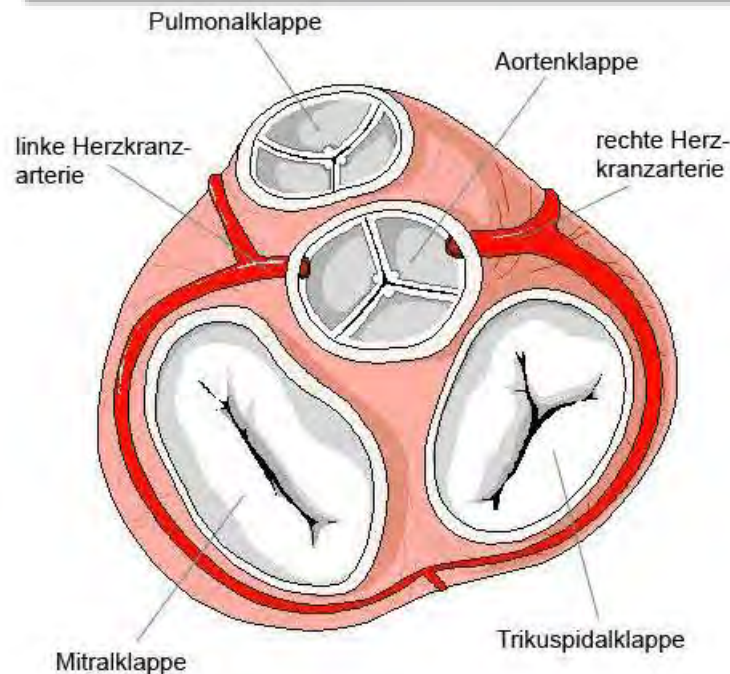
ultrasound Diagnostic plusTherapy →Embolysis

Basics: Embolic event monitoring/treatment by TPA and/or microbubbles



ultrasound Diagnostic plus Therapy → Emboli-Detection

Basics: Artificial heart valve and monitoring of embolism





Basics: Heart valve surgery

Solid Cerebral Microemboli and Cerebrovascular Symptoms in Patients With Prosthetic Heart Valves

Mona Skjelland, MD; Annika Michelsen, PhD; Frank Brosstad, MD, PhD;
Jan L. Svennevig, MD, PhD; Rainer Brucher, PhD; David Russell, FRCPE

Background and Purpose—Although cerebral microemboli are often detected by transcranial Doppler ultrasonography in mechanical heart valve patients, the clinical significance of such microemboli is unclear. The aim of this study was to determine the frequency and composition of cerebral microemboli in a prosthetic heart valve population and to correlate these findings to cerebrovascular symptoms, blood inflammation, and coagulation parameters.

Methods—Seventy-six consecutive patients with a total of 81 prosthetic (54 mechanical, 27 biologic) heart valves were monitored for cerebral microemboli by multifrequency transcranial Doppler ultrasonography 1 year after valve replacement. Cerebrovascular events in the first year were recorded by a neurologist. Inflammation and coagulation markers were measured by immunoassays.

Results—Microemboli were detected in mechanical heart valve patients only (28 patients, 56%). Twelve percent were solid, occurring in 17 (34%) of the mechanical heart valve population. The presence of solid cerebral microemboli was the only variable that was associated with cerebrovascular symptoms after a final regression analysis ($P=0.026$). The plasma monocyte chemotactic protein-1 level was raised in patients with solid microemboli ($P=0.014$).

Conclusions—Solid cerebral microemboli were detected by multifrequency transcranial Doppler ultrasonography in 35% of a mechanical heart valve population, and the frequency was higher in patients who experienced cerebrovascular events during the first year after valve replacement. The results suggest that the detection of solid cerebral microemboli may be helpful in predicting the risk of ischemic stroke in mechanical heart valve patients. (*Stroke*. 2008;39:1159-1164.)

Key Words: cerebral microemboli ■ embolic stroke ■ prosthetic heart valve
■ transcranial Doppler ultrasonography

Received May 6, 2007; final revision received August 7, 2007; accepted August 16, 2007.

From the Department of Neurology (M.S., D.R.), the Research Institute for Internal Medicine (A.M., F.B.), and the Department of Thoracic and Cardiac Surgery (J.L.S.), Rikshospitalet-Radiumhospitalet Medical Center, University of Oslo, Oslo, Norway, and the Department of Medical Engineering (R.B.), University of Applied Sciences, Ulm, Germany.

Correspondence to Mona Skjelland, MD, Department of Neurology, Rikshospitalet-Radiumhospitalet Medical Center, 0027 Oslo, Norway. E-mail: mona.skjelland@rikshospitalet.no

© 2008 American Heart Association, Inc.

Stroke is available at <http://stroke.ahajournals.org>

DOI: 10.1161/STROKEAHA.107.493031

Basics: Heart valve surgery

Institutional report - Cardiac general

Multifrequency transcranial Doppler for intraoperative automatic detection and characterisation of cerebral microemboli during port-access mitral valve surgery

Daniele Maselli*, Raffaella Pizio, Francesco Musumeci

Department of Cardiac Surgery, S. Camillo Hospital, Rome, Italy

Received 17 August 2005; received in revised form 18 October 2005; accepted 19 October 2005

Abstract

In 20 patients (6 male; age 56.5 ± 6.4 years; BSA 1.6 ± 0.1 m 2) undergoing port-access mitral valve surgery, automated intraoperative transcranial Doppler was used to monitor absolute amount, side distribution, and type of embolic events during selected phases of the procedure to evaluate the impact of specific surgical manoeuvres on cerebral microembolism. The rate of events per minute was acquired for the following five operative periods: from cardiopulmonary bypass (CPB) set-up to CPB start, from CPB start to aortic clamping, first minute after aortic endoclamp inflation, first minute after aortic endoclamp deflation, and first ten minutes from CPB weaning start. Endoclamp navigation into the aortic arch, CPB start and CPB weaning determined the highest absolute count of embolic events. When embolic rate was normalised for length of selected operation periods CPB start (1.58 ± 1.9 events/min), endoclamp inflation (1.42 ± 1.7 events/min) and endoclamp deflation (3.1 ± 3.5 events/min), resulted as the most critical phases. No side prevalence was observed. In conclusion, brain embolism during port-access mitral valve procedures occurs predominantly at CPB start and during ascending aorta clamping and unclamping. Aortic arch navigation with catheters exposes to the risk of cerebral embolic events.

© 2006 Published by European Association for Cardio-Thoracic Surgery. All rights reserved.

Keywords: Minimally invasive surgery; CPB complications; Embolism

*Corresponding author: Daniele Maselli, U.O. Cardiochirurgia, Azienda Ospedaliera Universitaria Pisana, Via Paradisa n 2, 56124 Pisa, Italy.
Tel.: +39050995261; fax: +39050995278.

E-mail address: dmaselli@tiscali.it (D. Maselli).

© 2006 Published by European Association for Cardio-Thoracic Surgery

Basics: Coronary surgery

Gaseous and solid cerebral microembolization during proximal aortic anastomoses in off-pump coronary surgery: The effect of an aortic side-biting clamp and two clampless devices

Lorenzo Guerrieri Wolf, MD, Yasir Abu-Omar, MRCS, Bikram P. Choudhary, MRCS, David Pigott, FRCA, and David P. Taggart, MD (Hons), PhD, FRCS

From the Department of Cardiothoracic Surgery, John Radcliffe Hospital, Oxford, United Kingdom.

Address for reprints: Professor David P. Taggart, MD, PhD, FRCS, Professor of Cardiovascular Surgery, University of Oxford, Department of Cardiothoracic Surgery, John Radcliffe Hospital, Headley Way, Headington, Oxford OX3 9DU, United Kingdom (E-mail: david.taggart@orh.nhs.uk).

J Thorac Cardiovasc Surg 2007;133:485-93

0022-5223/\$32.00

Copyright © 2007 by The American Association for Thoracic Surgery
doi:10.1016/j.jtcvs.2006.10.002

Objectives: Intraoperative cerebral microembolism is a cause of cerebral dysfunction after cardiac surgery, and particulate microemboli are the most damaging. Using a new-generation transcranial Doppler ultrasound, we compared the number and nature of microemboli in patients undergoing off-pump coronary artery bypass grafting during performance of proximal anastomoses with three techniques: an aortic side-biting clamp and two clampless devices (the Enclose II device [Novare Surgical Systems, Inc, Cupertino, Calif] and the Heartstring II device [Guidant Corporation, Santa Clara, Calif]) developed to obviate the need for an aortic side-biting clamp, thereby reducing the number of cerebral microemboli.

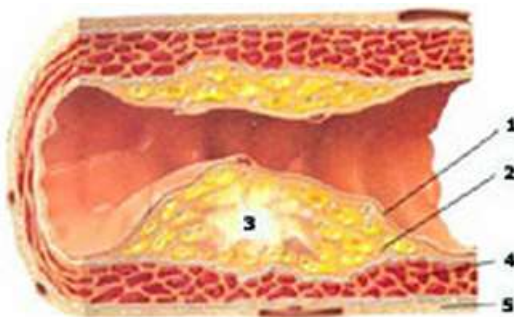
Methods: Bilateral continuous monitoring of the middle cerebral arteries was performed with a multirange, multifrequency transcranial Doppler device that both automatically rejects artifacts online and discriminates between solid and gaseous microemboli. Recordings were continuously undertaken during performance of 66 proximal aortic anastomoses in 42 patients. Thirty-five anastomoses were performed with an aortic side-biting clamp, 20 with the Enclose device, and 11 the Hearstring device.

Results: Most microemboli occurred during application/insertion and removal of each device from the ascending aorta. The median number (interquartile range) of total microemboli was 11 (6-32) during side clamping, 11 (6-15) with the Enclose device, 40 (31-48) with the Heartstring device ($P < .01$). The proportion of solid microemboli was significantly higher in the side-clamp group (23%) compared with 6% and 1% in the Enclose and Heartstring groups, respectively ($P < .01$).

Conclusions: Avoidance of aortic side clamping results in a significant reduction in the proportion of solid microemboli detected with transcranial Doppler. As solid microemboli are probably the most damaging, use of the Enclose and Heartstring devices may represent an important strategy for minimizing cerebral injury during proximal aortic anastomoses.

ultrasound Diagnostic plus Therapy → Emboli Detection

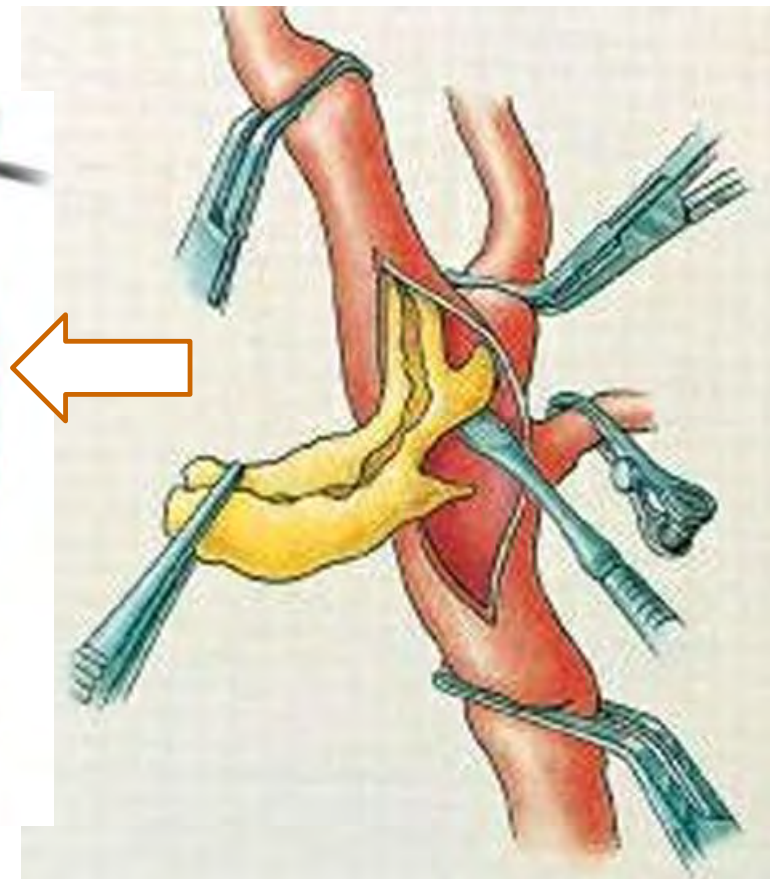
Basics: Carotis–Endarterectomy and Monitoring



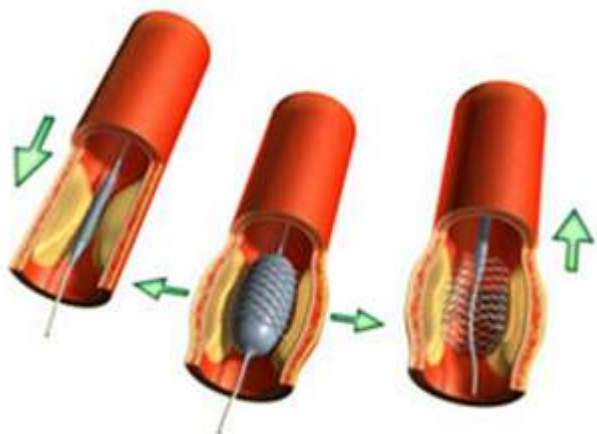
Carotis

1. Intima
2. Fat cells enclosures
3. Calcifications
4. Muscles of the wall
5. adventitia

I) surgical technique



II) stenting technique



Patch after surgery



Basics: stenting surgery

Carotid Plaque Surface Irregularity Predicts Cerebral Embolism during Carotid Artery Stenting

Michael Rosenkranz^a Arkadiusz Russjan^a Einar Goebell^b

Stefanie Havemeister^a Götz Thomalla^a Bastian Cheng^a Christoph Beck^a

Anna Krützelmann^a Jens Fiehler^b Christian Gerloff^a

Departments of ^aNeurology and ^bNeuroradiology, University Medical Center Hamburg-Eppendorf, Hamburg, Germany

Abstract

Background and Purpose: Carotid artery stenting (CAS) is associated with the risk of periprocedural embolic events.

The procedural risk may vary with plaque characteristics. We aimed at determining the impact of carotid plaque surface irregularity on the risk of cerebral embolism during CAS.

Methods: Solid microembolic signals (MES) during CAS for symptomatic carotid stenosis were assessed by means of dual-frequency transcranial Doppler ultrasound. Study endpoint was the number of solid MES during CAS in 12 patients with irregular carotid stenosis compared to 12 matched patients with smooth carotid stenosis. **Results:** A total of 438 solid MES were detected. The cumulative number of solid MES was 329 in patients with irregular plaques and 109 in those with smooth plaques. The proportion of subjects in whom solid MES were detected was higher in the irregular plaque group (11/12) than in the smooth plaque group (5/12) ($p = 0.030$). The numbers of solid MES per CAS procedure and per hour of CAS procedure were both higher in patients with irregular plaques than in those with smooth plaques ($p = 0.008$ and 0.015 , respectively). **Conclusions:** Carotid plaque surface irregularity predicts solid cerebral embolism during stenting of symptomatic carotid artery stenosis.

Copyright © 2011 S. Karger AG, Basel

Basics: stenting surgery

Cerebral Microemboli and Brain Injury During Carotid Artery Endarterectomy and Stenting

Mona Skjelland, MD; Kirsten Krohg-Sørensen, MD, PhD; Bjørn Tennøe, MD; Søren J. Bakke, MD;
Rainer Brucher, PhD; David Russell, MD, PhD, FRCPE

Background and Purpose—Cerebral microembolic signals detected by transcranial Doppler are frequent during carotid angioplasty with stenting and carotid endarterectomy (CEA). Their potential harmful effects on the brain are, however, unclear. The aim of this study was to relate the frequency and type of per-procedural microembolic signals to procedure-related ipsilateral ischemic strokes and new ipsilateral ischemic lesions on diffusion-weighted cerebral MRI.

Methods—Eighty-five patients who were prospectively treated with CEA (61) or carotid angioplasty with stenting (30) for high-grade ($\geq 70\%$) internal carotid artery stenoses were monitored during the procedures using multifrequency transcranial Doppler with embolus detection and differentiation. Pre- and postprocedural cerebral diffusion-weighted cerebral MRIs were performed on a subset of patients.

Results—Solid and gaseous microemboli were independently associated with procedure-related ipsilateral ischemic strokes (solid: $P=0.027$, gaseous: $P=0.037$) or new ipsilateral diffusion-weighted cerebral MRI lesions (solid: $P=0.043$, gaseous: $P=0.026$). Microembolic signals were detected during all procedures except one (CEA); 17% and 21% of all emboli were solid during carotid angioplasty with stenting and CEA, respectively. Patients undergoing carotid angioplasty with stenting had more solid ($P<0.001$) and gaseous ($P<0.001$) emboli and more new ipsilateral ischemic strokes ($P=0.033$) compared with patients undergoing CEA. Echolucent plaques ($P=0.020$) and preprocedural diffusion-weighted cerebral MRI ischemic lesions ($P=0.002$) were associated with increased numbers of solid emboli.

Conclusions—Solid and gaseous microemboli were increased in patients with procedure-related ipsilateral ischemic strokes or new diffusion-weighted cerebral MRI lesions, which suggests that both solid and gaseous emboli may be harmful to the brain during CEA and carotid angioplasty with stenting. (*Stroke*. 2009;40:230-234.)

Key Words: embolic stroke ■ embolism ■ endarterectomy ■ endovascular treatment ■ TCD ■ transcranial Doppler

Received January 8, 2008; final revision received May 6, 2008; accepted May 20, 2008.

From the Departments of Neurology (M.S., D.R.), Thoracic and Cardiovascular Surgery (K.K.-S.), and Radiology (B.T., S.J.B.), Rikshospitalet University Hospital, Oslo, Norway; and the Department of Medical Engineering (R.B.), University of Applied Sciences, Ulm, Germany.

Correspondence to Mona Skjelland, MD, Department of Neurology, Rikshospitalet University Hospital, 0027 Oslo, Norway. E-mail: mona.skjelland@rikshospitalet.no

© 2008 American Heart Association, Inc.

Stroke is available at <http://stroke.ahajournals.org>

DOI: 10.1161/STROKEAHA.107.513541

**ORIGINAL
RESEARCH**

M. Rosenkranz
J. Fiehler
W. Niesen
C. Waiblinger
B. Eckert
O. Wittkugel
T. Kucinski
J. Röther
H. Zeumer
C. Weiller
U. Sliwka

Basics: stenting surgery

The Amount of Solid Cerebral Microemboli during Carotid Stenting Does Not Relate to the Frequency of Silent Ischemic Lesions

BACKGROUND AND PURPOSE: Carotid artery stent placement (CAS) may be associated with clinically silent cerebral lesions. We prospectively evaluated the association of the number of solid cerebral microemboli during unprotected CAS with the frequency of silent cerebral lesions as detected by diffusion-weighted MR imaging (DWI).

METHODS: We performed multifrequency transcranial Doppler detection of solid microemboli in the ipsilateral middle cerebral artery (MCA) during CAS in 27 consecutive patients with symptomatic high-grade carotid stenoses. No embolus protection was used in any of the cases. DWI before and 24 ± 2 hours after CAS was used to detect new ischemic lesions.

RESULTS: We detected 484 solid microemboli in 17 patients (63%). On MR imaging 24 ± 2 hours after CAS, 6 patients (22%) had developed 13 new clinically silent DWI lesions within the ipsilateral MCA territory. In patients with Doppler evidence of solid emboli during CAS, the incidence of new DWI lesions was higher (29%) than in patients without Doppler evidence of solid emboli during the procedure (10%); this difference was not statistically significant ($P = .25$). The number of solid microemboli during CAS in patients with new ipsilateral DWI lesions was not significantly different from that in patients without new ipsilateral DWI lesions.

CONCLUSIONS: Solid microembolism is a common event during unprotected CAS; however, the frequency of procedure-related silent cerebral lesions appears to be independent of the number of solid cerebral microemboli during the procedure.

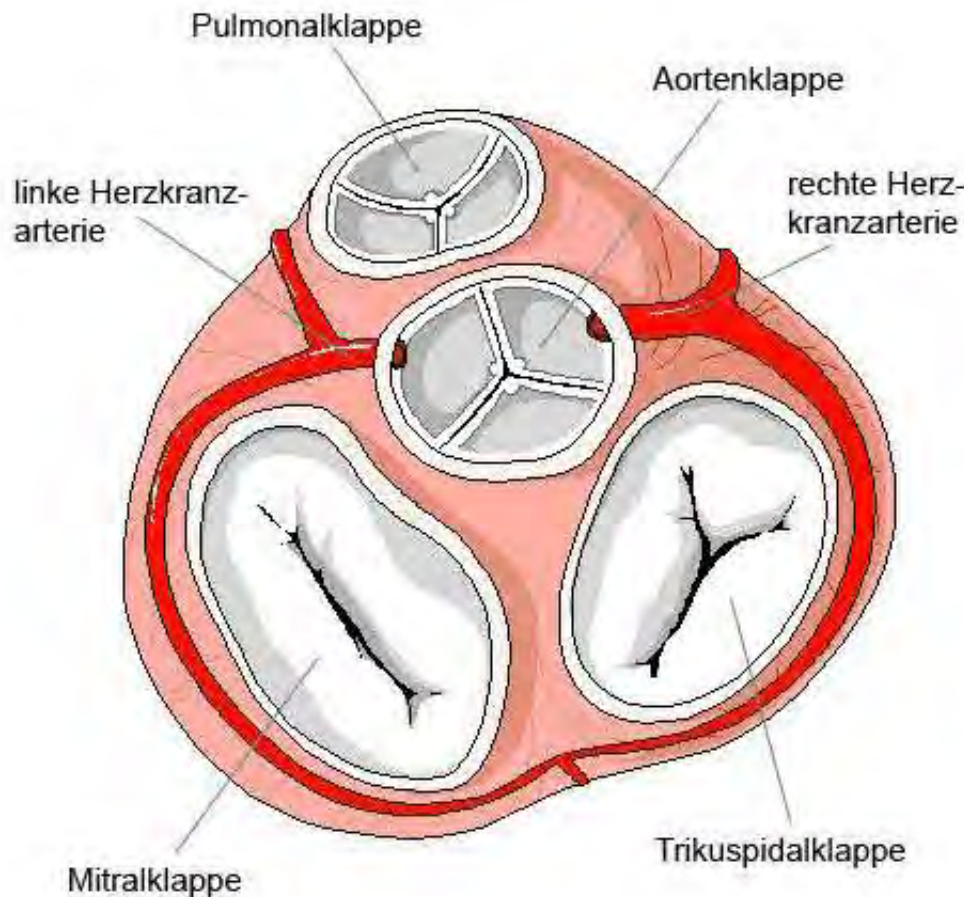
Received October 26, 2004; accepted after revision February 17, 2006.

From the Departments of Neurology (M.R., W.N., C.W., J.R., U.S.) and Neuroradiology (J.F., B.E., O.W., T.K., H.Z.), Universitätsklinikum Hamburg-Eppendorf, Hamburg, Germany.

This study was presented in part at the International Stroke Conference, February 5–7, 2004, San Diego, Calif, and at the European Stroke Conference, May 12–15, 2004, Mannheim, Germany.

Address correspondence to Michael Rosenkranz, MD, Department of Neurology, Universitätsklinikum Hamburg-Eppendorf, Martinistraße 52, D-20246 Hamburg, Germany.

Basics: Catheterization of coronary arteries



Basics: Left heart Catheterization

Cerebral emboli during left heart catheterization may cause acute brain injury

Christian Lund^{1*}, Ragnhild Bang Nes², Torhild Pynten Ugelstad³, Paulina Due-Tønnessen⁴,
Rune Andersen⁴, Per Kristian Hol⁵, Rainer Brucher⁶, and David Russell¹

¹ Department of Neurology, Rikshospitalet University Hospital, 0027 Oslo, Norway; ² Department of Psychosomatic Medicine, Rikshospitalet University Hospital, 0027 Oslo, Norway; ³ Department of Cardiology, Rikshospitalet University Hospital, 0027 Oslo, Norway; ⁴ Department of Radiology, Rikshospitalet University Hospital, 0027 Oslo, Norway; ⁵ The Interventional Centre, Rikshospitalet University Hospital, 0027 Oslo, Norway; and ⁶ Department of Medical Engineering, Ulm University of Applied Sciences, Ulm, Germany

Received 28 October 2004; revised 21 December 2004; accepted 5 January 2005; online publish-ahead-of-print 16 February 2005

KEYWORDS

Brain injury;
Cardiac catheterization;
Cerebral ischaemia;
Magnetic resonance imaging;
Microemboli;
Transcranial Doppler

Aims Left heart catheterization carries a risk for cerebral complications. The aims of this prospective study were to determine the frequency and composition of catheterization-related cerebral microemboli and to detect cerebral morphological changes and acute cognitive impairment due to catheterization.

Methods and results Forty-seven unselected patients undergoing elective left heart catheterization, either by transradial or by transfemoral access, were monitored for cerebral microemboli using multi-frequency transcranial Doppler. Cerebral magnetic resonance imaging (MRI) with diffusion-weighted imaging sequences and neuropsychological assessments were carried out on the day before and the day after catheterization. A median number of 754 cerebral microemboli were detected: 92.1% were gaseous and 7.9% were solid. New cerebral lesions were observed in 15.2% of the transradial, but none of the transfemoral, catheterization patients ($P = 0.567$). These lesions were significantly associated with a higher number of solid microemboli ($P = 0.016$) and a longer fluoroscopy time ($P = 0.039$). There was also a significantly higher number of solid microemboli during transradial than during transfemoral catheterization ($P = 0.012$). Cognitive impairment following the investigations was associated with the degree of pre-catheterization cerebral MRI injury ($P = 0.03$).

Conclusion During left heart catheterization, cerebral microemboli, especially those which are solid, may damage the brain. Cardiac catheterization may therefore pose a greater risk for the brain than previously acknowledged.



Basics: Coronary Angiography

Cerebral Microembolism During Coronary Angiography

A Randomized Comparison Between Femoral and Radial Arterial Access

Juliane Jurga, MD*; Jesper Nyman, MD*; Per Tornvall, MD, PhD; Maria Nastase Mannila, MD, PhD;
Peter Svenarud, MD, PhD; Jan van der Linden, MD, PhD; Nondita Sarkar, MD, PhD

Background and Purpose—Microemboli observed during coronary angiography can cause silent ischemic cerebral lesions. The aim of this study was to investigate if the number of particulate cerebral microemboli during coronary angiography is influenced by access site used.

Methods—Fifty-one patients with stable angina pectoris referred for coronary angiography were randomized to right radial or right femoral arterial access. The number of particulate microemboli passing the middle cerebral arteries was continuously registered with transcranial Doppler.

Results—The median (minimum–maximum range) numbers of particulate emboli were significantly higher with radial 10 (1–120) than with femoral 6 (1–19) access. More particulate microemboli passed the right middle cerebral artery with the radial access.

Conclusions—This study indicates that the radial access used for coronary angiography generates more particulate cerebral microemboli than the femoral access and thus may influence the occurrence of silent cerebral injuries. (*Stroke*. 2011; 42:1475–1477.)

Key Words: coronary angiography ■ microemboli ■ radial ■ transcranial Doppler

Received November 11, 2010; accepted November 26, 2010.

From Cardiology Unit, Department of Medicine (J.J., P.T., M.N.M., N.S.), and Department of Molecular Medicine and Surgery (J.N., P.S., J.v.d.L.), Karolinska University Hospital, Karolinska Institutet, Stockholm, Sweden.

*J.J. and J.N. contributed equally to this work.

Correspondence to Juliane Jurga, MD, Department of Cardiology, Karolinska University Hospital/ Solna, N3:05, SE 171 76 Stockholm, Sweden.
E-mail juliane.jurga@karolinska.se

© 2011 American Heart Association, Inc.

Stroke is available at <http://stroke.ahajournals.org>

DOI: 10.1161/STROKEAHA.110.608638

Basics: Coronary surgery

Gaseous and solid cerebral microembolization during proximal aortic anastomoses in off-pump coronary surgery: The effect of an aortic side-biting clamp and two clampless devices

Lorenzo Guerrieri Wolf, MD, Yasir Abu-Omar, MRCS, Bikram P. Choudhary, MRCS, David Pigott, FRCA, and David P. Taggart, MD (Hons), PhD, FRCS

From the Department of Cardiothoracic Surgery, John Radcliffe Hospital, Oxford, United Kingdom.

Address for reprints: Professor David P. Taggart, MD, PhD, FRCS, Professor of Cardiovascular Surgery, University of Oxford, Department of Cardiothoracic Surgery, John Radcliffe Hospital, Headley Way, Headington, Oxford OX3 9DU, United Kingdom (E-mail: david.taggart@orh.nhs.uk).

J Thorac Cardiovasc Surg 2007;133:485-93

0022-5223/\$32.00

Copyright © 2007 by The American Association for Thoracic Surgery
doi:10.1016/j.jtcvs.2006.10.002

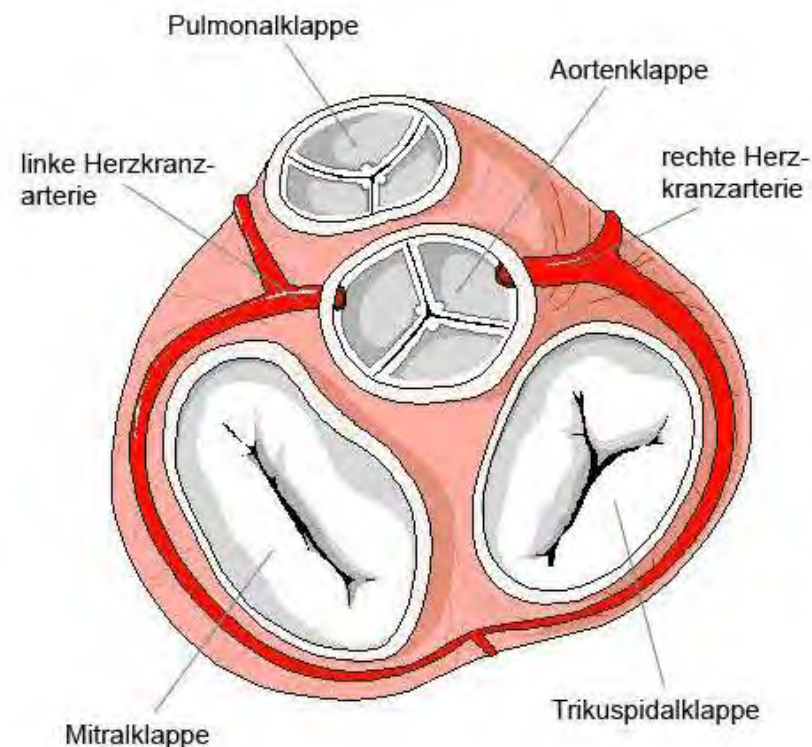
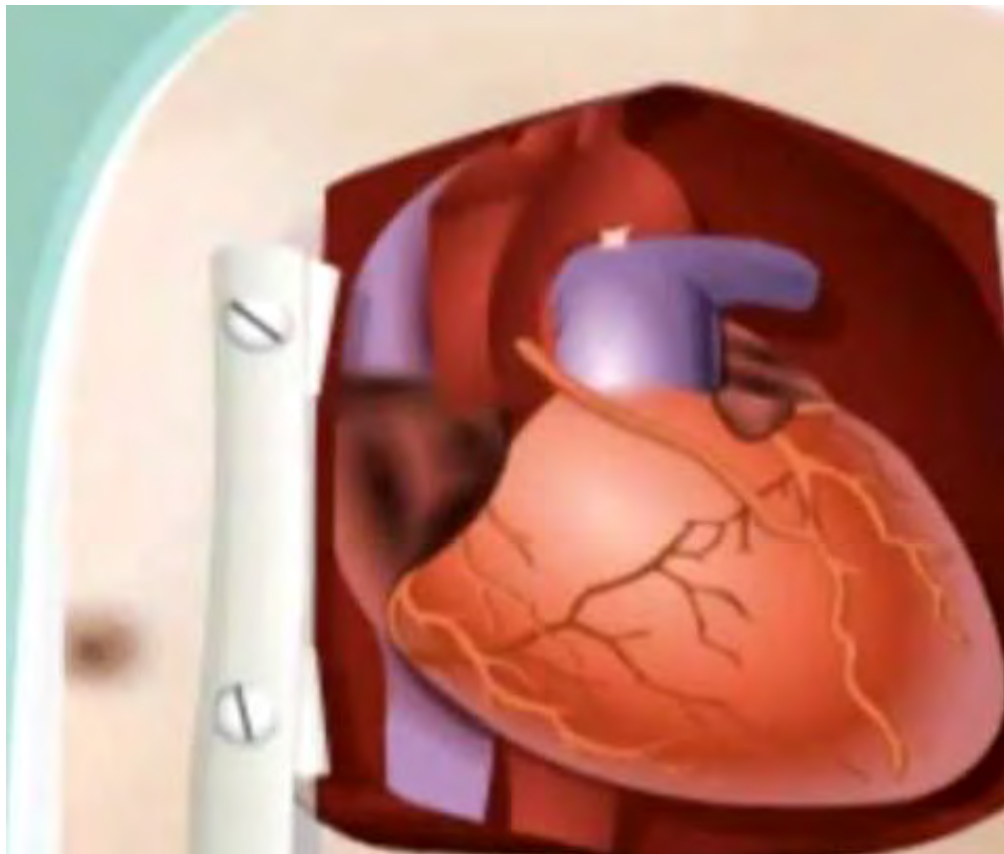
Objectives: Intraoperative cerebral microembolism is a cause of cerebral dysfunction after cardiac surgery, and particulate microemboli are the most damaging. Using a new-generation transcranial Doppler ultrasound, we compared the number and nature of microemboli in patients undergoing off-pump coronary artery bypass grafting during performance of proximal anastomoses with three techniques: an aortic side-biting clamp and two clampless devices (the Enclose II device [Novare Surgical Systems, Inc, Cupertino, Calif] and the Heartstring II device [Guidant Corporation, Santa Clara, Calif]) developed to obviate the need for an aortic side-biting clamp, thereby reducing the number of cerebral microemboli.

Methods: Bilateral continuous monitoring of the middle cerebral arteries was performed with a multirange, multifrequency transcranial Doppler device that both automatically rejects artifacts online and discriminates between solid and gaseous microemboli. Recordings were continuously undertaken during performance of 66 proximal aortic anastomoses in 42 patients. Thirty-five anastomoses were performed with an aortic side-biting clamp, 20 with the Enclose device, and 11 the Hearstring device.

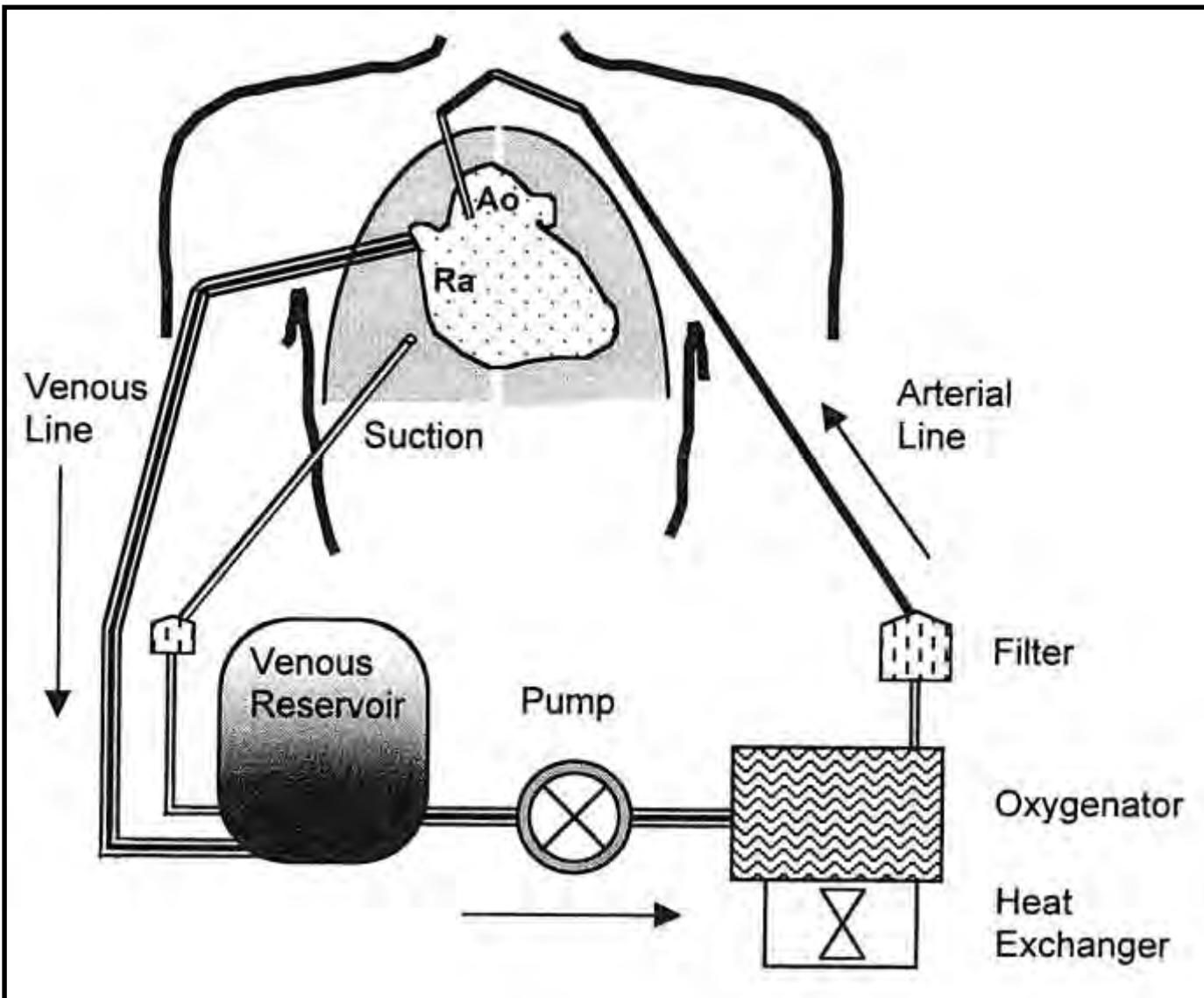
Results: Most microemboli occurred during application/insertion and removal of each device from the ascending aorta. The median number (interquartile range) of total microemboli was 11 (6-32) during side clamping, 11 (6-15) with the Enclose device, 40 (31-48) with the Heartstring device ($P < .01$). The proportion of solid microemboli was significantly higher in the side-clamp group (23%) compared with 6% and 1% in the Enclose and Heartstring groups, respectively ($P < .01$).

Conclusions: Avoidance of aortic side clamping results in a significant reduction in the proportion of solid microemboli detected with transcranial Doppler. As solid microemboli are probably the most damaging, use of the Enclose and Heartstring devices may represent an important strategy for minimizing cerebral injury during proximal aortic anastomoses.

Basics: Bypass Surgery



Basics: Bypass Surgery

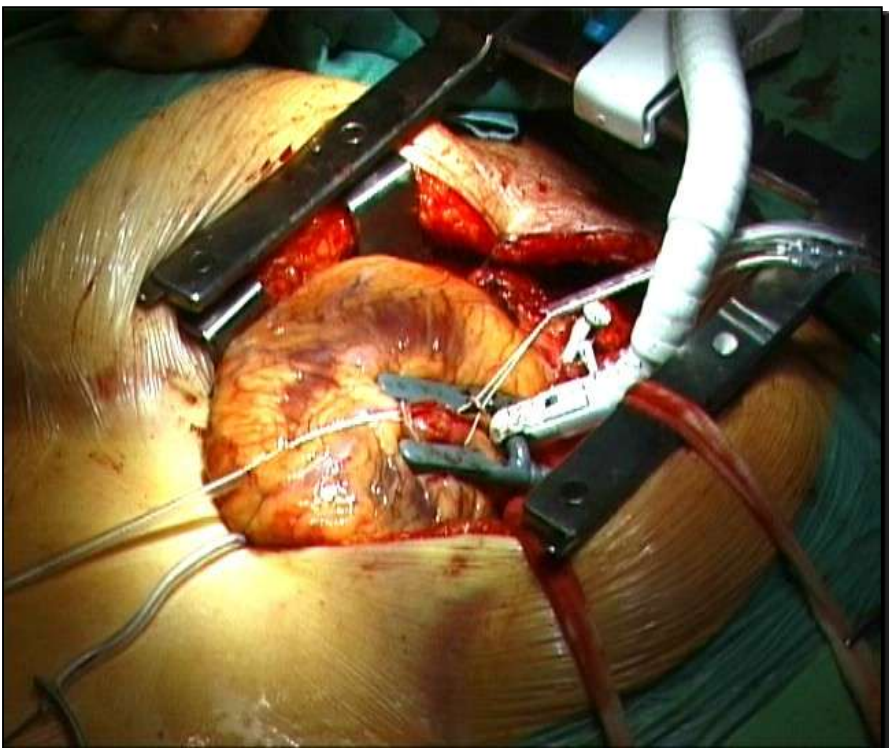




Basics: Bypass surgery

Cerebral microembolization during off-pump coronary artery bypass surgery with the Symmetry aortic connector device

Mona Skjelland, MD,^a Jacob Bergsland, MD,^b Runar Lundblad, MD, PhD,^c Per Snorre Lingaas, MD,^c Kjell Arne Rein, MD, PhD,^c Steinar Halvorsen, MD,^b Jan L. Svennavig, MD, PhD,^c Erik Fosse, MD, PhD,^b Rainer Brucher, PhD,^a and David Russell, MD, PhD, FRCPE^a



Objective: The use of aortic connector systems for proximal vein grafts in off-pump coronary artery bypass grafting might minimize aortic manipulation by eliminating the need for partial aortic clamping. The objective of this study was to assess whether use of a Symmetry connector (St Jude Medical, Inc, St Paul, Minn) reduced intraoperative cerebral embolization.

Methods: Thirty-two consecutive patients underwent off-pump coronary artery bypass grafting. Sixteen patients received at least one mechanical proximal vein graft anastomosis with a Symmetry aortic connector system. Sixteen patients representing the control group underwent operations with standard suturing techniques using partial aortic clamping. During surgical intervention, all patients were monitored continuously with multifrequency transcranial Doppler scanning, which detected and differentiated cerebral emboli.

Results: There were significantly more cerebral emboli in the Symmetry group (median, 36) compared with the control group (median, 11; $P = .027$). This was due to a higher number of gaseous emboli in the Symmetry group than in the control group (median, 27 vs 8; $P = .014$), whereas there was no significant difference regarding the number of solid emboli (median, 7 vs 3; $P = .139$).

Conclusion: Use of a Symmetry connector system during proximal vein graft anastomosis increased the number of emboli to the brain compared with a standard technique in coronary bypass surgery without cardiopulmonary bypass.

Ultraschall und Theragnostik

Ultraschall in Thera(pie) und (Dia)gnostik

Kapitel 9

Therapie mit hochdosiertem Ultraschall

Inhaltsangabe

1. Übersicht der Ultraschallanwendungen
2. Physikalische Grundlagen
3. Ultraschallsonden
4. Bildgebende Verfahren in der Diagnostik
5. Dopplerverfahren in der Diagnostik und Therapie
6. Artefakte und Diagnostik
7. Ultraschall und Kontrastmittel
8. Theragnostik mit Ultraschall
9. **Therapie mit hochdosierten Ultraschall**
10. Gewebecharakterisierung mittels shear waves
11. Dosierung und Sicherheitsaspekte

Keywords

Applications at very high intensity of ultrasound and dosis:

- Activation of metabolism of the cells a acceleration of wound healing e.g. Ulzera – diabetes foot
- Ultrasound Lithotripsy
 - of kidney stone
 - calcification of acromioclavicular joint (kleines Schultergelenk)
- Thermal demolition/damage of cancer cells or metastases
 - Kidney
 - Liver
 - Prostata

Wound healing



Treatment without anaesthesia

This treatment does not require anaesthesia. The broad surface distribution of the optimal treatment energy with the dermagold applicator significantly reduces the pain associated with shock wave treatment. The number of treatments needed for a skin lesion varies, depending on the indication and on the wound surface.



Therapeutic Focus fz (-6dB):
Energy Flux Density (ED):
Focus Energy (E total / -6dB):

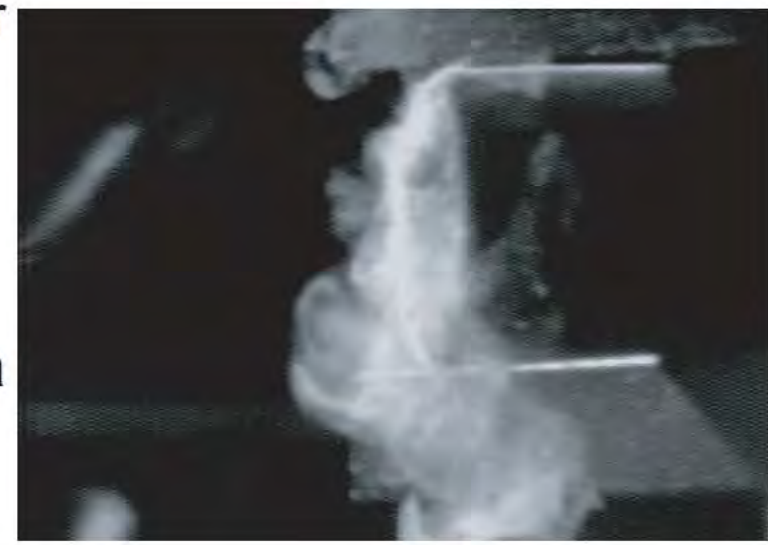
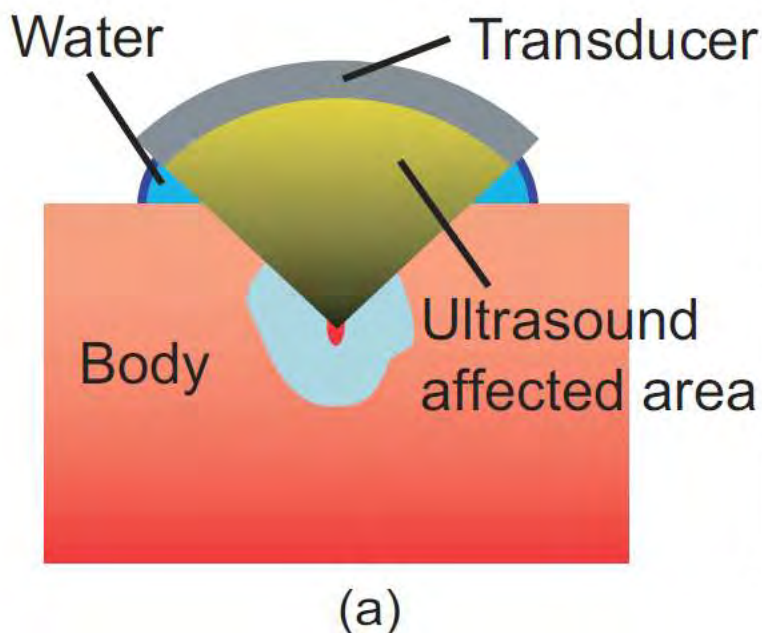
0 - 82 mm
0.01 - 0.19 mJ/mm²
0.40 - 3.88 mJ





High Intensity focused Ultrasound → applications

Physics: Extracorporele Shock Wave Therapy (ESWT)
 High Intenity Focused Ultrasound (HIFU)
 for Lithotripsy of kidney stones



(b)

Fig. (a) High-intensity focused ultrasound (HIFU). (b) Destruction of a kidney stone by HIFU.

High Intensity focused Ultrasound → applications

Physics: Extracorporeale Shock Wave Therapy (ESWT)

Es gibt Stoßwellen mit unterschiedlich starker Energie. Die niederenergetische Stoßwelle findet ihre Anwendung vor allem in der Schmerztherapie an eher oberflächlichen Sehnenansätzen. Die Wirkung wird durch wiederholte Anwendung verstärkt.

Mittelenergetische Wellen dringen tiefer in den Körper ein und werden vor allem bei der **Kalkschulter (Tendinitis calcarea)** eingesetzt. Wegen der dabei auftretenden **Schmerzen** ist in der Regel eine örtliche Betäubung unerlässlich.

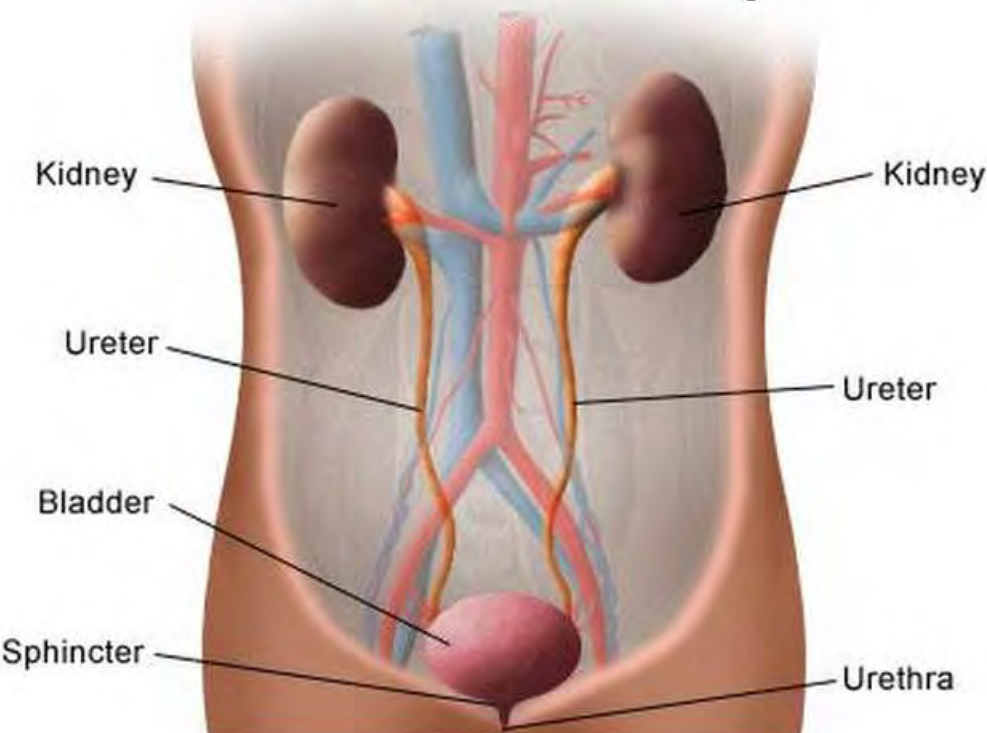


Wirkungen der ESWT

- Förderung des Knochenwachstums
- Förderung der Durchblutung (Vaskularisierung)
- Fördert Bildung von Wachstumsfaktoren
- Gewebeneubildung
- Förderung der Wundheilung
- Linderung von Schmerzsyndromen
- Verkürzung von Rehabilitationszeiten

Stones in Kidney or Ureter

Front View of Urinary Tract



Applications litotripsy

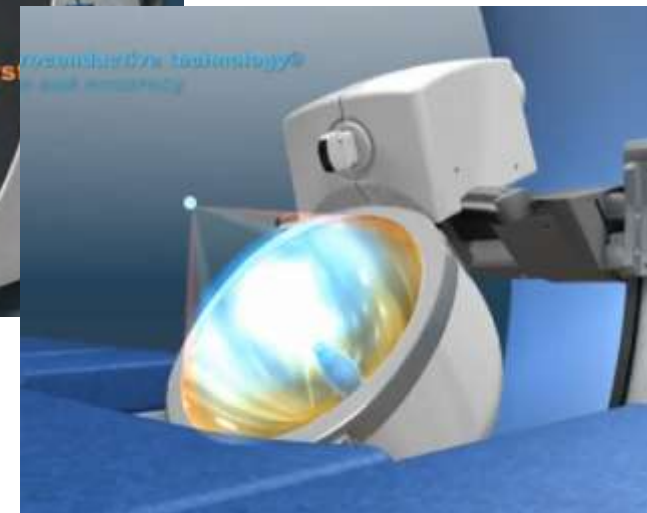
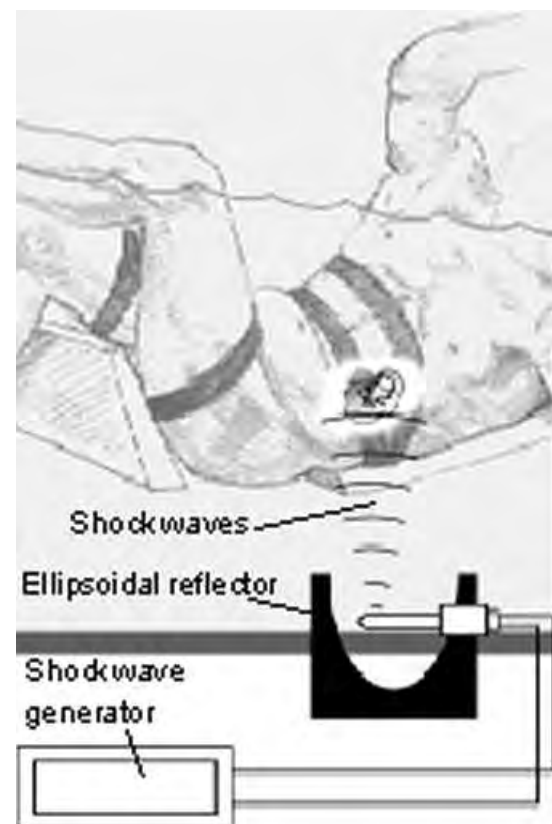
- Shock wave
- HIFU



Stein im rechten Harnleiter (Pfeil), mit Harnaufstau.
Computertomografie mit Kontrastmittel

High Intensity focused Ultrasound → applications

Kidney stone lithotripsy by shock waves ESWL (external shock wave lithotripsy)



Sonolith

Litotripter is a machine that pulverizes kidney stones by ultrasound as an alternative to their surgical removal

<http://www.youtube.com/watch?v=Z7cYuhpVeWw>

High Intensity focused Ultrasound → applications

Kidney stone tracking and lithotripsy by HIFU

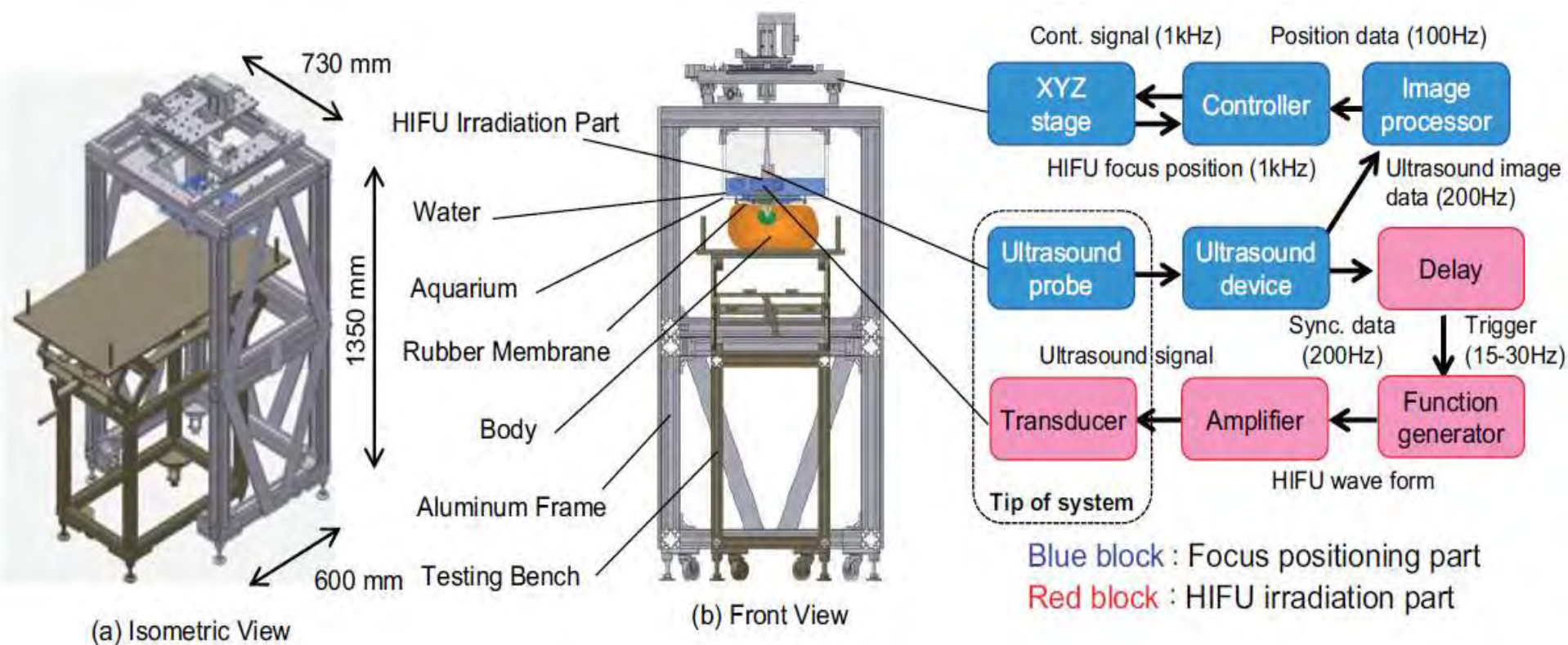


Fig.: System configuration of a non-invasive ultrasound theragnostic system.

High Intensity focused Ultrasound→applications

Kidney stone tracking and lithotripsy by HIFU

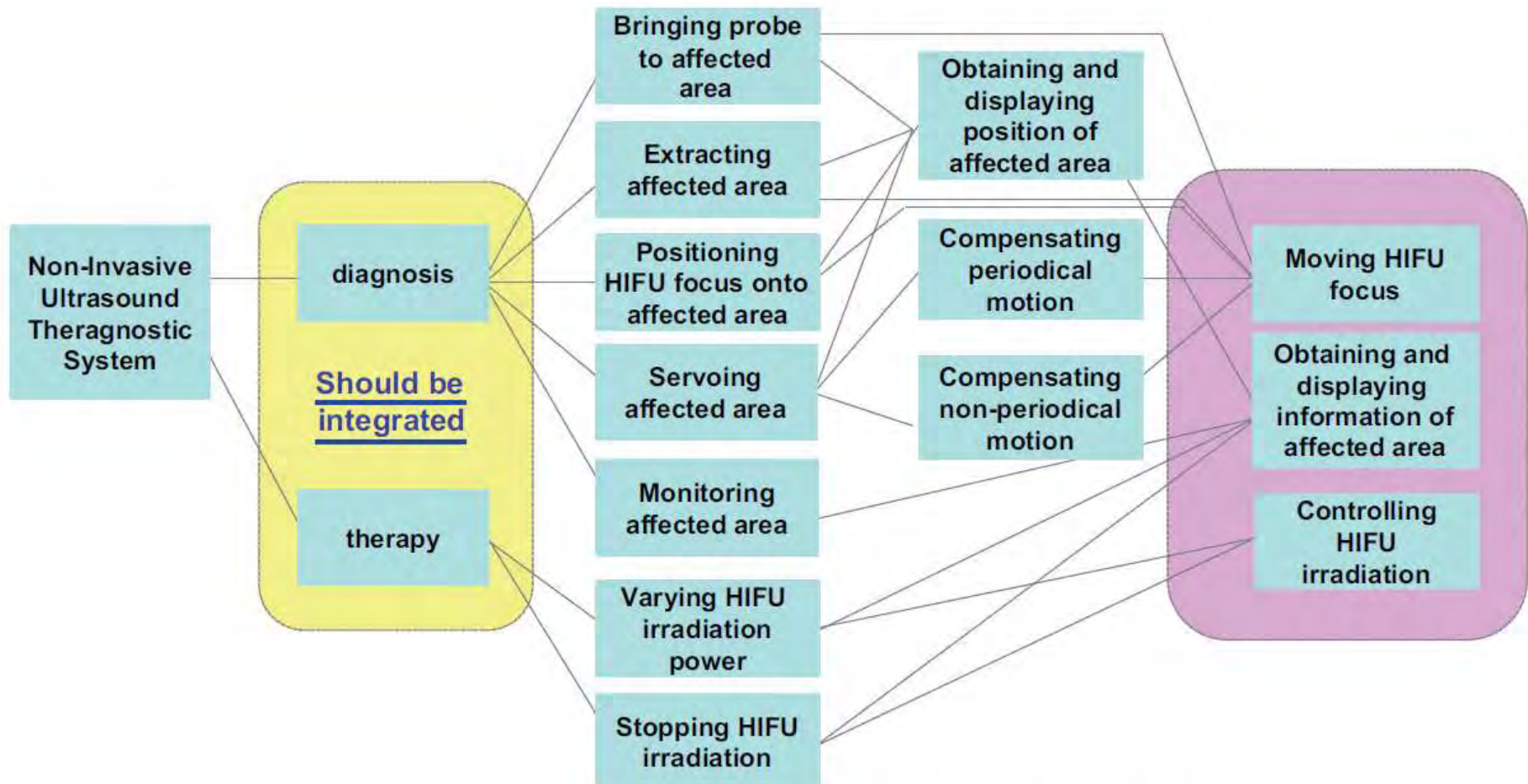


Fig. Required structuring functions for a non-invasive ultrasound theragnostic system.

High Intensity focused Ultrasound → applications

Kidney stone tracking and lithotripsy by HIFU

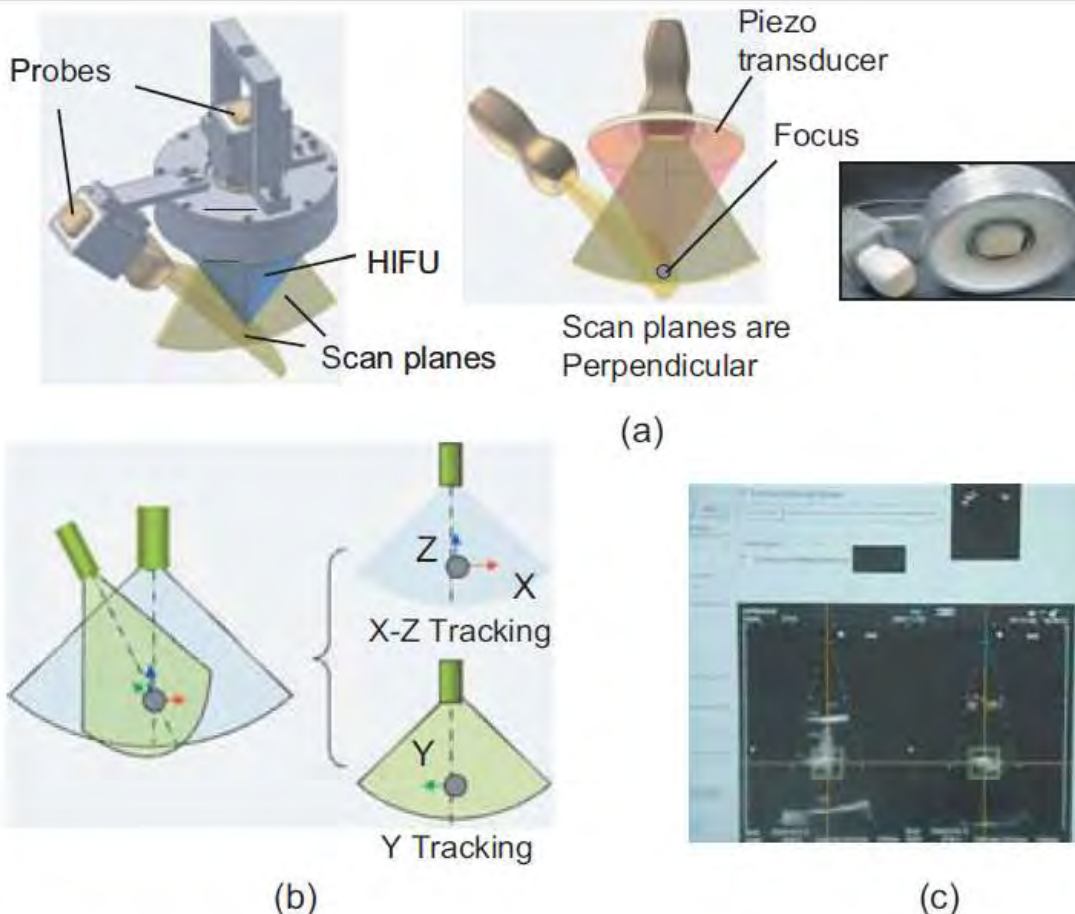


Fig. (a) Tip of the probe of the system with two ultrasound probes for diagnosis and a transducer for HIFU treatment. (b) Ultrasound image planes that are perpendicular to each other. (c) Ultrasound images acquired using the ultrasound probes.

High Intensity focused Ultrasound → applications

Kidney stone tracking and lithotripsy by HIFU

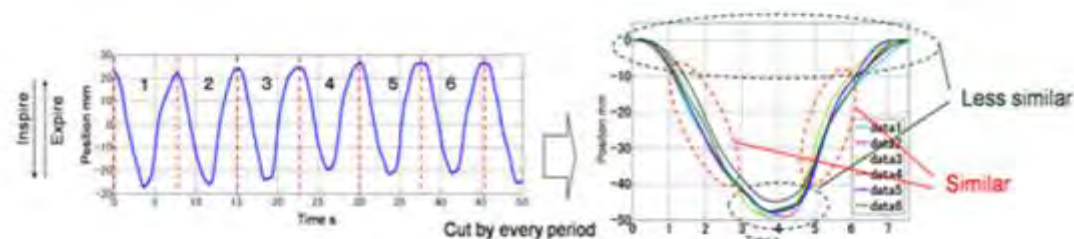


Fig. Quasi-periodical kidney motion

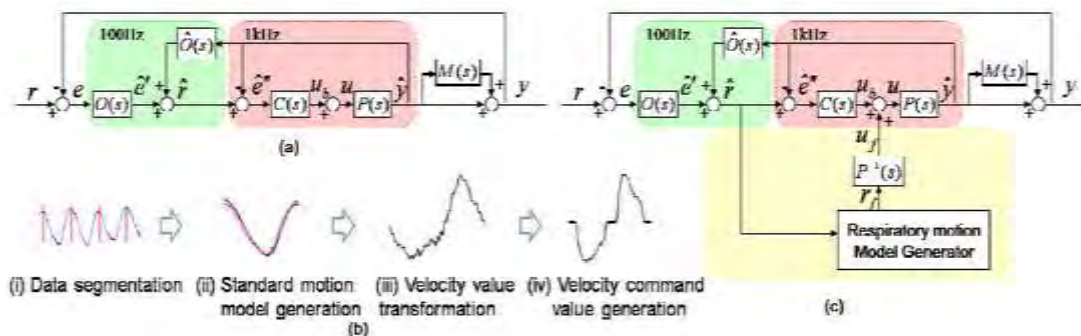
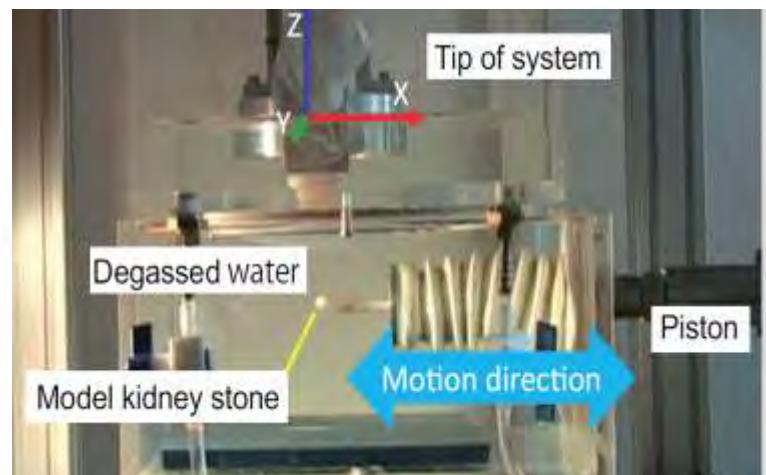
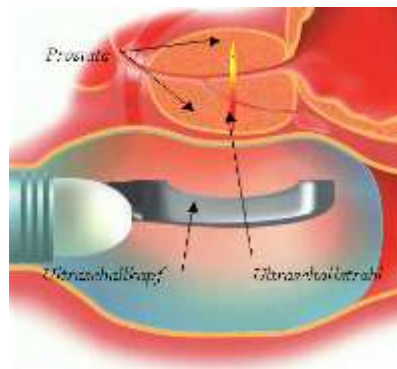
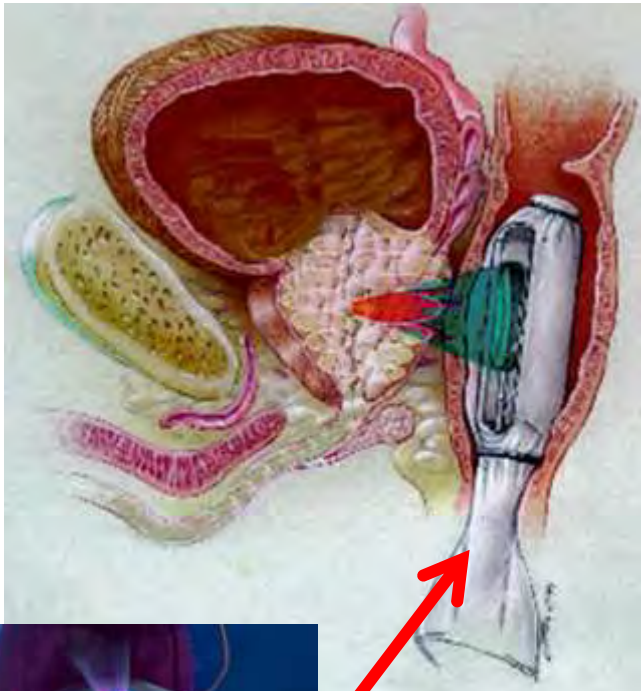


Fig. (a) Block diagram of the fundamental controller, (b) An algorithm to generate feed-forward term, (c) Block diagram of the proposed feed-forward controller

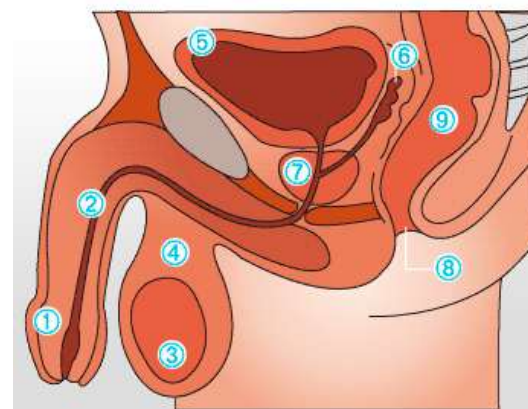
High Intensity focused Ultrasound → applications

HIFU zur Destruktion von Prostata Krebs (die dritthäufigste Krebsbedingte Todesursache bei Männern)



Die schematische Zeichnung macht die Funktionsweise des hochintensiven Ultraschalls deutlich: Der Ultraschall (blaugrün) wird so vom Schallkopf abgestrahlt, dass er sich im Brennpunkt bündelt und dort zur gewünschten Hitzewirkung führt (roter Bereich). Das zu beschallende Areal wird mit Ultraschallbildern und Computerhilfe exakt berechnet.

Anatomie



- 1 - Penis
- 2 - Harnröhre
- 3 - Hoden
- 4 - Hodensack
- 5 - Harnblase
- 6 - Samenblase
- 7 - Prostata
- 8 - Anus
- 9 - Enddarm

High Intensity focused Ultrasound → applications

Diagnostics: Elastography for localisation of prostate cancer



Using ultrasound elastographics an area of tumor can be fixed
(blue area within gray circle)

Ultraschall und Theragnostik

Ultraschall in Thera(pie) und (Dia)gnostik

Kapitel 10

Gewebecharakterisierung mittels „shear waves“

Inhaltsangabe

1. Übersicht der Ultraschallanwendungen
2. Physikalische Grundlagen
3. Ultraschallsonden
4. Bildgebende Verfahren in der Diagnostik
5. Dopplerverfahren in der Diagnostik und Therapie
6. Artefakte und Diagnostik
7. Ultraschall und Kontrastmittel
8. Theragnostik mit Ultraschall
9. Therapie mit hochdosierten Ultraschall
10. **Gewebecharakterisierung mittels shear waves**
11. Dosierung und Sicherheitsaspekte

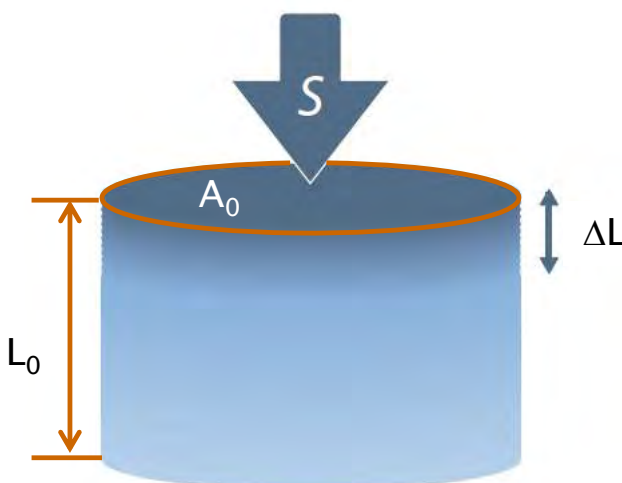
Keywords

Shear waves, elasticity and characterisation of tissue:

- Elasticity using longitudinal and shears (transversal) waves
- Supersonic generator
- Fast B-Mode Scan of shear wave propagation within tissue
- Map of shear wave velocities in respect to elasticities
- Application:
 - Masto carcinoma (Mammakarzinom)
 - Arteriosclerotics, Plaques
 - Prostate cancer

Physics: Stiffness module of material

- Characterizing of pathology using tissue stiffness (Young's Module E) by palpation



$$E = \frac{S}{e} = \frac{F / A_0}{\Delta L / L}$$

S: Stress

e: strain/displacement

	Art des Gewebes	Youngscher Modul (E in kPa)	Dichte (kg/m ³)
Brust	Normales Fettgewebe	18-24	1000 +/- 8% Wasser
	Normales Drüsengewebe	28-66	
	Fibröses Gewebe	96-244	
	Karzinom	22-560	
Prostata	Normal anterior	55-63	1000 +/- 8% Wasser
	Normal posterior	62-71	
	BPH	36-41	
	Karzinom	96-241	
Leber	Normal	0,4-6	1000 +/- 8% Wasser
	Zirrhose	15-100	

BPH: benigne Prostatahyperplasie (gutartige Prostatavergrößerung),

Physics: difference between longitudinal and transversal

- Longitudinal waves $c_L \approx 1500 \text{ m/s}$
- Shear waves (transversal) $c_s \approx 1-10 \text{ ms}$

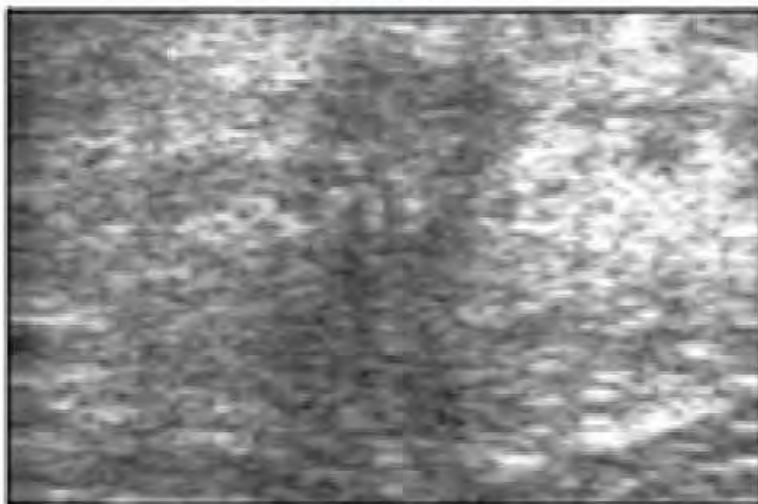
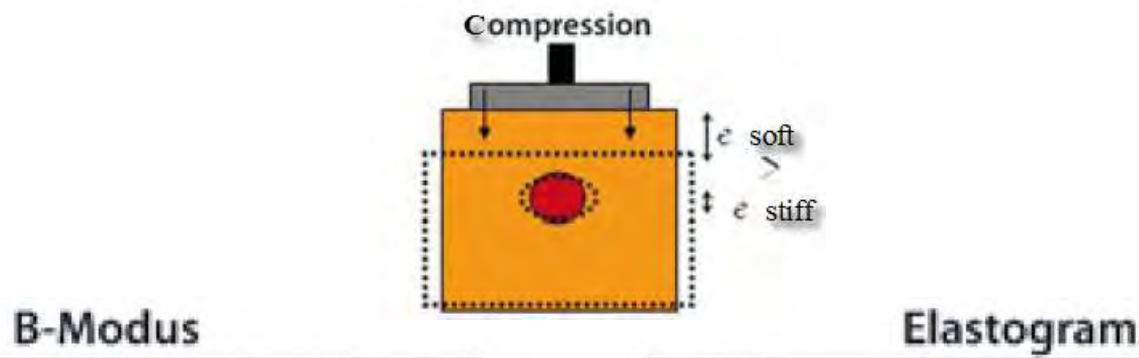
For transversal waves modul $E = 3\rho c_s^2$ ρ : density

Elastography: (3 steps)

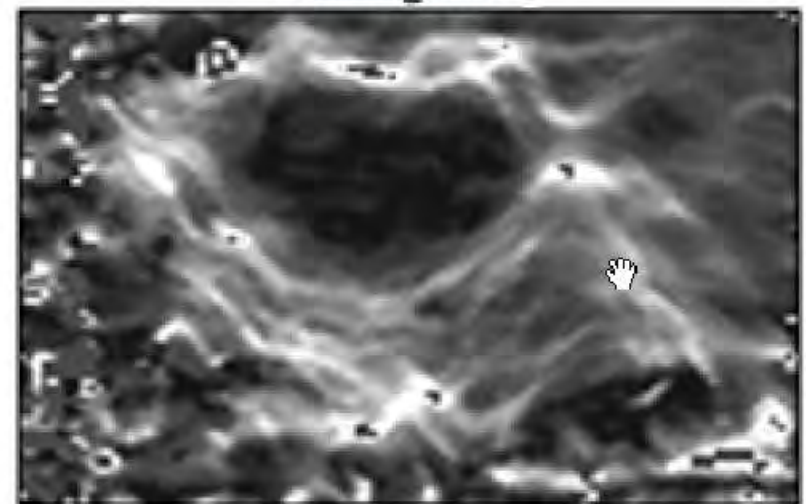
1. Generating low frequency vibrations for shear stress/strain
2. Fast ultrasound B-imaging for analyzing shear stress (c_s)
3. Parameter “E” extraction for tissue stiffness/elasticity

Physics: Types of Elastography

Static application → deformation of the material



Static elasticity: B-Mode imaging

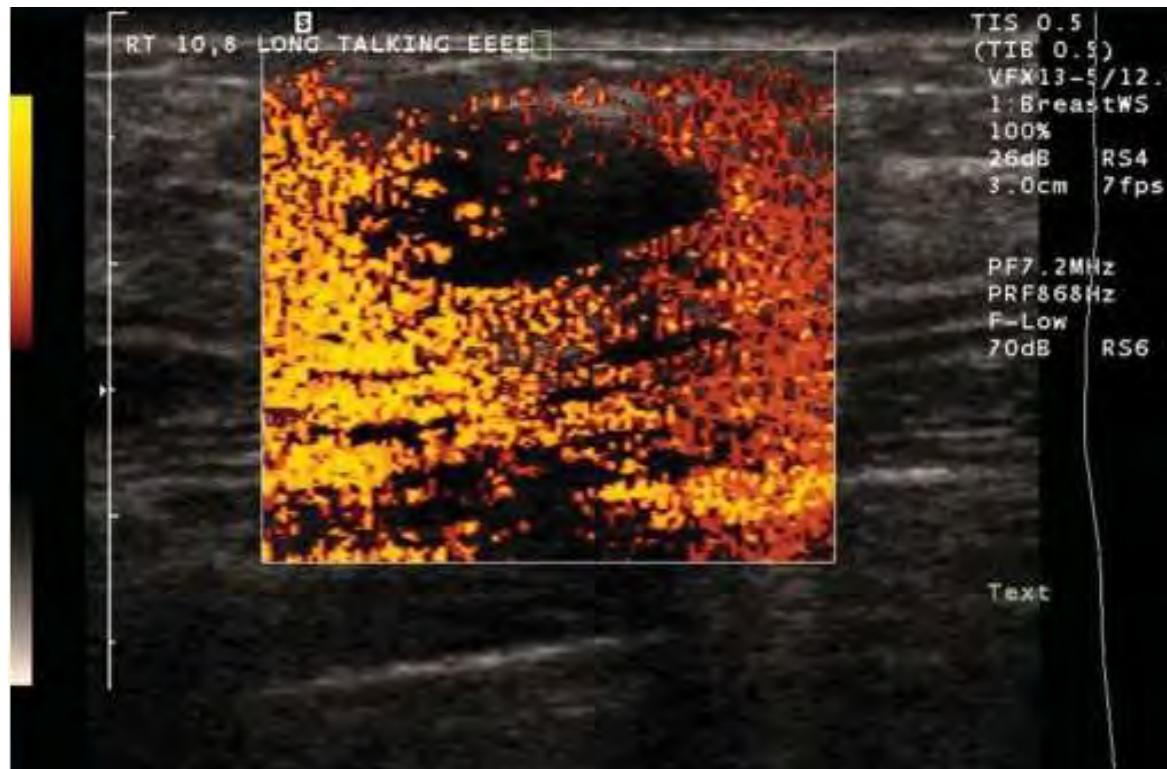


Elastogramm →
stiffness corresponds to dark

Tissue Characterisation by Elastograms

Physics: Types of Elastography

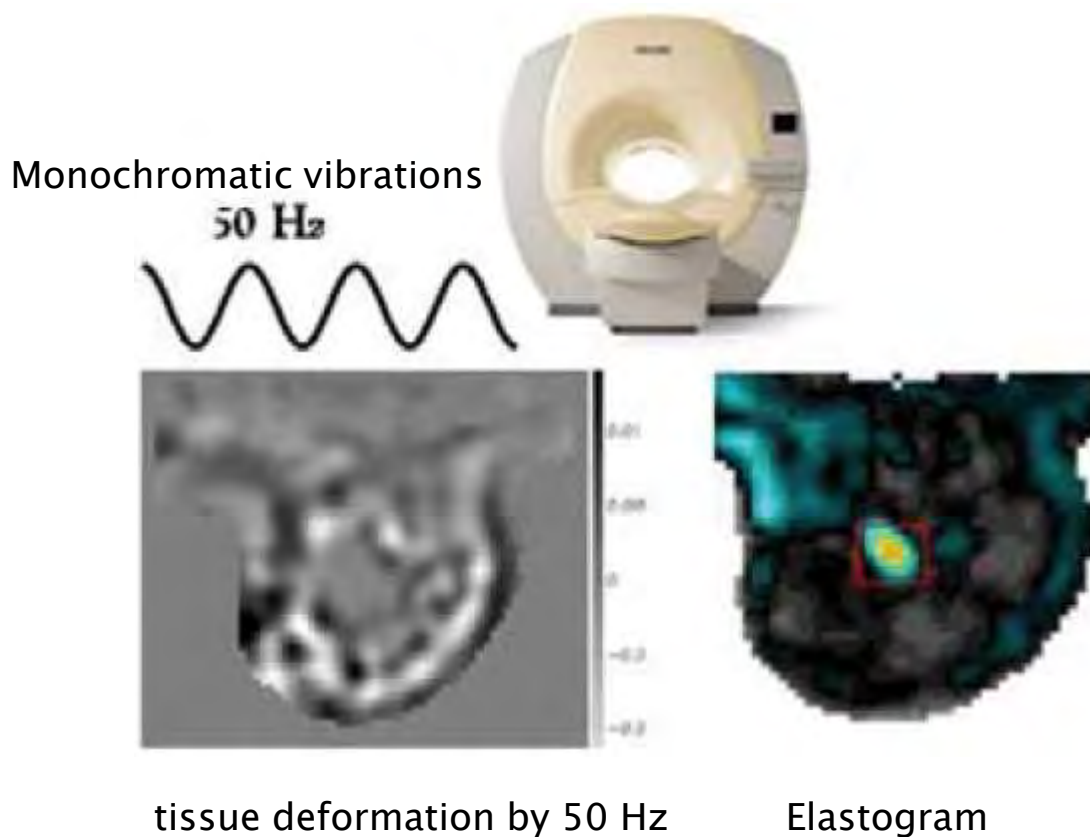
Physiological vibrations → B-Mode and Color coded Doppler



While using colour Doppler the patient is asked to say 'Eeeeeee'. The amount of vibration transmitted through the tissues is related to the elasticity of the tissues. The tissue movement is detected by the power Doppler. The lesion which is demonstrated is a fibroadenoma which is stiffer (and vibrates less) than the surrounding tissues.

Physics: Types of Elasticiography

Dynamic application → deformation by MRI

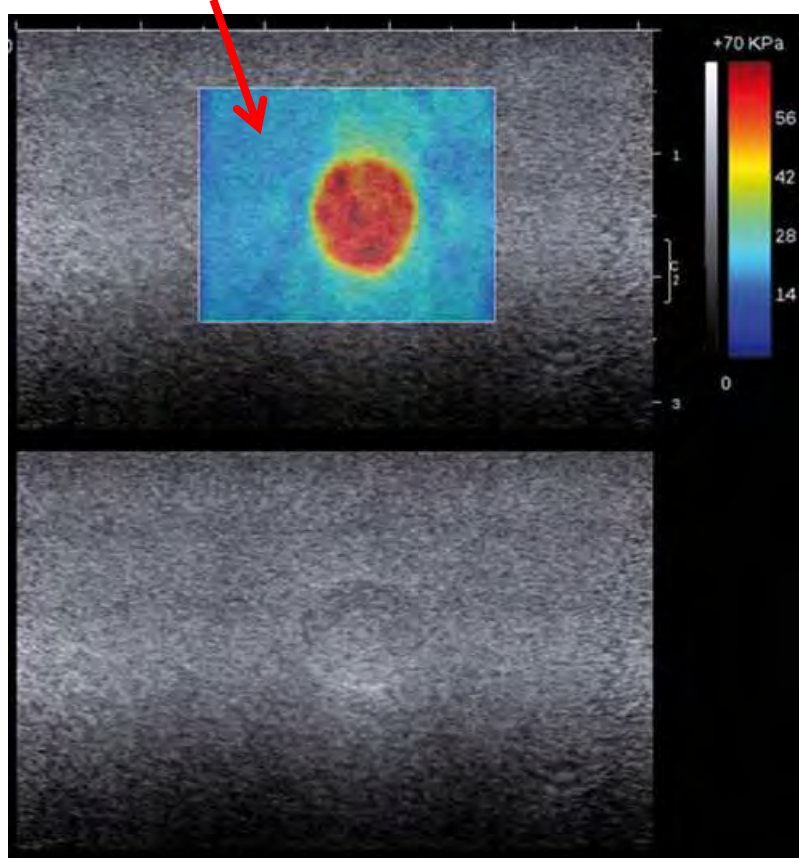


Physics: Types of Elastography

Dynamic application using transient pulses

Shear Waves Elastography (SWE) using B-Mode imaging

Colour coded elasticity

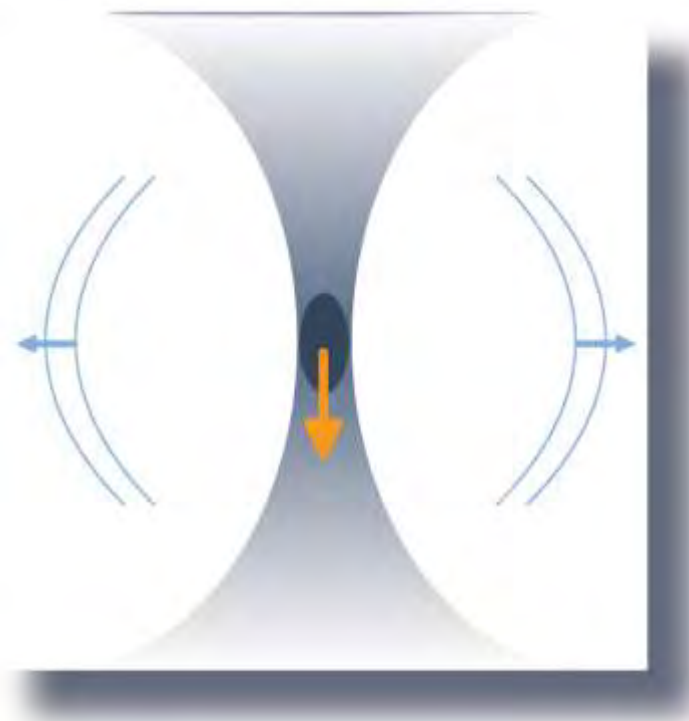


	Phantom 1	Phantom 2	Phantom 3	Phantom 4	Phantom 5
Referenzwert Elastizität	14	20	37	72	105
E mit SWE gemessen	15,1	21,3	37,4	74,7	105,7
STD-Abw.	2,3	3,1	5,4	9,6	11,5

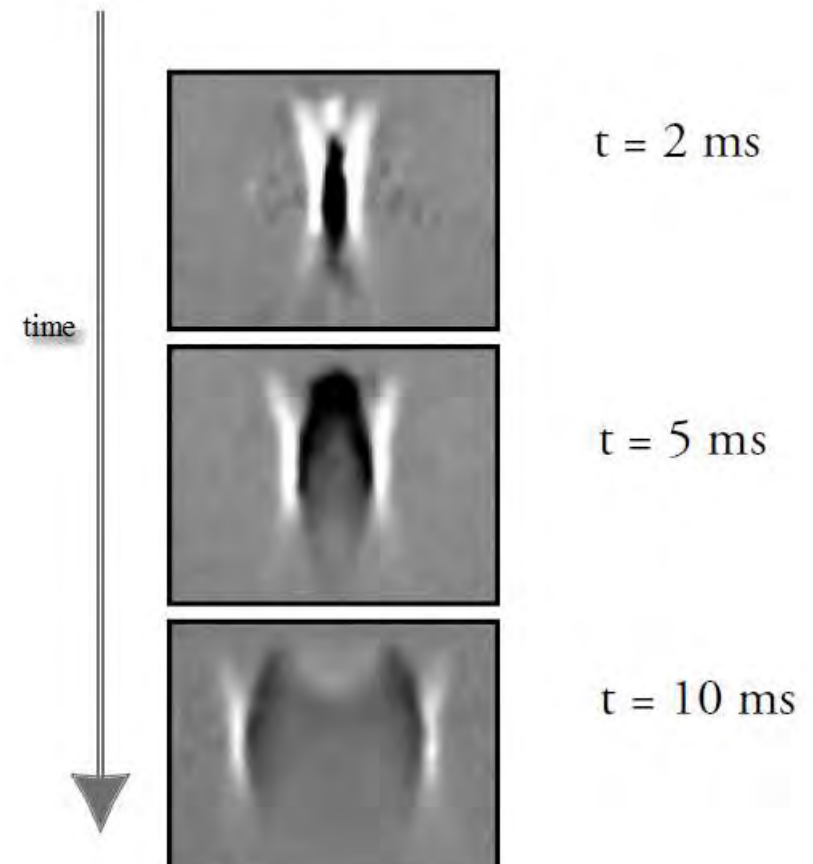
SWE measured at calibrated Phantoms

Tissue Characterization by Elastograms

Physics: Generation of ultrasound shear waves



Sound waves by conventional focused Beam
(only low intensity possible)



Focused beam as shear wave generator
only by one A-scan in the middle

Physics: Supersonic principle



Diagnostic intensities produce Mach'scher Cone of shear waves with increased amplitudes using quick dynamic focusing generates

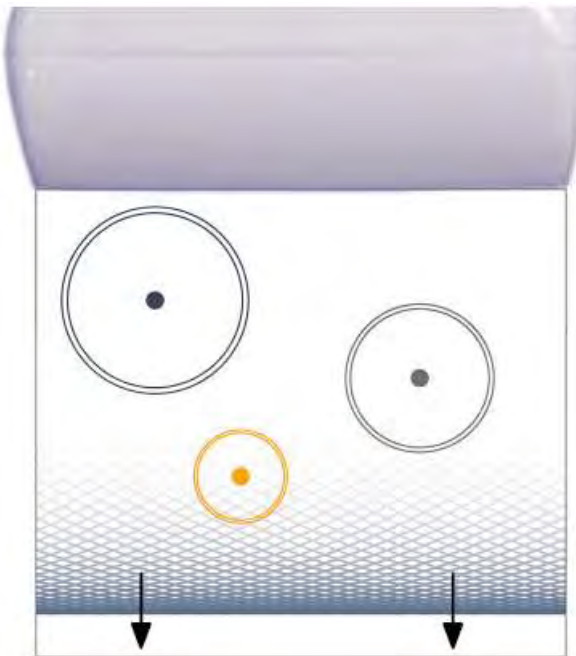
Ultrafast B-Mode imaging necessary $\leftarrow c=1-10\text{m/s} \rightarrow E=1-300\text{kPa}$

Propagation of shear waves: 3–6 cm depth within $dt=10-20\text{ms}$
 $\rightarrow 1/50\text{sec}$

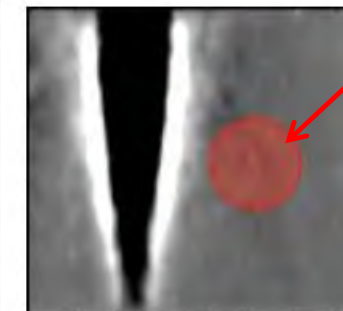
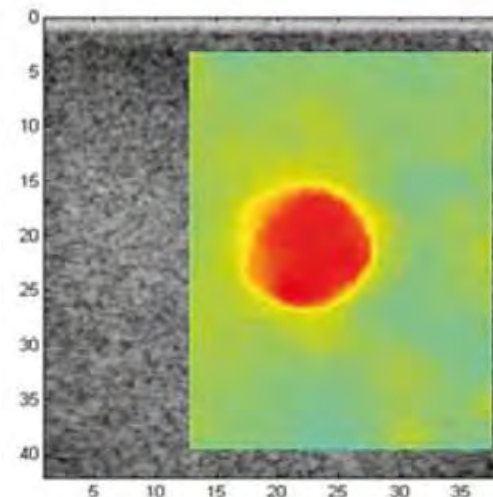
Requirements: Framerate = 1000–2000/sec for scanning shear stress

Tissue Characterisation by Elastograms

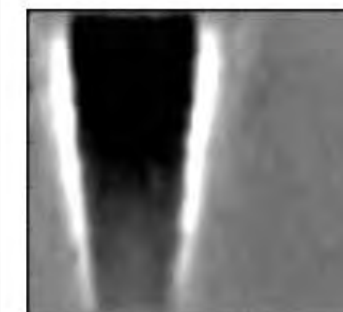
Physics: High frame rate of 1000–5000 per sec



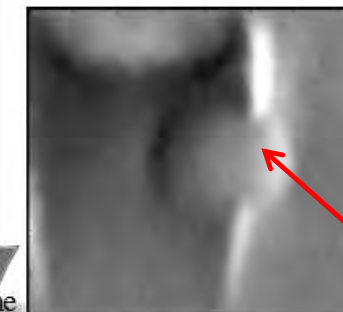
map of shear velocities m/s



stiff



t = 5 ms



t = 10 ms

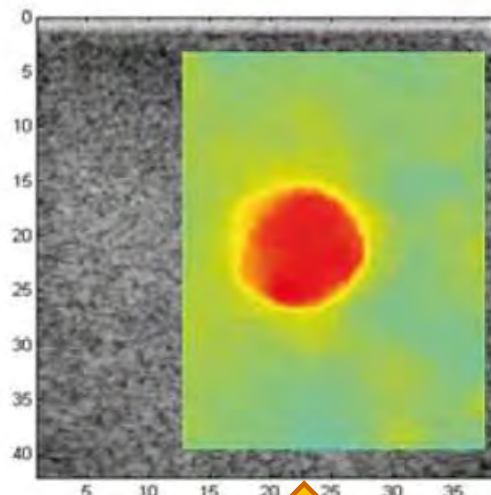
higher shear velocity

Simultaneous insonification of all A-Scans for B-Mode

→ Frame rate corresponds to travelling time in depth
→ 1000 – 5000 frames /sec

Tissue Characterisation by Elastograms

Physics: Map of elasticities or velocities c_s



$$E = 3\rho c_s^2$$

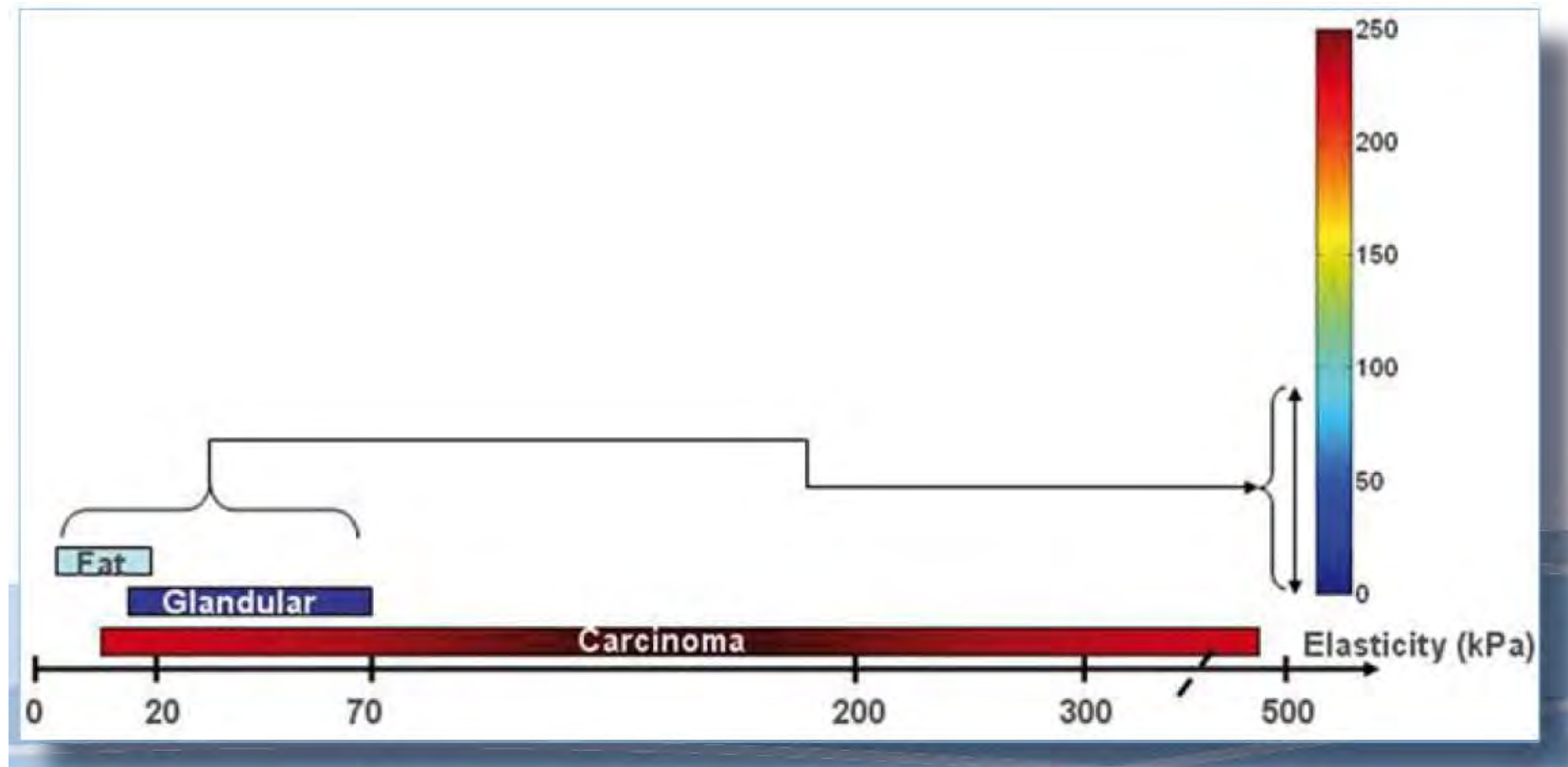


Each shear beam → one velocity map

Tissue Characterisation by Elastograms

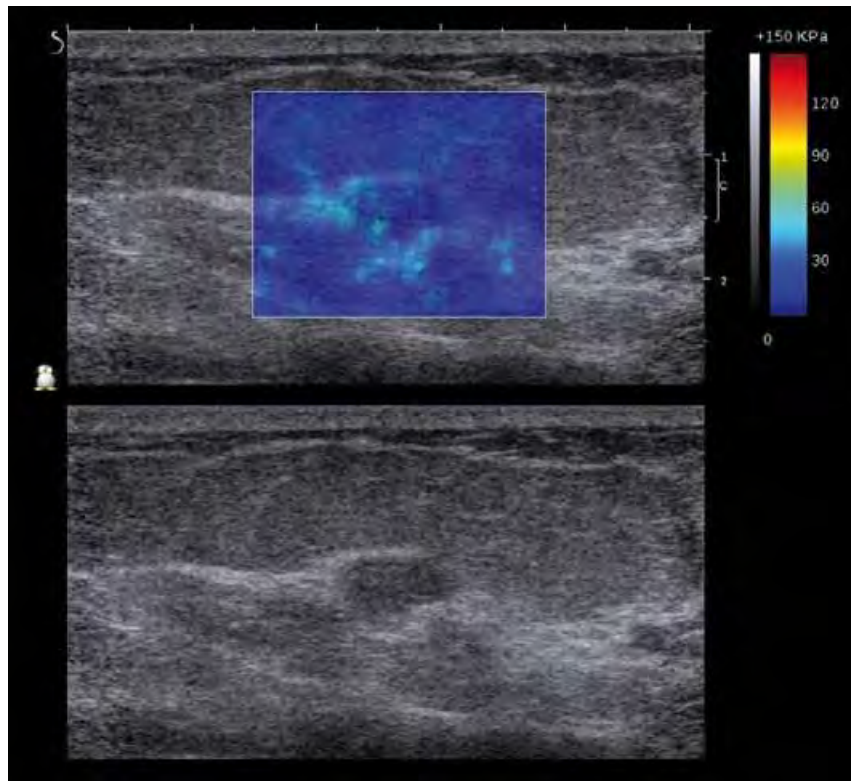
Clinical relevance: Elasticities of tissue (breast)

See also table on slide 4

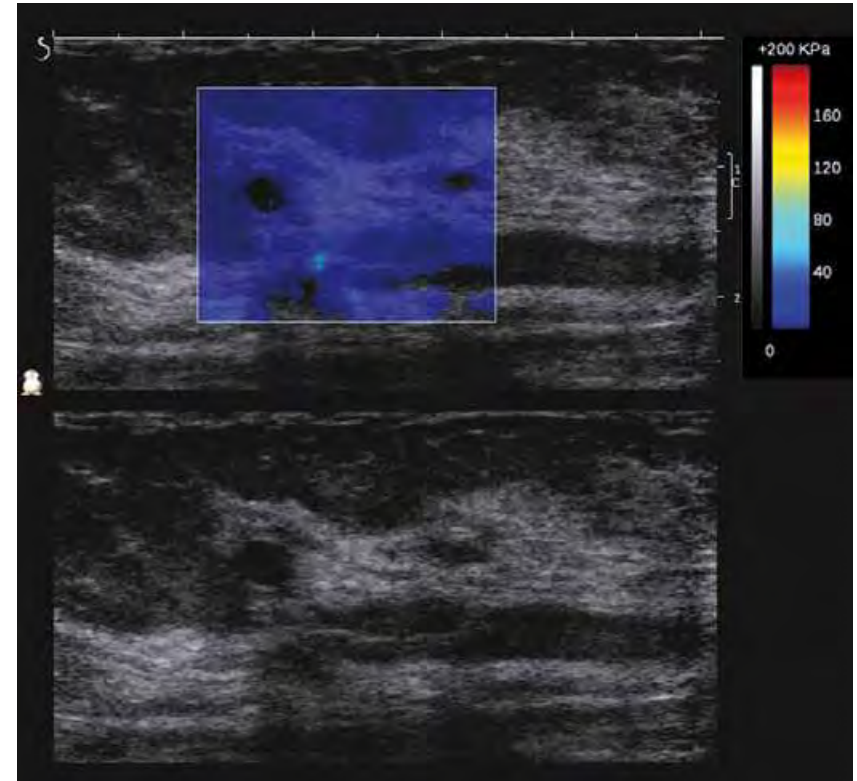


Tissue Characterisation by Elastograms

Clinical relevance: examples



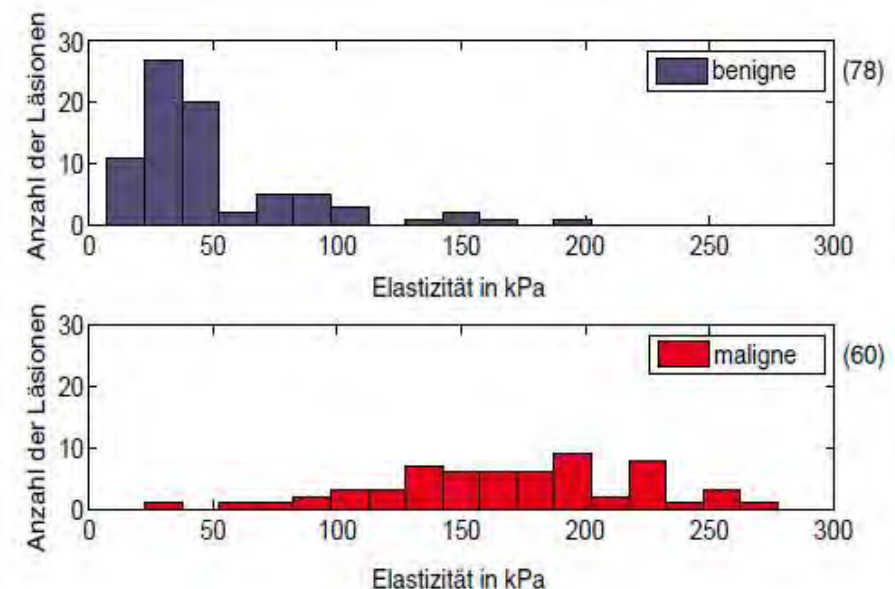
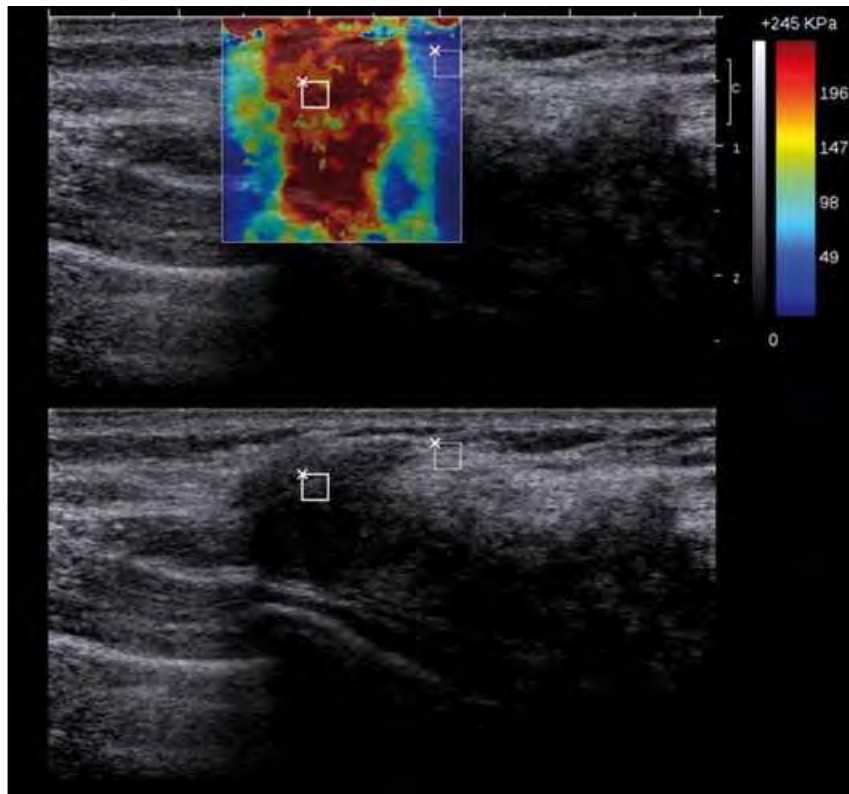
Elastogram of a Fibroadenoma
 $E_{\text{mean}} = 28 \text{kPa}$



SWE of two small cysts

Tissue Characterisation by Elastograms

Clinical relevance: examples

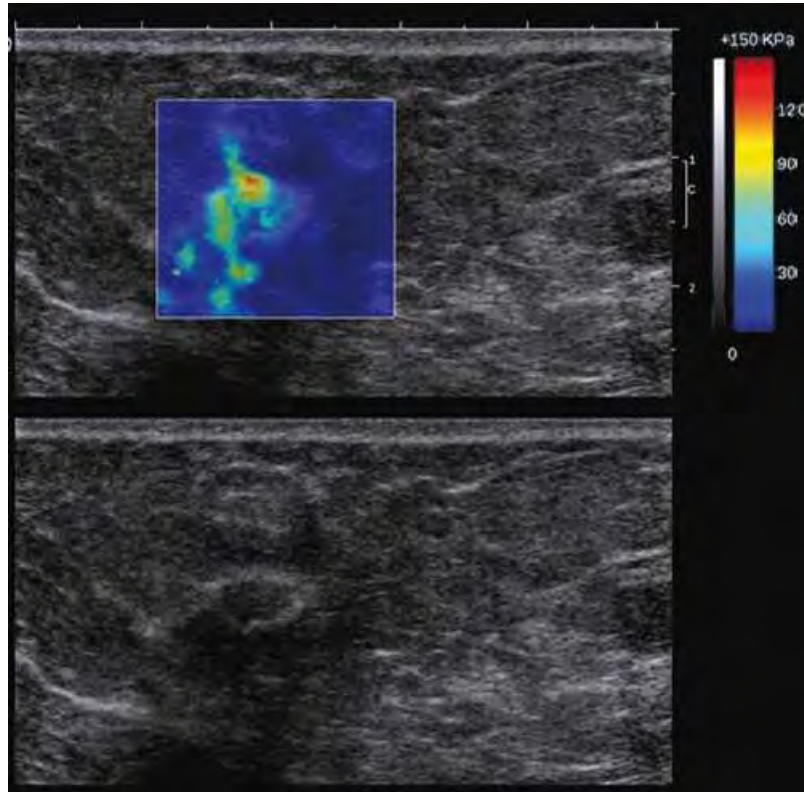


Elastizitätsverteilung als Funktion der Pathologie

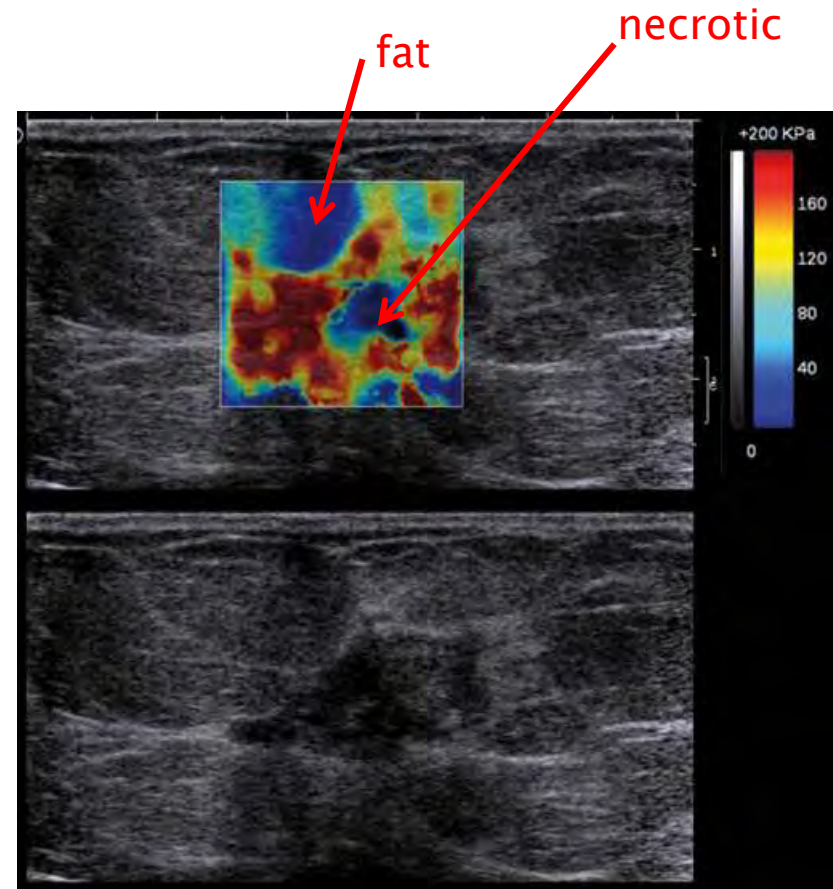
Study with 38 female Patients

$E_{\square} = >250 \text{ kPa}$
Invasive ductale carcinoma

Clinical relevance: examples

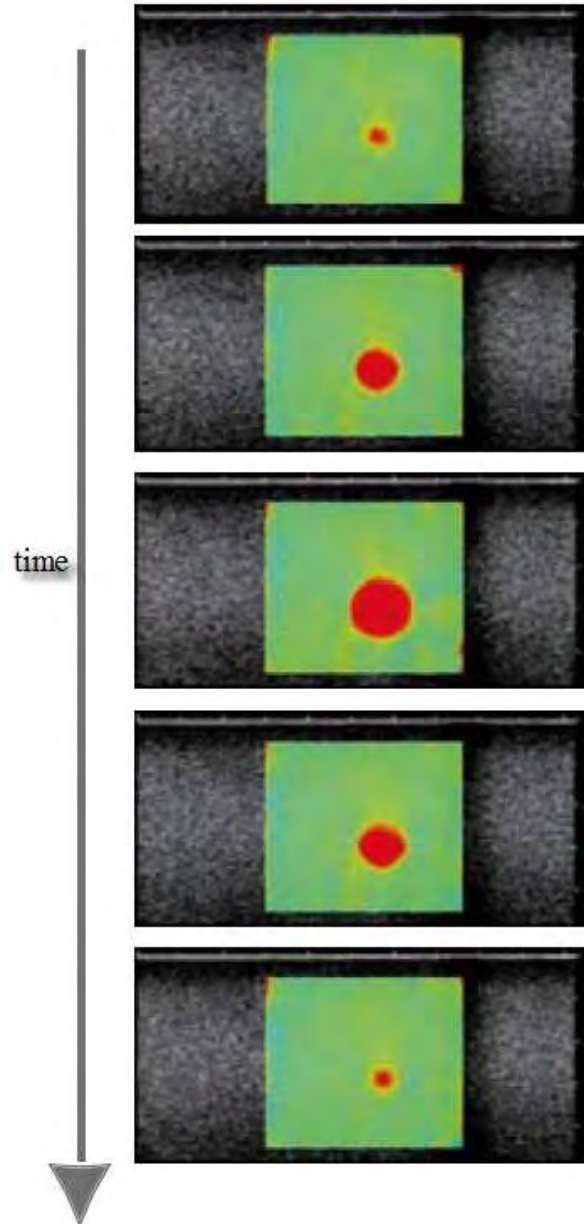


Very small lesion < 1mm



Difficult pattern of a lesion

Tissue Characterisation by Elastograms



Lateral resolution example:
spherical phantom

Several cross section picture
in the 3rd dimension
with a
stiff lesion
using a real-time SWE

Ultraschall und Theragnostik

Ultraschall in Thera(pie) und (Dia)gnostik

Kapitel 11

Dosierung und Sicherheitsaspekte

Inhaltsangabe

1. Übersicht der Ultraschallanwendungen
2. Physikalische Grundlagen
3. Ultraschallsonden
4. Bildgebende Verfahren in der Diagnostik
5. Dopplerverfahren in der Diagnostik und Therapie
6. Artefakte und Diagnostik
7. Ultraschall und Kontrastmittel
8. Theragnostik mit Ultraschall
9. Therapie mit hochdosierten Ultraschall
10. Gewebecharakterisierung mittels shear waves
11. **Dosierung und Sicherheitsaspekte**

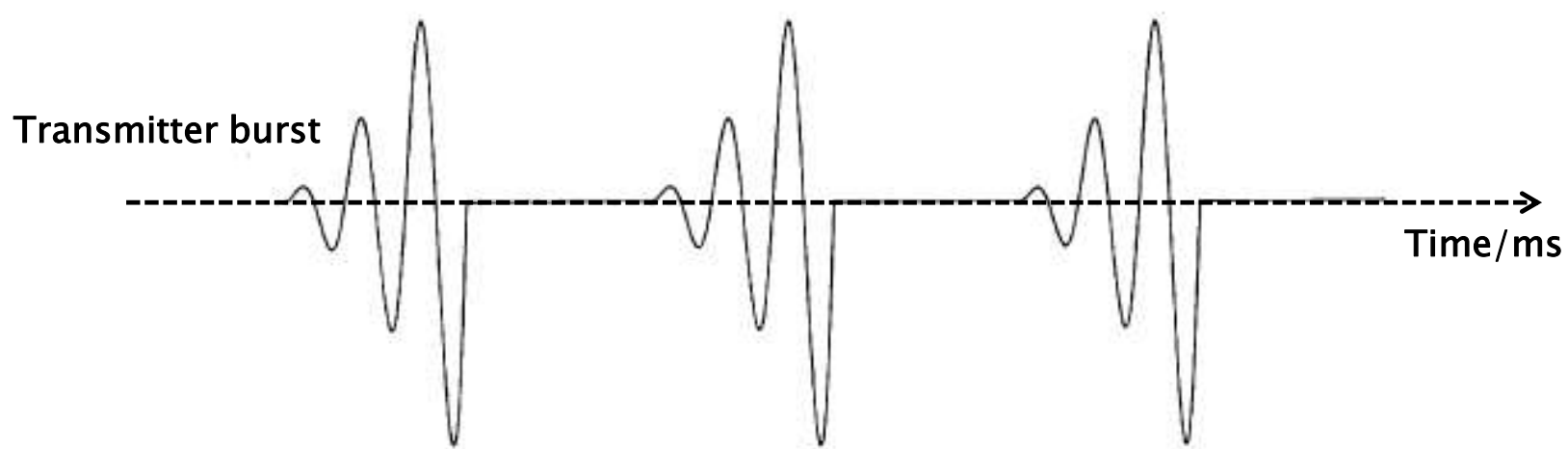
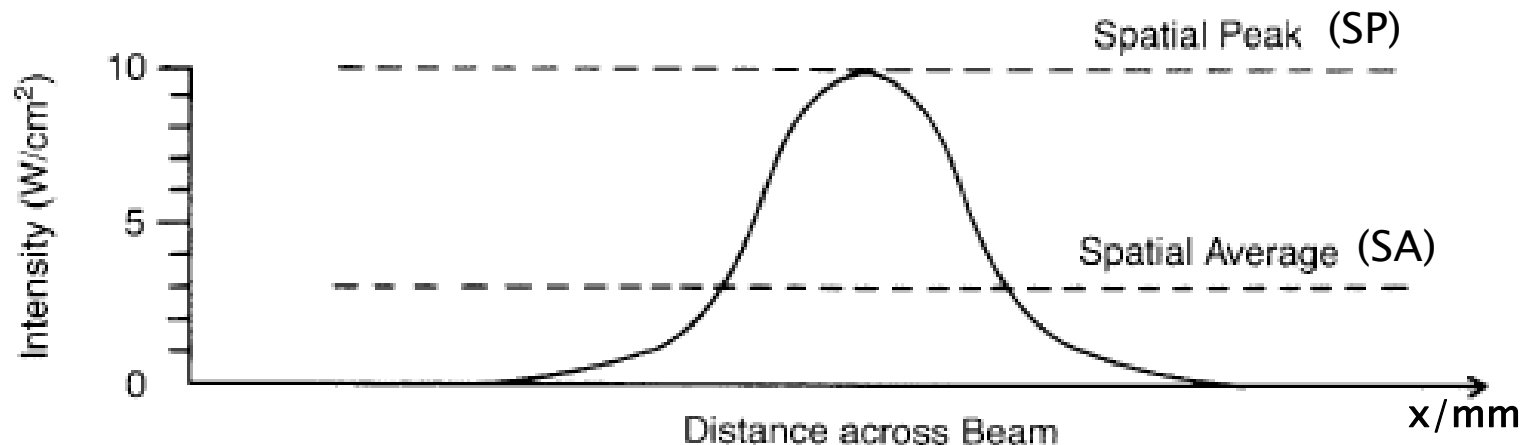
Keywords

Performance measurements and quality checks of ultrasound dosis:

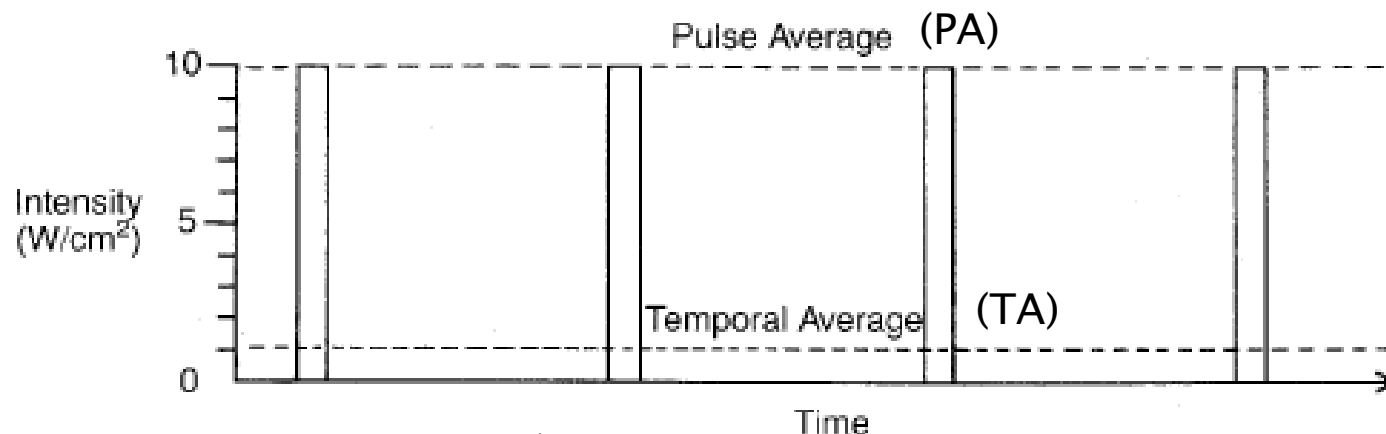
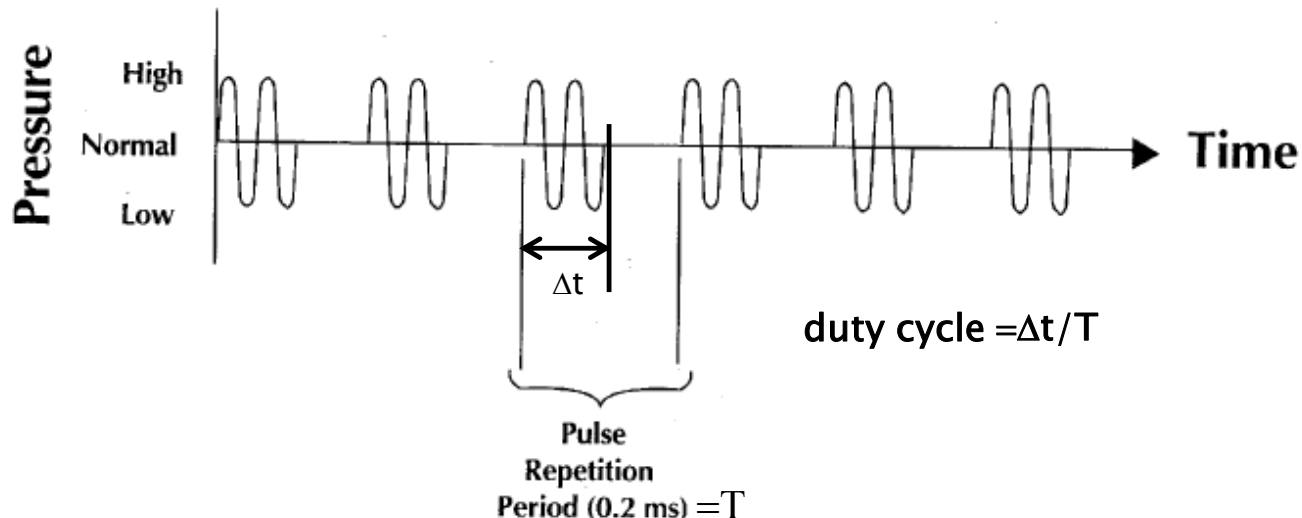
- Signal output (pulse shape and repetition e.g.)
- Performance measurements via phantoms
- Bioeffects, recommendations, limits, modelling and certification
- Measurement of power output
 - Force balance (total power)
 - Waterbath xyz-Scan (beam characteristics)
- Safety and prudence usage → minimized risk
- Regulatory activities

Performance, dosis, safety aspects

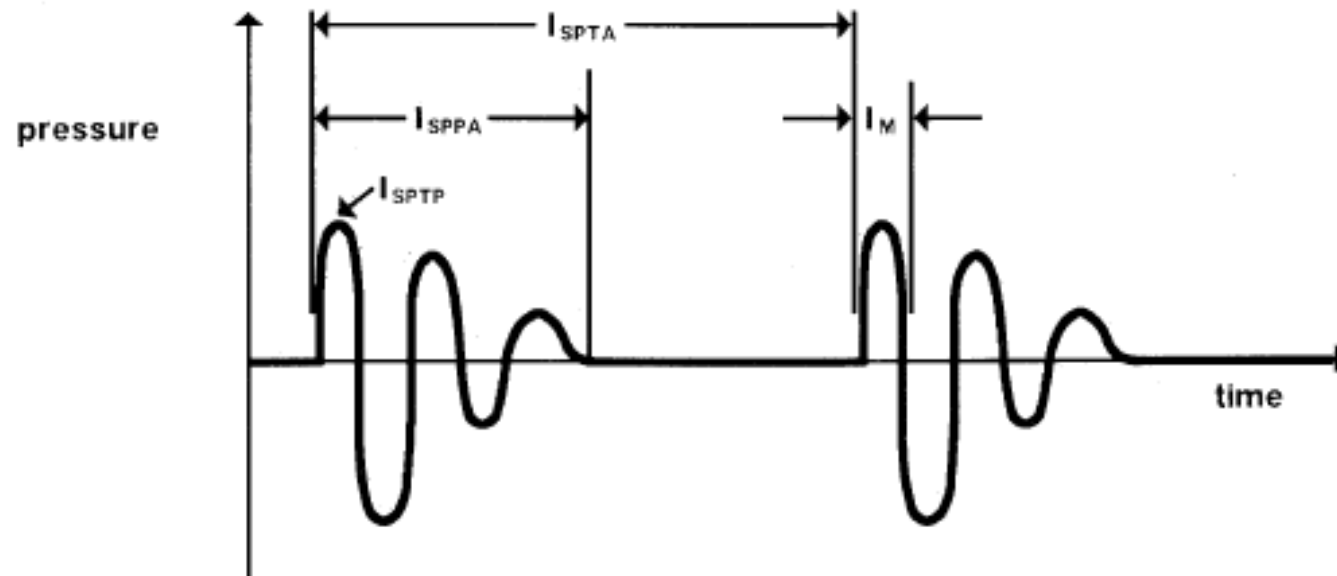
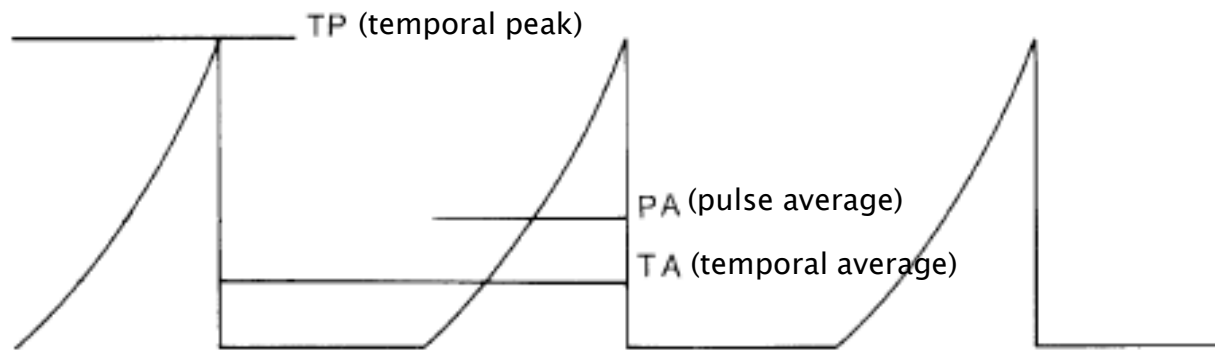
Power output signals



Power output signals

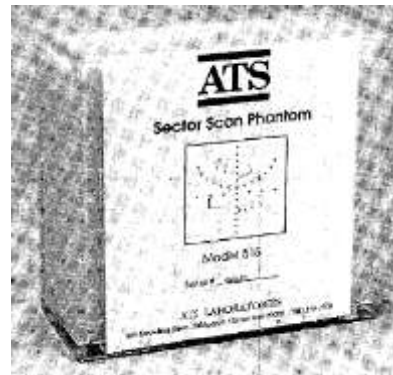
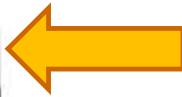
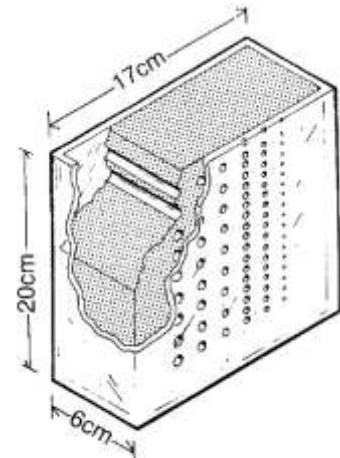


Power output signals

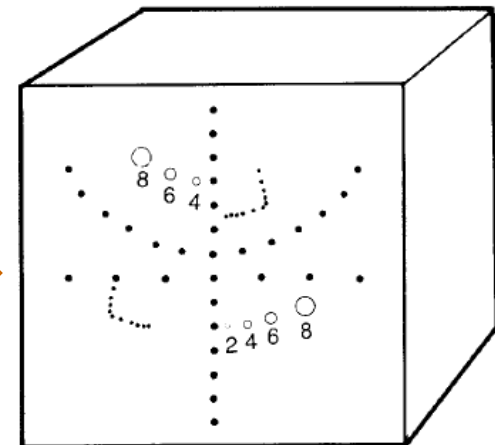


Performance, dosis, safety aspects

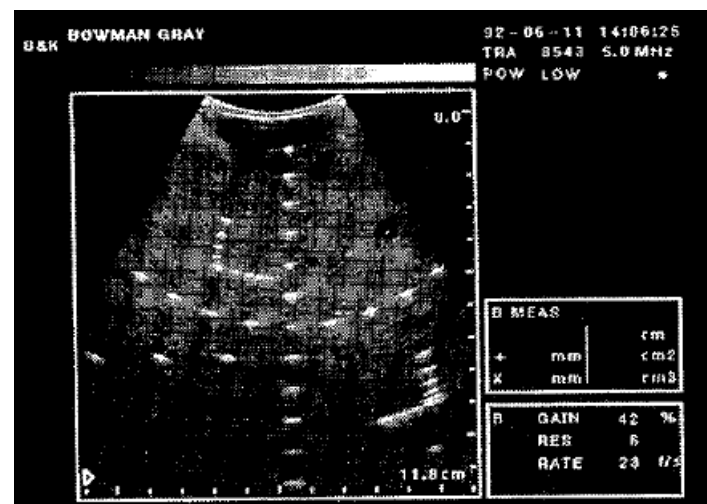
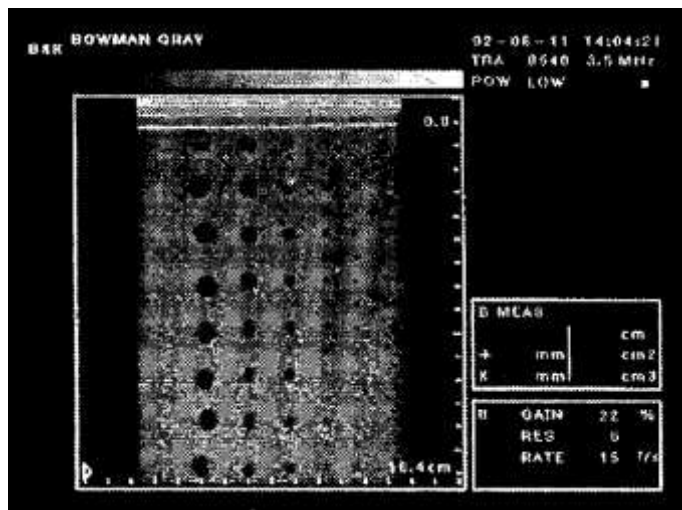
Performance measurements via Phantoms (tissue, B-Mode)



Sector Scan Phantom



Model 504 & 534

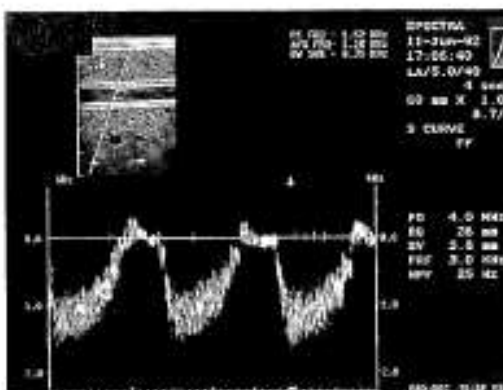


Performance, dosis, safety aspects

Performance measurements via Doppler phantoms (tube)



3



b

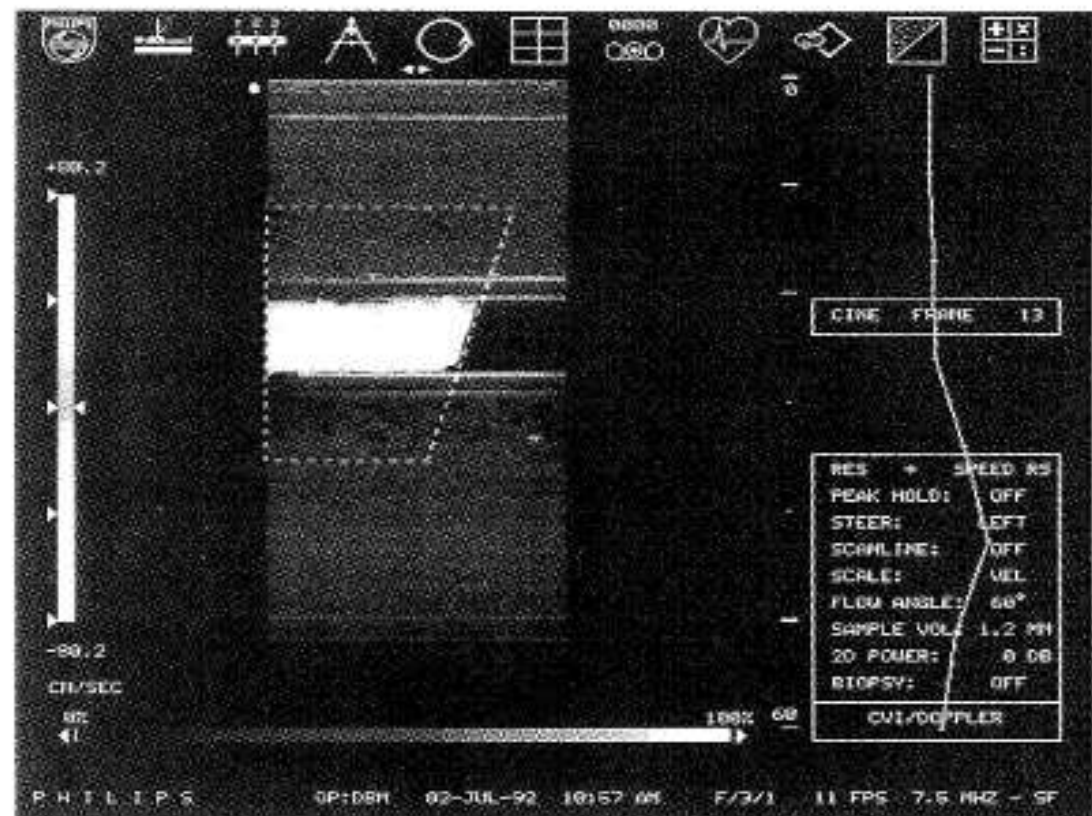
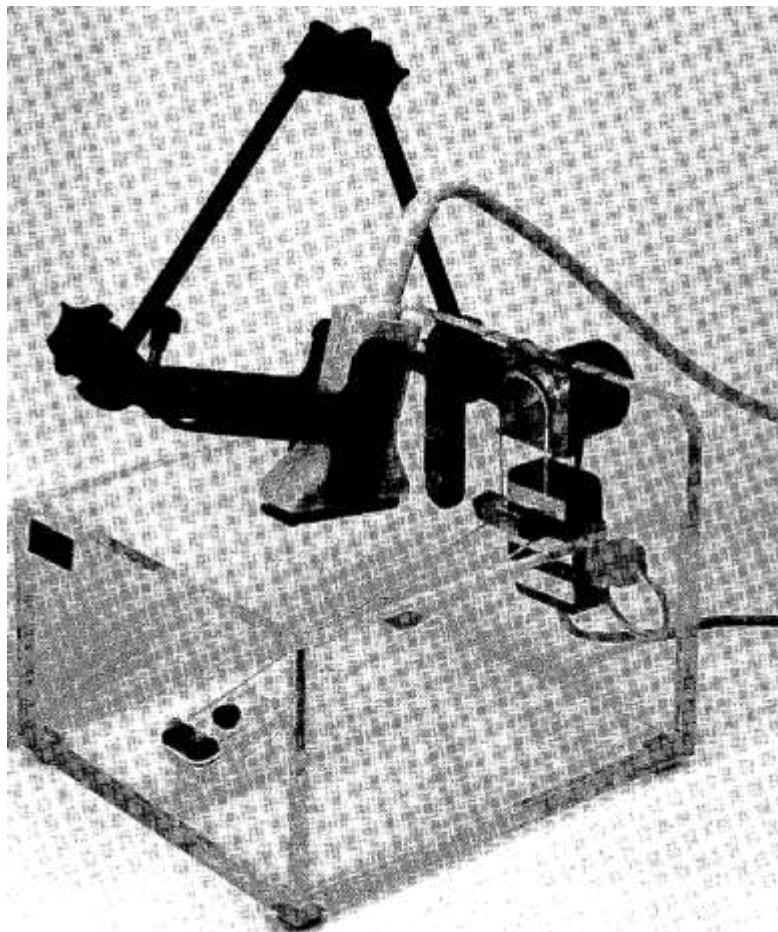


Figure (a) Doppler flow phantom (RMI Model 425). (b) Spectral display from flow phantom. (c) Color-flow image from flow phantom.

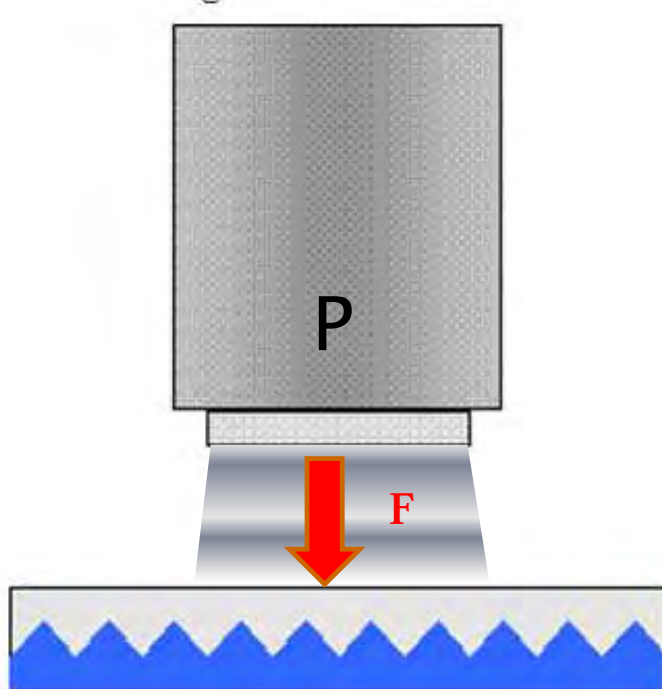
Performance measurements via Doppler phantoms (strings)



A motorized string with nodes (targets) is moving in the ultrasound beam (installed in a waterbath and multirelections can be expected)

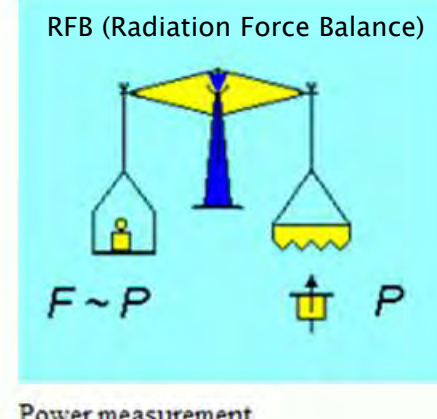
Power output via radiation force balance (IEC 61161)

Power output P causes micro streaming \rightarrow force $F = (2) \cdot c \cdot P$



$$F = \frac{P}{c} = \frac{5\text{W}}{1482\text{ms}^{-1}} \approx 3.4\text{mN}$$

$$m = \frac{F}{a} = \frac{34\text{mN}}{9.812\text{ms}^{-2}} \approx 0.34\text{g}$$



Acoustic Power	Change in mass
----------------	----------------

1 mW	68 µg
------	-------

50 mW	3.4 mg
-------	--------

250 mW	17.2 mg
--------	---------

2 W	0.14 g
-----	--------

10 W	0.68 g
------	--------

Performance, dosis, safety aspects

Power output via radiation force balance

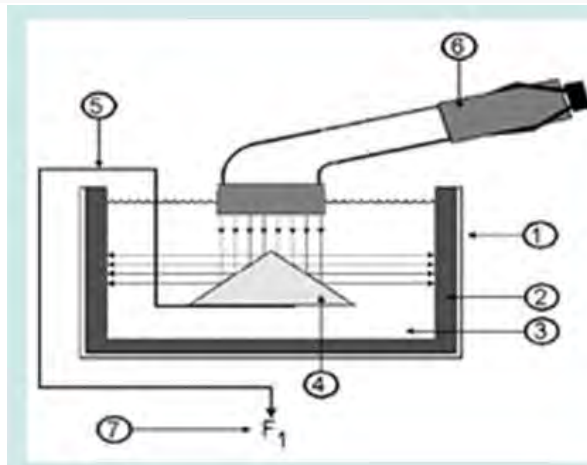


Figure 1.

RFB Construction Details

- 1) test tank
- 2) sonic sound absorber
- 3) test media: degassed water
- 4) sonic target
- 5) coupling target to scale
- 6) transducer under test (TUT) positioning and support
- 7) scale to measure force exerted on target

ULTRASOUND POWER METER MODEL UPM-DT-1AV & UPM-DT-10AV
TIME PROVEN WATTMETERS FOR DIAGNOSTIC & THERAPEUTIC APPLICATIONS

 Approved Electronics

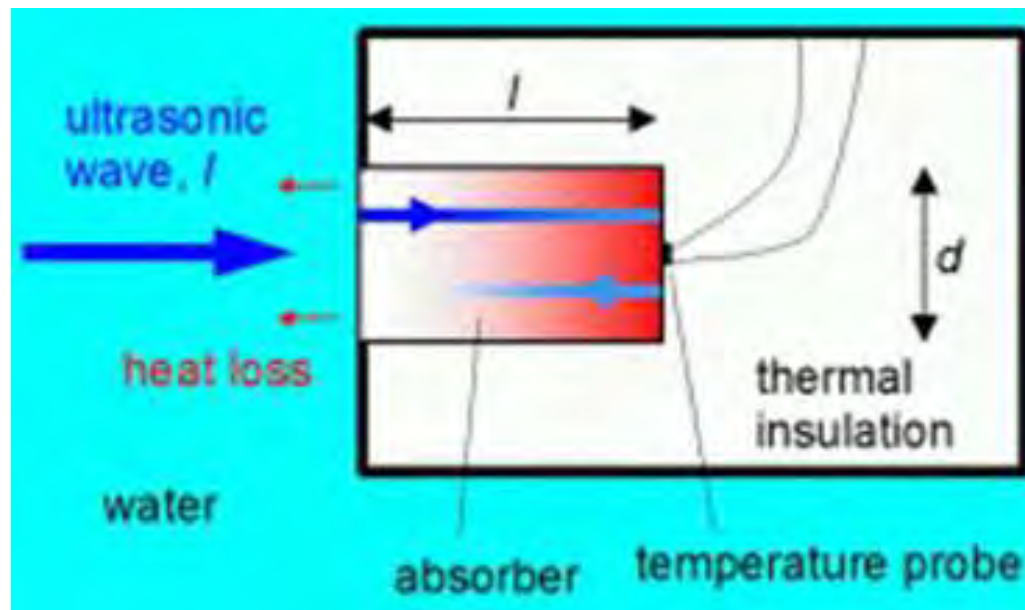
- FIVE POINT CERTIFICATION (NIST TRACEABLE)
- HIGH RESOLUTION: 2 OR 20mW (1.5 or 15 mW in grams mode)
- MEASUREMENT RANGE: 0-30 WATTS
- FREQUENCY RANGE: .5 TO 10MHZ
- MEASURES TOTAL PULSED OR CONTINUOUS POWER
- AUTOMATIC ZEROING & STABILIZATION
- DIGITAL DISPLAY & RS-232 INTERFACE
- EQUIPPED WITH CARRYING CASE



[IEC 61157](#) (diagnostic instruments)

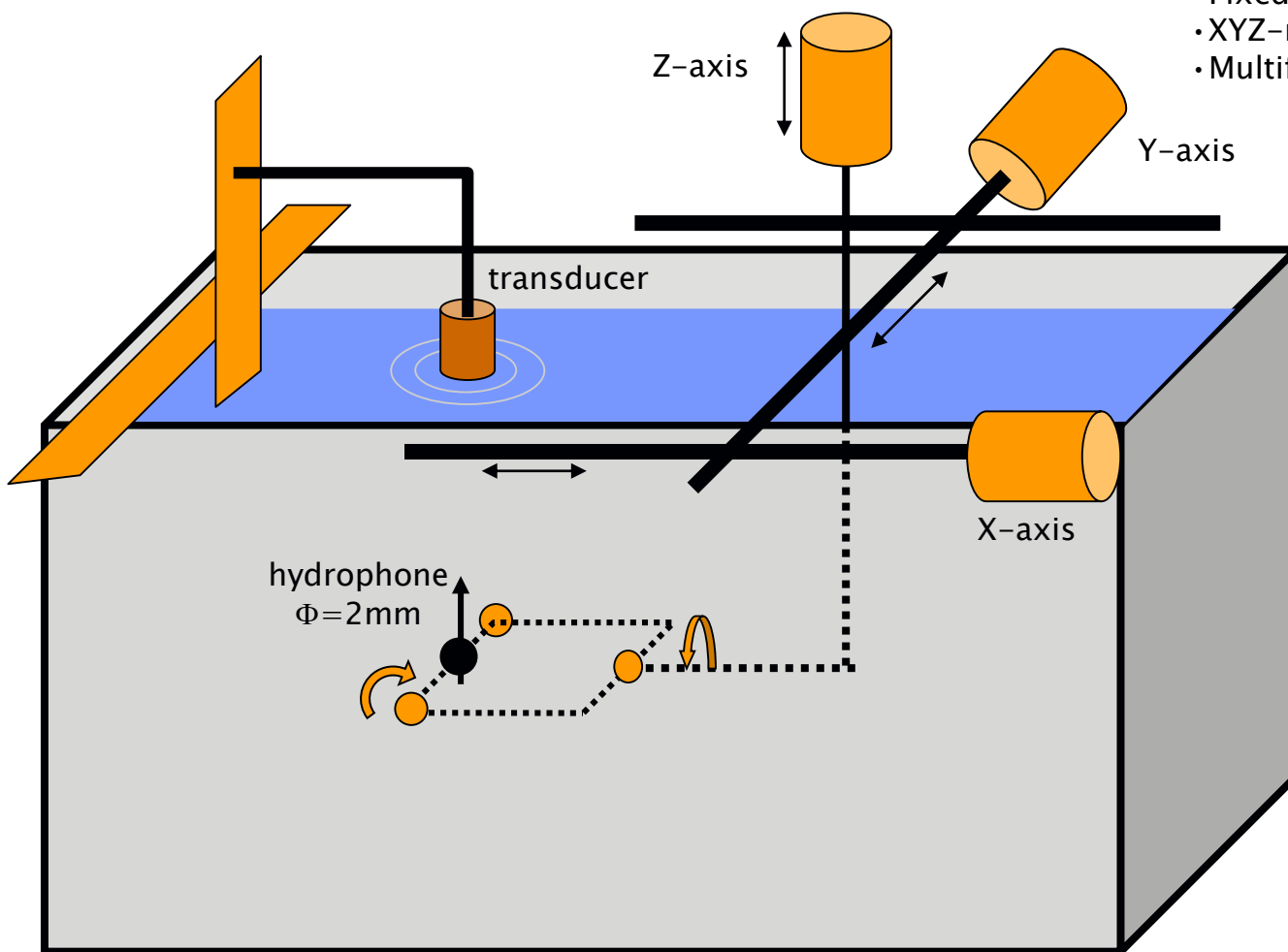
[IEC 61689](#) (therapeutic instruments).

Power output via thermal effect (IEC 61157)



Spatial-peak temporal-averaged output intensities of ultrasound machines

Power output characteristics via xyz-motor controlled hydrophone



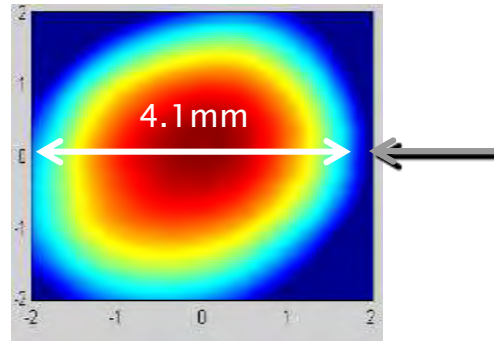
Legend: Scanning system

- Fixed transducer and bone-sample
- XYZ-movement of the hydrophone
- Multifrequency probe 2/2.5MHz

Power output characteristics via xyz-motor controlled hydrophone

Legend: XY-scan 2MHz + bone in the focal area

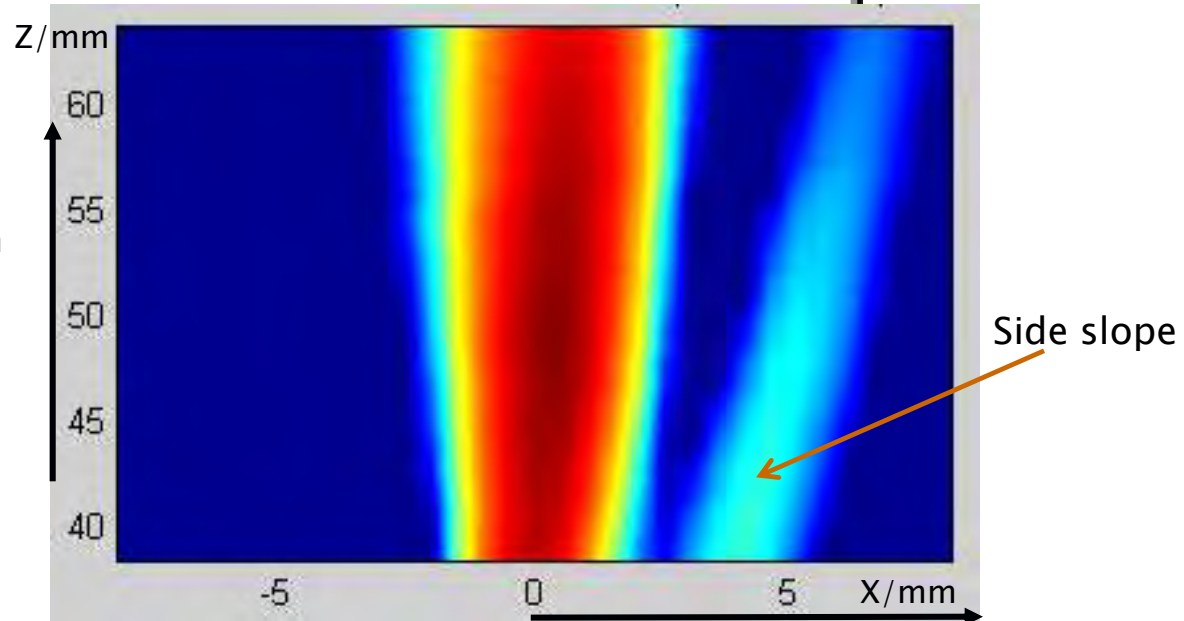
- Ranges $\Delta X = \pm 2\text{mm}$; $\Delta Y = \pm 2\text{mm}$
- Stepping $50\mu\text{m}$
- Colour scale 0...-6dB
- 6dB-limits = 4,1mm



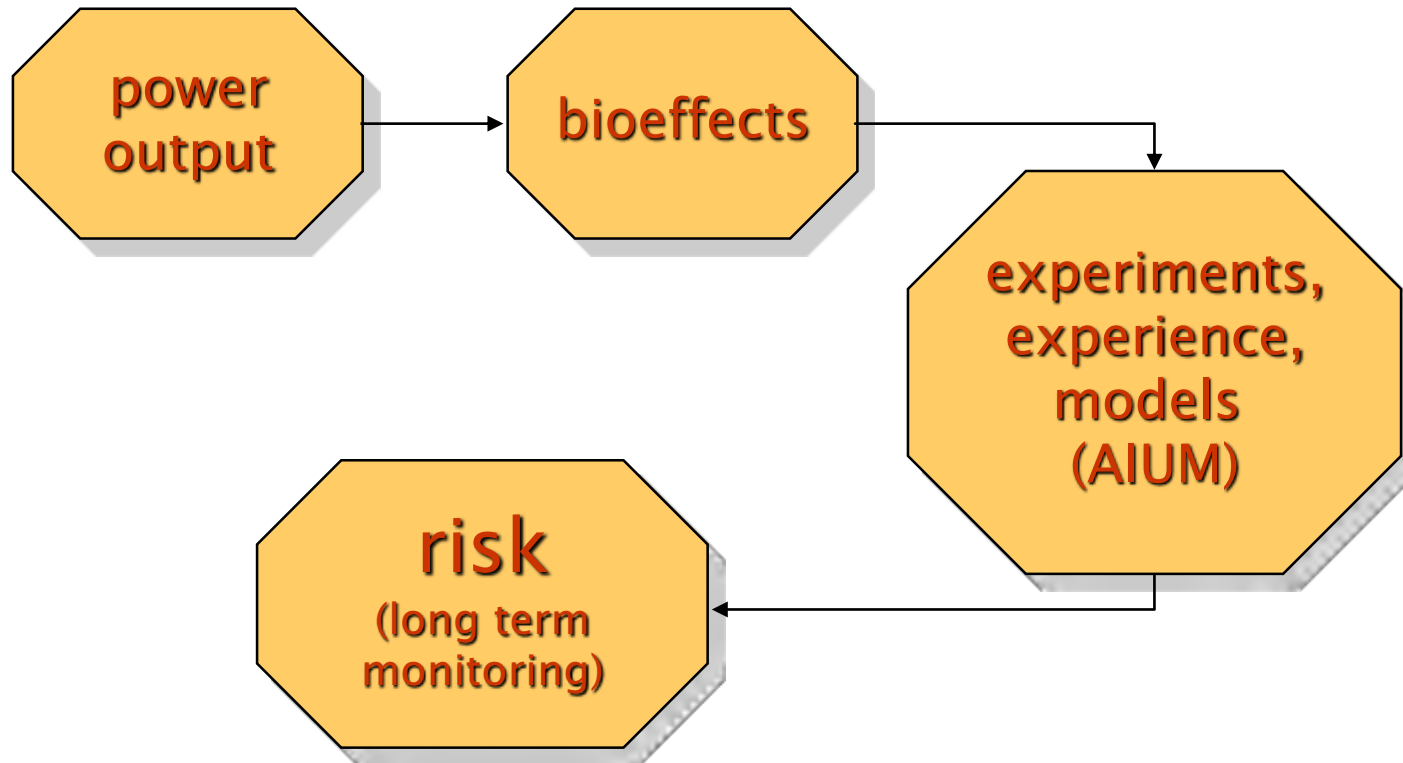
Legend: XZ-scan 2MHz + bone

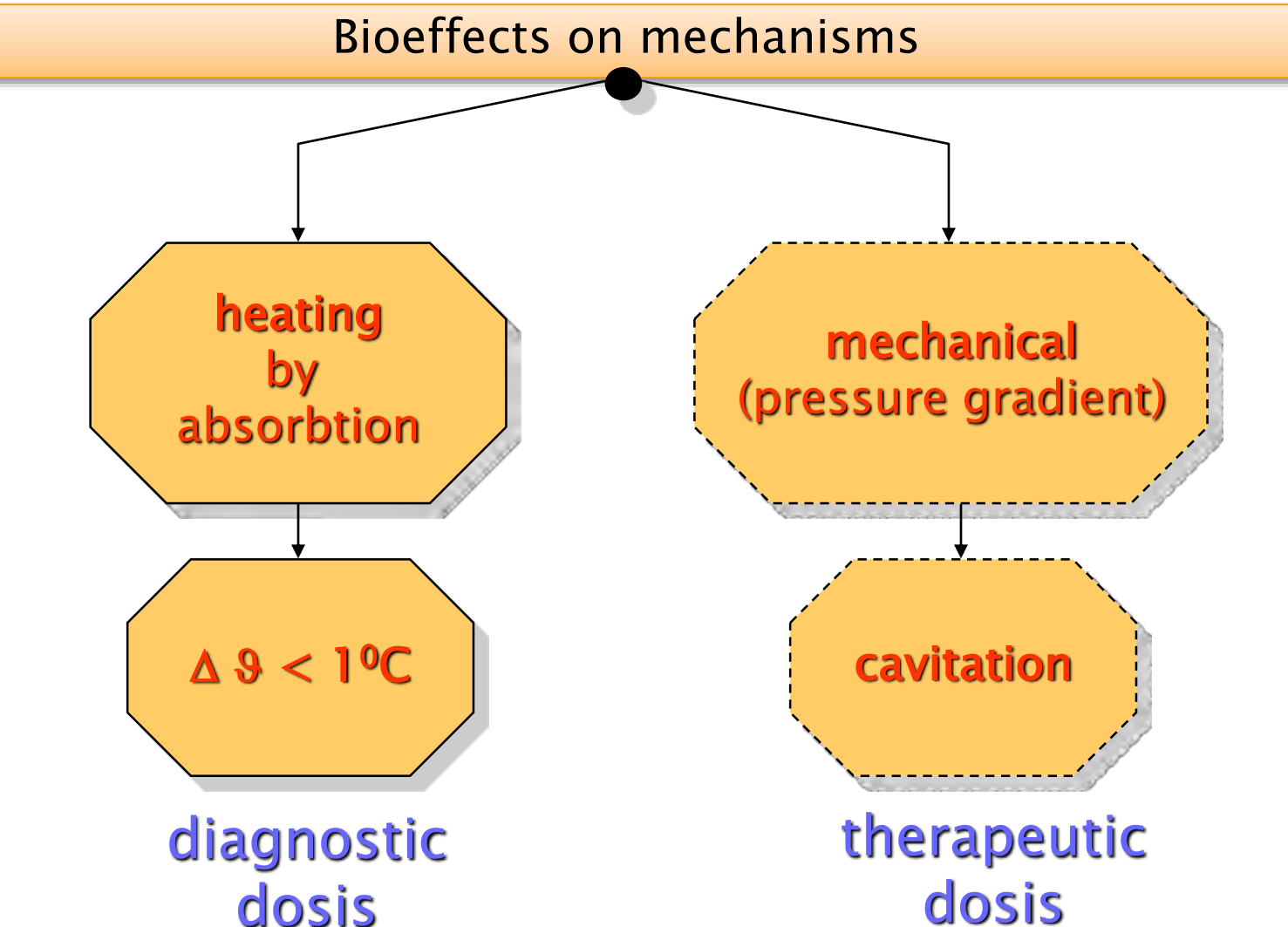
- Ranges $\Delta X = \pm 8\text{mm}$; $\Delta Z = 27\text{mm}$
- Stepping 0.1mm
- Color-scale 0...-6dB

side slope asymmetry →
due to temporal bone mimicking



Power output safety considerations

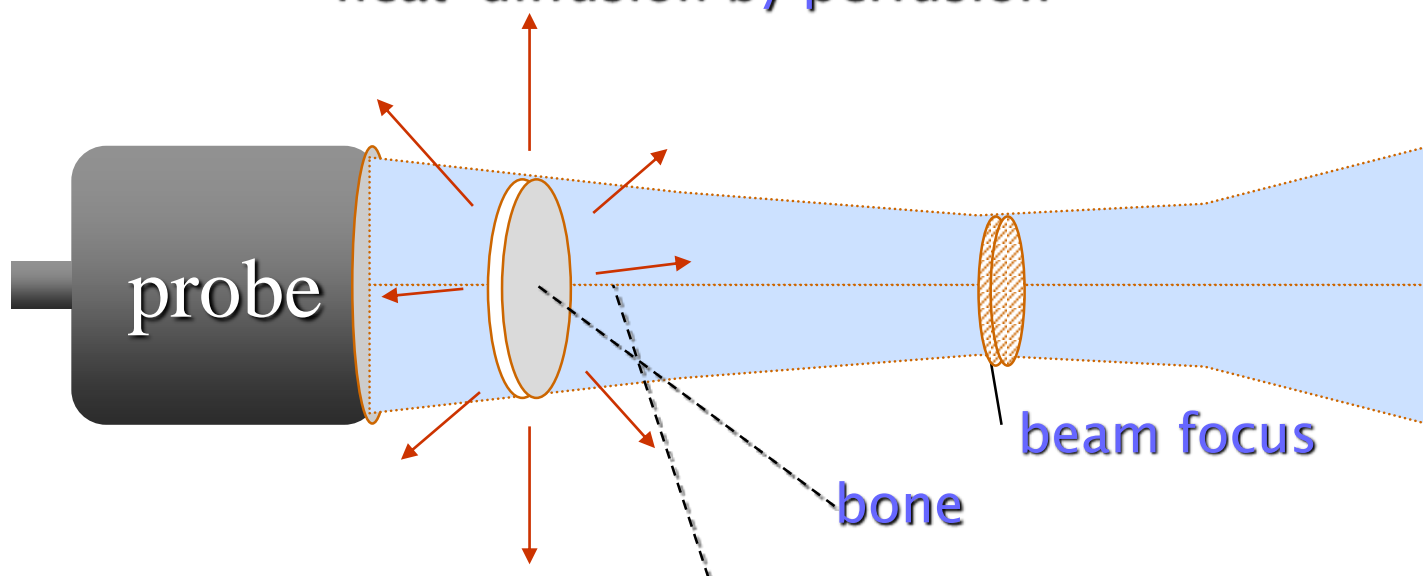




Modelling

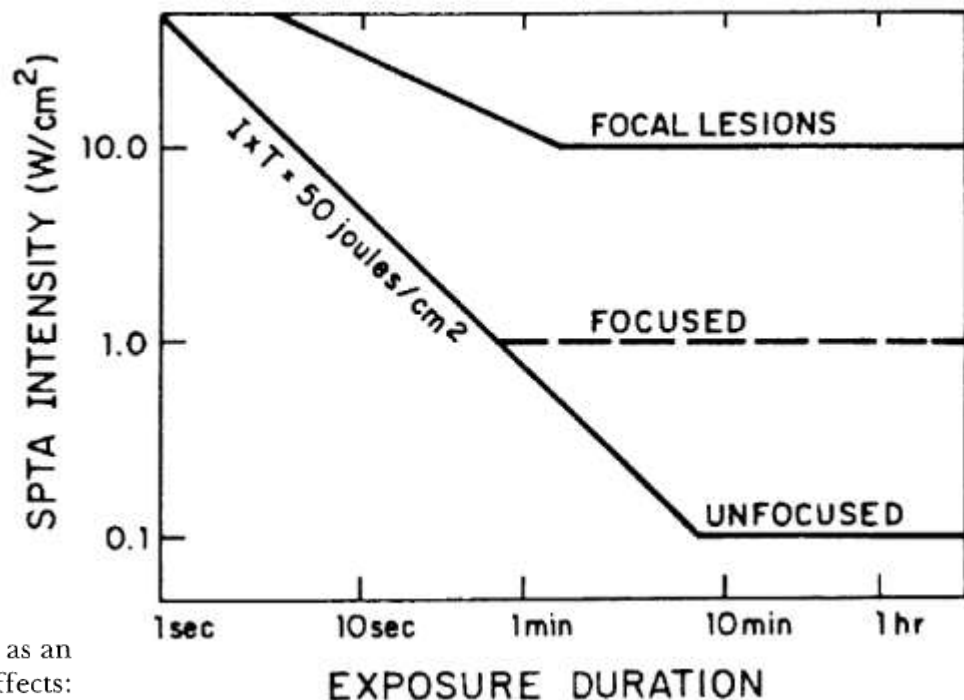
Heat-transfer model (worst case)

heat-diffusion by perfusion



heat generated by power output
 $TIC \leq 1 \leftarrow$ tissue heating $\leq 1^{\circ}C$

Recommendations



A review of bioeffects data supports the following statement as an update of the AIUM Statement on *In Vivo* Mammalian Bioeffects: In the low megahertz frequency range there have been (as of this date) no independently confirmed significant biological effects in mammalian tissues exposed *in vivo* to unfocused ultrasound with intensities* below 100 mW/cm, or to focused† ultrasound with intensities below 1 W/cm. Furthermore, for exposure times‡ greater than 1 second and less than 500 seconds (for unfocused ultrasound) or 50 seconds (for focused ultrasound), such effects have not been demonstrated even at higher intensities, when the product of intensity and exposure time is less than 50 joules/cm.

* Free-field spatial peak, temporal average (SPTA) for continuous-wave exposures and for pulsed-mode exposures with pulses repeated at a frequency greater than 100 Hz.

† Quarter-power (-6 dB) beam width smaller than four wavelengths or 4 mm, whichever is less at the exposure frequency.

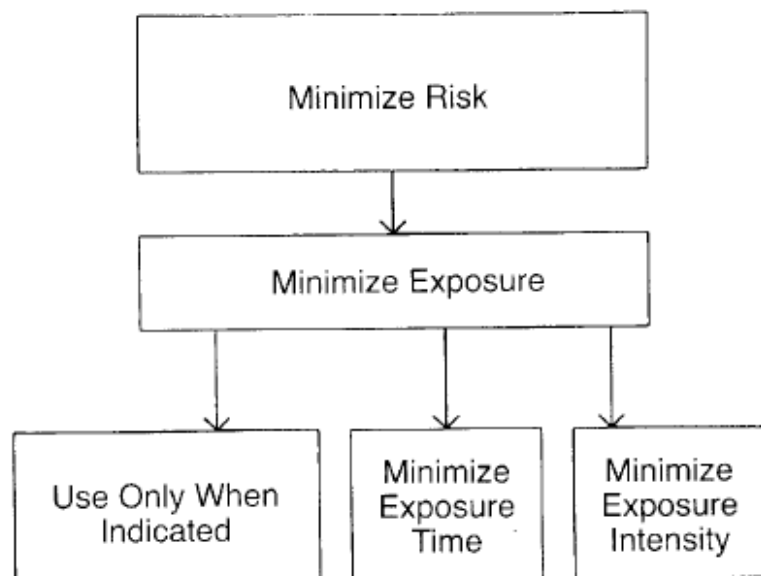
‡ Total time includes off-time as well as on-time for repeated pulse exposures.

Recommendations

Upper Limits of Attenuated* Spatial Peak–Temporal Average (SPTA) Output Intensities from Table 7.1

Type of Instrument	SPTA Output Intensity (mW/cm ²)
All instruments	500
Imaging instruments	136
Scanning	88
Stopped	136
Doppler instruments	500
Continuous wave	500
Pulsed	389

* 7 dB, to account for human tissue path



Minimization of power output → low risk:

- Minimum of PRF (velocity scale)
- Minimum of sample volume (pulse length)
- Focusing with about 6mm focus diameter
- Total power output (service by force balance)
- Display with Thermal Indicator Cranial (TIC≤1) according AIUM and FDA

Recommendations → Display of power output by indices
(based on Ultrasound Energy Absorbtion with heating)

Thermal Index (cranial) = TI(C)

$$TI = \frac{W_o}{W_{deg}}$$

where W_o is the total acoustic power (mW) arriving at the target tissue, and W_{deg} is the acoustic power necessary to raise the target tissue temperature by $1^{\circ}C$.

$$TIC = \frac{W_o}{40\sqrt{\frac{4A_{aprt}}{\pi}}}$$

where A_{aprt} (cm^2) is the active aperture at the beam entrance. In the computation it is used the following values: $W_o = 200$ mW (measured near the probe surface), and $A_{aprt} = 0.7^2\pi cm^2$. Consequently, the TIC was $3.57^{\circ}C$.

Recommendations → Display of power output by indices
(based on Ultrasound Energy Absorbtion with heating)

Thermal Index Soft Tissue = TIS

$$TIS = \frac{\left\{ [W'(z), I'(z) \times 1 \text{ cm}^2]_{\min} \right\}_{\max}}{\frac{210}{f}}$$

where z is the distance from the transducer, I' is the derated intensity over a designated area ($I' \times 1 \text{ cm}^2$), W' is the derated power evaluated along the beam axis, and f is the frequency (MHz).

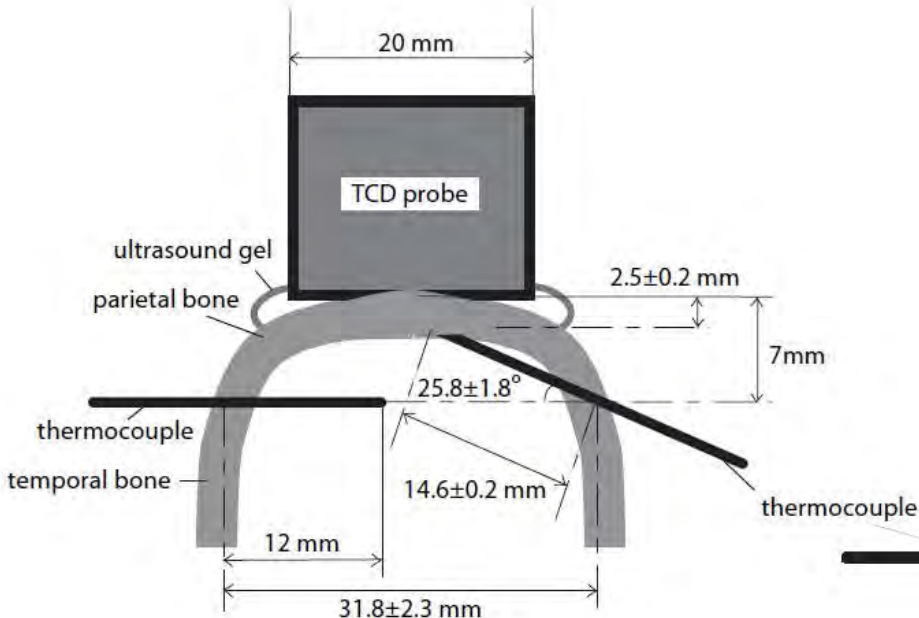
I' and W' are given by equations

$$I' = I \times 10^{-0.1f(ap + bq)}$$

where I is the time-averaged intensity measured in water (mW/cm^2), $10^{-0.1f(ap + bq)}$ is the derating factor, a is the attenuation coefficient of the skull (dB/cm/MHz), b is the attenuation coefficient of brain tissue (dB/cm/MHz), p is the distance along the beam axis from the transducer to the SBI (cm), q is the distance along the beam axis from the SBI to the CBT (cm).

Performance, dosis, safety aspects

Temperature increase during cranial insonification (experiments with New Zealand Rabbits)



Transducer:

$$P = 200\text{mW}; A_{\text{eff}} \rightarrow d = 14\text{mm}$$

$$\rightarrow W_0 = P/A_{\text{eff}} = 27\text{mW/cm}^2$$

CBTT
SBIT
ROT
RET

= Central Brain Tissue Temperature
= Skull Brain Interface Temperature
= Toom Temperature
= Rectal temperature

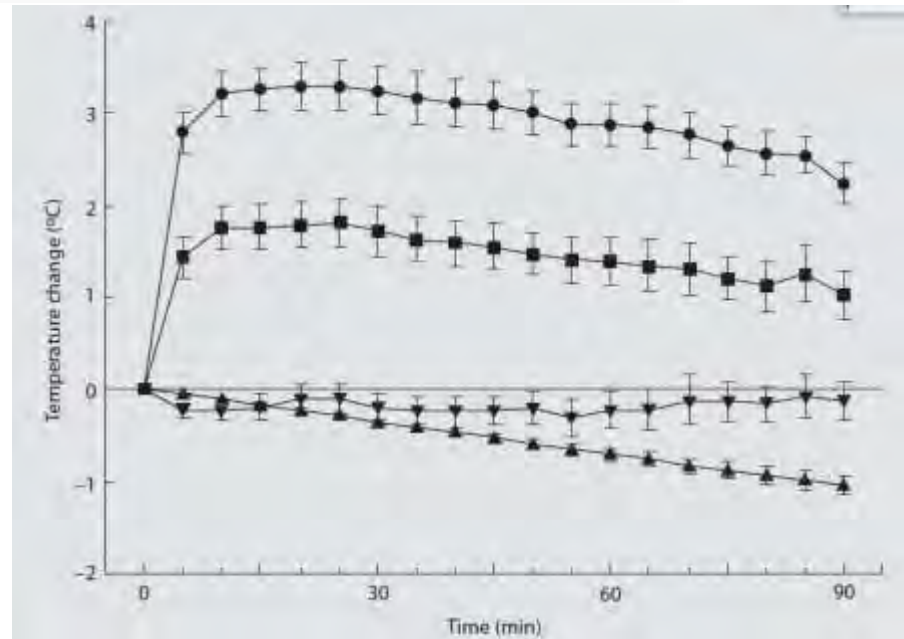


Fig. Temperature rise in the TCD application group during 90 min (experiment 2). TCD long-term irradiation increased SBIT, where the change value rose rapidly to $3.30 \pm 0.25^\circ\text{C}$ in 20 min and reached a plateau. CBTT showed a similar pattern: $1.80 \pm 0.26^\circ\text{C}$ in 25 min with a rise and a plateau. These temperature rises were significantly large in comparison with that of the control group ($p < 0.001$). ● = SBIT; ■ = CBTT; ▲ = RET; ▼ = ROT; error bar = SEM.

Ultraschall und Theragnostik

Ultraschall in Thera(pie) und (Dia)gnostik

Fragen

Inhaltsangabe: Fragen.....

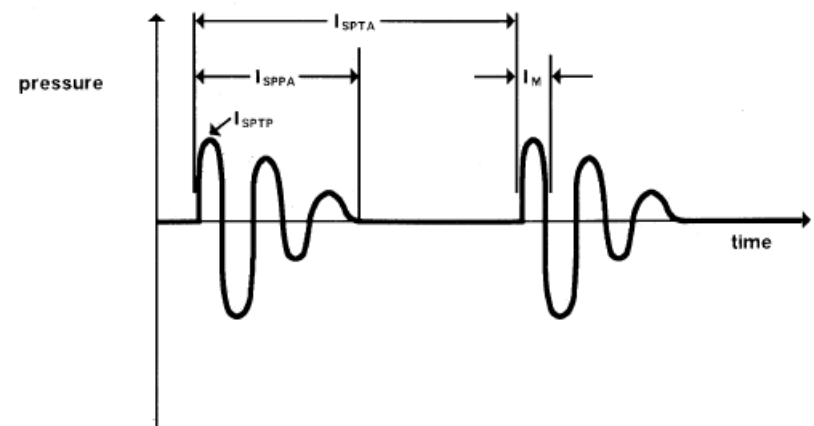
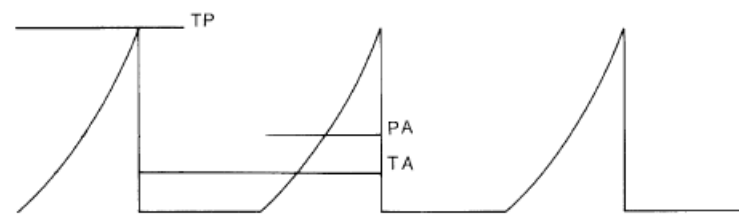
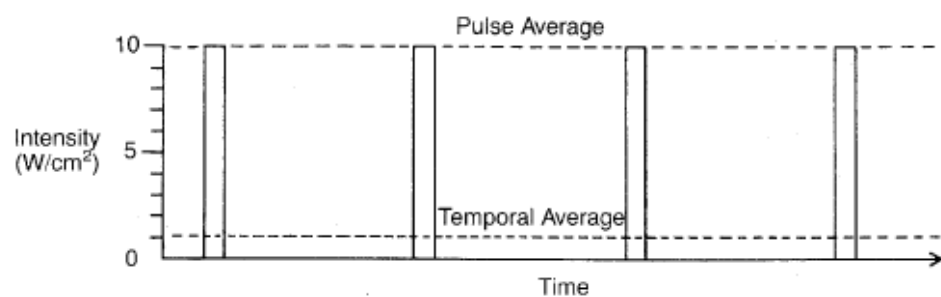
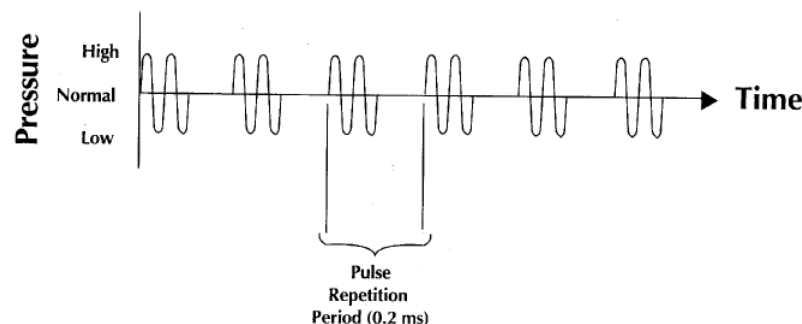
1. Übersicht der Ultraschallanwendungen
2. Physikalische Grundlagen
3. Ultraschallsonden
4. Bildgebende Verfahren in der Diagnostik
5. Dopplerverfahren in der Diagnostik und Therapie
6. Artefakte und Diagnostik
7. Ultraschall und Kontrastmittel
8. Theragnostik mit Ultraschall
9. Therapie mit hochdosierten Ultraschall
10. Gewebecharakterisierung mittels shear waves
11. Dosierung und Sicherheitsaspekte



Symbols

a	attenuation	NZL	near-zone length
a_c	attenuation coefficient	P	power, penetration
A	area	PD	pulse duration
A_B	beam area	PRF	pulse repetition frequency
BW	bandwidth	PRP	pulse repetition period
c	sound propagation speed	Q	quality factor
c_m	transducer element material propagation speed	R	resistance
d	distance to reflector	R_A	axial resolution
D_B	beam diameter	R_L	lateral resolution
D_T	transducer diameter	SPL	spatial pulse length
DF	duty factor	t	time, pulse round-trip time
f	frequency	T	period
f_D	Doppler shift	v	reflector speed
f_o	operating frequency	w	transducer thickness
f_e	echo frequency	z	impedance
FR	frame rate	λ	wavelength
I	intensity, current	ρ	density
I_i	incident intensity	θ	Doppler angle
I_r	reflected intensity	θ_i	incidence angle
I_{SA}	spatial average intensity	θ_r	reflection angle
I_{SP}	spatial peak intensity	θ_t	transmission angle
I_{TA}	temporal average intensity		
I_{PA}	pulse average intensity		
IRC	intensity reflection coefficient		
ITC	intensity transmission coefficient		
L	path length		
LPF	lines per frame		
n	number of cycles in a pulse		
NF	number of focuses		

Signals





Equations: Signals and attenuation

$$\text{distance to reflector (mm)} = \frac{1}{2}[\text{propagation speed (mm/}\mu\text{s)} \times \text{pulse round-trip time (}\mu\text{s)}] \quad d = \frac{1}{2} ct$$

$$\text{distance to reflector (mm)} \stackrel{*}{=} 0.77 \times \text{pulse round-trip time (}\mu\text{s)} \quad d \stackrel{*}{=} 0.77t$$

$$\text{period (}\mu\text{s)} = \frac{1}{\text{frequency (MHz)}} \quad T = \frac{1}{f}$$

$$\text{wavelength (mm)} = \frac{\text{propagation speed (mm/}\mu\text{s)}}{\text{frequency (MHz)}} \quad \lambda = \frac{c}{f}$$

$$\text{wavelength (mm)} \stackrel{*}{=} \frac{1.54}{\text{frequency (MHz)}} \quad \lambda \stackrel{*}{=} \frac{1.54}{f}$$

$$\text{impedance (rayl)} = \frac{\text{density}}{(\text{kg/m}^3)} \times \frac{\text{propagation speed (m/s)}}{} \quad z = \rho c$$

$$\text{pulse repetition period (ms)} = \frac{1}{\text{pulse repetition frequency (kHz)}} \quad \text{PRP} = \frac{1}{\text{PRF}}$$

$$\text{pulse duration (}\mu\text{s)} = \frac{\text{number of cycles in the pulse}}{} \times \text{period (}\mu\text{s)} \quad \text{PD} = nT$$

$$\text{pulse duration (}\mu\text{s)} = \frac{\text{number of cycles in the pulse}}{\text{frequency (MHz)}} \quad \text{PD} = \frac{n}{f}$$

$$\text{duty factor} = \frac{\text{pulse duration (}\mu\text{s)}}{\text{pulse repetition period (ms)} \times 1000} \quad \text{DF} = \frac{\text{PD}}{\text{PRP} \times 1000}$$

$$\text{duty factor} = \frac{\text{pulse duration (}\mu\text{s)} \times \text{pulse repetition frequency (kHz)}}{1000} \quad \text{DF} = \frac{\text{PD} \times \text{PRF}}{1000}$$

$$\text{spatial pulse length (mm)} = \frac{\text{number of cycles in the pulse}}{\times \text{wavelength (mm)}} \quad \text{SPL} = n\lambda$$

$$\text{spatial pulse length (mm)} = \frac{\text{number of cycles in the pulse}}{\times \text{propagation speed (mm/}\mu\text{s)}} \quad \text{SPL} = \frac{nc}{f}$$

$$\text{spatial pulse length (mm)} \stackrel{*}{=} \frac{\text{number of cycles in the pulse}}{\times \text{frequency (MHz)}} \quad \text{SPL} \stackrel{*}{=} \frac{n \times 1.54}{f}$$

$$\text{intensity (W/cm}^2) = \frac{\text{power (W)}}{\text{area (cm}^2)} \quad I = \frac{P}{A}$$

$$\text{temporal average intensity (W/cm}^2) = \frac{\text{duty factor} \times \text{pulse intensity (W/cm}^2)}{\text{average intensity (W/cm}^2)} \quad I_{TA} = DF \times I_{PA}$$

$$\text{attenuation (dB)} = \frac{\text{attenuation coefficient (dB/cm)}}{\times \text{path length (cm)}} \quad a = a_c l$$

$$\text{attenuation (dB)} \stackrel{*}{=} \frac{1}{2} \times \frac{\text{frequency (MHz)}}{\text{path length (cm)}} \quad a \stackrel{*}{=} \frac{1}{2} f L$$

$$\text{intensity reflection coefficient} = \frac{\text{reflected intensity (W/cm}^2)}{\text{incident intensity (W/cm}^2)} \quad \text{IRC} = \frac{I_r}{I_i}$$

$$\stackrel{**}{=} \left[\frac{\text{medium two impedance} - \text{medium one impedance}}{\text{medium two impedance} + \text{medium one impedance}} \right]^2 \quad \stackrel{**}{=} \left[\frac{z_2 - z_1}{z_2 + z_1} \right]^2$$

$$\text{intensity transmission coefficient} = \frac{\text{transmitted intensity (W/cm}^2)}{\text{incident intensity (W/cm}^2)} \quad \text{ITC} = \frac{I_t}{I_i}$$

$$\stackrel{**}{=} 1 - \text{intensity reflection coefficient} \quad \stackrel{**}{=} 1 - \text{IRC}$$

Equations: Beam, imaging resolution, Doppler

$$\text{operating frequency (MHz)} = \frac{\text{element propagation speed (mm/}\mu\text{s)}}{2 \times \text{thickness (mm)}} \quad f_o = \frac{c_m}{2w}$$

$$\text{quality factor} = \frac{\text{operating frequency (MHz)}}{\text{bandwidth (MHz)}} \quad Q = \frac{f_o}{BW}$$

$$\text{near-zone length (mm)} = \frac{[\text{transducer diameter (mm)}]^2}{4 \times \text{wavelength (mm)}} \quad NZL = \frac{D_T^2}{4\lambda}$$

$$\text{near-zone length (mm)} \doteq \frac{[\text{transducer diameter (mm)}]^2 \times \text{frequency (MHz)}}{6} \quad NZL \doteq \frac{D_T^2 f}{6}$$

$$\text{beam area (cm}^2) = 0.8 \times [\text{beam diameter (cm)}]^2 \quad A_B = 0.8 D_B^2$$

$$\text{axial resolution} = \frac{\text{spatial pulse length (mm)}}{2} \quad R_A = \frac{SPL}{2}$$

$$\text{axial resolution} \doteq \frac{0.77 \times \text{number of cycles in the pulse}}{\text{frequency (MHz)}} \quad R_A \doteq \frac{0.77n}{f}$$

$$\text{lateral resolution (mm)} = \text{beam diameter (mm)} \quad R_L = D_B$$

$$\frac{\text{pulse repetition frequency (Hz)}}{\text{per frame} \times \text{frame rate}} = \frac{\text{number of focuses} \times \text{lines}}{\text{per frame}} \quad PRF = NF \times LPF \times FR$$

$$\text{maximum unambiguous imaging depth (cm)} = \frac{77}{\text{pulse repetition frequency (kHz)}} \quad d_m = \frac{77}{PRF}$$

$$\frac{\text{penetration (cm)}}{\text{}} \times \frac{\text{number of focuses}}{\text{}} \times \frac{\text{lines per frame}}{\text{}} \times \frac{\text{frame rate}}{\text{}} \leq 77,000$$

$$P \times NF \times LPF \times FR \leq 77,000$$

$$\text{Doppler shift (MHz)} = \text{echo frequency (MHz)} - \text{operating frequency (MHz)}$$

$$= \frac{2 \times \text{operating frequency (MHz)} \times \text{reflector speed (m/s)} \times \cos \theta}{\text{propagation speed (m/s)}}$$

$$f_D = f_e - f_o = \frac{2 f_o v \cos \theta}{c}$$

$$\text{reflector speed} = \frac{\text{propagation speed} \times \text{Doppler shift}}{2 \times \text{operating frequency} \times \cos \theta}$$

$$v (\text{cm/s}) = \frac{77 f_D (\text{kHz})}{f_o (\text{MHz}) \cos \theta}$$

Equations: Beam, imaging resolution, Doppler

$$\text{operating frequency (MHz)} = \frac{\text{element propagation speed (mm/}\mu\text{s)}}{2 \times \text{thickness (mm)}} \quad f_o = \frac{c_m}{2w}$$

$$\text{quality factor} = \frac{\text{operating frequency (MHz)}}{\text{bandwidth (MHz)}} \quad Q = \frac{f_o}{BW}$$

$$\text{near-zone length (mm)} = \frac{[\text{transducer diameter (mm)}]^2}{4 \times \text{wavelength (mm)}} \quad NZL = \frac{D_T^2}{4\lambda}$$

$$\text{near-zone length (mm)} \doteq \frac{[\text{transducer diameter (mm)}]^2 \times \text{frequency (MHz)}}{6} \quad NZL \doteq \frac{D_T^2 f}{6}$$

$$\text{beam area (cm}^2) = 0.8 \times [\text{beam diameter (cm)}]^2 \quad A_B = 0.8 D_B^2$$

$$\text{axial resolution} = \frac{\text{spatial pulse length (mm)}}{2} \quad R_A = \frac{SPL}{2}$$

$$\text{axial resolution} \doteq \frac{0.77 \times \text{number of cycles in the pulse}}{\text{frequency (MHz)}} \quad R_A \doteq \frac{0.77n}{f}$$

$$\text{lateral resolution (mm)} = \text{beam diameter (mm)} \quad R_L = D_B$$

$$\frac{\text{pulse repetition frequency (Hz)}}{\text{per frame} \times \text{frame rate}} = \frac{\text{number of focuses} \times \text{lines}}{\text{per frame}} \quad PRF = NF \times LPF \times FR$$

$$\text{maximum unambiguous imaging depth (cm)} = \frac{77}{\text{pulse repetition frequency (kHz)}} \quad d_m = \frac{77}{PRF}$$

$$\frac{\text{penetration (cm)}}{\text{}} \times \frac{\text{number of focuses}}{\text{}} \times \frac{\text{lines per frame}}{\text{}} \times \frac{\text{frame rate}}{\text{}} \leq 77,000$$

$$P \times NF \times LPF \times FR \leq 77,000$$

$$\text{Doppler shift (MHz)} = \text{echo frequency (MHz)} - \text{operating frequency (MHz)}$$

$$= \frac{2 \times \text{operating frequency (MHz)} \times \text{reflector speed (m/s)} \times \cos \theta}{\text{propagation speed (m/s)}}$$

$$f_D = f_e - f_o = \frac{2 f_o v \cos \theta}{c}$$

$$\text{reflector speed} = \frac{\text{propagation speed} \times \text{Doppler shift}}{2 \times \text{operating frequency} \times \cos \theta}$$

$$v \text{ (cm/s)} = \frac{77 f_D \text{ (kHz)}}{f_o \text{ (MHz)} \cos \theta}$$



Questions

- 1** Increasing the frequency
 a. improves the resolution
 b. increases the imaging depth
 c. increases refraction
 d. both a and b
 e. both a and c
- 2** Increasing the pulse repetition frequency
 a. improves resolution
 b. increases maximum depth imaged unambiguously
 c. decreases maximum depth imaged unambiguously
 d. both a and b
 e. both a and c
- 3** Increasing the intensity produced by the transducer
 a. is accomplished by increasing the pulser voltage
 b. increases the sensitivity of the system
 c. increases the possibility of bioeffects
 d. all of the above
 e. none of the above
- 4** Increasing the spatial pulse length
 a. is accomplished by transducer damping
 b. is accompanied by decreased pulse duration
 c. improves the axial resolution
 d. all of the above
 e. none of the above
- 5** Dynamic imaging is made possible by
 a. scan converters
 b. mechanically driven transducers
 c. gray-scale display
 d. arrays
 e. both b and d
- 6** Phantoms with nylon lines measure
 a. detail resolution
 b. pulse duration
 c. SATA intensity
 d. wavelength
 e. all of the above
- 9** The diagnostic ultrasound frequency range is
 a. 2 to 10 mHz
 b. 2 to 10 kHz
 c. 2 to 10 MHz
 d. 3 to 15 kHz
 e. none of the above
- 10** Small transducers always produce smaller beam diameters. True or false?
- 11** No reflection occurs if media impedances are equal. True or false?
- 12** No refraction occurs if media impedances are equal. True or false?
- 14** Attenuation is corrected by
 a. demodulation
 b. desegregation
 c. decompression
 d. compensation
- 15** Time is one dimension on which type of display?
 a. B mode
 b. color-flow
 c. M mode
 d. a la mode
 e. none of the above
- 16** The Doppler effect for a scatterer moving toward the transducer causes scattered sound (compared with incident sound) received by the transducer to have _____.
 a. increased intensity
 b. decreased intensity
 c. increased impedance
 d. increased frequency
 e. increased wavelength



Questions

- 18 Continuous-wave sound is used in _____.
a. all imaging instruments
b. some imaging instruments
c. all Doppler instruments
d. some Doppler instruments
e. none of the above
- 19 What is the transmitted intensity if the incident intensity is 1 and the impedances are 1.00 and 2.64?
a. 0.2
b. 0.4
c. 0.6
d. 0.8
e. 1.0
- 20 A thin-scattering-layer test object measures:
a. contrast resolution
b. beam profile
c. axial resolution
d. section thickness
e. more than one of the above
- 21 An advantage of continuous-wave Doppler instruments is that they have _____.
a. no aliasing
b. depth information and selectivity
c. bidirectional information
d. amplitude information
e. all of the above
- 22 An advantage of pulsed Doppler instruments is that they have _____.
a. no aliasing
b. depth information
c. bidirectional information
d. amplitude information
e. all of the above
- 24 If a transducer element 19 mm in diameter is focused to produce a minimum beam diameter of 2 mm, the intensity at the focus is approximately _____ times the intensity at the transducer.
a. 2
b. 3
c. 19
d. 100
e. 500
- 27 Which of the following produce(s) a sector-scan format?
a. convex array
b. oscillating mechanical real-time transducer
c. phased array
d. vector array
e. all of the above
- 31 The axial resolution for a two-cycle pulse of 5 MHz in tissue is _____ mm.
a. 0.1
b. 0.2
c. 0.3
d. 0.4
e. 0.5
- 32 The best lateral resolution for an unfocused 13-mm transducer element is _____ mm.
a. 2.5
b. 4.5
c. 6.5
d. 815
e. 13

Questions

- 33** Which is not improved by multiple transmit focus?
- detail resolution
 - temporal resolution
 - lateral resolution
 - image detail
 - none of the above
- 34** If the frame rate with one focus is 30 Hz, what is the likely frame rate with 3 transmit focuses?
- 3
 - 10
 - 15
 - 20
 - 30
- 35** If pulse repetition frequency is increased, the SPTA intensity is _____.
- increased
 - unchanged
 - decreased
 - eliminated
 - none of the above
- 36** If the thickness of a transducer element is decreased, the frequency is _____.
- increased
 - unchanged
 - decreased
 - intensified
 - none of the above
- 37** In Exercise .36, the near-zone length is _____.
- increased
 - unchanged
 - decreased
 - intensified
 - none of the above
- 38** With increased damping, which of the following is increased?
- bandwidth
 - pulse duration
 - spatial pulse length
 - Q factor
 - all of the above
- 39** As frequency is increased, which of the following is (are) decreased?
- propagation speed
 - PRF
 - imaging depth
 - more than one of the above
 - none of the above
- 40** If the pulse repetition frequency is 3 kHz and the frame rate is 30 per second, there will be _____ scan lines in the image (single focus).
- 3
 - 100
 - 300
 - 3000
 - 30,000
- 45** Duplex Doppler instruments include _____.
- pulsed Doppler
 - continuous-wave Doppler
 - color-flow imaging
 - gray-scale imaging
 - more than one of the above
- 46** If the Doppler shifts from normal arteries and from stenotic carotid arteries are 4 kHz and 10 kHz, respectively, for which will a pulse repetition frequency of 7 kHz be a problem?
- normal
 - stenotic
 - both
 - neither



Questions

- 47** The problem in Exercise 46 is
- refraction
 - resolution
 - range ambiguity
 - aliasing
 - mirror
- 48** Compensation (swept gain) makes up for the fact that echoes from deeper reflectors arrive at the transducer later. True or false?
- 49** Which of the following affects contrast resolution the most?
- number of pixels
 - number of bits per pixel
 - pulse duration
 - frequency
 - focusing
- 50** Which of the following requires a phased array as a receiving transducer?
- dynamic range
 - dynamic imaging
 - dynamic focusing
 - dynamic personality
 - none of the above
- 55** Propagation speed increases with increasing
- stiffness
 - density
 - absorption
 - attenuation
 - both a and b
- 56** Reflections are produced by changes in
- stiffness
 - density
 - absorption
 - attenuation
 - both a and b
- 57** If no reflection occurs at a boundary, this always means that media impedances are equal in the case of
- perpendicular incidence
 - oblique incidence
 - refraction
 - both a and b
 - both b and c
- 58** If the propagation speeds in two media are unequal, the incidence angle equals the
- reflection angle
 - transmission angle
 - Doppler angle
 - both a and b
 - both b and c
- 59** At a distance of one near-zone length from a disk transducer, the beam diameter is equal to the disk diameter divided by
- one
 - two
 - three
 - four
 - one fourth
- 61** Decibels are _____ ratio units.
- amplitude
 - power
 - neper
 - more than one of the above
 - all of the above
- 62** Which of the following are real-time displays? (More than one correct answer)
- B mode
 - B scan
 - M mode
 - Doppler
 - color flow

Questions

65 Frame rate is _____ by dynamic focus.

- a. increased
- b. decreased
- c. strengthened
- d. unaffected
- e. doubled

66 Which of the following produce(s) a sector scan format?

- a. convex array
- b. oscillating mechanical transducer
- c. phased array
- d. linear array
- e. more than one of the above

68 Gray-scale displays present brightness corresponding to echo

- a. frequency
- b. amplitude
- c. bandwidth
- d. impedance
- e. more than one of the above

69 If approximately 100 different gray levels can be distinguished by a human observer, how many bits per pixel would be a good choice for an ultrasound memory?

- a. 4
- b. 6
- c. 8
- d. 10
- e. 12

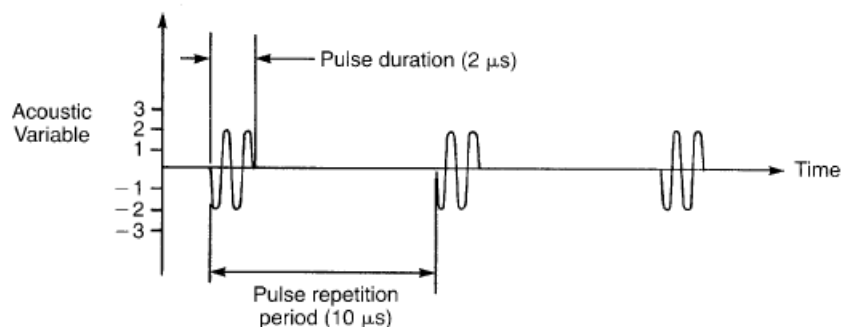
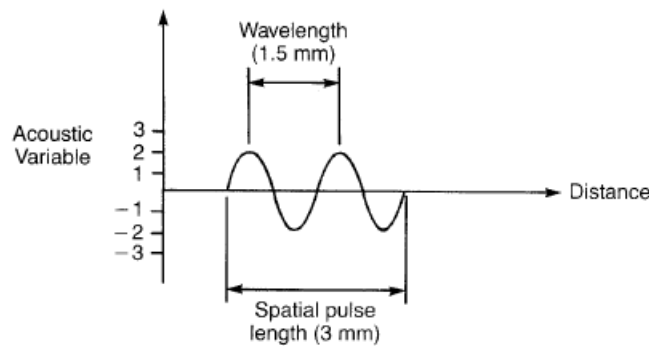
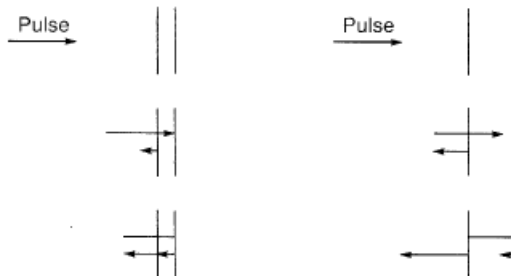
72 The intensity of returning echoes changes with the angle in Doppler flow measurements. True or false?

73 The intensity of returning echoes changes with the flow speed in Doppler ultrasound. True or false?

74 Figure 8.1 describes which type of resolution?

- a. axial
- b. lateral
- c. contrast
- d. detail
- e. a and d

75 In which part of Figure (a or b) are the two reflectors resolved?

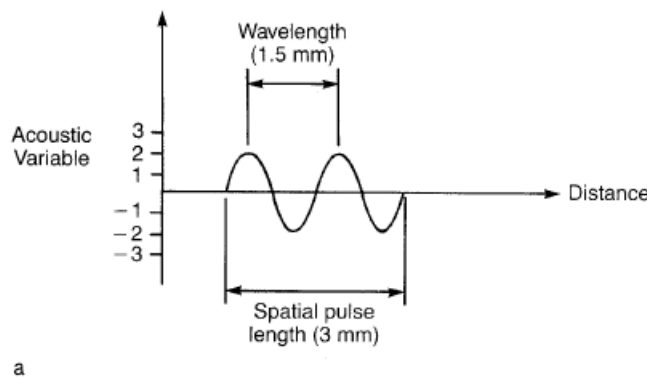




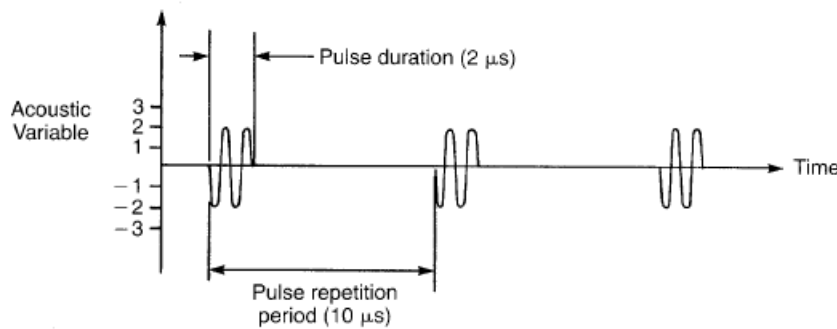
Questions

76 In Figure _____, give the following:

- number of cycles in a pulse
- amplitude
- wavelength
- spatial pulse length
- pulse repetition period
- pulse repetition frequency
- pulse duration
- period
- frequency
- duty factor
- propagation speed

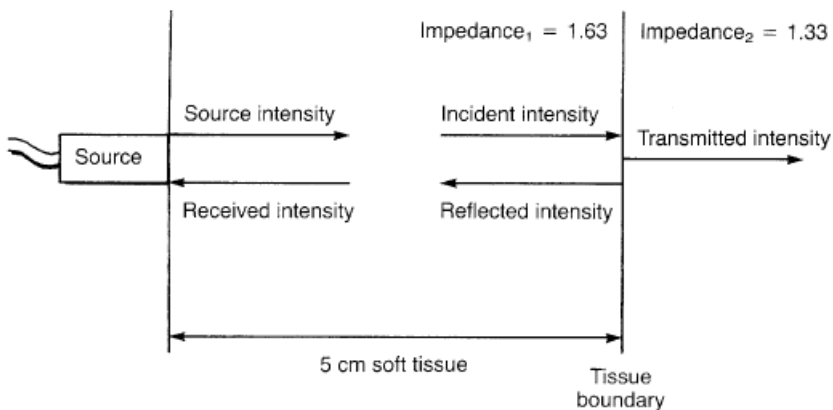


a

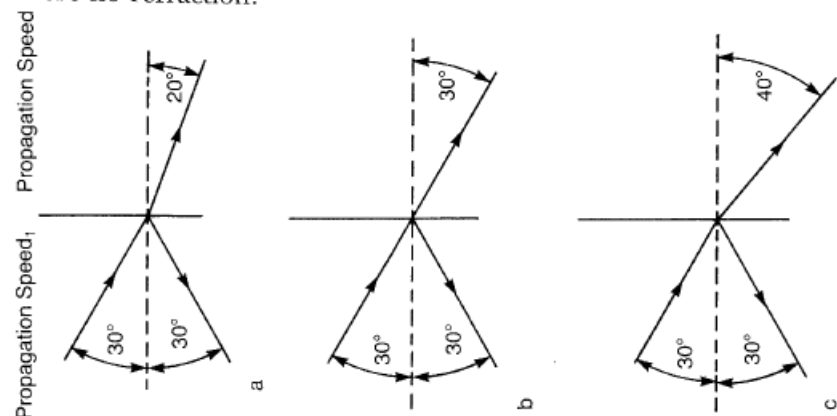


77 In Figure _____, if the frequency is 4 MHz, the attenuation from the source to the tissue boundary is _____ dB. If the intensity emitted by the source (transducer) is 10 mW/cm, the intensity arriving at the boundary (incident intensity) is _____ mW/cm.

The intensity reflection coefficient at the boundary is _____. The reflected intensity is _____ mW/cm and the received intensity at the source is _____ mW/cm.

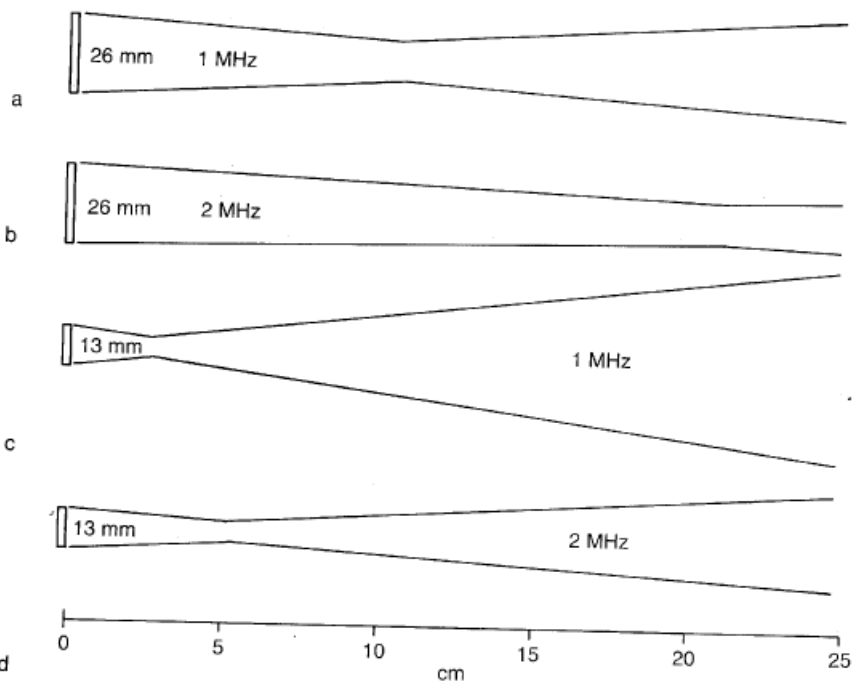


78 In which part of Figure 8.4 (a, b, or c) is speed 2 greater than speed 1? Is speed 2 less than speed 1? Is speed 2 equal to speed 1? Is there no refraction?

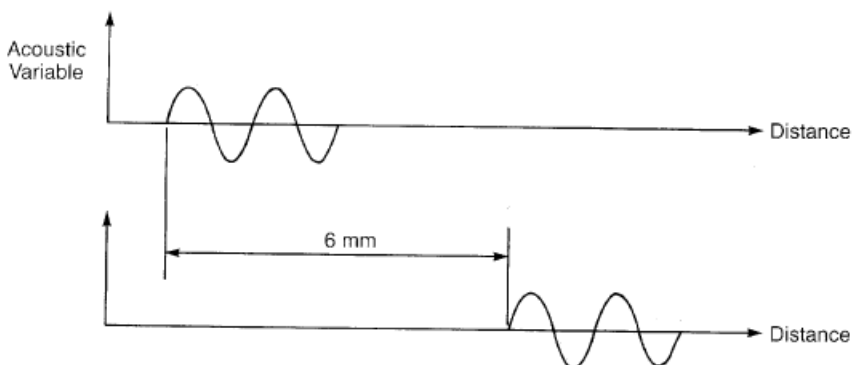


Questions

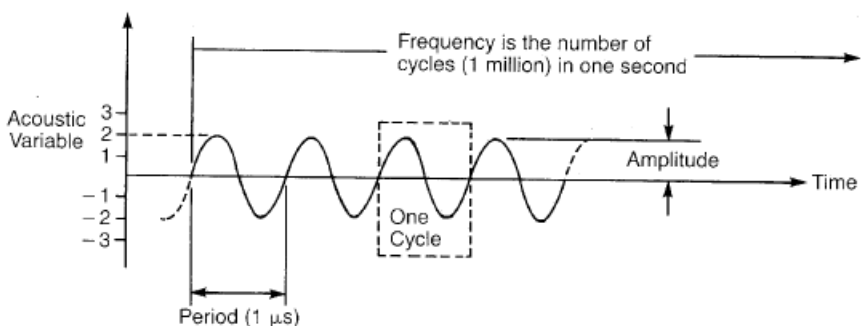
- 79 Figure shows that a higher frequency yields a (longer, shorter) near-zone length and that a larger transducer produces a (longer, shorter) near-zone length. By curving them, which of these transducers (a, b, c, or d) can be focused at 25 cm? at 15 cm? at 4 cm?



- 80 In Figure , the wave type is (continuous-wave, pulsed). If the lower portion of the figure represents 4 μs later than the upper portion, the propagation speed is _____ mm/ μs , the wavelength for a frequency of 1 MHz is _____ mm, and the spatial pulse length is _____ mm.



- .81 In Figure , the frequency is _____ MHz, the period is _____ μs , the amplitude is _____ units, the wave type is (continuous-wave, pulsed), and for soft tissue, the wavelength is _____ mm.

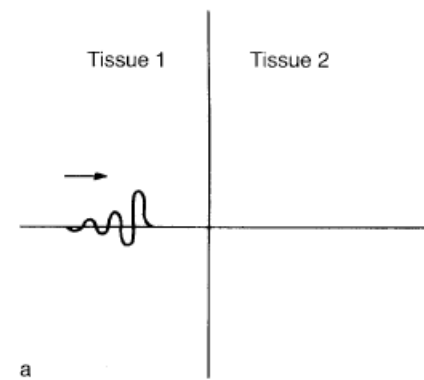




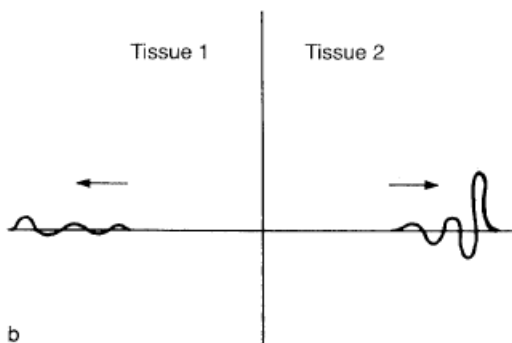
Questions

82 In Figure ..., which of the following have occurred?

- a. reflection
- b. refraction
- c. transmission
- d. a and b
- e. a and c

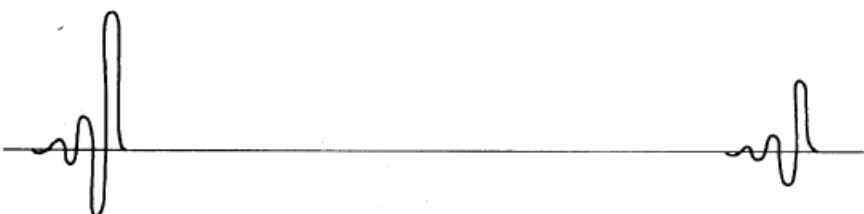


a



b

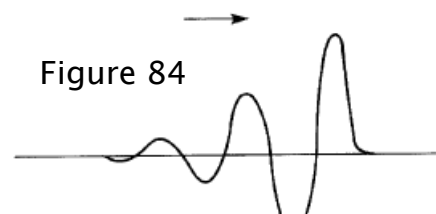
83 In Figure ..., as the pulse travels to the right, the amplitude decreases. This is called _____. If the amplitude at the right is one half the amplitude at the left, the attenuation is _____ dB.



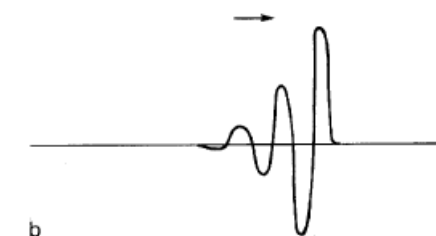
84 In Figure ..., which is the higher-frequency pulse (both in same medium)?

- a. a
- b. b
- c. neither

Figure 84



a



b

85 In Figure 84 ..., which pulse travels faster?

- a. a
- b. b
- c. neither

Questions

.86 In Figure 84 , which pulse travels farther (i.e., experiences less attenuation)?

- a. a
- b. b
- c. neither

87 In Figure 84 , which pulse has better axial resolution?

- a. a
- b. b
- c. neither

88 In Figure 84 , which pulse has the greater amplitude?

- a. a
- b. b
- c. neither

89 As frequency increases, which of the following (more than one) decrease?

- a. period
- b. wavelength
- c. propagation speed
- d. amplitude
- e. intensity
- f. attenuation coefficient
- g. penetration
- h. reflection coefficient
- i. transmission coefficient
- j. refraction
- k. pulse duration
- l. spatial pulse length
- m. pulse repetition frequency
- n. pulse repetition period
- o. duty factor
- p. near-zone length
- q. imaging depth
- r. axial resolution
- s. impedance

92 For a (flat) disk transducer element that is 13 mm in diameter, the lateral resolution at two times the near-zone length is:

- a. 6.5
- b. 13
- c. 19.5
- d. 26
- e. none of the above

93 As period increases, _____ increases.

- a. pulse duration
- b. frequency
- c. pulse repetition period

94 As duty factor increases, _____ increases.

- a. SPPA intensity
- b. SAPA intensity
- c. SATA intensity
- d. frequency
- e. amplitude

95 As PRF increases, _____ increases.

- a. penetration
- b. SPPA intensity
- c. amplitude
- d. pulse duration
- e. frame rate

96 Which produces a sector display that comes to a point at the top?

- a. linear array
- b. convex array
- c. phased array
- d. annular array
- e. vector array

Questions

97 A typical dynamic range for ultrasound instruments is:

- a. 1540 m/s
- b. 2–10 MHz
- c. 3 dB
- d. 50 dB
- e. 0.5 dB/cm

98 To maintain a comparable width focus as it moves deeper,
_____ must be increased.

- a. frequency
- b. aperture
- c. delays
- d. amplitude
- e. apodization

Answers

- .1 a
 .2 c
 .3 d
 .4 e
 .5 e
 .6 a
 .7 a
 .8 c
 .9 c (ophthalmic and intravascular are higher)
 .10 false (only true near the transducer)
 .11 false (only true for perpendicular incidence or oblique incidence when densities and propagation speeds of the media are equal)
 .12 false (see comment for 8.11)
 .13 c
 .14 d
 .15 c
 .16 d
 .17 false (6 bits)
 .18 d
 .19 d
 .20 e (b and d)
 .21 a
 .22 b
 .23 c
 .24 d (areas are 284 and 3 mm²)
 .25 c
- .26 d
 .27 e
 .28 c
 .29 a
 .30 d
 .31 c
 .32 c
 .33 b
 .34 b
 .35 a
 .36 a
 .37 a
 .38 a
 .39 c
 .40 b
 .41 c
 .42 d
 .43 c
 .44 c
 .45 e (a and d)
 .46 c
 .47 d
 .48 false
 .49 b
 .50 c
 .51
 .52
 .53
 .54
 .55 a
 .56 e
 .57 a
 .58 a
 .59 b
 .60 d
 .61 b
 .62 a, b, c, d, e
 .63 c
 .64 c
 .65 d
 .66 e (a, b, c)
 .67 d
 .68 b
- .69 c
 .70 d
 .71 a
 .72 false
 .73 false
 .74 e
 .75 b
 .76 a, 2; b, 2; c, 1.5 mm; d, 3 mm; e, 10 µs; f, 100 kHz; g, 2 µs; h, 1 µs;
 i, 1 MHz; j, 0.2; k, 1.5 mm/µs
 .77 10, 1, 0.01, 0.01, 0.001
 .78 c, a, b, b
 .79 longer; longer; none; b; a, b, and d
 .80 pulsed, 1.5, 1.5, 3
 .81 1, 1, 2, continuous-wave, 1.54
 .82 e
 .83 attenuation, 6, 2, 4
 .84 b
 .85 c
 .86 a
 .87 b
 .88 c
 .89 a, b, g, k, l, o, q, r (improved)
 .90 c
 .91 d
 .92 b
 .93 a
 .94 c
 .95 e
 .96 c
 .97 d
 .98 b
 .99



Futher Questions:

COMPREHENSIVE EXAMINATION

For each question, choose the best answer.

1. Which of the following frequencies is within the ultrasound range?
 - a. 15 Hz
 - b. 15 kHz
 - c. 15 MHz
 - d. 17,000 Hz
 - e. 17 km
2. The average propagation speed in soft tissues is
 - a. 1.54 mm/ μ s
 - b. 0.501 m/s
 - c. 1540 dB/cm
 - d. 37.0 km/min
 - e. 2 to 10 MHz
3. Pulse duration is the _____ for a pulse to occur.
 - a. space
 - b. time
 - c. delay
 - d. pressure
 - e. reciprocal
4. Spatial pulse length equals the number of cycles in the pulse times
 - a. period
 - b. impedance
 - c. beam width
 - d. resolution
 - e. wavelength
5. If pulse duration is 1 μ s and pulse repetition period is 100 μ s, duty factor is
 - a. 1 per cent
 - b. 10 per cent
 - c. 50 per cent
 - d. 90 per cent
 - e. 100 per cent
6. Which of the following depends significantly on frequency in soft tissues?
 - a. propagation speed
 - b. density
 - c. stiffness
 - d. attenuation
 - e. impedance
7. The attenuation of 5-MHz ultrasound in 4 cm of soft tissue is
 - a. 5 dB/cm
 - b. 10 dB
 - c. 2.5 MHz/cm
 - d. 2 cm
 - e. 5 dB/MHz
8. If the maximum value of an acoustic variable in a sound wave is 10 units and the normal (no sound) value is 7 units, the amplitude is _____ units.
 - a. 1
 - b. 3
 - c. 7
 - d. 10
 - e. 17
9. Impedance equals propagation speed multiplied by
 - a. density
 - b. stiffness
 - c. frequency
 - d. attenuation
 - e. path length
10. Which of the following cannot be determined from the others?
 - a. frequency
 - b. amplitude
 - c. intensity
 - d. power
 - e. beam area
11. For perpendicular incidence, in medium one, density = 1 and propagation speed = 3; in medium two, density = 1.5 and propagation speed = 2. What is the intensity reflection coefficient?
 - a. 0
 - b. 1
 - c. 2
 - d. 3
 - e. 4



Futher Questions:

COMPREHENSIVE EXAMINATION

- 12.** For perpendicular incidence, if the intensity transmission coefficient is 96 per cent, what is the intensity reflection coefficient?
- 2 per cent
 - 4 per cent
 - 6 per cent
 - 8 per cent
 - 10 per cent
- 13.** The quantitative presentation of frequencies contained in echoes is called
- preamplification
 - digitizing
 - optical encoding
 - spectral analysis
 - all of the above
- 14.** For oblique incidence and medium-two speed that is equal to twice medium-one speed, the transmission angle will be about _____ times the incidence angle.
- $\frac{1}{2}$
 - 17
 - 2
 - 4
 - 5
- 15.** The range equation describes the relationship of
- reflector distance, propagation time, and sound speed
 - distance, propagation time, and reflection coefficient
 - number of cows and sheep on a ranch
 - propagation time, sound speed, and transducer frequency
 - dynamic range and system sensitivity
- 16.** Axial resolution in a system equals
- four times the spatial pulse length
 - ratio of reflector size to transducer frequency
 - maximum reflector separation expected to be displayed
 - minimum reflector separation expected to be displayed
 - spatial pulse length
- 17.** The Doppler frequency shift is caused by
- relative motion between the transducer and the reflector
 - patient shivering in a cool room
 - a high transducer frequency and real-time scanner
 - small reflectors in the transducer beam
 - changing transducer thickness
- 18.** A small (relative to the transducer wavelength) reflector is said to _____ an incident sound beam.
- focus
 - speculate
 - scatter
 - shatter
 - amplify
- 19.** In soft tissue, two boundaries that generate reflections are separated in axial distance (depth) by 1 mm. With a two-cycle pulse of ultrasound, the minimum frequency that will axially resolve these boundaries is
- 1.0 MHz
 - 2.0 MHz
 - 3.0 MHz
 - 4.0 MHz
 - 5.0 MHz
- 20.** The frequency of an ultrasound transducer is determined primarily by which of the following:
- element diameter
 - element thickness
 - speed of sound in tissue
 - voltage applied
 - all of the above
- 21.** The fundamental operating principle of medical ultrasound transducers is
- Snell's law
 - Doppler's law
 - magnetostrictive effect
 - piezoelectric effect
 - impedance effect
- 22.** Transducers operating properly in pulse-echo imaging systems have a quality factor of approximately
- 1–3
 - 7–10
 - 25–50
 - 100
 - 500
- 23.** The axial resolution of a transducer is determined primarily by the
- spatial pulse length
 - the near-field limit
 - the transducer diameter
 - the acoustic impedance of tissue
 - density

24. The lateral resolution of a transducer is determined primarily by the
- spatial pulse length
 - damping
 - the transducer diameter
 - the acoustic impedance of tissue
 - applied voltage
25. Which of the following quantities varies most with distance from the transducer face?
- axial resolution
 - lateral resolution
 - frequency
 - wavelength
 - period
26. The near-zone length for a 13-mm diameter, unfocused, 5-MHz, circular transducer is greater than that for which of the following 5-MHz transducers with diameters as listed?
- 19 mm
 - 15 mm
 - 9 mm
 - depends on impedance
 - none of the above
27. If the near-zone length of an unfocused transducer that is 13 mm in diameter extends (in soft tissue) 6 cm from the transducer face, at which of the following distances from the face can the lateral resolution be improved by focusing the sound from this transducer?
- 13 cm
 - 8 cm
 - 3 cm
 - 9 cm
 - none of the above
28. The lateral resolution of an ultrasound system depends upon
- the transducer diameter
 - the transducer frequency
 - the speed of sound in soft tissue
 - memory and display
 - all of the above
29. Which of the following is a characteristic of a medium through which sound is propagating?
- impedance
 - intensity
 - amplitude
 - frequency
 - period
30. Which of the following cannot be determined from the others?
- frequency
 - period
 - amplitude
 - wavelength
 - propagation speed
31. For perpendicular incidence, if the impedances of the two media are the same, there will be no
- inflation
 - reflection
 - refraction
 - calibration
 - b and c
32. What is the transmitted intensity if the incident intensity is 1 and the impedances are 1.00 and 2.64?
- 0.2
 - 0.4
 - 0.6
 - 0.8
 - 1.0
33. Increasing frequency
- improves resolution
 - increases imaging depth
 - increases refraction
 - a and b
 - a and c
34. Increasing intensity produced by the transducer
- is accomplished by increasing pulser voltage
 - increases sensitivity of the system
 - increases the possibility of biologic effects
 - all of the above
 - none of the above
35. Ultrasound bioeffects
- do not occur
 - do not occur with diagnostic instruments
 - are not confirmed below 100 mW/cm^2 SPTA
 - b and c
 - none of the above
36. Diagnostic ultrasound frequency range is:
- 2 to 10 MHz
 - 2 to 10 kHz
 - 2 to 10 MHz
 - 3 to 15 kHz
 - none of the above

Futher Questions:

COMPREHENSIVE EXAMINATION

37. If propagation speeds of two media are equal, incidence angle equals
a. reflection angle
b. transmission angle
c. Doppler angle
d. a and b
e. b and c
38. If no reflection occurs at a boundary, it always means that media impedances are equal in the case of
a. perpendicular incidence
b. oblique incidence
c. refraction
d. a and b
e. b and c
39. Increasing spatial pulse length
a. accompanies increased transducer damping
b. is accompanied by decreased pulse duration
c. improves axial resolution
d. all of the above
e. none of the above
40. Place the media in order of increasing sound propagation speed.
a. gas, solid, liquid
b. solid, liquid, gas
c. gas, liquid, solid
d. liquid, solid, gas
e. solid, gas, liquid
41. What is the wavelength of 1-MHz ultrasound in tissue with a propagation speed of 1540 m/s?
a. 1×10^6 m
b. 1.54 mm
c. 1540 m
d. 1.54 cm
e. 0.77 cm
42. What is the spatial pulse length for two cycles of ultrasound having a wavelength of 2 mm?
a. 4 cm
b. 4 mm
c. 7 mm
d. 1.5 mm
e. 3 mm
43. Increased damping produces
a. increased bandwidth
b. decreased Q factor
c. decreased efficiency
d. all of the above
e. none of the above
44. The Doppler effect is a change in
a. intensity
b. wavelength
c. frequency
d. all of the above
e. b and c
45. What determines the lower and upper limits of the frequency range that is useful in diagnostic ultrasound?
a. resolution and imaging depth
b. intensity and resolution
c. intensity and propagation speed
d. scattering and impedance
e. impedance and wavelength
46. If no refraction occurs as an oblique sound beam passes through the boundary between two materials, what is unchanged as the boundary is crossed?
a. impedance
b. propagation speed
c. intensity
d. sound direction
e. b and d
47. If the spatial average intensity in a beam is 1 W/cm² and the transducer is 5 cm² in area, what is the total acoustic power?
a. 1 W
b. 2 W
c. 3 W
d. 4 W
e. 5 W
48. How does the propagation speed in bone compare to that in soft tissue?
a. lower
b. the same
c. higher
d. cannot say unless soft tissue is specified
e. b and c

Futher Questions:

COMPREHENSIVE EXAMINATION

49. Attenuation along a sound path is a decrease in
a. frequency
b. amplitude
c. intensity
d. b and c
e. impedance
50. Reverberation causes us to think there are reflectors that are too great in
a. impedance
b. attenuation
c. brightness
d. size
e. number
51. Doppler shift is zero when the angle between the sound direction and the movement (flow) direction is _____ degrees.
a. 30
b. 60
c. 90
d. 45
e. none of the above
52. A focused transducer that is 13 mm in diameter has a lateral resolution at the focus of better than (i.e., smaller than)
a. 26 mm
b. 13 mm
c. 6.5 mm
d. depends on frequency
e. none of the above
53. An important factor in the selection of a transducer for a specific application is the ultrasonic attenuation of tissue. Owing to this attenuation, a 7.5-MHz transducer should generally be used for
a. imaging deep structures
b. imaging superficial structures
c. imaging both deep and shallow structures
d. imaging adult intracranial structures
e. all of the above
55. Which of the following is determined by the pulser in an instrument?
a. amplitude
b. pulse repetition frequency
c. length of time required for a pulse to reach a specific reflector and return to the instrument
d. more than one of the above
e. none of the above
58. If the power at the output of an amplifier is 1000 times the power at the input, the gain is
a. 60 dB
b. 30 dB
c. 1000 dB
d. 1000 volts
e. none of the above
61. The compensation (swept gain) control serves to
a. compensate for machine instability in the warm-up time
b. compensate for attenuation
c. compensate for transducer aging and the ambient light in the examining room
d. decrease patient examination time
e. none of the above
66. Phased array systems involve the sequential switching of a small group of elements along the array.
a. true
b. false
67. Duplex Doppler presents:
a. anatomic (structural) information
b. physiologic (flow) information
c. impedance data
d. more than one of the above
e. all of the above
68. Doppler shift frequencies are usually in a relatively narrow range above 20 kHz.
a. true
b. false
69. Enhancement is caused by a
a. strongly reflecting structure
b. weakly attenuating structure
c. strongly attenuating structure
d. frequency error
e. propagation speed error
70. For a two-cycle pulse of 5 MHz in soft tissue, the axial resolution is
a. 0.1 mm
b. 0.3 mm
c. 0.5 mm
d. 0.7 mm
e. 0.9 mm

Futher Questions:

COMPREHENSIVE EXAMINATION

75. M-mode recordings have _____ dimension(s).
a. two spatial
b. one spatial and one temporal
c. one Doppler and one temporal
d. one Doppler and one spatial
e. b and c
77. Another name for rejection is
a. threshold
b. depth gain compensation
c. swept gain
d. compression
e. demodulation
80. If the propagation speed in a soft-tissue path is 1.60 mm/ μ s, a diagnostic instrument assumes a propagation speed too _____ and will show reflectors too _____ the transducer.
a. high, close to
b. high, far from
c. low, close to
d. low, far from
e. none of the above
81. The reflector information that can be obtained from an M-mode display includes
a. distance and motion pattern
b. transducer frequency, reflection coefficient, and distance
c. acoustic impedance, attenuation, and motion pattern
d. all of the above
e. none of the above
82. Increasing the gain generally produces the same effect
a. decreasing the attenuation
b. increasing the compression
c. increasing the rectification
d. both b and c
e. all of the above
83. A gray-scale display shows
a. gray color on a white background
b. reflections with one brightness level
c. a white color on a gray background
d. a range of reflection amplitudes or intensities
e. none of the above
84. Electric pulses from the pulser are applied to the
a. pulser
b. transducer
c. receiver
d. display
e. memory
85. Rectification and smoothing (filtering) are parts of
a. amplipression
b. rejection
c. a and b
d. compression
e. demodulation
86. Which of the following is performed in a receiver?
a. amplification
b. compensation
c. compression
d. demodulation
e. all of the above
87. Continuous-wave sound is used in
a. all ultrasound imaging instruments
b. only bistable instruments
c. all Doppler instruments
d. some Doppler instruments
e. some fourier instruments
88. If the gain of an amplifier is reduced by 3 dB and input power is unchanged, the output power of the amplifier is _____ what it was before.
a. equal to
b. twice
c. one half
d. greater than
e. none of the above
89. Increasing the pulse repetition frequency
a. improves detail resolution
b. increases maximum depth imaged unambiguously
c. decreases maximum depth imaged unambiguously
d. both a and b
e. both a and c
90. If gain was 30 dB and output power is reduced by one half, the new gain is _____ dB.
a. 15
b. 60
c. 33
d. 27
e. none of the above



Futher Questions:

COMPREHENSIVE EXAMINATION

- 93.** Phantoms with nylon lines measure
 a. resolution
 b. pulse duration
 c. SATA intensity
 d. wavelength
 e. all of the above
- 94.** The following measure acoustic output:
 a. hydrophone
 b. optical encoder
 c. 100-mm test object
 d. all of the above
 e. none of the above
- 96.** Gain and attenuation are usually expressed in
 a. dB
 b. dB/cm
 c. cm
 d. cm/dB
 e. none of the above
- 98.** An advantage of continuous-wave Doppler over pulsed Doppler is
 a. depth information
 b. bidirectional
 c. no aliasing
 d. b and c
 e. all of the above
- 99.** With which of the following is time on one axis?
 a. B mode
 b. B scan
 c. M mode
 d. a la mode
 e. none of the above
- 100.** In Doppler color-flow instruments, color represents
 a. sign (+ or -) of Doppler shift
 b. flow direction
 c. magnitude of the Doppler shift
 d. amplitude of the Doppler shift
 e. more than one of the above
- 101.** Attenuation is corrected by
 a. demodulation
 b. desegregation
 c. decompression
 d. compensation
 e. decompensation
- 102.** What must be known to calculate distance to a reflector?
 a. attenuation, speed, density
 b. attenuation, impedance
 c. attenuation, absorption
 d. travel time, speed
 e. density, speed
- 103.** Which of the following improve(s) sound transmission from the transducer element into the tissue?
 a. matching layer
 b. Doppler effect
 c. damping material
 d. coupling medium
 e. a and d
- 104.** Lateral resolution is improved by
 a. damping
 b. pulsing
 c. focusing
 d. reflecting
 e. absorbing
- 105.** Voltage pulses occur at the output of the
 a. pulser
 b. transducer
 c. receiver
 d. display
 e. a, b, and c
- 106.** The Doppler effect for a scatterer moving toward the sound source causes the scattered sound (compared to the incident sound) received by the transducer to have
 a. increased intensity
 b. decreased intensity
 c. increased impedance
 d. increased frequency
 e. decreased impedance
- 107.** Axial resolution is improved by
 a. damping
 b. pulsing
 c. focusing
 d. reflecting
 e. absorbing
- 108.** Which of the following is (are) dynamic (real-time)?
 a. Doppler
 b. B scan
 c. M mode
 d. all of the above
 e. none of the above



Futher Questions:

COMPREHENSIVE EXAMINATION

- 110.** If the Doppler shifts from normal and stenotic carotid arteries are 4 kHz and 10 kHz, respectively, for which will there be a problem with a pulse repetition frequency of 7 kHz?
- normal
 - stenotic
 - both
 - neither
- 111.** The receiver in a Doppler system compares the _____ of the voltage generator and the voltage from the receiving transducer.
- wavelength
 - intensity
 - impedance
 - frequency
 - all of the above
- 112.** A digital imaging instrument divides the cross-sectional image into _____.
- frequencies
 - bits
 - pixels
 - binaries
 - wavelengths
- 113.** Which of the following produce(s) a sector-scan format?
- rotating mechanical real-time transducer
 - oscillating mechanical real-time transducer
 - phased array
 - oscillating mirror
 - all of the above
- 114.** The piezoelectric effect describes how _____ is converted into _____ by a _____.
- electricity, an image, display
 - incident sound, reflected sound, boundary
 - ultrasound, electricity, transducer
 - ultrasound, heat, tissue
 - none of the above
- 115.** Propagation speed in soft tissues
- is directly proportional to frequency
 - is inversely proportional to frequency
 - is directly proportional to intensity
 - is inversely proportional to intensity
 - none of the above
- 116.** The frequencies used in diagnostic ultrasound imaging
- are much lower than those used in Doppler measurements
 - determine imaging depth in tissue
 - determine imaging resolution
 - all of the above
 - b and c
- 117.** As frequency is increased
- wavelength increases
 - a three-cycle ultrasound pulse decreases in length
 - imaging depth decreases
 - propagation speed decreases
 - b and c
- 118.** In the Doppler equation
- $$f_D = \frac{2 f \cos \theta}{c - v \cos \theta}$$
- which can normally be ignored?
- $v \cos \theta$ in the denominator
 - $v \cos \theta$ in the numerator
 - f
 - f_D
 - b and c
- 119.** For which of the following is the reflected frequency less than the incident frequency?
- advancing flow
 - receding flow
 - perpendicular flow
 - laminar flow
 - all of the above
- 120.** Focusing
- improves lateral resolution
 - improves axial resolution
 - increases beam width in the focal region
 - shortens pulse length
 - increases duty factor



Answers of comprehensive examination

Comprehensive Examination Answers

Some answers also have explanatory comments.

1. c. Ultrasound is sound having a frequency greater than 20 kHz (0.02 MHz). Answer e is not expressed in frequency units.
2. a. Propagation speeds in soft tissues are in the range of about 1.4 to 1.6 mm/ μ s. Answers c and e are not expressed in speed units.
3. b.
4. e. The wavelength is the length of each cycle in a pulse.
5. a. Duty factor is pulse duration divided by pulse repetition period.
6. d. Propagation speed and impedance increase only slightly with frequency.
7. b. The attenuation coefficient of 5-MHz ultrasound is approximately 2.5 dB/cm. The attenuation coefficient multiplied by the path length yields the attenuation in dB. Only answer b is given in attenuation (dB) units.
8. b. Amplitude is the maximum amount that an acoustic variable varies from the normal value. In this case, 10 minus 7 units.
9. a. This is the characteristic impedance.
10. a. Amplitude, intensity, power, and beam area are all related to each other. If two of these are known, the others can be found. Frequency is independent of these. All four of them can be known and yet frequency can remain undetermined.
11. a. Impedance 1 equals 3, which equals impedance 2; thus, there is no reflection.
12. b. If 96 per cent of the intensity is transmitted, 4 per cent was reflected because what is not reflected is transmitted (i.e., the two must add up to 100 per cent).
13. d. Spectral comes from "spectrum," referring to color spectrum. A prism is an optical spectrum analyzer that breaks down white light into its component colors.
14. c. If the second speed is twice the first speed, then the transmission angle is twice the incidence angle.
15. a. Reflector distance equals $1/2 \times$ speed \times time.
16. d. If reflectors are separated by less than the axial resolution, they are not separated on the display.
17. a.
18. c. Scattering occurs with rough surfaces and with hetero-

geneous media (made up of small particles relative to the wavelength). Large flat smooth surfaces produce specular reflections.

19. b. Axial resolution is equal to one half the spatial pulse length. Spatial pulse length is equal to the number of cycles in the pulse multiplied by wavelength. Wavelength is equal to propagation speed divided by frequency. For 1 MHz, wavelength is 1.54 mm, spatial pulse length is 2×1.54 , and axial resolution is 1.54 mm, so that two reflectors separated by 1 mm would not be resolved. For 2 MHz, the resolution is 0.77 and the reflectors will be resolved.
20. b. The operating frequency of a transducer is such that its thickness is equal to one half the wavelength in the transducer element material.
21. d. Transducer elements expand and contract when a voltage is applied, and, conversely, when returning echoes apply pressure to the element, a voltage is generated.
22. a. For highly damped transducers, the quality factor (Q) is approximately equal to the number of cycles in the pulse.
23. a. Axial resolution is equal to one half the spatial pulse length.
24. c. Lateral resolution is equal to beam width. Near-zone length is dependent on transducer diameter and, thus, so is the lateral resolution at any given distance from the transducer.
25. b. Beam width changes with distance from transducer and, thus, so does lateral resolution.
26. c. Near-zone length increases with transducer diameter so that the only transducer that would have a shorter near-zone length would be a transducer of smaller diameter.
27. c. Focusing can only be accomplished in the near zone of a beam.
28. e. Answers a, b, and c all affect the beam. Resolution of the system is also affected by the electronics of the instrument.
29. a. All the others are characteristics of the sound.
30. c. Frequency, period, wavelength, and propagation speed are all related to each other. However, all four of these can be known and yet the amplitude can remain undetermined.
31. e. For perpendicular incidence, there is no refraction. For equal impedances, there is no reflection.
32. d.

$$\text{IRC} = \left[\frac{2.64 - 1.00}{2.64 + 1.00} \right]^2 = \left[\frac{1.64}{3.64} \right]^2 = (0.45)^2 = 0.2$$



Answers of comprehensive examination

For an intensity reflection coefficient of 0.2 and an incident intensity of one, the reflected intensity is 0.2 and the transmitted intensity is 0.8.

33. a. Imaging depth decreases with increasing frequency and frequency has no effect on refraction.
34. d.
35. c. This is the AIUM statement on *in vivo* mammalian bioeffects.
36. c. Frequencies lower than this range do not provide the needed resolution, whereas frequencies greater than this range do not allow for adequate imaging depth for medical purposes.
37. d. Incidence angle always equals reflection angle and, for equal propagation speeds, it equals transmission angle as well.
38. a. For oblique incidence, it is possible to have no reflection, even if media impedances are unequal.
39. e. Increased transducer damping decreases the spatial pulse length. Increasing spatial pulse length is accompanied by increased pulse duration and degraded axial resolution.
40. c.
41. b. Wavelength is equal to propagation speed divided by frequency.
42. b. Spatial pulse length is equal to wavelength multiplied by the number of cycles in the pulse.
43. d.
44. e. If frequency changes, wavelength changes also.
45. a. See answer to Problem 36.
46. e. No refraction means that there is no change in sound direction. This is a result of no change in propagation speed (equal propagation speeds on both sides of the boundary).
47. e. If there is 1 W in each square centimeter of area, then there are 5 W in 5 cm² of area.
48. c. Speeds in solids are higher than in liquids. Soft tissue behaves acoustically as a liquid (it is mostly water).
49. d.
50. e. Reverberation adds additional reflectors on the display deeper than the true ones.
51. c
52. c. An unfocused 13-mm transducer has a beam width of 6.5 mm at the near-zone length. Focusing would reduce the lateral resolution below this value (i.e., improve it).
53. b. A 7.5-MHz transducer can image to a depth of only a few centimeters in tissue.

55. d. (a and b).

58. b. For each 10 dB, there is a factor of 10 increase in power.

61. b.

66. b. This is a description of a linear switched or sequenced array, rather than a phased array.

67. d. Answers a and b are both correct. Anatomic data are provided by the real-time B scan and physiologic data are provided by the pulsed Doppler portion of the instrument.

68. b. Physiologic Doppler shift frequencies are usually in the audible frequency range.

69. b.
70. b.

$$AR = \frac{1}{2}SPL = \frac{1}{2}n \times \frac{c}{f} = \frac{1}{2}(2) \frac{1.54}{5} = 0.3$$

75. b. In M mode, echo depth is displayed as a function of time.

77. a.

80. c. The instrument assumes a speed of 1.54 mm/ μ s. Echoes will arrive sooner because of their higher propagation speed and will be placed in closer proximity than they should be.

81. a.

Answers of comprehensive examination

82. a. Increasing gain and decreasing attenuation each increase echo intensity.
83. d.
84. b.
85. e.
86. e.
87. d. All imaging instruments and some Doppler instruments use pulsed ultrasound.
88. c. A reduction of 3 dB is a 50 per cent reduction.
89. c. Pulse repetition frequency has no effect on detail resolution.
90. d. See answer to Problem 88.
93. a.
94. a.
96. a.
98. c.
99. c.
100. e.
101. d.
102. d. The range equation relates these three quantities.
103. e. The matching layer improves sound transmission by reducing the reflection at the transducer-skin boundary. A coupling medium improves sound transmission by removing the air layer between the transducer and the skin.
104. c.
105. e.
106. d.
107. a.
108. d. All of these modes are updated many times each second.
110. c. Both Doppler shifts exceed one half the pulse repetition frequency. The problem is aliasing.
111. d.
112. c.
113. e.
114. c.
115. e. Propagation speed is independent of frequency and intensity.
116. e.
117. e.
118. a. Physiologic flow speeds are small compared to the speed of sound in tissues.
119. b.
120. a.